Laura J. Moore · A. Brad Murray
Editors

Barrier Dynamics and Response to Changing Climate

Springer

Barrier Dynamics and Response to Changing Climate

Laura J. Moore • A. Brad Murray
Editors

Barrier Dynamics and Response to Changing Climate

Springer

Editors
Laura J. Moore
Department Geological Sciences,
Curriculum for the Environment
and Ecology
University of North Carolina at Chapel Hill
Chapel Hill, NC, USA

A. Brad Murray
Division of Earth and Ocean Sciences,
Nicholas School of the Environment, Center
for Nonlinear and Complex Systems
Duke University
Durham, NC, USA

ISBN 978-3-319-68084-2 ISBN 978-3-319-68086-6 (eBook)
https://doi.org/10.1007/978-3-319-68086-6

Library of Congress Control Number: 2017960415

Cover Image:
Metmopkin Island, VA, USA
Metompkin Island – 633, ©Gordon Campbell, Gordon Campbell, https://ataltitudegallery.com/

Printed on acid-free paper

This Springer imprint is published by Springer Nature
The registered company is Springer International Publishing AG
The registered company address is: Gewerbestrasse 11, 6330 Cham, Switzerland

For Nia and Davin

And for all children, young and old, who love barrier beaches as much as they do

Preface

Motivation

Many of the world's coasts feature dynamic strips of sand and/or gravel, backed by shallow coastal bays and fronting mainland shores (e.g., Stutz and Pilkey 2002) (Fig. 1). Whether they are islands (separated from each other by tidal inlets) or long spits, these barriers often protect human development on the mainland, as well as valuable back-barrier ecosystems, from storm impacts. In addition, barriers themselves host unique ecosystems and economically important development and recreational opportunities. As low-lying collections of loose sediment (often inhabited by vegetation and/or the site of structures built by humans), barriers are vulnerable to increasing rates of relative sea-level rise (the additive effects of global sea-level rise and vertical motions of the land regionally; "RSLR") and increases in the frequency of major coastal storms. In this volume, we bring together chapters authored by internationally recognized barrier researchers, whose work collectively represents our state-of-the-art understanding of barrier dynamics and the ways in which these landforms respond to changing climate.

We intend this collection to be of use for researchers who study barriers and related coastal processes, for managers and policy-makers grappling with important decisions regarding the future of barrier coastlines, and for a broader audience of educated readers with a general interest in environmental processes in a changing world. Below we provide a brief overview of barrier dynamics to assist those who are less familiar with this topic in understanding the chapters that follow. We then provide an overview of the scope of the volume by summarizing chapter content, and we conclude with some general thoughts about barrier dynamics in a changing world based on what we have come to understand thus far.

Fig. 1 Examples of barrier systems. (**a**) Long Beach Peninsula, Washington, USA; (**b**) barriers along the Wadden Sea, the Netherlands and Germany; (**c**) barriers along the Gulf of Mexico, Mississippi and Alabama, USA; (**d**) Ria Formosa National Park, Portugal; (**e**) Virginia Barrier Islands, USA; (**f**) Outer Banks, North Carolina, USA; (**g**) Gold Coast and Stradbroke Island, Australia. All images: Google 2017 TerraMetrics; Data SIO, NOAA, U.S. Navy, NGA, Gebco

An Overview of Barrier Dynamics

The visible (or subaerial) portion of a barrier—the land above the normal high-tide level—continues to exist because of major storms: storm waves and elevated water levels ("storm surge") wash sediment landward from the beach and shallow seabed, depositing it on the barrier (or sometimes in the marshes or bays landward of the barrier; see chapters by Houser et al., Moore et al., Odezulu et al., Mallinson et al., and Rodriquez et al. for details). These "overwash" events build barriers vertically through the deposition of overwash sand (also more traditionally referred to as "washover"). Most barriers are comprised primarily of sand (although some are gravel), and on sandy barriers, wind is a primary driver of sediment transport when the beach is dry, sand is available for transport (e.g., not covered by a shell lag), and the wind is sufficiently strong to carry sand grains. Self-reinforcing interactions (i.e., feedbacks) between this wind-driven—aeolian—sand transport and vegetation growth lead to the development of coastal foredunes, the seaward-most line of dunes fronting most sandy barrier islands. Once present, dunes play an important role in determining the effect of storms on barriers. Where dunes are high relative to storm water level (which is determined by the combination of tides, storm surge, and wave action), they prevent overwash from occurring during all but the strongest of storms. Where dunes are low, even a moderate storm may be an overwash event. By controlling the delivery of overwashed sediment to the barrier interior, and beyond, the cycles of dune growth and destruction control how barriers and barrier environments evolve over time, especially at short time scales on the order of decades (see chapters by Moore et al., Houser et al., and Ruggiero et al. for details). On longer time scales (e.g., centuries and millennia), however, dunes are essentially transient features, and their effects are likely swamped by the effects of factors such as sea-level rise and changes in storminess that operate at larger spatial and longer temporal scales.

On some barriers, where the rate of sediment supply is high or where sea level is falling, accumulation of sediment leads to barrier widening, as the shoreline moves seaward (e.g., chapter by Cowell and Kinsella and Moore et al.). On most barriers throughout the world today and throughout the last several millennia, however, the shoreline moves landward in the long term, tending to result in barrier narrowing. When the width of a barrier becomes equivalent to the average extent of storm-driven overwash, further shoreline erosion leads to long-term landward migration of the barrier landform itself. Many barriers, especially barrier islands, initially formed farther seaward than their present-day location and have migrated to their current position as sea level continued to rise slowly over the last few thousand years. Evidence suggests that some barriers are already experiencing an increase in migration rate in response to recent increases in sea-level rise rates (e.g., see chapters by Rodriguez et al. and Odezulu et al.)—a response that is expected to become more widespread in the future (see chapters by Ashton and Lorenzo-Trueba, Moore and Murray, and FitzGerald et al.).

The subaerial portion of a barrier is intimately connected to a large region of the nearshore seabed, a region called the "shoreface" (see chapters by Ashton and

Lorenzo-Trueba, Cowell and Kinsela, and Murray and Moore). Waves in shallow water tend to sweep sand and gravel landward (because, in shallow water, the landward velocity of water under the crest of a wave is greater than the seaward velocity of water under the trough of a wave, leading to more sand moving landward under the crests than seaward under the troughs; Fredsoe and Deigaard 1992). Over time, this tendency for landward sweeping of sediment creates a pile of sediment and the seabed becomes sloped upward toward the land. This slope, in turn, tends to inhibit further landward motion of sediment. Given enough time, the slope of the seabed increases until the slope is steep enough to prevent further landward sediment transport (in a long-term averaged sense) and an "equilibrium slope" develops. Because wave motions at the bed (and asymmetry between landward and seaward velocities) are strongest in shallow water, equilibrium slopes are steepest near shore and become progressively gentler in the offshore direction. In other words, the equilibrium profile of the shoreface tends to be concave upward. This shoreface profile extends to do a depth below which wave-driven sediment transport becomes negligible (referred to as the shoreface depth when considered over long time scales and as the closure depth when considered on shorter time scales, especially in the coastal engineering literature). This depth depends on the typical wave characteristics as well as the time scales considered. Longer time scales are more likely to include larger storms and storm waves that affect the bed to greater depths (e.g., Ortiz and Ashton 2016). Longer time scales also and allow more time for the seabed to adjust (Cowell and Kinsella this volume). Considering the longest time scales (decades to millennia), the shoreface typically extends to depths of tens of meters, which are usually reached many kilometers from shore on barrier coastlines. (For simplicity, this description of the shoreface excludes the fascinating and complex dynamics that occur in the "surf zone"—the zone of breaking waves that is usually restricted to the upper-most portion of the shoreface; Fredsoe and Deigaard 1992.)

The visible portion of a barrier, then, represents the top of this shoreface profile. During storms, when water levels become elevated by wind and waves, the landward sweeping of sediment extends past the fair weather shoreline. The sediment deposited by storm overwash processes in the long term attains an elevation related to the water levels achieved during major storms. In other words, the pile of sediment created by wave processes extends from the base of the shoreface upward as far as the waves can reach during storms. As RSLR occurs, overwash tends to occur more frequently (as storm surge elevations tend to increase). As a result, the elevation to which sediment can be piled tends to increase. Thus, if RSLR is gradual enough, the elevation of a barrier will tend to increase at the rate of RSLR. And if the rate of RSLR is gradual enough, waves will tend to maintain an approximately equilibrium shoreface profile, relative to the moving sea-level frame of reference.

The transfer of sediment from the beach and shoreface to the top and landward portion of the visible portion of a barrier tends to cause erosion of the upper shoreface. If the shoreface slope is approximately an equilibrium slope, a reduction of the slope of the upper shoreface tends to cause onshore sediment transport on the upper shoreface. The transported sediment comes from lower portions of the shoreface, which lowers the slopes there. In this way, the erosion and lowering of the slopes

propagates offshore. Therefore, in the long term, the erosion of the upper shoreface that occurs during storms that produce overwash propagates to the base of the shoreface. Similarly, when sediment is gradually removed from the surf zone and upper shoreface by gradients in alongshore sediment transport, causing erosion of the beach and shoreline, that erosion propagates to the base of the shoreface. And if a gradient in alongshore sediment transport brings more sediment into a section of shoreline than it takes out, causing accretion of the beach and seaward movement of the shoreline, accretion propagates out to the base of the shoreface in the same manner.

If RSLR happens gradually enough for the shoreface profile to remain approximately in equilibrium, erosion of the beach and upper shoreface resulting from overwash processes produces a landward translation of the shoreface profile (at the same time the shoreface also translates upward in concert with sea level). In this scenario, the visible portion of a barrier and the shoreface can migrate upward and landward in unison allowing a barrier to persist indefinitely. However, many limitations, including a RSLR that is not sufficiently gradual, can cause barriers to founder, including the potential for the upper shoreface and subaerial portion of the barrier to become detached from the lower shoreface or for barriers to drown (see chapters by Ashton and Lorenzo-Trueba, Cowell and Kinsela, Fitzgerald et al., Houser et al, Mallinson et al., Mellett and Plater, Moore et al., Odezulu et al., and Rodriquez et al.). In addition to rapid RSLR, the management and manipulation of barrier environments by humans poses a threat to the continued existence of barrier landforms; actions taken to prevent or mitigate processes that represent hazards to coastal development and inhabitants can hinder the stabilizing feedbacks that tend to allow barriers to persist as sea level rises and shorelines erode (see chapters by Moore et al., Odezulu et al., and especially McNamara and Lazarus).

Scope of the Volume: An Overview of Chapters

Observation-Focused Contributions

Barriers cease to exist as subaerial landforms when RSLR rate is too high and/or too little sediment is available. A number of factors can combine to determine what rate of RSLR is "too high," and a number of processes can influence the rate sand (or gravel) is added to, or removed from, a barrier system—including storm impacts, the topographic setting, and gradients in alongshore sediment transport related to wave climate and coastline shape. In the first section of the book, the authors of six chapters mine observational data to explore how barriers respond to changing sea level and climate forcing and the conditions under which barriers may founder, or cease to exist.

In the opening chapter, *FitzGerald et al.* discuss observations from several different barrier settings throughout the world and synthesize them into a conceptual model called "runaway barrier island transgression," describing the potential response of barriers, and the back-barrier environments they are tied to, to high rates of RSLR. In this model, if back-barrier marshes do not keep up with high rates of

RSLR, they are replaced by open water, which triggers a cascade of effects—increases in the volume of water that must flow in and out through tidal inlets during each tidal cycle lead to consequent expansion of tidal deltas and the associated loss of sand that would otherwise be provided to barriers, leading to island narrowing, segmentation, and more frequent overwash. If the water behind a barrier becomes deep enough as RSLR outpaces back-barrier sedimentation, barriers in this scenario can eventually transition to subaqueous shoals. The case studies presented illustrate different aspects of this conceptual model, which paints a picture of what might occur in many regions as sea-level rise rates increase.

Mellet and Platter review studies of barriers from around the world that have drowned in the recent geologic past (since the last deglaciation). Geophysical observations of the seabed on continental shelves, which are becoming more widespread, reveal evidence of barriers that did not keep up with rising sea level. When a barrier migrates along a continental shelf as a persistent subaerial landform, typically little to none of the barrier sediment is left on the continental shelf. Extensive shelf deposits with the characteristics of barrier sediments—sometimes in which even the shape of the barrier remains intact—suggest that a barrier was left behind as sea level rose above it (presumably to be replaced by a new barrier farther landward). In a meta-analysis of studies of such drowned barriers, Mellett and Plater examine the prevalence of various potential causes of barrier drowning, which can be summarized as involving either high RSLR rates, low sediment supply rates, or influences of the topographic setting.

Mallinson et al. focus on geologic evidence for major changes in island configuration that occurred along a well-studied barrier island chain, the Outer Banks of North Carolina, USA. Combining analysis of the sedimentary record with numerical modeling of hydrodynamics in the back-barrier bay, Pamlico Sound, they demonstrate that the Outer Banks has, in the past, been severely segmented—separated by inlets that were much larger and more numerous than those that currently exist—more than once during the sea-level high stand of recent millennia. *Mallinson et al.* conclude that these pronounced changes in the barrier chain, and associated changes in the back-barrier environment, occurred in response to relatively minor but rapid changes in climate and/or RSLR rates, such as those that occurred during the Medieval Climate Anomaly and the Little Ice Age.

Rodriquez et al. examine the sedimentary record of overwash occurrences on a barrier on the East Coast of the USA (Onslow Beach, North Carolina) over the last two millennia. They find that the frequency and cross-shore extent of overwash deposition appear to have increased dramatically in the last century or so. Rodriquez et al. consider possible causes for the apparently anomalous overwash activity, including an unusually stormy period (a hypothesis they found to be unsupported by meteorological or historical data) and a change in alongshore sediment transport gradients that may have increased the rates of shoreline and dune erosion (possibly related to changes in wave climate). However, as the most likely explanation, they point to the global increase in sea-level rise rates since the industrial revolution—which, if true, would make these observations and analyses especially relevant to barriers worldwide.

Presenting a synthesis of their analysis of the stratigraphy of barrier deposits on Follets Island, TX, along the Gulf Coast of the USA, *Odezulu et al.* identify an order-of-magnitude increase in the rate of landward island migration during the historical period, relative to the rate estimated for the millennial (geologic) time scale. They attribute this change to a combination of increased RSLR rate and decreased rates of sediment supply from alongshore sources, caused by anthropogenic manipulations of a nearby tidal inlet and river mouth. Their analysis of stratigraphic data indicates that the barrier is undergoing a net loss of sand, because overwash sometimes extends well past the back of the barrier. The present shoreface is underlain mostly by muddy deposits that contribute little coarse sediment when eroded. Based on the depth of the water the barrier is migrating into and the volume of sediment making up the barrier presently, Odezulu et al. estimate that the barrier will likely transition to a subaqueous shoal on the time scale of a few centuries. Given the global ubiquity of anthropogenic manipulations of sediment pathways, as well as increased rates of RSLR, this study of the geologic record of a specific barrier likely has wide-ranging implications.

Houser et al. focus on the shorter time scales of dune recovery following a storm and the dependence of dune recovery on sediment availability both on the beach and the shallow seabed. Observations from the Gulf Coast (Padre Island, Texas, and Santa Rosa Island, Florida) and East Coast of the USA (Assateague Island, Virginia) indicate that the amount of sediment available for dune recovery can depend on the "geologic framework"—the material that underlies the barrier and the shallow seabed. Based on their observations, *Houser et al.* present conceptual models to explain the dependence of dune recovery on storm frequency and sediment availability and the influence of the extent of dune recovery between storms on overwash and therefore barrier response to sea-level rise.

Modeling-Focused Contributions

Theoretical considerations, in a synergy with observations, can assist in illuminating how barrier systems evolve and the ways in which they can respond to changing climate (or land-use) forcing. Theoretical investigations utilize conceptual, analytical, and numerical modeling, most often in combination with real-world observations and/or predictions of future conditions, which provide the bases for model parameterizations, scenarios to be explored, and tests of model results. Six chapters address fundamental constraints on barrier evolution and describe different aspects of the dynamics of barrier systems including conservation of mass; geometrical considerations; couplings among physical, ecological, and human processes; and how limits on the rates of change within different parts of a barrier system can affect overall system response to changing climate and land-use forcing.

In the first of the second six chapters, *Murray and Moore* examine how the considerations of mass conservation and an assumed time-invariant barrier geometry (averaged over major storm and recovery cycles) constrain barrier evolution, under

a series of thought experiments that include progressively more of the factors affecting barrier response to RSLR. They use conceptual/geometrical and analytical models, and they discuss numerical modeling used to address increasingly realistic scenarios. This chapter highlights the role of shoreface erosion (landward translation) in producing new sediment that is added to the nearshore system (possibly redistributed by alongshore sediment transport). Conceptual models often assume that barriers consist entirely of mobile sediment that moves landward across an underlying substrate such that shoreface erosion only entrains sediment that is already part of the barrier, which is then added to the top and landward side of the barrier during storms. In this picture, barrier sediment "rolls" (translates) across an unaffected substrate, with no net gain or loss. In contrast, *Murray and Moore* show that although a barrier will tend to evolve toward this state under some circumstances, more generally, the lower part of the shoreface erodes into the underlying substrate, producing new sediment as a barrier responds to RSLR.

Whereas Murray and Moore's analyses assume that the barrier profile, including the lower shoreface, retains a constant geometry over long time scales, *Cowell and Kinsella* use a numerical model to address what happens when the rate at which the lower shoreface can respond to changes in sea level and barrier position is too slow for the shape of the whole shoreface profile to remain constant. These numerical experiments, in concert with geological observations from the data-rich Tuncurry Coast, in Australia, help to define an "active" upper portion of the shoreface that retains a constant geometry. This active portion extends to shallower and shallower depths as the rate of RSLR increases. The response of the shoreface below the active portion becomes time lagged, resulting in cross-shore sediment fluxes—net additions or subtractions to the sediment stored in the upper parts of the barrier profile—not related to present rates of RSLR. In these cases, barriers will respond to a combination of present and past rates of RSLR.

In a complementary numerical modeling endeavor, *Ashton and Lorenzo-Trueba* also consider how limitations on response rates can affect how barriers evolve. They include limitations on the rates of shoreface sediment fluxes as well as limits on overwash fluxes, showing that barriers could potentially drown under either limitation if overwash rates can't keep pace with RSLR or if rates of landward sediment transport on the shoreface can't keep pace with overwash. This chapter demonstrates that instead of the continuous barrier response to sea level that has typically been assumed, punctuated landward migration, alternating with extended periods in which a barrier remains stationary, may be the most common response to RSLR.

Moore et al. provide a synthesis of model findings—tested against observations—that yield insights into the role of interactions between ecological processes (vegetation dynamics) and patterns of sediment erosion, transport, and accretion, in shaping barrier environments and their response to changing climate forcing. Specifically, the work described in this chapter numerically addresses the different, sometimes species-specific, characteristics of vegetation that influence the alongshore and cross-shore shape of coastal foredunes and multiple dune fields. The authors also summarize recent work that demonstrates the importance of a competition between factors that

build dunes (e.g., vegetation recovery, sand flux) and the factors that erode dunes (e.g., storms, sea-level rise) in determining local dune, or island, elevation and thus the degree of connectivity between sandy barriers and the back-barrier marshes and bays behind them. This chapter highlights the importance of feedbacks between vegetative and sediment transport processes in shaping the barrier landscape and the importance of couplings between and among landscape units, in influencing the overall evolution of barrier-marsh-bay systems as climate conditions change.

Ruggiero et al. combine field observations from the US Pacific Northwest with laboratory, field, and numerical-modeling experiments to investigate what controls dune shape. The deeply interdisciplinary body of work they synthesize addresses how the species-specific morphological characteristics and growth patterns of dune-building vegetation, in combination with physical influences (chiefly shoreline-change rates), help to determine whether dunes are low and wide versus tall and narrow. These dune and dune-field characteristics, in turn, determine how much storm protection dunes provide for landward environments and development. The authors find that the ongoing spread of invasive dune-building grass species is accompanied by changes in dune shape—and therefore changes in coastal vulnerability to storm impacts.

In the final chapter of the volume, *McNamara and Lazarus* make the case that barrier evolution and human dynamics are thoroughly coupled on developed coastlines. Engineering and management actions to protect humans and infrastructure from storm hazards and beach erosion are reactions to physical and ecomorphodynamic coastal processes. On the other hand, human actions also affect physical and ecomorphodynamic coastal processes: shoreline stabilization (chiefly through beach nourishment in recent decades) tends to prevent barriers from moving landward, and constructed dunes or seawalls tend to prevent the moderate overwash events that would otherwise increase island elevation as sea level rises. These manipulations of barrier environments alter the evolution of barrier morphology and therefore alter the hazards humans and infrastructures are exposed to—influencing future hazard mitigation efforts. Because mitigation of coastal hazards tends to be expensive, the dynamics of human decision making are inextricably interwoven with physical and ecomorphodynamic processes in barrier environments. McNamara and Lazarus review newly emerging research addressing the dynamics of this coupled system and discuss how the resulting understanding could help to guide more intentional, holistic coastal management—especially as the pressures of increasing RSLR rate, changing storm climate, and limited reservoirs of nearshore sand make continued sustainability of the current pattern of coastal land use in developed regions challenging.

State of the Science and Future Directions

Understanding the dynamics that shape barriers, and determining their fates as RSLR rate and storms change, has become the focus of much scientific inquiry. Because this scientific focus has arisen relatively recently, our understanding is evolving quickly. Given this, it is not surprising to find that leading experts, approaching barrier dynamics from different disciplinary perspectives and through the use of different case studies, may sometimes come to conclusions that are less than completely consistent. A careful comparison of the chapters in this volume reveals some contrasting interpretations and apparent contradictions, which attest to the exciting state of this field of research and point to the areas of greatest insight and learning yet to come. However, much more prominent upon review of this collection are the areas of overlap that depict an emerging collective understanding about how and why barriers come to be and how and why they change over time as the influences of physical processes, vegetative processes, climate, and human activities, as well as the interactions among these factors, shift. The newer elements of this emerging collective understanding that appear in this volume include the following:

It is becoming increasingly clear that shoreface characteristics and shoreface processes play important roles in the dynamics of barrier migration. The shoreface represents an important source of sediment to barriers, and the importance of this role is partially determined by the composition and erodibility of the material that comprises the shoreface and the degree to which the upper and lower parts of the shoreface, and the subaerial barrier, migrate in unison as conditions change. This migration may proceed continuously in some cases but is perhaps more likely to occur as periods of migration alternating with periods of relative stability. In some cases, barriers do not keep up with changing conditions and they drown, becoming subaqueous shoals. In other cases, changes in RSLR rate or storminess can segment a barrier island chain, greatly increasing the connection between the ocean and the back-barrier environment.

On long time scales, the feedbacks between vegetation and sediment transport that determine dune shape and the vulnerability of barrier environments and infrastructure to storms are likely to be swamped by the effects of rising sea level and changes in storminess. On the decadal, and perhaps centurial, scale, however, the absence or the presence and height of coastal foredunes is important in determining what the impact of storms will be. How reliably and how thoroughly dunes re-form after a strong storm depends on factors including sediment supply from the shoreface, the characteristics of the material below the sandy surface (the geologic framework), and how often strong storms occur relative to the time scale for vertical dune growth—which depends on the vegetation present as well as climatic influences. Foredune height plays an important role in determining how well connected the sandy part of a barrier is to back-barrier marsh or bay environments. These connections are important in determining how barrier-marsh-bay systems evolve overall and how vulnerable they are to increased rates of RSLR. Where humans have built dunes that are higher than natural dunes would be for a given set of conditions,

overwash events may be filtered, making it harder for barriers to keep pace with rising sea level. This is only one example of the way in which the natural coastal system and the human coastal system are tightly coupled—each affecting the other repeatedly through time.

A growing number of examples highlight how RSLR, changes in storm activity, and shifts in the geographic distribution of important dune-building grasses are affecting barrier island behavior today. Often, under these influences, barriers tend to become lower and narrower and to migrate more rapidly. We can learn about barrier dynamics by studying examples of barrier response to changing conditions in the more distant past. A new influence on barrier evolution has arisen in recent centuries, however: the role of humans. As conditions begin to change more rapidly, so too will our response to coastal processes that constitute hazards to humans and development. An emerging insight of critical importance to future generations is that the management decisions we make today may unintentionally destabilize barrier landforms by preventing them from migrating and gaining elevation to keep pace with changing RSLR rates or by interrupting sediment supply pathways—potentially hastening segmentation or the conversion of barrier landforms to shoals. Where it occurs, this would lead not only to the loss of barriers but also to the increased vulnerability of mainland shores to potentially more intense coastal storms. We are well poised with our current understanding of the eco-physical system to more fully understand the ways in which couplings with the human system will affect barrier evolution in the future. This important area of future research could provide the basis for more intentional, forward-looking, and holistic management of barriers as the important natural resource—and unique landforms—that they are.

Chapel Hill, NC, USA Laura J. Moore
Durham, NC, USA A. Brad Murray

References

Cowell PJ, Kinsela MA (2018) Shoreface controls on barrier evolution and shoreline change. In: Moore LJ, Murray AB (eds) Barrier dynamics and response to changing climate. Springer, New York. https://doi.org/10.1007/978-3-319-68086-6_8

Fredsoe J, Deigaard R (1992) Mechanics of coastal sediment transport, vol. 3. World Scientific Publishing, Singapore

Ortiz AC, Ashton AD (2016) Exploring shoreface dynamics and a mechanistic explanation for a morphodynamic depth of closure. J Geophys Res Earth Surf. https://doi.org/10.1002/2015JF003699

Stutz ML, Pilkey OH (2002) Global distribution and morphology of deltaic barrier island systems. J Coast Res 36(1):694–707

Contents

Contributors

John B. Anderson Department of Earth Sciences, Rice University, Houston, TX, USA

Andrew D. Ashton Department of Geology and Geophysics, Woods Hole Oceanographic Institution, Woods Hole, MA, USA

Patrick Barrineau Department of Geography, Texas A&M University, College Station, TX, USA

Peter J. Cowell School of Geosciences, The University of Sydney, Sydney, NSW, Australia

Stephen Culver Department of Geological Sciences, East Carolina University, Greenville, NC, USA

Duncan M. FitzGerald Department of Earth and Environmental Sciences, Boston University, Boston, MA, USA

Ioannis Georgiou Department of Earth and Environmental Sciences, University of New Orleans, New Orleans, LA, USA

Evan B. Goldstein Department of Geological Sciences, University of North Carolina at Chapel Hill, Chapel Hill, NC, USA

Sally Hacker Department of Integrative Biology, Oregon State University, Corvallis, OR, USA

Brianna Hammond Department of Geography, Texas A&M University, College Station, TX, USA

Christopher J. Hein Department of Physical Sciences, Virginia Institute of Marine Science, College of William and Mary, Gloucester Point, VA, USA

Chris Houser Department of Earth and Environmental Sciences, University of Windsor, Windsor, ON, Canada

Zoe Hughes Department of Earth and Environmental Sciences, Boston University, Boston, MA, USA

Department of Biology and Biochemistry, University of Houston, Houston, TX, USA

Michael A. Kinsela School of Geosciences, The University of Sydney, Sydney, NSW, Australia

Department of Coastal and Marine Science, Office of Environment and Heritage, Sydney, NSW, Australia

Matthew Kirwan Department of Physical Sciences, Virginia Institute of Marine Sciences, Gloucester Point, VA, USA

Mark Kulp Department of Earth and Environmental Sciences, University of New Orleans, New Orleans, LA, USA

Rebecca Lauzon Division of Earth and Ocean Sciences, Nicholas School of the Environment, Duke University, Durham, NC, USA

Eli D. Lazarus Environmental Dynamics Lab, Geography and Environment Unit, University of Southampton, Highfield, Southampton, UK

Eduardo Leorri Department of Geological Sciences, East Carolina University, Greenville, NC, USA

Jorge Lorenzo-Trueba Earth and Environmental Studies, Montclair State University, Montclair, NJ, USA

David Mallinson Department of Geological Sciences, East Carolina University, Greenville, NC, USA

Dylan E. McNamara Department of Physics and Physical Oceanography, Center for Marine Science, University of North Carolina, Wilmington, NC, USA

Claire L. Mellett British Geological Survey, The Lyell Centre, Research Avenue South, Edinburgh, UK

Michael Miner Bureau of Ocean Energy Management, Gulf of Mexico Region, New Orleans, LA, USA

Siddhartha Mitra Department of Geological Sciences, East Carolina University, Greenville, NC, USA

Laura J. Moore Department of Geological Sciences, University of North Carolina at Chapel Hill, Chapel Hill, NC, USA

Ryan Mulligan Department of Civil Engineering, Queen's University, Kingston, ON, Canada

A. Brad Murray Division of Earth and Ocean Sciences, Nicholas School of the Environment, Duke University, Durham, NC, USA

Christopher I. Odezulu Department of Earth Sciences, Rice University, Houston, TX, USA

Andrew J. Plater School of Environmental Sciences, University of Liverpool, Liverpool, UK

Elizabeth Rentschler Department of Geography, Texas A&M University, College Station, TX, USA

Stanley Riggs Department of Geological Sciences, East Carolina University, Greenville, NC, USA

Antonio B. Rodriguez Institute of Marine Sciences, University of North Carolina at Chapel Hill, Morehead City, NC, USA

Peter Ruggiero College of Earth, Ocean, and Atmospheric Sciences, Oregon State University, Corvallis, OR, USA

Brooke Saari Department of Environmental Studies, University of West Florida, Pensacola, FL, USA

Eric Seabloom Department of Ecology, Evolution, and Behavior, University of Minnesota, St. Paul, MN, USA

Ethan J. Theuerkauf Institute of Marine Sciences, University of North Carolina at Chapel Hill, Morehead City, NC, USA

Illinois State Geological Survey, Champaign, IL, USA

Sarah Trimble Department of Geography, Texas A&M University, College Station, TX, USA

Orencio Durán Vinent Department of Physical Sciences, Virginia Institute of Marine Sciences, Gloucester Point, VA, USA

Davin J. Wallace Division of Marine Science, University of Southern Mississippi, Stennis Space Center, Kiln, MS, USA

David Walters Department of Physical Sciences, Virginia Institute of Marine Sciences, Gloucester Point, VA, USA

Phil Wernette Department of Geography, Texas A&M University, College Station, TX, USA

Bradley Weymer Department of Geology and Geophysics, Texas A&M University, College Station, TX, USA

Shelby Young Department of Geography, Texas A&M University, College Station, TX, USA

Winnie Yu Institute of Marine Sciences, University of North Carolina at Chapel Hill, Morehead City, NC, USA

Phoebe Zarnetske Department of Forestry, Fisheries and Wildlife, Michigan State University, East Lansing, MI, USA

Ecology, Evolutionary Biology, and Behavior Program, Michigan State University, East Lansing, MI, USA

Part I
Observations and Conceptual Models of Barrier Response to Changing Climate

Runaway Barrier Island Transgression Concept: Global Case Studies

Duncan M. FitzGerald, Christopher J. Hein, Zoe Hughes, Mark Kulp, Ioannis Georgiou, and Michael Miner

Abstract The regime of accelerating sea-level rise forecasted by the IPCC (2013) suggests that many platform marshes and tidal flats may soon cross a threshold and deteriorate/drown as back-barrier basins transform to intertidal and subtidal areas. This chapter explores how marshes may succumb to rising sea level and how the loss of wetlands will increase the extent and the overall depth of open water in the back-barrier, causing greater tidal exchange. Here, we present a conceptual model that depicts how increasing tidal prism enlarges the size of tidal inlets and sequesters an increasingly larger volume of sand in ebb-tidal delta shoals. The conceptual model is based on empirical relationships between tidal prism and inlet parameters, as well as field and theoretical hydraulic studies of tidal inlets showing that long-term basinal deepening intensifies the flood dominance of existing inlet channels and transforms some ebb-dominated channels to flood-dominated channels. This condition leads to sand movement into the back-barrier, which builds and enlarges flood-tidal deltas, filling the newly created accommodation space. The model hypothesizes that sand contributed to the growth of the ebb and flood tidal delta shoals will be at the expense of barrier reservoirs. This will result in diminished

D.M. FitzGerald, B.A., M.S., Ph.D. (✉)
Department of Earth and Environmental Sciences, Boston University, Boston, MA, USA
e-mail: dunc@bu.edu

C.J. Hein, B.S., Ph.D.
Department of Physical Sciences, Virginia Institute of Marine Science, College of William and Mary, Gloucester Point, VA, USA
e-mail: hein@vims.edu

Z. Hughes, Ph.D.
Department of Earth and Environmental Sciences, Boston University, Boston, MA, USA

Department of Biology and Biochemistry, University of Houston, Houston, TX, USA
e-mail: zoeh@bu.edu

M. Kulp, B.S., M.S., Ph.D. • I. Georgiou, B.Sc., M.Sc., Ph.D.
Department of Earth and Environmental Sciences, University of New Orleans, New Orleans, LA, USA
e-mail: mkulp@uno.edu; igeorgio@uno.edu

M. Miner, B.S., M.S., Ph.D.
Bureau of Ocean Energy Management, Gulf of Mexico Region, New Orleans, USA
e-mail: michael.miner@boem.gov

L.J. Moore, A.B. Murray (eds.), *Barrier Dynamics and Response to Changing Climate*, https://doi.org/10.1007/978-3-319-68086-6_1

sand supplies along the coast, eventually leading to fragmentation of barrier island chains and the transition from stable to transgressive coastal systems. Several historical studies of barrier island systems throughout the world demonstrate barrier response to changing tidal prism and illustrate different stages of this conceptual model.

Keywords Barrier island • Tidal inlets • Transgressive shoreline • Sea-level rise • Saltmarsh deterioration • Tidal prism • Sediment transport • Inlet hydrodynamics • Coastal sand-reservoirs • Ebb-tidal delta • Flood-tidal delta • Back-barrier feedbacks • Lagoons • Virginia barrier islands • Nauset Spit • New Inlet, MA • Assateague Island • Barataria Islands • Chandeleur Islands • Copper River • Friesian Islands

1 Introduction

The future of the world's barrier coasts is dependent upon how barriers respond to climate change, specifically global warming and the ensuing acceleration in sea-level rise (Jevrejeva et al. 2012), as well as possible increased storm magnitude (Knutson et al. 2010; Grinsted et al. 2013). Most barrier coasts contain a finite volume of sediment with little net sand contributed via cross-shore or alongshore transport. Exceptions include those with contributions from nearby rivers (e.g., South African rivers, Cooper et al. 1990; Long Beach in Washington fed by the Columbia River, Dingler and Clifton 1994; northern New England barriers nourished by rivers during spring freshets and floods; Fenster et al. 2001; FitzGerald et al. 2005; Hein et al. 2012, 2014a); the movement of sand onshore from the inner continental shelf (e.g., Fire Island, Schwab et al. 2013; Hapke et al. 2010a); the erosion of updrift bluffs (e.g., Sandy Neck, Cape Cod, MA; van Heteren and van de Plassche 1997), or erosion of the barrier shoreface into a sandy substrate (e.g., Moore et al. 2010; Cowell and Kinsela this volume; Murray and Moore this volume). The lack of new sand sources coupled with the effects of sea-level rise had led to the vast majority of the world's barrier shorelines eroding (70% as estimated by Bird 1985). For example, Hapke et al. (2010b) determined that 65% of the sandy shoreline stretching from central Maine to northern North Carolina has undergone net erosion over the long-term (1800s to ~2000), at rates ranging from 0.2 m/year in Maine to 3.7 m/year in southern Delmarva/northern North Carolina. Globally, erosion has driven the expenditure of billions of private and public dollars to fund widespread beach nourishment projects, revetment construction, and rebuilding efforts associated with increasing loss of real estate and infrastructure (Nicholls et al. 2007; Doran et al. 2013).

The sand comprising barrier systems can be compartmentalized into several reservoirs including the barrier lithosome, the ebb-tidal delta, flood-tidal delta shoals, and channel deposits. Dunes, washovers, spit platforms, and recurved spits are all considered part of the barrier lithosome, which also extends seaward to the depth of closure. The depth of closure for a characteristic time interval is the most landward depth

seaward of the beach for which there is no significant change in bottom elevation and no significant net sediment transport between the nearshore and the offshore (Kraus et al. 1998). The long-term loss of sand from these systems is normally a gradual process punctuated by major storms. Erosion is attributed to a variety of processes including, but not limited to: (1) sand transported offshore to regions beyond the closure depth by downwelling currents during large-magnitude storms (Niedoroda and Swift 1981; Field and Roy 1984; Snedden et al. 1988); (2) sand moved alongshore into estuaries where it becomes trapped in intertidal and subtidal shoals (Harris 1988; Dalrymple et al. 1992), thereby reducing the volume of sand bypassed to down-drift barrier shorelines; and (3) sand deposited in channels at migrating tidal inlets below the depth of the erosional shoreface. This latter reservoir will not be exhumed during the proceeding transgression and will therefore remain buried as a channel deposit on the inner shelf (Rieu et al. 2005; FitzGerald et al. 2012).

Along with these sediment sinks, sand tends to be lost to the offshore to compensate for rising sea level as the equilibrium profile deepens (Bruun 1988). Although scientists have criticized Bruun's (1988) equilibrium equation as being impractical in actual usage due to various complicating factors (e.g., grain-size variability, alongshore sediment losses, and geologic controls; Cooper and Pilkey 2004), the concept provides a valuable tool for understanding why sand is lost to the offshore, especially for periods of rising sea level before a barrier begins to migrate landward (for further discussion see: Wolinsky and Murray 2009; Rosati et al. 2013).

In addition to long-term sediment loss, rising sea level will undoubtedly alter the hypsometry of back-barrier bays and marsh systems. This will result in changes in inlet and tidal channel hydraulics, accommodation space, and net sediment transport directions. In a regime of accelerating sea-level rise (Donnelly et al. 2004; Jevrejeva et al. 2012), these responses will be most dramatic when certain thresholds are crossed, particularly those relating to wetland loss, causing rapid bay expansion and/or deepening of bay hypsometry. Coastal marshes maintain their surface elevation relative to high tide by accumulating organic sediment (predominantly plant roots) and trapping inorganic sediment delivered by tides. Both processes are dependent on the presence of vegetation. If a marsh can no longer produce enough belowground biomass and/or import enough sediment through tidal exchange to keep pace with rising high tides, it will become inundated below mean sea level (Kirwan et al. 2010). Considering the projected rate of sea-level rise during this century (Church et al. 2013), and despite possible ameliorating effects of increased sediment influx (Morris et al. 2002) or biomass production (Langley et al. 2009), the future duration of tidal inundation at many marshes will exceed the local critical period of flooding with each tidal cycle. In this case, marsh plants will perish, transforming marshes to tidal flats or open water (Kirwan et al. 2010). This is likely to occur in combination with increased marsh-edge erosion resulting from greater wave energy associated with expanding, deeper open-water areas (Mariotti et al. 2010; Mariotti and Carr 2014). Because most platform marshes behind barrier systems have low relief (commonly less than 30 cm; Eiser and Kjerfve 1986; Cahoon and Reed 1995; Silvestri et al. 2005), deterioration of marshes, once initiated, is likely to occur rapidly. The wetlands comprising Barataria Bay (behind the

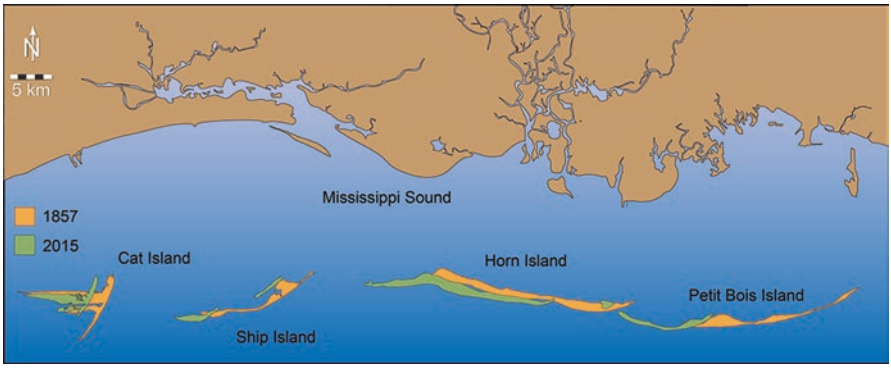

Fig. 1 Mississippi barrier footprints decreasing with time. Constructed using historical maps and aerial photographs

Grand Isle–Grand Terre barrier chain along the central Louisiana coast) provide an example of marsh collapse in just this manner. Here submergence, excavation by hurricanes, and edge erosion have led to extensive conversion of marshlands to open water at an average rate of 22 km^2/year between 1956 and 1990 (Barras et al. 1994). These changes to bay area and the consequent increase in tidal prism have produced a profound response of the barrier system, resulting from a redistribution of sediment among the coastal sand reservoirs (FitzGerald et al. 2007; and discussed below).

The long-term loss of sand from barrier chains is well illustrated along the Mississippi barrier system west of Mobile Bay, including Dauphin Island in Alabama, where a 29% decrease in the collective areas of the five islands was observed between 1840s and 2007 (Morton 2008; Byrnes et al. 2012; Fig. 1). Morton (2008) attributes much of the erosion during the past century to progressive dredging and deepening of navigation channels that decreased the volume of sand, which otherwise would have naturally bypassed the inlets and fed downdrift barriers. However, a sediment budget study of the Mississippi barriers by Byrnes et al. (2012) showed that much of the long-term loss of sand from barriers can be attributed to sand sequestered on ebb-tidal deltas and moved offshore during storms. The net loss of sand due to storm erosion is documented along many barrier islands, including the Chandeleur Islands (Sallenger et al. 2009).

In addition to the long-term loss of sand due to the combined effects of major storms, sea-level rise, and human modifications, it appears inevitable that barrier erosion will accelerate in the future as the rate of sea-level rise increases. This trend will likely be most apparent along mixed-energy barriers (sensu: Hayes 1979) as stability thresholds are crossed in back-barrier marshes due to increased inundation (FitzGerald et al. 2008). Likewise, barriers fronting bays and lagoons with tidal flats will undergo increased erosion due to flood dominance within inlet channels and the creation of bay sediment sinks (Dissanayake et al. 2012; van Goor et al. 2003). In this chapter we explore the projected loss of sand from barrier lithosomes as sand is

transferred to other reservoirs within the barrier system, including ebb- and flood- tidal shoals and bays. Because this relocation of sand will be largely forced by changes to back-barrier environments, our discussion begins with a review of back-barrier marsh processes and modeling efforts. Next, we explore barrier response to changes in back-barrier hypsometry, using examples from historical records, and demonstrating how barrier sand reservoirs undergo substantial redistribution in relatively short time spans. From these illustrations, we form a conceptual evolutionary model of barrier erosion and transgression, resulting in the transformation of a barrier chain to a system of mainland-attached beaches, proximal mainland barriers, or inner shelf shoals. The processes and factors governing barrier rollover and landward migration are covered in other chapters in this book (see chapters by Ashton and Lorenzo-Trueba this volume; Cowell and Kinsela this volume; Murray and Moore this volume). Barrier systems along active deltaic shorelines are not considered in this analysis, because they consist either primarily of spit systems (e.g., Danube, Rhone, Ebro) or lack detailed historical and process data (e.g., Niger).

2 Methodology

Projecting the future response of barriers to anticipated increases in the rate of sea-level rise is difficult because most barrier chains originally evolved during periods of slow relative sea-level rise (RSLR). Even today, most barrier systems are experiencing much slower RSLR rates than those expected in the same regions by the end of this century (Church et al. 2013). During the last 100 years, global sea level has been rising at 1.2 ± 0.2 mm/year (Hay et al. 2015). The future rate is projected to be as much as four times this value (Church et al. 2013). Excepting the Grand Isle–Grand Terre barrier system in Louisiana (discussed later in the chapter), where RSLR is 9.05 mm/year (NOAA 2015a, b), there are few natural laboratories in which to study the effects of rapid RSLR on barrier systems. Compounding the difficulties of studying the impacts of accelerating RSLR is the short length of historical databases, which rarely extend back in time prior to the mid-1800s; the earliest provide only a qualitative assessment of barrier morphology and adjacent bathymetry. Despite these limitations, we have assembled historical documents from several sites that provide insights into how barriers, tidal inlets, tidal deltas, and bays have responded to changes in inlet channel dimensions, tidal prism, and bay hypsometry brought about by storms, changes in sediment supply, human alterations, and tectonic events (physical settings summarized in Table 1). At many of these sites, the cumulative effect of various forcings is the formation of a new tidal inlet (and its attendant tidal prism) or a change in tidal prism volume. These historic changes in tidal prism mimic the changes expected to occur when wetlands and/or tidal flats can no longer keep pace with RSLR and convert to open water. The morphologic responses of the barrier chains described herein, therefore, provide insight into future outcomes. We note that in some of these analyses the scenario occurs in reverse, demonstrating how the barrier system responded as tidal prism decreased.

Table 1 Study sites

	Nauset Spit and New Inlet, Cape Cod, MA	Ocean City Inlet and Assateague Island, MD	Virginia Eastern Shore Barriers	Chandeleur Islands (CI) and Isle Derniers (ID), LA	Grand Isle (GI)-East Grand Terre (EGT), LA	Copper River Delta Barriers, AK	Friesian Islands, Germany
Coastal setting							
Tectonic coastal setting (Inman and Nordstrom 1971)	Amero-trailing edge	Amero-training edge	Amero-training edge	Marginal sea	Marginal sea	Collision coast	Amero-training edge
Barrier type (Davis and Hayes 1984)	Mixed energy	Wave-dominated	Mixed energy	Wave dominated	Wave dominated	Mixed energy	Mixed energy
Sediment source	Erosion of proximal updrift sandy glacial deposit	Erosion of proximal headlands composed of Pleistocene coastal deposits	Reworking of lowstand shelf deposits; limited alongshore input from erosion of updrift headlands	Reworking of former Mississippi River delta lobes CI: St. Bernard Delta 4.6–1.8 ka; ID: Lafourche Delta 3.5–0.4 ka deposits	Reworking of former Mississippi River delta lobe Lafourche Delta; 3.5–0.4 ka deposits	Glacially liberated sediments from proximal Copper River	Reworked glacio-fluvial deposits on shelf
Spring tidal range (m)	2.3	1.2	1.7	0.5	0.5	3.5–6.5	2.7–2.9
Deep-water significant wave height (m)	2	1.6	1.2	1.6	1	3.1	1.0
Dominant waves	Northeast (winter storms)	Northeast (winter storms)	Northeast (winter storms)	CI: East-southeast; ID: Southeast	GI, EGT: South-southeast	Southeast	Northwest
Dominant alongshore transport direction	South	South	South	CI: North-South; ID: West-East	Northeast	West	East

Anthropogenic alterations	None	Jetties, nourishment	Stabilization and nourishment at Wallops Island	CI: Nourishment, north end; ID: nourishment, breakwaters	GI: Nourished, breakwaters, Terminal Jetties EGT: Nourished	None	Poldering of back-barrier, Jetties
Barrier system							
Individual barrier length (km)	2–13	40–60	3–13	2–22	4–12	14–30	25–50
Individual barrier width (km)	0.1–0.5	0.1–0.3	0.1–1.0	0.1–0.4	0.2–0.8	0.6–2.5	500–800 0.8–1.5
Barrier thickness (m)	4–6	3–8	2–8	2–8	1–12	2–8	5–24

3 Background

3.1 Marsh Deterioration Processes and Existing Modeling Results

The timeframe and rate at which future changes will occur along barrier islands, in response to accelerating RSLR, will correspond with the stability and persistence of marshes in the back-barrier. Ultimately, barrier change will be related to the rate at which marshes are converted to intertidal flats and open water areas, thereby producing a larger tidal prism, increasing back-barrier accommodation space, and changing tidal hydrodynamics throughout the system. How quickly the marsh erodes, submerges, or becomes segmented once critical thresholds of marsh inundation have been crossed (Morris et al. 2002) will depend on a number of factors that we explore in this section. Adding to the complexity of predicting marsh evolution, many of these factors will, themselves, be impacted by climate change (Kirwan et al. 2009; Kirwan and Megonigal 2013) or respond to changes in marsh area (Mariotti and Fagherazzi 2013), creating feedbacks that enhance or buffer their effects.

The areal extent of saltmarsh platform is the result of a balance between vertical and horizontal processes (Fig. 2). The vertical elevation of a marsh platform (ζ), with respect to sea level (η), is a balance between mineral and organic deposition, shallow compaction processes, and deeper subsidence processes.

$$\Delta\zeta = D_{\mathrm{i}} + D_{\mathrm{o}} - a - s - \Delta\eta \tag{1}$$

where D_{i} represents the deposition of inorganic sediment, D_{o} is organic accumulation, a represents shallow autocompaction, s is deeper subsidence, and $\Delta\eta$ is the eustatic change in sea level. On the horizontal plane, coastal wetlands are subject to both lateral erosion and deposition depending on the hydrodynamic forcing and sediment availability, including the translation of wetland boundaries and the elaboration of channel networks. All of these processes may occur simultaneously within the same system, some areas being exposed and others sheltered, with the net difference dictating whether marsh area is lost or gained (e.g., van Proosdij et al. 2005; and see Fig. 3).

Inorganic deposition varies geographically based on suspended sediment availability, but, locally, it is well correlated with marsh platform elevation (deep areas accrete faster than shallow areas; Richards 1934; Stoddart et al. 1989; French and Spencer 1993; Cahoon and Reed 1995; Temmerman et al. 2003) and proximity to a creek or water body (French and Spencer 1993; Temmerman et al. 2003). The latter is due to a rapid reduction in carrying capacity as tidal flows or waves are slowed by the marsh grass canopy (Leonard and Croft 2006; Christiansen et al. 2000; Temmerman et al. 2003), and to the direct trapping of sediment on leaf surfaces (Stumpf 1983; French and Spencer 1993). Inorganic sediment accumulation is thus dependent on type, height, and density of vegetation (Gleason et al. 1979; Mudd et al. 2004, 2010; Palmer et al. 2004; Ortiz et al. 2017), which varies based on platform elevation and flooding frequency (high marshes are dominated by plants such

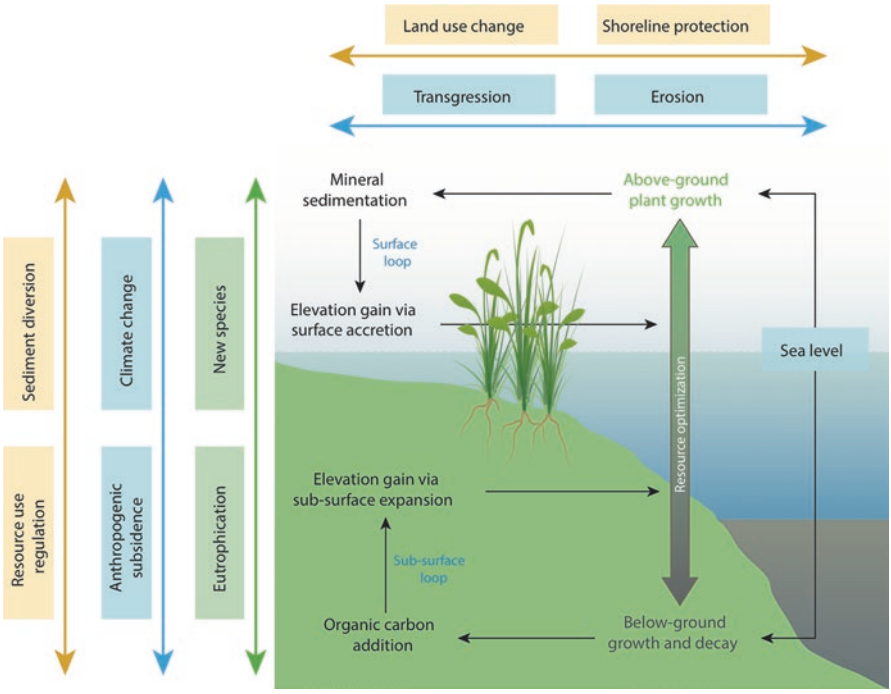

Fig. 2 The area of a wetland is determined by a balance among processes that operate vertically and horizontally on different scales; these include local factors related to the wetland's elevation and proximity to creeks (shown in *green* on left of image), regional or system scale factors related to climatic and geomorphic forcings (shown in *blue*), and anthropogenic factors (shown in *orange*). The surface and sub-surface "loops" demonstrate the feedbacks impacting marsh elevation (modified from Kirwan and Megonigal 2013)

as *Spartina patens*, and low marshes are dominated by plants such as *Spartina alterniflora*). Organic accumulation also relates to wetland vegetation; the majority of plant biomass forms belowground (Whittaker 1975; Chmura et al. 2003; Darby and Turner 2008), boosting platform elevations and creating highly organic soils (Cherry et al. 2009; Kirwan and Guntenspergen 2012; Chmura et al. 2003; Neubauer 2008). Feeding back into these relationships, biomass of *Spartina alterniflora* is linked to inundation depth through a parabolic relationship between platform elevation and plant productivity (Morris et al. 2002). This provides a buffer to RSLR, with increasing biomass production and thus, increased organic and inorganic deposition at deeper water levels, up until the apex of the parabolic relationship, after which point the marsh will deteriorate (Kirwan and Murray 2007).

Similar feedbacks occur in lateral variations of the marsh platform. Lateral expansion seaward requires low-energy conditions and an ample sediment supply sourced locally through erosion (e.g., van Proosdij et al. 2006; Fagherazzi and Priestas 2010) or from tidal exchange with the coastal ocean. Colonization by marsh vegetation stabilizes sediments, enhances deposition, and focuses erosive flows into

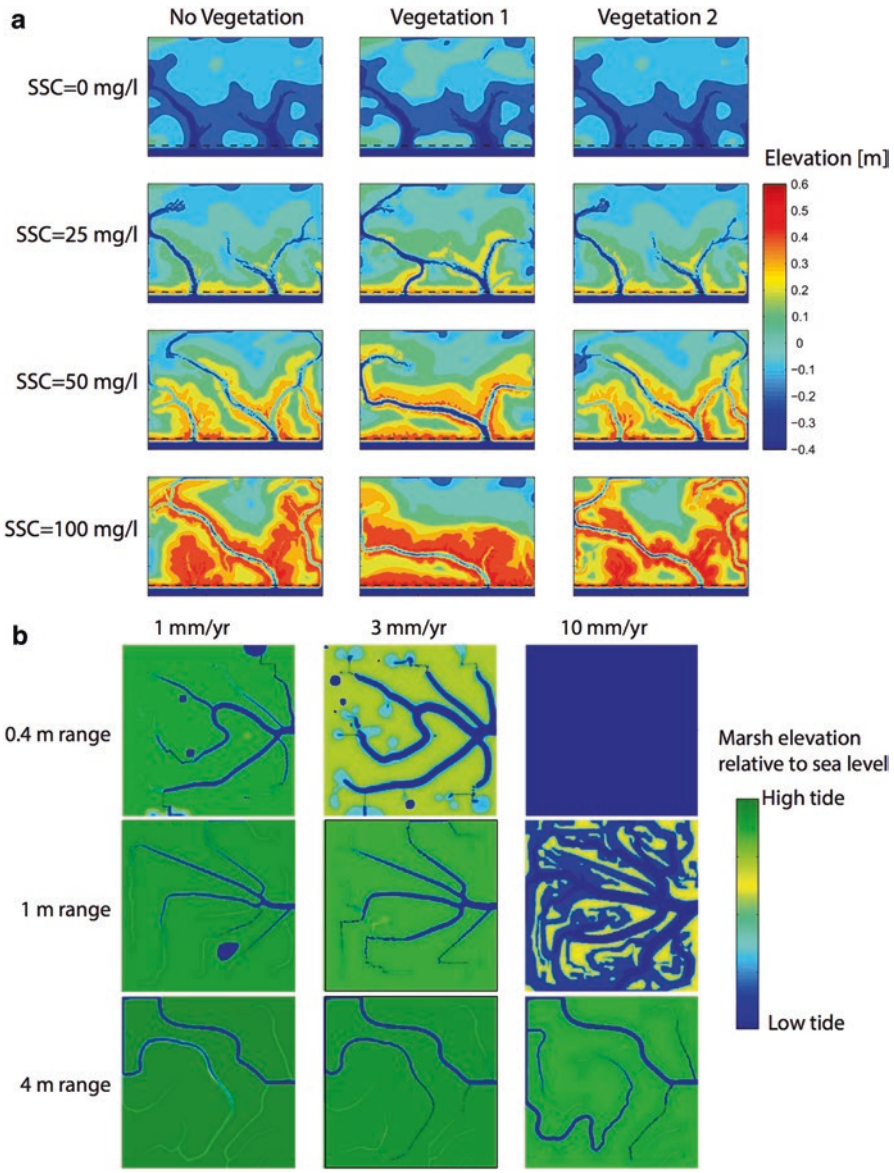

Fig. 3 Example outputs from models of integrated marsh platform—channel evolution: *Upper panel*: the results of a model incorporating feedbacks between vegetation, suspended sediment, channel evolution, and marsh platform elevation (from Belliard et al. 2015). *Lower panel*, the results of a model incorporating feedbacks between vegetation, sea level rise, tidal range, channel evolution, and marsh platform elevation (modified from Kirwan and Guntenspergen 2010). Both models provide interesting insights into the sensitivities of marsh systems, yet neither provide (nor aimed to provide) a realistic, holistic, representation of wetland systems

certain areas (Van der Koppel et al. 2005; Temmerman et al. 2007). As a barrier system evolves, and spits prograde, previously exposed, high-energy areas may become sheltered, encouraging the accumulation of sediment and, eventually, the incursion of marsh vegetation. Figure 4 shows an example from Cape Romain in South Carolina, where the breach and subsequent reformation of the barrier island caused a cycle of marsh platform erosion and extension over a period of 25 years. Landward encroachment of a marsh is a function of vertical change in accommodation space, as well as sediment availability and competition between species, changing the dominant vegetation type (from upland to high marsh and, eventually, low marsh species). As sea level rises and tidal flooding extends across the upland margin, the area affected depends on the slope of the upland coastal plain and anthropogenic impediments (Brinson et al. 1995; Torio and Chmura 2015).

Lateral losses through retreat of the marsh edge or the expansion of ponds and bays occur predominantly as a result of wind-waves (Stevenson et al. 1985; Nyman et al. 1994; van Proosdij et al. 2006). A linear relationship links marsh-edge erosion and wave power (a function of fetch and water depth) (Schwimmer 2001; Fagherazzi and Priestas 2010; Stevenson et al. 1985; Mariotti and Fagherazzi 2013), scaled according to local soil characteristics (Marani et al. 2011), which will reflect grain size and vegetation type, density, and live rooting depth (Richards 1934; Feagin et al. 2009; Marani et al. 2011; Silliman et al. 2012). Rates of platform retreat are therefore complex and site-specific, but observations along the US Gulf and East coasts range between 0.3 and 4.0 m/year (Schwimmer 2001; Wilson and Allison 2008; Silliman et al. 2012; Trosclair 2013). Marsh edge erosion coupled with tidal flat scour together enhance wave power by expanding and deepening the open water area. However, these same erosive processes also create a sediment source for the marsh surface. This concept of "cannibalization" of flats or marsh platform provides a mechanism for marshes in regions with low ambient suspended sediment concentrations to maintain elevation, possibly leading to marsh persistence.

Channel elaboration, during which expanding creeks dissect the marsh and effectively reduce platform area, occurs in response to increase in tidal prism (D'Alpaos et al. 2007; Kirwan and Guntenspergen 2010). The rate and geometry of the response are often modulated by vegetation presence and type, or other biotic factors, such as crab burrowing and biomass consumption (Hughes et al. 2009; Wilson et al. 2013; Belliard et al. 2015). While channel network expansion decreases platform area, increases in channel network length or overall cross-sectional area leads to better drainage for the marsh, thereby shortening inundation periods, even while inundation depth increases as sea level rises (Wright 2012). This means channel elaboration can help to maintain vegetation (and, thus, marsh) in an area of deeper inundation.

This multitude of complex feedbacks and site-specific controls involved in maintaining the marsh platform create immense challenges for predicting the future of marsh platforms through observations alone. Numerical modeling has provided a useful and effective tool to explore future climate scenarios, replacing or supplementing difficult, intensive manipulative field experiments. These tools can be used either to predict marsh behavior at specific sites based on existing observations,

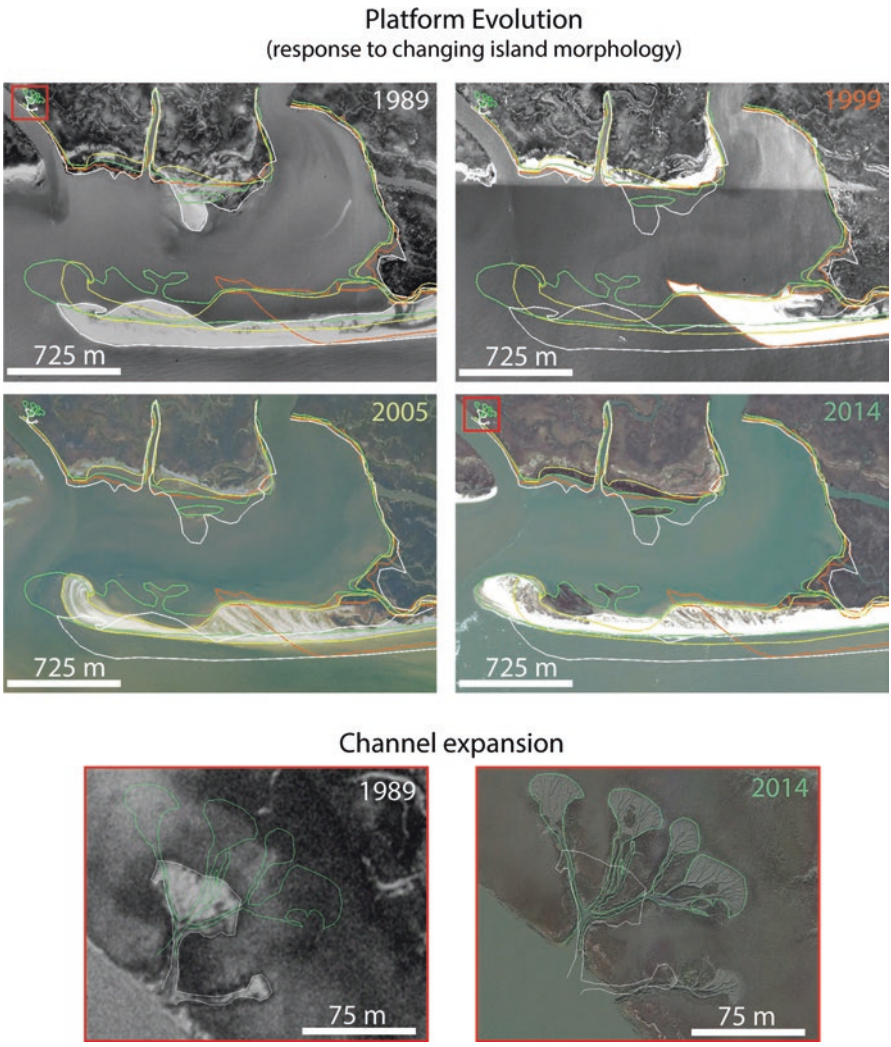

Fig. 4 *Upper panels*: A time series of barrier island and marsh platform evolution in Cape Romain, South Carolina, illustrating the cycle of platform evolution in response to changes in barrier island configuration. Initial marsh platform erosion is followed by reestablishment through both sheltering and overwash. *Lower panels*: An example of channel enlargement at the same site. Headward expansion of the channel network implies an increase in the marsh tidal prism in response to relative sea level rise. These changes are superimposed on the fluctuations in marsh area arising in response to barrier island dynamics

semi-empirical relationships, and parameterizations through some form of Eq. 1, or to explore, in a more theoretical manner, ecogeomorphic feedbacks and thresholds to improve our understanding of these processes on longer temporal and larger spatial scales than would otherwise be possible (for a full review of marsh models, including the assumptions and numerical approach of each, see Fagherazzi et al. 2012).

Kirwan et al. (2010) present a quantitative comparison of five of the more commonly used marsh elevation models (Morris et al. 2002; Temmerman et al. 2003; D'Alpaos et al. 2007; Kirwan and Murray 2007; Mudd et al. 2010), examining marsh platform persistence under moderate and high rates of RSLR. Each model uses a slightly different method of assessing platform elevation; the earlier models focus on interactions between elevation and vegetation, the later models include the effects of tidal range and decomposition. The models show similar behavior under IPCC (2013) predictions of moderate sea-level rise (~0.4 m rise by 2100) with accretion rate increasing in response to sea-level change. All the models predict marsh survival under these conditions, yet the platform elevation at the end of the simulations is 7–15 cm deeper within the tidal frame than present (the equivalent of increasing accommodation space and tidal prism by 50–100%). This, in turn, equates to shifts in ecotones, increased channelization, and wave-related edge erosion. Under higher rates of predicted SLR (~1.2 m by 2100), three of the five models predict marsh collapse sometime between 2050 and 2100; the other two predict marsh persistence at 2100 but at the very limit of vegetation tolerance, with submergence occurring before 2110. By compiling a series of model scenarios, Kirwan et al. (2010) conclude that there is potential for marshes to survive if suspended sediment supply is sufficient, but this potential is linked to tidal range. Microtidal marshes require a higher suspended sediment input as compared to those with larger tidal ranges, in order to maintain elevation under similar RSLR rates. However, the buffer provided by a large tidal range is limited, and, if ambient sediment supply is very low (such as in Plum Island Sound, Massachusetts) marshes could be threatened by sea-level rise rates of only 5 mm/year.

Building on these model assessments, Kirwan et al. (2016) carry out a meta-analysis of existing marsh accretion and elevation change data using a global data set. They conclude that high marsh settings seem, on average, to be pacing global sea level rise (3 mm/year), and that low marshes (next in the ecological succession as the marsh landscape lowers in the sea-level frame) currently accrete at rates more than double that of sea-level rise (6.9 mm/year), suggesting that marshes are less vulnerable than previously predicted. Specifically, they compare the dynamic landscape models used by Kirwan et al. (2010) with more traditional "static landscape" models (such as the Sea Level Affecting Marsh Model; SLAMM), which do not incorporate all of the positive and negative feedbacks between increasing rising sea level and elevation change. The comparison shows that while static marsh models predict catastrophic marsh losses, dynamic models predict resilience of marshes up to sea-level rise rates of 10 mm/year or more. It should be noted, though, that while the model results suggest that marshes may survive high rates of sea-level rise, this will be associated with an ecosystem shift as many areas with supratidal (high) platform marshes will transition to intertidal (low) marshes, dramatically changing the appearance, function, and suspended sediment demands of the marsh. Additionally, a switch from high to low marsh will still lead to lowering of the platform relative to the tidal datum and, thus, a large increase in tidal prism in the back-barrier system (Kirwan et al. 2010).

A fundamental challenge in predicting future marsh evolution is that many existing models have been designed to consider only the wetlands, rather than the larger landscape setting. The presence of a protective barrier is not relevant to all estuarine marshes, but in a back-barrier setting (especially in the case of a transgressive island), breaching and overwashing will impact the wetland planform area and persistence (Fig. 4). Where significant rollover of barrier units occurs, models including feedbacks between the geomorphic units are needed. The model of Walters et al. (2014) begins to address this by combining an existing model of barrier island dynamics and stratigraphy (GEOMBEST; Stolper et al. 2005; Moore et al. 2010) with the marsh edge model of Mariotti et al. (2010). The results highlight the dynamic response of back-barrier marshes to barrier islands, demonstrating that the presence of back-barrier marshes can decrease island migration rates and that barrier islands can increase marsh persistence through contributions of overwash sand (see Moore et al. this volume for more detail). The model only addresses these relationships in two dimensions along a cross-shore transect, but these results indicate the importance of feedbacks among the geomorphic components of the back-barrier system that need further investigation. Regardless, it is clear that many predicted future scenarios involve extensive loss or deepening of wetland platforms within barrier systems.

3.2 Effects of Sea-level Rise on Hydrodynamics and Sediment Transport

Studying the impact of RSLR on coastal systems including tidal inlets and back-barrier basins (lagoons, marsh and tidal creeks, estuaries) is difficult by observation alone, due to the long timescales of their evolution. In addition, not all sea-level-related thresholds have been identified, and those that have are yet to be quantified. Finally, despite the fact that hydrodynamics and sediment transport in coastal systems are becoming increasingly quantifiable, there remain practical limitations on the spatial and temporal resolutions of field-surveyed data that limit the degree to which process links can be established. As a result, predicting how these systems will respond to forcings often relies upon RSLR projections coupled with empirical or numerical models. Validation of geomorphic model results, however, can only be based on the limited existing historic data, and the timeframe of coverage is often insufficient to match the time period required for the modeled system to reach equilibrium. Moreover, important model inputs, such as RSLR, do not compare historically to the existing or future projected rates that are used in the models. Thus, geomorphic and hydrodynamic models cannot account for as-of-yet unknown linear and non-linear (possibly threshold) geomorphic responses of barriers to rates of RSLR higher than those experienced during historic time.

Historically, there has been a gradual scientific progression in the approach to studying the effect of RSLR on tidal inlets and back-barrier systems, from initial conceptual models based on historical trends, commonly for site-specific areas (FitzGerald et al. 2007), to quantitative physics-based models. In addition, large-scale

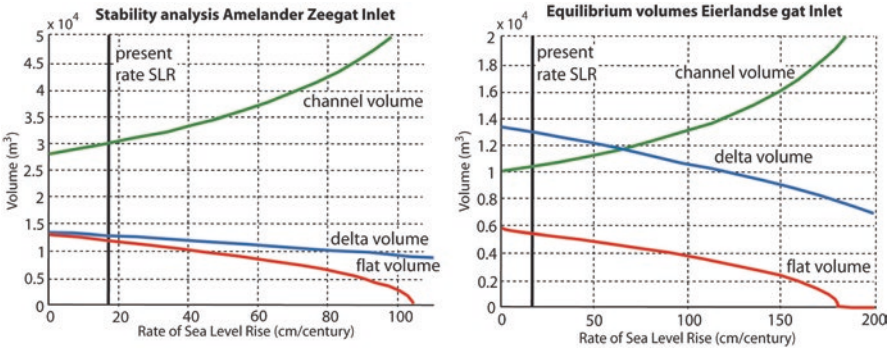

Fig. 5 Equilibrium volumes of tidal inlet elements as a function of SLR rates for two Dutch inlets. *Vertical line* represents present conditions (after Van Goor et al. 2003)

physical modeling studies have also been attempted, such as those of Stefanon et al. (2012) who performed laboratory experiments to explore channel network development in a back-barrier lagoon setting in response to changes in water level (essentially replicating rising sea level). They found a very close relationship between increasing tidal prism and drainage network expansion. This suggests that as rising sea level increasingly inundates back-barrier flats and marshes, tidal creeks will increase their drainage density through headward erosion and new creek formation, an implication that has been supported by some field observations (e.g., Hughes et al. 2009).

One simple mathematical approach is to model the geomorphic response to hydrodynamic forcings using empirical relationships (De Vriend et al. 1993). Van Goor et al. (2003) modeled two tidal inlets along the Netherlands coast using a three-element (ebb-tidal delta, inlet channel, interior tidal flats) sediment equilibrium model. The model assumes a continuous supply of sand from the adjacent barrier and sand exchange among the three components, and is based on equilibrium volumes tied to empirical relationships (obtained from regression analyses). The study shows that, at Amelander Gat, inlet channel size increases as the rate of SLR increases, whereas the volume of sand contained in the ebb-tidal delta and tidal flats decreases (Fig. 5). Likewise, the smaller-sized Eierlandse Gat increases in dimensions with rising sea level, but the shoals inside tend to be more stable because less sand is required to maintain a dynamic equilibrium (Fig. 5). These analyses suggest that, in a regime of rising sea level, the two inlets will experience different volumes and rates of sediment exchange, however both basins will import sediment from adjacent beaches and associated ebb-tidal deltas. They also indicate that both inlets will drown (widen and deepen until they can no longer be considered an inlet) during high rates of RSLR, which is consistent with the work of Beets et al. (1992) who showed that inlets on the Netherlands inner shelf drowned when sea level rose by 0.8–3.0 m/century.

In recent years, studies of the impacts of RSLR on tidal inlet systems and back-barrier basins have become more refined by utilizing models based on the physical processes governing hydrodynamics and sediment transport. van der Wegen (2013),

for example, used a two-dimensional process-based model (DELFT3D used in two dimensions with vertical averaging) to explore how different rates of RSLR affect sedimentation in an elongated basin with dimensions similar to the Western Scheldt estuary located along the Netherlands southwestern coast. The results indicate that, despite a seaward influx of sediment into the estuary, RSLR will ultimately drown intertidal flats, albeit at a slower rate for estuaries with higher tidal ranges. Likewise, Dissanayake et al. (2012) demonstrate that basins in large inlet/basin systems will import sediment at a rate commensurate with the rate of RSLR due to increasing flood-dominance of tidal currents and the consequent erosion of ebb-tidal deltas. Under a low rate of RSLR (0.2 m by 2100), the study projects that tidal flats will be maintained, whereas for high-rate scenarios, they will drown. This study was modeled after Ameland Inlet (Dutch Wadden Sea); historical records corroborate this tendency of these same basins to import sediment, showing that the presence and extent of tidal flats in the Middle Ages was similar to what it is today, despite the higher modern rate of RSLR (Louters and Gerritsen 1994).

Process-based, RSLR modeling studies of the Netherland coast consider large tidal inlets with expansive back-barrier tidal flats and channel systems, reflecting the nature of that particular coast. They uniformly predict that the basins will import sand, ebb-tidal deltas will erode, and, once rates of RSLR exceed a certain threshold, tidal flats will become permanently submerged. The exchange of sand among the various sand reservoirs, and net sediment transport directions in the channels are based on time and velocity asymmetries that will be altered by changes in tidal wave propagation as relative sea level rises; given the relationship between wave celerity and water depth (Boon and Byrne 1981; Aubrey and Speer 1985; Dronkers 1998). Higher water levels will induce changes in back-barrier hypsometry, hydraulics, and erosional-depositional patterns, which will initiate both positive and negative feedbacks until the system equilibrates to the new conditions.

The response to rising sea level of small tidal inlet systems (width <0.5 km) or systems with large inlets and with back-barriers dominated by marsh and tidal creeks is much less well studied and modeled (FitzGerald et al. 2007; Lovering and Adams 2009). We note that our understanding of thresholds governing the ability of marshes to keep pace with RSLR is in its infancy; until we know how, and at what rates, platform marshes will deteriorate, it will be difficult to predict changes in back-barrier hypsometry with rising water levels. Finally, process-based models predicting the erosion of ebb-tidal deltas due to RSLR and increasing tidal prism may be ignoring some basic tenants concerning the formation and stability of ebb deltas (e.g., Dissanayake et al. 2012). With increasing tidal prism, greater discharge at an inlet will tend to move sand further offshore and deposit it into deeper water. The distal end of the ebb delta will grow vertically due to this deposition of sand until shoaling and breaking waves, in combination with flood currents, move it back onshore. Thus, as sea level rises and tidal prism increases, ebb-tidal deltas will likely capture more sand from the littoral transport system, thereby causing these deltas to enlarge rather than erode (Walton and Adams 1976). Moreover, it should be emphasized that most existing large ebb-tidal delta systems are 1000–4000 years old and were constructed during a period of rising sea level, albeit slower than

today, lending credence to this conceptual framework of ebb delta growth, and therefore to the hypothesis set forth in this paper.

3.3 Barrier/Tidal Inlet Response to Various Forcings: Basic Relationships

In this section, we use historical datasets to illustrate erosional-depositional patterns along barrier islands caused by changes in tidal prism volumes or in locations in which storms created new pathways of tidal exchange between bays and the coastal ocean (tidal inlets). We trace the pathway of sand movement among the different sand reservoirs and, when possible, discuss the rates at which changes to the system have occurred. Changes in tidal prism are a major factor affecting the sand budget of barrier islands because tidal prism dictates: (1) the size of tidal inlets (O'Brien 1931; Jarrett 1976; Stive et al. 2009) expressed by the general equation:

$$A = CP^q \tag{2}$$

in which A = cross-sectional area of the inlet channel (m^2), P = tidal prism (m^3), and C and q are empirically derived parameters, and (2) the volume of sand comprising the ebb-tidal delta (Walton and Adams 1976; Hicks and Hume 1996; Fontolan et al. 2007) described by the general relationship:

$$V = CP^q \tag{3}$$

in which V = volume of the ebb-tidal delta (m^3), P = spring tidal prism (m^3), and C and q are again, empirical parameters determined from field measurements. For barrier island chains, the tidal prism of the entire back-barrier controls the size/number of tidal inlets along the chain (Roos et al. 2013). Tidal prism can increase through the conversion of wetlands to open water and by decreasing frictional resistance of tidal exchange through channel enlargement and/or bay deepening (Fig. 6). When barriers are breached during a storm, the sustainability of the new tidal inlet is dependent upon the inlet accessing a large enough tidal prism to keep it open (Escoffier 1940, 1977; Tran et al. 2012; Roos et al. 2013). As the new inlet equilibrates to reversing tidal flow and wave conditions, sand is transported seaward and landward building ebb- and flood-tidal deltas, respectively. This represents a loss of sand from the barrier lithosome. Using the tidal prism relationships, we explore how alterations in basinal hypsometry can lead to changes in inlet hydraulics and creation of a sediment sink inside a deepening bay.

Barrier chains most affected by the loss of wetlands—and the ensuing increase in tidal prism—are those along mixed-energy shorelines (Hayes 1979), which have numerous tidal inlets connected to broad back-barrier marshes that are incised by tidal creeks. These types of coasts tend to occur along mesotidal shores (tidal range = 1.5–4.0 m) and primarily in coastal plain settings. Hayes (1979) has also

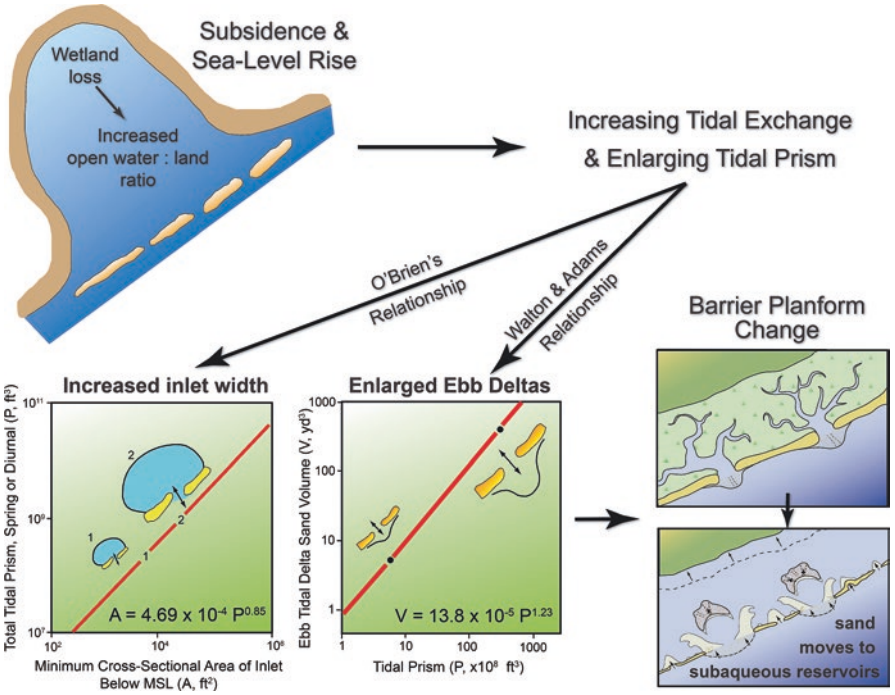

Fig. 6 Flowchart illustrating how wetland loss leads to increasing tidal prism, larger tidal inlets, and enlarging ebb-tidal deltas. Ultimately, sand from barrier reservoirs is transferred to ebb- and flood-tidal deltas causing barrier transgression

shown that tidal flats supplant marshes along some mixed-energy barrier coasts, including the Friesian Islands bordering the North Sea and the Copper River delta barrier system in the northern Gulf of Alaska. The impacts of increasing tidal prism, which results in the enlargement of ebb-tidal deltas and the siphoning of sand away from adjacent barrier islands, will tend to be greater in regions of higher tidal range. This is because platform marshes exist near or above the mean high water elevation; the volume of marsh that is potentially converted to an intertidal or subtidal environment will increase with increasing tidal range because marsh peats tend to be thicker in settings with higher tidal ranges (Redfield and Rubin 1962). This point does not discount the fact that marshes in areas of greater tidal range may reach threshold at later times than lower tidal range marshes.

In mixed-energy settings, ebb-tidal deltas contain large quantities of sand that can be comparable in volume to the adjacent barrier islands (Hayes and Kana 1976a). For example, along the mixed-energy South Carolina coast, the barriers are relatively short and tidal inlets comprise an increasingly greater proportion of the shoreline to the south, coinciding with an increase in tidal range (Hayes 1994; Hayes and FitzGerald 2013). South of Charleston Harbor, Stono and North Edisto Inlets have a combined ebb-tidal delta volume that is approximately four-fifths the volume of intervening Kiawah-Seabrook Island barrier lithosome (Fig. 7; Hayes

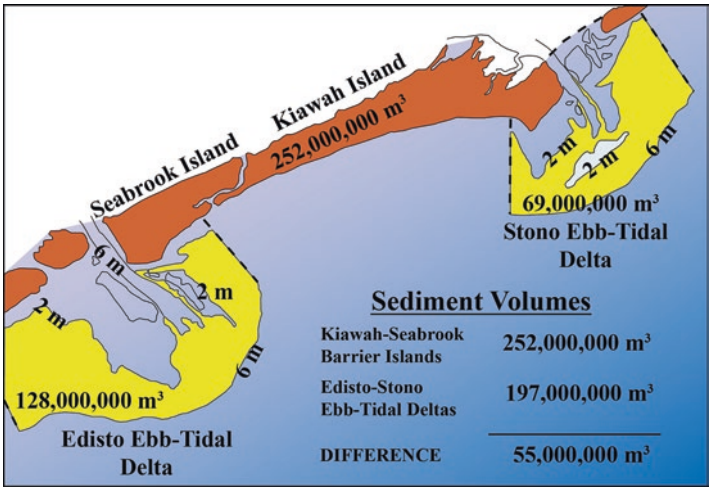

Fig. 7 Along mixed-energy coasts, such as this example from Seabrook and Kiawah islands in South Carolina, ebb-tidal deltas contain a volume of sand comparable to the volume of the intervening barrier lithosome (after Hayes et al. 1976)

and Kana 1976a, b). For the sake of illustration, if the tidal prisms of Stono and North Edisto Inlets increased by 1%, then the combined volume of the ebb-tidal deltas would increase by approximately 2.2 million cubic meters of sand would be sourced predominantly from erosion of the adjacent barrier islands and to a lesser extent channel enlargement (see Eq. 2).

4 Case Studies

We discuss a series of historical accounts of barrier island/tidal inlet systems below to explore how changes to back-barrier marsh, tidal flats, and channels areas affect inlet dimensions, and how coastal sand reservoirs are redistributed. We use the insights gained from these studies to present a conceptual model of barrier evolution in a regime of accelerating RSLR.

4.1 Nauset Spit-New Inlet, Cape Cod, Massachusetts

The 30-km long Nauset barrier system is composed of a series of spits and barrier islands that form the southern outer coast of Cape Cod, Massachusetts. Nauset Spit breached during a moderate northeast storm on January 2, 1987 after overwash had formed an incipient channel across the barrier and then return flow, accompanying a wind shift to the northwest as the storm passed, scoured a deep channel. New Inlet

was actually a product of long-term erosion that narrowed the barrier, storm waves that dismantled the foredune ridge, and a hydraulic head across the barrier that reached 0.70 m and 0.86 m at high and low tide, respectively (Friedrichs et al. 1993; FitzGerald and Pendelton 2002).

One day after the storm, the channel was 100-m wide. It grew to 0.5 km after two months and to 2.0 km wide a year later as the inlet captured and equilibrated to an increasingly large tidal prism. During this process, barrier sands washed into the bay enlarging the flood-tidal delta and other sand shoals (Stauble 2001; FitzGerald and Montello 1993). FitzGerald and Montello (1993) estimated that during the first year approximately 0.7–1.0 million cubic meters of sand were transported into the bay (Fig. 8). Initially, the inlet widened through erosion and retreat of the northern and southern shorelines, but after 1.5 years the inlet reached a stable configuration and continued to narrow due to spit accretion. At that time, a 1.6-km wide shallow spit platform extended south from Nauset Beach and the channel thalweg was positioned at the very southern side of the inlet, a consequence of the dominant southerly alongshore transport direction and the northerly approach of the main bay channel toward the inlet. In subsequent years, the main inlet channel periodically breached an easterly, more-direct channel through the spit platform, expanding the extent of ebb-tidal delta seaward (Liu et al. 1993). The new channel dominated the former southern channel because it was a more hydraulically efficient pathway for tidal flow into and out of the inlet.

Between 1988 and 1999, the ebb-tidal delta grew in volume (Fig. 8) as New Inlet equilibrated to its tidal prism, as predicted by the Walton and Adams (1976) relationship. The sequestration of sand on the ebb delta coupled with sand movement into the inlet, added to the growth of the bay shoals and led to a reduction in sand bypassing the inlet thereby starving the downdrift South Beach shoreline. During this period of ebb-delta growth (1990–2000), South Beach retreated 200–300 m. Following a period of relative stability, another inlet formed north of New Inlet in April 2007, which again disrupted the alongshore transport system causing shoreline recession and ultimately, formation of a third inlet along South Beach.

The pattern of tidal inlet development along the Nauset Spit system during the past three decades illustrates the strong coupling effect between barrier breaching and tidal inlet formation and the loss of sand from the barrier lithosome. Moreover, the historical morphological changes demonstrate that the sequestration of sand on ebb-tidal deltas represents a short- to long-term loss of sand from the barrier system, whereas sand transport into bays represents an important long-term loss. This sand will not re-enter the barrier/littoral system until the barrier transgression reaches this landward site.

4.2 Ocean City Inlet–Assateague Island, Maryland

Fenwick and Assateague Islands were once a continuous island along the Maryland coast prior to a 1933 hurricane that breached the barrier and formed Ocean City Inlet. Initially, the inlet was 3 m deep and 76 m wide (Underwood and Hiland 1995).

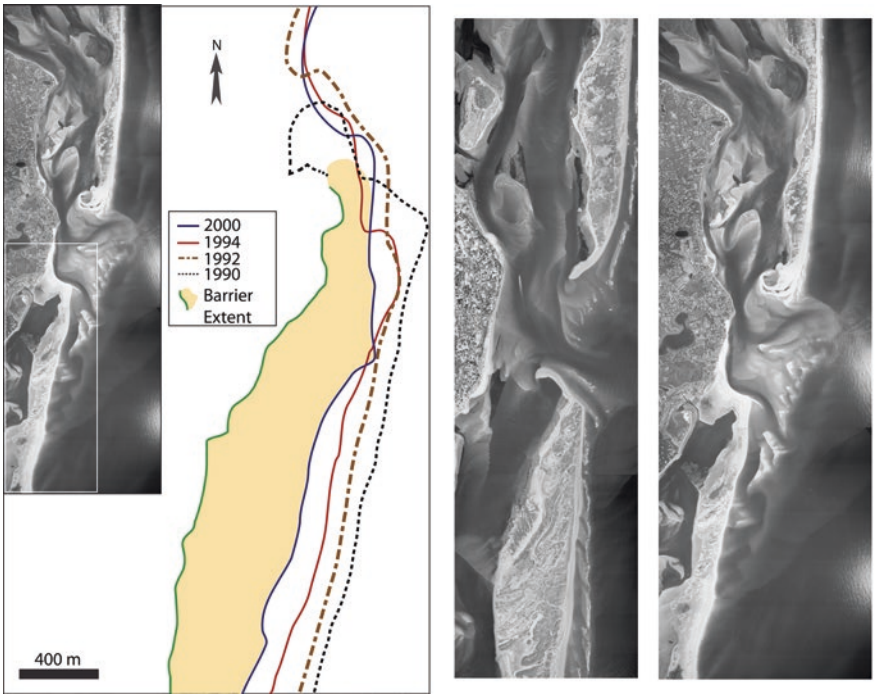

Fig. 8 New Inlet, Cape Cod. Historical shoreline data documents retreat of the downdrift beach as sand was sequestered on ebb-tidal delta (after Stauble 2001). During the period between 1990 and 2000 the shoreline retreated 200–400 m

Within a month the US Army Corps of Engineers began construction of jetties to stabilize the inlet's location and prevent southerly alongshore transport from closing the channel. The inlet is now 330 m wide narrowing to 200 m at the seaward end of the jetties. Numerous authors have detailed shoreline changes, channel characteristics, and a sediment budget for the inlet area (Dean and Perlin 1977; Stauble et al. 1993; Rosati and Ebersole 1996; Stauble 1997).

Immediately following completion of the jetties, erosion rates along northern Assateague Island, extending ~14 km south of the inlet, essentially doubled (average rate = 2.9 ± 2.7 m/year; Rosati and Ebersole 1996). Northern Assateague Island migrated almost two barrier widths onshore (0.5 km) between 1850 and 1980 (Fig. 9a; Dean and Perlin 1977) and most of this movement occurred following inlet formation. During the same period, the Fenwick shoreline immediately north of the inlet prograded approximately 250 m with accretion tapering northward for about 2 km (Dean and Perlin 1977). This accretion was attributed to trapping of the southerly alongshore transport of sand by the north jetty as well as several beach nourishment projects (volume = 2.2×10^6 m^3; USACOE 1998).

The dramatic erosion of northern Assateague Island was due to the disruption of the natural alongshore transport system caused by inlet formation, leading to the sequestration of sand on ebb- and flood-tidal deltas, initial accretion next to the

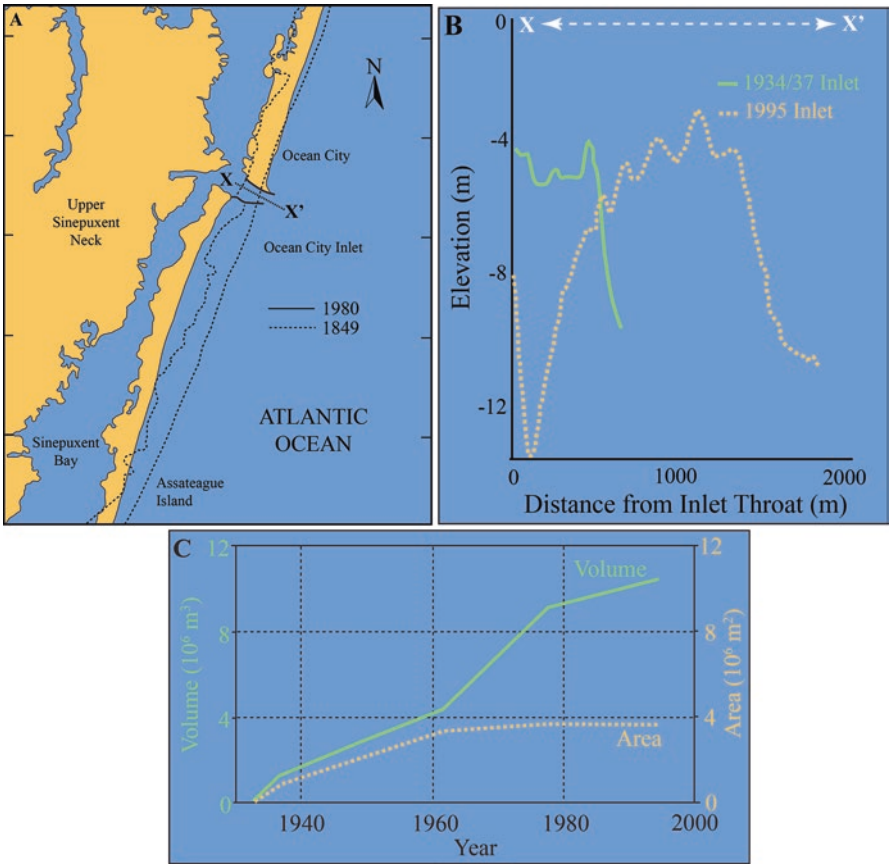

Fig. 9 Ocean City Inlet, MD. (**a**) Shoreline changes showing the landward migration of Assateague Island. (**b**) Cross-sectional changes of Ocean City Inlet from 1934/1937 to 1995 demonstrating deepening of the inlet and seaward progradation of the ebb-tidal delta (after Stauble 1997). Cross section location is shown on panel (**a**). (**c**) Growth of the ebb-tidal delta (10×10^6 m^3) from inlet formation to 1995 (after Stauble 1997)

north jetty, and removal of sand from the jettied navigation channel during numerous dredging projects (Rosati and Ebersole 1996; Stauble 1997). The evolution of the inlet channel and ebb-tidal delta are depicted in Fig. 9b, c. During the 1937–1995 period, the inlet throat deepened from 5 to more than 14 m coincident with a substantial increase in cross-sectional area as the inlet accessed an increasingly large bay tidal prism.

Following the formation of a new tidal inlet, it commonly takes several years for new channels to fully develop and efficiently connect to back-barrier bays and capture the entire potential tidal prism inlet (Liu et al. 1993). During this phase at Ocean City Inlet, the inlet channel increased in dimensions, eventually reaching an equilibrium size predicted by Eq. 2. Sand was transported into the proximal back-barrier.

Likewise, sand entering the inlet via alongshore transport and scoured from the channel was transported seaward building the ebb-tidal delta and moved landward, enlarging flood-tidal shoals. A profile along the inlet channel and across the ebb-tidal delta demonstrates that following inlet formation and extending to a period when the ebb delta reached a dynamic equilibrium (sometime after 1995), the ebb-delta accumulated sediment and accreted seaward. Using the terminal lobe as a reference point (seaward apex of the ebb delta, Fig. 9b), it is clear that the delta built seaward by ~1 km and increased to a volume $>10 \times 10^6$ m^3 (Fig. 8c; Stauble 1997).

The delta appeared to have reached an equilibrium volume by the late 1990s as indicated by large swash bars bypassing the inlet and migrating from the delta landward to Assateague Island (Kraus 2000). However, there continues to be a deficit of sand along northern Assateague Island, requiring continued beach nourishment (US Army Corps of Engineers 1998). Nonetheless, the evolution of this area clearly demonstrates that inlet formation can drastically impact the barrier sediment budget, particularly when the growth of ebb- (and to a lesser extent flood-) tidal deltas sequesters sand from the alongshore transport system that otherwise would nourish the downdrift barrier island.

4.3 Virginia Barriers

The Virginia coast along the Delmarva Peninsula, south of Assateague Island, is composed of mixed-energy barrier islands (Fig. 10) dominated by fine-grained beaches with frequent overwash (McGee 1890; Rice et al. 1976; Halsey 1979; Oertel and Kraft 1994). Barriers are backed by a network of tidal channels, subtidal to intertidal mudflats, shallow (<2 m) open bays, and salt marsh (Fig. 10). The northern islands are located 1–3 km offshore of the mainland and are predominantly backed by extensive marsh. Farther south, the distance between the barriers and the mainland and the area of open water behind individual barriers both increase, reaching a maximum at Hog and Cobb islands of 13–14 km and >80%, respectively. Modern rates of RSLR along this coast are among the highest on the US East Coast, with estimates ranging from 3.6 to 6.0 mm/year in recent decades (Boon 2012; Ezer and Corlett 2012; Boon and Mitchell 2015). This rate exceeds that determined for vertical accretion of mid and high marsh in this region (0.7 ± 1.2 and 1.4 ± 0.2 mm/year, respectively), leading to reversal of marsh growth trends inferred from the late Holocene, and the loss of marsh, particularly adjacent to open water (Kastler and Wiberg 1996; Erwin et al. 2004, 2006; Priestas et al. 2015). These effects are compounded by marsh-edge erosion driven by wave action in some of the larger back-barrier bays (Mariotti and Fagherazzi 2013), albeit some progradation of marsh has occurred into shallow ponds and tidal flats (Erwin et al. 2006) as well as onto low-lying sections of barrier islands themselves (Deaton et al. 2017). The net result has been a loss of >9% of marsh area behind the Virginia barriers (Assawoman to Smith islands) since 1870 (Fig. 10; Deaton et al. 2017).

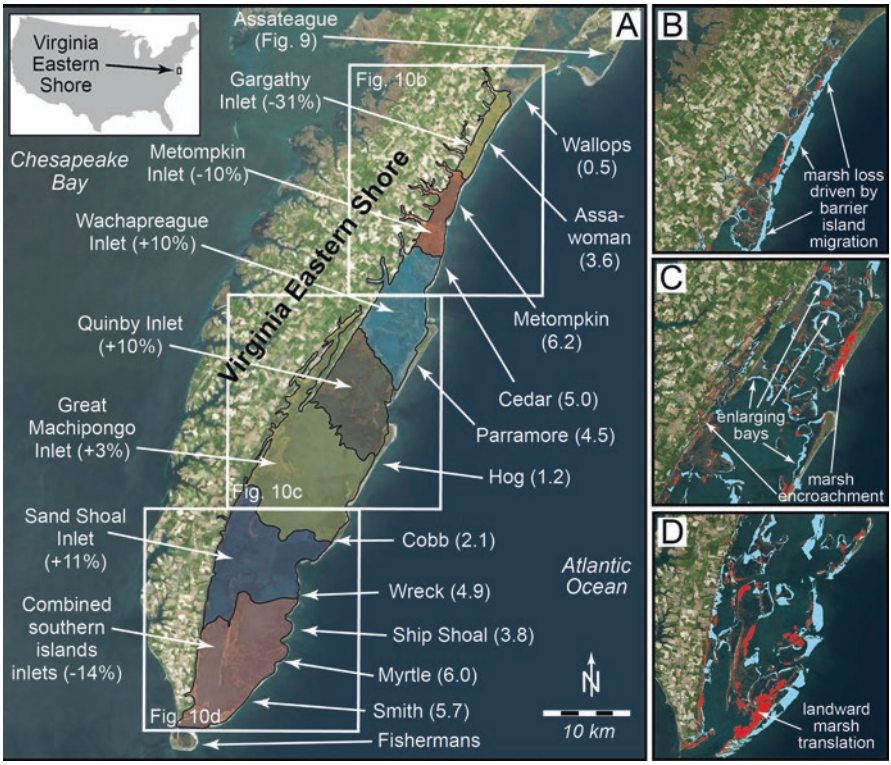

Fig. 10 Historical changes along the Virginia barrier islands. All data are from Deaton et al. (2017) and individual panels are modified from Deaton et al. (2017). (**a**) Site map of the Virginia Eastern Shore barrier islands. Colored regions behind each barrier island indicate the "bayshed" for each tidal inlet (area flooded/drained by that tidal inlet); values are change in tidal prism between 1870 and 2009 (negative values represent loss in tidal prism). Note large decreases in tidal prism associated with northern rollover-dominated barrier islands and increases associated with back-barrier marsh loss along southern islands. Barrier island names are given on the right; numbers in parentheses are long-term shoreline-migration (1851/2 to 2010) rates determined from linear regression analysis after Hapke et al. (2010b). (**b**–**d**) Maps of marsh gain (*red*) and loss (*blue*) associated with bay expansion, upland migration, and landward migration of Wallops through Smith islands between the mid- to late-1800s and 2009

Despite the overall loss of marsh from the back-barrier, the rapid onshore migration of the Virginia barrier islands plays a role in marsh loss and in determining the extent of open-water area along the Virginia Eastern Shore (Kastler and Wiberg 1996; Deaton et al. 2017). Recent work has demonstrated that exposure and erosion of marsh along the shoreface due to the landward migration of the islands accounts for ~32 km^2 of marsh loss during the last 150 years (Deaton et al. 2017); this is ~5% greater than the net area lost due to back-barrier processes. The barrier rollover process has not only consumed marsh, it has also filled open-water areas. The net result of back-barrier marsh loss and landward barrier migration has been a slight increase in back-barrier open water area of only 9 km^2, <2% of the total open water area

(Deaton et al. 2017). This analysis suggests that any gain in tidal prism from marsh loss along this barrier chain is countered by the "squeezing" of the back-barrier by barrier migration. Although some inlets have experienced a small increase in tidal prism (e.g., Wachapreague Inlet increased by 6–10% between the late 1800s and early twenty-first century; Fenster et al. 2011; Richardson 2012; McBride et al. 2015), other inlets have undergone a marked decrease in tidal prism of >30% due to landward barrier migration (Fig. 10; Deaton et al. 2017).

Overall, the tidal inlets associated with the Virginia barriers are maintaining a quasi-stable state: the ongoing disintegration of back-barrier marshes (20% total loss due to barrier migration and back-barrier processes [e.g., edge erosion] in the last 150 years) and slow migration of marshes onto uplands, although increasing bay area, is negated by the landward migration of the barriers, which is reducing system-wide back-barrier area at an approximately same rate.

4.4 Barataria Barriers, Louisiana

The barriers fronting Barataria Bay along the central Louisiana coast formed from sand delivered from two former distributary headlands, Bayou Lafourche to the west and Plaquemine Delta to the east (Fig. 11). The Barataria coast is low-energy with diurnal tides and a spring tidal range of 0.46 m; however, circulation at the inlets within Barataria Bay is commonly dominated by wind-generated set-up and set-down. Generally, breaking waves are small along the coast (<0.4 m), except during the passage of winter storms nearshore when waves as high as 3.0 m can prevail for days (Stone et al. 2003; Stone and Orford 2004). Infrequent hurricanes (1 every 7 years; Muller and Stone 2001) cause the greatest impact on the shoreline, resulting in widespread erosion, overwash, and breaches that can evolve into tidal inlets (Boyd and Penland 1981; Stone et al. 2003).

The Barataria barriers provide a natural laboratory in which to study the effects of accelerated SLR because this region is experiencing one of the highest rates of relative SLR in the world (9.03 mm/year for 1947–2015; Fig. 12; NOAA 2015a, b) due to a variety of causes including deep-seated crustal adjustments (Mitrovica and Milne 2002; Yu et al. 2012), fluid withdrawal associated with hydrocarbon production (Morton et al. 2005); compaction of Holocene deltaic sediments (Penland and Ramsey 1990; Törnqvist et al. 2008), and reduced sediment supply due to leveeing and channelization of the Mississippi River.

During the past 80 years rapid RSLR and erosional processes within Barataria Bay have led to substantial wetland loss, converting more than 1100 km^2 of wetlands to open water (14 km^2/year; Couvillion et al. 2011; Fig. 12). Conversion of wetlands to intertidal and subtidal environments is a product of several linked processes including subsidence, marsh front erosion (Schwimmer 2001; Wilson and Allison 2008; Mariotti et al. 2010; Mariotti and Fagherazzi 2013), and catastrophic scour during large magnitude hurricanes (e.g., Katrina; Barras 2006; FitzGerald et al. 2007). The multiple causes of wetland loss appear to be dominated by RSLR;

Fig. 11 Barataria barriers and tidal inlet systems formed from reworking of former distributary headlands Lafourche and Plaquemine Deltas

a temporal plot of wetland loss and RSLR shows similar trends during the past 50 years. However, they are slightly out of phase, indicating other processes are likely operative (Fig. 12). For example, Morton et al. (2005) and Morton et al. (2006) demonstrated convincingly that accelerated wetland loss in adjacent Terrebone Basin is related to rapid subsidence following peak volume fluid withdrawal from nearby oil and gas fields. A large number of oil and gas fields also exists in the Barataria Basin and may have contributed to subsidence in this region as well (Morton et al. 2006).

Long-term conversion of wetlands to open water over the last >125 years has steadily increased tidal exchange between Barataria Bay and the Gulf of Mexico resulting in larger inlet tidal prisms. Two direct consequences of the increasing tidal discharge are the enlarging tidal inlet geometry and growth of ebb-tidal delta shoals (List et al. 1994; FitzGerald et al. 2004). Data collected during the summers of 2006 and 2011 allow updating of hydraulic and morphologic trends previously established for the Barataria Bay barrier system for the period between 1880 and 1980. As shown in Fig. 13a and Table 2, the inlets have collectively more than quadrupled in size, accommodated in part by the formation of Pass Abel in 1920s and a widening of the other inlets, but primarily by a deepening of the inlet throats. It is noteworthy that during the 26 years between 1980 and 2006, the combined cross-sectional areas of the inlets increased by almost 70%, coinciding with a period of significant

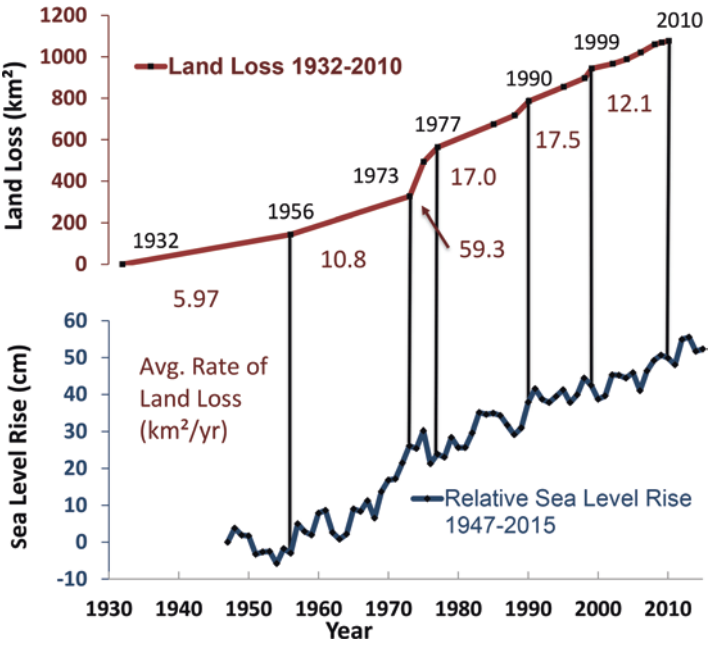

Fig. 12 Temporal changes in sea level at Grand Isle (gage # 8761724, NOAA 2015a, b) and wetland loss in Barataria Bay (after Couvillion et al. 2011)

wetland loss in Barataria Bay (Fig. 12). During this time, the inlets deepened from 5 to 10 m (Fig. 13a). Collectively, the historical inlet combined cross sections all plot well within the 95% confidence limits of Jarrett's (1976) regression equation of tidal prism versus throat cross section (Fig. 13b), indicating that they have remained in equilibrium with the increasing tidal prism.

Significant in the evolution of the Barataria barriers is how sediment reservoirs are being redistributed as the inlet tidal prisms are enlarging. As predicted by Eq. 2, there has been a growth in the volume of ebb-tidal deltas as evidenced by a significant increase in the ebb-delta footprint through time (Fig. 14) and by the seaward excursion of the 5-m contour at Barataria Pass (Figs. 13a and 14). During the same approximate time period (1880s–1988), the intervening barriers underwent dramatic erosion with average shoreline retreat rates between 1 and 15 m/year (Williams 1992). An exception to this trend is the accretion that occurred along the east end of Grand Isle, which is protected by a system of offshore breakwaters and has been the site of beach nourishment projects. The response of the Barataria barriers to wetland loss and a growing tidal prism has been an increase in the dimensions of the tidal inlets, and growth of ebb-tidal delta volumes at the expense of the barriers, which have drastically decreased in size, resulting in the formation of a new tidal inlet (Pass Abel). This case study clearly shows the end-result of large-scale wetland loss ultimately translating to the redistribution of coastal sand reservoirs and severe erosion along this coast, leading to numerous state and federally funded beach nourishment projects to maintain the integrity of this barrier chain.

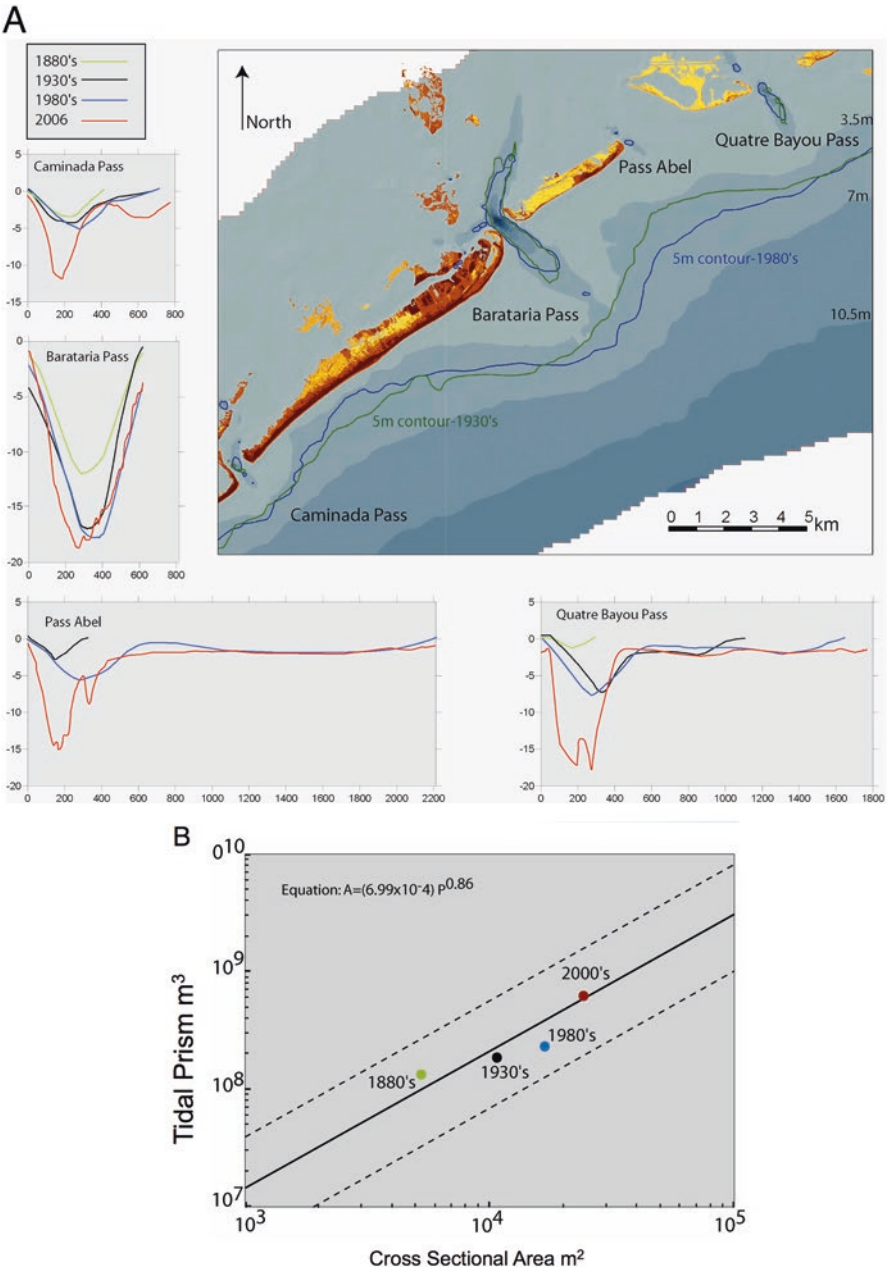

Fig. 13 (**a**) Changes in tidal inlet cross section (1880s–2006) of Barataria Bight. (**b**) Plot of combined inlet cross-sectional areas (Table 2) versus their combined tidal prism for the 1880–2006 period using Jarrett's (1976) equation for Gulf Coast inlets

Table 2 Inlet cross-sectional areas (m^2)[a]

Year	Caminada	Barataria	Pass Abel	Quatre Bayou	Total X-sect area
1880s	809	4304	0	133	5646
1930s	1353	6271	395	2590	10609
1980s	1532	7182	4193	3777	16,684
2006	3372	7374	6669	6726	24,141

[a]Note that all inlets of this section of the Louisiana coast have shown a net increase in cross-sectional area

4.5 Chandeleur Islands and Isle Dernieres, Louisiana

These two island chains are located along the east and south-central portion of the Mississippi River delta plain (MRDP). We treat them separately from the Barataria system because most of islands along these chains have reached a phase of rapid erosion and their back-barrier wetlands have collapsed to the extent that the barriers are migrating landward into deepening sounds. Their tidal inlets are small, with insignificant ebb-tidal deltas. The evolution of these systems provides insights into the factors controlling landward barrier migration. These barriers are a product of the delta cycle, which involves a regressive stage of delta building and then a transgressive component when marine processes dominate over the previous fluvial processes because of distributary abandonment (Penland et al. 1988; Roberts 1997; Coleman et al. 1998). Consequently, wave and tidal currents rework and laterally distribute sands that were originally deposited within and proximal to the distributary, forming erosional headlands with flanking barrier islands. RSLR and wave and tidal current erosion in the back-barrier drives mainland detachment and development of a fully transgressive barrier system. Lateral sand transport away from the original, centralized fluvial depocenter point source and redeposition as spit platforms at the flanks of the barrier chain ultimately depletes sand available for the system to maintain exposure in a regime of rapid RSLR. Ultimately, the barrier system is transformed into a subaqueous sand shoal on the inner continental shelf (Penland et al. 1988).

4.5.1 The Chandeleur Islands

The Chandeleur Islands represent remnants of the St Bernard delta complex (fluvial abandonment ~1800 years BP; Frazier 1967) and are now separated from the mainland marsh by the ~40-km wide Chandeleur-Breton Sound. In this late stage of barrier island evolution, large tidal inlets typical of the younger central coast barrier systems (e.g., Barataria barrier chain) are absent. Instead, tidal currents primarily flow through deep, broad troughs around the flanks of the island chain (Hart and Murray 1978). However, the loss of sand from the system due to the impact of repeated hurricanes has thinned the barrier arc, rendering it prone to breaching. Periodic inlet development has facilitated landward sand transport and the building

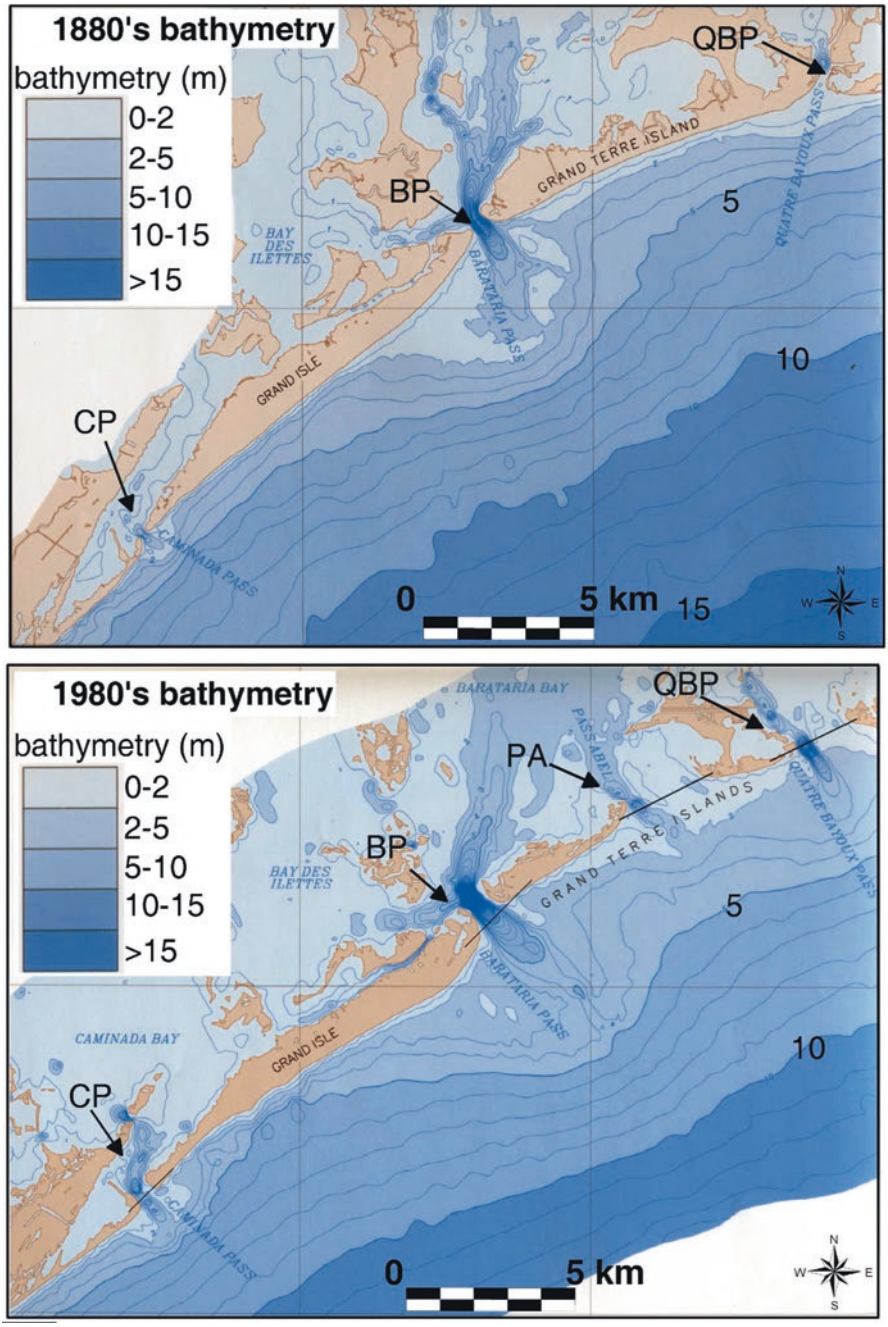

Fig. 14 Bathymetric maps for inlets in 1880s and 1980s (after List et al. 1994). Note the growth of the ebb deltas and formation of Pass Abel. CP Caminada Pass, BP Barataria Pass, PA Pass Abele, QBP Quatre Bayou Pass

of recurved spits and flood-tidal deltas. Most new inlets are ephemeral closing within 2–3 years, but one inlet (~1 km wide) has remained open, primarily due to the sand-starved nature of the southern portion of the barrier arc.

Most of the sand eroded from the front side of the Chandeleur Islands is transported alongshore and deposited in deepwater sinks at the flanks of the island chain rather than being sequestered at ebb-tidal deltas (Miner et al. 2009a; Georgiou and Schindler 2009). Because these islands are far removed (temporally) from the headland-detachment process, they are no longer effectively fed relict deltaic sands except by excavation of subsurface deposits intercepted by tidal inlet and shoreface ravinement. Sand lost alongshore to deepwater sinks has led to a long-term reduction in island area from 44.5 km^2 in 1855 to 4.7 km^2 in 2005 (Miner et al. 2009a; Fearnley et al. 2009). Deterioration of the barrier arc significantly accelerated after 1998 due to an increase in frequency of large magnitude hurricanes (e.g., Ivan in 2004, Katrina and Rita in 2005; Gustav in 2008; Sallenger et al. 2009). On the basis of regression-forecasting models of the barrier footprint area, the islands are predicted to undergo transgressive submergence and conversion to an inner shelf shoal within the next three decades (Fearnley et al. 2009). The majority of the southern Chandeleur Island system is dominated by wave-generated cross-shore sediment transport rather than alongshore transport and has already converted to shoals and ephemeral islands (Miner et al. 2009b).

Using time-series bathymetric data and sediment cores, Miner et al. (2009b) have shown a correlation between shoreface slope angle and barrier evolution (Fig. 15). The southern Chandeleurs have a relatively gentle shoreface slope and are experiencing landward retreat of short-lived barrier islands and barrier shoals, with no well-established back-barrier marsh. The northern Chandeleurs have a relatively steep shoreface and are undergoing shoreline erosion and limited landward barrier island migration. These islands are backed by well-established back-barrier marshes that serve as nucleation sites for sand deposition during storm recovery. This resistant substrate inhibits total destruction of islands during storms. It also serves to slow the rate of shoreline erosion because it forms a barrier beyond which sand transported by waves cannot pass. Thus, it accumulates and, during recovery, forms bars that weld to the shoreline. In contrast, where no back-barrier marsh is present or where it is destroyed during storms, sand from the nearshore zone is transported landward by waves forming flood tidal deltas and recurved spits. Parts of the islands that are backed by marsh migrate landward slowly, and the shoreface matures and becomes steeper. Parts of the islands that are not backed by marsh are destroyed during storms and reemerge during calm weather in a position landward of their pre-storm location (Fig. 15).

The ongoing storm-induced loss of back-barrier marsh is forcing a shift in the sediment transport regime from the previously dominant alongshore direction to one dominated by cross-shore processes. The system is becoming more efficient at recycling sediment during landward retreat by overwash activity and through the formation and expansion of flood-tidal deltas at tidal inlets. The development of recurved spits along the borders of inlets also moves sand onshore. Tidal inlet formation and persistence are controlled by storm frequency and magnitude. In other regions, particularly the southern portion of the chain, storms inhibit island reemergence and

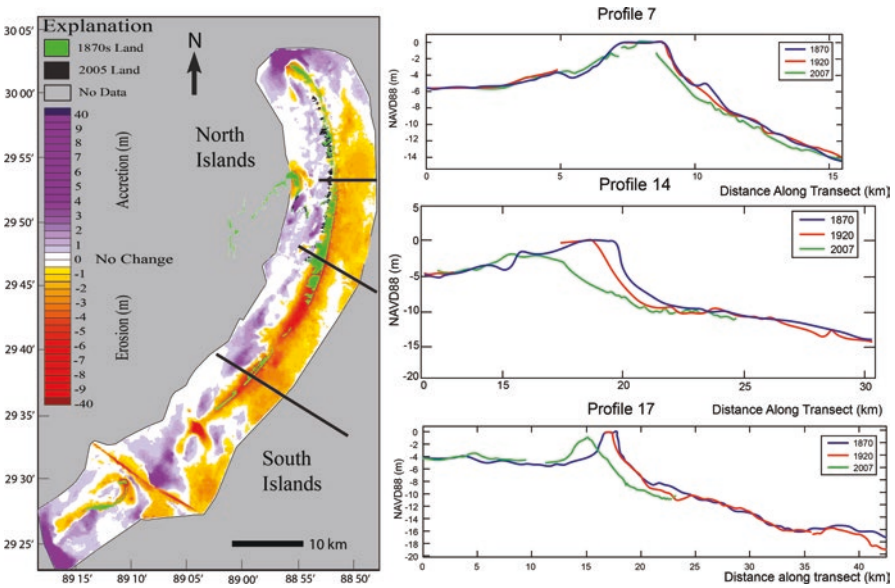

Fig. 15 Shoreline and bathymetric changes along the Chandeluer Island chain between the 1870s and 2007 (after Miner et al. 2009a)

subaerial expansion, processes that occur during extended calm weather periods. In a regime of frequent storms, sand transported offshore by storm waves and return flow does not have sufficient time to move back onshore and reorganize into a linear shoal before being impacted by a subsequent storm. This results in a net loss of sand to the offshore and development of an offshore sand sheet in the retreat path of the landward-migrating ephemeral barrier islands/shoals.

4.5.2 The Isles Dernieres

The Isles Dernieres are another highly transgressive Louisiana barrier chain that has undergone complete detachment from the mainland. Stratigraphic evidence, historic maps, and vertical aerial photographs show that the Isles Dernieres formed from the reworking of a delta lobe that was abandoned approximately 400 year BP (Kulp et al. 2005). By the mid-1800s, the island chain was a continuous barrier system backed by Pelto Bay and Big Pelto Bay (Fig 16). Initially, these lakes that became bays were surrounded by nearly continuous marshland; however, during the next 100 years, RSLR, tidal scour, wave erosion of marsh platforms, and canal construction transformed the lakes into a single, large open sound connecting to Caillou Bay to the west and Terrebonne Bay to the east (Fig. 16). Locally, the barriers have migrated >2 km landward since the 1800s (McBride et al. 1992), but the rate of northward translation has not kept pace with the landward retreat of the mainland marshes, leading to an increasingly larger and deeper back-barrier bay area (Fig. 16).

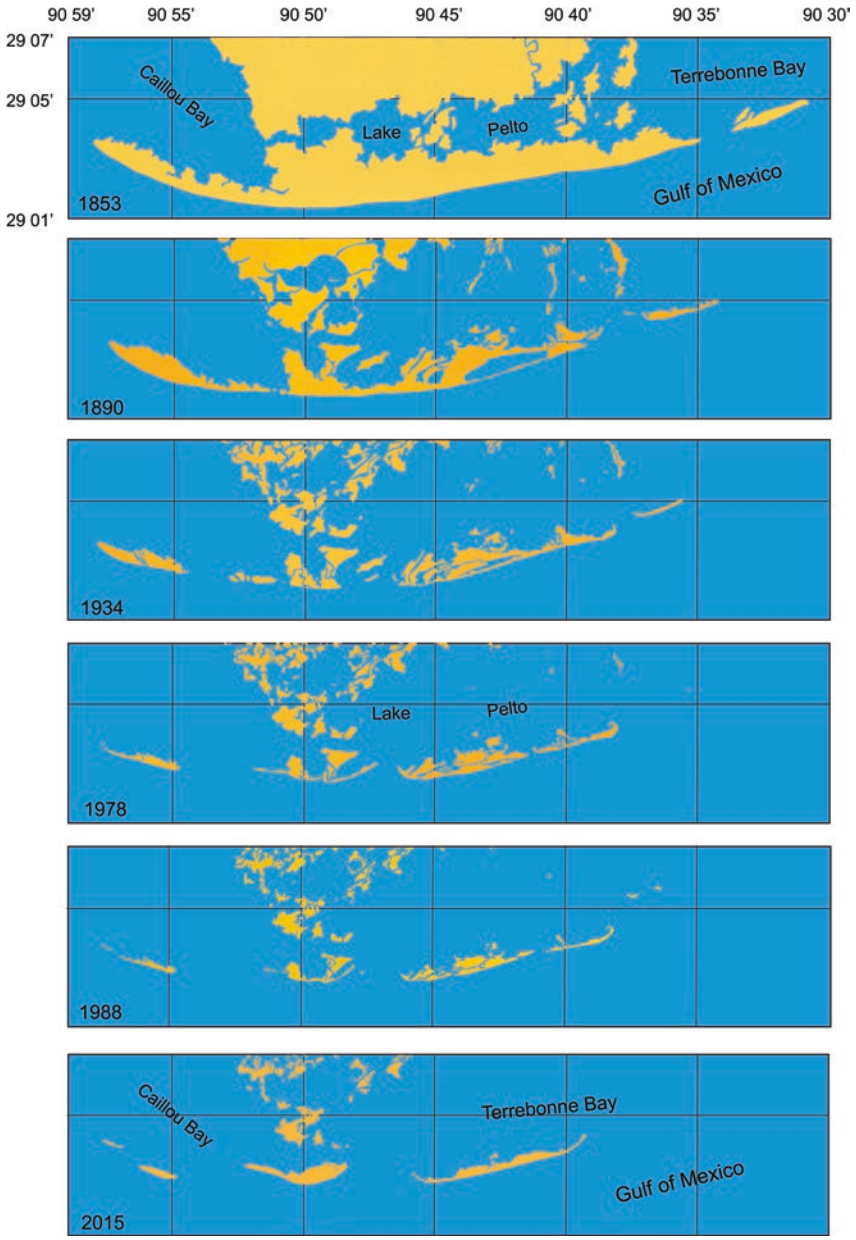

Fig. 16 Morphologic evolution of the Isles Dernieres, Louisiana, showing thinning of the barriers and widening of the tidal inlets. Between 1988 and 2015 several sediment renourishment projects took place along the island system, locally resulting in a more continuous shoreline (modified from McBride et al. 1992, and updated from Kindinger et al. 2013)

Eventually, the alongshore continuity of the system was compromised and the barrier chain segmented due to the diminished sand reservoirs. Gradually, tidal inlets that formed during major storms stabilized because of increasing tidal prism that resulted from wetland loss in the back-barrier. Sand once comprising a robust barrier system moved offshore, became sequestered in ebb-tidal deltas, and moved landward to form flood-tidal deltas. As the Isle Dernieres migrated onshore, much of the ebb-delta sand moved onshore as well, but some was permanently lost to the inner shelf (Miner et al. 2009b).

The landward migration of the barrier system into a deepening bay is an ongoing process, causing the decrease in areal extent of the barrier chain. As barrier sand moves onshore during major storm overwash events, sand must fill an increasingly deeper water column to maintain a subaerial footprint. A positive feedback also exists whereby increasingly thicker barrier sand results in greater compaction of the underlying bay and deltaic mud (Rosati et al. 2010), further exacerbating the high rate of RSLR in the area. Bathymetric and seafloor-change analysis by Miner et al. (2009a, b) demonstrates that much of the back-barrier has undergone an increase in water depth from 0 to 1 m during the last century, attributed to the erosion of bay sediment and RSLR. Using historical charts and aerial photographs, McBride et al. (1992) documented that between the 1890s and 1988, the width of the island system decreased by approximately 0.8 km at an average rate of 8.6 m/year, which contributed toward a total reduction in island area of 27.6 km^2, or 78% of the 1890s island foot-print. Like the Chandeleurs, this barrier chain is evolving rapidly toward becoming an inner shelf sand shoal (*sensu*: Penland et al. 1988), but the influx of sand from the barrier chain to the east and from barrier island restoration projects, slows the process to a small degree.

4.6 Copper River Barriers, Alaska

This case study illustrates a condition of tidal prism reduction. The Copper River barriers are located on a collision coast (Inman and Nordstrom 1971) in the Gulf of Alaska (Fig. 17). Their presence is a consequence of significant sediment discharge from the glaciated Alaska Range and Chugach Mountains via the Copper River and several other smaller rivers (40×10^6 m^3/year; Reimnitz 1966). The barrier chain is 80 km long and sits atop deltaic sediment as much as 180 m in thickness (Reimnitz 1966). Modern sea level along this coast is a product of deltaic subsidence (2.5–3.8 cm/year; Reimnitz and Marshall 1965) and infrequent tectonic uplift (Ferrians 1966; Plafker 1969; National Research Council 1972). A wave study by Nummedal and Stephen (1976) showed that frequent storm winds from the south and southeast produce a net westerly alongshore transport rate of more than 6×10^6 m^3/year. The barriers vary in length from 6 to 14 km and are backed by an extensive system of tidal flats (5–10 km wide) incised by a network of tidal channels.

A field study of the region between 1969 and 1975 by Hayes et al. (1976) and Hayes and Ruby (1994) showed that the strong westerly movement of littoral sedi-

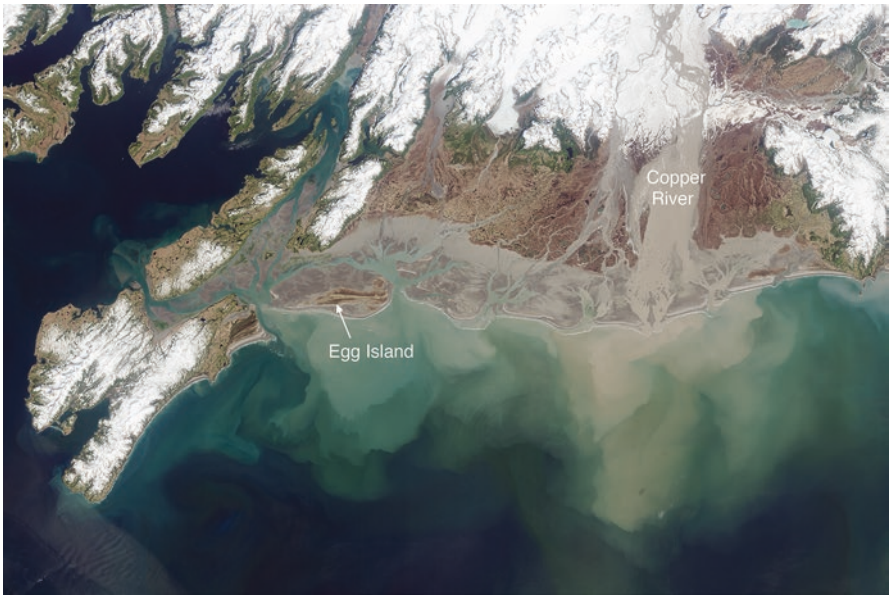

Fig. 17 Vertical aerial photograph of the Copper River delta barriers (from http://earthobservatory.nasa.gov/IOTD/view.php?id=81784)

ment produced spits at the western ends of the barriers and a slight westerly migration of the inlets. In addition, the proximity of the eastern back-barrier to the Copper River and wave sheltering of the eastern barrier flank by Kayak Island have led to a lagoon that is largely filled with sediment. Lagoonal width and open water area increase westerly along the rest of the chain resulting in larger tidal prisms that generate wider tidal inlets having larger inlet offsets and larger ebb-tidal deltas (Fig. 18; Hayes and Ruby 1994).

A dramatic historical impact to the island chain occurred on March 27, 1964 when the Good Friday Earthquake (magnitude 9.2; http://earthquake.usgs.gov/earthquakes/events/alaska1964) uplifted the Copper River delta region by 2.5–3.0 m (Fig. 19a; Plafker 1969). A map of Egg Island at the western end of the chain depicts the footprint of island after the uplift event in 1964 and its progradation during an 11-year period following the earthquake (Fig. 19b, Hayes and Ruby 1994). The overall increase in areal extent of Egg Island is characteristic of the other barriers along this coast during the same time span. The rapid growth of the islands is difficult to reconcile after the uplift event given their previous history of slow shoreline accretion. Only a large influx of sediment would explain the rapid lengthening of spits and addition of new beach ridges to the front side of the barriers. Presumably, the uplift event did not significantly increase the discharge of sediment from Copper River and, thus, cause greater accretionary patterns along the islands, because the production of riverine sediment is closely related to glacial erosion of unweathered bedrock and meltwater discharge delivering this sediment to the coast. Within short time spans these processes are climatic and not related to tectonics.

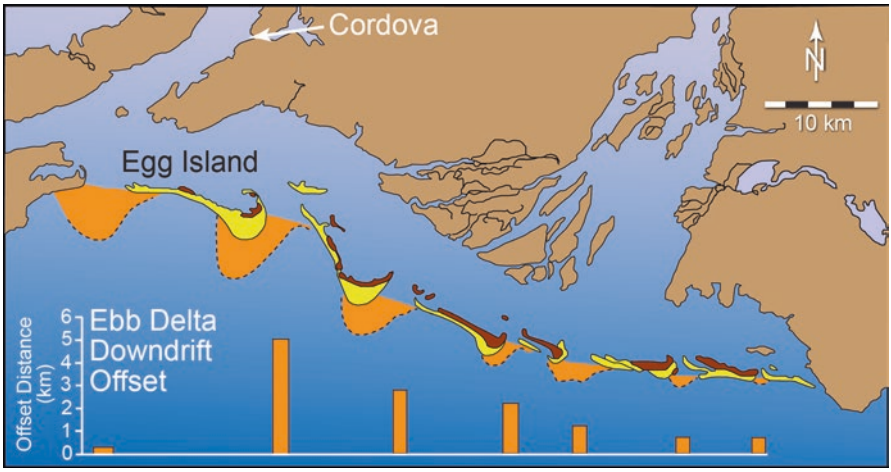

Fig. 18 Barriers of the Copper River delta show an increase in inlet size and ebb-tidal delta extent from west to east. The bulbous updrift nature (drumstick shape; Hayes 1979) of the barriers produces an increasing downdrift alignment of the inlet shoreline (modified after Hayes 1979)

A plausible explanation for rapid island growth is a decrease in tidal prism arising from changes in lagoonal hypsometry resulting from the 1964 uplift that transformed subtidal areas to intertidal flats and tidal flats to supratidal wetlands. The end product of these changes was a decrease of open-water area in the lagoon leading to reduced tidal prisms, which ultimately resulted in smaller equilibrium-sized tidal inlets and ebb-tidal delta volumes (as predicted by Eqs. 2 and 3, respectively). Although some of the sand comprising the ebb deltas may have been lost offshore during storms, it is likely that much of the excess sand was driven onshore by the strong wave energy of this region, causing an enlargement of the barriers. Sand moved landward from the nearshore and sediment eroded from entrenching tidal channels in the back-barrier due to the uplift also may have contributed sand to the barriers during this period. Finally, some sand may have moved onshore due to a re-equilibration of the under-steepened shoreface (reverse of "Bruun Rule") caused by the uplift event. This case study demonstrates the interplay among changes in bay hypsometry, tidal prism, and sand reservoirs.

4.7 East Friesian Islands, Germany

The East Frisian Islands provide another opportunity to observe how tidal prism changes impact coastal sand reservoirs, again through observing barrier island growth associated with reductions in back-barrier open-water area. This chain consists of seven barrier islands located in the southeast North Sea between the Ems River to the west and Jade Bay to the east (Fig. 20). This coast is subjected to strong,

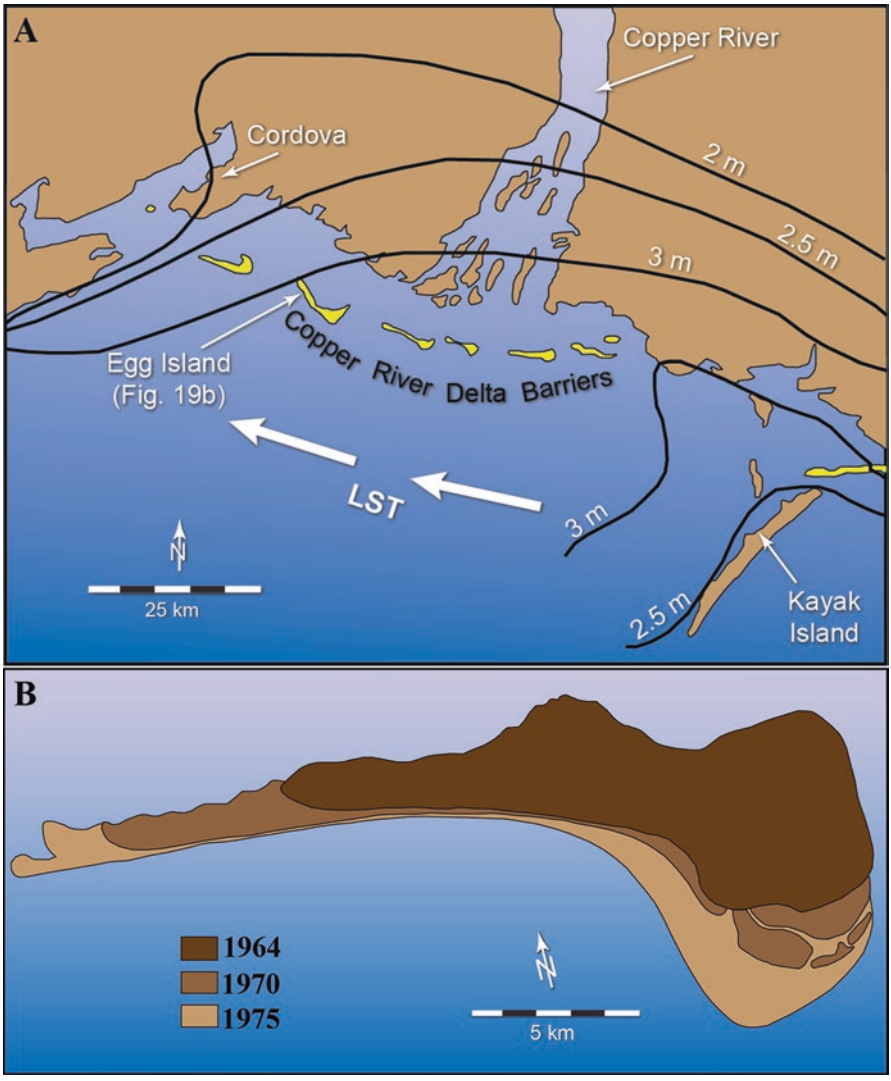

Fig. 19 (**a**) Contour map showing uplift along the Copper River Delta resulting from the Good Friday Earthquake of March 27, 1964 (after Plafker 1969). (**b**) Egg Island (see location in panel above) illustrating accretionary history following the Good Friday Earthquake. The continued increase in areal extent of the island was due to sand moving onshore from the nearshore and ebb-tidal delta (after Hayes and Ruby 1994)

persistent winds from the westerly quadrant that produce a deepwater significant wave height of 1.6 m, resulting in an easterly alongshore transport rate of 2.7×10^5 m^3/year (FitzGerald et al. 1984). Spring tidal ranges increase in an easterly direction from 2.5 m at Borkum to 2.9 m at Wangerooge. The back-barrier is composed of broad tidal flats separated by tidal channels that shoal toward the drainage

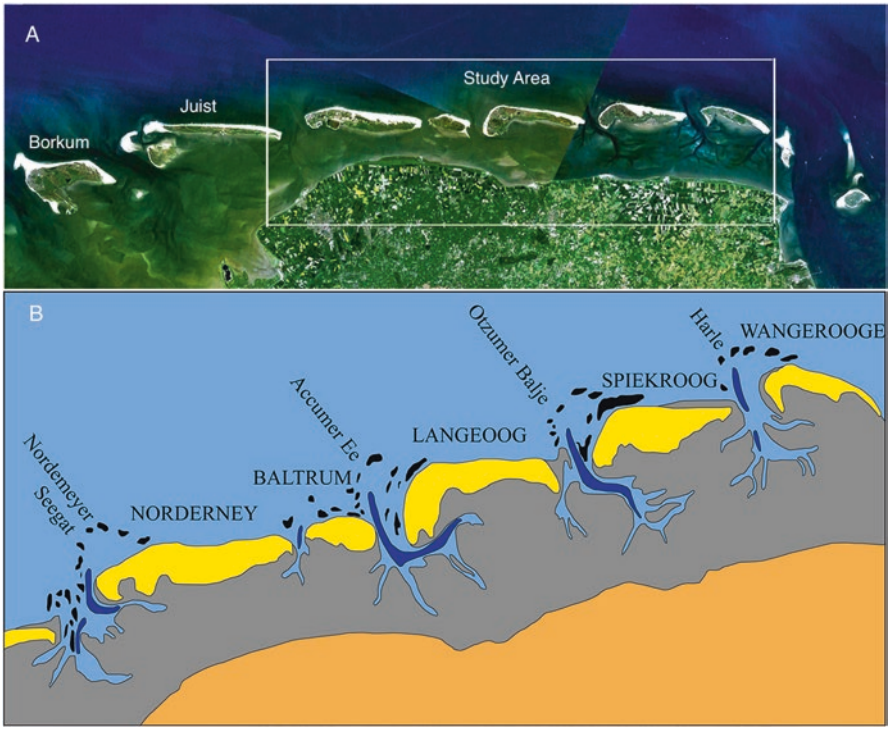

Fig. 20 East Friesian Islands. (**a**) A satellite image showing the extent of the East Friesian Islands along the north coast of Germany. (**b**) Area indicated by *white box* in (**a**), which shows the distribution of barrier islands (*yellow*) tidal inlet thalwegs (*dark blue*), shoals (*black*), back-barrier marsh (*gray*) and mainland (*orange*)

divides behind the middle of the barriers. Inlets vary in width from 0.87 to 3.19 km and are fronted by well-developed ebb-tidal deltas. Sand bypasses the inlets through the landward migration of large swash bars (0.5–1.0 km long), which dictates erosional and accretional patterns along the shore as well as the planform of individual barriers (FitzGerald et al. 1984).

Detailed morphological changes of the East Frisian Islands, tidal inlets, and back-barrier environment for years: 1660, 1750, 1860, and 1960 (Table 3; FitzGerald et al. 1984) were determined using historical maps produced by Homeier and Luck (1969); we did not update these analyses here, because the trends were clearly apparent in the 310-year record. Between 1650 and 1960, an abundant sand supply coupled with the strong easterly alongshore transport system caused extensive spit development at the eastern end of the barriers. During this period, the total length of the barriers increased by 14.1 km, largely at the expense of the inlets, which narrowed by a combined 10.6 km (Table 3, Fig. 21a). The 3.5 km net increase in length of the barrier-inlet system was due to Juist accreting westward and Wangerooge building eastward into Jade Bay (Fig. 20).

Table 3 Summary of morphological changes of East Friesian Islands (after FitzGerald et al. 1984)

Morphological unit	1650	1750	1960	1960	Difference between 1650 and 1960
Total barrier Island length (m)	48,840	52,870	59,830	62,940	+14,100
Total tidal Inlet width (m)	20,360	17,310	11,920	9,740	−10,620
Total barrier Island area (km^2)	52.14	57.91	73.83	93.61	+41.47 (18.07)[a]
Total tidal Inlet drainage area (km^2)	497	433	372	348	−149

[a]This value is the combined area of the barriers minus the polder areas along the backside of the barriers

The historic narrowing of the tidal inlets since 1650 can be explained by a reduction in tidal prism. It was a long-term practice of early inhabitants along the German coast to reclaim land from sea (Goeldner 1999). These parcels, called polders, consist of dikes constructed around former marshland and tidal flats. During the 1650–1960 period, poldering resulted in a 30% decrease in back-barrier drainage areas (Table 3), leading to a reduction in tidal exchange and a decrease in tidal prism. Note in Fig. 21b, the gradual conversion of tidal flat and marsh in the reentrant area behind Harle Inlet that reduced its drainage area and tidal prism, resulting in an eastward progradation of Spiekeroog and a narrowing of the inlet throat.

During the 1650–1960 period, poldering took place along the entire mainland shoreline backing the barriers, as well as the landward side of the barriers. The decrease in drainage area of the inlets and attendant decrease in tidal prism produced smaller equilibrium ebb-tidal delta volumes. Thus, as tidal prism decreased at the inlets, sand from the ebb deltas was moved onshore by the strong wave energy in this location, supplying sediment to the barriers that resulted in spit accretion as well as a collective lengthening of the barriers and an increase in their areal extent. In a regime of accelerating RSLR, if rising tidal waters convert polders back to intertidal flats and marshes, we can expect that the barrier chain will revert to its former morphology due to increasing tidal prism resulting in dramatic erosion (FitzGerald et al. 2008).

5 Runaway Transgression Model

5.1 Presentation of Concept and Stages

Given the prediction of accelerating sea-level rise (IPCC 2013), it appears that marshes (Kirwan et al. 2010) and tidal flats (Dissanayake et al. 2012; Van der Wegen 2013) will ultimately succumb to flooding and will be supplanted by intertidal areas and eventually open water. The history of the Barataria barriers may be a good

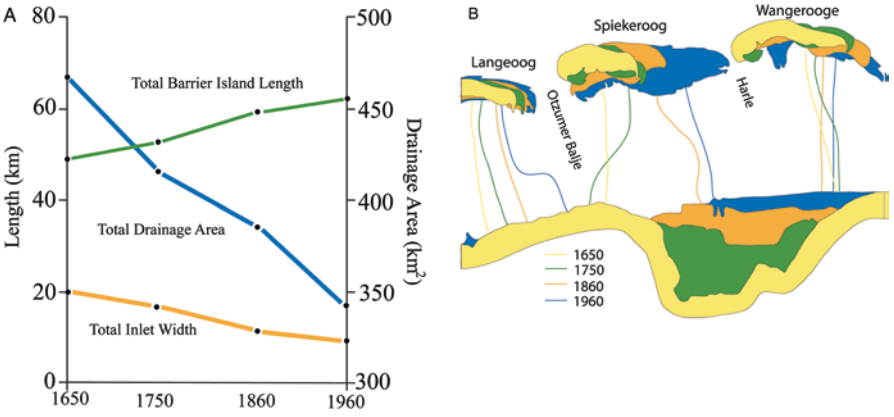

Fig. 21 (**a**) Plot of the historical changes in drainage area, barrier length, and tidal inlet width for the East Friesan Islands (after FitzGerald et al. 1984). As the total drainage area decreased through time as a result of back-barrier poldering, there was a concomitant increase in total barrier length and decrease in total inlet width; a result of the reduced tidal prism created by back-barrier poldering. (**b**) Illustration of changes in morphology and size of the barrier islands and back-barrier drainage area from 1650 to 1960

example of how other barrier coasts will evolve, as this coast has experienced extremely high rates of RSLR, wholesale loss of wetlands, expanding tidal inlets and ebb deltas, and rapid deterioration of the barriers in a timeframe of approximately 150 years. We present below (and in Fig. 22) a conceptual model of how mixed-energy barrier coasts may evolve in a regime of accelerated RSLR from a stable barrier through three progressive stages of barrier disintegration.

5.1.1 Stable Barrier

Accretion rates suggest that many marshes and mangroves are relatively stable and keeping pace with the present trend of eustatic sea-level rise (FitzGerald et al. 2007). Thus, we use the present general configuration of mixed-energy regimes (Hayes 1979) as the initial phase in the conceptual model. This morphology consists of a barrier chain backed by expansive high tide or supratidal marsh incised by numerous tidal creeks, though the extent of intertidal and subtidal environments in the back-barrier varies substantially in mixed energy settings. For example, the Virginia barrier coast exhibits considerable variability along the entire chain, and tidal flats, instead of marshes, occupy the back-barriers of the Copper River delta barriers and Friesian Islands. Inlets along mixed-energy coasts are fronted by well-developed ebb-tidal deltas, although their intertidal exposure varies greatly depending upon tidal range, inner-shelf slope, wave energy, and other factors (Smith and FitzGerald 1994).

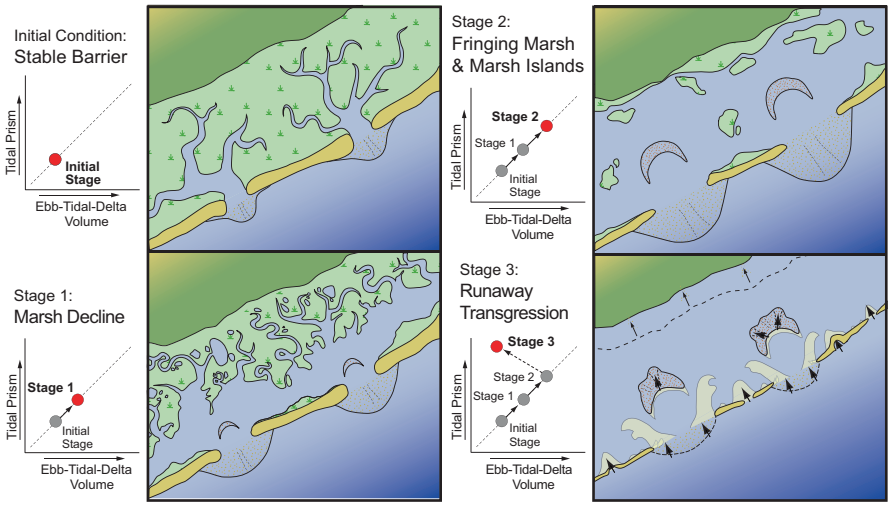

Fig. 22 Conceptual model of barrier evolution on a mixed-energy coast in a regime of accelerated SLR (after FitzGerald et al. 2008)

5.1.2 Disintegrating Barrier

In this conceptual model, marsh loss triggers barrier disintegration, which proceeds through three stages:

Stage 1. High Marsh Loss—This stage of the model represents a period when the rate of RSLR has accelerated sufficiently to transform portions of the supratidal and high-tide marsh to intertidal and subtidal environments, including low marsh. Similarly, this stage also includes the drowning of back-barrier tidal flats such as those that currently exist along the Copper River Delta barrier chain, the East and West Friesian Islands, and contained within Willipa Bay (Mariotti and Fagherazzi 2013) and Grays Harbor barrier system in southern Washington. The resulting increase in tidal discharge strengthens tidal flow at the inlet, leading to scouring of tidal creeks and an enlargement of the main inlet channel. Increasing tidal prism causes a growth in the equilibrium volume of the ebb-tidal delta. The expansion of open water landward of the inlet creates accommodation space, leading to the formation of new flood-tidal deltas and growth of existing deltas and shoals. Sand sequestered on the ebb delta is sourced partially from sediment eroded from back-barrier tidal creeks and at the inlet as these channels enlarge in response to increasing tidal flow. However, most of the sediment transferred to the ebb-tidal delta, and moved landward into the bay leading to enlargement of flood deltas, is captured from the sand transported to the inlet via the alongshore transport system (see Barataria Barriers, Figs. 13a and 14). Tidal inlet capture of sand and growth of ebb and flood deltas is demonstrated well at the Nauset Spit-New Inlet system on Cape Cod (Fig. 7) and at Ocean City Inlet-Assateague Island in Virginia (Fig. 8). In this location, growth of tidal deltas occurs because

of the establishment of tidal discharge at a new inlet, but is comparable to an inlet where wetland loss causes an increase in tidal prism, thereby increasing tidal discharge.

Stage 2. Fringing Marsh and Marsh Islands—By Stage 2 most of the marsh has been converted to open water and intertidal environments. In addition, encroaching tidal waters flood portions of the mainland, and subtidal and intertidal environments comprise most of the back-barrier. Increasing tidal prism continues to enlarge the size of the tidal inlets and increase the volume of sand contained in ebb-tidal deltas. Changes in the dimensions of the inlet channel, combined with alterations in back-barrier hypsometry, produce a tidal regime that favors flood dominance of tidal currents in the inlet channel leading to the landward transport of sand. The work of Mota Oliveira (1970), Boon and Byrne (1981), Aubrey and Speer (1985), and Dronkers (1988) demonstrates that as a back-barrier is transformed from marsh and tidal creeks to an open-water basin with deep-water connectivity to the ocean, the hydraulics of the inlet change from dominance by ebb currents and natural sand flushing to dominance by flood tidal currents and landward bedload transport (e.g., Wadden Sea inlets; Van Goor et al. 2003). Thus, during this stage, flood-tidal deltas and other back-barrier shoals grow in size as sand is siphoned from the littoral system, further depleting sand nourishment to adjacent barrier shorelines. At the end of Stage 2, thinning barriers occasionally breach and ephemeral and permanent tidal inlets form. This scenario has occurred at Grand Terre, along the Barataria system in LA (Fig. 13).

Stage 3. Runaway Transgression—Stage 3 occurs after the barriers have been starved of sediment and undergone long-term erosion such that many new tidal inlets have developed. During this stage, moderate to large storms move sand landward by overwash (see Rodriguez et al. this volume; Odezulu et al. this volume), enlarge flood deltas, and extend or form recurved spits (e.g., southern Chandeleurs, Fig 15; Isle Dernieres, Fig. 16). Barriers denude and narrow in place before barrier sand begins moving onshore as a discrete sediment packet. Sand shoals and vestiges of marsh may act as stabilization points where landward migrating barriers may re-establish; indeed recent modeling studies demonstrate the role played by marsh immediately backing a barrier in the stability of the barrier-marsh system (Walters et al. 2014). Marshes have served this purpose along sections of the Chandeleurs and Isle Dernieres (Figs. 15 and 16). During this stage, multiple new tidal inlets along the barrier chain (e.g., Mallinson et al. this volume) effectively reduce tidal prisms at many of the formerly large inlets causing the partial collapse of these ebb-tidal deltas onshore, providing a temporary source of sand for the ephemeral barriers. A different evolutionary tract is illustrated along the Virginia barriers where a system-wide back-barrier conversion of wetland to open water has been compensated by barrier rollover, thereby reducing bay area at approximately the same rate as it is being created (Deaton et al. 2017; Fig. 10). This evolution has led to near-constant system-wide inlet tidal prisms.

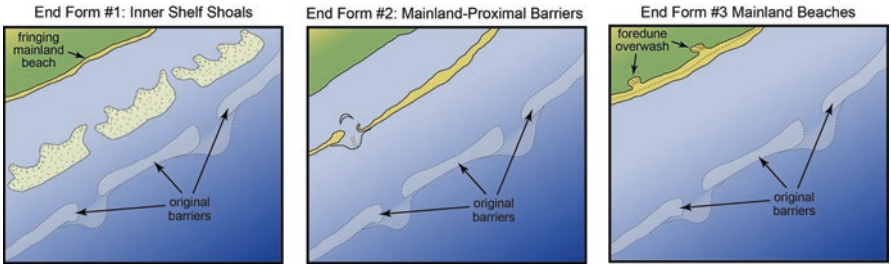

Fig. 23 Possible barrier end forms of a transgressive barrier evolutionary scheme

5.2 Final Disposition of Barrier Sand

Once the barrier system becomes fully transgressive and is migrating across the back-barrier bay, the ultimate fate of the sand comprising the barrier chains depends on the trend of RSLR, existing sand volumes, efficiency of coastal processes in recycling sand from collapsed ebb-tidal deltas, extent of wetlands/tidal flat, accommodation space of the bay (depth) across which barriers transgress, and intensity and frequency of major storms. The variety of forms that resulting sand bodies can take range from inner-shelf shoals, to barriers with narrow lagoons, or mainland beaches (Fig. 23).

At the most extreme, inner-shelf shoals provide examples of barriers reworking and overstepping (drowning) by rising sea level (Fig. 23a) (see chapter by Mellett and Plater this volume). For example, Ship Shoal is located in 10 m of water, 20 km offshore of the Isles Dernieres on the central Louisiana inner shelf (Penland et al. 1989). It is 50 km long, 8–10 km wide, and 4–6 m thick. The shoal crest, which reaches to within 3–8 m of the water surface, is slightly asymmetric in cross section and appears to be migrating very slowly onshore (Penland et al. 1988). Proximal Trinity Shoal demonstrates a similar pattern of behavior. Conditions promoting the development of inner shelf shoals from landward migrating barrier systems include: (1) high rates of RSLR, where subsidence and erosion of back-barrier wetlands (e.g., Louisiana delta plain) lead to significant deepening of the bay and (2) insufficient sand available to fill the back-barrier accommodation space. The southern Chandeluer Islands are a present-day example of a location where this process is ongoing (see also Odezulu et al. this volume).

A second possible scenario for barrier evolution involves the formation of a barrier close to the mainland with a narrow lagoon (Fig. 23b). The Virginia barrier islands, most of which have been migrating landward throughout historic time and appear to be maintaining a system-wide consistent tidal prism through time via a combination of island migration, back-barrier marsh loss, and very slow upland marsh migration (Deaton et al. 2017), provide an example of how barrier island migration can counter effects of back-barrier marsh loss. Elsewhere, this process may occur through complete barrier disintegration and re-formation in a landward position. In this latter scenario, barrier washover sand, including flood-tidal delta

and inner-bay shoal deposits, would be transported onshore as subtidal to intertidal sand sheets that would stabilize after reaching a critical depth, bathymetric high, or subaerial landform. The barrier system would re-form in a state of at least short-term equilibrium with its new, smaller tidal prism. Wave action would feed new sand to the system, as well as elongate the barrier parallel to shore. Although there are several important dissimilarities, the drumlin coast of the Eastern Shore of Nova Scotia is a region where such serial destructive and constructive phases of barrier evolution have been documented (Boyd et al. 1987). Researchers studying this coast describe the formation of barrier spits and nourishment by eroding drumlins until the glacial sediment is exhausted and the subsequent loss of sediment by washover and alongshore transport which produce a landward-migrating sand sheet. The mostly subtidal sand sheet moves onshore and stabilizes at a landward drumlin-anchoring site where a new barrier spit is established (Boyd et al. 1987). These studies provide evidence to suggest that the presence of sand shoals can lead to reestablishment of barriers. Barrier reestablishment could also be a product of a deceleration of sea-level rise, under conditions similar to the Late Holocene sea-level deceleration that is tied to the formation of many barrier systems throughout the world (Hein et al. 2014b; Frueergaard et al. 2015).

A final possible evolutionary scenario is the formation of mainland beaches (Fig. 23c). In this model, it is assumed that most of the sediment comprising the transgressing barrier is left on the inner shelf or in partially infilled former back-barrier bays (now exposed on the ocean side of beaches), but a limited amount of sand is transported across the entire bay to the mainland. Such a scenario is a long-term (century or longer) possibility for rapidly migrating barriers along parts of the Virginia coast. Modern examples of such mainland beaches are found in a 46-km stretch of shoreline along Myrtle Beach, South Carolina—the only interruption in the barrier island system that extend from North Carolina to Winyah Bay in South Carolina. The shoreline here is perched on limestone and there is much less sand contained in the nearshore with no rivers feeding into this region since the late Pleistocene (Barnhardt 2009). The offshore of this region is somewhat steeper than areas to the northeast and southwest, which may also explain why mainland beaches have formed here preferentially (Wolinsky and Murray 2009; Murray and Moore this volume). This site may be an example of where barrier sand has been transported onshore during the late Holocene.

6 Summary and Conclusions

Research to date suggests that barrier chains worldwide will undergo significant erosion and deterioration due to the forecasted acceleration in sea-level rise and the ensuing transfer of sand from barrier lithosomes to ebb-tidal deltas and into back-barrier bays. RSLR will deepen back-barrier wetlands eventually converting then to open water and will drown tidal flats, producing larger tidal prisms.

Changes in basin hypsometry will lead to flood-tidal dominance or an increase in flood-tidal dominance in the inlet channel. Major exceptions to this scenario include the Copper River delta barriers where tectonics produced uplift, decreasing the amount of open water, and the East Friesian Islands, where poldering has created the same effect. If the gains in supra and intertidal areas at these two systems were to be reversed to their former condition, then future barrier loss would likely occur. An interesting case occurs along the Virginia barrier coast where deteriorating wetlands have not led to larger tidal prisms, and greater sequestration of sand on ebb-tidal deltas. Rather, wetland loss and increase in open water have been balanced system-wide by a landward migration of the barrier system primarily through overwash.

One of the major unknowns concerning the evolution of barrier coasts is how quickly thresholds for marsh drowning or marsh deterioration will be reached. It is assumed that marshes receiving less inorganic sediment will reach a tipping point before marshes receiving higher suspended sediment loads. For example, barriers in the US northeast will likely undergo a faster rate of geomorphic change (high marsh to low marsh; low marsh to tidal flat) than those along the southeastern US. This is because northeastern marshes receive very low suspended loads from the coastal ocean compared to the southeastern marshes due to the very low suspended loads discharged by the major northeast rivers (Meade 1969). If marsh models are to realistically project future evolutionary changes, they will require detailed data on sediment delivery to marsh platforms and knowledge of how marsh platforms will accommodate and respond to increasing inundation and tidal prism.

To fully understand the fate of barriers, we need to quantify the long-term sand losses to the offshore, back-barrier (via overwash), ephemeral inlets, and alongshore as a result of RSLR, storms, and human activities. Additionally, we need to determine how much sand will be transferred from the barriers to ebb- and flood-tidal deltas to equilibrate the volume increases caused by enlarging tidal prisms and changes in basinal hypsometry during different stages of marsh loss/tidal flat drowning. To determine the impact of these sand losses, they need to be compared to the volumes of sand contained in the adjacent barrier lithosomes. However, this is not an easy task because of the large range in the size and sand volume of barriers throughout the world and the fact that barrier lithosomes vary considerably along their length due to changes in width, elevation, and depth (Table 1). This research, combined with a better understanding of how marsh systems will evolve, is required before accurate predictions of the impact of RSLR on long-term erosional trends and the longevity of barrier systems can be made.

Acknowledgements The authors would like to thank the many graduate students whose research helped develop the ideas presented in this chapter. The paper has been substantively improved with suggestions and editorial comments by Andrew Ashton, Laura Moore, Brad Murray, and one anonymous reviewer.

References

Ashton AD, Lorenzo-Trueba J (2018) Morphodynamics of barrier response to sea-level rise. In: Moore LJ, Murray AB (eds) Barrier dynamics and response to changing climate. Springer, New York

Aubrey D, Speer P (1985) A study of non-linear tidal propagation in shallow inlet/estuarine system. In: Aubrey D, Weishar L (eds) Estuarine, coastal and shelf science, vol 21, pp 185–205

Barnhardt W (ed) (2009) Coastal change along the shore of northeastern South Carolina—the South Carolina coastal erosion study: U.S. Geological Survey Circular 1339:77

Barras J (2006) Land area change in coastal Louisiana after the 2005 hurricanes—a series of three maps: U.S. Geological Survey Open-File Report 2006-1274. http://pubs.usgs.gov/of/2006/1274/

Barras J, Bourgeois P, Handley L (1994) Land loss in coastal Louisiana 1956-90. National Biological Survey, National Wetlands Research Center Open File Report 94:4

Beets D, van der Valk L, Stive M (1992) Holocene evolution of the coast of Holland. Mar Geol 103:423–443

Belliard J et al (2015) An ecogeomorphic model of tidal channel initiation and elaboration in progressive marsh accretion contexts. J Geophys Res 120:1040–1064

Bird E (1985) Coastline changes. A global review. Wiley, New York

Boon J (2012) Evidence of sea level acceleration at U.S. and Canada Tide Stations, Atlantic Coast, North America. J Coast Res 28:1437–1445

Boon J, Byrne R (1981) On basin hypsometry and the morphodynamic response of coastal inlet systems. Mar Geol 40:27–48

Boon JD, Mitchell M (2015) Nonlinear change in sea level observed at North American tide stations. J Coast Res 31(6):1295–1305. https://doi.org/10.2112/JCOASTRES-D-15-00041.1

Boyd R, Penland S (1981) Washover of deltaic barriers on the Louisiana coast. Trans Gulf Coast Assoc Geol Soc 31:243–248

Boyd R, Bowen A, Hall R (1987) Evolutionary model for transgressive sedimentation on the eastern shore of Nova Scotia. Glaciated coasts. Academic Press Inc., New York, pp 87–114

Brinson MM, Christian RR, Blum LK (1995) Multiple states in the sea-level induced transition from terrestrial forest to estuary. Estuaries 18:648–659

Bruun P (1988) The Bruun rule of erosion by sea-level rise: a discussion on large-scale two- and three-dimensional usages. J Coast Res 4:627–648

Cahoon D, Reed D (1995) Relationships among marsh surface topography, hydro-period, and soil accretion in a deteriorating Louisiana salt marsh. J Coast Res 11:357–369

Cherry JA, McKee KL, Grace JB (2009) Elevated CO2 enhances biological contributions to elevation change in coastal wetlands by offsetting stressors associated with sea-level rise. J Ecol 97:67–77

Chmura G et al (2003) Global carbon sequestration in tidal, saline wetland soils. Glob Biogeochem Cycles 17

Christiansen T, Wiberg P, Milligan T (2000) Flow and sediment transport on a tidal salt marsh surface. Estuar Coast Shelf Sci 50:315–331

Church JA, Clark PU, Cazenave A, Gregory JM, Jevrejeva S, Levermann A, Merrifield MA, Milne GA, Nerem RS, Nunn PD, Payne AJ, Pfeffer WT, Stammer D, Unnikrishnan AS (2013) Sea level change. In: Stocker TF, Qin D, Plattner G-K, Tignor M, Allen SK, Boschung J, Nauels A, Xia Y, Bex V, Midgley PM (eds) Climate change 2013: the physical science basis. Contribution of working group I to the fifth assessment report of the intergovernmental panel on climate change. Cambridge University Press, Cambridge and New York

Coleman J, Roberts H, Stone G (1998) Mississippi river delta: an overview. J Coast Res 14:698–716

Cooper J, Pilkey O (2004) Sea-level rise and shoreline retreat: time to abandon the Bruun rule. Glob Planet Change 43:157–171

Cooper J et al (1990) Ephemeral stream mouth bars at flood-breach river mouths: comparison with tidal deltas at barrier inlets. Mar Geol 95:57–70
Couvillion B et al (2011) Land area change in coastal Louisiana from 1932 to 2010: U.S. Geological Survey Scientific Investigations Map 3164, scale 1:265,000, 12 p. pamphlet
Cowell PJ, Kinsela MA (2018) Shoreface controls on barrier evolution and shoreline change. In: Moore LJ, Murray AB (eds) Barrier dynamics and response to changing climate. Springer, New York
D'Alpaos A, Lanzoni S, Marani M, Rinaldo A (2007) Landscape evolution in tidal embayments: modeling the interplay of erosion sedimentation and vegetation dynamics. J Geophys Res 112(1)
Dalrymple R, Zaitlin B, Boyd R (1992) Estuarine facies models: conceptual basis and stratigraphic implications: perspective. J Sediment Petrol 62:1130–1146
Darby FA, Turner RE (2008) Below- and aboveground biomass of Spartina alterniflora: response to nutrient addition in a Louisiana Salt Marsh. Estuar Coasts 31:326–334
Davis R, Hayes M (1984) What is a wave dominated coast? Mar Geol 60:313–329
De Vriend H et al (1993) Approaches to long-term modeling of coastal morphology: a review. Coast Eng 21:225–269
Dean R, Perlin M (1977) Coastal engineering study of Ocean City Inlet, Maryland. In: Proceedings, coastal sediments 1977, American Society of Civil Engineers, pp 520–540
Deaton CD, Hein CJ, Kirwan ML (2017) Barrier-island migration dominates ecogeomorphic feedbacks and drives salt marsh loss along the Virginia Atlantic Coast, USA. Geology 45:123–126
Dingler J, Clifton H (1994) Barrier systems of California, Oregon, and Washington. In: Davis R (ed) Geology of Holocene barrier island systems. Springer, Berlin, pp 115–165
Dissanayake D, Ranasinghe R, Roelvink J (2012) The morphological response of large tidal inlet/basin systems to relative sea level rise. Clim Change 113:253–276
Donnelly J et al (2004) Coupling instrumental and geological records of sea-level change: evidence from southern New England of and increase in the rate of sea-level rise in the late 19th century. Geophys Res Lett 31. https://doi.org/10.1029/2003GL018933
Doran K et al (2013) National assessment of hurricane-induced coastal erosion hazards: Mid-Atlantic Coast: U.S. Geological Survey Open-File Report 2013–1131, 28 p
Dronkers J (1988) Inshore/offshore water exchange in shallow coastal systems. Coast Offshore Ecosyst Interact 22:3–39
Dronkers J (1998) Morphodynamics of the Dutch delta. Phys Estuar Coast Seas 297–304
Eiser W, Kjerfve B (1986) Marsh topography and hypsometric characteristics of a South Carolina salt marsh basin. Estuar Coast Shelf Sci 23:595–605
Erwin R, Sanders G, Prosser D (2004) Changes in lagoonal marsh morphology at selected northeastern Atlantic coast sites of significance to migratory waterbirds. Wetlands 24:891–903
Erwin R et al (2006) Surface elevation dynamics in vegetated Spartina marshes versus unvegetated tidal ponds along the Mid- Atlantic Coast, USA, with implications to waterbirds. Estuar Coast 29:96–106
Escoffier F (1940) The stability of tidal inlets. Shore Beach 8:114–115
Escoffier F (1977) Hydraulics and stability of tidal inlets. U.S. Army Corps of Engineers, Coastal 75
Ezer T, Corlett W (2012) Is sea level rise accelerating in the Chesapeake Bay? A demonstration of a novel new approach for analyzing sea level data. Geophys Res Lett 39. https://doi.org/10.1029/2012GL053435
Fagherazzi S, Priestas A (2010) Sediments and water fluxes in a muddy coastline: interplay between waves and tidal channel hydrodynamics. Earth Surf Process Landform 35:284–293
Fagherazzi S et al (2012) Numerical models of salt marsh evolution: ecological, geomorphic, and climatic factors. Rev Geophys 50
Feagin R et al (2009) Does vegetation prevent wave erosion of salt marsh edges? Proc Natl Acad Sci U S A 106:10109–10113
Fearnley S et al (2009) Hurricane impact and recovery shoreline change analysis of the Chandeleur Islands, Louisiana, USA: 1855 to 2005. Geo-Mar Lett 29:445–466

Fenster MS, FitzGerald DM, Kelley JT, Belknap DF, Buynevich IV, Dickson SM (2001) Net ebb sediment transport in a rock-bound, mesotidal estuary during spring-freshet conditions: Kennebec River Estuary, Maine. Geol Soc Am Bull 113:1522–1531

Fenster MS, McBride RA, Trembanis A, Richardson T, Nebel SH (2011) A field test of the theoretical evolution of a mixed-energy barrier coast to a regime of accelerated sea-level rise. The proceedings of the coastal sediments 2011, American Association of Civil Engineers, Miami, FL, pp 216–229

Ferrians O (1966) Effects of the earthquake of March 27, 1964, in the Copper River basin area, Alaska. U.S. Geological Survey Professional Paper 543-E 28

Field M, Roy P (1984) Offshore transport and sand-body formation: evidence from a steep, high-energy shoreface, Southeastern Australia. J Sediment Res 54:1292–1302

FitzGerald D, Montello T (1993) Back-barrier and inlet sediment response to the breaching of Nauset Spit and formation of New Inlet, Cape Cod, Massachusetts. From: coastal and estuarine studies. American Geophysical Union, Washington, DC

FitzGerald D, Pendelton E (2002) Inlet formation and evolution of the sediment bypassing system: New Inlet, Cape Cod, Massachusetts. J Coast Res 36:290–299

FitzGerald D, Penland S, Nummedal D (1984) Control of barrier island shape by inlet sediment bypassing: East Frisian Islands, West Germany. Mar Geol 60:355–376

FitzGerald D et al (2004) Morphologic and stratigraphic evolution of muddy ebb-tidal deltas along a subsiding coast: Barataria Bay, Mississippi River delta. Sedimentology 51:1157–1178

FitzGerald D et al (2005) Coarse-grained sediment transport in Northern New England Estuaries: a synthesis. Coast Syst Cont Margin 8:195–213

FitzGerald D et al (2007) Impacts of rising sea level to back-barrier Wetlands, Tidal Inlets, and Barrier Islands: Barataria Coast, Louisiana. Coast Sediment 7:1179–1192

FitzGerald D et al (2008) Coastal impacts due to sea-level rise. Annu Rev Earth Planet Sci 36:601–647

FitzGerald D, Buynevich I, Hein C (2012) Morphodynamics and facies architecture of tidal inlets and tidal deltas. In: Davis R, Dalrymple R (eds) Principles of tidal sedimentology. Springer, New York, pp 301–333

Fontolan G et al (2007) Sediment storage at tidal inlets in Northern Adriatic Lagoons: ebb-tidal delta morphodynamics, conservation and sand use strategies. Estuar Coast Shelf Sci 75:261–277

Frazier D (1967) Recent deltaic deposits of the Mississippi River; their development and chronology. Gulf Coast Assoc Geol Soc Trans 17:287–315

French J, Spencer T (1993) Mar Geol 110:315–331

Friedrichs C et al (1993) Hydrodynamic modeling of a multiple-inlet estuary/barrier system: insight into tidal inlet formation and stability. In: Aubrey D, Giese G (eds) Formation and evolution of multiple tidal inlet systems. American Geophysical Institute, Washington, DC, pp 95–112

Frueergaard M et al (2015) Stratigraphy, evolution, and controls of a Holocene transgressive–regressive barrier island under changing sea level: Danish north sea coast. J Sediment Res 85:820–884

Georgiou I, Schindler J (2009) Wave forecasting and longshore sediment transport gradients along a transgressive barrier island: Chandeleur Islands, Louisiana. Geo-Mar Lett 29:467–476

Gleason M et al (1979) Effects of stem density upon sediment retention by salt marsh cord grass, Spartina alterniflora loisel. Estuar Coast 2:271–273

Goeldner L (1999) The German Wadden sea coast: reclamation and environmental protection. J Coast Conserv 5:23–30

Grinsted A, Moore J, Jevrejeva S (2013) Projected Atlantic hurricane surge thread from rising temperatures. Proc Natl Acad Sci U S A 110:5369–5373

Halsey S (1979) New model of barrier island development. In: Leatherman S (ed) Barrier islands: from the Gulf of St. Lawrence to the Gulf of Mexico. Academic Press, New York, pp 185–210

Hapke C et al (2010a) A review of sediment budget imbalances along Fire Island, New York: can nearshore geologic framework and patterns of shoreline change explain the deficit? J Coast Res 26:510–522
Hapke C et al (2010b) National assessment of shoreline change: historical shoreline change along the New England and Mid-Atlantic coasts: U.S. Geological Survey Open-File Report 2010-1118, 57p
Harris P (1988) Large-scale bedforms as indicators of mutually evasive sand transport and the sequential infilling of wide-mouthed estuaries. Sediment Geol 57:273–298
Hart W, Murray S (1978) Energy balance and wind effects in a shallow sound. J Geophys Res 83:4097–4106
Hayes M (1979) Barrier island morphology as a function of tidal and wave regime. In: Leatherman S (ed) Barrier islands. Academic, New York, pp 1–28
Hayes M (1994) The Georgia bight barrier system. In: Davis R (ed) Geology of Holocene barrier island system. Springer, Berlin, pp 233–304
Hayes M, FitzGerald D (2013) Origin, evolution, and classification of tidal inlets, symposium in applied coastal geomorphology to honor miles O. Hayes. J Coast Res Special Issue 69:14–33
Hayes M, Kana T (1976a) Terrigenous clastic depositional environments: some modern example: a field course. Coastal Research Division, Department of Geology, University of South Carolina. No. 11
Hayes M, Kana T (eds) (1976b) Terrigenous clastic depositional environments. Tech. Rept. No.11-CRD. Coastal Research Division. Dept. Geol., Univ. South Carolina, 306 p
Hayes M, Ruby C (1994) Barriers of Pacific Alaska. In: Davis R (ed) Geology of Holocene barrier island systems. Springer, Berlin, pp 395–433
Hayes M et al (1976) Geomorphology of the Southern Coast of Alaska. Coast Eng Proc 1:15
Hein C et al (2012) Refining the model of barrier island formation along a paraglacial coast in the Gulf of Maine. Mar Geol 307:40–57
Hein C et al (2014a) Evolution of paraglacial coasts in response to changes in fluvial sediment supply. Geol Soc Lond Spec Publ 388:247–280
Hein C et al (2014b) Coastal response to late-stage transgression and sea-level highstand. Geol Soc Am Bull 126:459–480
Hicks D, Hume T (1996) Morphology an size of ebb tidal deltas at natural inlets on open-sea and pocket-bay coasts, North Island, New Zealand. Coast Res 12:47–63
Homeier H, Luck G (1969) Das historische Kartenwerk 1: 50000 der Niedersächsischen Wasserwirtschaftsverwaltung als Ergebnis historisch-topographischer Untersuchungen und Grundlage zur kausalen Deutung hydrologisch-morphologischer Gestaltungsvorgänge im Küstengebiet. Wurm
Hughes Z et al (2009) Rapid headward erosion of marsh creeks in response to relative sea level rise. Geophys Res Lett 36:L03602. https://doi.org/10.1029/2008GL036000
Inman D, Nordstrom C (1971) On the tectonic and morphologic classification of coasts. J Geol 79:1–21
IPCC (2013) Climate change 2013: the physical science basis. Contribution of Working Group I to the Fifth Assessment Report of the IPCC
Jarrett J (1976) Tidal prism-inlet area relationships. GITI Rep. 3, U.S. Army Engineer Waterw. Exp. Stn., Vicksburg, MS
Jevrejeva S, Moore J, Grinsted A (2012) Sea level projections to AD2500 with a new generation of climate change scenarios. Glob Planet Change 80:14–20
Kastler J, and Wiberg P, 1996, Sedimentation and boundary changes of Virginia salt marshes: Estuar Coast Shelf Sci, v. 42, p. 683–700, doi:https://doi.org/10.1006/ecss.1996.0044.
Kindinger J, Buster N, Flocks J, Bernier J, Kulp M (2013) Louisiana barrier island comprehensive monitoring (BICM) program summary report: data and analyses 2006 through 2010: U.S. Geological Survey Open-File Report 2013–1083, 86 p
Kirwan M, Guntenspergen G (2010) Influence of tidal range on the stability of coastal marshland. J Geophys Res 115

Kirwan M, Guntenspergen G (2012) Feedbacks between inundation, root production, and shoot growth in a rapidly submerging brackish marsh. J Ecol 100:764–770
Kirwan M, Megonigal J (2013) Tidal wetland stability in the face of human impacts and sea-level rise. Nature 504:53–60
Kirwan M, Murray A (2007) A coupled geomorphic and ecological model of tidal marsh evolution. Proc Natl Acad Sci U S A 104:6118–6122
Kirwan M, Guntenspergen G, Morris J (2009) Latitudinal trends in *Spartina alterniflora* productivity and the response of coastal marshes to global change. Glob Change Biol 15:1982–1989
Kirwan M et al (2010) Limits on the adaptability of coastal marshes to rising sea level. Geophys Res Lett 37. https://doi.org/10.1029/2010GL045489
Kirwan M et al (2016) Overestimation of marsh vulnerability to sea level rise. Nat Clim Change 6:253–260
Knutson T et al (2010) Tropical cyclones and climate change. Nat Geosci 3:157–163
Kraus NC, Larson ML, Wise RA (1998) Depth of closure in beach-fill design, Coastal Engineering Technical Note. U.S. Army Engineer Waterways Experiment Station, Vicksburg, MS, 13p
Kraus N (2000) Reservoir model of ebb-tidal shoal evolution and sand bypassing. J Waterway Port Coast Ocean Eng 126:305–313
Kulp M, FitzGerald D, Penland S (2005) Sand-rich lithosomes of the Holocene Mississippi River delta plain. In: Giosan L, Bhattacharya J (eds) River deltas-concepts, models, and examples, Society of Economic Mineralogists and Paleontologists Special Publication 83:277–291
Langley A et al (2009) Elevated CO_2 stimulates marsh elevation gain, counterbalancing sea-level rise. Proc Natl Acad Sci U S A 106:6182–6186
Leonard L, Croft A (2006) The effect of standing biomass on flow velocity and turbulence in S*partina alterniflora* canopies. Estuar Coast Shelf Sci 69:325–336
List J et al (1994) Louisiana barrier island erosion study: atlas of seafloor changes from 1878 to 1989. Miscellaneous Investigations Series I-2150-B. US Geological Survey and Louisiana State University, Reston, VA, 81 p
Liu J et al (1993) Morphodynamics evolution of a newly formed tidal inlet. In: Aubrey D, Giese G (eds) Formation and evolution of multiple tidal inlets. American Geophysical Union, Washington, DC. https://doi.org/10.1029/CE044p0062
Louters T, Gerritsen F (1994) The riddle of the sands: a tidal system's answer to a rising sea level. Public works and water management. National Institute for Coastal and Marine Management, The Hague, Netherlands
Lovering J, Adams R (2009) Exploring the interplay of wave climate and terrestrial sediment supply in the geomorphic evolution of sandy coasts with a numerical model. Abstract Presented at the AGU Fall Meeting 1:644
Mallinson D, Culver S, Leorri E, Mitra S, Mulligan R, Riggs S (2018) Barrier island and estuary co-evolution in response to Holocene climate and sea-level change: Pamlico Sound and the Outer Banks Barrier Islands, North Carolina, USA. In: Moore LJ, Murray AB (eds) Barrier dynamics and response to changing climate. Springer, New York
Marani M et al (2011) Understanding and predicting wave erosion of marsh edges. Geophys Res Lett 38
Mariotti G, Carr J (2014) Dual role of slat marsh retreat: long-term loss and short-term resilience. Water Resour Res 50:2963–2974
Mariotti G, Fagherazzi S (2013) Critical width of tidal flats triggers marsh collapse in the absence of sea-level rise. PNAS 110:5353–5356
Mariotti G et al (2010) Influence of storm surges and sea level on shallow tidal basin erosive processes. J Geophys Res 115(C11). https://doi.org/10.1029/2009JC005892
McBride R, Penland S, Hilands M, Williams S, Westphal K, Jaffe B, Sallenger A Jr (1992) Chapter 4: Analysis of barrier shoreline change in Louisiana from 1853 to 1989. In: Williams S, Penland S, Sallenger AH (eds) Atlas of shoreline changes in Louisiana from 1853 to 1989, USGS Miscellaneous Investigations Series I-2150-A, 108 p

McBride R, Fenster M, Seminack C, Richardson T, Sepanik J, Hanley J, Bundick J, Tedder E (2015) Holocene barrier-island geology and morphodynamics of the Maryland and Virginia open-ocean coasts: Fenwick, Assateague, Chincoteague, Wallops, Cedar, and Parramore Islands. Field Excursions for the GSA Annual Meeting, Baltimore, 2015: GSA Field Guide 40, pp 392–401. https://doi.org/10.1130/2015.0040(10)

McGee W (1890) Encroachments of the sea. The Forum 9:437–449

Meade R (1969) Landward transport of bottom sediments in estuaries of the Atlantic Coastal Plain. J Sedim Petrol 39:222–234

Mellett CL, Plater AJ (2018) Drowned barriers as archives of coastal-response to sea-level rise. In: Moore LJ, Murray AB (eds) Barrier dynamics and response to changing climate. Springer, New York

Miner M et al (2009a) Chapter D. Historical (1869-2007) sea floor evolution and sediment dynamics along the Chandeleur Islands. In: Lavoie D (ed) Sand resources, regional geology, and coastal processes of the Chandeleur Islands coastal system—an evaluation of the Breton National Wildlife Refuge. U.S. Geological Survey Scientific Investigations Report 47-74

Miner M et al (2009b) Hurricane-associated ebb-tidal delta sediment dynamics. Geology 37:851–854

Mitrovica J, Milne G (2002) On the origin of late Holocene sea-level highstands within equatorial ocean basins. Quat Sci Rev 21:2179–2190

Moore LJ, List JH, Williams SJ, Stolper D (2010) Complexities in barrier island response to sea-level rise: insights from model experiments. J Geophys Res Earth Surf. https://doi.org/10.1029/2009JF001299

Moore LJ, Goldstein EB, Vinent OD, Walters D, Kirwan M, Lauzon R, Murray AB, Ruggiero P (2018) The role of ecomorphodynamic feedbacks and landscape couplings in influencing the response of barriers to changing climate. In: Moore LJ, Murray AB (eds) Barrier dynamics and response to changing climate. Springer, New York

Morris J et al (2002) Responses of coastal wetlands to rising sea level. Ecology 83:2869–2877

Morton R (2003) Morphological impacts of extreme storms on sandy beaches and barriers. J Coast Res 19:560–573

Morton R (2008) Historical changes in the Mississippi-Alabama barrier-island chain and the roles of extreme storms, sea level, and human activities. J Coast Res 24:1587–1600

Morton RA, Bernier JC, Barras JA, Ferina NF (2005) Rapid subsidence and historical wetland loss in the south-central Mississippi delta plain: likely causes and future implications. U.S. Geological Survey Open-file Report 2005–1216. http://www.pubs.usgs.gov/of/2005/1216

Morton R, Bernier JC, Barras JA (2006) Evidence of regional subsidence and associated interior wetland loss induced by hydrocarbon production, Gulf Coast region, USA. Environ Geol 50:261–274

Mota Oliveira I (1970) Natural flushing ability in tidal inlets. In: Am. Soc. Civ. Eng., Proc. 12th Coastal Eng. Conf., Washington, DC, pp 1827–1845

Mudd S et al (2004) Flow, sedimentation, and biomass production on a vegetated salt marsh in South Carolina: toward a predictive model of marsh morphologic and ecologic evolution. Ecogeomorphol Tidal Marshes Coast Estuar Stud 59:165–187

Mudd S, D'Alpaos A, Morris J (2010) How does vegetation affect sedimentation on tidal marshes? Investigating particle capture and hydrodynamic controls on biologically mediated sedimentation. J Geophys Res 115

Muller R, Stone G (2001) A climatology of tropical storm and hurricane strikes to enhance vulnerability prediction for the Southeast U.S. Coast. J Coast Res 17:949–956

Murray AB, Moore LJ (2018) Geometric constraints on long-term barrier migration: from simple to surprising. In: Moore LJ, Murray AB (eds) Barrier dynamics and response to changing climate. Springer, New York

National Research Council (1972) Committee on the Alaska Earthquake of the Division of Earth Sciences, 1972. The Great Alaska Earthquake of 1964: oceanography and coastal engineering. National Academy of Sciences, Washington, DC

Neubauer S (2008) Contributions of mineral and organic components to tidal freshwater marsh accretion. Estuar Coast Shelf Sci 78:78–88
Nicholls R et al (2007) Coastal systems and low-lying areas. Climate change 2007: impacts, adaptation and vulnerability. Contribution of Working Group II to the Fourth Assessment Report of the Intergovernmental Panel on Climate Change, Parry M, et al. Cambridge University Press, Cambridge, UK, pp 315–356
Niedoroda A, Swift D (1981) Maintenance of the shoreface by wave orbital currents and mean floe: observations from the long island coast. Geophys Res Lett 8:337–340
NOAA (2015a) http://tidesandcurrents.noaa.gov/sltrends/sltrends_station.shtml?stnid=8761724
NOAA (2015b) http://www.ndbc.noaa.gov/station_history.php?station=46001
Nummedal D, Stephen M (1976) Coastal dynamics and sediment transportation, Northeast Gulf of Alaska. Geology 12
Nyman JA, Carloss M, DeLaune RD, Patrick WH Jr (1994) Erosion rather than plant dieback as the mechanism of marsh loss in an estuarine marsh. Earth Surf Process Landf 19:69–84
O'Brien M (1931) Estuary tidal prisms related to entrance areas. Civil Eng 1:738–739
Odezulu CI, Lorenzo-Trueba J, Wallace DJ, Anderson JB (2018) Follets Island: a case of unprecedented change and transition from rollover to subaqueous shoals. In: Moore LJ, Murray AB (eds) Barrier dynamics and response to changing climate. Springer, New York
Oertel G, Kraft J (1994) New Jersey and Delmarva barrier islands. In: Davis R (ed) Geology of Holocene barrier island systems. Springer, Berlin, pp 207–232
Ortiz AC, Roy S, Edmonds DA (2017) Land loss by pond expansion on the Mississippi River Delta Plain. Geophys Res Lett 44:3635–3642. https://doi.org/10.1002/2017GL073079
Palmer M et al (2004) Observations of particle capture on a cylindrical collector: implications for particle accumulation and removal in aquatic systems. Limnol Oceanogr 49:76–85
Penland S, Boyd R, Suter J (1988) Transgressive depositional systems of the Mississippi Delta Plain: a model for barrier shoreline and shelf sand development. J Sediment Petrol 58:932–949
Penland S et al (1989) Holocene sand shoals offshore of the Mississippi River Delta plain. Gulf Coast Assoc Geol Soc Trans 39:471–480
Penland S, Ramsey KE (1990) Relative sea-level rise in Louisiana and the Gulf of Mexico. J Coast Res 2:323–342
Plafker G (1969) Tectonics of the March 27, 1964 Alaska Earthquake. U.S. Geological Survey Professional Paper 543:74
Priestas AM, Mariotti G, Leonardi N, Fagherazzi S (2015) Coupled wave energy and erosion dynamics along a salt marsh boundary, Hog Island Bay, Virginia, USA. J Mar Sci Eng 3:1041–1065. https://doi.org/10.3390/jmse3031041
Proosdij V, Davidson-Arnott R, Ollerhead J (2006) Controls on spatial patterns of sediment deposition across a macro-tidal salt marsh surface over single tidal cycles. Estuar Coast Shelf Sci 69:64–86
Redfield A, Rubin M (1962) Age of salt marsh peat in relation to recent changes in sea level. Science 136:328
Reimnitz E (1966) Late Quaternary history and sedimentation of the Copper River Delta and Vicinity, Alaska. Thesis, Scripps Institute of Oceanography, La Jolla, California. Unpublished
Reimnitz E, Marshall N (1965) Effects of the Alaska Earthquake and Tsunami on recent deltaic sediments. J Geophys Res 70:2363–2376
Rice T, Niedoroda A, Pratt A (1976) The coastal processes and geology: Virginia Barrier Islands. Virginia coast reserve study: ecosystem description 117–388
Richards (1934) The salt marshes of the Dovey Estuary. Ann Bot 1:225–259
Richardson T (2012) Morphodynamic changes of the Parramore-Cedar barrier island system and Wachapreague Inlet, Virginia from 1852 to 2011: a model of barrier island and tidal inlet evolution along the southern Delmarva Peninsula, USA. Ph.D. thesis. Fairfax, George Mason University, 306 p
Rieu R, van Heteren S, Van Der Spek AJ, De Boer PL (2005) Development and preservation of a mid-Holocene tidal-channel network offshore the Western Netherlands. J Sediment Geol 75:409–419

Roberts H (1997) Dynamic changes of the Holocene Mississippi river delta plain: the delta cycle. J Coast Res 13:605–637

Rodriguez AB, Yu W, Theuerkauf EJ (2018) Abrupt increase in washover deposition along a transgressive barrier island during the late nineteenth century acceleration in sea-level rise. In: Moore LJ, Murray AB (eds) Barrier dynamics and response to changing climate. Springer, New York

Roos PC, Schuttelaars HM, Brouwer RL (2013) Observations of barrier island length explained using an exploratory morphodynamic model. Geophys Res Lett 40:4338–4343. https://doi.org/10.1002/grl.50843

Rosati J, Ebersole B (1996) Littoral impact of Ocean City Inlet, Maryland, USA. Coast Eng Proc 1:25

Rosati J, Dean R, Stone G (2010) A cross-shore model of barrier island migration over a compressible substrate. Mar Geol 271:1–16

Rosati J, Dean R, Walton T (2013) The modified Brunn rule extended for landward transport. Mar Geol 340:71–81

Sallenger A, Wright C, Howd P, Doran K, Guy K (2009) Extreme coastal changes on the Chandeleur Islands, Louisiana, during and after Hurricane Katrina. In: Lavoie D (ed) Sand resources, regional geology, and coastal processes of the Chandeleur islands coastal system: an evaluation of the Breton National Wildlife Refuge. U.S. Geological Survey, Denver, CO, pp 27–36

Schwab W et al (2013) Geologic evidence for onshore sediment transport from the inner continental shelf: Fire Island, New York. J Coast Res 29:526–544

Schwimmer R (2001) Rates and processes of marsh shoreline erosion in Rehoboth Bay, Delaware, U.S.A. J Coast Res 17:672–683

Silliman B et al (2012) Degradation and resilience in Louisiana salt marshes after the BP-*Deepwater Horizons* oil spill. Proc Natl Acad Sci U S A 109:11234–11239

Silvestri S, Defina A, Marani M (2005) Tidal regime, salinity and salt marsh plant zonation. Estuar Coast Shelf Sci 62:119–130

Smith J, FitzGerald D (1994) Sediment transport patterns at the Essex River Inlet Ebb-Tidal Delta, Massachusetts, U.S.A. J Coast Res 10:752–774

Snedden J, Nummedal D, Amos A (1988) Storm- and fair-weather combined flow on the Central Texas continental shelf. J Sediment Res 58:580–595

Stauble D (1997) Ocean City, Maryland and Vicinity water resources study. Draft integrated feasibility report and environmental impact statement. US Army Engineer District, Baltimore, Baltimore, MD

Stauble D (2001) Morphodynamic evaluation of a highly dynamic inlet to improve channel navigation: Chatham Harbor Massachusetts, USA. Coast Dyn 1:232–241

Stauble D et al (1993) Beach nourishment response and design evaluation: Ocean City, Maryland. Coastal Engineering Research Center, Vicksburg, MS

Stefanon L et al (2012) Signatures of sea level changes on tidal geomorphology: experiments on network incision and retreat. Geophys Res Lett 39

Stevenson J, Kearney M, Pendleton E (1985) Sedimentation and erosion in a Chesapeake Bay brackish marsh system. Mar Geol 67:213–235

Stive M et al (2009) Empirical relationships between tidal inlet cross sections and tidal prism: a review. In: Mizuguchi M (ed) Proceedings of the conference on coastal dynamics, Tokyo, Japan 1:1–10

Stoddart R, Reed D, French J (1989) Understanding salt-marsh accretion, Scolt Head Island, Norfolk, England. Estuar Coast 12:228–236

Stolper D, List JH, Thieler ER (2005) Simulating the evolution of coastal morphology and stratigraphy with a new morphological-behavior model (GEOMBEST). Mar Geol 218:17–36

Stone GW, Sheremet A, Zhang X, Braud D (2003) Coastal landloss and wave-surge predictions during hurricanes in Coastal Louisiana: implications for the oil and gas industry. Report prepared for Louisiana Department of Natural Resources, Minerals Management Service, and U.S. Geological Survey, 61p

Stone, G. and Orford, J. 2004, Storms and their significance in coastal morphosedimentary dynamics: Marine Geology, v. 210, nos. 1–4, p. 1–362.
Stumpf R (1983) The process of sedimentation on the surface of a salt marsh. Estuar Coast Shelf Sci 17:495–508
Temmerman S et al (2003) Modeling long-term tidal marsh growth under changing tidal conditions and suspended sediment concentrations, Scheldt estuary, Belgium. Mar Geol 193:151–169
Temmerman S et al (2007) Vegetation causes channel erosion in a tidal landscape. Geology 35:631–634
Torio D, Chmura GL (2015) Impact of sea level rise on tidal marsh as fish habitat. Estuar Coasts 38:1288–1303
Törnqvist T et al (2008) Mississippi delta subsidence primarily caused by compaction of Holocene strata. Nat Geosci 1:173–176
Trosclair KJ (2013) Wave transformation at a saltmarsh edge and resulting marsh edge erosion: observations and modeling. Department of Earth and Environmental Science, University of New Orleans Theses and Dissertations, 134 p
Tran T et al (2012) Cross-sectional stability of tidal inlets: a comparison between numerical and empirical approaches. Coast Eng 60:21–29
Underwood S, Hiland M (1995) Historical development of Ocean City Inlet ebb shoal and its effect on Northern Assateague Island. U.S. Army Engineer Waterways Experiment Station, Coastal Engineering Research Center, Vicksburg, MS. 128p
U.S. Army Corps of Engineers (1998) Ocean City, Maryland, and vicinity water resources study final integrated feasibility report and environmental impact statement, Appendix D, Restoration of Assateague Island, Baltimore, Maryland
Van der Koppel J et al (2005) Self-organization and vegetation collapse in salt marsh ecosystems. Am Nat 165
van der Wegen M (2013) Numerical modeling of the impact of sea level rise on tidal basin morphodynamics. J Geophys Res Earth Surf 118:447–460. https://doi.org/10.1002/jgrf.20034
Van Goor M et al (2003) Impact of sea-level rise on the morphological equilibrium state of tidal inlets. Mar Geol 202:211–227
van Heteren S, van de Plassche O (1997) Influence of relative sea-level change and tidal-inlet development on barrier-spit stratigraphy, Sandy Neck, MA. J Sediment Res 67:350–363
Van Proosdij D et al (2005) Monitoring seasonal changes in surface elevation of intertidal environments near the Windsor Causeway. Final report prepared for the Nova Scotia Department of Transportation
Walters D et al (2014) Interactions between barrier islands and back-barrier marshes affect island system response to sea level rise: Insights from a coupled model. J Geophys Res Earth Surf 119:2013–2031. https://doi.org/10.1002/2014jf003091
Walton T, Adams W (1976) Capacity of inlet outer ears to store sand. In: Proceedings of the 15th conference on coastal engineering, Honolulu, Hawaii
Whittaker R (ed) (1975) Communities and ecosystems, 2nd edn. Macmillan, New York
Williams J (1992) USGS Research Contributes to Assateague Island Restoration—Mitigating 70 Years of Coastal Erosion Due to Ocean City Inlet Jetties, Sound Waves, USGS Pub. U. S. Department of the Interior
Wilson CA, Allison MA (2008) An equilibrium profile model for retreating marsh shorelines in southeast Louisiana. Estuar Coast Shelf Sci 80(4):483–494
Wilson CA et al (2013) Marsh pool and tidal creek morphodynamics: dynamic equilibrium of northern saltmarshes? Geomorphology 213:99–115
Wolinsky MA, Murray AB (2009) A unifying framework for shoreline migration: 2. Application to wave-dominated coasts. J Geophys Res 114:F01009. https://doi.org/10.1029/2007JF000856
Wright S (2012) Understanding the mechanisms behind surface elevation loss in ditched marshes. Master's Thesis, Department of Earth Sciences, Boston University, Boston, 125 p
Yu S, Törnqvist T, Hu P (2012) Quantifying Holocene lithospheric subsidence rates underneath the Mississippi. Earth Planet Sci Lett 331:21–30

Drowned Barriers as Archives of Coastal-Response to Sea-Level Rise

Claire L. Mellett and Andrew J. Plater

Abstract Advances in submarine technologies and increased exploration of continental shelves are revealing increasingly more submerged barriers that have drowned in response to early- to mid-Holocene sea-level rise. These coastal archives, when combined with information on sea-level trends, oceanographic conditions and palaeogeography, are valuable palaeo-evidence that can be used to understand the processes and drivers of coastal change. In this chapter, we synthesize documented examples of drowned barriers preserved on continental shelves across the world. Using these examples, we examine the relative significance of controls on barrier drowning (aka overstepping) whereby the barrier becomes drowned offshore of the advancing shoreline. Relative sea-level rise (RSLR), sediment supply and topography are the principal controls on shoreline retreat, but the interaction between these factors cannot readily be deconstructed as they are not in operation simultaneously, nor present along all coasts. However, it is possible to recognize local conditions that make barriers vulnerable to overstepping. It is shown that barrier retreat through overstepping is enhanced by one or more of the following; coarse grain size, cemented sediment, high sediment supply rates, topographic pinning and a rapid increase in accommodation. We emphasize that to gain a better understanding of the likely response of barrier coastal systems to future RSLR and to better constrain numerical models, we need to fully utilize the geological record left behind by former coastal systems that underwent accelerated RSLR in the past.

Keywords Barrier • Coast • Overstepping • Rollover • Drowned • Sea level • Transgression • Holocene • Submerged landscape • Coastal retreat • Sediment supply • Palaeoshoreline

C.L. Mellett
British Geological Survey, The Lyell Centre, Research Avenue South, Edinburgh, UK
e-mail: cmell@bgs.ac.uk

A.J. Plater (✉)
School of Environmental Sciences, University of Liverpool, Liverpool, UK
e-mail: gg07@liverpool.ac.uk

L.J. Moore, A.B. Murray (eds.), *Barrier Dynamics and Response to Changing Climate*, https://doi.org/10.1007/978-3-319-68086-6_2

1 Introduction

In essence, barriers respond to relative sea-level rise (RSLR) by migrating landward when the creation of accommodation (space that sediment can occupy) by rising sea levels is outpaced by the availability and rate of sediment supply to the shoreline. With respect to observed accelerations in historical and modern sea-level data (Haigh et al. 2014; Jevrejeva et al. 2014) and projected rates of future sea-level rise (SLR) (Church et al. 2013), globally, barriers are expected to enter a phase of rapid landward retreat and begin encroaching (along with the shallow coastal bays behind them) on our heavily populated and strategically important coastal zones. Coastal degradation due to RSLR is already being observed at various locations around the world (e.g. Saito 2001; Thanh et al. 2004; Gibbons and Nicholls 2006; Blum and Roberts 2009) and the economic, environmental and social impacts of such 'coastal squeeze' are staggering. In order to plan strategically and to deploy resources effectively for the future resilience of coastal economies, it is essential to better understand the timescales and geomorphological response of barriers to rising sea levels.

Determining barrier response to RSLR on historical timescales (ca. the last 150 years) from cartographic, photographic and instrumental data (e.g. Fenster et al. 1993; McBride and Byrnes 1997; Lentz et al. 2013) provides only a snapshot of entire system response to longer term changes in relative sea-level (RSL). Whilst these data are of considerable importance in quantifying rates and scales of coastal geomorphic processes, there is a need for geological analogues in which barrier response to past RSLR can be examined in relation to other determinants. As the nature of transgression is commonly erosional, preservation of former shorelines is rare and typically biased towards scenarios where transgression was superseded by a regression of the shoreline (e.g. Goodman et al. 2008; Hein et al. 2014).

Renewed exploration of continental shelves due to the development of offshore renewable energy and mineral resource prospecting has led to the collection of high-resolution geophysical data that is uncovering a wealth of subaqueous geomorphic and sedimentary evidence of former barriers that were drowned below sea level during rapid post-glacial SLR. As the early Holocene is the most recent time period when rates of SLR were of similar magnitude to those predicted for the future under various emissions scenarios (Church et al. 2013), it is drowned barriers of this age that should be targeted as analogues to understand how modern barrier coasts will respond to projected global SLR.

This chapter provides a synthesis of known drowned barriers preserved on the continental shelf and uses them to identify a variety of scenarios/controls that determine the style of barrier shoreline retreat to RSLR.

2 Barrier Coastal-Response to Transgression

Shorelines have considerable capacity to respond to RSLR by migrating landward and upward (Cattaneo and Steel 2003). In barrier-dominated coastal settings, waves generally erode sediment from the shoreface and transport it landward to the

back-barrier (e.g. Kraft 1971; Belknap and Kraft 1981; Roy et al. 1994), i.e. transgressive ravinement. If a barrier is in a state of equilibrium and there are no topographic constraints, the landward translation of sediment keeps pace with rising sea level and the barrier-lagoon system retreats landward in concert. In a state of equilibrium (or net sediment loss), the record of coastal retreat offshore is represented in the form of an erosion surface, or ravinement surface (Swift and Moslow 1982; Leatherman et al. 1983) (Fig. 1a). This style of coastal process-response to transgression is predominantly referred to as *rollover* (Swift 1968; Belknap and Kraft 1981; Swift et al. 1991) and coasts along the Gulf of Mexico and the US Atlantic are already displaying characteristics of this style of retreat (Pilkey et al. 1998; Feagin et al. 2005; Morton et al. 2005; FitzGerald et al. 2008; Odezulu et al. this volume; Rodriguez et al. this volume).

Conversely, if a barrier coast is in disequilibrium with rising sea level, there is potential for all or part of the barrier to drown in-situ, becoming abandoned on the continental shelf seaward of the advancing shoreline (Fig. 1). This style of coastal-response is referred to as overstepping (a term we use synonymously with "drowning" throughout) (Curray 1964; Rampino and Sanders 1980), which can be recognized by the preservation of barrier-lagoon landforms and sediments offshore (Rampino and Sanders 1980, 1982; Leatherman et al. 1983; Forbes et al. 1991). Typically, only back-barrier sediments or landward-dipping barrier beach sediments are preserved during overstepping (low preservation; Rampino and Sanders 1980, 1982; Leatherman et al. 1983; Forbes et al. 1991) (Fig. 1b). However, there are scenarios in which the entire barrier-lagoon system is preserved (high preservation; Fig. 1c) with minimal reworking (e.g. Mellett et al. 2012a). While a barrier may re-establish landward of an overstepped barrier, this is not a requirement of the overstepping process; for example, re-establishment of a barrier landward where coastal slopes are steep (Fig. 1d) would be restricted. The extent (spatial and temporal) of preserved barrier-lagoon systems can provide information on the processes occurring during and after overstepping, and help to identify the controls driving this style of coastal change.

Here, we have defined the style of coastal retreat according to the presence (overstepping) or absence (rollover) of former barrier deposits or morphology offshore of the advancing shoreline. In this instance, any morphological or sedimentary remnant of the former barrier position is interpreted as barrier response through overstepping. However, it is important to recognize that barrier response to RSLR is dynamic on both spatial and temporal scales and it is expected during overall transgression a barrier has potential to switch between the two modes depending on local conditions. From a morphodynamic perspective, a barrier may be considered to be in a continuous state of rollover as sediment is translated from the nearshore to the backshore. However, here we assess the longer term response of barriers to relative sea-level rise over geological, rather than historical, timescales.

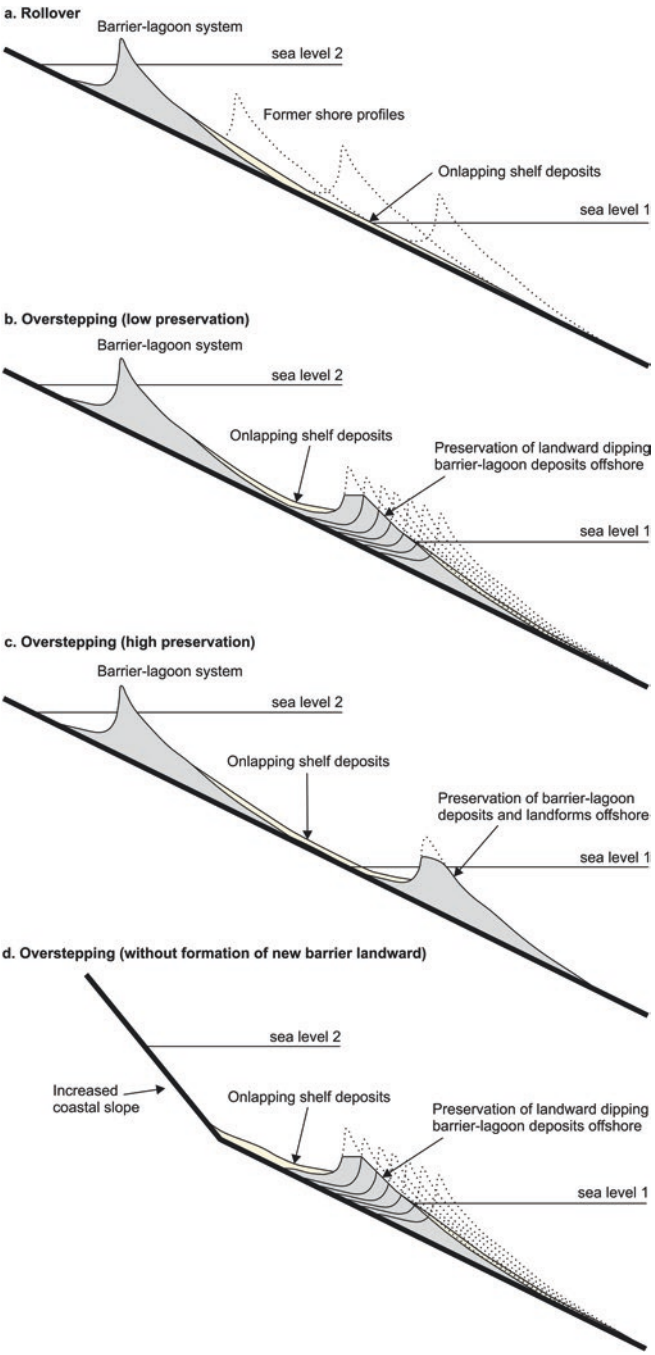

Fig. 1 Schematic illustration of different styles of barrier shoreline retreat during RSLR

3 Synthesis of Drowned Barriers

Here, we undertook a systematic review of scholarly articles to identify examples of drowned barriers using a combination of the following keywords; "Drowned Barrier", "Overstepping", "Drowned Shoreline", "Early Holocene Barrier", and "Transgressive Barrier". Further articles were identified from citations within the returned results.

The systematic review returned examples of early Holocene transgressive barriers that are preserved onshore due to subsequent regression of the shoreline (e.g. Hein et al. 2014). These were not included in the review as, despite responding to a transgression initially, they have a different post-depositional history and are not directly comparable with transgressive barriers that have been overstepped. Literature searches also revealed a scenario in which sediments interpreted as being deposited in back-barrier or tidal inlet environments, thus indicating the presence of a former barrier, are preserved within incised valleys (e.g. Rodriguez et al. 2010). The distinction between back-barrier/tidal inlet and open estuarine sediments within an incised valley can be problematic; therefore, these examples were not included in the review.

A total of 25 examples of drowned barriers were discovered based on information published in 28 peer-reviewed articles. The articles were reviewed and the key information used in this synthesis is summarized in Tables 1 and 2.

The examples presented here are the preserved remnants of barrier-lagoon systems from open to embayed coastal settings or those representing the position of former shorelines in enclosed-lake or inland-sea basins. For each barrier example, the location was recorded—the distribution of drowned barriers presented in this review is given in Fig. 2. The maximum and minimum elevation of the barrier deposits/landforms was also documented (Table 1). Elevations have not been adjusted to a single datum and are assumed to be relative to mean sea level (MSL).

The reported age of the drowned barriers is shown in Table 1. Where radiocarbon (^{14}C) dates were available, the age of the drowned barriers was given in calibrated (cal. ka) or radiocarbon (^{14}C ka) years before present (BP). For examples dated using optical stimulated luminescence (OSL), ages were reported in ka. Where possible, the ages were quoted as documented by the authors in the literature. However, in some cases (e.g. Kelley et al. 2010) chronological information had to be interrogated in relation to core and seismic data to establish the age of the drowned barriers. In the absence of chronological information, an age estimate (e.g. early Holocene) was extracted from the relevant manuscript according to elevation and local RSL history. It is important to note that the ages quoted in the literature are depositional ages and are not a representation of the timing of barrier drowning.

Careful attention was paid to the seismic and lithological evidence underpinning drowned barrier interpretations and articles that did not present a convincing argument or sufficient raw data to test interpretations were excluded from the review. The sedimentological and/or geomorphological evidence used to support interpretations of features as drowned barriers is summarized in Table 2. However, it is advised that original articles are consulted for more comprehensive descriptions.

Table 1 Drowned barriers documented in the published literature

ID	Location	Latitude	Longitude	Coastal setting	Reported Age	Elevation range of coastal deposits*	References
1	Gulf of Maine, USA	43°N	68°W	Lake/ inland sea	9.5–8.2 cal. ka BP *	−28 m to −22 m	Kelley et al. (2010, 2013)
2	Adriatic Sea, Italy	44°N	14°E	Barrier-lagoon (Site A)	~14.3 cal. ka BP *	−82 m to −78 m	Storms et al. (2008); Maselli et al. (2011)
	Adriatic Sea, Italy	44°N	15°E	Barrier-lagoon (Site B)	~10.5 cal. ka BP *	−39 m to −16 m	
3	Bras d'Or Lakes, Canada	46°N	60°W	Lake/ inland sea	Mid Holocene	−25 m to −15 m	Shaw et al. (2009)
4	Baltic Sea, Germany	54°N	11°E	Lake/ inland sea	After 9.2 ^{14}C ka BP *	−17 m to −15 m	Novak (2002)
5	West-central Florida shelf, USA	28°N	83°W	Barrier-lagoon	8.3 to 5.9 ^{14}C ka BP *	~−12 m	Brooks et al. (2003); Hill et al. (2003)
6	KwaZulu-Natal shelf, South Africa	28°S	33°E	Barrier-lagoon	Late glacial to early Holocene	−100 m and −60 m to −50 m	Salzmanm et al. (2013)
7	KwaZulu-Natal shelf, South Africa	29°S	31°E	Barrier-lagoon	Early Holocene	−65 m to −50 m	Green et al. (2012, 2013)
8	De Soto Canyon, Gulf of Mexico, USA	30°N	87°W	Barrier-lagoon	Early Holocene	−51 m to −26 m	Gardner et al. (2007)
9	De Soto Canyon, Gulf of Mexico, USA	29°N	85°W	Barrier-lagoon (shelf-edge delta)	Unresolved	−85 m to −55 m	Gardner et al. (2005)
10	Baltic Sea, Germany	55°N	12°E	Lake/ inland sea	Early Holocene	−19 m to −12 m	Jensen and Stecher (1992)
11	New Jersey shelf, USA	40°N	70°W	Barrier-lagoon	Late glacial to early Holocene	~−70 m and −60 m to −50 m	Nordfjord et al. (2009)

(continued)

Table 1 (continued)

ID	Location	Latitude	Longitude	Coastal setting	Reported Age	Elevation range of coastal deposits*	References
12	Kattegat, Southern Scandinavia	56°N	11°E	Barrier-lagoon system	10.5 cal. ka BP to 9.5 cal. ka BP *	−35 m to −24 m	Bennike et al. (2000)
13	Southwest Florida margin, USA	25°N	83°W	Barrier-lagoon (capped with biogenic reef)	14.5 to 13.8 ^{14}C ka BP *	−72 m to −60 m	Jarrett et al. (2005)
14	Black Sea	43°N	31°E	Lake/ Inland Sea	8.5 ka BP to 9.5 ka BP *	−100 m to −85 m	Lericolais et al. (2007)
15	New South Wales shelf, Australia	32°S	153°E	Barrier-lagoon	Early Holocene	Unknown	Browne (1994)
16	Rhine-Meuse, The Netherlands	52°N	5°E	Barrier-lagoon	8.3 cal. ka BP to 7.4 cal. ka BP *	−31 m to −14 m	Hijma et al. (2010)
17	English Channel, UK	51°N	0°E	Barrier-lagoon	8.4 ka to 5.3 ka *	−24 m to −14 m	Mellett et al. (2012a, b)
18	Chedabucto Bay, Canada	45°N	61°W	Barrier-lagoon	Early Holocene	~−38 m	Forbes et al. (1995)
19	Chezzetcook Inlet, Canada	45°N	63°W	Barrier-lagoon	Recent	−5 m to −2 m	Forbes et al. (1991)
20	Western Korea	35°N	126°E	Barrier-lagoon	Early Holocene	−27 m to – 8 m	Yang et al. (2006)
21	Sabine Bank, Gulf of Mexico, USA	29°N	94°W	Barrier-lagoon	~5.3 to 4.7 ^{14}C ka BP *	~−12 m	Rodriguez et al. (1999)
22	Heald Bank, Gulf of Mexico, USA	29°N	94°W	Barrier-lagoon	~8.4 to 7.5 ^{14}C ka BP *	~−15 m	Rodriguez et al. (1999)
23	Gulf of Valencia, Mediterranean	39°N	0°E	Barrier-lagoon	Pleistocene	~−60 m	Albarracín et al. (2013)
24	Old Rhine, The Netherlands	52°N	4°E	Barrier-lagoon	7.3 to 5.2 ^{14}C ka BP *	−15 to −31 m	Rieu et al. (2005)

ID refers to locations presented in Fig. 2. In reported age column * refers to examples that have been dated using chronometric methods (^{14}C or OSL)

Table 2 Evidence used to identify drowned barriers

ID	Location	Evidence	References
1	Gulf of Maine, USA	Cores reveal glaciagenic deposits overlain by tidal flat deposits, washover fan deposits and marine sand. Rip up clasts of peat are present. Bathymetry shows ridges interpreted as spits and tombolos	Kelley et al. (2010, 2013)
2	Adriatic Sea, Italy	Channels observed in seismic showing oblique reflectors. Channel filled with interbedded silt and clay. Channels are erosionaly truncated by a ravinement surface. Channels interpreted as tidal inlets	Storms et al. (2008); Maselli et al. (2011)
	Adriatic Sea, Italy	Bathymetry reveals a ridge interpreted as a barrier island. Cores from the ridge show coarsening upwards sediments. Barrier sediments are truncated by a ravinement surface	
3	Bras d'Or lakes, Canada	Coastal landforms (tombolos, spits and barrier beaches) observed in bathymetry	Shaw et al. (2009)
4	Baltic Sea, Germany	Buried ridges with mound and oblique reflectors observed in seismic. Cores reveal coarsening upward sequences of interbedded sand, silt and clay. Deposits interpreted as back-stepping barrier islands	Novak (2002)
5	West-central Florida shelf, USA	Cores reveal mud, organic muddy sand and muddy sand facies interpreted as back barrier deposits based on lithology and fauna assemblages. These are overlain by a coarse shell and sand facies with a sharp lower erosional boundary interpreted as a ravinement surface	Brooks et al. (2003); Hill et al. (2003)
6	KwaZulu-Natal shelf, South Africa	Buried ridges separated by depressions comprising draped reflectors are observed in seismic. These features are interpreted as barrier-lagoons and they are truncated by a strong reflector interpreted as a ravinement surface. Cores show the ridges comprise cemented shelly sand (beachrock/ aeolianite). The ridge features are also visible in bathymetry	Salzmanm et al. (2013)
7	KwaZulu-Natal shelf, South Africa	Bathymetry reveals a series of arcuate ridges and associated depressions. The ridges and depressions are also observed in seismic data	Green et al. (2012, 2013)
8	De Soto Canyon, Gulf of Mexico, USA	Ridges interpreted as barrier islands identified from bathymetry	Gardner et al. (2007)
9	De Soto Canyon, Gulf of Mexico, USA	Ridges interpreted as barrier islands identified from bathymetry	Gardner et al. (2005)

(continued)

Table 2 (continued)

ID	Location	Evidence	References
10	Baltic Sea, Germany	Seismic facies show oblique landward prograding clinoforms that are truncated by an erosional surface. Cores comprise laminated clayey silt and coarsening upward sand. Both seismic and lithology are interpreted as a sequence of barrier beach ridges closely connected to back barrier lagoon/pond deposits	Jensen and Stecher (1992)
11	New Jersey shelf, USA	Topographic lows observed in seismic data interpreted as back barrier morphology filled with transparent seismic facies interpreted as tidal inlet facies	Nordfjord et al. (2009)
12	Kattegat, Southern Scandinavia	Seismic data reveal landward oblique dipping reflectors which comprise laminated clays and silts and contain macrofossils characteristic of lagoon sediments. These are interpreted as backstepping barrier-lagoon sediments and they are truncated by an erosional reflector representing a ravinement surface	Bennike et al. (2000)
13	Southwest Florida margin, USA	Ridges with oblique reflectors are observed in seismic. Recurved spit, tidal inlet channel and prograding beach ridges observed on bathymetry	Jarrett et al. (2005)
14	Black Sea	Linear ridges and depressions observed in bathymetry. Cores reveal laminated mud overlain by a shell hash and sand. Ridges interpreted as remnant beaches	Lericolais et al. (2007)
15	New South Wales shelf, Australia	Seismic data show seaward prograding oblique reflectors interpreted as shoreface deposits overlain by landward prograding oblique reflectors interpreted as washover fan, lagoonal and tidal deposits. An erosional reflector interpreted as a ravinement surface truncates deposits. Cores comprise interbedded sand and clay, peat beds, muddy sand and fine sand	Browne (1994)
16	Rhine-Meuse, The Netherlands	Channels observed in seismic data are infilled with interbedded sand and mud comprising fauna typical of back barrier environments. These deposits are overlain by lower shoreface sediment	Hijma et al. (2010)

(continued)

Table 2 (continued)

ID	Location	Evidence	References
17	English Channel, UK	Recurved ridge and associated landward depression observed in bathymetry. The ridge is represented in seismic by a mound deposit comprising convex reflectors. Cores from the ridge comprise gravel-pebbles and coarsening. These deposits rest unconformable on a seaward prograding sand unit. In the depression behind the ridge, parallel to draped reflectors on lap against the ridge facies. Cores in this unit comprise interbedded sand and mud. All facies are truncated by an erosional boundary interpreted as a ravinement surface	Mellett et al. (2012a, b)
18	Chedabucto Bay, Canada	A ridge/mound of sediment comprising seaward prograding oblique reflectors observed in seismic data. Feature interpreted as a gravel barrier/ foreland	Forbes et al. (1995)
19	Chezzetcook Inlet, Canada	Morphological profiles reveal a ridge preserved offshore of the present day barrier. Samples of pebbles recovered from the ridge. Ridge interpreted as relict barrier	Forbes et al. (1991)
20	Western Korea	Seismic data show channels with oblique reflectors and cores show an overall coarsening upwards sequence and the presence of tidal rythmites. The channels are interpreted as back barrier tidal inlets. The channels are truncated by a sharp erosional boundary interpreted as ravinement surface	Yang et al. (2006)
21	Sabine Bank, Gulf of Mexico, USA	Banks observed in bathymetry. Seaward dipping seismic units comprising muddy sand rest unconformably on a seismic unit of landward dipping reflectors comprising interbedded mud and sand. Fauna assemblages in the lower unit are typical of bay/inlet environments	Rodriguez et al. (1999)
22	Heald Bank, Gulf of Mexico, USA	Shows the same characteristics as Sabine Bank	Rodriguez et al. (1999)
23	Gulf of Valencia, Mediterranean	Seismic data show buried mounds interpreted as barriers	Albarracín et al. (2013)
24	Old Rhine, The Netherlands	Channels recognized from seismic data with some oblique reflectors. Channels comprise fine to medium sand with cross-laminae and fauna characteristic of a back barrier setting. Channels interpreted as tidal inlets	Rieu et al. (2005)

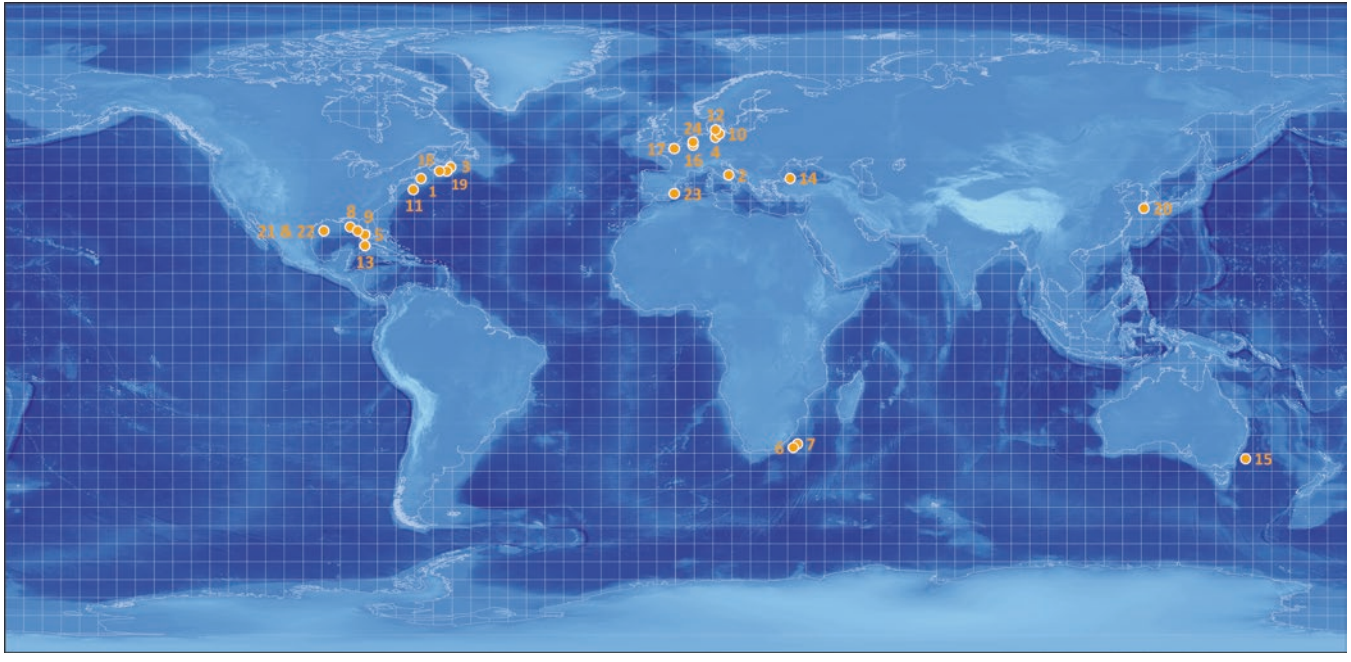

Fig. 2 Location of drowned barriers presented in this review. Bathymetry source: GEBCO_08 Grid, version 20091120, http://www.gebco.net. (*1*) Kelley et al. (2010, 2013). (*2*) Storms et al. (2008); Maselli et al. (2011). (*3*) Shaw et al. (2009). (*4*) Novak (2002). (*5*) Brooks et al. (2003); Hill et al. (2003). (*6*) Salzmanm et al. (2013). (*7*) Green et al. (2013a, b). (*8*) Gardner et al. (2007). (*9*) Gardner et al. (2005). (*10*) Jensen and Stecher (1992). (*11*) Nordfjord et al. (2009). (*12*) Bennike et al. (2000). (*13*) Jarrett et al. (2005). (*14*) Lericolais et al. (2007). (*15*) Browne (1994). (*16*) Hijma et al. (2010). (*17*) Mellett et al. (2012a). (*18*) Forbes et al. (1995). (*19*) Forbes et al. (1991). (*20*) Yang et al. (2006). (*21*) Rodriguez et al. (1999). (*22*) Rodriguez et al. (1999). (*23*) Albarracín et al. (2013). (*24*) Rieu et al. (2005)

4 Characteristics of Drowned Barriers

Drowned barriers have a morphological and stratigraphic expression that can be determined from geophysical data (multibeam bathymetry and sub-bottom seismic) and/or borehole data and sediment cores (Fig. 3). In addition, fauna and flora assemblages can be used to characterize depositional environment (e.g. Hill et al. 2003).

Multibeam bathymetry is used to distinguish the morphology of a barrier-lagoon system, although it would be possible to identify morphological components buried in the sub-surface using high-resolution 2D or 3D seismic data. The barrier beach element of the depositional system is represented morphologically by one or more elongate to recurved ridges (e.g. Jarrett et al. 2005; Mellett et al. 2012a; Salzmanm et al. 2013). The ridges are commonly parallel to the palaeoshoreline and may be segmented alongshore and/or cross-shore, showing evidence of breaching or shoreline retreat (Storms et al. 2008). Topographic depressions corresponding to the back-barrier environment may be present on the landward side of the ridges (Fig. 3). It is important to recognize that relict barrier ridges can exhibit a similar morphological expression to shelf sediment ridges forming underwater in response to hydrodynamic processes operating post-transgression (e.g. Lericolais et al. 2007) and therefore interpretation of landforms using morphology alone is ambiguous. Furthermore, landforms are not always recognizable on the seabed due to poor data resolution or full/partial burial.

Sub-bottom seismic data are used to recognize barrier-lagoon features that are buried, or to unravel the internal structures and stratigraphy of barrier-lagoon systems. Using high-resolution seismic data, cross-shore seismic profiles of the barrier beach exhibit oblique reflectors that dip both landward and seaward (Fig. 3). If data are of lower resolution, the barrier beach is represented by a mound in cross-shore profiles (e.g. Kelley et al. 2010; Salzmanm et al. 2013). In scenarios where the barrier has been partially reworked and the shoreface eroded, oblique landward-dipping reflectors represent the transgressing barrier (e.g. Browne 1994). These can rest unconformably on pre-transgression deposits (Storms et al. 2008; Kelley et al. 2010) or shoreface deposits characterized by seaward-dipping reflectors (Browne 1994; Rodriguez et al. 1999) that are the product of deposition in relatively deeper water when the shoreline was farther landward, prior to emergence of the barrier beach and creation of the back-barrier environment.

Washover (or overwash) fans are another component of the barrier-lagoon system that can be preserved, i.e. the barrier beach backshore (Mellett et al. 2012a; Kelley et al. 2013). Chaotic seismic reflectors that dip predominantly landward are diagnostic of these fans and borehole data show poorly sorted coarse sediments become thinner and finer landward. These may be recognizable using multibeam bathymetry as topographic lows or breaches in the barrier. However, blow outs in dune systems have a similar morphological expression (Lericolais et al. 2007).

Preservation of entire barrier-lagoon systems is rare; typically, the existence of a former barrier is inferred from the presence of lagoon or tidal inlet sediments below a ravinement surface that can be diagnosed from sub-bottom seismic data and/or

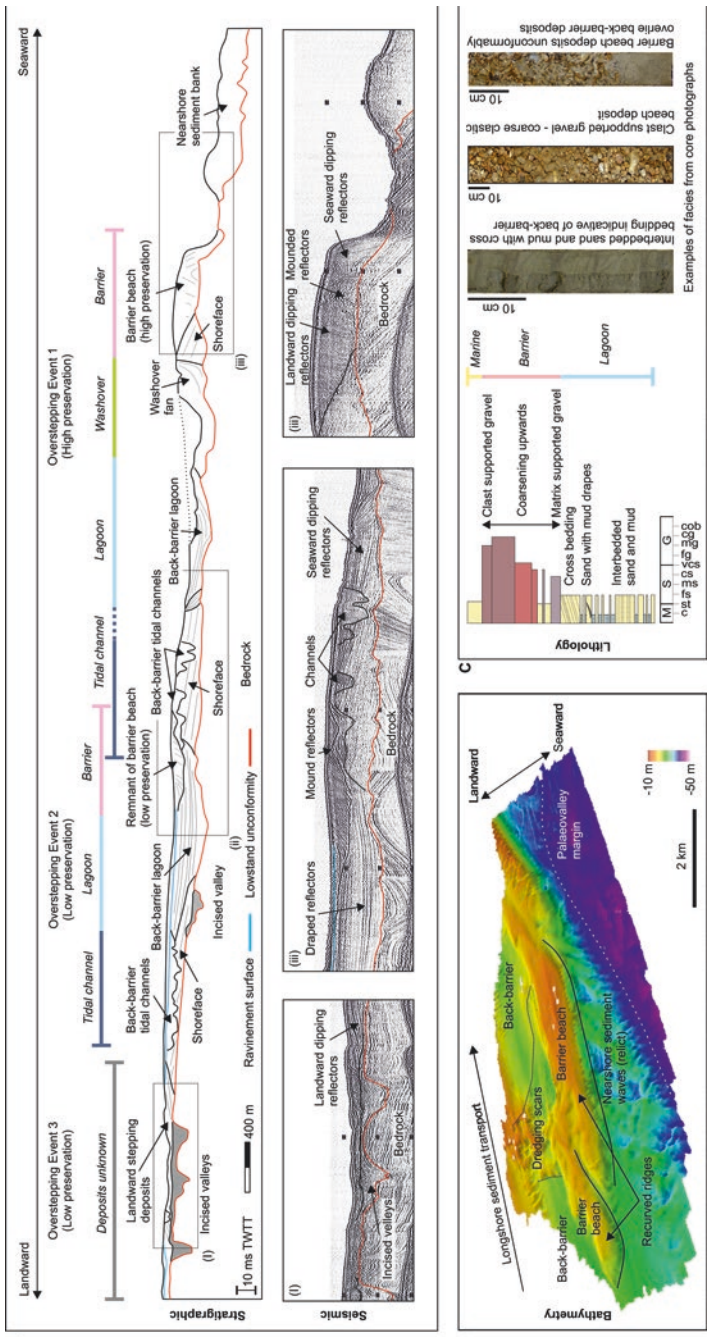

Fig. 3 Example of key morphological, stratigraphic, seismic and lithological features of a representative drowned barrier. Images modified from Mellett et al. (2012a). (**a**) Annotated seismic cross section running onshore–offshore perpendicular to the shoreline. Key seismic reflector patterns are highlighted and three phases of overstepping are documented. (**b**) Bathymetry of the most seaward ridge (Overstepping Event 1). (**c**) Representative lithostratigraphically extracted from core records (note: not all facies are present in each core). Core photographs show key facies and erosion surfaces

boreholes (e.g. Fig. 3). In seismic data, these deposits exhibit low amplitude, parallel to low-angle oblique landward-dipping reflectors. Where the back-barrier is dissected by tidal inlets, multiple lateral and stacked channels can be recognized (e.g. Rieu et al. 2005; Hijma et al. 2010). In boreholes, fine grained sediments with structures indicative of tidal influence or organic deposits are characteristic of back-barrier lagoon and tidal inlet environments. Stratigraphically, vertical deepening of facies (lagoon-shoreface-marine) is diagnostic of barrier-lagoon systems that have been overstepped (Cattaneo and Steel 2003).

During transgression, barrier-lagoon systems are at least partly reworked through ravinement as the shoreline advances. This erosion surface is represented in seismic data by a strong reflector that truncates underlying strata (e.g. Storms et al. 2008). In cores it can be identified by a sharp erosional contact above which lies a shell hash or coarse shelly sand which can exhibit fining upwards representing water deepening (e.g. Brooks et al. 2003).

Identification of drowned barriers should ideally be carried out through the integration of morphological, sub-bottom seismic, lithological and palaeoecological data and a lesser degree of confidence is placed on interpretations underpinned by a single line of evidence. An example of an integrated approach has been given in Fig. 3. While the characteristics of seismic, bathymetry and lithofacies at this site are not representative of all drowned barriers, they clearly demonstrate the key morphologicical, seismic and lithological signatures of drowned barriers. It is important to bear in mind that coastal barrier systems are highly dynamic and their style of retreat can switch on many timescales during an overall transgression leading to high degrees of spatial variability and preservation potential. This was demonstrated at Hastings Bank, UK (Fig. 3) where at least three phases of overstepping were recognized and preservation of barrier-lagoon deposits became progressively lower as the shoreline retreated (Mellett et al. 2012a).

5 Patterns of Drowned Barrier Distribution and Behaviour

5.1 Distribution of Drowned Barriers in Space and Time

The majority of the drowned barrier examples are located in the Northern Hemisphere (Fig. 2). This hemispheric bias may be related to the availability of suitable geophysical and borehole data which is used to underpin interpretations of drowned barrier. It is perhaps also due to the greater areas of shallow shelf seas that comprise significant accumulations of sand and gravel to support barrier development.

The elevation range of drowned barrier landforms and sediments was plotted against latitude (Fig. 4). A clustering of drowned barriers (Group 1; Fig. 3) is observed at elevations between ca. −35 m and −15 m and latitudes of 43–56°N, i.e. shallow shelf seas that might be regarded as experiencing both RSL fall and rise

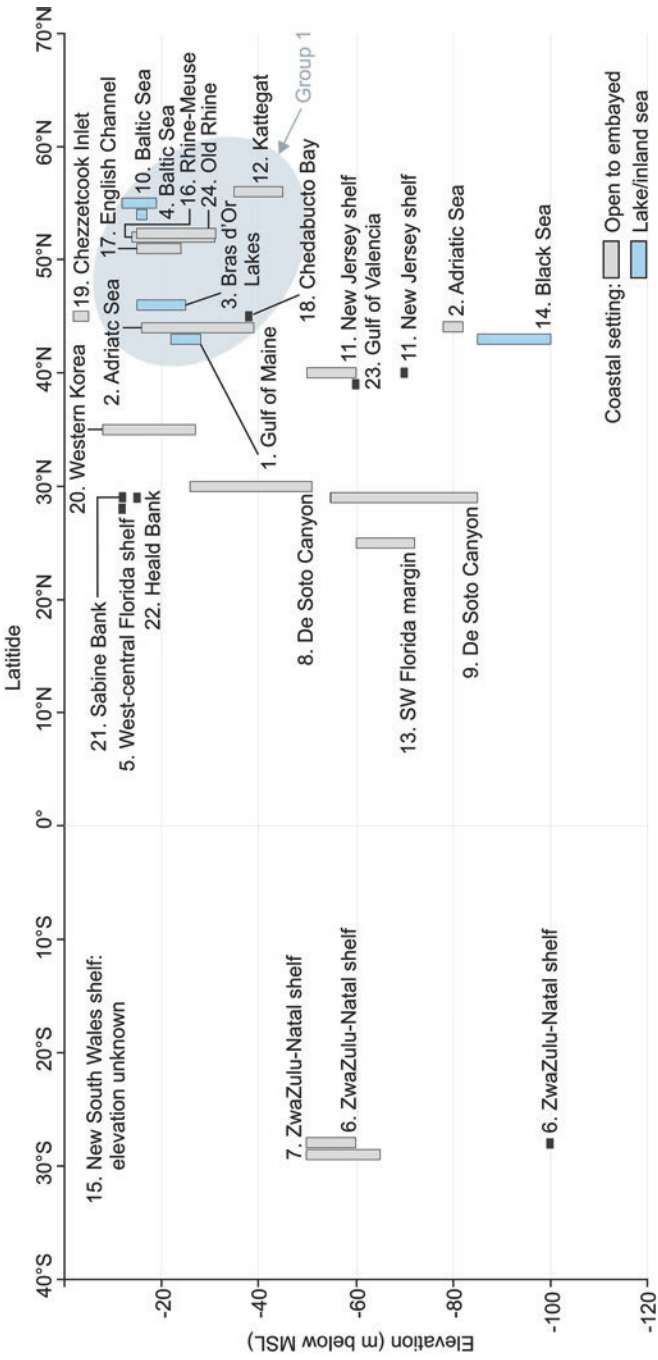

Fig. 4 Elevation of drowned barriers in relation to latitude. ID numbers and locations are presented in Fig. 2 and Table 1

over glacial-interglacial timescales (cf. Zone II from Clark et al. 1978), suggesting a potential temporo-spatial control on drowning and/or preservation of barriers. No barriers were identified in water depths <15 m as these correspond to a period of time in the late Holocene when the rate of RSLR was very low, allowing sufficient time for reworking through ravinement of any former barrier systems. Elsewhere there are no strong relationships between elevation and latitude.

As noted in Sect. 3, where no chronological information is available, the age of drowned barriers is often estimated by comparing the elevation of the feature to local RSL history (e.g. Green et al. 2013). If high-resolution local RSL data are available and there has been minimal post-depositional reworking then a degree of confidence can be placed in these age estimates. However, preservation is often partial and, given reworking, it is unlikely the elevation of the feature preserved today reflects the original barrier morphology and elevation prior to submergence. Furthermore, the relationship between RSL and the morphology and elevation of any given barrier is difficult to establish unequivocally without accompanying palaeoecological or sedimentary evidence (Rodriguez and Meyer 2006; Tamura 2012; Hede et al. 2013; Billy et al. 2015). The drowned barriers discussed here are from a period of time (Early Holocene) where local RSL data are often sparse as these sites occupy elevations that are now submerged. This must be considered when interpreting sea level-related controls on barrier response where chronological data are absent.

Of the documented drowned barriers included in the systematic review, 13 have been dated using chronological methods (see Table 1). The reported ages and elevations are presented in Fig. 5. With the exception of The Black Sea (ID 14.), there is a relationship between elevation and age with those located at greater depths being the oldest. This broad relationship is likely a function of post-glacial SLR. The drowned barrier preserved in the Black Sea is an outlier in this respect due to changes in water(sea) level being controlled by intermittent connection to the Mediterranean Sea and water balance in the surrounding drainage basin (Lericolais et al. 2007). Ten of the drowned barriers span the time period from early Holocene to mid− to late Holocene, whilst two are of Late Glacial age.

Evolution of a barrier coast during RSLR can be broadly split into three phases: (1) barrier formation; (2) barrier retreat; and (3) preservation post-submergence. The role of RSL, sediment supply and topographic/antecedent controls in governing each of these evolution phases, as described in the cited articles following interpretation of the presented evidence, are given in Table 3.

5.2 Barrier Formation

Twelve of the 24 drowned barrier examples acknowledged that RSL stillstand or slowdown was required to enable the barrier to form (Table 3). However, barrier systems can develop during RSLR where the rate of sediment supply is greater than the rate at which accommodation is created by the rising sea (e.g. Mellett et al.

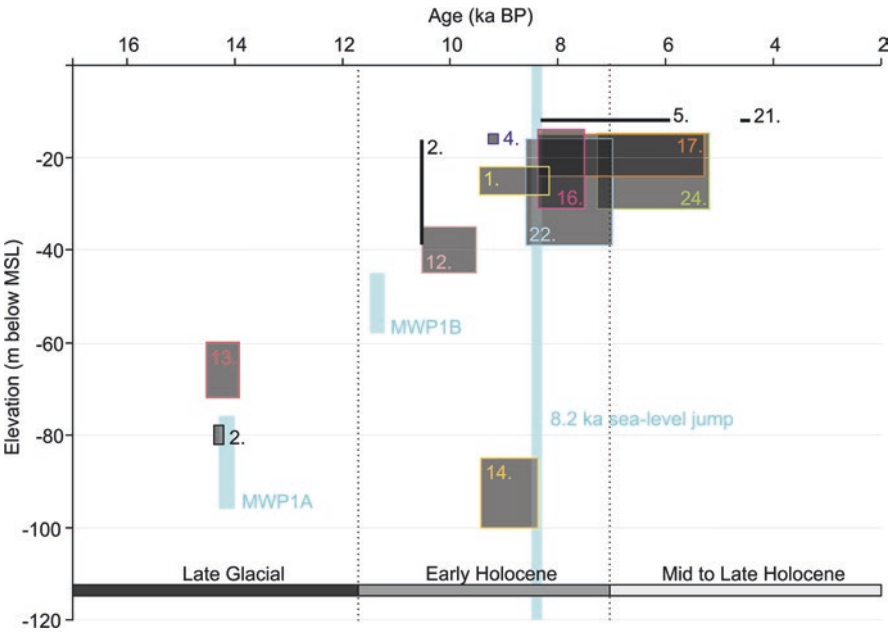

Fig. 5 Age of chronometrically constrained (^{14}C and OSL) drowned barriers and their elevation. (*1*) Kelley et al. (2010, 2013). (*2*) Storms et al. (2008); Maselli et al. (2011). (*4*) Novak (2002). (*5*) Brooks et al. (2003); Hill et al. (2003). (*12*) Bennike et al. (2000). (*13*) Jarrett et al. (2005). (*14*) Lericolais et al. (2007). (*16*) Hijma et al. (2010). (*17*) Mellett et al. (2012b). (*21*) Rodriguez et al. (1999). (*22*) Rodriguez et al. (1999). (*24*) Rieu et al. (2005). MWP1A: −96 m to −76 m from 14.3 to 14.0 ka BP (Liu and Milliman 2004). MWP1B: −58 m to −45 m from 11.5 to 11.2 ka BP (Liu and Milliman 2004). 8.2 ka sea-level jump: 8.5–8.3 ka (Tornqvist and Hijma 2012). Early Holocene defined as 11,650–7000 years BP after Smith et al. (2011)

2012a). Sediment supply is highlighted as an important control, particularly in high latitudes where the supply of coarse clastic sediment from previously glaciated terrains supports barrier formation (Jensen and Stecher 1992; Jarrett et al. 2005; Storms et al. 2008; Kelley et al. 2010, 2013).

5.3 Barrier Retreat Through Overstepping

The role of RSLR in driving barrier retreat through overstepping is complex. High rates of RSLR (or shoreline transgression driven by RSLR) is the most commonly cited driver of barrier retreat through overstepping (Table 3). At two locations, barrier overstepping has been attributed to high rates of RSLR associated with post-glacial meltwater pulses (Storms et al. 2008; Green et al. 2012, 2013; Salzmanm et al. 2013).

Table 3 Controls on barrier formation, drowning and preservation determined from drowned barrier examples

ID	Location	Barrier Formation			Barrier retreat (overstepping)											High preservation post-submergence			
		RSL slow-stand or still stand	Supply of sediment from glacial/paraglacial terrain	Increase in sediment supply	High rate of RSLR associated with MWP1A	High rate of RSLR associated with MWP1B	High RRSLR/Rapid SLR	Rapid transgression (unspecified)	Rapid transgression driven by large back barrier accommodation	Rapid transgression driven by shallow slope	Rapid transgression through driven by breaching of topography	Trapped by topography	'Sediment surplus' overstepping	'Sediment deficit' overstepping	High sedimentation due to small tidal prism	Regression prior to transgression	Sheltered by topography	Large volumes of sediment and/or coarse grain size	Cemented prior to drowning
1	Gulf of Maine, USA																		
2	Adriatic Sea, Italy																		
	Adriatic Sea, Italy																		
3	Bras d'Or Lakes, Canada																		
4	Baltic Sea, Germany																		
5	West-central Florida shelf, USA																		
6	KwaZulu-Natal shelf, South Africa																		
7	KwaZulu-Natal shelf, South Africa																		
8	De Soto Canyon, Gulf of Mexico, USA																		
9	De Soto Canyon, Gulf of Mexico, USA																		
10	Baltic Sea, Germany																		

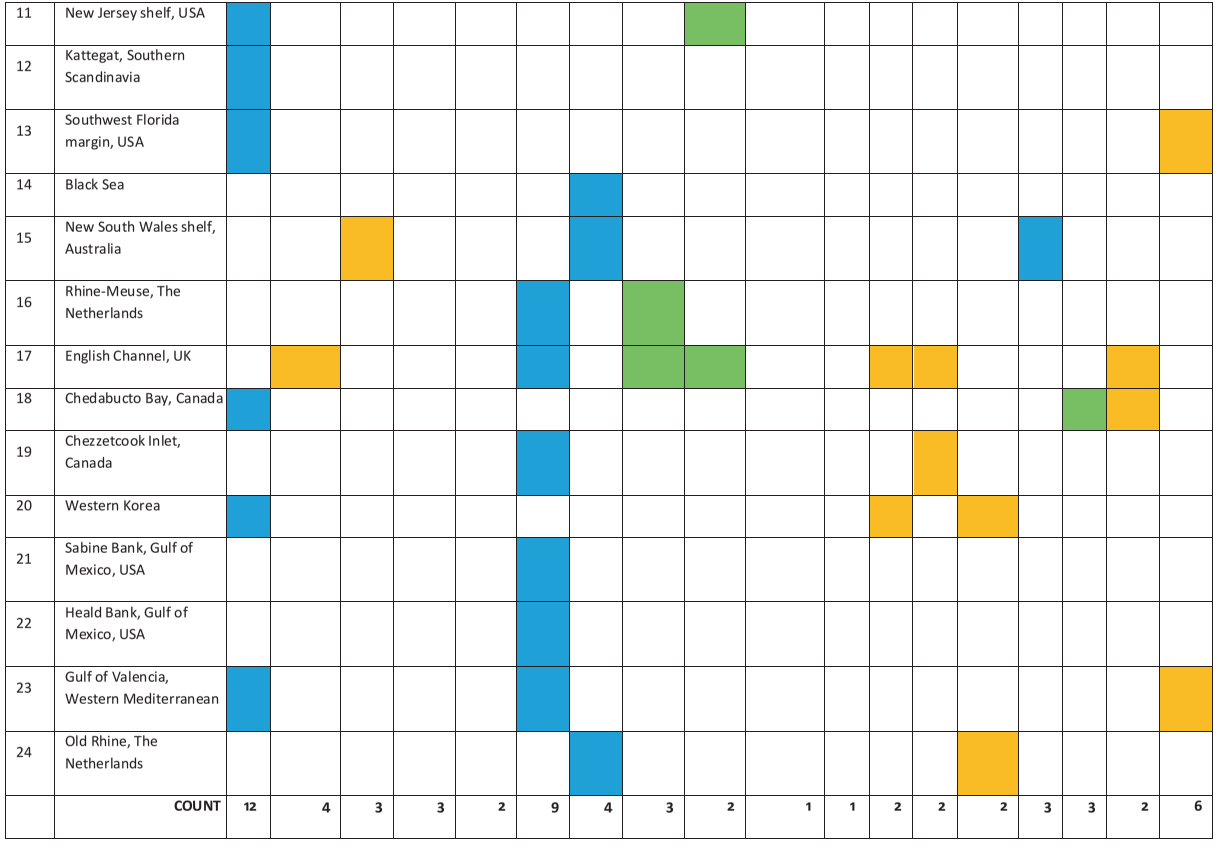

11	New Jersey shelf, USA																		
12	Kattegat, Southern Scandinavia																		
13	Southwest Florida margin, USA																		
14	Black Sea																		
15	New South Wales shelf, Australia																		
16	Rhine-Meuse, The Netherlands																		
17	English Channel, UK																		
18	Chedabucto Bay, Canada																		
19	Chezzetcook Inlet, Canada																		
20	Western Korea																		
21	Sabine Bank, Gulf of Mexico, USA																		
22	Heald Bank, Gulf of Mexico, USA																		
23	Gulf of Valencia, Western Mediterranean																		
24	Old Rhine, The Netherlands																		
	COUNT	12	4	3	3	2	9	4	3	2	1	1	2	2	2	3	3	2	6

RSL components given in blue, topographic components in green and sediment supply controls represented in orange

Transgression is the landward movement of the shoreline and whilst it can be driven by RSLR, it can be moderated by sediment budget (Curray 1964). Under any given rate of RSLR where there is no significant change in sediment supply, transgression will be more rapid on a shallow slope when compared to a steep slope. This important topographic influence on the rate of transgression has been acknowledged as a driver of barrier overstepping (Nordfjord et al. 2009; Mellett et al. 2012a). Rapid transgression can also occur if a topographic barrier is breached/overtopped. For example, barrier overstepping in Bras d'Or Lakes, Canada is interpreted to have occurred when a topographic sill was exceeded or breached, allowing the basin in which the barrier was located to flood rapidly (Shaw et al. 2009).

Based on the systematic review, the role of sediment supply is considered subordinate to topographic and RSL controls in driving barrier retreat. Sediment supply is recognized as a control at only four locations (Table 3). Two modes of sediment supply are identified as a driver of overstepping. Traditionally, barriers are interpreted to drown when RSLR outpaces sediment supply (Curray 1964; Swift 1968; Rampino and Sanders 1980). This mode of overstepping is referred to here as 'sediment deficit' overstepping and has been identified at two locations (Forbes et al. 1991; Mellett et al. 2012a). A 'sediment surplus' mode was also recognized by Mellett et al. (2012a) where sediment supply to the shoreface during transgression is sufficient to prevent substantial reworking of the barrier, and retreat is achieved through overstepping (i.e., in this case a new barrier rapidly becomes established at a more landward position, see additional discussion in Sect. 6.2). High sediment supply in relation to accommodation driven by a small tidal amplitude or prism was recognized as a driver of barrier overstepping at two locations (Rieu et al. 2005; Yang et al. 2006). In these examples, local hydrodynamics are considered alongside the more common drivers of barrier response.

Whilst topography (coastal slope) can influence the rate of transgression, the morphology of the back-barrier, which partly governs accommodation and rate of transgression, is acknowledged for its role in influencing barrier retreat. When back-barrier accommodation is large, sediment reworked from the shoreface, and transported across-shore, fills the space, preventing the barrier from retreating through *rollover*, effectively pinning the barrier in place (Mellett et al. 2012a). Tidal amplitude moderates back-barrier accommodation and, as a result, is recognized as a control on barrier retreat (Storms et al. 2008; Hijma et al. 2010).

5.4 Barrier Preservation

The style of barrier retreat in part governs the preservation of the barrier during RSLR (Sect. 2). However, a number of conditions have been identified that increase the preservation potential of the barrier during drowning or after submergence. These conditions create a bias that is independent of the processes that drive barrier overstepping.

A scenario in which overall RSLR is punctuated by a short-lived phase of RSL fall has been interpreted to increase preservation of barrier systems (Jensen and Stecher 1992; Browne 1994). In this case, as the shoreline moves seaward (regression) the barrier system becomes stranded on land and becomes at least partly disconnected from the sea (or lake). If the subsequent transgression is rapid and the barrier does not have time to equilibrate morphodynamically (i.e. retreat by rollover), the barrier is drowned and becomes stranded offshore of the advancing shoreline. After submergence, near- and offshore hydrodynamics rework the barrier system, removing or degrading evidence of its existence. Local topography can enhance preservation potential where it shelters a barrier from, or modifies, the hydrodynamic regime (tides and waves) (Jensen and Stecher 1992; Forbes et al. 1995; Kelley et al. 2010, 2013).

The characteristics of sediment can support preservation of the barrier either during or after submergence. Coarse clastic (gravel-dominated) barrier systems have greater morphological resilience to rising sea levels which must be overcome for the barrier to retreat through *rollover* (Forbes et al. 1995; Orford and Anthony 2011). As a result gravel barriers are more likely to retreat by overstepping when compared to sand-dominated ones. Barriers preserved in subtropical latitudes have been cemented by biological and chemical processes (Albarracín et al. 2013; Green et al. 2012, 2013; Salzmanm et al. 2013) or capped by reef communities (Jarrett et al. 2005). This geochemical or biogenic cementation has been interpreted to increase barrier preservation, making it more difficult to rework the barrier during or after transgression.

6 Relative Significance of Controls on Barrier Overstepping

Reflecting on the examples outlined in Sect. 5, and the evidence on which barrier response has been interpreted, here we consider the relative importance of RSLR, sediment supply, and topography/antecedence in determining the style of barrier retreat.

6.1 Relative Sea-Level Rise

A general assumption is that barriers drown when the rate of RSLR is high (Swift and Moslow 1982; Leatherman et al. 1983). Eleven of the 13 dated examples described in Sect. 5 have depositional ages ranging from 10.5 to 4.5 ka spanning both the early Holocene when rates of RSLR were high, and the mid Holocene when rates began to slow (Fig. 4). As is it not always possible to date drowning events due to their erosive nature, these ages record the existence of a barrier prior to overstepping, hence the minimum age of drowning is taken as the maximum age of deposition of barrier sediments. It is recognized that this assumption does not

account for spatial variations in barrier behaviour (e.g. alongshore progradation or erosion). The age of drowning may also be overestimated due to removal of younger sediment during and after submergence. Furthermore, the lag time between forcing and barrier response is unknown; some barriers may respond immediately to enhanced forcing from RSLR, others might exhibit substantial delay before breaking down, thus making it hard to constrain the timing or duration of overstepping. In light of this, it can be inferred from the examples presented here that barrier drowning occurred during the early to mid-Holocene transition, incorporating episodes of both rapidly rising and decelerating global sea-level rise. The compilation of barrier age and elevation in relation to relative sea-level history is of interest as: a) it implies that barriers are able to develop even under rapid RSLR, as occurred in the early Holocene, although their persistence and thickness is expected to be low; and b) barrier overstepping can occur when rates of RSLR are slowing. These observations can be tested through further research into the threshold RSLR rates for retreat through overstepping.

Aside from sediment supply and topography, regional RSLR can explain the variability observed in the age of drowned barriers shown in Fig. 4, particularly when the effects of glacio-isostasy are considered. For example, in the Gulf of Maine, despite rapidly rising global sea level during the early Holocene, isostatic rebound generated a local relative sea-level stillstand that lasted ca. 3.5 ka (Kelley et al. 2010). During this stillstand the barrier system developed and was later overstepped as rates of RSLR began to rise. At this location, local RSLR can be isolated as a driver of barrier overstepping (Kelley et al. 2010, 2013). However, this control can only be identified where well-constrained (vertical and temporal) RSLR data are available.

The timing of barrier drowning identified above overlaps with the timing of initiation of worldwide marine deltas from ca. 8.5 to 6.5 ka (Stanley and Warne 1994), where radiocarbon-dated deltaic sequences document the landward migration or ‘pinning’ of coastal depositional environments. The dated barrier sequences reviewed here corroborate this global landward advance of shorelines during the early- to mid-Holocene transition as rates of SLR decelerate and ‘modern’-day barrier systems become established.

Chronological information implies that some of the barriers drowned in the mid-Holocene when rates of RSLR were waning. Despite this deceleration, it is likely that rates of RSLR remained high enough during this time to exceed a modelled threshold for overstepping of c.3 mm/year (cf. Storms et al. 2002). Whilst the rate in itself is important in controlling the mode of barrier response, a change in rate driven by a sudden pulse or ‘jump’ in sea level, such as those associated with meltwater events (Liu and Milliman 2004), may provide additional impetus for barrier overstepping. To test ‘sea-level jumps’ as drivers of barrier process-response, a high-resolution barrier chronology (e.g. Hijma and Cohen 2010) is essential. In the absence of such chronological constraint, it is not possible to exclude other factors in moderating barrier drowning.

6.2 Sediment Supply

During transgression, sediment supply rates can substantially alter barrier response to RSLR (cf. Curray 1964; Murray and Moore this volume). For example, during sea-level rise, continued barrier rollover is in part driven by a net sediment loss where the barrier has to migrate landward to extract sediment from the shoreface to maintain its geometry despite the rising sea level (Moore et al. 2010; Murray and Moore this volume). Using the drowned barrier examples in Sect. 5, sediment supply can be separated into a number of components that condition overstepping, namely sediment availability, sediment transport (wave and tide regime), sediment volume (relative to accommodation) and sediment properties (grain size and cementation). However, the relative significance—or, indeed, combination—of these sediment-related factors in governing the style of barrier retreat cannot be determined from the sedimentological or stratigraphic evidence alone.

The elevations at which the drowned barrier examples are found implies that they formed during post-glacial RSLR and are not relicts from sea-level stillstand(s) during the last glacial (Fig. 4). Sediment supply to these barriers must therefore have been sufficient to outpace rapidly rising post-glacial RSLR, allowing the barrier systems to aggrade or even prograde (e.g. Mellett et al. 2012a). During transgression when the overall trajectory of shoreline migration is from offshore to onshore, the availability of sediment on the continental shelf can be of greater importance than that being delivered from land due to coastal erosion and/or riverine input (e.g. Long et al. 1996; Cowell and Kinsela this volume). These seabed sediment 'reserves' are the product of processes and environments that prevailed before and during RSLR. For example, sediment availability is high in formerly glaciated or paraglacial areas (Forbes et al. 1995; Kelley et al. 2010, 2013) and in basins connected to large deltas where significant thicknesses of sediment associated with falling stage systems tracts have accumulated on the continental shelf (e.g. Anderson et al. 2014), though deltaic sediments may contain limited sand. These environments may be predisposed to barrier retreat through overstepping in that full recycling of the barrier sediment volume, i.e. rollover, is not a requirement as there are large volumes of sediment available to facilitate coastal-response without significant reworking.

Prevailing nearshore and coastal hydrodynamics are also an important consideration in relation to barrier sediment supply. For example, significant vertical and shore-normal changes in water level associated with a large tidal amplitude (or prism) can encourage barrier overstepping (Rieu et al. 2005; Storms et al. 2008). Reconstructing past hydrodynamics to understand their interaction with different styles of barrier retreat is difficult, because there is little evidence of past hydrodynamic conditions available in the geologic record.

With respect to sediment grain size, it is expected that gravel-dominated barriers will be more morphologically resistant to RSLR (Orford 2011), because their larger grain size makes rollover less likely. Thus, these barrier systems exhibit greater potential for overstepping. In cases, where a barrier system has been overstepped

during post-glacial RSLR and the barrier beach component of the system is preserved, it is possible to determine the predominant sediment composition (gravel vs. sand). However, when a barrier retreats and only back-barrier sediments are preserved, i.e. the barrier beach component has been removed, it is not possible to establish the sediment composition of the former barrier. The best preserved drowned barriers are gravel dominated (e.g. Forbes et al. 1995; Mellett et al. 2012a) or have been cemented into beachrock (e.g. Green et al. 2012, 2013; Salzmanm et al. 2013).

When sufficient sediment is available and nearshore/coastal hydrodynamics have the ability to transport it, the evolution of a barrier system—and, indeed, its preservation on the sea bed—depends on the interaction between sediment supply and RSLR. Where there is a deficit in sediment supply (or translation potential) relative to RSLR, the barrier degrades and drowns as it cannot meet the pace of retreat through rollover, which relies on sediment translation from the shoreface to the back-barrier. Alternatively, barrier overstepping can be supported by a 'surplus' of sediment where high sediment supply maintains the shoreface and prevents the barrier from recycling itself through erosion of the underlying substrate. Under these conditions, the barrier shoreface maintains its seaward position and elevation despite rising sea levels. Meanwhile, overwash continues to transport sediment landward increasing barrier width until a morphodynamic threshold is reached and the barrier 'jumps' landward. In this case, a new barrier begins to form landward and the former features become stranded below the influence of waves and tidal currents (e.g. Mellett et al. 2012a). This 'sediment surplus' mode of overstepping appears to support exceptional preservation of drowned barriers. The thickness or volume of sediment within the barrier-system deposits relative to the depth of reworking (or depth of ravinement) during transgression also plays a role in determining preservation of the barrier. It is apparent that there is no single style of barrier response with respect to interactions between RSLR and sediment supply, especially as the latter can be both a limiting and enabling factor.

6.3 Topography/Antecedence

Topography that is largely an artefact of past geological and glacial-interglacial processes is considered antecedent and is a fixed control on barrier evolution. Antecedent topography governs substrate slope which, for a given rate of RSLR, determines the rate of transgression (cf. Curray 1964), i.e. the pace and distance over which a barrier migrates. Many of the barriers discussed in this review rest unconformably on different types of deposits from the last glacial stage (e.g., bedrock planation surfaces, Mellett et al. 2012a; undulating glacigenic landscapes, Kelley et al. 2010, 2013; incised valleys, Rodriguez et al. 1999; and deltaic systems, Gardner et al. 2005) and thus barrier form and thickness vary considerably. This variation in substrate slope and antecedent lithology, which is a local phenomenon, plays a significant role in determining the style of coastal retreat.

In addition to being static, topography can also be dynamic, changing as the barrier morphodynamically adjusts to RSLR (Rieu et al. 2005). Topography essentially provides the 'space' for sediment to occupy as a barrier responds to RSLR, i.e. accommodation. In this respect, barrier retreat is fundamentally governed by the balance between the evolving back-barrier accommodation and sediment supply. Rapid barrier drowning by overstepping can be assisted by large back-barrier accommodation due to disequilibrium between sedimentation at the shoreface and in the back-barrier (e.g. Storms et al. 2008; Hijma et al. 2010). In this case, the barrier becomes anchored as any overwash sedimentation is lost to the accommodation space, whilst RSLR continues, relocating the shoreline further landward.

Accommodation created by tidal inlets may be antecedent if the barrier occupies former lowstand fluvial valleys (Rodriguez et al. 1999; Anderson et al. 2014), or may become modified as the barrier evolves morphodynamically (Rieu et al. 2005). In either case, the presence of a large inlet can restrict sediment in both cross-shore and alongshore directions and act as a sink in a similar way to a back-barrier lagoon (FitzGerald et al. 2008, this volume; Mellett et al. 2012a). Whilst the inlet remains unfilled, barrier migration is interrupted. If RSLR continues whilst cross-barrier sediment flux is diverted to inlet infilling, accommodation in the back-barrier is maintained or increases. Therefore, depending on the duration of this infilling phase, barrier overstepping may be encouraged by creation of 'excess' accommodation that would otherwise be met by sediment supply if it were not being diverted to infilling.

Topography can therefore play an important role in barrier response by 'trapping' the barrier in place and preventing retreat through rollover. Furthermore, should a barrier experience progradation, for example due to an increase in sediment supply, the topography offshore can also pin a barrier in place if shoreface accommodation is too great (Mellett et al. 2012a).

7 Prerequisites for Barrier Retreat Through Overstepping

A number of conditions have been identified that lead to barrier retreat through *overstepping*. Isolating a single, predominant driver or control is problematic because the sedimentological, stratigraphic and chronological data obtained from the offshore geological record provide evidence of net landform response. In short, the interaction of RSLR, sediment supply and topography cannot readily be deconstructed, especially as wave climate and storm magnitude/frequency have an important moderating effect on barrier response. Despite this limitation, it is still possible to recognize local conditions that make barriers vulnerable to overstepping.

In a shore-normal sense, barrier response to SLR can be framed simply as an interaction between barrier forcing and barrier inertia (cf. Carter 1988). Barrier forcing mechanisms include coastal hydrodynamics (waves and tides), superimposed on an underlying trend in RSLR and punctuated by aperiodic storms (and in some locations, tsunami). As such, not all forcing mechanisms produce the same barrier response because they operate over different scales of time and space

(Cowell and Thom 1994) and induce different morphodynamic responses (Wright and Thom 1977; Prime et al. 2016). For example, a change in storm regime and/or wave climate is likely to cause significant changes in the translation of sediment from the shoreface to the back-barrier. Where cross-shore sediment transport is enhanced, or depth of ravinement is higher, retreat through *rollover* would be expected. However, while one component of barrier forcing can encourage *rollover*, another component, RSLR, has the potential to drown a barrier through overstepping in the absence of any substantial landward translation of sediment (Roy et al. 1994; Plater et al. 2009).

Barrier inertia is largely controlled by local topography and sediment grain size (Cowell et al. 1991; Roy et al. 1994). These are factors that moderate the translation of sediment from the foreshore to the backshore either geometrically, e.g. barrier elevation and cross-section, or dynamically, by slowing sediment-transport rates. Barrier *rollover* occurs when the landward translocation of sediment by waves and storms (a component of barrier forcing) exceeds barrier inertia, enabling coastal hydrodynamics to relocate and reshape a transgressing barrier without any restrictions from topographic constraints or grain size limitations. In comparison, overstepping is facilitated when conditions support high barrier inertia, making it difficult for a barrier system to be translated dynamically under any given combination of forcing factors, and especially when rates of RSLR are high. First order controls considered to enhance barrier inertia include; (1) coarse grain size, (2) cemented barrier sediments, (3) high sediment supply (positive net sediment budget), (4) topographic pinning (e.g. morphological obstruction, barrier thickness), and (5) rapid increase in accommodation driven by back-barrier topography and coastal slope. In this respect, the morphological resistance of barriers to RSLR is not directly comparable to barrier 'resilience' because any dynamic response is limited by high barrier inertia. Resilient barriers are those that can respond dynamically to perturbations such as change in the rate of RSLR and return to their pre-existing state, hence they have a greater chance to retreat by *rollover*.

Here, we demonstrate that the relationship between barrier forcing and barrier inertia is complex, making it difficult to predict coastal-response under given conditions. However, we recognize that forcings can both encourage (e.g. via high waves and frequent storms) and limit (e.g. via high RSLR rates) the dynamic, landward translation of barrier sediment, and we predict that barriers with high inertia are more likely to be overstepped under the same barrier forcing as those with low inertia.

Because the examples we present are early- to mid-Holocene drowned barriers from the continental shelf, the influence of human activity on the coast has not been recognized in this review. However, it is possible to evaluate scenarios in which human activity can potentially increase barrier inertia by modifying one or more of the first order controls. For example, coastal defence strategies such as beach replenishment provide an additional supply of sediment of potentially more resistant grain size that may enhance barrier inertia, increasing the potential for overstepping and making coastal resources more vulnerable to catastrophic exceedance/breakdown. In addition, emplacement of engineering structures, such as rock armouring or seawalls, can 'pin' a barrier, preventing it from responding to RSLR dynamically; this

activity increases barrier resistance whilst reducing its resilience (see also McNamara and Lazarus this volume; Murray and Moore this volume).

To ensure sustainable management of the coast, it is important to identify environmental conditions that would cause barrier retreat through overstepping. It is possible to parameterize antecedent topography (onshore and offshore) and apply RSLR projections to calculate accommodation. The much greater challenge lies in understanding sediment regimes and how they interact with accommodation under different RSLR scenarios, especially where the rate of RSLR is potentially punctuated and sediment supply is modified by human intervention. The dynamic component of sediment supply in terms of the ability of the barrier to rework and resupply itself through ravinement (governed by hydrodynamics and barrier inertia), and the availability of sediment determined by barrier size and thickness, needs to be considered (see Murray and Moore this volume). Furthermore, the relative importance of dynamic vs. antecedent topography in moderating barrier retreat needs to be evaluated. Predicting barrier retreat relies heavily on numerical and simulation models (Moore et al. 2010; Williams et al. 2012; Lorenzo-Trueba and Ashton 2014; McCall et al. 2014; Brenner et al. 2015) but these should be calibrated with geomorphological and sedimentological evidence from drowned barrier archives preserved on the continental shelf.

The role of barrier forcing processes other than RSLR, such as wave climate and storm magnitude/frequency, is underrepresented in this review. Whilst the importance of waves in determining barrier behaviour is widely recognized (e.g. Orford et al. 1991, 2002; Roy et al. 1994; Masselink et al. 2010), it is not possible to resolve storm history using the offshore evidence base and palaeotidal and palaeowave models are replied upon (e.g. Storms et al. 2008). Here, we consider RSLR, sediment supply and topography/accommodation as the main drivers of barrier response. However, this is because our analysis does not capture event-based (storm-driven) coastal-response. Indeed, this is a general shortcoming of current chronological constraints on submerged barriers and is a key limitation of applying lessons over geological and glacial/interglacial timescales to contemporary, resource management timescales. Despite this limitation, we can still provide detail on coastal settings where barrier retreat through overstepping is more likely, although it is not possible to predict whether this overstepping will be temporary (storm impacts, mendable breaches) or permanent (longer-term change that is beyond the reach of engineering solutions).

Overstepping as a scenario of shoreline retreat is currently not considered in shoreline management strategies and the impact of such process-response to RSLR on the coastal zone is unknown. Depending on the coastal setting, overstepping may have a positive or negative influence. For example, a barrier stranded offshore of the shoreline may act as a shoal, intercepting and dissipating incoming wave energy and hence offering natural morphological protection. Alternatively, a barrier (or barrier sediments) that become stranded would serve to remove large volumes of sand from the coastal sediment budget (e.g. Anderson et al. 2014) which can perturb the system with feedback implications.

8 Conclusions

There are increasingly more examples of drowned barriers being discovered on continental shelves suggesting these features are not as rare as once thought. This style of coastal process-response to RSLR, i.e. in situ drowning by overstepping, which was previously relatively poorly understood due to a lack of suitable examples, should be considered in shoreline management plans. Evidence from drowned barriers preserved on the continental shelf shows there is no predominant driver of barrier overstepping. Whilst it is possible to identify conditions that would facilitate barrier retreat through overstepping, these conditions are not in operation simultaneously nor are they evident across all coastal settings. Site-specific local conditions, such as antecedent topography and sediment supply, may therefore outweigh any widespread forcing of change, e.g. global SLR. Barrier drowning can be facilitated by the rapid rates of sea-level rise that may be achieved under future climate change projections. However, it is the interaction between RSLR, topography and sediment supply on a local scale that conditions the style of retreat. As such, it is difficult to establish a widely applicable 'recipe' for barrier overstepping. Aside from the value of submerged, offshore examples in framing our understanding of barrier overstepping and testing numerical models, resolving system interactions should be a priority for coastal research to improve the reliability of predictions of barrier response to RSLR and thus ensure sustainable management of the coast.

Acknowledgements The authors would like to thank the editors of this volume for inviting this review and their comments on the manuscript. We would also like to thank John Anderson and an anonymous reviewer for their input which improved the manuscript. Chris Thomas is thanked for his review. This research is published with the permission of the Executive Director of the British Geological Survey (BGS) and was supported in part by BGS's Marine Geoscience research programme.

References

Albarracín S, Alcántara-Carrió J, Barranco A, García MJS, Bouzas AF, Salgado JR (2013) Seismic evidence for the preservation of several stacked Pleistocene coastal barrier/lagoon systems on the Gulf of Valencia continental shelf (western Mediterranean). Geo-Mar Lett 33:217–223

Anderson JB, Wallace DJ, Simms AR, Rodriquez AB, Miliken KT (2014) Variable response of coastal environments of the northwestern Gulf of Mexico to sea-level rise and climate change: implications for future change. Mar Geol 352:348–366

Belknap DF, Kraft JC (1981) Preservation potential of transgressive coastal lithosomes on the US Atlantic shelf. Mar Geol 42:429–442

Bennike OLE, Jensen JBO, Konradi PB, Lemke W, Heinemeier JAN (2000) Early Holocene drowned lagoonal deposits from the Kattegat, southern Scandinavia. Boreas 29:272–286

Billy J, Robin N, Hein CJ, Certain R, FitzGerald DM (2015) Insight into the Late Holocene sea-level changes in the NW Atlantic from a paraglacial beach-ridge plain south of Newfoundland. Geomorphology 248:134–146

Blum MD, Roberts HH (2009) Drowning of the Mississippi Delta due to insufficient sediment supply and global sea-level rise. Nat Geosci 2:488–491

Brenner OT, Moore LJ, Murray AB (2015) The complex influences of back-barrier deposition, substrate slope and underlying stratigraphy in barrier island response to sea-level rise: insights from the Virginia Barrier Islands, Mid-Atlantic Bight, USA. Geomorphology 246:334–350

Brooks GR, Doyle LJ, Suthard BC, Locker SD, Hine AC (2003) Facies architecture of the mixed carbonate/siliciclastic inner continental shelf of west-central Florida: implications for Holocene barrier development. Mar Geol 200:325–349

Browne I (1994) Seismic stratigraphy and relict coastal sediments off the east coast of Australia. Mar Geol 122:81–107

Carter RWG (1988) Coastal environments. Academic Press, London

Cattaneo A, Steel RJ (2003) Transgressive deposits: a review of their variability. Earth Sci Rev 62:187–228

Church JA, Clark PU, Cazenave A, Gregory JM, Jevrejeva S, Levermann A, Merrifield MA, Milne GA, Nerem RS, Nunn PD, Payne AJ, Pfeffer WT, Stammer D, Unnikrishnan AS (2013) Sea level change. In: Stocker TF, Qin D, Plattner JK, Tignor M, Allen SK, Boschung J, Nauels A, Xia Y, Bex V, Midgley PM (eds) Climate change 2013: the physical science basis. Contribution of Working Group I to the Fifth Assessment Report of the Intergovernmental Panel on Climate Change. Cambridge University Press, Cambridge

Clark JA, Farrell WE, Peltier WR (1978) Global changes in postglacial sea level: a numerical calculation. Quat Res 9:265–281

Cowell PJ, Kinsela MA (2018) Shoreface controls on barrier evolution and shoreline change. In: Moore LJ, Murray AB (eds) Barrier dynamics and response to changing climate. Springer, New York

Cowell PJ, Thom BG (1994) Morphodynamics of coastal evolution. In: Carter RWG, Woodroffe CD (eds) Coastal evolution: late quaternary shoreline morphodynamics. Cambridge University Press, Cambridge, pp 33–86

Cowell PJ, Roy PS, Jones RA (1991) Shoreface translation model: application to management of coastal erosion. In: Brierley G, Chappell J (eds) Applied quaternary studies, biogeography and geomorphology. Australian National University, Canberra, pp 57–73

Curray JR (1964) Transgression and regression. In: Miller RL (ed) Papers in marine geology. Macmillan Company, New York, pp 175–203

Feagin RA, Sherman DJ, Grant WE (2005) Coastal erosion, global sea-level rise, and the loss of sand dune plant habitats. Front Ecol Environ 3:359–364

Fenster MS, Dolan R, Elder JF (1993) A new method for predicting shoreline positions from historical data. J Coast Res 9(1):147–171

FitzGerald DM, Fenster MS, Argow BA, Buynevich IV (2008) Coastal impacts due to sea-level rise. Annu Rev Earth Planet Sci 36:601–647

FitzGerald DM, Hein C, Hughes Z, Kulp M, Georgiou I, Miner M (2018) Runaway barrier island transgression concept: global case studies. In: Moore LJ, Murray AB (eds) Barrier dynamics and response to changing climate. Springer, New York

Forbes DL, Taylor RB, Orford JD, Carter RWG, Shaw J (1991) Gravel-barrier migration and overstepping. Mar Geol 97:305–313

Forbes DL, Orford JD, Carter RWG, Shaw J, Jennings SC (1995) Morphodynamic evolution, self-organisation, and instability of coarse-clastic barriers on paraglacial coasts. Mar Geol 126:63–85

Gardner JV, Dartnell P, Mayer LA, Hughes Clarke JE, Calder BR, Duffy G (2005) Shelf-edge deltas and drowned barrier island complexes on the Northwest Florida outer continental shelf. Geomorphology 64:133–166

Gardner JV, Calder BR, Hughes Clarke JE, Mayer LA, Elston G, Rzhanov Y (2007) Drowned shelf-edge deltas, barrier islands and related features along the outer continental shelf north of the head of De Soto Canyon, NE Gulf of Mexico. Geomorphology 89:370–390

Gibbons SJA, Nicholls RJ (2006) Island abandonment and sea-level rise: An historical analog from the Chesapeake Bay, USA. Glob Environ Change 16:40–47

Goodman B, Reinhardt E, Dey H, Boyce J, Schwarcz H, Sahoglu V, Erkanal H, Artzy M (2008) Evidence for Holocene marine transgression and shoreline progradation due to barrier development in Iskele, Bay of Izmir, Turkey. J Coast Res 245:1269–1280

Green A, Leuci R, Thackeray Z, Vella G (2012) Number One Reef: an overstepped segmented lagoon complex on the KwaZulu-Natal continental shelf. S Afr J Sci 108:1–5

Green AN, Cooper JAG, Leuci R, Thackeray Z (2013) Formation and preservation of an overstepped segmented lagoon complex on a high-energy continental shelf. Sedimentology 60:1755–1768

Haigh ID, Wahl T, Rohling EJ, Price RM, Pattiaratchi CB, Calafat FM, Dandendorf S (2014) Timescales for detecting a significant acceleration in sea level rise. Nat Commun 5:3635

Hede MU, Bendixen M, Clemmensen LB, Kroon A, Nielsen L (2013) Joint interpretation of beach-ridge architecture and coastal topography show the validity of sea-level markers observed in ground-penetrating radar data. The Holocene 23(9):1238–1246

Hein CJ, FitzGerald DM, Thadeu de Menezes J, Cleary WJ, Klein AHF, Albernaz MB (2014) Coastal response to late-stage transgression and sea-level highstand. GSA Bull 126(3–4):459–480

Hijma MP, Cohen KM (2010) Timing and magnitude of the sea-level jump preluding the 8200 yr event. Geology 38:275–278

Hijma MP, van der Spek AJF, van Heteren S (2010) Development of a mid-Holocene estuarine basin, Rhine–Meuse mouth area, offshore The Netherlands. Mar Geol 271:198–211

Hill TM, Brooks GR, Duncan DS, Medioli FS (2003) Benthic foraminifera of the Holocene transgressive west-central Florida inner shelf: paleoenvironmental implications. Mar Geol 200:263–272

Jarrett BD, Hine AC, Halley RB, Naar DF, Locker SD, Neumann AC, Twichell D, Hu C, Donahue BT, Jaap WC, Palandro D, Ciembronowicz K (2005) Strange bedfellows—a deep-water hermatypic coral reef superimposed on a drowned barrier island; southern Pulley Ridge, SW Florida platform margin. Mar Geol 214:295–307

Jensen JB, Stecher O (1992) Paraglacial barrier—lagoon development in the late pleistocene Baltic Ice Lake, southwestern Baltic. Mar Geol 107:81–101

Jevrejeva S, Moore JC, Grinsted A, Matthews AP, Spada G (2014) Trends and acceleration in global and regional sea levels since 1807. Glob Planet Chang 113:11–22

Kelley JT, Belknap DF, Claesson SH (2010) Drowned coastal deposits with associated archaeological remains from a sea-level "slowstand": Northwestern Gulf of Maine, USA. Geology 38:695–698

Kelley JT, Belknap DF, Kelley AR, Claesson SH (2013) A model for drowned terrestrial habitats with associated archeological remains in the northwestern Gulf of Maine, USA. Mar Geol 338:1–16

Kraft KC (1971) Sedimentary facies patterns and geologic history of a Holocene marine transgression. GSA Bull 82:2131–2158

Leatherman SP, Rampino MR, Sanders JE (1983) Barrier island evolution in response to sea level rise; discussion and reply. J Sediment Res 53:1026–1033

Lentz EE, Hapke CJ, Stockdon HF, Hehre RE (2013) Improving understanding of near-term barrier island evolution through multi-decadal assessment of morphologic change. Mar Geol 337:125–139

Lericolais G, Popescu I, Guichard F, Popescu SM (2007) A Black Sea lowstand at 8500 yr B.P. indicated by a relict coastal dune system at a depth of 90 m below sea level. In: Harff J, Hay WW, Tetzlaff DM (eds) Coastline changes: interrelation of climate and geological processes. GSA Special Paper 426

Liu JP, Milliman JD (2004) Reconsidering melt-water pulses 1A and 1B: global impacts of rapid sea-level rise. J Ocean Univ China 3:183–190

Long AJ, Plater AJ, Waller MJ, Innes JB (1996) Holocene coastal evolution in the Eastern English Channel: new evidence from the Romney Marsh region, United Kingdom. Mar Geol 136:97–120

Lorenzo-Trueba J, Ashton A (2014) Rollover, drowning, and discontinuous retreat: Distinct modes of barrier response to sea-level rise arising from a simple morphodynamic model. J Geophys Res Earth Surf 119:779–801

Maselli V, Hutton EW, Kettner AJ, Syvitski JPM, Trincardi F (2011) High-frequency sea level and sediment supply fluctuations during Termination I: an integrated sequence-stratigraphy and modeling approach from the Adriatic Sea (Central Mediterranean). Mar Geol 287:54–70

Masselink G, Russell P, Blenkinsopp C, Turner I (2010) Swash zone sediment transport, step dynamics and morphological response on a gravel beach. Mar Geol 274(1):50–68

McBride RA, Byrnes MR (1997) Regional variations in shore response along barrier island systems of the Mississippi River delta plain: historical change and future prediction. J Coast Res 13(3):628–655

McCall RT, Masselink G, Poate TG, Roelvink JA, Almeida LP, Davidson M, Russell PE (2014) Modelling storm hydrodynamics on gravel beaches with XBeach-G. Coast Eng 91:231–250

McNamara DE, Lazarus ED (2018) Barrier islands as coupled human–landscape systems. In: Moore LJ, Murray AB (eds) Barrier dynamics and response to changing climate. Springer, New York

Mellett CL, Hodgson DM, Lang A, Mauz B, Selby I, Plater AJ (2012a) Preservation of a drowned gravel barrier complex: a landscape evolution study from the north-eastern English Channel. Mar Geol 315–318:115–131

Mellett CL, Mauz B, Plater AJ, Hodgson DM, Lang A (2012b) Optical dating of drowned landscapes: a case study from the English Channel. Quat Geochronol 10:201–208

Moore LJ, List JH, Williams SJ, Stolper D (2010) Complexities in barrier island response to sea-level rise: insights from model experiments. J Geophys Res Earth Surf 115:F03004

Morton RA, Miller T, Moore L (2005) Historical shoreline changes along the US Gulf of Mexico: a summary of recent shoreline comparisons and analyses. J Coast Res 21(4):704–709

Murray AB, Moore LJ (2018) Geometric constraints on long-term barrier migration: from simple to surprising. In: Moore LJ, Murray AB (eds) Barrier dynamics and response to changing climate. Springer, New York

Nordfjord S, Goff JA, Austin JA Jr, Duncan LS (2009) Shallow stratigraphy and complex transgressive ravinement on the New Jersey middle and outer continental shelf. Mar Geol 266:232–243

Novak B (2002) Early Holocene brackish and marine facies in the Fehmarn Belt, southwest Baltic Sea: depositional processes revealed by high-resolution seismic and core analysis. Mar Geol 189:307–321

Odezulu CI, Lorenzo-Trueba J, Wallace DJ, Anderson JB (2018) Follets Island: a case of unprecedented change and transition from rollover to subaqueous shoals. In: Moore LJ, Murray AB (eds) Barrier dynamics and response to changing climate. Springer, New York

Orford JD (2011) Gravel-dominated coastal-barrier reorganisation variability as a function of coastal susceptibility and barrier resilience. In: Ping W (ed) Proceedings of the coastal sediments, vol 2. World Scientific Publishing Company, Singapore, pp 1257–1270

Orford JD, Anthony EJ (2011) Extreme events and the morphodynamics of gravel-dominated coastal barriers: strengthening uncertain ground. Mar Geol 290:41–45

Orford JD, Carter RWG, Forbes DL (1991) Gravel barrier migration and sea level rise: some observations from Story Head, Nova Scotia, Canada. J Coast Res 7(2):477–489

Orford JD, Forbes DL, Jennings SC (2002) Organisational controls, typologies and time scales of paraglacial gravel-dominated coastal systems. Geomorphology 48(1):51–85

Pilkey OH, Neal WJ, Riggs SR, Webb CA, Bush DM, Pilkey DF, Bullock J, Cowan BA (1998) The North Carolina shore and its barrier islands: restless ribbons of sand. Duke University Press, Durham. 344p

Plater AJ, Stupples P, Roberts HM (2009) Evidence of episodic coastal change during the Late Holocene: the Dungeness barrier complex, SE England. Geomorphology 104(1–2):47–58

Prime T, Brown JM, Plater AJ (2016) Flood inundation uncertainty: the case of a 0.5% annual probability flood event. Environ Sci Policy 59:1–9

Rampino MR, Sanders JE (1980) Holocene transgression in South-central Long Island, New York. J Sediment Res 50:1063–1079
Rampino MR, Sanders JE (1982) Holocene transgression in South-central Long Island, New York; reply. J Sediment Res 52:1020–1025
Rieu R, Van Heteren S, Van der Spek AJF, De Boer PL (2005) Development and preservation of a mid-Holocene tidal-channel network offshore the western Netherlands. J Sediment Res 75:409–419
Rodriguez AB, Meyer CT (2006) Sea-level variation during the Holocene deduced from the morphologic and stratigraphic evolution of Morgan Peninsula, Alabama, U.S.A. J Sediment Res 76(2):257–269
Rodriguez AB, Anderson JB, Fernando PS, Taviani M (1999) Sedimentary facies and genesis of Holocene sand banks on the East Texas inner continental shelf. In: Sneddin J, Bergman K (eds) Isolated shallow marine sand bodies, vol 64, SEPM Special Publication, pp 165–178
Rodriguez AB, Simms AR, Anderson JB (2010) Bay-head deltas across the northern Gulf of Mexico back step in response to the 8.2 ka cooling event. Quat Sci Rev 29:3983–3993
Rodriguez AB, Yu W, Theuerkauf EJ (2018) Abrupt increase in washover deposition along a transgressive barrier island during the late nineteenth century acceleration in sea-level rise. In: Moore LJ, Murray AB (eds) Barrier dynamics and response to changing climate. Springer, New York
Roy PS, Cowell PJ, Ferland MA, Thom BG (eds) (1994) Wave-dominated coasts. Coastal evolution: late quaternary shoreline morphodynamics. Cambridge University Press, Cambridge, pp 121–186
Saito Y (2001) Deltas in Southeast and East Asia: their evolution and current problems. In: Proceedings of the APN/SURVAS/LOICZ joint conference on coastal impacts of climate change and adaptation in the Asia–Pacific Region, 14–16th November 2000, Kobe, Japan, Asia Pacific Network for Global Change Research, pp 185–191
Salzmanm L, Green A, Cooper JAG (2013) Submerged barrier shoreline sequences on a high energy, steep and narrow shelf. Mar Geol 346:366–374
Shaw J, Fader GB, Taylor RB (2009) Submerged early Holocene coastal and terrestrial landforms on the inner shelves of Atlantic Canada. Quat Int 206:24–34
Smith DE, Harrison S, Firth CR, Jordan JT (2011) The early Holocene sea level rise. Quat Sci Rev 30:1846–1860
Stanley DJ, Warne AG (1994) Worldwide initiation of Holocene marine deltas by deceleration of sea-level rise. Science 265:228–231
Storms JEA, Weltje GJ, van Dijke JJ, Geel CR, Kroonenberg SB (2002) Process response modelling of wave-dominated coastal systems: simulating evolution and stratigraphy on geological timescales. J Sediment Res 72:226–239
Storms JEA, Weltje GJ, Terra GJ, Cattaneo A, Trincardi F (2008) Coastal dynamics under conditions of rapid sea-level rise: Late Pleistocene to Early Holocene evolution of barrier-lagoon systems on the northern Adriatic shelf (Italy). Quat Sci Rev 27:1107–1123
Swift DJP (1968) Coastal erosion and transgressive stratigraphy. J Geol 76:444–456
Swift DJP, Moslow TF (1982) Holocene transgression in south-central Long Island, New York; discussion. J Sediment Res 52:1014–1019
Swift DJP, Phillips S, Thorne JA (1991) Sedimentation on continental margins, V: parasequences. In: Swift DJP, Oertel GF, Tillman RW, Thorne JA (eds) Shelf sand and sandstone bodies—geometry. Facies and sequence stratigraphy. International Association of Sedimentologists Special Publication 14, pp 153–187
Tamura T (2012) Beach ridges and prograded beach deposits as palaeoenvironment records. Earth Sci Rev 114(3–4):279–297
Thanh TD, Saito Y, Huy DV, Nguyen VL, Oanh TKO, Tateishi M (2004) Regimes of human and climate impacts on coastal changes in Vietnam. Reg Environ Chang 4:49–62
Tornqvist TE, Hijma MP (2012) Links between early Holocene ice-sheet decay, sea-level rise and abrupt climate change. Nat Geosci 5:601–606

Williams JJ, Ruiz de Alegría-Arzaburu A, McCall RT, Van Dongeren A (2012) Modelling gravel barrier profile response to combined waves and tides using XBeach: laboratory and field results. Coast Eng 63:62–80

Wright LD, Thom BG (1977) Coastal depositional landforms: a morphodynamic approach. Prog Phys Geogr 1:412–459

Yang B, Dalrymple RW, Chun S, Lee H (2006) Transgressive sedimentation and stratigraphic evolution of a wave-dominated macrotidal coast, western Korea. Mar Geol 235:35–48

Barrier Island and Estuary Co-evolution in Response to Holocene Climate and Sea-Level Change: Pamlico Sound and the Outer Banks Barrier Islands, North Carolina, USA

David Mallinson, Stephen Culver, Eduardo Leorri, Siddhartha Mitra, Ryan Mulligan, and Stanley Riggs

Abstract Barrier islands and associated back-barrier estuaries and lagoons interact via hydrodynamic and sedimentary processes, affecting the evolution of both systems. Understanding coupled dynamic processes between both systems is vital to forecasts of future coastal morphologic and hydrodynamic changes in response to such factors as sea-level rise and storm patterns. The Pamlico Sound and the Outer Banks barrier islands of North Carolina, USA have co-evolved in response to Holocene climate and sea-level change, and autogenic processes. Recent data and models illustrate the dynamic response of this system to minor, but rapid, climate changes occurring throughout the Holocene, including the Medieval Climate Anomaly and Little Ice Age. Periods of extreme barrier segmentation occurred during times of rapid climate change, affecting tidal energy and salinity conditions within the Pamlico Sound. Hydrodynamic models aid in understanding the magnitude of changes, and the impact on barrier morphology. Future changes to coastal systems may be anticipated based upon changes that have occurred in the past.

Keywords Barrier island • Pamlico Sound • Outer Banks • North Carolina coast • Coastal evolution • Sea-level rise • Climate change • Hydrodynamic model • Coastal geology • Inlets

D. Mallinson (✉) • S. Culver • E. Leorri • S. Mitra • S. Riggs
Department of Geological Sciences, East Carolina University, Greenville, NC, USA
e-mail: mallinsond@ecu.edu; culvers@ecu.edu; leorrie@ecu.edu; mitras@ecu.edu; riggss@ecu.edu

R. Mulligan
Department of Civil Engineering, Queen's University, Kingston, ON, Canada
e-mail: ryan.mulligan@queensu.ca

L.J. Moore, A.B. Murray (eds.), *Barrier Dynamics and Response to Changing Climate*, https://doi.org/10.1007/978-3-319-68086-6_3

1 Introduction

More than 20,000 km of barrier islands with accompanying back-barrier estuaries or lagoons occur along the world's open ocean coasts (Stutz and Pilkey 2011) and are imminently vulnerable to the effects of projected climate change. The morphodynamics of barrier islands and associated estuaries or lagoons are linked via multiple feedbacks operating on subannual to millennial time-scales. Barrier systems (herein defined as the subaerial and subaqueous portions of barrier islands, barrier spits, inlets, and associated tidal deltas) exhibit variations in morphological and sedimentological characteristics in response to wave and tidal energy, the geologic framework, and sediment supply (Hayes 1979; Kraft et al. 1987; Inman and Dolan 1989; Oertel et al. 1992; Fenster and Dolan 1993; Riggs et al. 1995, 2009; Otvos and Carter 2008; Moran et al. 2015). The barrier system, in turn, controls the hydraulic connectivity between the back-barrier lagoon or estuary and the ocean, which imparts a control on the back-barrier processes (tides, waves, currents, salinity) and resultant morphology and ecosystems. Thus, geomorphic changes to barrier systems, particularly the number and width of inlets, or overtopping, greatly affect the hydrodynamics within the entire coastal system and have significant impacts on the characteristics of adjacent estuaries, mainland shorelines, and associated ecosystems. In short, changes to the barrier system may affect areas far-removed from the barriers themselves.

Changes to barrier-fronted coastal systems, resulting from climate processes (storminess, wind patterns, precipitation, etc.) or sea-level rise driven by climate change (see also Ashton and Lorenzo-Trueba this volume; Cowell and Kinsela this volume; FitzGerald et al. this volume; Murray and Moore this volume; Odezulu et al. this volume; Rodriguez et al. this volume), will likely have serious economic ramifications related to the disruption of biological, hydrological, and terrestrial resources, and accelerated mainland shoreline erosion. One way to understand the fate of coastal environments is to examine the changes that occurred in the past in response to sea-level rise and variability in storm patterns. Here, we describe the evolution of the Pamlico Sound estuary in North Carolina (NC) (Fig. 1a) in response to Holocene sea-level rise, climate changes, and barrier island changes, based on a synthesis of previous studies (e.g., Culver et al. 2007; Grand Pre et al. 2011; Mallinson et al. 2011; Clunies 2014; Zaremba et al. 2016). These studies used geological data, geomorphic models, and hydrodynamic models to evaluate the potential magnitude of change to tides and currents in response to known past major erosional episodes that have altered barrier island geomorphology.

2 Study Area

2.1 Modern Setting

Pamlico Sound (Figs. 1 and 2) is a composite estuary comprising the drowned river valleys of the Pamlico and Neuse Rivers, and the completely submerged paleodrainage system of paleo-Pamlico Creek (Riggs et al. 1995, 2000; Riggs and Ames 2003;

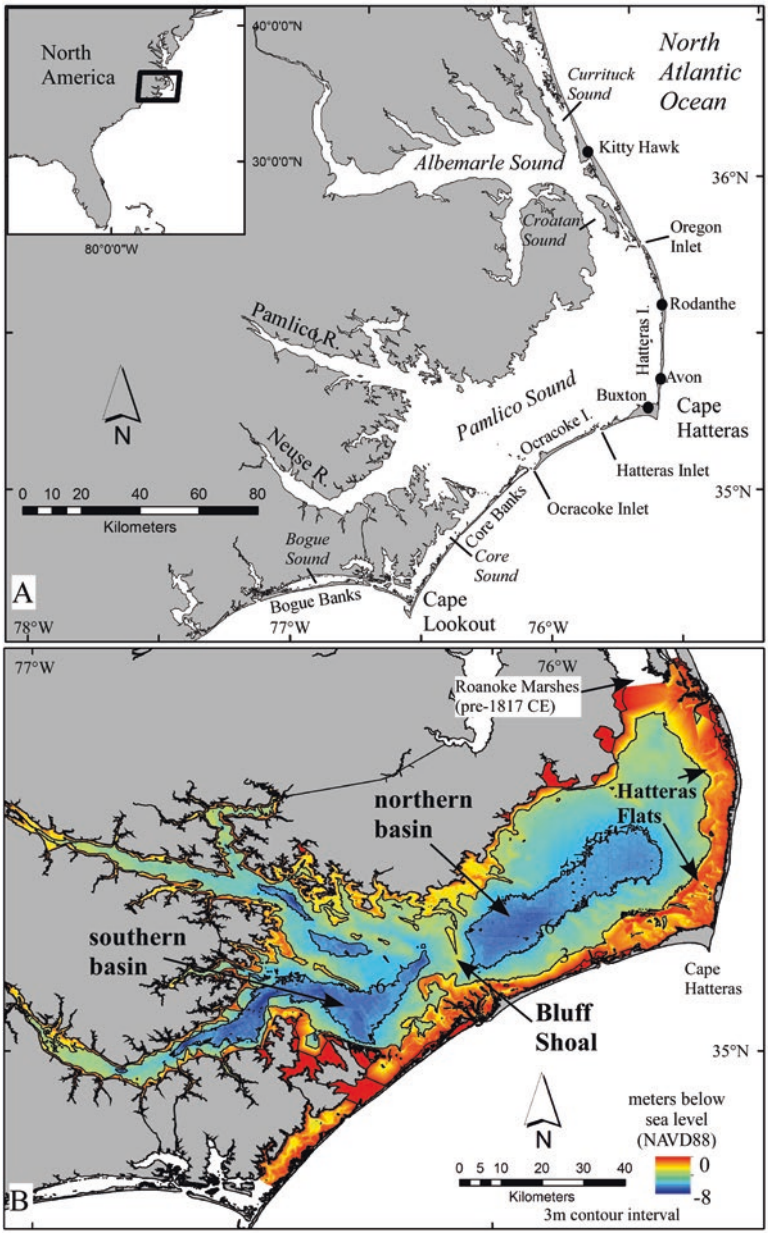

Fig. 1 (**a**) Location map showing the Albemarle-Pamlico estuarine system and the Outer Banks barrier islands of North Carolina. (**b**) Map showing the modern bathymetry within Pamlico Sound and important geomorphic features

Mallinson et al. 2010a, b). The two main basins (the northern and southern basins; Fig. 1b) of Pamlico Sound are related to the underlying paleotopographic surface (Fig. 2a), and together create a large estuary constrained by the wave-dominated southern Outer Banks barrier islands including, from north to south, Hatteras Island, Ocracoke Island and northern Core Banks (Fig. 1a). Albemarle and Pamlico Sounds were isolated drainage systems until the early nineteenth century (Riggs et al. 2000).

Salinity within Pamlico Sound varies seasonally, but generally ranges from nearly fresh in the upper regions of the Pamlico and Neuse Rivers to 34 PSU (Practical Salinity Unit) depending on river discharge and proximity to inlets (Wells and Kim 1989). Pamlico Sound is characterized by an astronomical tidal range of approximately 0.1 m, and basin-scale water level variations that are dominated by wind-forcing (Luettich et al. 2002). In contrast, the seaward side of the barriers is subject to tidal ranges of 0.3–1 m (microtidal), depending on location. These estuarine salinity and tidal characteristics arise from the combination of freshwater influx and presence of the Outer Banks barrier islands, which serve as a boundary to normal-marine-salinity waters and tides.

The Outer Banks barrier islands (here, defined as extending from the Virginia border to Cape Lookout) are separated by three major inlets (Oregon Inlet, Hatteras Inlet, and Ocracoke Inlet; Fig. 1a) that have remained active for >100 years, and a variable number of smaller inlets active on subannual to decadal timescales. A greater number of inlets were active during the Little Ice Age (LIA; Mallinson et al. 2011). However, it is not known to what extent the inlets temporally overlapped in terms of their activity. Most of these inlets had closed by 1817 AD (Stick 1958; Mallinson et al. 2011). The closure of these inlets impacted the hydrodynamics of the estuarine systems by restricting the influx of marine waters, which altered the circulation, salinity, and current patterns, and allowed hydraulic interchange between the Albemarle and Pamlico Sounds through the opening of Croatan Sound by 1817 (Riggs et al. 2000; Riggs and Ames 2003; Corbett et al. 2007).

The barrier islands fronting Pamlico Sound experience variations in energy (wave and tidal), morphology, and histories, depending on location. Inman and Dolan (1989) provide an excellent analysis of the sediment budget and processes impacting these islands. Mean significant wave height at Cape Hatteras is 1.2–1.3 m (Pendleton et al. 2004), and drives a net southerly longshore current and littoral transport that affects shoreline characteristics (Inman and Dolan 1989). The majority of the islands (70%) are erosional, with ocean shoreline retreat rates averaging circa (ca) 1.6 m/year between Oregon Inlet and Cape Hatteras (Inman and Dolan 1989; Riggs et al. 2011). Localized areas of accretion occur, most notably along the south-facing shore of Cape Hatteras (to 7 km west of the Cape).

2.2 Antecedent Topography

Antecedent topography strongly influences the morphology of the modern coastal system (Fig. 2a). The antecedent topographic surface is the flooded landscape shaped by surface processes during subaerial exposure in the late Pleistocene, and

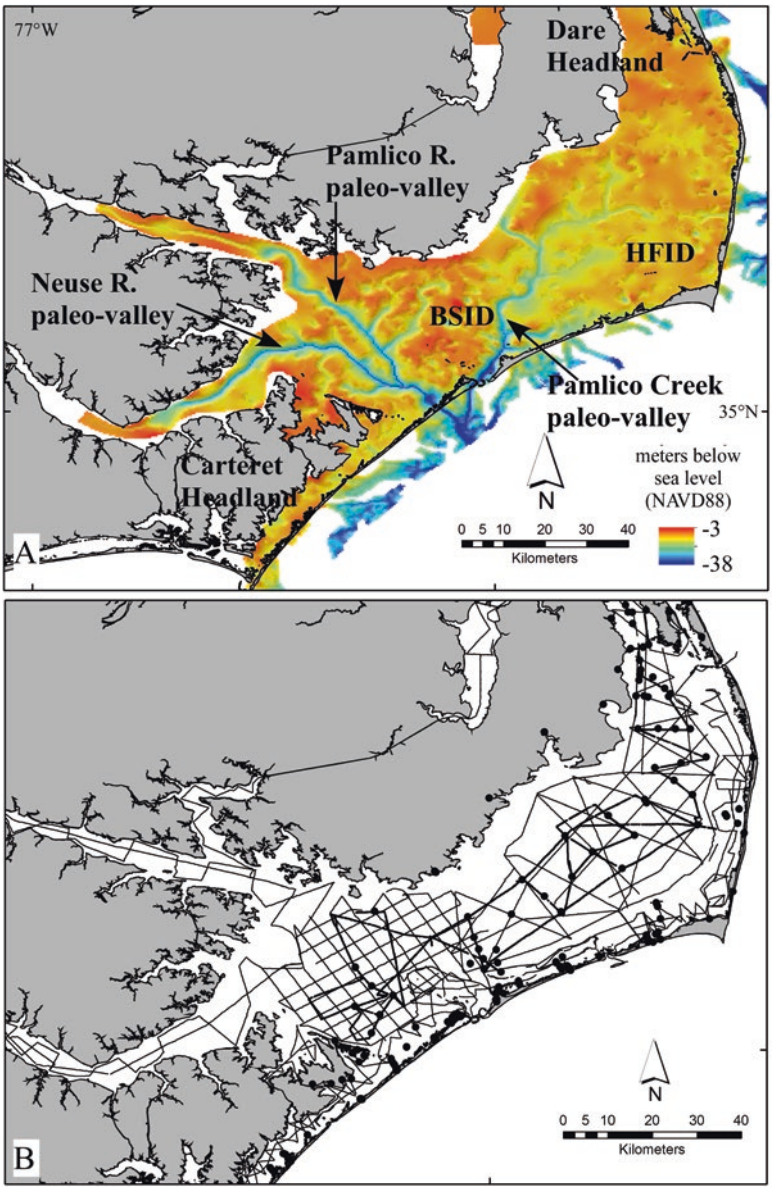

Fig. 2 (**a**) Map showing the paleotopographic surface formed during the late Pleistocene lowstand, based upon seismic data (data from Mallinson et al. 2010a; Thieler et al. 2013). Note the incised paleo-valleys associated with the Neuse and Pamlico Rivers, and Pamlico Creek paleovalley, a completely submerged drainage system. The Bluff Shoal interstream divide (BSID), controls the modern position of Bluff Shoal and separates the northern and southern basins of Pamlico Sound. HFID is the Hatteras Flats interstream divide. (**b**) Map showing the location of seismic track-lines and cores (black dots) used to define the geologic framework of Pamlico Sound

especially the lowstand associated with the Last Glacial Maximum (ca 26,500–19,000 calendar years before present–cal year BP; Clark et al. 2009). Beneath the antecedent topographic surface, the stratigraphic framework includes fluvial, coastal, and shelf facies deposited during the late Pleistocene (Riggs et al. 1992, 1995; Mallinson et al. 2005, 2008, 2010a, b; Parham et al. 2007, 2013). These deposits provide a source of sediment to the modern system via erosion of the estuarine shoreline and marine shoreface.

The paleodrainage systems incised into this landscape include valleys (now filled and submerged) associated with the Pamlico River, Neuse River, and Paleo-Pamlico Creek (Fig. 2a; Riggs et al. 1995; Mallinson et al. 2010a, b). Not only are the incised valleys important in defining the estuaries, but the interfluves are likewise just as significant in defining the geomorphic/bathymetric evolution and resultant processes. For example, interfluves of the flooded landscape control the location of shoals and paleo-marshes (e.g., Bluff Shoal; Roanoke Marshes; Fig. 1b) and shallow lagoons, such as Currituck Sound, Croatan Sound, Core Sound, and Bogue Sound (Fig. 1a), which are defined by the extent of the fronting barrier and the mainland. Deeper basins and drowned river estuaries are associated with the paleo-valleys.

The topographic relief (elevations and slopes) of the flooded landscape affected the timing of inundation associated with sea-level rise, as well as the rate of shoreline transgression (i.e., transgression is more rapid where slopes are lower). Flat-topped interfluves flooded rapidly as sea level reached and exceeded their elevation (ca 5000–4000 cal year BP; Zaremba et al. 2016). Rapid expansion of estuaries increased fetch and wave energy within the basins, as well as tidal energy, both of which affected the sedimentological and stratigraphic character (i.e., grain size distributions, stratigraphic boundary development, etc.) of the estuarine sediments. These relationships are discussed in the context of sea-level rise and climate change in the following sections.

3 Evolution in Response to Climate and Sea-Level Change

The Holocene evolution of this coastal system has been defined based upon a variety of analyses of >100 vibracores (penetrating up to 8.5 m) and deep rotasonic cores (with penetration up to 70 m) collected by numerous researchers over three decades (Fig. 2b), and further informed by many previous studies (referenced herein). Cores were analyzed for sedimentology (grain-size, structures, bedding characteristics, etc.), microfossils (foraminifera, diatoms, and pollen) and macrofossils, bulk magnetic susceptibility, isotopic geochemistry on foraminifera and total organic carbon (TOC), and elemental geochemistry (not all analyses were done on all cores). Holocene geochronology was derived from a compilation of >300 radiocarbon analyses, ^{210}Pb analyses on recent sediments, and optically stimulated luminescence (OSL) analyses, applied to cores collected from numerous locations. Geophysical data include ca 150 km of ground-penetrating radar data for the Outer Banks (between Kitty Hawk and Ocracoke; Fig. 1) and approximately 3400 km of boomer

seismic and 2800 km of chirp seismic data within Albemarle, Pamlico, Croatan, and Core Sounds (Fig. 2b; Thieler et al. 2013; Zaremba et al. 2016). Geomorphic models corresponding to specific times were created using seismic data constrained by radiocarbon analyses from cores, with bathymetry calculated using the Kopp et al. (2015) relative sea-level curve. Hydrodynamic modeling utilized Delft3D software, with boundary conditions determined by the paleobathymetry and paleogeomorphology datasets (Clunies 2014; Clunies et al. 2017). Many results from these studies have been published in the references provided in the following discussion.

3.1 Early Holocene to ca 4000 Cal Year BP

The early- to mid-Holocene was characterized by greater seasonality in the northern hemisphere creating the Hypsithermal (a.k.a. Holocene Climate Optimum or Holocene Thermal Maximum) from ca 9000 to 4000 cal year BP (Wright 1976; Wright et al. 1993). Although minimal paleoclimate data exist in the region for this time period, data from Lake Tulane, Florida (Grimm et al. 1993), and the Adirondacks in New York (Davis et al. 1980; Jackson 1989) indicate warmer and drier summers than at present in eastern North America. Warm, dry conditions are indicated in the southeastern U.S. by the desiccation of ponds and lakes in eastern Tennessee between 8500 and 4000 cal year BP (Delcourt and Delcourt 1980).

Between 11,000 cal year BP and 4500 cal year BP the rate of sea-level rise in NC decreased substantially, from 6.8 ± 1.2 mm/year to 0.8 ± 1.0 mm/year (Kopp et al. 2015). During the same time interval, sea-level elevation changed from ca −30 ± 2 m to ca −4.5 ± 1 m (Kopp et al. 2015). The principal semi-diurnal lunar tide component (M_2) along the NC coast was approximately 75% greater than today at ca 5000 cal year BP, which likely enhanced tidal circulation within the early estuaries, and perhaps the number of inlets through any existing barrier island chain (Hill et al. 2011), the extent of which remains uncertain.

3.1.1 Coastal Evolution

The existence of barrier islands along the NC coast is suggested by relict flood tide delta and back-barrier sand flat deposits dating from approximately 6000 to 4000 cal year BP, found in the vicinity of Rodanthe on Hatteras Island (Smith et al. 2009) and Bogue Banks (Fig. 1; Timmons et al. 2010; Lazar et al. 2016), and Holocene barrier shoreface deposits dated to 4500 cal year BP beneath Currituck Sound (Fig. 1; Moran et al. 2015). Formation of extensive barrier islands beginning at ca 6000 cal year BP may have been in response to the decreasing rate of relative sea-level rise. In the region of Hatteras Island and Ocracoke Island, the occurrence of estuarine conditions in Pamlico Sound, based upon foraminiferal and diatom paleoenvironmental data (Culver et al. 2007; Grand Pre et al. 2011), suggests the existence of barrier islands, as the Hatteras Flats Interstream Divide was submerged

by this time (Zaremba et al. 2016). It is not clear whether the shoreline was west or east of the modern shoreline prior to 4000 cal year BP, and there are insufficient data to understand the barrier characteristics at this time.

Although estuarine conditions prevailed, $\delta^{13}C$ and $\delta^{18}O$ data from foraminifera (*Elphidium excavatum*) in core PS-03 exhibit larger variability (1.5–2.5‰ excursions; Lauback et al. 2012; Fig. 3a) than the following time period from 4000 to 3500 cal year BP (ca 0.5‰ excursions). Likewise, $\delta^{13}C_{TOC}$ data also show rapid excursions between ca −23.5‰ and −22‰, suggesting alternating sources of organic material from terrestrial and marine environments, respectively (Fig. 3b; Minnehan 2014). These geochemical excursions suggest more variable salinity conditions within the Sound (relative to 4000–3500 cal year BP, and present conditions). Greater variability was likely related to several factors, including Hypsithermal conditions (e.g., greater seasonality and drier conditions; Delcourt and Delcourt 1980; Wright et al. 1993) affecting freshwater flux to the estuary, and greater tidal influence affecting barrier continuity and seawater influx, combined with a smaller estuary volume (i.e., smaller residence time).

3.2 ca 4000–3500 Cal Year BP

Rapid climate change (defined as changes in regional to global meteorological conditions occurring within a few hundred years; Mayewski et al. 2004) is indicated from 4200 to 3800 cal year BP, with glacial advances in North America and Central Asia, and weak North Atlantic Deepwater (NADW) formation (Mayewski et al. 2004; Wanner et al. 2008). Weakened NADW formation may have contributed to an increased rate of relative sea-level rise along the U.S. east coast (Levermann et al. 2005), which may have influenced barrier island evolution. Several studies suggest low El Niño Southern Oscillation (ENSO) activity between ca 5000 and ca 3000 cal year BP (Cobb et al. 2013; McGregor et al. 2013; Carré et al. 2014), which has been shown to enhance hurricane activity in the North Atlantic (Goldenberg and Shapiro 1996; Bove et al. 1998). Data from deMenocal et al. (2000) show that sea surface temperatures off the northwest African coast were at a peak (as warm as during the Medieval Climate Anomaly, and present), which also may have contributed to greater hurricane activity. Changes to the barrier islands and estuaries are also evident and occur coevally with these more widespread climate fluctuations. Relative sea level in NC at the time was ca −4.5 to −3.5 m relative to modern mean sea level (msl). The rate of relative sea-level rise is poorly understood for this time, but Kopp et al. (2015) show a general rate of ca 2–3 mm/year, and decreasing.

3.2.1 Coastal Evolution

Based on the mapped elevation of the Pleistocene surface (i.e., the antecedent topographic surface) in the Pamlico Sound region (Mallinson et al. 2010a, b; Zaremba et al. 2016), and the relative sea-level curve of NC (Horton et al. 2009; Kopp et al.

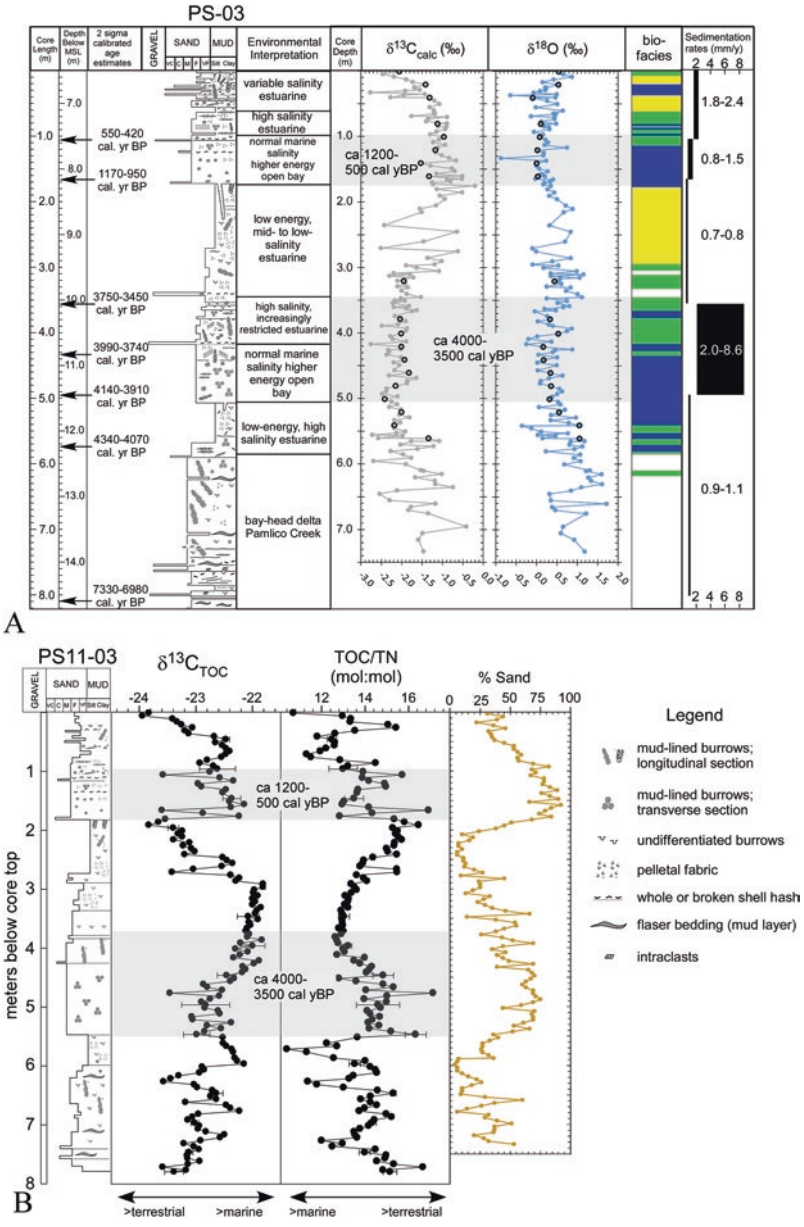

Fig. 3 (**a**) Carbon and oxygen isotopic data from *Elphidium excavatum* samples from core PS03 in the northern basin of Pamlico Sound (Lauback et al. 2012). *Black circles* represent replicate sample averages. Biofacies are also indicated (refer to Fig. 4b for explanation). Note that biofacies are mixed downward by bioturbation. Sedimentation rates are calculated using maximum and minimum 2-sigma ages from radiocarbon analyses. (**b**) Graphic log, carbon isotopic data from total organic carbon and C:N, and percent sand from core PS11-03, a duplicate core of PS-03 (Minnehan 2014)

2015), the local interstream divides (e.g., Hatteras Flats, Bluff Shoals, etc.; Fig. 2a) should have been overtopped at ca 5000–4000 cal year BP (Zaremba et al. 2016). At this time, the southern Pamlico Sound exhibited normal-marine-salinity conditions suggesting the existence of a large opening through the Outer Banks. These conditions are evidenced by sediments containing 35 species of benthic foraminifera typical of the inner shelf today, and 22 species of planktonic foraminifera (Fig. 4; e.g., *Buccella inusitata*, *Elphidium subarcticum*, *Hanzawaia strattoni*, *Nonionella atlantica, Trifarina angulosa, Globigerinoides ruber, Globorotalia menardii*; Culver et al. 2007; Grand Pre et al. 2011). This assemblage is in stark contrast to the modern assemblage within Pamlico Sound, which is low diversity and consists of benthic foraminifera dominated by *Elphidum excavatum, Ammotium salsum* and *Ammonia parkinsoniana*, and no planktonic foraminifera (Abbene et al. 2006). The largest apparent gap within the Outer Banks appears to have been in the Ocracoke Island and North Core Banks area (Fig. 5a, b). Deposits containing normal-marine-salinity shelf foraminifera occur up to 10 km behind the modern barrier island. These data suggest that much of Ocracoke Island was reduced to a subtidal shoal at this time, likely with deeper tidal passes allowing for the introduction of shelf waters and Gulf Stream filaments carrying planktonic foraminifera into the northern and southern Pamlico basins. Segmentation in other areas of the Outer Banks is less clear, thus the geomorphic model (Fig. 5b, c) only includes the large gap at Ocracoke, and an inlet near present-day Oregon Inlet (Smith et al. 2009).

Several factors may have contributed to this reduction in barrier island continuity and increased tidal exchange. First, warmer surface water temperatures in the North Atlantic (deMenocal et al. 2000) may have contributed to an increase in hurricane activity (Donnelly and Woodruff 2007), although more data (e.g., spatial and temporal distribution of hurricane deposits) are needed to test this hypothesis. Increased hurricane impacts may have caused multiple breaches in the barriers, enhancing the tidal prism, and allowing more and/or larger inlets to persist, resulting in barrier segmentation (Giese 1988). Tidally driven sediment flux into the sound and shoaling may have ultimately reduced the tidal prism and shut down the inlets. Alternatively, a minor increase in the rate of sea-level rise may have taken place along the Atlantic coast as a result of the weaker North Atlantic Deep Water (NADW) production (Mayewski et al. 2004; Levermann et al. 2005; Wanner et al. 2008), causing increased rates of erosion and breaching during storms. Finally, the rapid enlargement of the sound as interstream divides were overtopped, may have also increased the tidal prism, causing barrier fragmentation as described by Fitzgerald et al. (2004, 2008, this volume). Reduction of friction, as more area is converted to open water, increases tidal range and the tidal prism, and tidal inlet size (O'Brien 1969; Oliveira 1970).

Pamlico Sound at this time exhibited much greater exchange with marine waters and more energetic conditions. By 4000 cal year BP, the northern and southern estuaries had merged across the shallow Bluff Shoal Interstream Divide (BSID). Zaremba et al. (2016) mapped a prominent seismic reflection, H_{4000}, within Pamlico Sound (primarily the northern basin) that is constrained to ca 5000–3000 cal year BP by multiple radiocarbon ages (Fig. 5e, f). This reflection is interpreted to represent

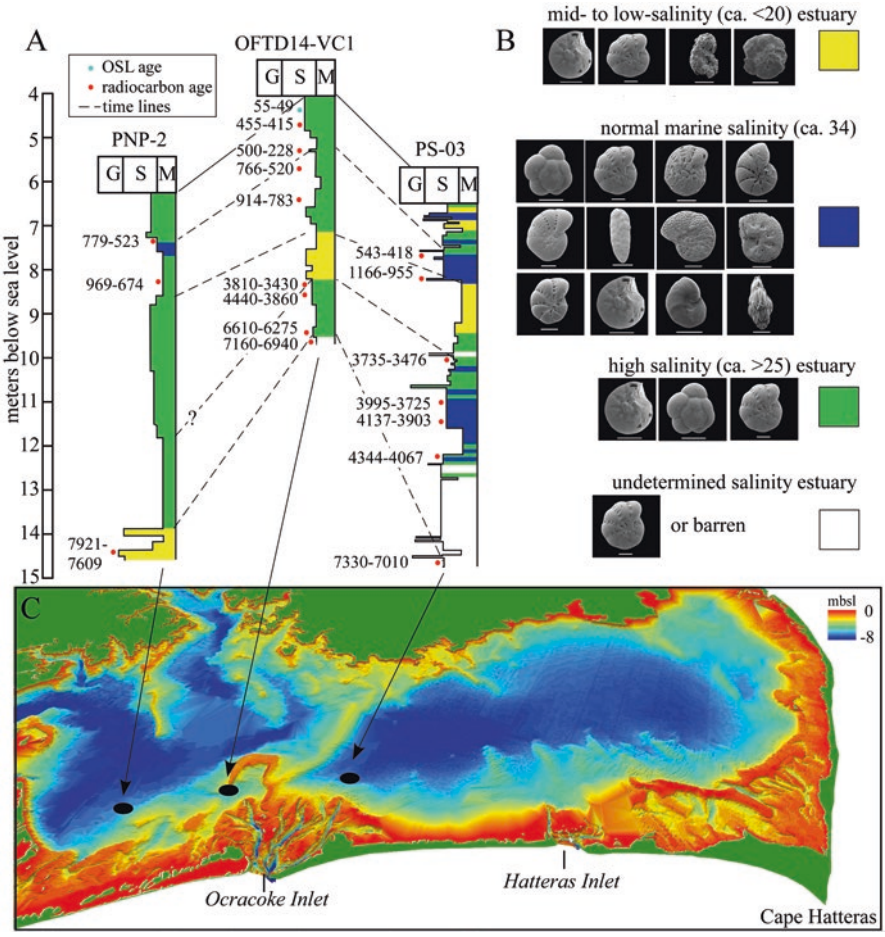

Fig. 4 (**a**) Graphic logs showing modal grain size (*G* gravel, *S* sand, *M* mud) and foraminiferal biofacies from cores PNP-2 (Metger 2009), OFTD14-VC1 (Smith 2015), and PS-03 (Grand Pre et al. 2011). (**b**) Representative foraminifera that compose the biofacies shown in (**a**) (Grand Pre et al. 2011). Top assemblage from *left* to *right*: *Ammonia parkinsoniana, Elphidium excavatum, Ammotium salsum, Deuterammina ochracea.* Second assemblage from *left* to *right* each row: *Ammonia tepida, Elphidium excavatum, Elphidium gunteri, Elphidium mexicanum, Elphidium translucens, Bolivina lowmani, Cibicides lobatulus, Hanzawaia strattoni Elphidium poeyanum, Ammonia parkinsoniana, Valvulineria* sp., *Trifarina angulosa.* Third assemblage from *left* to *right Ammonia parkinsoniana, Ammonia tepida, Elphidium excavatum.* Fourth assemblage: *Elphidium excavatum.* (**c**) Perspective view of Pamlico Sound showing the location of the cores in (**a**)

erosion associated with greater fetch, and increased wave and current activity within Pamlico Sound. A more energetic hydrodynamic state likely occurred either as a result of the final overtopping of interfluves and rapid expansion of the estuary, or extensive barrier island segmentation, or both. The greater influence of marine conditions is supported by the foraminiferal assemblages as described above, as well as an increase in the sand/mud ratio of sediments correlated to the H_{4000} reflection.

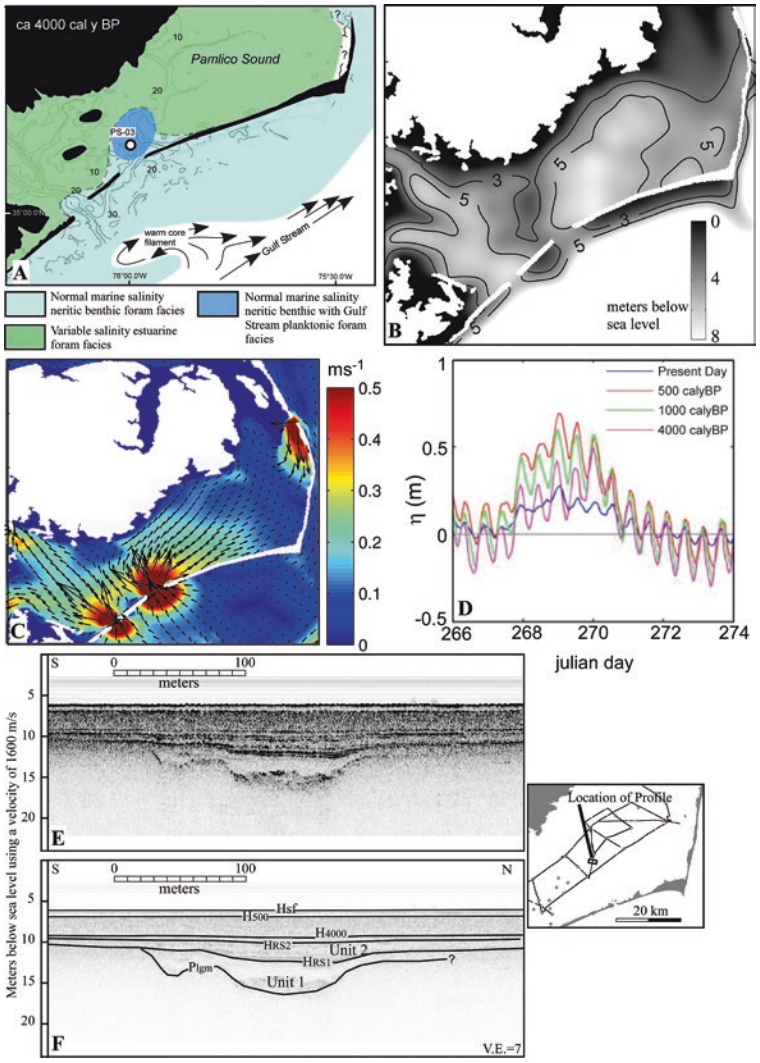

Fig. 5 (**a**) Paleo-environmental reconstruction of Pamlico Sound at ca 4000 cal year BP based upon foraminiferal assemblages within cores, and sedimentological data (modified from Grand Pre et al. 2011). (**b**) Paleo-geomorphic reconstruction of Pamlico Sound at ca 4000 cal year BP based upon geological data. (**c**) Delft3D model of flood tidal currents within Pamlico Sound corresponding to the paleo-geomorphic reconstruction. (**d**) Delft3D model of water surface elevation (η) at the location of PS03 (shown in **a**) given the paleo-geomorphic reconstruction as input. The elevated water level between day 168 and 171 is due to an imposed wind event. Note the higher tidal range (up to 30 cm) corresponding to the three paleo-geomorphic reconstructions (4000, 1200, 500 cal year BP), as compared to the modern range (ca 5 cm). (**e**) Chirp seismic data (see small map for location) illustrating seismic reflections within the Holocene section (from Zaremba et al. 2016). P_{lgm} is the subaerial unconformity formed during the Last Glacial Maximum. H_{RS1} and H_{RS2} are interpreted as tidal and wave ravinement surfaces, respectively. H_{4000} is the reflection corresponding to the ca 4000 cal year BP barrier segmentation. H_{500} is a regional reflection that formed during the Little Ice Age

Between 4000 and 3500 cal year BP, Pamlico Sound was shallower than present (Fig. 5b), particularly in the north, across Bluff Shoal, and across the Hatteras Flats Interstream Divide (HFID; Fig. 2a). At this time, erosion of the recently flooded bay shoals and the mainland shoreline, as well as the segmentation of the barrier islands, as sea level rose, resulted in high rates of sediment accumulation (ca 2.0–8.6 mm/year at PS-03), compared to earlier or later rates (Fig. 3a). Increased tidal range and tidal exchange through inlets likely advected sand into the sound from the shoreface.

Values of $\delta^{13}C_{TOC}$ exhibit a more constant trend and enriched values (ca −22‰) (Fig. 3b) relative to the previous time (>4000 cal year BP), suggesting that this was a period of greater marine influx and more constant water conditions. However, C:N ratios of organic matter (Fig. 3b) suggest a more complicated scenario, possibly with a contribution of organic carbon from marsh grasses (e.g., *Spartina* spp.) as interstream divides were overtopped and eroded (Minnehan 2014).

Clunies (2014) modeled the hydrodynamics of the Pamlico Sound based upon a geomorphic reconstruction derived from geological and geophysical data (Fig. 5b,c). Modeling suggests that a large opening in the barrier island system near Ocracoke Island likely resulted in significantly greater tidal currents in Pamlico Sound relative to present tidal conditions. The hydrodynamic model predicts flood-tide currents in excess of 0.3 m/s over large portions of southern and northern Pamlico Sound (Fig. 5c), and the tidal range may have been enhanced (to ca 0.3 m). The increased sand/mud ratio of sedimentary deposits, increased sediment accumulation rates, and the occurrence and extent of seismic reflection H_{4000} (Zaremba et al. 2016) support the tidal model and suggest advection of nearshore sand into the sound.

3.3 ca 3500–1200 Cal Year BP (750 CE–Common Era)

The Northern Hemisphere was characterized by a general cooling trend between ca 3500 and 1200 cal year BP (750 CE) (Wanner et al. 2008). Data from deMenocal et al. (2000) show generally cooler sea surface temperature (SST) than present in the eastern North Atlantic during this time interval, whereas $\delta^{18}O$ from *Globigerinoides ruber* on the Bermuda Rise suggest a cycle of rapid warming at ca 3500 cal year BP followed by slow cooling until ca 1500 cal year BP (450 CE) (Keigwin 1996). This cooling may have limited hurricane formation in the North Atlantic, resulting in a lower rate of barrier breaching and inlet formation, and allowing former inlets to close. The average rate of relative sea-level rise ranged from ca 0.3 to 0.9 mm/year in the study area (Kemp et al. 2017).

3.3.1 Coastal Evolution

Few data exist to understand the location or condition of the southern Outer Banks during this time interval. Ricardo (2005) found open marine/inner shelf sands beneath Hatteras Island and Hatteras Flats between Rodanthe and Avon (Fig. 1a)

that have an age of ca 2900 cal year BP to 1200 cal year BP (750 CE). However, it is not clear whether these deposits represent a large inlet region, or if they represent shoreface deposits to the east of a barrier system. If the latter is correct, then the barrier may have formed west of the present location, and prograded seaward before becoming transgressive. However, Pierce and Colquhoun (1970) show generally transgressive deposits beneath Hatteras Island (north of Cape Hatteras). Regressive barrier islands are indicated in regions to the north (i.e., the Kitty Hawk beach ridges; Mallinson et al. 2008; Moran et al. 2015), at Buxton (Cape Hatteras region; Peek et al. 2013) and to the south (Bogue Banks; Timmons et al. 2010; Lazar et al. 2016) at this time. Seismic data behind southernmost Hatteras Island reveal seaward dipping clinoforms that indicate shoreface progradation and a regressive barrier (Fig. 6a). Peek et al. (2013) identified beach ridges on the northernmost portion of the Buxton area dating to ca 1600 cal year BP (350 CE) (Fig. 6b) indicating that the paleo-shoreline in this area was north and west of the modern shoreline. Pierce and Colquhoun (1970) also propose that initial Holocene barrier island formation occurred to the north of the modern shoreline at Cape Hatteras. Presently, this area is experiencing southward progradation as erosion on the east facing shore, and accretion on the south facing shore have caused Cape Hatteras to migrate in a southwesterly direction (Inman and Dolan 1989; Peek et al. 2013). This long-term progradation is evidenced by the occurrence of the east–west trending beach ridges (the Buxton Beach Ridges; Peek et al. 2013) that form the bulk of the island at Cape Hatteras.

Within the Pamlico Sound basin, estuarine conditions were likely similar to today, if not more restricted, between 3500 cal year BP and 1200 cal year BP (750 CE). Sediments exhibit a fining-upward trend consisting of muddy fine sands at ca 3500 cal year BP grading to organic-rich mud with minimal sand component prior to 1200 cal year BP (750 CE). The associated biofacies consists solely of *E. excavatum* at ca 3500 cal year BP, grading-upward to a lower salinity *A. salsum*-dominated facies prior to 1200 cal year BP (750 CE) (Grand Pre et al. 2011). These data indicate a decrease in energy and salinity during this time interval. $\delta^{13}C_{TOC}$ data show a change from enriched values to depleted values during the second half of this interval (Fig. 3b), indicating a dominantly terrestrial source of carbon with $\delta^{13}C$ values of ca −23‰ to −24‰. Likewise, the C:N exhibits a trend toward greater values (ca 16) which are also indicative of a terrestrial source (Fig. 3b; Minnehan 2014). Thus, the estuary appears to have experienced decreasing marine influence during this period, suggesting development of a continuous barrier system with few inlets. A minor disruption of this barrier system is suggested at ca 2500 cal year BP in the vicinity of Ocracoke Inlet, based on the limited occurrence of normal-marine-salinity, shelf, benthic foraminifera behind northern Core Banks (Grand Pre et al. 2011).

Zaremba et al. (2016) suggest that the decrease in inlet activity may have been related to the decrease in the M_2 (dominant semi-diurnal lunar) tidal component (Hill et al. 2011). An equilibrium exists between the total cross-sectional area of inlets within a barrier, and the tidal range, with fewer inlets necessary to accommodate a smaller tidal prism (O'Brien 1969). More limited hurricane impacts also would have limited the creation of breaches that could have developed into inlets.

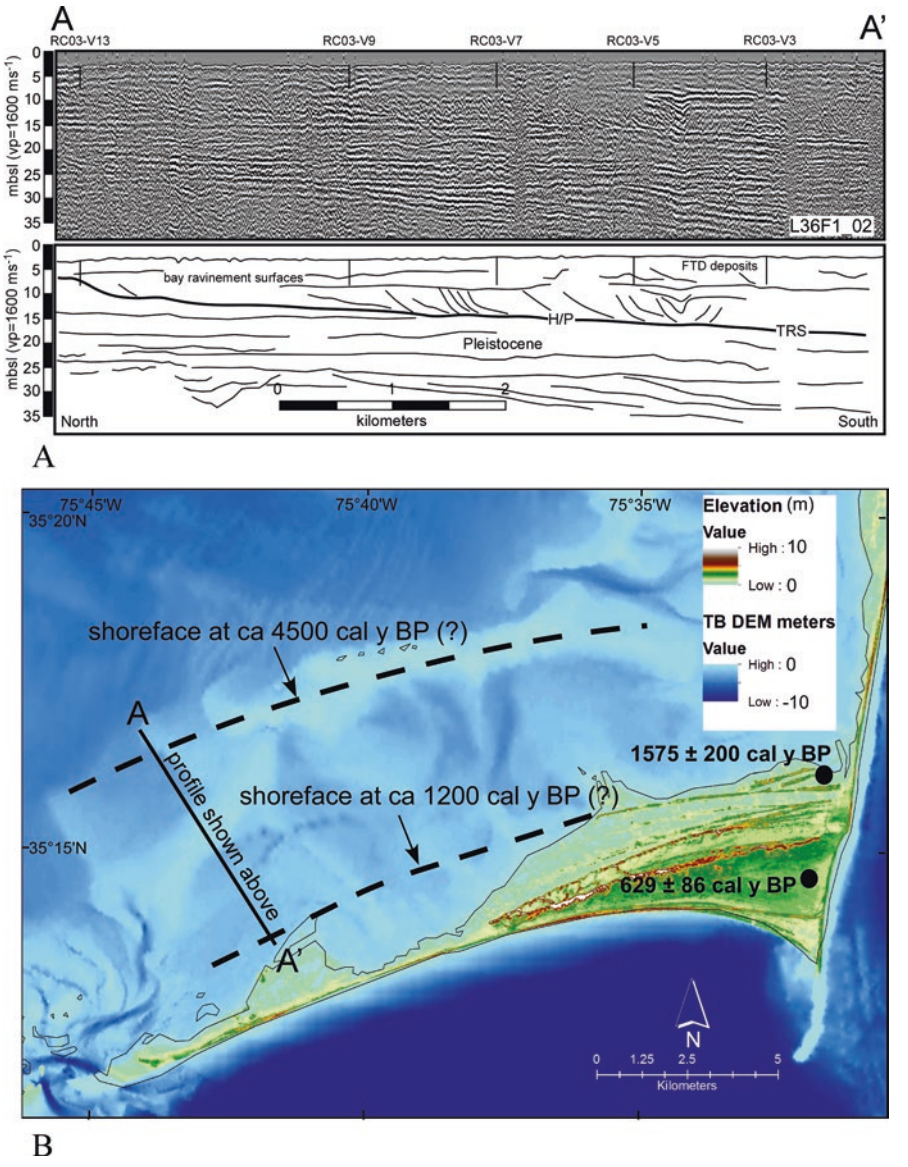

Fig. 6 (**a**) Seismic data along transect A–A′ (see **b**) illustrating the transgressive ravinement surface (TRS) associated with Holocene sea-level rise, and seaward dipping clinoforms in the shallow subsurface, suggesting barrier progradation. (**b**) Present-day bathymetry of the Hatteras Flats and Cape Hatteras region showing the transect location for (**a**), and the inferred shoreface positions at 4500 cal year BP and 1200 cal year BP based upon the seismic data, modern geomorphology, core data, and geochronology (OSL ages) from the beach ridge complex at Buxton. Note the eastward extension of the proposed 1200 cal year BP shoreline along the trend of a prominent beach ridge that cross-cuts older ridges (dated to ca 1575 cal year BP) to the north. Ages shown are based on optically stimulated luminescence (OSL) analyses

Furthermore, inlet closure may have allowed onshore migration of ebb-tidal delta sediments, contributing to barrier progradation at this time (FitzGerald et al. 2004; Zaremba et al. 2016).

3.4 The Medieval Climate Anomaly (ca 1200 Cal Year BP to ca 800 Cal Year BP; 750–1150 CE)

During the Medieval Climate Anomaly (MCA), Sargasso Sea surface waters were characterized by relatively high temperatures (ca 24 °C; Keigwin 1996) in comparison to centuries before and after. Likewise, sea-surface temperature in the eastern North Atlantic was at a peak during the MCA (deMenocal et al. 2000). Cronin et al. (2003) provided an assessment of conditions in the Chesapeake Bay region, north of the study region. Their data suggest that Chesapeake Bay water temperatures, based upon Mg/Ca paleothermometry, were ca 2 °C warmer than the pre-twentieth century average, and roughly correlate with North Atlantic sea surface temperatures in terms of trends (Keigwin 1996; deMenocal et al. 2000). An increase in hurricane activity in the North Atlantic, relative to pre-MCA conditions, has been proposed (Mann et al. 2009; Donnelly et al. 2015) and may be responsible for increased breaching of the Outer Banks. Kemp et al. (2011) show that the rate of relative sea-level rise in NC increased at this time by +0.6 mm/year, to ca 1.6 mm/year, but the significance of this minor rate change is unclear.

3.4.1 Coastal Evolution

A major erosional event or events, characterized by widespread barrier island segmentation occurred during the MCA (Fig. 7). This is supported by several lines of evidence including geophysical data (both ground penetrating radar and seismic), paleo-environmental analyses (foraminiferal biofacies), and isotope geochemistry. Inlet facies, identified using GPR and core samples, occur in Rodanthe, Kinnikeet, and Ocracoke Island areas (Fig. 1). These have been dated to the MCA period using OSL (Fig. 8; Mallinson et al. 2011). The area that was affected most was the Ocracoke Island and southern Hatteras Island area (Fig. 7; Culver et al. 2007; Grand Pre et al. 2011; Mallinson et al. 2011). Peek et al. (2013) recognized a major erosional boundary marking a change in the orientation of the beach ridges, which compose the cuspate foreland at Cape Hatteras (Fig. 6b). This change in orientation is constrained to between ca 1500 cal year BP and 700 cal year BP (450–1250 CE) and is interpreted as corresponding to the ca 1200 cal year BP (750 CE) erosional event(s) that reduced much of Ocracoke Island to subtidal shoals. Likewise, basal ages of the Hatteras Flats deposits range from 1155 ± 210 cal year BP to 1060 ± 115 cal year BP (Fig. 9; Peek et al. 2013), suggesting major segmentation of Hatteras Island at this time and deposition of many large flood tide deltas which coalesced to form the Hatteras Flats (Fig. 1b). The formation of these numerous flood tide deltas

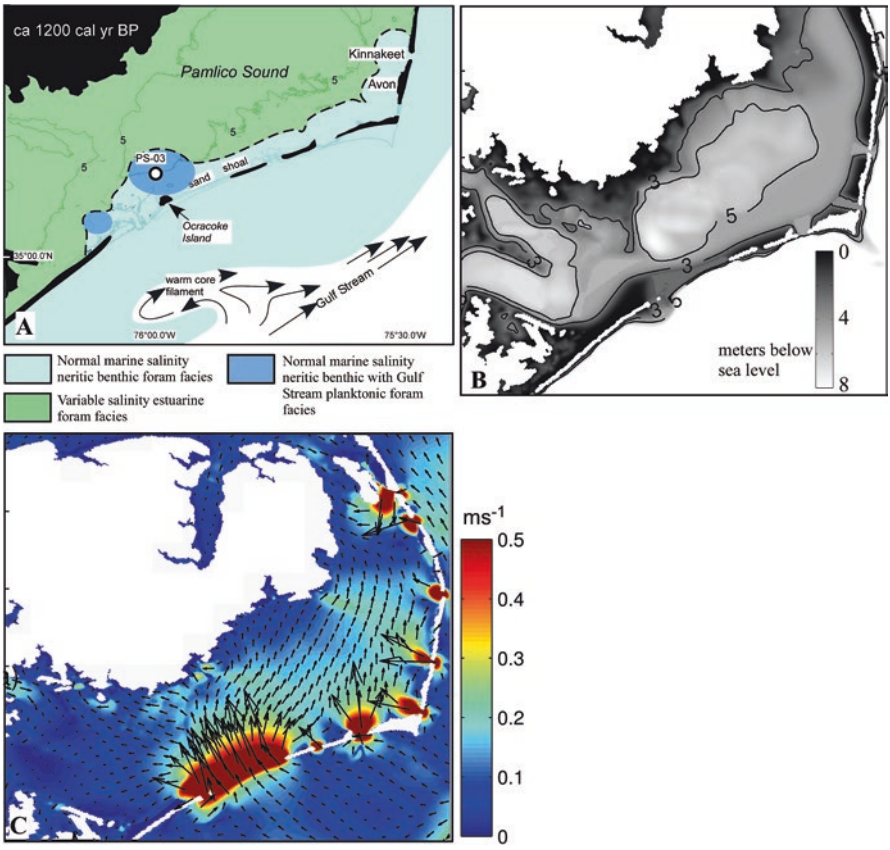

Fig. 7 (**a**) Paleo-environmental reconstruction of Pamlico Sound at ca 1200 cal year BP based upon foraminiferal assemblages within cores, and sedimentological data (modified from Grand Pre et al. 2011). (**b**) Paleo-geomorphic reconstruction of Pamlico Sound at ca 1200 cal year BP based upon geological data. (**c**) Delft3D model of flood tidal currents within Pamlico Sound corresponding to the paleogeomorphic reconstruction. The color scale is in meters per second

during this time represents a significant loss of sand from the longshore transport system. This should have resulted in rapid shoreline erosion and transgression (see Fitzgerald et al. 2008, this volume).

Increased salinity within the Pamlico Sound is indicated by the occurrence of normal-marine-salinity, shelf, benthic, and planktonic foraminifera within core samples (Culver et al. 2007; Grand Pre et al. 2011; Figs. 3a and 7a). The assemblage exhibits high diversity and consists of well-preserved, relatively small, unsorted specimens suggesting they are in situ (i.e., minimal reworking and transport occurred). Foraminifera include *Asterigerinata mamilla, Bolivina* spp.*, Eoeponidella pulchella, Cibicides fletcheri, Fursenkoina fusiformis, Hanzawaia strattoni, Trifarina angulosa*, and *Valvulineria* sp. A. Twenty-two planktonic species were identified (Grand Pre et al. 2011), including *Globigerinoides ruber* and *Globorotalia menardii,* which are typical of Gulf Stream-influenced waters (Bé and Hamlin 1967).

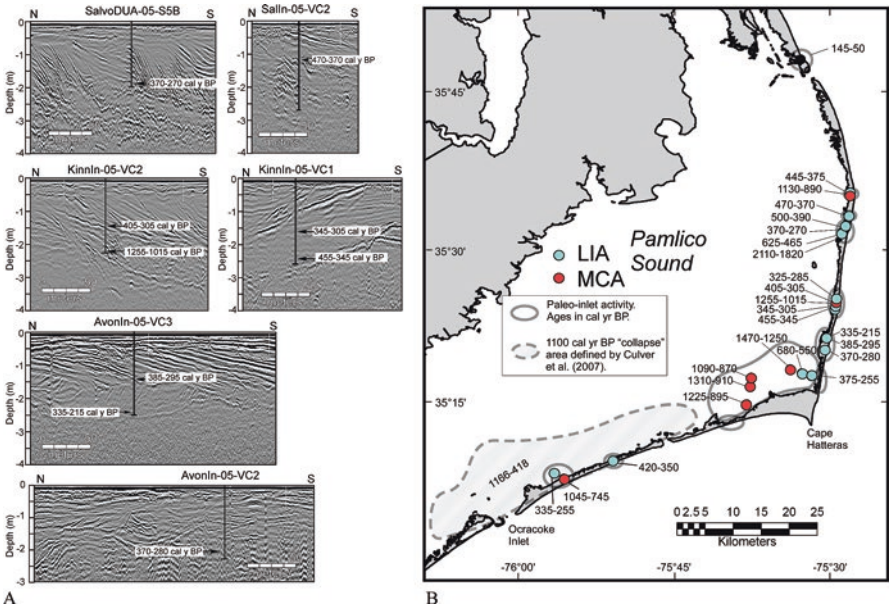

Fig. 8 (**a**) Examples of ground penetrating radar data from the Outer Banks showing core locations and OSL ages (from Mallinson et al. 2011). (**b**) Map showing the locations of paleo-inlets based on ground penetrating radar data and cores, and ages (cal year BP) of paleo-inlet activity based on radiocarbon and optically stimulated luminescence data (from Mallinson et al. 2011). MCA refers to inlet ages corresponding to the Medieval Climate Anomaly whereas LIA refers to inlet ages corresponding to the Little Ice Age

Increased sediment grain size (dominance of sand-size material) is seen in four cores from eastern Pamlico Sound and indicated by a low bulk-magnetic-susceptibility (BMS) value that can be correlated between cores (Zaremba et al. 2016). This BMS low is found throughout Pamlico Sound and is correlated to seismic reflection H_{1000} (Fig. 10; Zaremba et al. 2016), interpreted as a ravinement surface (i.e., a surface scoured by waves and/or tidal currents), with the age constrained to between 1400 and 950 cal year BP (550 and 1000 CE) by seven radiocarbon age estimates in five cores. Thus, the coincidence of coarser grain sizes and a ravinement surface suggests increased energy (wave or current activity) within the Pamlico Sound at this time.

At ca 1200 cal year BP (750 CE), $\delta^{13}C_{TOC}$ data exhibit a positive shift (ca +2‰) to values of ca −22‰, suggesting a slightly greater contribution of marine organic matter (Fig. 3b; Minnehan 2014) than in the previous time period. C:N ratios also show a decrease toward more marine-like values, although with substantial variability. Carbon isotope data from *E. excavatum* also exhibit a positive shift toward more marine-like values (Fig. 3a; Lauback et al. 2012). Thus, the geochemical signature corroborates the foraminiferal data in suggesting that the eastern Pamlico Sound experienced substantial marine influence, indicating a highly segmented barrier system (Fig. 7).

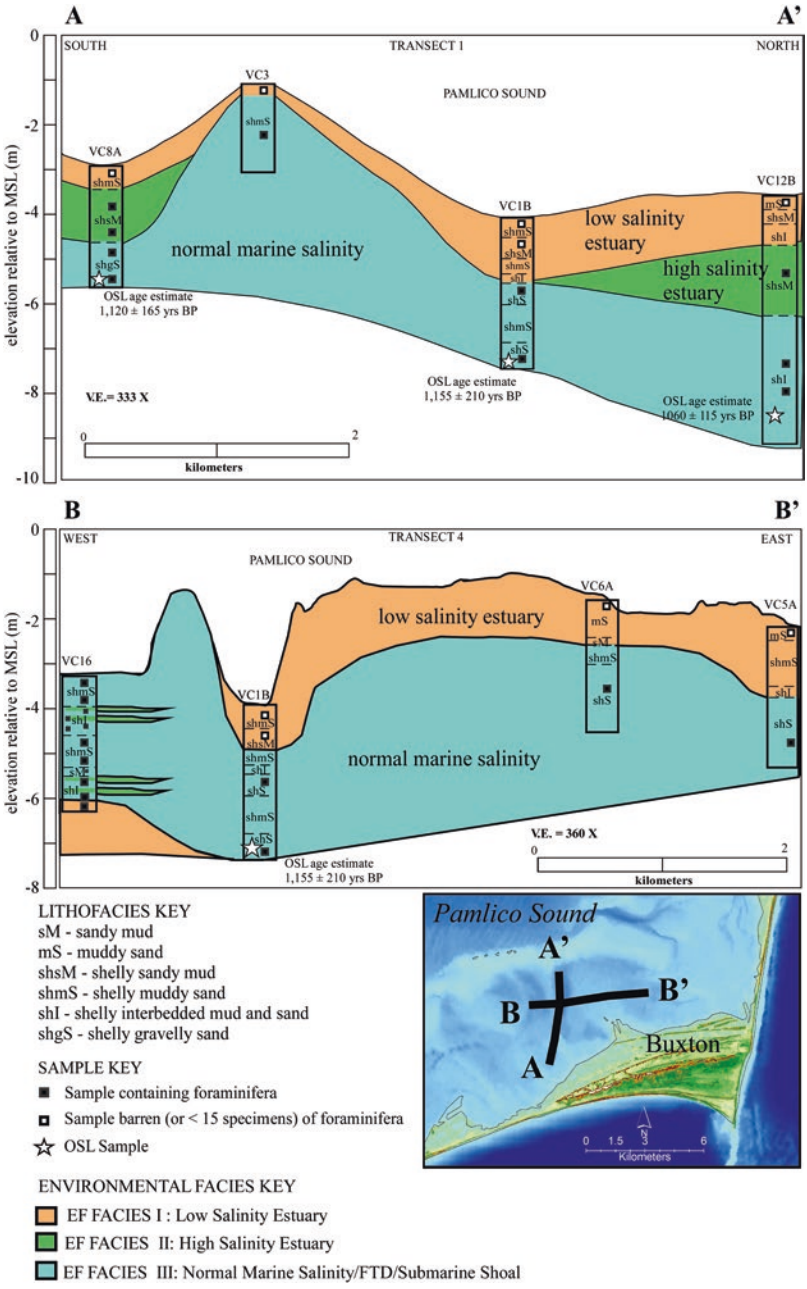

Fig. 9 Geological cross-section showing the paleoenvironments and ages associated with the Hatteras Flats (modified from Peek et al. 2013). Note that the basal ages of the Hatteras Flats correspond to the Medieval Climate Anomaly and the segmentation of the Outer Banks as described by Culver et al. (2007), Mallinson et al. (2011), and Grand Pre et al. (2011)

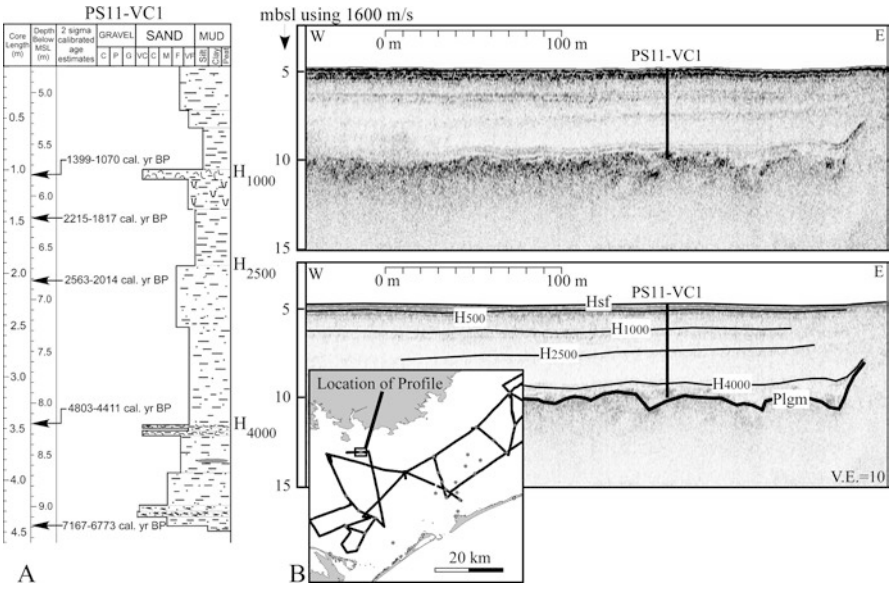

Fig. 10 (**a**) PS11-VC1 core log with radiocarbon ages showing the position of reflectors H_{1000} and H_{fs}. (**b**) Chirp seismic data from western Pamlico Sound (see *inset* map) illustrating reflectors at the PS11-VC1 site

Reconstructed flood-tide currents derived from the hydrodynamic model, with boundary conditions set using the geomorphic reconstruction, are shown in Fig. 7c. Similar to the 4000 cal year BP scenario, the model suggests that the highly segmented barrier island resulted in significantly greater tidal currents in Pamlico Sound relative to present tidal conditions. In the model simulation, flood tide currents in excess of 0.5 m/s are predicted over portions of southern and northern Pamlico Sound and are particularly strong over the shoals where the greatest segmentation occurred (Fig. 7c). This enhanced current activity likely produced the ravinement surface mapped as H_{1000} in chirp seismic data (Zaremba et al. 2016), and increased the sand/mud ratio of the sedimentary deposits (Fig. 10). Additionally, the currents would have likely caused channelization across the shoals, though the model does not provide this degree of detail. The modeled tidal range (ca 0.3 m) is also similar to the 4000 cal year BP scenario (Fig. 5d) and greater than the modern range of ca 0.1 m.

Barrier island segmentation at this time has been attributed to increased hurricane activity and associated breaching of the barriers (Culver et al. 2007; Grand Pre et al. 2011; Mallinson et al. 2011). A minor acceleration in the rate of sea-level rise may have also contributed. An alternative hypothesis is that the barriers were impacted by a tsunami capable of causing numerous breaches (Culver et al. 2007),

although there is more evidence for an increase in hurricane impacts (Mann et al. 2009; Donnelly and Woodruff 2007; Donnelly et al. 2015).

Following initial breaching during one or more closely timed events, the barriers may have followed a path similar to the segmentation described for Nauset Spit, Massachusetts (FitzGerald and Montello 1993). Nauset Spit was breached by a nor'easter in January 1987, resulting in an increase in the back-barrier tidal range and currents, and a corresponding increase in inlet size and sediment flux to the back-barrier. Along the Outer Banks, breaching and inlet formation, if occurring in multiple locations at nearly the same time, may have enhanced the tidal range within the sound sufficiently to enlarge and maintain multiple inlets. The persistence of normal-marine-salinity conditions in Pamlico Sound indicates that these were not ephemeral inlets, but must have been sustained in equilibrium with the tidal prism for up to ca 500 years (Culver et al. 2007). Transfer of sand to the back-barrier resulted in the formation of multiple coalescing flood tide deltas producing the Hatteras Flats during this time, at least in the area of southern Hatteras Island (Peek et al. 2013). Additionally, the transfer of a large volume of sand to the back-barrier estuary may have caused rapid transgression (see Fitzgerald et al. this volume). Eventual shoaling and closure of these inlets may have been in response to increased tidal friction associated with the formation of the Hatteras Flats, and the associated decrease in estuary volume, which would serve to decrease the tidal prism.

3.5 The Little Ice Age (ca 500 Cal Year BP) to Present

Data from Cronin et al. (2003) indicate that Chesapeake Bay waters during the LIA were as much as 4.7 °C cooler than the twentieth century mean. Likewise, sea-surface temperature in the North Atlantic, and the Caribbean Sea, was cooler than present by 2–4 °C (Keigwin 1996; deMenocal et al. 2000; Winter et al. 2000). However, centennial-scale oscillations in temperature are evident, and a warm interval at ca 300 cal year BP (1650 CE) separated LIA-I (500–420 cal year BP; 1450–1530 CE) from LIA-II (230–100 cal year BP; 1720–1850 CE) (Cronin et al. 2003). This warm interval is also seen in SST above the Bermuda Rise (Keigwin 1996) and in the eastern North Atlantic (deMenocal et al. 2000). Following LIA-II, Chesapeake Bay water temperatures increased rapidly to ca 15 °C, warmer than the previous 2000 years.

Relative sea level in the Pamlico Sound region rose approximately 0.7 m between 500 cal year BP and present. Initially (500–100 cal year BP), the rate of rise was ca 1 ± 0.5 mm/year, and driven by glacio-isostatic adjustment. However, the rate of rise accelerated near the beginning of the twentieth century to an average of 3.5 mm/year in southern Pamlico Sound (Kemp et al. 2009, 2011; Kopp et al. 2015).

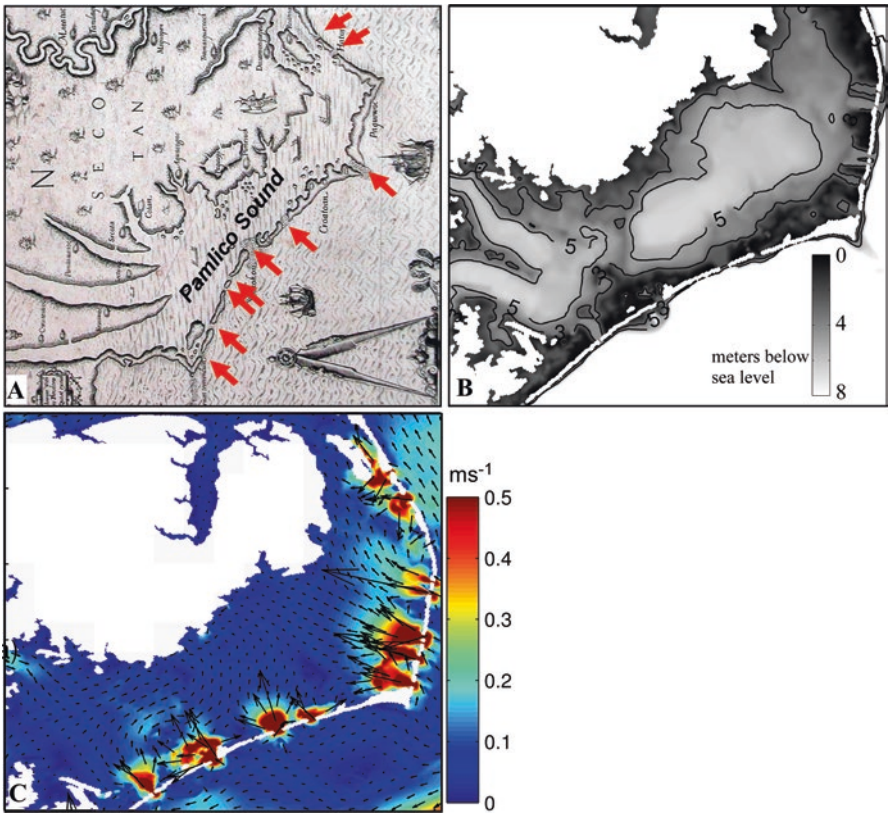

Fig. 11 (**a**) White-De Bry map of 1590 AD (Cumming 1966; Courtesy of the State Archives of North Carolina) with arrows added to show the location of inlets. (**b**) Paleo-geomorphic reconstruction of Pamlico Sound at 1590 AD based upon historical and geological data. (**c**) Delft3D model of flood tidal currents within Pamlico Sound corresponding to the paleogeomorphic reconstruction. The color scale is in meters per second

3.5.1 Coastal Evolution

Historical documentation (e.g., the White-De Bry map of 1590 CE; Cumming 1966; Fig. 11a) and geological and geophysical data (Fig. 8; Mallinson et al. 2011) indicate widespread inlet activity throughout the Outer Banks during the LIA. It is not clear if these inlets represent a distinct short-lived period of inlet activity, as suggested by Mallinson et al. (2011), or if they represent a healing phase of the barriers following the high degree of segmentation during the MCA. Donnelly and Woodruff (2007) and Donnelly et al. (2015), based on data from Puerto Rico and New York, proposed an increase in hurricane frequency along the North American east coast between 1400 and 1675 CE. This activity may have corresponded with the increase in sea surface temperature observed for the Atlantic and Chesapeake Bay (Keigwin 1996; Cronin et al. 2003), and the Cariaco Basin (Wurtzel et al. 2013). Thus, the

increase in inlet activity relative to earlier time periods, as seen in historical and geological data may stem from hurricane impacts. Although there appears to be more inlet activity during the LIA, there is no corresponding increase in salinity within the sound, in contrast to the normal-marine-salinity conditions seen during the 4000 cal year BP or 1200 cal year BP periods. This suggests that tidal conditions were not as enhanced as they were during earlier segmentations, thus inlets may have been more ephemeral with minimal overlap in activity.

Geophysical data and optically stimulated luminescence dating of core samples indicate that inlets were present in the areas of Rodanthe, Avon, and Buxton (Figs. 1a, 8, and 11). The White-De Bry map (Cumming 1966) suggests multiple inlets through Core Banks (Fig. 11a). These inlets were used as input to the hydrodynamic model (Fig. 11b, c; Clunies 2014) in a scenario where they occur coevally (which may not have been the case). The high degree of segmentation produces higher current velocities in Pamlico Sound relative to today (Fig. 11c), although not as high as during the 4000 or 1200 cal year BP scenarios. The tidal range produced (at the PS03 core site) is ca 0.2 m; intermediate between the modern range and the modeled range for the 1200 cal year BP scenario. This enhanced current activity relative to today may have contributed to the formation of the H_{500} surface in chirp seismic data (Fig. 5e, 10b; Zaremba et al. 2016); however, the hydrodynamic model (Fig. 11c) suggests that the increased current activity, and the associated erosional surface, was limited to the eastern portion of the Pamlico Sound, in the immediate vicinity of the inlets. The widespread occurrence of H_{500} thus suggests the occurrence of a larger-scale erosional event, such as one or more major storms.

From ca 350 cal year BP (1600 CE) to present, most of the inlets closed resulting in the present relatively restricted conditions of Pamlico Sound, with only three major active inlets. In recent years, shoreline erosion has narrowed the barrier islands significantly, with as much as 76% of barrier width lost in specific areas (e.g., between Buxton and Avon) over the last 150 years (Riggs et al. 2011). If trends of increasing intense (category 3–5) hurricane activity continue, and rates of sea-level rise accelerate as anticipated (Rahmstorf et al. 2012; Kopp et al. 2015), it is expected that the southern Outer Banks barrier islands may return to a more segmented condition in the near future. Thus, the modeled conditions that occurred during the MCA, or the LIA may once again dominate the NC coastal system, including greater tidal range, greater wave and current activity, increased salinity, and higher storm surges impacting the mainland.

4 Summary

A multidisciplinary and multiproxy approach shows that the evolution of barrier islands represents a fundamental control on the evolution of associated estuaries and lagoons. The Pamlico Sound region exhibits biofacies, lithofacies, and geophysical facies beneath the islands and within the sound that reveal complex paleoenvironmental changes occurring to the system throughout its evolution. Major coastal

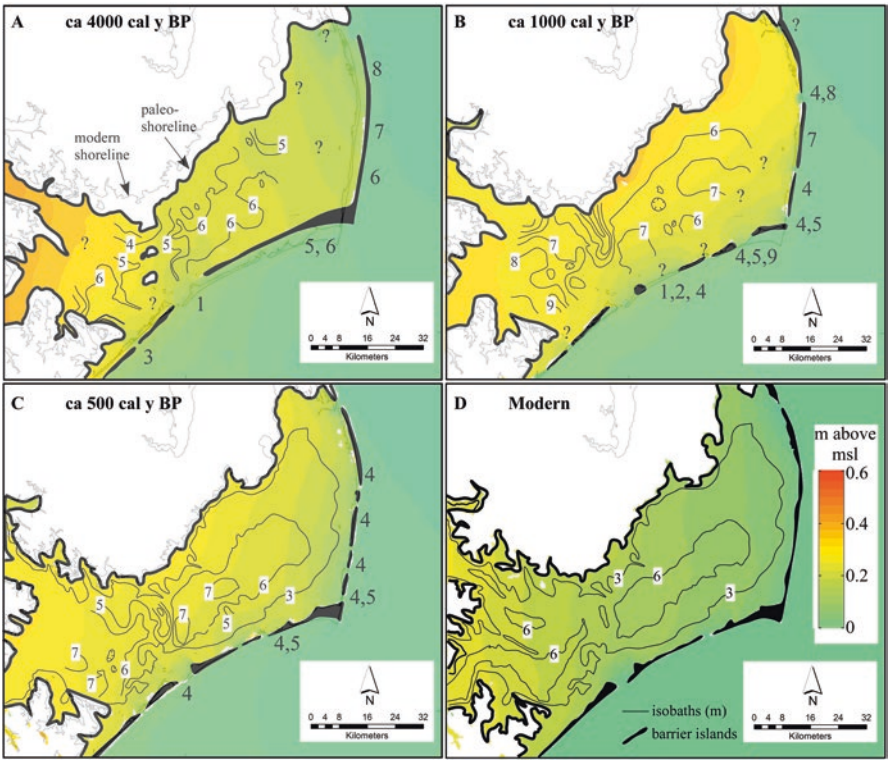

Fig. 12 (**a**–**c**) Maps showing paleo-geomorphic reconstructions based upon data from geophysics and cores (lithofacies and microfossils), and modeled water surface elevation (on a falling tide corresponding with mean tide level on the ocean side of the barriers). Isobaths are based on seismic data (from Zaremba et al. 2016). Large numbers refer to references for barrier island reconstructions at corresponding locations: (*1*) Grand Pre et al. (2011), (*2*) Hale (2008), (*3*) Heron et al. (1984), (*4*) Mallinson et al. (2011), (*5*) Peek et al. (2013), (*6*) Pierce and Colquhoun (1970), (*7*) Ricardo (2005), (*8*) Smith et al. (2009), (*9*) Twamley (2006). (**d**) Modern geomorphic conditions and tides. Note that the 4000 cal year BP scenario (**a**), with a major inlet in southern Pamlico Sound, shows amplified tides (relative to today) in the southwestern Sound (the river estuaries). However, little is known about the occurrence of inlets to the north of Cape Hatteras at 4000 cal year BP. The 1000 cal year BP scenario (**b**) exhibits amplified tides throughout the Sound (up to 40 cm). The 500 cal year BP scenario (**c**) also exhibits amplified tides, but to a lesser extent

geomorphic change, characterized by a high degree of barrier segmentation and normal-marine-salinity waters in southern Pamlico Sound occurred at ca 4000–3500 cal year BP and ca 1200–550 cal year BP (750–1400 CE) (Fig. 12; Culver et al. 2007; Grand Pre et al. 2011; Mallinson et al. 2011). A third period of greater inlet activity (relative to today) occurred during the LIA, ca 500–350 cal year BP (ca 1450–1600 CE), but was not characterized by normal-marine-salinity waters in the sound. These changes were driven by a combination of factors, including processes

that are internal to the coastal system itself (e.g. autogenic processes such as interfluve overtopping, tidal prism changes), and processes external to the coastal system (e.g., climate changes that influence regional storm energy, and relative sea-level rise).

Hydrodynamic modeling based on geologic data and geomorphic reconstructions suggest that increased segmentation of the islands resulted in much greater current activity (Figs. 5 and 7) and an increase in the tidal range within Pamlico Sound (Fig. 12), confirming observations and models of barrier fragmentation described by Fitzgerald et al. (2004, 2008, this volume). The hydrodynamic models agree with geological observations (seismic, sedimentological, and paleoenvironmental data), except for the LIA period. An extensive seismic reflection is seen throughout much of the Pamlico Sound that has been dated to the LIA, but the hydrodynamic model does not show a significant increase in current energy that might be responsible for the erosion and production of the reflection. Likewise, paleoenvironmental data do not indicate increased salinities at this time. This suggests that LIA inlets, although more numerous (based on historical documents and geological data), may have been small, ephemeral, and ineffective at enhancing tidal conditions within the Sound.

An important result of this work, with respect to barrier island evolution, is the recognition that a substantial portion of the submerged back-barrier system (the Hatteras Flats) was likely emplaced in a very short period (within the last 1000 years) in response to widespread segmentation of the barrier islands at ca 1200 cal year BP (750 CE). An additional important result is the recognition that the modern transgressive barrier islands were not always transgressive, but in some areas (i.e., south of Cape Hatteras at least) went through an earlier regressive phase, followed by extensive erosion (at ca 1200 cal year BP), then progradation once again. Finally, these modern wave-dominated barriers appear to have evolved in response to a changing energy regime that included greater tidal influence (relative to today; Fig. 12).

Results of multiple studies along the NC coast illustrate that very rapid and large magnitude changes to the coastal system occurred in the past, and will likely occur in the future, as a result of morphodynamic feedbacks accompanying geomorphic changes to the barrier islands. Given projected rates of sea-level rise and forecasts of increased hurricane activity, it is expected that the future state of the Outer Banks and Pamlico Sound will eventually return to conditions that prevailed during the MCA. Similar responses to changing storminess and sea-level rise can likely be expected for other coastal systems composed of barrier islands and associated back-barrier estuaries and lagoons. Coastal community planning for, and adaptation to (see McNamara and Lazarus this volume), future sea-level rise must take into account not only realistic scenarios of sea-level rise acceleration (e.g., Rahmstorf et al. 2012; Jevrejeeva et al. 2010, 2012) and storm surge, but also significant changes to the regional tidal regime, wave energy, mainland shoreline erosion rates, and ecosystem changes, all of which will have widespread economic impacts.

Acknowledgements The authors would like to acknowledge the extensive contributions from many graduate and undergraduate students that participated in the acquisition and interpretation of data throughout the study area, over a period of nearly three decades. We would also like to acknowledge the contributions of Dorothea Ames, Jim Watson, and John Woods. This paper was improved by the reviews of Antonio Rodriguez and an anonymous reviewer. Financial support was provided by NSF OCE-1130843, and the United States Geological Survey pursuant to cooperative agreement 02ERAG0044.

References

Abbene J, Culver SJ, Corbett DR, Buzas MA, Tully LS (2006) Foraminifera of Pamlico Sound, North Carolina, over the past century. J Foraminifer Res 36:135–151

Ashton AD, Lorenzo-Trueba J (2018) Morphodynamics of barrier response to sea-level rise. In: Moore LJ, Murray AB (eds) Barrier dynamics and response to changing climate. Springer, New York

Bé A, Hamlin WH (1967) Ecology of recent planktonic foraminifera, Part 3, Distribution in the North Atlantic during the summer of 1962. Micropaleontology 13:87–106

Bove MC, Elsner JB, Landsea CW, Niu X, O'Brien JJ (1998) Effect of El Niño on U.S. landfalling hurricanes revisited. Bull Am Meteorol Soc 79:2477–2482

Carré M, Sachs JP, Purca S, Schauer AF, Braconnot P, Falcón RA, Julien M, Lavallee D (2014) Holocene history of ENSO variance and asymmetry in the eastern tropical Pacific. Science 345:1045–1048

Clark PU, Dyke AS, Shaku JD, Carlson A, Clark J, Wohlfarth B, Mitrovica J, Hostetler SW, McCabe AM (2009) The last glacial maximum. Science 325:710–714

Clunies G (2014) Hydrodynamics of a large and shallow back-barrier estuarine system and responses to long-term changes in geomorphology. MS Thesis, Queen's University, Kingston, Ontario, Canada 99 pp

Clunies GJ, Mulligan RP, Mallinson DJ, Walsh JP (2017) Modelling hydrodynamics of large lagoons: insights from the Albemarle-Pamlico Estuarine System. Estuar Coast Shelf Sci 189:90–103

Cobb KM, Westphal N, Sayani HR, Watson JT, Di Lorenzo E, Cheng H, Edwards RL, Charles CD (2013) Highly variable El Niño-Southern Oscillation throughout the Holocene. Science 339:67–70

Corbett DR, Vance D, Letrick E, Mallinson D, Culver S (2007) Decadal-scale sediment dynamics and environmental change in the Albemarle Estuarine System, North Carolina. Estuar Coast Shelf Sci 71:717–729

Cowell PJ, Kinsela MA (2018) Shoreface controls on barrier evolution and shoreline change. In: Moore LJ, Murray AB (eds) Barrier dynamics and response to changing climate. Springer, New York

Cronin TM, Dwyer GS, Kamiya T, Schwede S, Willard DA (2003) Medieval Warm Period, Little Ice Age and 20th century temperature variability from Chesapeake Bay. Glob Planet Chang 36:17–29

Culver SJ, Grand Pre CA, Mallinson DJ, Riggs SR, Corbett DR, Foley J, Hale M, Metger L, Ricardo J, Rosenberger J, Smith CG, Smith CW, Snyder SW, Twamley D (2007) Late Holocene barrier island collapse: Outer Banks, North Carolina, USA. Sediment Rec 5:4–8

Cumming WP (1966) North Carolina in maps, plate II. Division of Archives and History, North Carolina Department of Cultural Resources, Raleigh, NC

Davis MB, Spear RW, Shane LCK (1980) Holocene climate of New England. Quat Res 14:240–250

Delcourt PA, Delcourt HR (1980) Pollen preservation and Quaternary environmental history in the Southeastern United States. Palynology 4:215–231

deMenocal P, Ortiz J, Guilderson T, Sarnthein M (2000) Coherent high- and low-latitude climate variability during the Holocene warm period. Science 288:2198–2202

Donnelly JP, Woodruff JD (2007) Intense hurricane activity over the past 5,000 years controlled by El Niño and the West African monsoon. Nature 447:465–468

Donnelly JP, Hawkes AD, Lane P, MacDonald D, Shuman BN, Toomey MR, van Hengstum PJ, Woodruff JD (2015) Climate forcing of unprecedented intense-hurricane activity in the last 2000 years. Earth's Future 3(2):49–65. https://doi.org/10.1002/2014EF000274

Fenster MS, Dolan R (1993) Historical shoreline trends along the Outer Banks, North Carolina: processes and responses. J Coast Res 9:172–188

FitzGerald DM, Montello TM (1993) Backbarrier and inlet sediment response to the breaching of Nauset Spit and formation of New Inlet, Cape Cod, MA. In: Aubrey DG, Giese GS (eds) Formation and evolution of multiple tidal inlet systems. Am. Geophys. Inst, Washington, DC, pp 158–185

FitzGerald DM, Kulp M, Penland P, Flocks J, Kindinger J (2004) Morphologic and stratigraphic evolution of ebb-tidal deltas along a subsiding coast: Barataria Bay, Mississippi River Delta. Sedimentology 15:1125–1148

Fitzgerald DM, Fenster MS, Argow BA, Buynevich IV (2008) Coastal impacts due to sea-level rise. Annu Rev Earth Planet Sci 36:601–647

Fitzgerald DM, Georgiou I, Hein C, Hughes Z, Kulp M, Miner M (2018) Runaway barrier island transgression concept: global case studies. In: Moore L, Murray B (eds) Barrier dynamics and the impact of climate change on barrier evolution. Springer, New York

Giese GS (1988) Cyclical behavior of the tidal inlet at Nauset Beach, Chatham, Massachusetts. In: Aubrey L, Weishar DG (eds) Hydrodynamics and sediment dynamics of tidal inlets. Springer, New York, pp 269–283

Goldenberg SB, Shapiro LJ (1996) Physical mechanisms for the association of El Niño and West African rainfall with Atlantic major hurricane activity. J Clim 9:1169–1187

Grand Pre C, Culver SJ, Mallinson DJ, Farrell KM, Corbett DR, Horton BP, Hillier C, Riggs SR, Snyder SW, Buzas MA (2011) Rapid Holocene coastal change revealed by high-resolution micropaleontological analysis, Pamlico Sound, North Carolina, USA. Quat Res 76:319–334

Grimm EC, Jacobson GL, Watts WA, Hansen BCS, Maasch K (1993) A 50,000 year record of climate oscillations from Florida correlated with North Atlantic Heinrich events. Science 261:198–200

Hale ME (2008) Late Holocene geologic evolution of Central Ocracoke Island, Outer Banks, North Carolina. M.S. thesis, Greenville, North Carolina, East Carolina University, 213 p

Hayes MO (1979) Barrier island morphology as a function of tidal and wave regime. In: Leatherman SP (ed) Barrier Islands from the Gulf of St. Lawrence to the Gulf of Mexico. Academic Press, New York, pp 1–27

Heron SD Jr, Moslow TF, Berelson WM, Herbert JR, Steele GA III, Susman KR (1984) Holocene sedimentation of a wave-dominated barrier-island shoreline: Cape Lookout, North Carolina. Mar Geol 60:413–434

Hill DF, Griffiths SD, Peltier WR, Horton BP, Tornqvist TE (2011) High-resolution numerical modeling of tides in the western Atlantic, Gulf of Mexico, and Caribbean Sea during the Holocene. J Geophys Res 116:1–16. https://doi.org/10.1029/2010JC006896

Horton BP, Peltier WR, Culver SJ, Drummond R, Engelhart SE, Kemp AC, Mallinson D, Thieler ER, Riggs SR, Ames DV (2009) Holocene sea-level changes along the North Carolina coastline: implications for glacial adjustment models and current rates of sea-level change. Quat Sci Rev 28:1725–1736

Inman D, Dolan R (1989) The Outer Banks of North Carolina: budget of sediment and inlet dynamics along a migrating barrier system. J Coast Res 5:193–237

Jackson ST (1989) Postglacial vegetational changes along an elevational gradient in the Adirondack Mountains (New York). Biological Survey Museum Bulletin 465. The New York State Museum, New York, p 29

Jevrejeeva S, Moore JC, Grinsted A (2010) How will sea level respond to changes in natural and anthropogenic forcings by 2100? Geophys Res Lett 37:L07703. https://doi.org/10.1029/2010GL042947

Jevrejeeva S, Moore JC, Grinsted A (2012) Sea level projections to AD2500 with a new generation of climate change scenarios. Glob Planet Chang 80–81:14–20

Keigwin LD (1996) The Little Ice Age and Medieval Warm Period in the Sargasso Sea. Science 274:1504–1508

Kemp AC, Horton BP, Culver SJ, Corbett DR, van de Plassche O, Gehrels WR, Douglas BC, Parnell AC (2009) Timing and magnitude of recent accelerated sea-level rise (North Carolina, United States). Geology 37:1035–1038

Kemp AC, Horton BP, Donnelly JP, Mann ME, Vermeer M, Rahmstorf S (2011) Climate related sea-level variations over the past two millennia. Proc Natl Acad Sci U S A 108:11017–11022

Kemp AC, Kegel JJ, Culver SJ, Barber DC, Mallinson DJ, Leorri E, Bernhardt CE, Cahill N, Riggs SR, Woodson AL, Mulligan RP, Horton BP (2017) Extended late Holocene relative sea-level histories for North Carolina, USA. Quat Sci Rev 160:13–30

Kopp RE, Horton BP, Kemp AC, Tebaldi C (2015) Past and future sea-level rise along the coast of North Carolina, USA. Clim Chang 132(4):693–707. https://doi.org/10.1007/s10584-015-1451-x

Kraft JC, Chrzastowski MJ, Belknap DF, Toscano MA, Fletcher CH III (1987) The transgressive barrier–lagoon coast of Delaware: morphostratigraphy, sediment sequences and responses to relative rise in sea level. In: Nummedal D, Pilkey OH, Howard JD (eds) Sea-level fluctuations and coastal evolution. Special Publication No. 41. Society of American Paleontologists and Mineralogists, Tulsa, OK, pp 129–143

Lauback C, Culver S, Leorri E, Mallinson D, Mitra S, Minnehan J, Mulligan R (2012) Isotopic evidence for episodic marine water incursions into Pamlico Sound, NC during the Holocene. GSA Abstracts with Programs, Annual Meeting, Charlotte, NC, vol 44 No. 7

Lazar K, Mallinson D, Culver S (2016) Late Quaternary development of the Croatan Beach Ridge Complex, Bogue Sound, and Bogue Banks, NC, USA and implications for coastal evolution. Estuar Coast Shelf Sci 174:49–64

Levermann A, Griesel A, Hofmann M, Montoya M, Rahmstorf S (2005) Dynamic sea level changes following changes in the thermohaline circulation. Clim Dyn 24:347–354

Luettich RA Jr, Carr SD, Reynolds-Fleming JV, Fulcher CW, McNinch JE (2002) Semi-diurnal seiching in a shallow, micro-tidal lagoonal estuary. Cont Shelf Res 22:1669–1681

Mallinson DJ, Riggs SR, Thieler ER, Culver SJ, Farrell K, Foster DS, Corbett DR, Horton B, Wehmiller JF (2005) Late Neogene and Quaternary evolution of the northern Albemarle Embayment (mid-Atlantic continental margin, USA). Mar Geol 217:97–117

Mallinson DJ, Burdette K, Mahan S, Brook G (2008) Optically stimulated luminescence age controls on late Pleistocene and Holocene lithosomes, North Carolina, USA. Quat Res 69:97–109

Mallinson DJ, Culver SJ, Riggs SR, Thieler ER, Foster D, Wehmiller J, Farrell K, Pierson J (2010a) Regional seismic stratigraphy and controls on the Quaternary evolution of the Cape Hatteras region of the Atlantic passive margin, USA. Mar Geol 268:16–33

Mallinson DJ, Smith CW, Culver SJ, Riggs SR, Ames DV (2010b) Geological characteristics and spatial distribution of paleo-inlet channels beneath the Outer Banks barrier islands, North Carolina, USA. Estuar Coast Shelf Sci 88:175–189

Mallinson DJ, Smith CW, Mahan S, Culver SJ, McDowell K (2011) Barrier island processes and response to late Holocene climate patterns: Outer Banks barrier islands, North Carolina, USA. Quat Res 76:46–57

Mann ME, Woodruff JD, Donnelly JP, Zhang Z (2009) Atlantic hurricanes and climate over the past 1,500 years. Nature 460:880–883

Mayewski PA, Rohling EE, Stager JC, Karlen W, Maasch KA, Meeker LD, Meyerson EA, Gasse F, van Kreveld S, Holmgren K, Lee-Thorp J, Rosqvist G, Rack F, Staubwasser M, Schneider RR, Steig EJ (2004) Holocene climate variability. Quat Res 62:243–255

McGregor HV, Fisher MJ, Gagan MD, Fink D, Phipps SF, Wong H, Woodroffe CD (2013) A weak El Nino/Southern Oscillation with delayed seasonal growth around 4,300 years ago. Nat Geosci 6:949–953. https://doi.org/10.1038/NGEO1936

McNamara DE, Lazarus ED (2018) Barrier islands as coupled human–landscape systems. In: Moore LJ, Murray AB (eds) Barrier dynamics and response to changing climate. Springer, New York

Metger L (2009) Holocene paleoenvironmental change in southern Pamlico Sound, North Carolina. MS Thesis, East Carolina University

Minnehan J (2014) Using sediment organic geochemistry to interpret late Holocene barrier island and estuarine evolution, North Carolina, USA. MS Thesis, East Carolina University

Moran KL, Mallinson DJ, Culver SJ, Leorri E, Mulligan RP (2015) Late Holocene evolution of Currituck Sound, North Carolina, USA: environmental change driven by sea-level rise, storms, and barrier island morphology. J Coast Res 31:827–841

Murray AB, Moore LJ (2018) Geometric constraints on long-term barrier migration: from simple to surprising. In: Moore LJ, Murray AB (eds) Barrier dynamics and response to changing climate. Springer, New York

O'Brien MP (1969) Equilibrium flow areas of inlets on sandy coasts. J Waterway Port Coast Ocean Eng 95:43–55

Odezulu CI, Lorenzo-Trueba J, Wallace DJ, Anderson JB (2018) Follets Island: a case of unprecedented change and transition from rollover to subaqueous shoals. In: Moore LJ, Murray AB (eds) Barrier dynamics and response to changing climate. Springer, New York

Oertel GF, Kraft JC, Kearney MS, Woo HJ (1992) A rational theory for barrier–lagoon development: Quaternary coasts of the United States. SEPM Special Publication. Mar Lacustrine Syst 48:77–87

Oliveira I (1970) Natural flushing ability in tidal inlets. Coast Eng 1970:1827–1845. https://doi.org/10.1061/9780872620285.111

Otvos EG, Carter GA (2008) Hurricane degradation–barrier development cycles, northeastern Gulf of Mexico: landform evolution and island chain history. J Coast Res 24:463–478

Parham PR, Riggs SR, Culver SJ, Mallinson DJ, Rink WJ, Burdette K (2013) Quaternary coastal lithofacies, sequence development and stratigraphy in a passive margin setting, North Carolina and Virginia, USA. Sedimentology 60:503–547

Parham PR, Riggs SR, Culver SJ, Mallinson D, Wehmiller JF (2007) Quaternary depositional patterns and sea-level fluctuations, northeastern North Carolina. Quat Res 67:83–99

Peek KM, Mallinson DJ, Culver SJ, Mahan SA (2013) Holocene geologic development of the Cape Hatteras Region, Outer Banks, North Carolina, USA. J Coast Res 30(1):41–58

Pendleton EA, Thieler ER, Williams SJ (2004) Coastal vulnerability assessment of Cape Hatteras National Seashore (CAHA) to sea-level rise. Open-file report 2004-1064, U.S. Department of the Interior, US Geological Survey, 20 p

Pierce JW, Colquhoun DJ (1970) Holocene evolution of a portion of the North Carolina Coast. Geol Soc Am Bull 81:3697–3714

Rahmstorf S (2007) A semi-empirical approach to projecting future sea-level rise. Science 315:368–370

Rahmstorf S, Perrette M, Vermeer M (2012) Testing the robustness of semi-empirical sea level projections. Climate Dynam 39:861–875

Ricardo JP (2005) Late Holocene Paleoenvironmental Change of the Salvo–Gull Island–Little Kinnekeet Area, Outer Banks, North Carolina. M.S. thesis, East Carolina University, Greenville, North Carolina, 188 p

Riggs SR, Ames DV (2003) Drowning of North Carolina: Sea-level rise and estuarine dynamics. University of North Carolina Sea Grant Publication, Raleigh, NC, UNC-SG-03-04

Riggs SR, York LL, Wehmiller JF, Snyder SW (1992) Depositional patterns resulting from high-frequency Quaternary sea-level fluctuations in Northeastern North Carolina. Quaternary coasts of the United States: marine and lacustrine systems. SEPM Spec Publ 48:141–153

Riggs SR, Cleary WJ, Snyder SW (1995) Influence of inherited geologic framework on barrier shoreface morphology and dynamics. Mar Geol 126:213–234

Riggs, SR, Rudolph, GL, Ames, DW (2000) Erosional scour and geologic evolution of Croatan Sound, Northeastern North Carolina. North Carolina Department of Transportation, Raleigh, NC, Rept. No. FHWA/NC/2000-02, 115 p

Riggs SR, Ames DV, Culver SJ, Mallinson DJ, Corbett DR, Walsh JP (2009) In the eye of a human hurricane: Oregon Inlet, Pea Island, and the northern Outer Banks of North Carolina. In: Kelley JT, Young RS, Pilkey OH (eds) Identifying America's most vulnerable oceanfront communities: a geological perspective. Geological Society of America, Special Publication, Boulder, CO, pp 43–72

Riggs S, Ames D, Culver S, Mallinson D (2011) The battle for North Carolina's coast: evolutionary history, present crisis & vision for the future. UNC Press, Chapel Hill, NC. 142 p

Rodriguez AB, Yu W, Theuerkauf EJ (2018) Abrupt increase in washover deposition along a transgressive barrier island during the late nineteenth century acceleration in sea-level rise. In: Moore LJ, Murray AB (eds) Barrier dynamics and response to changing climate. Springer, New York

Schnitker D (1971) Distribution of foraminifera on the North Carolina continental shelf. Tulane Stud Geol Paleontol 8:169–215

Smith CF (2015) Holocene development of the Ocracoke Inlet flood-tide delta region, Outer Banks, North Carolina. MS Thesis, East Carolina University

Smith CG, Culver SJ, Mallinson DJ, Riggs SR, Corbett DR (2009) Using foraminifera to recognize former flood-tide deltas in the Holocene stratigraphic record: examples from the Outer Banks, North Carolina. Stratigraphy 6:61–78

Stick, D., 1958. The Outer Banks of North Carolina. Van Rees Press, New York. 352 p.

Stutz ML, Pilkey OH (2011) Open-ocean barrier islands: influence of climatic, oceanographic and depositional settings. J Coast Res 27:207–222

Thieler ER, Foster DS, Mallinson DJ, Himmelstoss EA, McNinch JE, List JH, Hammar-Klose ES (2013) Quaternary geophysical framework of the northeastern North Carolina coastal system. U.S. Geological Survey Open-File Report 2011–1015, https://pubs.usgs.gov/of/2011/1015/

Timmons EA, Rodriguez AB, Mattheus CR, DeWitt R (2010) Transition of a regressive to a transgressive barrier island due to back-barrier erosion, increased storminess, and low sediment supply: Bogue Banks, North Carolina, USA. Mar Geol 278(1–4):100–114

Twamley DF (2006) Holocene geologic development of the Hatteras Village Area, Outer Banks, North Carolina. M.S. thesis, East Carolina University, Greenville, North Carolina, 173 p

Wanner H, Beer J, Butikofer J, Crowley TJ, Cubasch U, Fluckiger J, Goosse H, Grosjean M, Joos F, Kaplan J, Kuttel M, Muller S, Prentice I, Solimina O, Stocker T, Tarasov P, Wagner M, Widmann M (2008) Mid- to late Holocene climate change: an overview. Quat Sci Rev 27:1791–1828

Wells JT, Kim S-Y (1989) Sedimentation in the Albemarle-Pamlico lagoonal system: synthesis and hypothesis. Mar Geol 88:263–284

Winter A, Ishioroshi H, Watanabe T, Oba T, Christy J (2000) Caribbean sea surface temperatures: two-to-three degrees cooler than present during the Little Ice Age. Geophys Res Lett 27:3365–3368

Wright HE Jr (1976) The dynamic nature of Holocene vegetation, a problem in paleoclimatology, biogeography, and stratigraphic nomenclature. Quat Res 6:581–596

Wright HE, Kutzbach JE, Webb T III, Ruddiman WF, Street-Perrot EA, Bartlein PJ (eds) (1993) Global climates since the last glacial maximum. University of Minnesota Press, Minneapolis, MN

Wurtzel JB, Black DE, Thunell RC, Peterson LC, Tappa EJ, Rahman S (2013) Mechanisms of southern Caribbean SST variability over the last two millennia. Geophys Res Lett 40(22):5954–5958

Zaremba N, Mallinson D, Leorri E, Culver S, Riggs S, Mulligan R, Horsman E (2016) Controls on the stratigraphic record and paleoenvironmental change within a Holocene estuarine system: Pamlico Sound, North Carolina, USA. Mar Geol 379:109–123

Abrupt Increase in Washover Deposition Along a Transgressive Barrier Island During the Late Nineteenth Century Acceleration in Sea-Level Rise

Antonio B. Rodriguez, Winnie Yu, and Ethan J. Theuerkauf

Abstract Determining the magnitude of barrier-island geomorphologic change and response time to an increase in the rate of sea-level rise is important because sea-level rise is accelerating, many barriers islands are urban centers, and barriers buffer mainland shorelines and estuaries from ocean processes, especially during storms. Here, we show that Onslow Beach, NC, a sediment-starved transgressive barrier island located along a cuspate shoreline, had an immediate increase in apparent frequency and landward extent of washover deposition during the late nineteenth century increase in the rate of relative sea-level rise. The evolution of the barrier at millennial to decadal time scales was reconstructed from sediment cores, radiocarbon dates, and remote sensing. Those data show that the oldest washover deposit preserved in the stratigraphy of the island is approximately AD 722 and at that time the island was seaward of its present location and an open-water lagoon separated it from the mainland. Barrier-island transgression progressed mainly through overwash processes and saltmarsh replaced the lagoon by AD 1500. During the nineteenth century, the number and landward extent of washover deposits increased abruptly along the island concurrently with a threefold increase in the rate of relative sea-level rise. This was not a period of increased storminess in the Atlantic. Rather, the increase in number and landward extent of washover deposits is interpreted to have been caused by an increase in the rate of island transgression. The increase in the rate of relative sea-level rise, and possibly other contemporaneous mechanisms such as changes in wave climate, likely caused island narrowing through landward movement of the shoreline, lowered the elevation of the island

A.B. Rodriguez (✉) • W. Yu
Institute of Marine Sciences, University of North Carolina at Chapel Hill, Morehead City, NC, USA
e-mail: abrodrig@email.unc.edu; wnnyu13@gmail.com

E.J. Theuerkauf
Institute of Marine Sciences, University of North Carolina at Chapel Hill, Morehead City, NC, USA

Illinois State Geological Survey, Champaign, IL, USA
e-mail: ejtheu@illinois.edu

L.J. Moore, A.B. Murray (eds.), *Barrier Dynamics and Response to Changing Climate*, https://doi.org/10.1007/978-3-319-68086-6_4

principally through erosion of the dunes and made the island more vulnerable to overwash. These data suggest that transgressive barriers, especially those at the center of a coastal embayment, are extremely sensitive to increases in water level, which cause an abrupt decrease in resistance to overwash. The response of other barrier islands to accelerating sea-level rise may well be similarly rapid, but the degree of geomorphic change will vary depending on island morphology, rates of sediment supply, and physical processes.

Keywords Barrier island • Onslow Beach • Sea-level rise • Washover • Overwash • Climate change • Coastal resilience • Storm impact • Paleotempestology • Coastal evolution Coastal hazard

1 Introduction

Over the next 100 years, projections show an acceleration in sea-level rise (Rahmstorf 2007; Jevrejeva et al. 2008; Church et al. 2013) and an increase in the intensity of tropical cyclones in the Atlantic (Knutson et al. 2010; Bender et al. 2010). Determining the effects of such changes on coastal environments is a research priority because globally there is a high concentration of people, infrastructure, and investment in low-lying coastal areas (Gornitz 1991; Titus et al. 1991; Nicholls et al. 1999; Thieler and Hammar-Klose 2000; Ashton et al. 2008; FitzGerald et al. 2008; Woodruff et al. 2013). Improving predictions of the vulnerability and response of barrier islands to projected climate change is particularly important because in addition to this depositional environment's socioeconomic value, it buffers inland areas and fragile estuarine ecosystems against tropical-cyclone induced storm surges and waves. Coastal vulnerability is a function of an environment's resistance and/or resilience to climate change, storms, or human impacts. Resiliency refers to the ability of a landscape to recover after a disturbance; while resistance refers to its ability to maintain its state during a disturbance. While barrier islands are effective at buffering against individual storms, they are not highly resistant to increases in storminess and the rate of sea-level rise, or changes to coastal sediment budgets and sediment-transport pathways, because barrier islands are composed of unconsolidated sandy sediment that is easily eroded (Rodriguez et al. 2004; FitzGerald et al. 2008; Wallace et al. 2009; Timmons et al. 2010; Mallinson et al. 2011). The unconsolidated nature of barrier islands makes them prone to changes in morphology and shoreline position in response to prolonged periods (i.e., longer than individual storms) of higher water level and wave conditions that transfer wave energy to higher elevations promoting erosion of the backshore and dunes (Theuerkauf et al. 2014; Johnson et al. 2015). As barrier islands narrow and decrease in elevation, they become more vulnerable to flooding and overwash during storms and their effectiveness as buffers to inland-area flooding can decrease (Wamsley et al. 2009; Irish et al. 2010; Bilskie et al. 2014).

It is well documented that barrier-island evolution over millennial time scales is impacted by changes in sea-level rise and storminess. During the last deglaciation, increases in the rate of sea-level rise resulted in episodes of rapid shoreline retreat, as evidenced by preserved barrier-island sequences on low-energy broad continental shelves (Rodriguez et al. 1999; Gardner et al. 2007; Storms et al. 2008; Mellett and Plater this volume) as well as high-energy steep continental shelves (Salzmann et al. 2013). Increased hurricane activity during the medieval climate anomaly (1100–900 cal year BP; Cronin et al. 2003; Mann et al. 2009) resulted in an increase in the number of tidal inlets along the northern and central Outer Banks barrier-island chain of North Carolina, USA (Mallinson et al. 2011, this volume; Culver et al. 2007) and increased backbarrier erosion along the southern Outer Banks (Timmons et al. 2010). Most field studies of long-term barrier-island evolution lack the necessary stratigraphic resolution to address morphologic response to changes in sea-level rise and storminess that occur over centennial and shorter time scales making models extremely important for predicting changes in coastal morphology.

Morphologic models parameterized to run over yearly to centennial time periods indicate that those 100-year predictions for sea-level rise and tropical-cyclone intensity could result in dramatic changes to barrier-island morphology and position (Slott et al. 2006; Lorenzo-Trueba and Ashton 2014; Moore et al. 2014; Walters et al. 2014; Cowell and Kinsela this volume; Murray and Moore this volume; Ashton and Lorenzo-Trueba this volume); however, there are few comparative field studies that can be used to corroborate and advance model parameterization. Challenges associated with anthropogenic modifications to the coast overprinting the sedimentary record, such as beach nourishment, development, and shoreline stabilization, have led to a lack of field-data-based reconstructions of barrier-island morphology and shoreline position over centennial time scales with changing climatic conditions (Wallace and Anderson 2013; Johnson et al. 2015) and short time periods being represented by thin strata that is easily bioturbated and/or eroded.

While there is little evidence that the frequency of tropical cyclone activity has increased over the past 150 years (Vecchi and Knutson 2008), saltmarsh proxy records of relative sea level from around the world show an abrupt increase in the rate of rise at the end of the nineteenth century from <1 mm/year to ~2 mm/year (e.g., van de Plassche et al. 1998; Donnelly et al. 2004; Gehrels et al. 2008; Leorri et al. 2008; Kemp et al. 2011; García-Artola et al. 2015). This more than doubling of the rate of sea-level rise should have affected the morphology and/or shoreline position of barrier islands, but few studies that resolve coastal landscape change during that abrupt acceleration in sea level exist. Wallace and Anderson (2013) interpreted that the historical acceleration in relative sea-level rise resulted in an increase in the flux of sediment from Galveston Island, TX, USA to laterally-adjacent and offshore environments. This was based on a comparison of sediment flux averaged over the last 3 millennia, estimated from the volume and age of sediment in the shoreface, inner shelf, and tidal delta (~130,000 m^3/year), and sediment flux estimated using historic shoreline-erosion rates (~240,000 m^3/year; Wallace and Anderson 2013). Here, our aim is to increase the fidelity of coastal-change records by measuring the frequency and extent of washover deposition. Washover

deposition occurs during barrier-island overwash, when the water level of the ocean exceeds the height of the beach berm and/or dune crest resulting in the flow of water and sediment landward across a barrier island (Donnelly et al. 2006).

We hypothesize that an increase in the rate of sea-level rise will manifest as an increase in the flux of sand landward across transgressive barrier islands, which commonly have low dune elevations and narrow widths (Galloway and Hobday 1983). Increases in the flux of landward transport of sand would occur because the height of storm surge would increase concomitantly with sea-level rise, thus increasing the frequency of barrier-island overwash. Additionally, an increase in the rate of sea-level rise results in an increase in the rate of beach erosion and shoreline transgression (Brunn 1962), which could narrow and/or lower the elevation of barrier islands making them less resistant to overwash. Here, we examine impacts of the late nineteenth century increase in the rate of sea-level rise on the cross-shore transport and deposition of washover sand on a transgressive barrier island. We test our hypothesis by developing a record of washover deposition, which should be preserved in back-barrier sediments and can be extracted by collecting transects of cores to sample, map, and date washover deposits.

2 Study Area and Background

The study area is Onslow Beach, a northeast–southwest trending barrier island located in Onslow Bay, southeast North Carolina, USA (Fig. 1). Onslow Beach is a 12-km long and 90–600 m wide wave-dominated barrier that borders Browns Inlet to the northeast and the New River Inlet to the southwest (Fig. 1). The tidal range is about 1 m, the nearshore average annual significant wave height and wave period is 0.91 m and 4.7 s, respectively, and the island is impacted by tropical systems in the summer and fall and extratropical systems in the winter (Theuerkauf et al. 2014). The island is part of Marine Corps Base Camp Lejeune and the northernmost part of the island was not accessible for study due to the presence of unexploded ordinance. There is limited human modification of the island; the few small buildings that exist are confined to a 2.5 km-long sector (Fig. 1), driving on the dunes is prohibited and Marine Corps amphibious training is mainly confined to intertidal areas around the southwestern end.

The barrier shoreline has a central headland, which intersects the island (Riggs et al. 1995). The headland corresponds with a transition in shoreline evolution from transgression in the southwest, to regression in the northeast (Rodriguez et al. 2012; Theuerkauf and Rodriguez 2014). The morphology along the length of the island is variable, characterized by a low-elevation (1–2 m) discontinuous foredune ridge along with washover fans and terraces in the southwest and a high-elevation (>7 m) continuous dune ridge backed by a well-developed maritime forest in the northeast (Fig. 1).

The site is ideal for investigating barrier-island response to an increase in the rate of sea-level rise and/or storminess because the shoreline has been predicted to

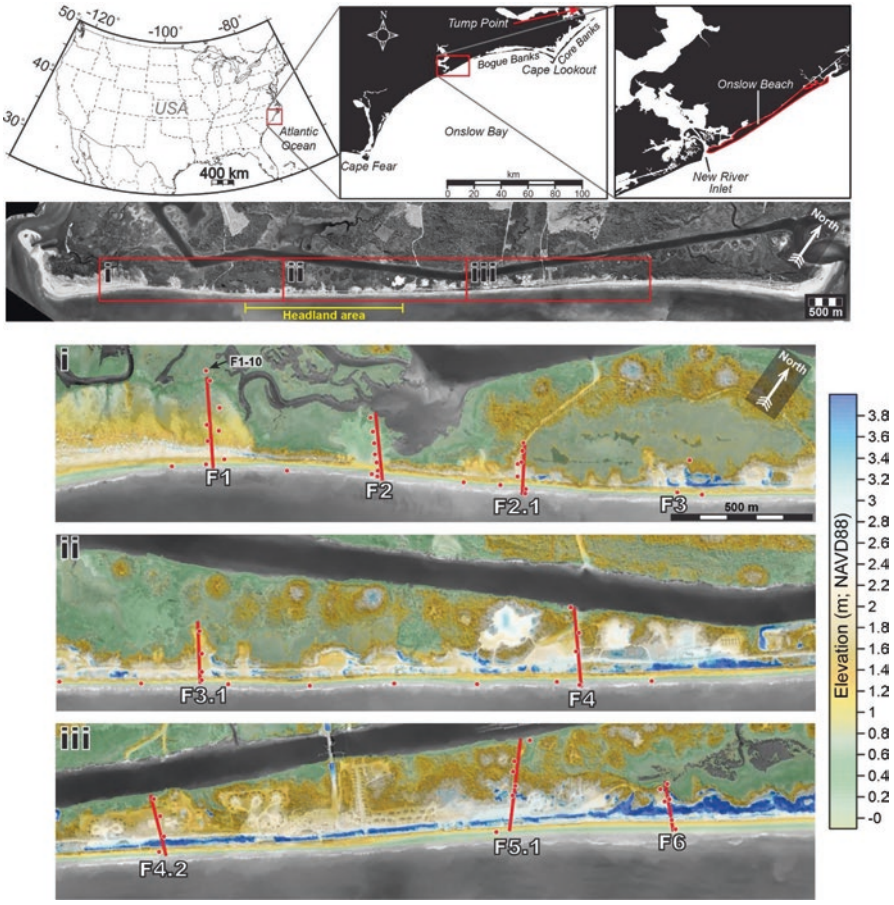

Fig. 1 Study area map. Onslow Beach is centrally located between Cape Fear and Cape Lookout and ~100 km southwest of Tump Point, where Kemp et al. (2011) reconstructed sea level from a saltmarsh sedimentary record. Elevation data and imagery, provided by Marine Corps Base Camp Lejeune, is from April 2013

respond rapidly to changes in water level (Theuerkauf et al. 2014) and wave conditions (Slott et al. 2006). The island is positioned in the middle of an embayment, half-way between Cape Lookout and Cape Fear. The model of Ashton et al. (2001) suggests erosion rates along this shoreline over millennial time scales were higher in cuspate bays than at cape headlands. These large-scale (10–100 km) along-shore variations in erosion rates are due to the predominance of oblique high-angle waves in Onslow Bay that transported sand away from Onslow Beach to the adjacent accreting capes (Ashton et al. 2001). Slott et al. (2006) used Ashton et al.'s (2001) model to examine shoreline response to changing storm patterns in Onslow Bay and found that an increase in tropical and extra-tropical storms cause more erosion in cuspate bays (maximum erosion in the area of Onslow Beach) than adjacent cape

headlands. Based on a salt-marsh sedimentary record from Tump Point, located 100 km northeast of Onslow Beach, the rate of relative sea-level rise in the area fluctuated during the last 2000 years (Kemp et al. 2009, 2011). Kemp et al. (2009) identified an increase in the rate of relative sea level (not corrected for background Holocene rates of sea-level rise and glacial isostatic rebound) from ~1.0 mm/year to 3.2 mm/year that began between A.D. 1865 and 1892 in response to twentieth century warming (Kemp et al. 2011) in North Carolina, which is similar to other studies along the Atlantic coast (Engelhart et al. 2011; Kemp et al. 2014). As sea-level rise accelerates, higher-elevation portions of Onslow Beach, such as the backshore and foredune areas, should experience increased wave erosion.

3 Methods

3.1 Coring

To sample the stratigraphy of Onslow Beach and identify washover deposits, we collected 47 cores from 9 cross-island transects. We tried to space transects equally along the island, but dense vegetation limited access; hence, transect spacing averaged 899 m ± 327 m (± standard deviation). An additional 13 cores were collected between transects along the southwestern and central parts of Onslow Beach to assess whether sampling based only on the cross-shore transects were missing washover deposits. Those supplementary cores reduced our along-beach sample spacing to 250 ± 135 m (± standard deviation) for that portion of the barrier (Fig. 1). Most transects were sampled with 6 or 7 cores, except sites F3 and F4, where only 2 and 4 cores were collected, respectively (Fig. 1). Most of the cores were obtained using the vibracoring method, which resulted in cores that were 0.62–3.94 m in length. We had difficulty penetrating through the upper ~75 cm of dry sand, which necessitated digging a hole to the water table at most of the sites using a post-hole digger. The excavated sediment was described in the field and at each site the depth of the hole was recorded before vibracoring. Due to dense vegetation, the most landward core at Site F3 was collected using an Edelman Auger and sediment down to 3-m depth was described in the field. The locations and elevations of all cores as well as topographic profiles crossing the barrier at the 9 transects were surveyed with a Trimble R8/5800 Real-Time Kinematic GPS unit. Average horizontal and vertical precisions were 0.015 m and 0.020 m, respectively.

The cores were split, photographed, described, and sampled in the lab. Interpretations of sedimentary facies relied on lithologies, sedimentary structures, bedding, and macrofossil assemblages. Approximately 370 subsamples were collected from the cores for grain-size analyses. A 2000-μm sieve was used to determine the >2000 μm fraction and a Cilas laser particle-size analyzer for the 2000 μm to 0.04 μm component. Shore-perpendicular stratigraphic cross sections were created from facies interpretations.

3.2 Radiocarbon Dating

Inorganic and organic materials sampled from the cores were selected for radiocarbon dating by accelerator mass spectrometry. Articulated bivalves, large pieces of wood, and seeds were preferentially chosen over bulk organic samples, multiple small wood fragments, and unpaired valves to minimize the adverse effects of reworking on developing an accurate chronostratigraphy. Radiocarbon analysis of 22 samples was performed by Woods Hole Oceanographic Institution and Beta Analytic. Ages were calibrated to years before present (AD 1950 = 0 BP) and calendar years at the 95.45% confidence interval (2 sigma) obtained by using the CALIB 7.1 program (Stuiver and Reimer 1993; Reimer et al. 2013). The two estuarine bivalves that were dated were treated as marine samples during calibration (Hughen et al. 2004).

3.3 Washover Measurements

To constrain the timing of washover deposition, we sampled and radiocarbon dated saltmarsh organic material directly below (T1) and above (T2) the washover deposit and assumed that the washover was deposited during the midpoint time ± (T1 − T2)/2. We used the median probability calibrated radiocarbon ages, as opposed to the 2-sigma age ranges (which there can be a number of), for T1 and T2. This method assumes that T1 is older than the washover, because of saltmarsh erosion during island overwash and T2 is younger than the washover due to the time lag between washover deposition and subsequent saltmarsh colonization. We used historical aerial photography from 1938 to constrain the minimum age (T2) of washover deposits with calibrated age ranges of T1 that included AD 1950, based on the presence or absence of the washover in the photo. The historical record (including personal observation for washovers deposited during the last decade) and the presence or absence of the washover on aerial photographs from 1938 and 1956 were employed to constrain T1 and T2 for washover deposits that presently exist at the surface across transects F1, F2, F3.1, and F4.

The landward extent of each washover deposit was measured as the distance between a straight baseline and the landward edge of the washover. We defined the baseline as the best-fit linear regression through the 2006 digitized Onslow Beach shoreline (defined as the wet-dry line). This approach averages out the sinusoidal shape of the shoreline, which is likely variable through time, resulting in a straight baseline. The landward edge of each washover was measured from aerial photos (for historical washovers) or the landward pinch-out measured from the stratigraphic cross sections for the older washover deposits. The landward pinch out of washover deposits was estimated to be the midpoint between the core that sampled the deposit and the adjacent landward core that did not sample the deposit and error on this measurement is equal to the distance between the midpoint and an adjacent core location.

4 Results and Interpretations

4.1 Depositional Environments and Lithologic Facies

The depositional environments along Onslow Beach, including beach (foreshore and backshore), dune, washover, and marsh were sampled in the tops of the cores. Lithologic-facies descriptions of those modern environments were used to help interpret the older sedimentary units, including the identification of old buried washover deposits. Lithologic facies A and B were only sampled at depth and were not similar to any of the modern depositional environments that exist at Onslow Beach.

4.1.1 Beach Facies

The beach facies is characterized by fine to medium quartz sand (0.91–2.38 Φ) with gently dipping heavy-mineral laminae and beds and gravelly sand beds (Figs. 2a and 3a). The average gravel content is 6.75% but can be as high as 41.72% within those coarse-grained beds, which were predominantly sampled in the foreshore and contain abraded shells and well-rounded oblate lithoclasts. The backshore is predominantly influenced by aeolian processes, which results in finer grained and better sorted sand than found in foreshore deposits. The beach facies ranges in thickness from 32 cm to >204 cm (in places the core was not long enough to sample the entire thickness). Overall, the thickness of the beach facies decreases, and the percent gravel and the mean grain size of the sand fraction increases toward the southwest and from the toe of the foredune seaward (Rodriguez et al. 2012).

4.1.2 Dune Facies

The dune facies is a well-sorted, pale orange (10YR 8/2) fine-grained siliciclastic sand with highly spherical and rounded grains (Fig. 2b). Plant roots and organic detritus were sampled, commonly near the top of the unit where dune grasses are present, but also at depth near organic-rich beds interpreted as paleosols (Fig. 2b). Steeply dipping heavy mineral cross laminae and bedding are common sedimentary structures sampled and are typical of coastal dunes (Davis 1978). The mean grain size of the dune sand decreases slightly toward the northeast from 1.81 Φ at transect F1 to 2.30 Φ at cross section F6 (Fig. 3a). The thickness of this unit ranges from 83 cm to >274 cm and generally increases toward the northeast.

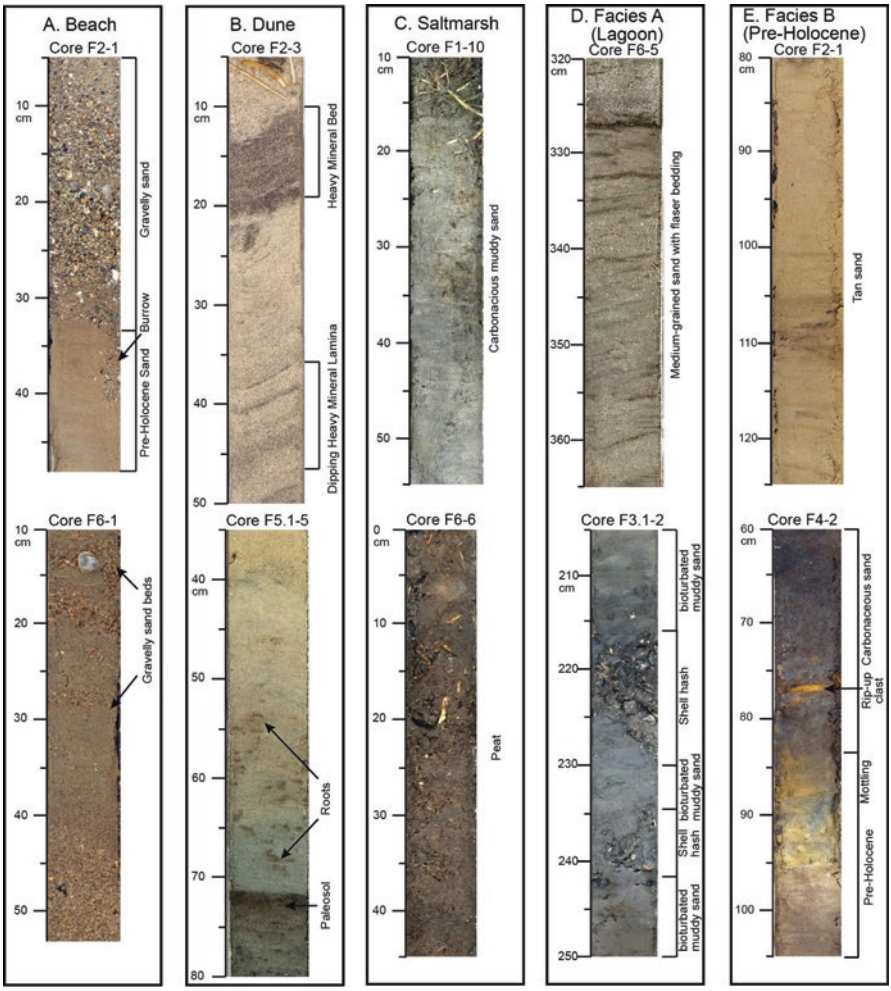

Fig. 2 Core photos of the depositional environments and facies sampled at Onslow Beach. Depth scale (cm) is relative to the surface. See Figs. 1 and 5 for core locations

4.1.3 Saltmarsh Facies

The marsh facies is an olive gray (5Y 3/2) to brownish gray (5YR 4/1) bioturbated carbonaceous muddy sand to sandy silt (Figs. 2c and 3a). Dense mats of *Spartina alterniflora* and *Juncus roemerianus* plant, roots, and woody material contribute to the organic sediment fraction within the marsh facies, which can be as high as 50% carbon (Rodriguez et al. 2013). Marsh sediments have variable mean grain sizes and contain a sand component that is transported from the dunes by aeolian processes (Rodriguez et al. 2013; Fig. 3) or overwash processes. Active burrowing from back-barrier species such as fiddler crabs and mud crabs frequently destroy primary

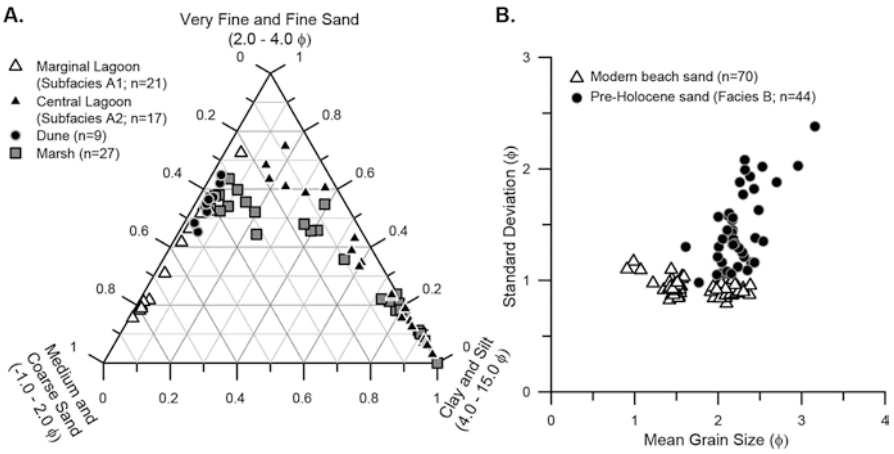

Fig. 3 Ternary diagram showing distinct grain-size distributions for lagoon, dune, and marsh depositional environments (**a**). Pre-Holocene sand is distinguished from modern beach sand by its lower sorting or higher mean standard deviation (**b**)

sedimentary structures that may be present, resulting in poorly sorted sediment with intermixed clay, silt, and fine sand (Staub and Cohen 1979; Fig. 3).

4.1.4 Washover Facies

Transects F1, F2, F3.1, and F4 are located where washover fans or terraces are at the surface. These washovers formed in September 1996 by Hurricane Fran (F1 and F3.1), in August 2011 by Hurricane Irene (F2) and sometime between AD 1839 and AD 1938, based on a radiocarbon date below the washover deposit and its presence on 1938 aerial photography (F4). Those washovers are characterized by the same sedimentary facies and we use the washover terrace at Site F1 as a type example (Fig. 4). Washover deposits are composed of fining-upward beds of gravelly coarse sand at the base to medium-grained sand at the top with heavy-mineral laminae (Fig. 4). The basal gravelly sand is predominately composed of shell fragments and contains up to 7.18% gravel. This facies is similar to the "stratified sand" and "normal-graded sand" washover subfacies identified by Sedgwick and Davis (2003). Each fining-upward bed is interpreted to have been deposited during an individual overwash event that occurred after the initial washover terrace formed. After the washover terrace at Site F1 initially formed during Hurricane Fran in 1996, it extended landward in the northeast an additional 120 m during the period between 1998 and 2002 (Fig. 4). During that period, the barrier was impacted by multiple tropical and extratropical storms, including Hurricane Bonnie in 1998, that could have overwashed the island and deposited the fining-upward beds (Fig. 4).

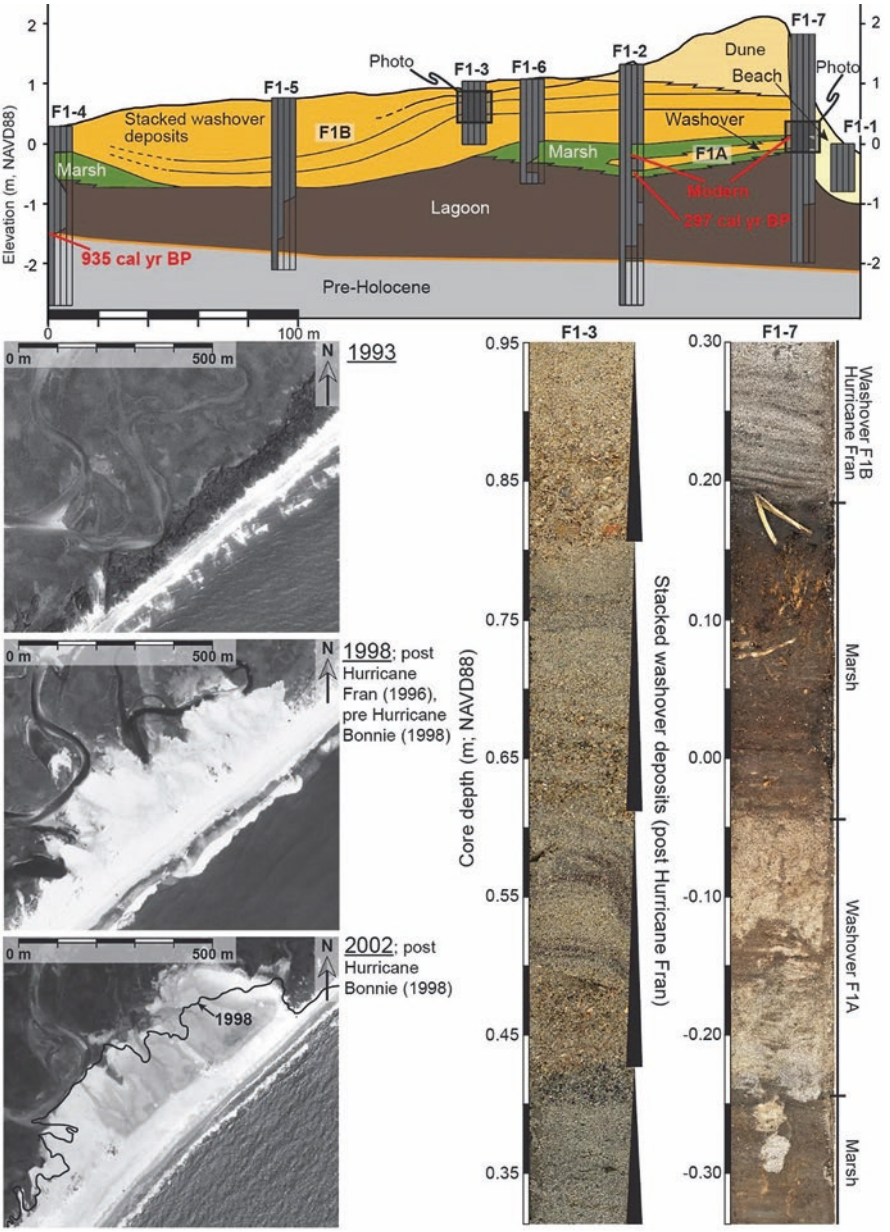

Fig. 4 Cross section across the washover terrace that initially formed during Hurricane Fran (Transect 1). The photo of core F1-7 shows an old washover (F1A) deposited above marsh sediment. That washover deposit was colonized by saltmarsh, which was subsequently buried by another washover deposited during Hurricane Fran (F1B). The photo of core F1-3 shows fining upward sand beds that were deposited during multiple overwash events that occurred after Hurricane Fran. Overhead photos show that Hurricane Bonnie, which overwashed the area in 1998, extended the washover terrace landward and likely formed one of the observed fining upward sand beds. See Fig. 1 for locations

4.1.5 Facies A

Facies A was sampled below the modern depositional environments of Onslow Beach in all transects except F2.1. The facies typically thickens seaward and in places is >2.3 m thick (some cores were not long enough to sample its entire thickness). The whole shells sampled in this unit were always back-barrier fauna such as *Tagelus plebius*, *Ilyanassa obsolete*, *Crassostrea virginica*, and *Macoma balthica*. Facies A is composed of two lithologically distinct subfacies, A1 and A2.

Subfacies A1 is medium light gray (N6) to olive gray (5Y 4/1) sand with silty laminae (Fig. 2d; core F6-5). The sediment is 97% sand with a mean grain size of 1.77 Φ (Fig. 3a). Flaser bedding and sand-sized shell fragments are common in this subfacies. Based on the macrofauna assemblages and the flaser bedding interpreted as tidal-bedding structures, this subfacies is interpreted as a marginal lagoon environment (Reineck and Wunderlich 1968; Davis 1978). Facies A is currently being deposited adjacent to the Bogue Bank barrier island in Bogue Sound, a shallow lagoon located approximately 40 km northeast of Onslow Beach (Timmons et al. 2010).

Subfacies A2 is a light gray (N7) to grayish black (N2) muddy sand with abundant articulated shells and sand burrows (Fig. 2d; core F3-2). Subfacies A2 has a greater clay and silt fraction (61%) and a finer-grained sand fraction (mean grain size of 4.0 Φ) than Subfacies A1 (Fig. 3a). A 25-cm thick oyster reef was sampled in core F1-5. The high mud content, excellent preservation of estuarine fauna and bioturbation indicates a low-energy, central lagoon environment. A silty clay unit with abundant *Crassostrea virginica*, similar to Subfacies A2, was also sampled by Timmons et al. (2010) at the bottom of central Bogue Sound.

4.1.6 Facies B

Facies B was sampled at the base of 6 transects and displays a wide range of textural characteristics that are distinct from those observed in the two lagoonal subfacies or in the modern depositional facies. The cores did not penetrate the entire unit and sampled Facies B at variable depths that generally decrease landward and toward the southern end of the island. This facies is primarily composed of a massive moderate yellowish brown (10 YR 5/4) sand (Fig. 2e; core F2-1). The facies is easily distinguished from beach sand by its distinct color, finer-grained texture (mean grain size of 2.19 Φ versus 1.75 Φ for the beach), and poorer sorting, which is caused by a minor silt component (Fig. 3b). Stiff light gray (N7) clay with yellow mottling was also sampled and the mottling is indicative of oxidation (Fig. 2e; core F4-2). Although samples from Facies B were not radiocarbon dated, the homogenous, indurated, and oxidized nature of the upper part of the facies suggests subaerial exposure and the unit is interpreted to be pre-Holocene in age.

4.2 Stratigraphy

The stratigraphic cross sections through Onslow Beach show a typical transgressive facies succession (Fig. 5). The contact between the basal pre-Holocene unit and the overlying lagoonal mud is sharp and shows evidence of subaerial exposure and soil formation indicating that it is associated with a significant hiatus when sea level was lower. This disconformity was sampled at variable depths in the alongshore direction and generally slopes seaward. The disconformity is shallow (>0 m NAVD88) in the middle of transect F2.1, where pre-Holocene strata outcrops in the foreshore (Riggs et al. 1995) but away from transect F2.1, in the southwest and northeast, it is deeper and overlain by thick (>5 m) coastal deposits. This disconformity represents the antecedent topography that was inundated during Holocene sea-level rise and where that surface is at a lower elevation, water depth below sea level was deeper and therefore local sediment accommodation was greater.

At transects F2.1 and F4, carbonaceous sand to sandy mud (20–90 cm thick) overlies the disconformity (Fig. 5). That unit is interpreted as fringing marsh based on its similar lithology to the modern marsh facies sampled in transects F1 and F6, the presence of wood, and its superposition above the upland pre-Holocene unit. Marsh adjacent to mainland shorelines represents the leading edge of marine incursion during sea-level rise. Roots extend from the marsh unit into the pre-Holocene strata and radiocarbon dates of wood found at the bottom and top of this marsh in the F4 transect are 3561–3823 cal year BP and 2156–2351 cal year BP, respectively (Table 1).

Where the disconformity is deep and accommodation was increased, at an elevation <−1.25 m NAVD88, lagoonal sands and mud were sampled either in contact with the disconformity (transects F1, F2, F4.2, F5.1) or above the fringing marsh (Transect F4). The lagoonal unit is wedge-shaped, pinches out landward toward the modern back-barrier marsh and thickness is dictated by the topography of the seaward-dipping disconformity (Fig. 5). Lagoonal deposition initiated in the area sometime before 1000 cal year BP, based on a *Macoma constricta* valve sampled at the base of the unit at Transect F1 (886–1001 cal year BP; Table 1) and other dates from the middle of the lagoonal unit at Transects F5.1 (801–931 cal year BP) and F6 (526–641 cal year BP); however, the deepest and oldest part of the lagoonal unit was not sampled. Based on the sea-level reconstruction of Kemp et al. (2011), ~1000 years ago sea level in the area was ~1.5 m below present mean sea level. At that time, the barrier island was located further offshore.

A discontinuous organic-rich muddy sand and peat unit, interpreted as a back-barrier marsh, was sampled above the lagoon unit. This carbonaceous unit correlates with the modern back-barrier marsh sampled at the surface in transects F1 and F6. Radiocarbon dates from the base of the marsh range from 1716 to 1833 cal year BP (F4) to sometime after AD 1950 (F1). Sharp-based sand beds, ranging from 12 to 80 cm thick, that pinch out in a landward direction were sampled within the marsh unit at the seaward and middle portions of the transects (Figs. 4 and 5). The sand beds are bioturbated, contain root traces, and have a higher concentration of

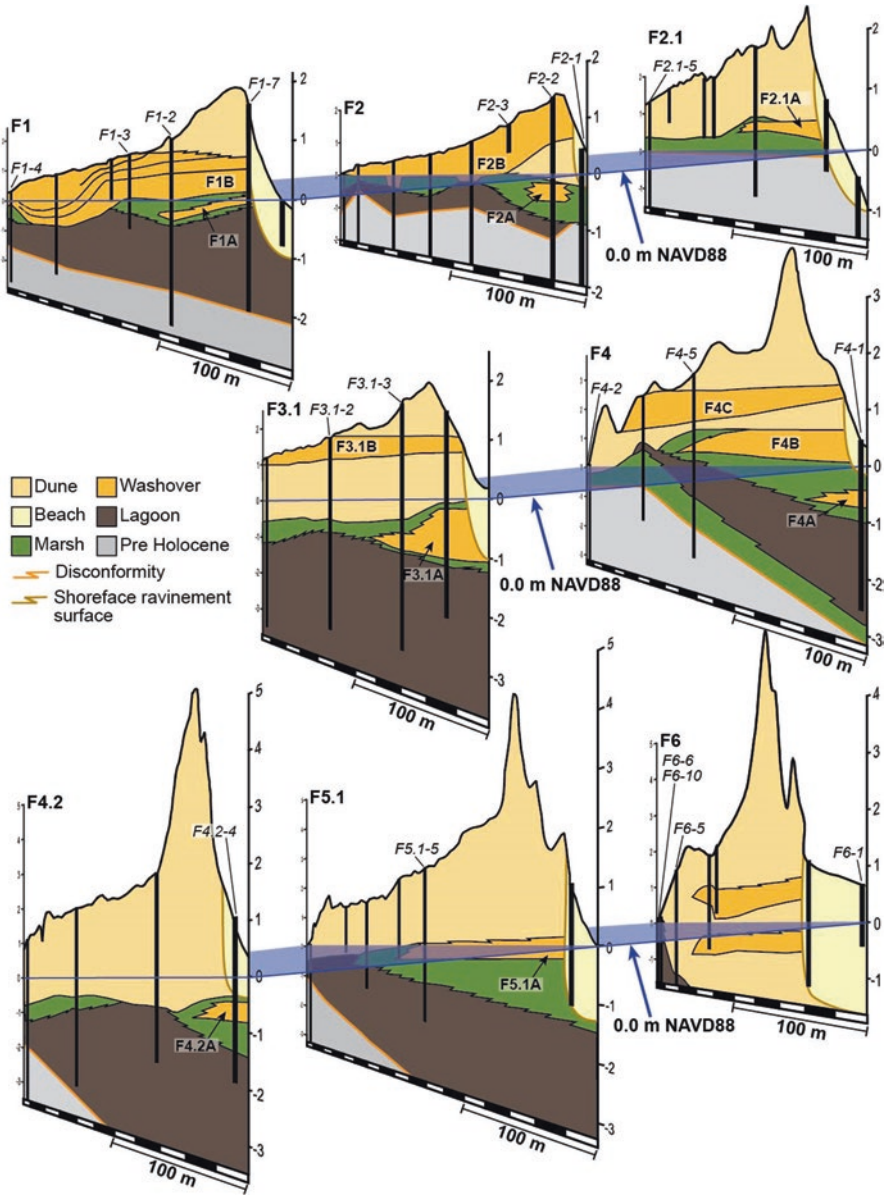

Fig. 5 Cross sections along Onslow Beach. Each transect sampled at least one old washover deposit (*orange*). Vertical axis is elevation, m NAVD88. Notice profiles are foreshortened and no cross section was created for F3 because only 2 cores were collected there. Washover labels correspond with Table 2. See Fig. 1 for locations

Table 1 Radiocarbon dates

Core	Depth (cm)	Material type	Context	14C Age	Cal year BP age[a] (median probability)
F1-4	177–179	*Macoma constricta*	Base of lagoon	1390 ± 20	886–1001 (935)
F1-2	187–190	Plant fragments	Base of F1A	250 ± 40	0–436 (297)
F1-2	158–160	Plant fragments	Top of F1A	>Modern	Na
F1-7	192–193	Plant fragments	Top of F1A	>Modern	Na
F2-2	195–198	Plant fragments	Base of F2A	205 ± 25	145–301 (175)
F2-2	154–159	Plant fragments	Top of F2A	140 ± 30	6–281 (143)
F2.1-5	70–73	Plant fragments	Base of marsh	115 ± 20	19–267 (112)
F3-4	135–137	Plant fragments	Base of F3A	660 ± 25	560–671 (611)
F3-4	93–95	Plant fragments	Top of F3A	250 ± 25	0–424 (296)
F3.1-3	96–98	Plant fragments	Base of F3.1A	640 ± 30	554–667 (599)
F3.1-3	53–55	Plant fragments	Top of F3.1A	290 ± 30	288–457 (384)
F4-1	115–117	Plant fragments	Base of F4A	1850 ± 25	1716–1833 (1784)
F4-1	63–66	Plant fragments	Top of F4A	715 ± 35	564–725 (671)
F4-5	445–447	Wood	Base of old marsh	3400 ± 40	3561–3823 (3647)
F4-5	327–329	Wood	Top of old marsh	2270 ± 40	2156–2351 (2249)
F4-5	227–229	Plant fragments	Base of F4B	115 ± 15	23–264 (110)
F4-5	202–204	Plant fragments	Top of F4B	105 ± 15	28–259 (113)
F4.2-4	198–200	Plant fragments	Base of F4.2A	1430 ± 30	1293–1375 (1328)
F4.2-4	144–146	Plant fragments	Top of F4.2A	520 ± 35	505–630 (536)
F5.1-5	219–221	Plant fragments	Base of F5.1A	100 ± 15	31–257 (114)
F5.1-5	322–324	Plant fragment	Lagoon	975 ± 15	801–931 (913)
F6-10	130–133	*Tagelus Plebeius*	Lagoon	1000 ± 30	526–641 (584)

[a]2-sigma range

heavy minerals at their base (Fig. 4). Based on textural and compositional similarities between these beds and the modern washover facies, they are interpreted to be old washover deposits and 8 such old washovers were sampled in the core transects. Cores taken along the beach between transects only sampled old washover deposits if they were collected <250 m from a transect. We assumed that those washover deposits correlated with the washover deposits sampled in the adjacent cross-island transects, given close proximity and similar depth of the deposit. The presence of saltmarsh below the washover and bioturbation indicates deposition in the intertidal zone and preservation of distal washover deposits. Waves and currents in the shoreface most likely eroded the corresponding proximal part of the old washover deposits. The leading edge of the shoreface ravinement surface is located seaward of the

Table 2 Washover-deposit metrics

Washover	Median age (AD)	Minimum age (AD)	Maximum age (AD)	Landward distance (m)
F1A	1726	1938	1514	171 ± 20
F1B	1996	1998	1996	400 ± 5
F2A	1791	1807	1775	120 ± 15
F2B	2012	2012	2012	350 ± 5
F2.1A	1888	1938	1838	97 ± 25
F3A	1497	1654	1339	54 ± 70
F3.1A	1459	1566	1351	20 ± 30
F3.1B	1996	1998	1996	185 ± 5
F4A	722	1279	166	10 ± 60
F4B	1838	1839	1837	101 ± 35
F4C	1889	1938	1839	125 ± 5
F4.2A	1018	1414	622	29 ± 25
F5.1A	1893	1938	1839	239 ± 20

dunes and is defined by erosional truncation of old washover deposits and underlying facies (Rodriguez et al. 2013). Distal portions of the old washover deposits were re-colonized by marsh vegetation, which was preserved as an overlaying carbonaceous muddy sand bed. Depositional timing of the 9 buried washover deposits, sampled in all transects except F6, was determined from radiocarbon dates obtained below and above the sand beds (technique described in methods). Those washover deposits formed between 1784 cal year BP and ~100 cal year BP (Table 1). At F6, two sharp-based fining upward sand beds, interpreted as proximal washover deposits, were sampled within the thick (>700 cm) dune sand, but these deposits were not dated due to a lack of suitable material for radiocarbon analyses. Historical washover fans and terraces were deposited over backbarrier saltmarsh at F1 and F2, and over dunes at F3.1 and F4.

5 Discussion

The multiple washover deposits preserved in the stratigraphy of Onslow Beach formed during a time period that includes the increase in rate of relative sea-level rise at AD 1865–1892 from 1.0 mm/year to 3.2 mm/year (Kemp et al. 2011; Fig. 6). We sampled 7 washover deposits emplaced between AD 700 and AD 1865 and 6 washover deposits emplaced after AD 1865 (using the median probability age; Fig. 6). The frequency of washover deposition increased from 0.6 washovers per century to 4.1 washovers per century after the increase in the rate of relative sea-level rise. In addition, the average landward extent of washover deposition increased between the time period AD 700–1865 (mean of 72 m) and post AD 1865 (mean of 232 m; Fig. 6). Given the spacing between cores along the northeastern end of the

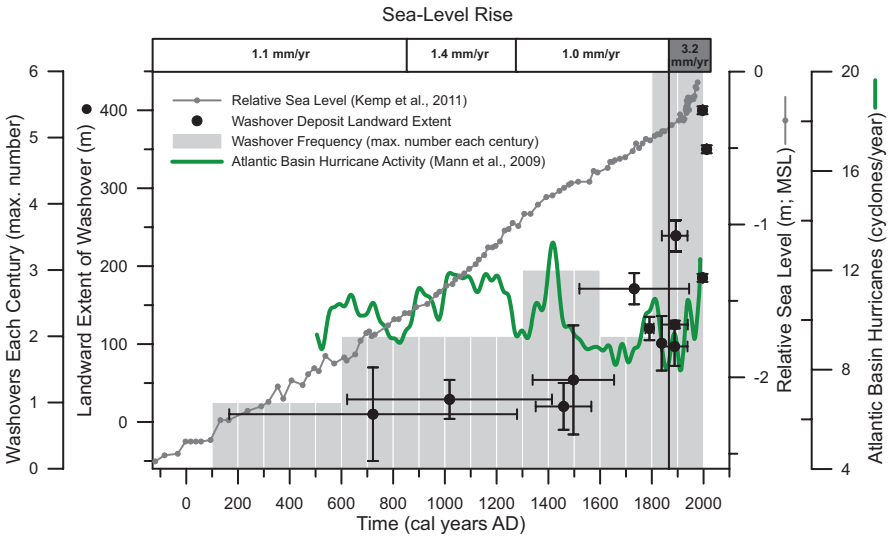

Fig. 6 Comparison of landward extent of washover deposit and age shows an abrupt increase in frequency and extent of washover deposition around the same time as sea-level rise accelerated. Atlantic basin tropical cyclone activity based on a regional composite of washover deposits from Mattapoisett, Massachusetts; Succotash, Rhode Island; Alder, New York; Whales, New Jersey; Brigantine, New Jersey; Singleton Swash, South Carolina; Western Lake, Florida; and Vieques, Puerto Rico shows periods of high activity AD 900–1100 and a general decrease in the level of activity after AD 1200 (Mann et al. 2009)

island and arbitrary transect placement, it is likely that we did not sample every washover deposit preserved in the island stratigraphy; however, given our large sample size and closely spaced cores between transects along the southwestern part of the island that did not sample additional washover deposits, changes in the frequency and landward extent of washover deposition during the record should be similar to what would be calculated from sampling every preserved washover deposit.

While we are confident that our sampling and measuring techniques are robust, there are significant challenges associated with measuring washover frequency and landward extent along any transgressive barrier island and these challenges introduce uncertainty in the dataset, which is difficult to quantify. The ocean shoreline moved landward continuously throughout the record. This means that the fidelity of our washover record increased through time as the shoreline moved closer to our sampling locations. The recent part of the record should have captured more of the smaller washovers than the older part of the record because the ocean shoreline could have moved beyond the landward extent of small old washovers and eroded them away. Another challenge with measuring the landward extent of washover deposits is using a stationary baseline as a benchmark, which makes older washovers appear shorter in landward extent than younger washovers. This is because the coeval ocean shoreline for older washovers is located some unknown distance sea-

ward of the stationary baseline. Old and young washovers of exactly the same landward extent would present themselves as being shorter and longer, respectively, on Fig. 6 because the present location of the shoreline is closer to the landward edge of the old washover deposits than the young washover deposits due to shoreline transgression. Our measurements of the frequency and landward extent of washover fans are not truly a reflection of what occurred, rather because of shoreline transgression, they are apparent measurements.

Although both the apparent frequency and landward extent of washover deposition increased abruptly around 1865–1892, this does not necessarily indicate that the sudden increase in the rate of sea-level rise at that time was the direct cause. An increase in the size and/or frequency of storms around AD 1800–1900 could also explain the observed pattern of washover deposition; however, historical and geological records, as well as statistical models of Atlantic tropical cyclone activity, do not support an increase in storminess at that time (Fig. 6; Vecchi and Knutson 2008; Mann et al. 2009). A peak in Atlantic tropical cyclone activity was recognized during medieval times (~AD 1000) and although this impacted the morphology of the adjacent Outer Banks (Culver et al. 2007; Timmons et al. 2010; Mallinson et al. 2011, this volume), that peak occurred ~865 years earlier than the observed change in the apparent landward extent and frequency of washover deposits at Onslow Beach. Based on the age of backbarrier saltmarsh sediment preserved below the backshore at F4, Onslow Beach reached its present location sometime after 671 cal year BP (Table 1), making it >1000 years younger than the Outer Banks (Culver et al. 2007; Mallinson et al. 2008; Timmons et al. 2010). Onslow Beach must have been positioned further offshore during the Medieval Warm Period because widespread lagoon deposits were being deposited in the area at that time. It is likely that only the largest washovers that formed during the Medieval Warm Period are still preserved because they extended the furthest landward and were not entirely removed by waves and currents as the shoreface migrated landward. Smaller washovers deposited during the Medieval Warm Period would have been completely removed by shoreface ravinement processes during island transgression. Onslow Beach is too young to have recorded the increase in storminess during the Medieval Warm Period in its back barrier sedimentary record.

Our data show an abrupt increase in the frequency of washover deposition around the nineteenth century as opposed to a continuous increase through time, the latter of which would be expected for a barrier island that is transgressing at a steady rate. The abrupt increase in the frequency of washover deposition suggests that an external oceanographic mechanism changed abruptly (increase in water level and/or wave energy) increasing the frequency of overwash, and/or Onslow Beach abruptly became less resistant to overwash as island morphology changed (e.g., decreased height and/or width). Humans did not modify island morphology in the nineteenth century and the only access to Onslow Beach and adjacent Topsail Island, to the southwest, was by boat until the middle twentieth century. While the abrupt increase in the frequency of washover deposition could not have been the result of human modifications or an increase in the number of hurricanes in the Atlantic Basin (Mann et al. 2009), it could have been associated with a localized persistent increase in

wave energy (Komar and Allan 2008), wave direction (Ashton et al. 2001; Slott et al. 2006; Moore et al. 2013), storminess (Mallinson et al. 2011), and/or sea-level anomalies (Theuerkauf et al. 2014), for which no independent record extending over multiple centuries exists.

Onslow Beach reached its modern position no earlier than 671 cal year BP (Table 1), making it 2329 years younger than Bogue Banks, a regressive barrier located in northeastern Onslow Bay near Cape Lookout (Timmons et al. 2010). As the cuspate morphology of the coastline implies, barriers located at the center of a coastal embayment, such as Onslow Beach, transgressed more rapidly and across a longer distance of continental shelf than barriers located along the cape flanks (Bogue Banks), given a presumed straight shoreline configuration near the continental shelf break during the sea-level lowstand. Along with the Timmons et al. (2010) study of Bogue Banks that shows island regression during its early formation, the transgressive stratigraphy of the much younger Onslow Beach supports the numerical model of Ashton et al. (2001) and Ashton and Murray (2006) (Table 1 and Fig. 5). Slott et al. (2006) suggest that the central embayment of cuspate coastlines can experience greater shoreline retreat rates and transgress larger distances than cape flanks due to more frequent high-angle waves. If a change in wave climate toward more frequent high-angle waves were to have occurred at Onslow Beach around the end of the nineteenth century, this could have caused or contributed to the increase in frequency and apparent landward extent of washover deposits there.

The full dimensions of the older washover deposits preserved in the subsurface could not be measured; however, all of the old washovers in our record were large enough to extend beyond the dunes on top of backbarrier-fringing marsh. Since the landward extent of washover deposition is measured from a linear stationary baseline, as opposed to from each washover's coeval shoreline position on the beach, the increase in landward extent of washover deposition does not necessarily indicate that the size of washovers and their associated storms increased abruptly around the nineteenth century (Fig. 6).

A constant increase in the frequency and apparent landward extent of washovers sampled through time can be produced simply by a shoreline continuously transgressing at a constant rate and moving closer to the sampling location, but such a scenario does not explain an abrupt increase, as recorded in the sediments of Onslow Beach. That abrupt increase in washover frequency and apparent landward extent occurred at the same time as the rate of sea-level rise increased threefold. It is possible that the sudden increase in the rate of sea-level rise caused an increase in the vulnerability of the barrier island to overwash by increasing the rate of landward-shoreline movement, which narrowed the island and decreased the elevation of the island through dune erosion, allowing smaller storms to overwash the island and either create new washovers or enlarge existing washovers. We observed such an increase in the size of the washover at F1 after Hurricane Fran when smaller storms overwashed the island, transported sand onto the backbarrier marsh and increased the landward extent of the terrace (Fig. 4).

Barrier islands with a low rate of sediment supply and composed of a thin (<1–2 m) accumulation of sand, like the transgressive southwestern end of Onslow

Beach (and Follets Island, TX; see Odezulu et al. this volume), are likely less resilient to storm erosion than barriers with a higher rate of sediment supply and composed of thicker accumulation of (>5 m) sand, like the northeastern end of Onslow Beach where no washover deposits on top of back-barrier marsh were sampled (Riggs et al. 1995; Rodriguez et al. 2012). This is because barrier islands with a low sand supply that experience overwash, washover deposition, and beach erosion during a storm likely have longer post-storm recovery periods than higher sediment-supply areas where the barrier island is composed of a thicker sand unit. The finer grained lagoon and marsh sediment, which underlies the thin veneer of beach sand in the central and southwestern areas of Onslow Beach, is likely transported in suspension away from the littoral zone during storms, leaving less sediment available for post-storm recovery than if the beach were underlain by sand. It is unknown if there were other forcing mechanisms, in addition to the well-defined sudden increase in the rate of sea-level rise, that contributed to the abrupt apparent increase in frequency and landward extent of washover deposits on Onslow Beach, such as an increase in sea-level anomalies (Theuerkauf et al. 2014), changes in the wave climate (Ashton et al. 2001; Komar and Allan 2008; Moore et al. 2013), and/or an increase in local storminess (Mallinson et al. 2011). Nevertheless, the abrupt increase in washover deposition along Onslow Beach demonstrates that transgressive barriers are highly sensitive to either morphologic thresholds and/or oceanographic changes.

6 Conclusions

Onslow Beach is a transgressive barrier island that moved landward rapidly during the late Holocene and reached its modern position no earlier than 671 cal year BP (Table 1). Core transects sampled nine old washover deposits and four historical washovers that span the time period between AD 722 and AD 2012. The frequency and landward extent of the sampled washovers increased in the nineteenth century, about the same time that the rate of sea-level rise in the area increased from 1.0 mm/year to 3.2 mm/year (Kemp et al. 2011). A contemporaneous increase in storminess throughout the Atlantic, which could explain such a trend in washover deposition, has not been observed. Further, our observations of an abrupt increase are not consistent with increases in the fidelity of the record through time that would arise simply from continuous shoreline retreat. Rather, decreased resistance to overwash more likely occurred because the abrupt increase in the rate of sea-level rise accelerated landward-shoreline movement, which narrowed the island and decreased the elevation of the island through dune erosion. It is possible that other forcing mechanisms, such as a localized increase in storminess, change in wave climate, and/or increase in the frequency of sea-level anomalies contributed to the increase in apparent frequency and landward extent of washover deposits, but records of those forcing mechanism span a more recent and shorter time period than the change in the washover record presented here.

Rates of sea-level rise are predicted to increase in the future and our findings for Onslow Beach suggest that future sea-level rise can be expected to cause a decrease in the resistance of other barrier islands to storms. Decreased storm resistance will inevitably lead to an increase in barrier-island overwash, but the amount of time over which that change occurs will vary based on rates of sediment supply and island morphology. Our record of washover deposition shows that those morphologic changes to barrier islands, which affect resistance to storms, can occur over decadal time scales and possibly in response to increases in the rate of sea-level rise of only a few millimeters/year. Barrier islands that are wide, high in elevation and have high rates of sediment supply will maintain resistance to overwash the longest; however, even these islands will still experience some geomorphic impacts from an increased rate of sea-level rise, such as increased rates of shoreline transgression and dune erosion. Barriers that are low in elevation and that have low rates of sediment supply, such as Onslow Beach, may be the most susceptible to storm overwash; however, such barriers also have the highest potential of preserving a record of impacts from accelerated sea-level rise in intertidal back barrier sedimentary strata.

Acknowledgements This research was supported by funding from the Defense Coastal/Estuarine Research Program (DCERP; dcerp.rti.org), funded by the Strategic Environmental Research and Development Program (SERDP). Views, opinions, and/or findings contained in this manuscript are those of the authors and should not be construed as an official U.S. Department of Defense position or decision unless so designated by other official documentation. The authors would like to thank Robin Mattheus, Justin Ridge, Patricia Rodriguez, Erin Fegley, Dan Hood, Richard Browne, Noel Anderson, and Joe Purifoy for their help in the field and in the lab. We thank Laura Moore, Brad Murray, and two anonymous reviewers for generously providing constructive criticisms and edits, which greatly improved the manuscript.

References

Ashton AD, Lorenzo-Trueba J (2018) Morphodynamics of barrier response to sea-level rise. In: Moore LJ, Murray AB (eds) Barrier dynamics and response to changing climate. Springer, New York

Ashton AD, Murray AB (2006) High-angle wave instability and emergent shoreline shapes: 1. Modeling of sand waves, flying spits, and capes. J Geophys Res Earth Surf 111(F4):F04011. https://doi.org/10.1029/2005jf000422

Ashton A, Murray AB, Arnault O (2001) Formation of coastline features by large-scale instabilities induced by high-angle waves. Nature 414:269–300

Ashton A, Donnelly J, Evans R (2008) A discussion of the potential impacts of climate change on the shorelines of the Northeastern USA. Mitig Adapt Strateg Glob Chang 13(7):719–743. https://doi.org/10.1007/s11027-007-9124-3

Bender MA, Knutson TR, Tuleya RE, Sirutis JJ, Vecchi GA, Garner ST, Held IM (2010) Modeled impact of anthropogenic warming on the frequency of intense Atlantic Hurricanes. Science 327(5964):454–458. https://doi.org/10.1126/science.1180568

Bilskie MV, Hagen SC, Medeiros SC, Passeri DL (2014) Dynamics of sea level rise and coastal flooding on a changing landscape. Geophys Res Lett 41(3):927–934. https://doi.org/10.1002/2013gl058759

Brunn P (1962) Sea-level rise as a cause of shore erosion. Proceedings of the American Society of Civil Engineers. J Waterway Harb Div 88:117–130

Church JA, Clark PU, Cazenave A, Gregory JM, Jevrejeva S, Levermann A, Merrifield MA, Milne GA, Nerem RS, Nunn PD, Payne AJ, Pfeffer WT, Stammer D, Unnikrishnan AS (2013) Sea level change. In: Stocker TF, Qin D, Plattner G-K et al (eds) Climate change 2013: the physical science basis. Contribution of Working Group I to the Fifth Assessment Report of the Intergovernmental Panel on Climate Change. Cambridge University Press, New York

Cowell PJ, Kinsela MA (2018) Shoreface controls on barrier evolution and shoreline change. In: Moore LJ, Murray AB (eds) Barrier dynamics and response to changing climate. Springer, New York

Cronin TM, Dwyer GS, Kamiya T, Schwede S, Willard DA (2003) Medieval Warm Period, Little Ice Age and 20th century temperature variability from Chesapeake Bay. Glob Planet Change 36(1–2):17–29. https://doi.org/10.1016/S0921-8181(02)00161-3

Culver SJ, Grand Pre CA, Mallinson DJ, Riggs SR, Corbett DR, Foley J, Hale M, Metger L, Ricardo J, Rosenberger J, Smith CG, Smith CW, Snyder SW, Twamley D (2007) Late Holocene barrier island collapse: Outer Banks, North Carolina, USA. Sediment Rec 5:4–8

Davis RA (1978) Coastal sedimentary environments. Springer, Berlin

Donnelly JP, Cleary P, Newby P, Ettinger R (2004) Coupling instrumental and geological records of sea-level change: evidence from southern New England of an increase in the rate of sea-level rise in the late 19th century. Geophys Res Lett 31:GL018933

Donnelly C, Kraus N, Larson M (2006) State of knowledge on measurement and modeling of coastal overwash. J Coast Res 224:965–991

Engelhart SE, Horton BP, Kemp AC (2011) Holocene sea level changes along the United States' Atlantic Coast. Oceanography 24(2):70–79

FitzGerald DM, Fenster MS, Argow BA, Buynevich IV (2008) Coastal impacts due to sea-level rise. Annu Rev Earth Planet Sci 36:601–647. https://doi.org/10.1146/annurev.earth.35.031306.140139

Galloway WE, Hobday DK (1983) Terrigenous clastic depositional systems. Springer, Berlin

García-Artola A, Cearreta A, Leorri E (2015) Relative sea-level changes in the Basque coast (northern Spain, Bay of Biscay) during the Holocene and Anthropocene: the Urdaibai estuary case. Quat Int 364:172–180. https://doi.org/10.1016/j.quaint.2014.06.040

Gardner JV, Calder BR, Hughes Clarke JE, Mayer LA, Elston G, Rzhanov Y (2007) Drowned shelf-edge deltas, barrier islands and related features along the outer continental shelf north of the head of De Soto Canyon, NE Gulf of Mexico. Geomorphology 89(3–4):370–390. https://doi.org/10.1016/j.geomorph.2007.01.005

Gehrels WR, Hayward BW, Newnham RM, Southall KE (2008) A 20th century acceleration of sea-level rise in New Zealand. Geophys Res Lett 35(2):L02717. https://doi.org/10.1029/2007gl032632

Gornitz V (1991) Global coastal hazards from future sea level rise. Palaeogeogr Palaeoclimatol Palaeoecol 89(4):379–398. https://doi.org/10.1016/0031-0182(91)90173-O

Hughen KA, Baillie MGL, Bard E, Bayliss A, Beck JW, Bertrand CJH, Blackwell PG, Buck CE, Burr GS, Cutler KB, Damon PE, Edwards RL, Fairbanks RG, Friedrich M, Guilderson TP, Kromer B, McCormac FG, Manning SW, Bronk Ramsey C, Reimer PJ, Reimer RW, Remmele S, Southon JR, Stuiver M, Talamo S, Taylor FW, van der Plicht J, Weyhenmeyer CE (2004) Marine04 Marine radiocarbon age calibration 26–0 ka BP. Radiocarbon 46:1059–1086

Irish JL, Frey AE, Rosati JD, Olivera F, Dunkin LM, Kaihatu JM, Ferreira CM, Edge BL (2010) Potential implications of global warming and barrier island degradation on future hurricane inundation, property damages, and population impacted. Ocean Coast Manage 53(10):645–657. https://doi.org/10.1016/j.ocecoaman.2010.08.001

Jevrejeva S, Moore JC, Grinsted A, Woodworth PL (2008) Recent global sea level acceleration started over 200 years ago? Geophys Res Lett 35

Johnson JM, Moore LJ, Ells K, Murray AB, Adams PN, MacKenzie RA, Jaeger JM (2015) Recent shifts in coastline change and shoreline stabilization linked to storm climate change. Earth Surf Process Landf 40(5):569–585. https://doi.org/10.1002/esp.3650

Kemp AC, Horton BP, Culver SJ, Corbett DR, van de Plassche O, Gehrels WR, Douglas BC, Parnell AC (2009) Timing and magnitude of recent accelerated sea-level rise (North Carolina, United States). Geology 37:1035–1038

Kemp AC, Horton BP, Donnelly JP, Mann ME, Vermeer M, Rahmstorf S (2011) Climate related sea-level variations over the past two millennia. Proc Natl Acad Sci U S A 108(27):11017–11022. https://doi.org/10.1073/pnas.1015619108

Kemp AC, Bernhardt CE, Horton BP, Kopp RE, Vane CH, Peltier WR, Hawkes AD, Donnelly JP, Parnell AC, Cahill N (2014) Late Holocene sea- and land-level change on the U.S. southeastern Atlantic coast. Mar Geol 357:90–100. https://doi.org/10.1016/j.margeo.2014.07.010

Knutson TR, McBride JL, Chan J, Emanuel K, Holland G, Landsea C, Held I, Kossin JP, Srivastava AK, Sugi M (2010) Tropical cyclones and climate change. Nat Geosci 3(3):157–163. http://www.nature.com/ngeo/journal/v3/n3/suppinfo/ngeo779_S1.html

Komar PD, Allan JC (2008) Increasing hurricane-generated wave heights along the U.S. East coast and their climate controls. J Coast Res 24:479–488

Leorri E, Horton BP, Cearreta A (2008) Development of a foraminifera-based transfer function in the Basque marshes, N. Spain: implications for sea-level studies in the Bay of Biscay. Mar Geol 251(1–2):60–74. https://doi.org/10.1016/j.margeo.2008.02.005

Lorenzo-Trueba J, Ashton AD (2014) Rollover, drowning, and discontinuous retreat: distinct modes of barrier response to sea-level rise arising from a simple morphodynamic model. J Geophys Res Earth 119(4):779–801. https://doi.org/10.1002/2013jf002941

Mallinson D, Burdette K, Mahan S, Brook G (2008) Optically stimulated luminescence age controls on late Pleistocene and Holocene coastal lithosomes, North Carolina, USA. Quat Res 69:97–109

Mallinson DJ, Smith CW, Mahan S, Culver SJ, McDowell K (2011) Barrier island response to late Holocene climate events, North Carolina, USA. Quat Res 76(1):46–57. https://doi.org/10.1016/j.yqres.2011.05.001

Mallinson D, Culver S, Leorri E, Mitra S, Mulligan R, Riggs S (2018) Barrier Island and estuary co-evolution in response to Holocene climate and sea-level change: Pamlico Sound and the Outer Banks Barrier Islands, North Carolina, USA. In: Moore LJ, Murray AB (eds) Barrier dynamics and response to changing climate. Springer, New York

Mann ME, Woodruff JD, Donnelly JP, Zhang Z (2009) Atlantic hurricanes and climate over the past 1,500 years. Nature 460:880–883

Mellett CL, Plater AJ (2018) Drowned barriers as archives of coastal-response to sea-level rise. In: Moore LJ, Murray AB (eds) Barrier dynamics and response to changing climate. Springer, New York

Moore LJ, McNamara DE, Brad Murray A, Brenner O (2013) Observed changes in hurricane-driven waves explain the dynamics of modern cuspate shorelines. Geophys Res Lett 40(22):5867–5871. https://doi.org/10.1002/2013gl057311

Moore LJ, Patsch K, List JH, Williams SJ (2014) The potential for sea-level-rise-induced barrier island loss: insights from the Chandeleur Islands, Louisiana, USA. Mar Geol 355:244–259. https://doi.org/10.1016/j.margeo.2014.05.022

Murray AB, Moore LJ (2018) Geometric constraints on long-term barrier migration: from simple to surprising. In: Moore LJ, Murray AB (eds) Barrier dynamics and response to changing climate. Springer, New York

Nicholls RJ, Hoozemans FMJ, Marchand M (1999) Increasing flood risk and wetland losses due to global sea-level rise: regional and global analyses. Glob Environ Change 9(Suppl 1):S69–S87. https://doi.org/10.1016/S0959-3780(99)00019-9

Odezulu CI, Lorenzo-Trueba J, Wallace DJ, Anderson JB (2018) Follets Island: a case of unprecedented change and transition from rollover to subaqueous shoals. In: Moore LJ, Murray AB (eds) Barrier dynamics and response to changing climate. Springer, New York

Rahmstorf S (2007) A semi-empirical approach to projecting future sea-level rise. Science 315:368–370

Reimer PJ, Bard E, Bayliss A, Beck JW, Blackwell PG, Bronk Ramsey C, Buck CE, Cheng H, Edwards RL, Friedrich M, Grootes PM, Guilderson TP, Haflidason H, Hajdas I, Hatté C, Heaton TJ, Hoffmann DL, Hogg AG, Hughen KA, Kaiser KF, Kromer B, Manning SW, Niu M, Reimer RW, Richards DA, Scott EM, Southon JR, Staff RA, CSM T, van der Plicht J (2013) IntCal13 and Marine13 radiocarbon age calibration curves 0–50,000 years cal BP. Radiocarbon 55(4):1869–1887

Reineck H-E, Wunderlich F (1968) Classification and origin of flaser and lenticular bedding. Sedimentology 11(1–2):99–104. https://doi.org/10.1111/j.1365-3091.1968.tb00843.x

Riggs SR, Cleary WJ, Snyder SW (1995) Influence of inherited geologic framework on barrier shoreface morphology and dynamics. Mar Geol 126:213–234

Rodriguez AB, Anderson JB, Siringan FP, Taviani M (1999) Sedimentary facies and genesis of Holocene sand banks on the east Texas inner continental shelf. In: Snedden J, Bergman K (eds) Isolated shallow marine sand bodies: sequence stratigraphic analysis and sedimentologic interpretation. SEPM, Special Publication 64. SEPM, Tulsa, pp 165–178

Rodriguez AB, Anderson JB, Siringan FP, Taviani M (2004) Holocene evolution of the east Texas coast and inner continental shelf: along-strike variability in coastal retreat rates. J Sediment Res 74:406–422

Rodriguez AB, Rodriguez PL, Fegley SR (2012) One-year along-beach variation in the maximum depth of erosion resulting from irregular shoreline morphology. Mar Geol 291–294:12–23

Rodriguez AB, Fegley SR, Ridge JT, VanDusen BM, Anderson N (2013) Contribution of aeolian sand to backbarrier marsh sedimentation. Estuar Coast Shelf Sci 117:248–259. https://doi.org/10.1016/j.ecss.2012.12.001

Salzmann L, Green A, Cooper JAG (2013) Submerged barrier shoreline sequences on a high energy, steep and narrow shelf. Mar Geol 346:366–374. https://doi.org/10.1016/j.margeo.2013.10.003

Sedgwick PE, Davis RA Jr (2003) Stratigraphy of washover deposits in Florida: implications for recognition in the stratigraphic record. Mar Geol 200(1–4):31–48. https://doi.org/10.1016/S0025-3227(03)00163-4

Slott JM, Murray AB, Ashton AD, Crowley TJ (2006) Coastline responses to changing storm patterns. Geophys Res Lett 33(18):L18404. https://doi.org/10.1029/2006gl027445

Staub JR, Cohen AD (1979) The Snuggedy Swamp of South Carolina, a back-barrier coal forming environment. J Sediment Petrol 49:133–144

Storms JEA, Weltje GJ, Terra GJ, Cattaneo A, Trincardi F (2008) Coastal dynamics under conditions of rapid sea-level rise: Late Pleistocene to Early Holocene evolution of barrier–lagoon systems on the northern Adriatic shelf (Italy). Quat Sci Rev 27(11–12):1107–1123. https://doi.org/10.1016/j.quascirev.2008.02.009

Stuiver M, Reimer PJ (1993) Extended 14C database and revised CALIB radiocarbon calibration program. Radiocarbon 35:215–230

Theuerkauf EJ, Rodriguez AB (2014) Evaluating proxies for estimating subaerial beach volume change across increasing time scales and various morphologies. Earth Surf Process Landf 39(5):593–604. https://doi.org/10.1002/esp.3467

Theuerkauf EJ, Rodriguez AB, Fegley SR, Luettich RA (2014) Sea level anomalies exacerbate beach erosion. Geophys Res Lett 41(14):5139–5147. https://doi.org/10.1002/2014gl060544

Thieler ER, Hammar-Klose ES (2000) National assessment of coastal vulnerability to future sea-level rise, U.S. Gulf of Mexico Coast. U.S. Geological Survey, Open-File Report 00-179

Timmons EA, Rodriguez AB, Mattheus CR, DeWitt R (2010) Transition of a regressive to a transgressive barrier island as a function of back-barrier erosion, climate change, and low sediment supply, Bogue Banks, North Carolina, USA. Mar Geol 278:100–114

Titus JG, Park RA, Leatherman SP, Weggel JR, Greene MS, Mausel PW, Brown S, Gaunt C, Trehan M, Yohe G (1991) Greenhouse effect and sea level rise: the cost of holding back the sea. Coast Manag 19(2):171–204. https://doi.org/10.1080/08920759109362138

van de Plassche O, van der Borg K, de Jong AFM (1998) Sea level-climate correlation during the past 1400 yr. Geology 26(4):319–322. https://doi.org/10.1130/0091-7613(1998)026<0319:slccdt>2.3.co;2

Vecchi GA, Knutson TR (2008) On estimates of historical North Atlantic tropical cyclone activity*. J Clim 21(14):3580–3600

Wallace DJ, Anderson JB (2013) Unprecedented erosion of the upper Texas coast: response to accelerated sea-level rise and hurricane impacts. Geol Soc Am Bull 125(5–6):728–740. https://doi.org/10.1130/b30725.1

Wallace DJ, Anderson JB, Rodriguez AB (2009) Natural versus anthropogenic mechanisms of erosion along the upper Texas coast. Geol Soc Am Spec Pap 460:137–147

Walters D, Moore LJ, Duran Vinent O, Fagherazzi S, Mariotti G (2014) Interactions between barrier islands and backbarrier marshes affect island system response to sea level rise: insights from a coupled model. J Geophys Res Earth 119(9):2013–2031. https://doi.org/10.1002/2014jf003091

Wamsley T, Cialone M, Smith J, Ebersole B, Grzegorzewski A (2009) Influence of landscape restoration and degradation on storm surge and waves in southern Louisiana. Nat Hazards 51(1):207–224. https://doi.org/10.1007/s11069-009-9378-z

Woodruff JD, Irish JL, Camargo SJ (2013) Coastal flooding by tropical cyclones and sea-level rise. Nature 504(7478):44–52. https://doi.org/10.1038/nature12855

Follets Island: A Case of Unprecedented Change and Transition from Rollover to Subaqueous Shoals

Christopher I. Odezulu, Jorge Lorenzo-Trueba, Davin J. Wallace, and John B. Anderson

Abstract Follets Island, a transgressive island located on the upper Texas coast, is an ideal location to study barrier island transition from a rollover subaerial barrier to subaqueous shoals. This system also allows for an examination of coastal response to accelerated sea-level rise, storms, and sediment supply. The landward shoreline retreat rate during historical time is similar to the landward retreat rate of the bay shoreline, hence its current classification as a rollover barrier. However, the island has a limited and diminishing sand supply, which makes it even more vulnerable to erosion during storms and relative sea-level rise. Four core transects that extend from the upper shoreface to the back barrier bay are used to constrain the thickness of washover, barrier and upper shoreface deposits and to estimate sediment fluxes in the context of the overall sand budget for the island over centennial timescales. Stratigraphic architecture reveals two prominent transgressive surfaces. A lower flooding surface separates red fluvial-deltaic clay from overlying bay mud and an upper erosional surface separates back-barrier deposits from overlying shoreface and foreshore deposits.

Radiocarbon ages are used to constrain the evolution of the barrier and its long-term rate of island migration whereas ^{210}Pb dates are used to constrain the modern sand overwash flux. Results show that significant washover sands are deposited in the bay and about twice this volume is deposited as subaerial washover deposits. The total sand washover volume shows that overwash processes account for about half of the sand produced by shoreline erosion in historical time. Our results also indicate that the historical rate of shoreline retreat is about an order of magnitude

C.I. Odezulu (✉) • J.B. Anderson
Department of Earth Sciences, Rice University, Houston, TX, USA
e-mail: christopher.i.odezulu@rice.edu; johna@rice.edu

J. Lorenzo-Trueba
Earth and Environmental Studies, Montclair State University, Montclair, NJ, USA
e-mail: lorenzotruej@mail.montclair.edu

D.J. Wallace
Division of Marine Science, University of Southern Mississippi, Stennis Space Center, MS, USA
e-mail: davin.wallace@usm.edu

L.J. Moore, A.B. Murray (eds.), *Barrier Dynamics and Response to Changing Climate*, https://doi.org/10.1007/978-3-319-68086-6_5

faster than the geologic rate. We estimate back-barrier accommodation space to be about three times greater than the volume of the barrier. Hence, given the current shoreline erosion and overwash flux rate, Follets Island will eventually transition from a subaerial rollover barrier to subaqueous shoals. The frequency of severe storms along the Texas coast is not believed to have varied significantly in recent time, but the rate of sea-level rise has increased approximately five-fold and sand supply to the island is minimal. This leads us to suggest that accelerated sea-level rise and diminished sand supply are the main causes of this unprecedented change.

Keywords Rollover • Overwash • Transgressive barrier • Coastal erosion • Sea level • Flooding surface • Sediment flux • Texas coast • Numerical modeling • Antecedent topography

1 Introduction

Barrier rollover is the progressive erosion of the beach and shoreface as eroded sand is recycled and transported to the back-barrier via overwash and tidal inlet processes (Leatherman 1983; Niedoroda et al. 1985; Swift et al. 1985; Inman and Dolan 1989; Cowell et al. 2003; Stéphan et al. 2012). A barrier is assumed to maintain constant width during rollover, thereby providing stabilization during transgression (Dean and Maurmeyer 1983). However, a negative sediment budget and back-barrier accommodation space can reduce the volume of subaerial barriers during rollover processes, leading to frequent overwash and disintegration or break-up of barriers as seen in the Chandeleur Islands (Boyd and Penland 1984; McBride and Byrnes 1997; Moore et al. 2014). This process of barrier transition has wide reaching impacts because barrier islands serve as buffers to storm impacts, shielding mainland and coastal ecosystems from the full force of storm surge.

Two-thirds of the northern Gulf of Mexico coast is occupied by barrier islands (Morton et al. 2004). In Texas, 35% of barriers are progradational, 45% retrogradational, and 20% aggradational (Morton 1994). These differences reflect variable response of these barriers to relative sea-level rise and other factors since the time of their formation (Anderson et al. 2014), and this variability continues today. Historical data show that 88% of the barriers of the upper Texas coast are experiencing net shoreline retreat, but rates vary spatially and temporally along the coast (Gibeaut et al. 2000; Paine et al. 2012, 2017). Sea-level rise, limited sand supply, and storm impacts are assumed to be the main drivers of these shoreline changes (Morton et al. 2004; Wallace et al. 2009; Wallace and Anderson 2013). Sea-level and sediment supply rates control long-term shoreline changes while storms punctuate the long-term processes by shaping the morphology of barriers (Morton et al. 1995; Anderson et al. 2010, 2014; Wallace and Anderson 2013; Paine et al. 2017).

Anderson et al. (2014) suggest that modern rates of shoreline retreat along the upper Texas coast are unprecedented, arguing that the current shoreline would be

located kilometers inland of its current location if these rates had occurred since these barriers first began migrating landward. For example, Galveston Island formed ~5.5 ka and experienced an extended period of progradation that ended around 1.8 ka (Bernard et al. 1959, 1970; Rodriguez et al. 2004). Today, the west end of the island, which is not protected by a seawall, is retreating at short-term rates between 1.4 and 3.9 m/year (Paine et al. 2012). If the long-term landward retreat rate since 1.8 ka was the same as the current average rate, the shoreline would be located about 4.7 km landward of its current location. By determining the sequestration location of eroded material from Galveston Island beaches and nearshore environments through time, Wallace and Anderson (2013) were able to quantify short-term and long-term volumetric erosion. Consistent with observations elsewhere by FitzGerald et al. (this volume), Wallace and Anderson (2013) demonstrated that unprecedented historic erosion of Galveston Island is supported by accelerated growth of the San Luis Pass tidal delta in historical time, as this tidal delta is the ultimate sink for most of the sand eroded from the island. They further argued that this unprecedented change was due to accelerated sea-level rise punctuated by storm events.

South Padre Island is an even more dramatic case of unprecedented shoreline retreat in modern time. Distal overwash deposits in Laguna Madre and barrier island sands date back to ~4 ka, indicating that the island has not moved significantly during the late Holocene (Wallace and Anderson 2010), while the current rate of shoreline retreat of ~1.90 m/year would have resulted in ~7.6 km of retreat over this time interval.

Follets Island is a relatively small barrier located west of Galveston Island (Fig. 1). It is classified as a low-gradient retrogradational barrier in a rollover phase, based on sediment cores that have sampled back-barrier deposits below modern barrier and shoreface deposits (Bernard et al. 1970; Morton 1994; Wallace et al. 2010; Anderson et al. 2014). Indeed, it is one of the fastest retreating barriers of the Texas coast. The historical shoreline retreat rate averages ~2.0 m/year (Morton 1994; Gibeaut et al. 2000; Paine et al. 2012).

Though the causes of Follets Island's historic shoreline retreat are known to be both natural (limited sand supply, relative sea-level rise, and storm impacts) and anthropogenic (diversion of the Brazos River mouth and construction of jetties at the old river mouth), the impact of each factor alone has not been quantified. Numerical modeling is needed to evaluate the individual contributions of these agents to current shoreline retreat and to predict future changes to the island. But, quantitative prediction of the island's response to sea-level rise and storms is difficult due to the complex nature of these processes and stochastic storm frequency. To gain further insight, detailed stratigraphic resolution is needed to match specific events with historical records. In addition, the high-resolution, short-term sand budget of the island must be determined; specifically the amount of sand being transported offshore and backshore versus the amount of sand moving within the longshore transport system. Furthermore, the thickness of barrier sands must be determined to quantify the rate of sand generated by erosion and cannibalization of the island.

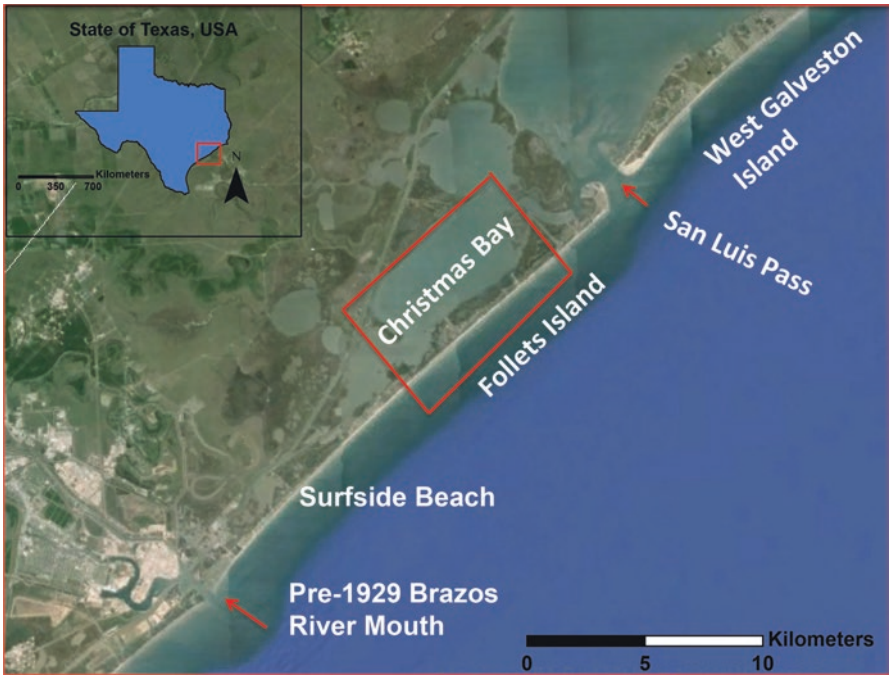

Fig. 1 Location of Follets Island and nearby coastal features. Study area (Fig. 3) shown by *red box*

Here, our objectives are (1) to determine the thickness of sand composing Follets Island and the adjacent shoreface, (2) to determine the modern overwash flux for the island as it relates to the volume of sand that has been eroded from the island during historical time, (3) to compare current rates of shoreline erosion to the geological rate in order to assess the magnitude of change over time, (4) to determine if and when Follets Island will transition from a rollover subaerial barrier to subaqueous shoals, and (5) to describe the response of the island to external forcings and predict the island's future.

2 Study Area

Follets Island is a long (10 km), narrow (average 350 m), low-lying (<2 m high, excluding artificial dunes) barrier bounded by the Gulf of Mexico to the south and Christmas Bay to the north (Fig. 1). It is a diurnal, micro-tidal (less than 0.5 m tidal amplitude), wave-dominated environment (Morton et al. 2004). Southeasterly winds are prevalent most of the year, with prevailing longshore currents toward the west. During winter, cold fronts result in a reversal in longshore currents, from west to east (Morton et al. 1995).

The average rate of long-term subsidence for the upper Texas coast is low, averaging ~0.05 mm/year (Paine 1993). However, this rate varies along the coast due to compaction of Holocene sediments, which vary in thickness from <1 to 50 m, a reflection of the relief on the Pleistocene surface that underlies the coast (Anderson et al. 2014). Follets Island is situated above the eastern margin of the Brazos River incised river valley and is flanked on its eastern and western sides by Holocene Brazos River channels belts; the Bastrop Channel belt and Oyster Creek channel belt, respectively (Bernard et al. 1959; Morton 1994; Rodriguez et al. 2004; Wallace et al. 2010). Drill cores and shallow seismic data indicate an average thickness of Holocene fluvial sediments of ~10 m beneath the island (Bernard et al. 1970; Taha and Anderson 2008; unpublished data). So, the rate of subsidence related to compaction of these Holocene sediments is contributing to the overall relative sea-level rise in the area and is believed to be higher than the average regional rate.

Sand is supplied to Follets Island mainly through episodic recycling of the San Luis Pass tidal inlet, located just east of the island (Morton et al. 1995) (Figs. 1 and 2). During the past three decades, the island has experienced high rates of erosion (Fig. 2a) indicating that sand delivery from the tidal inlet through alongshore transport (westward) is providing negligible amounts of sand to maintain the island. Sand supply from the west has been decreased by diversion of the Brazos River mouth to the west of its pre-1929 location and construction of jetties at the former river mouth at Surfside, Texas (Morton and Pieper 1975) (Fig. 2b).

3 Methodology

Thirty-four vibracores, between 100 and 520 cm in length, and 40 surface samples were collected along four transects extending from the upper shoreface across the barrier and Christmas Bay (Fig. 3). Immediately after acquisition the cores were split, photographed, and described for lithology, macrofossil content, and sedimentary structures. Grain size analyses were conducted using a Malvern Mastersizer 2000. This instrument utilizes laser diffraction in sediment suspended in water to obtain measurements. All 34 vibracores were sampled for grain size analysis. The sampling interval depended on the core length and objective of the analysis. Most cores from Christmas Bay and the upper shoreface were sampled at 10 cm intervals to determine sand fluxes through time as a function of distance from the barrier. Cores from the beach and subaerial part of the barrier were sampled at targeted intervals to help distinguish facies.

LiDAR was used to map the barrier topography and backshore water depths. Carlin et al. (2015) conducted a detailed side-scan sonar and CHIRP survey offshore of Follets Island and their data were used for establishing the offshore profile and sub-bottom geology.

A total of 21 macrofossils were radiocarbon dated from 14 cores (Fig. 3; Table 1) using the continuous flow gas bench accelerator mass spectrometer method at the Woods Hole Oceanographic Institution (NOSAMS). Where possible, we used

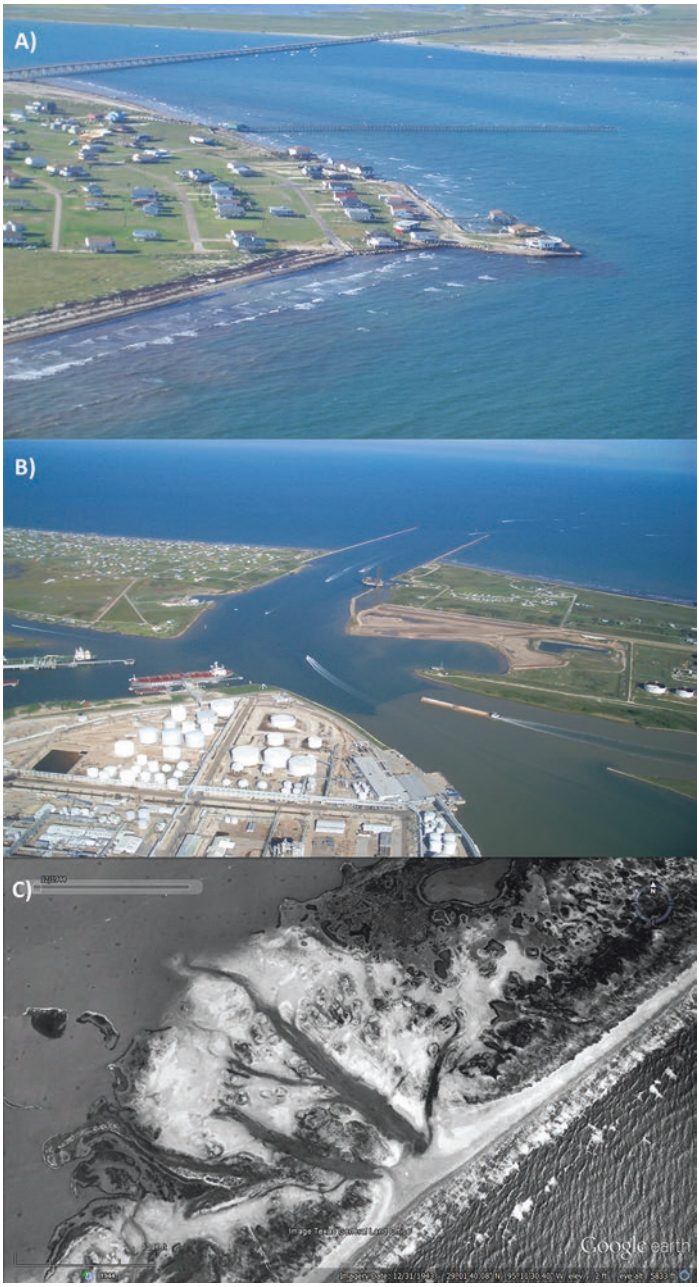

Fig. 2 (**a**) Photo showing beach erosion at the east end of Follets Island. The houses located on the spit of land protruding into the Gulf were previously located behind a dune line. (**b**) Photo facing south showing Freeport jetties, which block longshore transport of sand from the west and the Brazos River. (**c**) Breach in the island and overwash that resulted from an unnamed storm event in December 1944

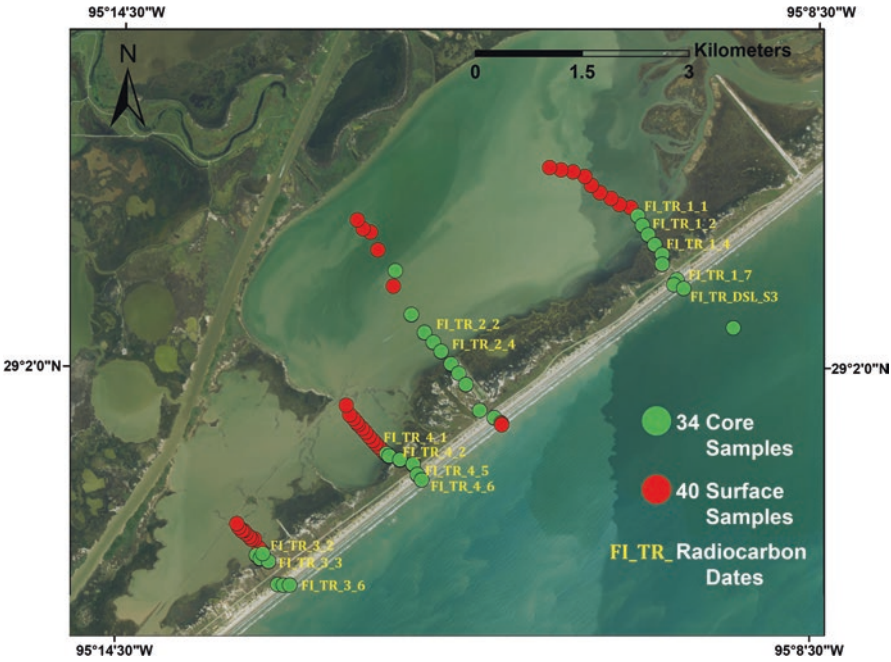

Fig. 3 Locations of sediment cores (*green circles*), cores sampled for radiocarbon dating (*yellow letters*), and surface samples (*red circles*) used for this study

articulated *Rangia cuneata* and *Ensis directus* (Razor clams), indicating largely in situ samples (Fig. 4). Table 1 provides details of the radiocarbon analyses. Radiocarbon ages were reported as calibrated years before present (where present is CE 1950). Using the standard 400-year marine reservoir correction, the ^{14}C ages were converted to calibrated calendar years at the 95.5% confidence interval (2 sigma ranges) with Marine 13 using the CALIB.Rev. 5.0 program (Reimer et al. 2013).

In addition to radiocarbon dating, ^{210}Pb analysis was conducted on cores 2-4 and 4-1 to constrain the age of modern overwash deposits (Fig. 5). The top 14 cm and 21 cm of core 2-4 and 4-1, respectively, were sampled for ^{210} Pb activity. The two cores were collected using a short transparent plastic tube. The samples were carefully cut on site immediately after extrusion to avoid mixing at the sediment–water interface. Core 2-4 was sampled entirely at a 2 cm interval whereas Core 4-1 was sampled at a 2 cm interval for the first 10 cm and at a 4 cm interval for the remaining 11 cm of the extruded core. Samples were analyzed at Core Scientific International. With a half-life of 22.3 years, ^{210}Pb can effectively date sediments younger than ~150 years (Faure 1986). Constant Rate of Sedimentation (CRS) and Constant Initial Concentration (CIC) are two major models for ^{210}Pb analysis, but CRS is the most widely used (Appleby 1998). It is a reliable method for calculating ^{210}Pb ages when the rate of sediment accumulation is not constant (Appleby and Oldfield 1983). Independent validation of the chronology is necessary for a high level of confidence in the result. We could not conduct ^{137}Cs and ^{241}Am to validate the ages

Table 1 Radiocarbon ages from cores used for this study

Core ID	Material	Depth (cm)	Age	±	2 Sigma start (BP)	2 Sigma end (BP)
			Uncalibrated 14C years BP		Calibrated 14C years BP	Calibrated 14C years BP
FI_TR_2-4	*Rangia cuneata* fragment	50	530	172	0	448
FI_TR_4-1	*Ensis directus*	90	496	173	0	431
FI_TR_1-1	*Chione elevata*	130	945	175	241	894
FI_TR_DSL_S3	*Rangia cuneata*	300	3160	177	2527	3403
[a]FI_TR_1-2	*Argopectin irradians*	190	1665	174	856	1595
FI_TR_1-7	*Perna perna*	260	2540	180	1804	2691
FI_TR_3-3	*Rangia cuneata*	115	507	173	0	436
[a]FI_TR_5-1	Articulated *Ensis directus*	290	1330	176	565	1238
FI_TR_1-2	*Ensis directus* fragment	160	1436	177	652	1315
FI_TR_3-3	*Rangia cuneata*	170	1794	182	960	1754
[a]FI_TR_3-6	*Crassostrea virginica*	265	4228	181	3854	4806
FI_TR_4-6	*Ensis directus* fragment	205	2355	176	1543	2401
FI_TR_2-2	Articulated *Rangia cuneata*	265	3734	179	3222	4144
FI_TR_3-6	*Rangia cuneata*	360	3724	183	3201	4144
[a]FI_TR_5-2	*Crassostrea virginica*	250	1783	175	958	1719
FI_TR_1-4	*Ensis directus* fragment	165	1619	175	795	1526
[a]FI_TR_1-6	*Perna perna*	145	3286	179	2723	3545
FI_TR_3-2	*Ensis directus* fragment	100	504	173	0	435
FI_TR_4-1	*Crassostrea virginica*	100	1028	176	292	929
FI_TR_4-5	*Rangia cuneata*	300	3724	189	3179	4157
FI_TR_4-2	Articulated *Ensis directus*	90	542	179	0	462

[a]Rejected due to unlikely age-depth relationship

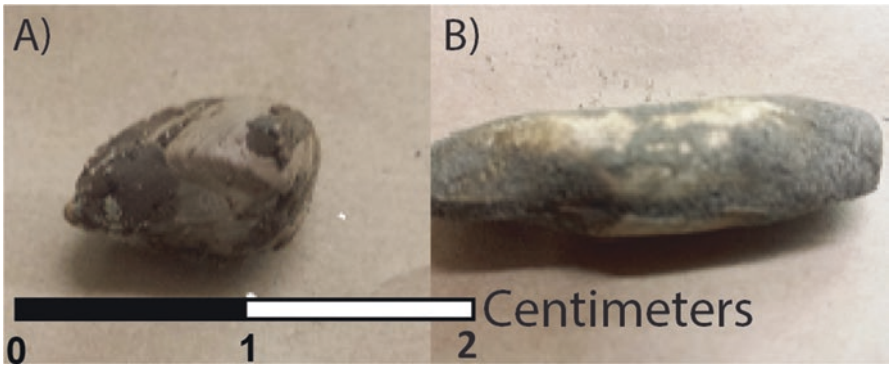

Fig. 4 (**a**) Photo showing Articulated *Rangia cuneata* and (**b**) *Ensis directus* clams targeted for radiocarbon dating

but we compared results from both CRS and CIC models for more accurate estimates. It is assumed that ^{210}Pb activity of lakes and bays has a supported component that was generated in situ within the sediment column, and the unsupported component came from the atmosphere (Appleby 1998) (Fig. 5).

4 Results

4.1 Lithofacies

Lithologic logs for sediment cores collected along four transects are shown in Fig. 6. Based on modern distribution patterns and visual descriptions of cores augmented by grain size data (Fig. 7), lithofacies were differentiated into upper shoreface sand, beach sand, proximal and distal washover deposits, bay mud, and fluvial/delta plain red clay (Fig. 8a–d). A brief description of these lithofacies follows:

Upper shoreface sands are fine (120–150 μm), well-sorted, with abundant shell debris and rare stratification (Fig. 8a).

Beach sands consist of well-sorted, yellowish-brown, structureless, fine sand (140–200 μm). Shells are common, including shell lags up to 10 cm thick (Fig. 8c, d).

The proximal overwash environment is a subaerial zone that occurs just bayward of aeolian dunes, which are mostly less than 2 m in elevation. The overwash zone is marked by a change to relatively flat relief and includes much of the back-barrier intertidal zone. The lithofacies consists dominantly (>90%) of very fine to fine (size range from 70 to 190 μm), moderately to well-sorted sand, with root casts and a virtual absence of shells (Fig. 8b, c).

The distal overwash facies is a subaqueous facies that extends bayward from the bay shoreline to where overwash transitions into bay mud. It is a poorly sorted, muddy-sand/sandy-mud and ranges in color from brown to gray. It is burrowed and

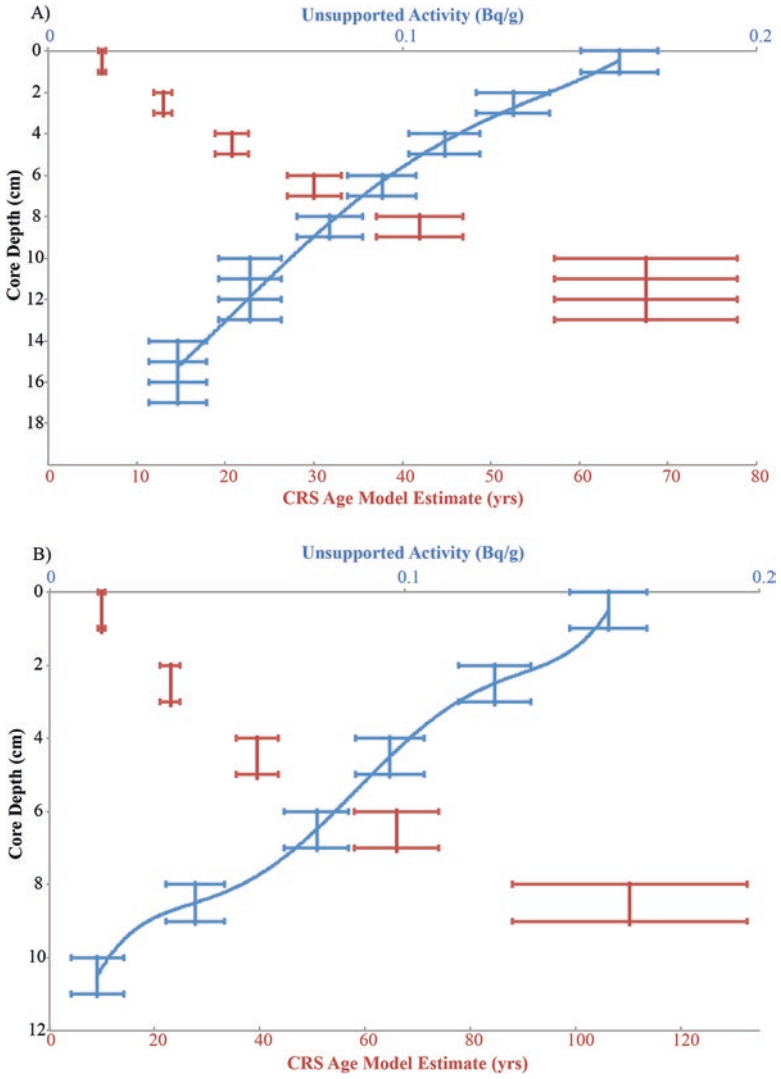

Fig. 5 Plot showing unsupported ^{210}Pb decreasing with depth for cores 4-1 (**a**) and 2-4 (**b**). Plotted are the unsupported ^{210}Pb activity (Bq/g) represented by *blue* and the CRS age model estimate (years) represented by *red* for both sample range depths

characterized by isolated shells, mainly *Rangia cuneata*, *Ensis directus* (razor clams), *Chione elevate*, and *Argopecten irradians* (scallop) (Fig. 8b, c). Results from grain size analyses show that it is a mixture of very fine sand and coarse silt (40–120 μm, Fig. 7).

Bay mud is a gray to dark gray mixture of sand and mud, which includes more fine silt and clay than the distal overwash facies (Fig. 8b). This facies is characterized by abundant shells; most abundant are *Crassostrea virginica* (oysters) and *Rangia cuneata*.

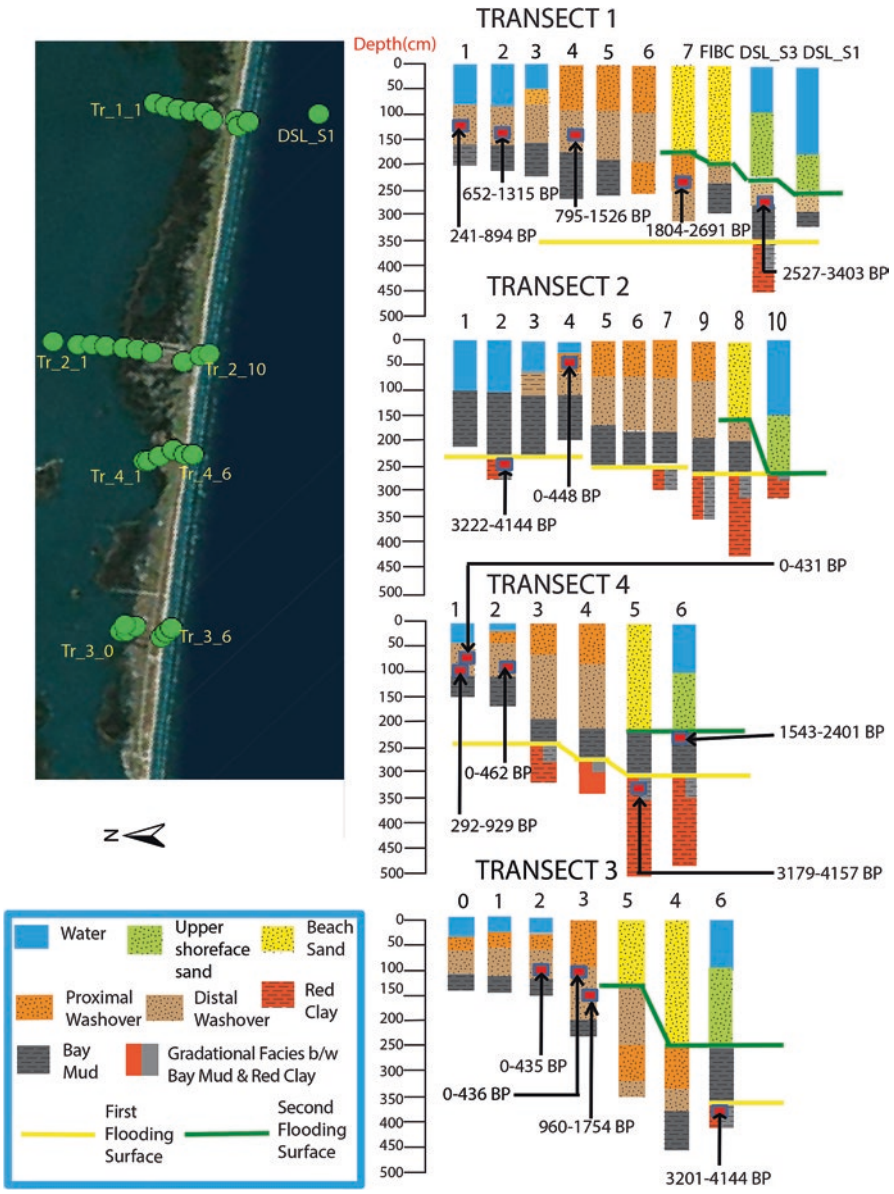

Fig. 6 Core locations and lithologic logs. Also shown are 2 sigma radiocarbon age ranges. Two flooding surfaces are identified. The younger (*green*) surface separates modern beach and foreshore sands from underlying back-barrier overwash deposits and bay mud. An older (*yellow*) surface is the initial bay shoreline flooding surface and separates bay mud from underlying fluvial and delta plain deposits

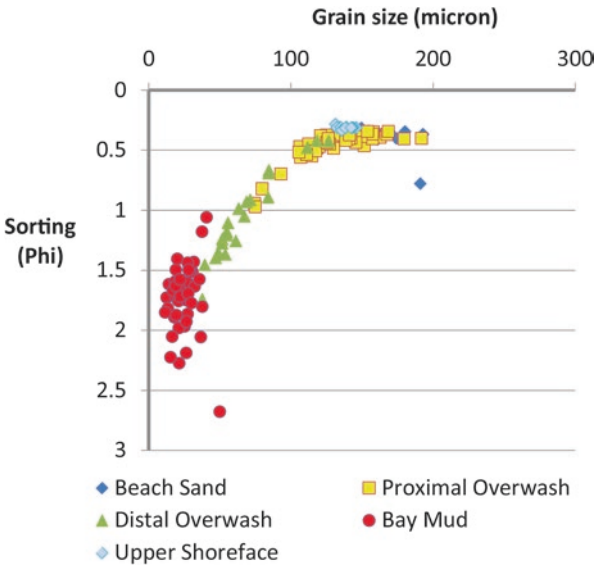

Fig. 7 Sorting versus mean grain size data for samples from different lithofacies

The oldest facies consists of compacted red clay that is mostly barren of fossils and root casts (Fig. 8a). This is a flood plain-delta plain facies associated with the ancestral Brazos River, which occupied channels on either end of Follets Island during the late Holocene (Bernard et al. 1970).

4.2 Stratigraphy

CHIRP profiles collected offshore of Follets Island by Carlin et al. (2015) show a thin upper shoreface unit resting on older strata. Our sediment cores from the upper shoreface sampled a thin (less than ~1.5 m thick) sand unit resting above the red fluvial-deltaic clay, bay, and washover lithofacies (Fig. 6). Radiocarbon ages from cores indicate that the red clay is older than ~4.1 ka, which is consistent with radiocarbon ages obtained onshore from Brazos paleo-channel deposits (Bernard et al. 1970).

The red clay unit is overlain by, and in sharp contact with, bay mud. This contact is the bay shoreline flooding surface, which represents initial flooding and creation of Christmas Bay. Radiocarbon ages from cores 2-2, 3-6 and 4-5 indicate initial bay flooding began between approximately 4.2 and 3.2 ka (Fig. 6; Table 1), which is consistent with the sea-level record for the northwestern Gulf of Mexico (Milliken et al. 2008).

Cores through Follets Island penetrated between ~2.0 and 2.5 m of beach sand. Beneath the barrier sand, cores sampled back-barrier washover and bay deposits (Fig. 6). Cores from the subaerial back-barrier zone sampled proximal washover

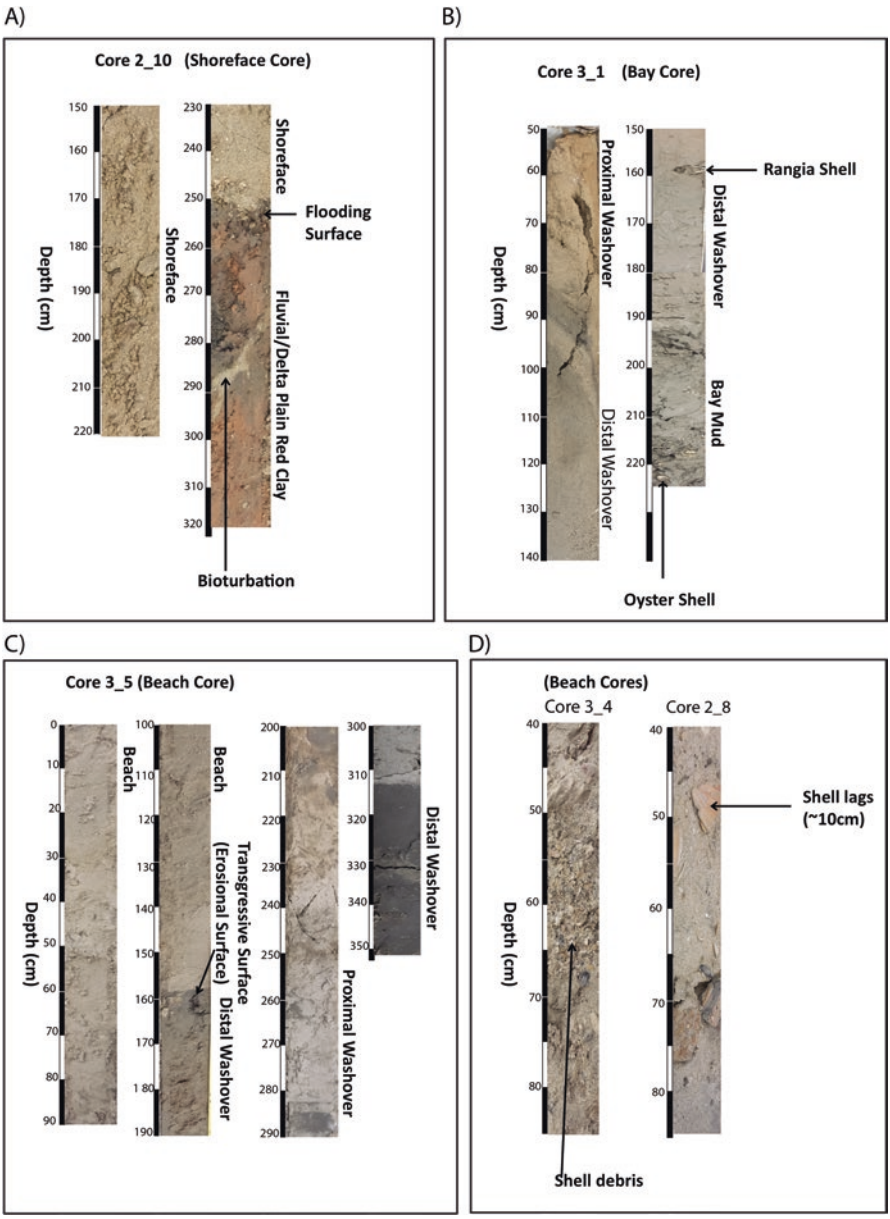

Fig. 8 Core photos of (**a**) shoreface facies, (**b**) bay facies, (**c**) and (**d**) beach facies sampled in sediment cores

deposits resting in sharp contact on distal washover deposits, which rest on, and have a gradational contact with, bay muds (Fig. 8b, c).

The observed stratigraphic architecture recorded by our sediment cores reveals two prominent transgressive surfaces. The lower surface occurs at a depth of between ~2.5 and 4 m (yellow line in Fig. 6) and separates red clay (Holocene delta plain and flood plain deposits of the Brazos River) from overlying bay mud. The contact between these units is gradational, indicating little or no erosion. The upper transgressive surface is a planar, sharp surface at a depth between ~1.5 and ~3 m (green line in Fig. 6) separating back-barrier sediments from overlying upper shoreface and/or beach deposits.

The Transgressive Ravinement Surface (TRS) occurs at an average depth between 8 and 12 m along the upper Texas coast (Siringan and Anderson 1994; Rodriguez et al. 2001; Wallace et al. 2010). We did not sample this surface, but CHIRP profiles from offshore Follets Island show that at approximately −8 m marine muds onlap older Pleistocene and Holocene deposits (Carlin et al. 2015).

Thin upper shoreface sands off Follets Island are unique in the context of the Texas coast. Offshore Follets, sand thicknesses are only ~1 m thick compared to at least 5 m thick upper shoreface sands for other Texas barriers (Siringan and Anderson 1994; Rodriguez et al. 2001; Wallace et al. 2010). This suggests that the Follets Island shoreface is starved of sand, which is supported by grain size data. Upper shoreface sands are notably finer than beach sands, indicating minimal offshore sand transport of beach material (Fig. 7).

4.3 Sand Budget and Flux Analysis

To predict future changes to Follets Island accurately, the sand budget of the island must be determined. Sand budgets can be used to investigate the overwash flux of sediments eroded from the shoreface (Inman and Dolan 1989), and to understand the dynamics of sand sources and sinks for a barrier environment. Precise sand budget analyses involve well-constrained sand volumes. Most published data on washover sediment budgets are derived from field measurements and aerial photographs to quantify washover. Specifically, washover penetration distances and thicknesses determined for modern events (Morton and Paine 1985; Morton and Sallenger 2003) or time series of beach profiles (Park and Edge 2011) form the basis for conclusions when there is little sediment core chronology available. The greatest uncertainty in deriving washover fluxes using these methods arises from the limited information on unit thickness and age. Good core coverage and improved chronostratigraphic resolution, coupled with information gained from aerial photographs and detailed topographic data, have provided sufficient detail to relate pre-historic and historic overwash rates (Donnelly et al. 2006; Carruthers et al. 2013; Rodriguez et al. this volume). The results from these later studies provided motivation for our work.

4.3.1 Sand Overwash Estimate

Long-term, millennially averaged sand fluxes have been quantified for Follets Island over the past ~3000 years (Wallace et al. 2010). These longer-term values can help put the historic values into context and allow for a better understanding of short-term coastal morphologic change.

We can constrain modern accumulation rates for distal overwash using ^{210}Pb (Fig. 5a, b). For core 4-1, the measured unsupported activities for the topmost 17 cm of the core range from 0.161 to 0.037 Bq/g (Fig. 5a). Measured unsupported activity (Bq/g) values in the uppermost 11 cm of core 2-4 range from 0.157 to 0.013 Bq/g (Fig. 5b). The accumulation rate was calculated using the constant rate of supply (CRS) model of Appleby and Oldfield (1983), which assumes a constant flux of unsupported ^{210}Pb but varying rate of sediment accumulation over time. From the age model, the oldest reliable associated age for core 2-4 of ~70 years occurs as shallow as 6 cm (using the shallowest depth interval), and this same age occurs in core 4-1 as deep as 13 cm (using the deepest depth interval). Therefore, the maximum spread of calculated sedimentation/accumulation rates from the ^{210}Pb results range between ~0.86 and 1.86 mm/year (6–13 cm/~70 years).

To determine the volume of modern sand overwash, we first estimated the thickness and extent of proximal overwash deposits using aerial photographs and sediment cores. The average total thickness of proximal overwash sand varies between transects from 1.5 m to a few decimeters and decreases bayward (Fig. 6). The area of the proximal overwash was estimated to be 3,500,000 m^2 (10 km length by 350 m width). We determined a 0.19 m thickness for modern overwash based on the assumption that proximal overwash is twice the highest average value from the distal overwash for the last ~70 years (thickness of distal overwash estimated from ^{210}Pb is between 6–13 cm for the last ~70 years). This is likely a minimum value based on the observation of rapid thinning of modern overwash deposits at the bay shoreline, the approximate boundary between proximal and distal overwash deposits. Based on this analysis, we estimate the modern proximal overwash sand volume to be ~665,000 m^3 (3,500,000 m^2 × 0.19 m).

The next step was to measure the concentration of 100–200 μm sand within distal washover and bay sediments in the tops of the cores and in grab samples. This size range encompasses the sand that comprises Follets Island and its shoreface (Fig. 7). Our radiocarbon dates differentiate the overwash deposits into modern (<500 years), intermediate (~1200 years), and paleo overwash (between ~2000 and ~3700 years) units (Fig. 9). The long-term accumulation rate is roughly linear at ~1.0 mm/year.

We measured the volume of sand in modern distal washover and bay sediments using core tops and grab samples. As expected, the concentrations decrease with increasing distance from the bay shoreline (Fig. 10). A surprising outcome of this analysis is that 20–30% sand (between 100 and 200 μm) comprises Christmas Bay sediments for distances of up to 1.5 and 2.3 km from the bay shoreline in transects 1 and 2, respectively. Note that surface samples collected more than 1.5 km from the bay shoreline along transect 1 contain ~25% sand. We attribute these relatively high

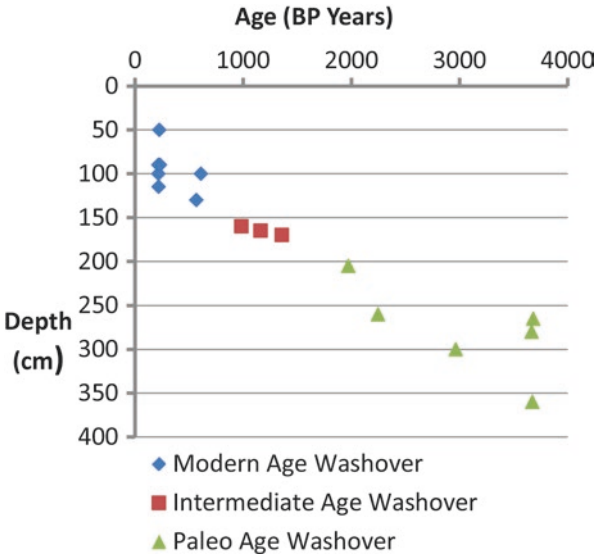

Fig. 9 Radiocarbon age clusters are used to subdivide washover deposits into units by age: modern (<500 years), intermediate (average 1200 years), and paleo washover (between ~2000 and 3700 years)

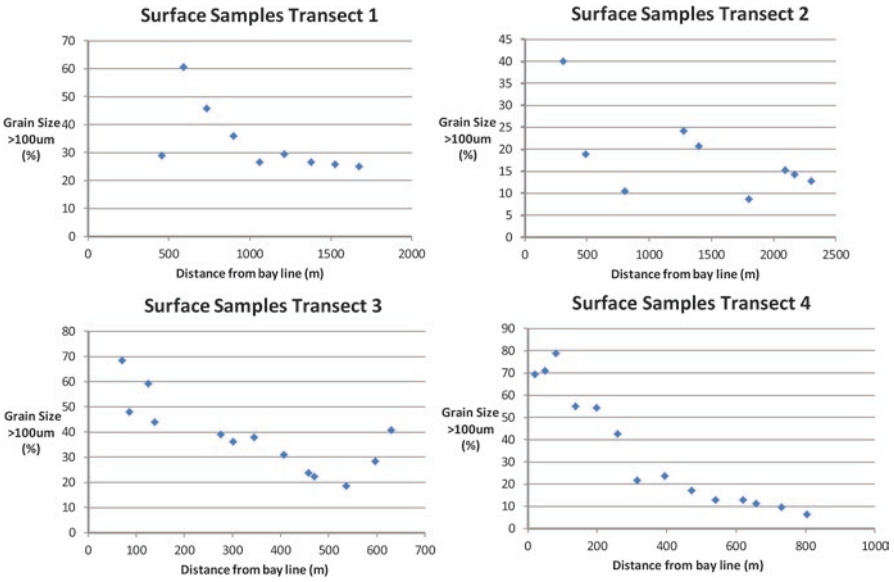

Fig. 10 Sand (100–200 μm) concentration, representing lower limit of sand concentration that makes up Follets Island and the shoreface, with increasing distance (northward and into Christmas Bay) from the bay shoreline (bay line) for each sample transect

concentrations to the proximity of the San Luis Pass tidal delta within the eastern part of Christmas Bay (Fig. 3). Transects 3 and 4 also show the expected decrease in sand volume with distance from the bay shoreline, but the distances are less than in transects 1 and 2. Note that transect 3 shows a decrease and then an increase in sand with distance from the bay shoreline. This increase is attributed to the close proximity of a dredge spoil area where sand concentrations increase. These samples were not included in our overwash sand flux calculations. The difference in transport distance between transects 1 and 2 versus transect 3 and 4 is attributed to the shallower water depths of transects 3 and 4. We made grids that range from 950,000 to 1,175,000 m^2 in areal extent (500 m length, distance interval from the bay shoreline, and the distance between two transects) and then multiplied by the sand (100–200 μm) concentration in the grid (Fig. 11). Based on this analysis, we estimate the modern distal overwash sand flux into Christmas Bay to be ~399,000 m^3 (10 km barrier length by average of 420 m width and 0.095 m average overwash thickness for the last ~70 years). The 0.095 m thickness was the average of 0.13 m and 0.06 m, the maximum and minimum overwash flux in 70 years for cores 4-1 and 2-4 respectively. Again, the modern proximal overwash sand volume is ~665,000 m^3 (0.95 m^3/m/year), which yields a total modern overwash volume of ~1,064,000 m^3 for the last ~70 years (1.52 m^3/m/year). Flux units are presented as m^3/m/year (average flux per meter of shoreline) and m^3/year (total volumetric accumulation).

The next step is to see how this total modern overwash volume compares with the total volume of sand eroded from the island in historical time. A key assumption is that the total thickness of sediment eroded is ~1.5 m. The 1.5 m thickness used is the average of proximal overwash, beach, and upper shoreface sands sampled in cores. Though the ravinement surface is about 8–10 m water depth, the acoustic back scatter from the CHIRP data shows that there is no sand below ~4 m water depth (Carlin et al. 2015).

Using these values, we are able to relate the total volume of ~2,100,000 m^3 (3.0 m^3/m/year) sand eroded (2.0 m/year modern erosion rate × 10,000 m length × 1.5 m thickness × 70 years) from the shoreface and beach over the period of observation (70 years) with the overwash volume. (The calculation of sand eroded neglects erosion of the bay sediments outcropping on the shoreface because grain size analysis indicates sand content is negligible in this facies where it outcrops on the shoreface.) Total modern sand overwash volume is ~1,064,000 m^3 (1.52 m^3/m/year) for the same time interval, suggesting that a little over half of the sand eroded from Follets Island in recent decades can be accounted for in the sand overwash estimates.

4.3.2 Drowning Time Estimate

Based on the flux of sand eroded from the foreshore and shoreface (3.0 m^3/m/year) and the total overwash flux (1.52 m^3/m/year), we estimate that the sand volume of Follets Island has been reduced at a rate of 1.48 m^3/m/year over the past 70 years.

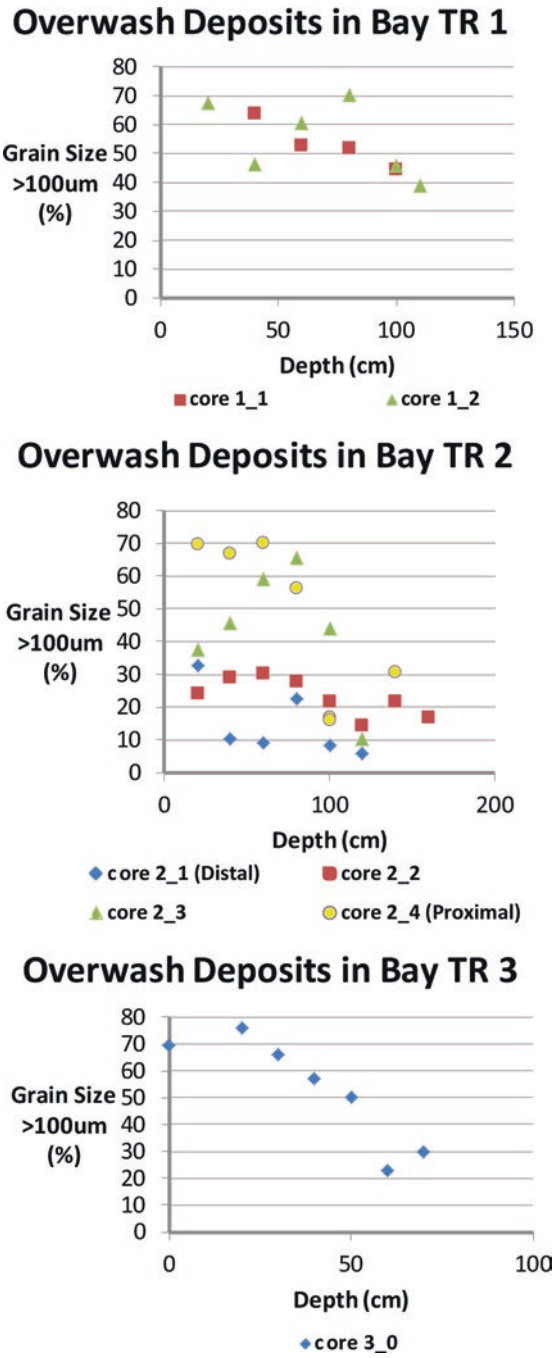

Fig. 11 Sand (100–200 μm) concentration trends with depth in cores

Additionally, we note that a significant fraction of the total overwash flux is deposited into Christmas Bay, far from the back-barrier shoreline, where it cannot contribute to maintaining the sand volume of Follets Island in the near future. In particular, assuming that only the proximal overwash flux (0.95 m^3/m/year) contributes to the landward migration of Follets Island, the future rate of sand loss will be 2.05 m^3/m/year. At this rate, and given that the volume of Follets Island is 525 m^3/m (350 m width × 1.5 m thick), we estimate the time of drowning to be ~260 years.

We consider 260 years an upper limit estimate because it does not incorporate the effect of future sea-level rise rates or future barrier narrowing, which can potentially result in a significant increase in sand flux to Christmas Bay. Future numerical modeling efforts will explore these effects.

4.3.3 Modern Versus Long-Term Overwash Flux

Cores collected within the upper shoreface to beach zones along transects 1, 2, and 3 sampled beach and shoreface sands resting unconformably on paleo overwash and bay deposits (Fig. 6). Cores DSL S3 (Transect 1) yielded a two-sigma calibrated ^{14}C age range of 2527 to 3403 and core 1-7 yielded a two-sigma calibrated ^{14}C age range of 1804 to 2691 BP for these deposits (Fig. 6). Thus, the current island location was a back-barrier bay during this time interval. There is a cluster of radiocarbon ages from mostly paleo overwash deposits at ~3 ka (Fig. 9), which supports the previously known age of the barrier (Wallace et al. 2010). The modern proximal overwash occurs between 500 and 800 m from the present-day Gulf of Mexico shoreline. This implies that the barrier was within 500–800 m of its current location around 3 ka. Based on these distances and ages, we estimate the long-term rate of shoreline retreat of the barrier to be in the range of 0.17–0.27 m/year (500–800 m over 3 ka), compared to a modern measured rate of 2.0 m/year, or about an order of magnitude difference.

We attempted to independently constrain the pre-modern rate of bay shoreline retreat (landward movement of the bay shoreline) by examining down-core sand concentrations (100–200 μm) as compared to the concentrations of sand in surface sediments from Christmas Bay (Fig. 10). Cores collected nearest the bay shoreline (e.g. core 3-0) show a clear decrease with depth while the cores distal to the bay shoreline show less variability with depth, probably due to bioturbation. Whereas most cores show a decrease in sand concentration with depth, there is no clear trend that allows us to estimate bay shoreline retreat rates through time from these data.

4.3.4 Back-Barrier Accommodation

Christmas Bay has an areal extent of ~27,000,000 m^2 and an average depth of 1.5 m. Thus, the bay has a total accommodation of 40,500,000 m^3.

5 Discussion

The rate of shoreline retreat for Follets Island is nearly equal to the rate of bay shoreline retreat as measured by the Bureau of Economic Geology (Morton et al. 2004; Paine et al. 2012). Our data show exposure of back-barrier sediments in the shoreface. Our results also show that the washover accumulation rate accounts for a little over half the volume of sand estimated from the shoreline erosion rate.

Cores that penetrated Follets Island reveal that the sand that composes the island is less than 2 m thick (similar to Onslow Beach discussed in Rodriguez et al. this volume). Compared to other Texas barriers (Bernard et al. 1959; Morton and Amdurer 1974; Wilkinson 1975; Wilkinson and Basse 1978; Rodriguez et al. 2001; Simms et al. 2006; Wallace and Anderson 2010; Anderson et al. 2014), it is the thinnest barrier island on the Texas coast. Likewise, cores from the upper shoreface sampled no more than 1.5 m of sand and CHIRP profiles indicate very thin to no lower shoreface deposits below approximately 4 m water depth (Carlin et al. 2015). This is in stark contrast to other portions of the Texas coast where shoreface deposits are thicker and extend to the toe of the shoreface between approximately 8 and 12 m water depth (Siringan and Anderson 1994; Rodriguez et al. 2004). These observations suggest that the barrier has been sand-starved in historical time.

Sediment cores sampled two transgressive surfaces, a flooding surface (lower) and an erosional shoreface surface (upper). The upper surface places beach facies and upper shoreface deposits on top of back-barrier and fluvial-deltaic deposits. Both surfaces occur above the level of transgressive ravinement for the upper Texas coast, which is at about −8 m in this area (Siringan and Anderson 1994; Rodriguez et al. 2001; Wallace et al. 2010). The Transgressive Ravinement Surface (TRS) generally coincides with the toe of the shoreface and is marked by marine mud that onlaps Pleistocene deposits. The depth of the TRS indicates that it is coincident with storm wave base (Wallace et al. 2010).

Most models for shoreface and shoreline retreat rely on transgressive ravinement and assume an equilibrium shoreface configuration to account for translation (e.g. Bruun 1954, 1962; Swift 1976; Thieler et al. 2000). These models are applicable to Galveston Island and Mustang Island, where offshore core coverage allows detailed stratigraphic analysis (Siringan and Anderson 1994; Rodriguez et al. 2004; Wallace et al. 2010). But, in the case of Follets Island, the shoreface ravinement surface shows a decoupling between the upper and lower shoreface, and a coupling between upper shoreface and back-barrier (e.g., Stive and de Vriend 1995; Cowell et al. 2003). The equilibrium shoreface profile assumption does not hold in this case, at least over short timescales (i.e., the shoreface might be out-of equilibrium: Moore et al. 2010; Lorenzo-Trueba and Ashton 2014). Sediments from the upper shoreface are reworked landwards, exposing back-barrier deposits buried only by a thin veneer of upper shoreface and beach sand. This is consistent with observations of Carlin et al. (2015), who examined beach and offshore profiles collected before and after Hurricane Ike, which made landfall in 2008 approximately 20 km east of Follets Island but breached the island in 75 places (Harter et al. 2015). They noted little

change in the lower shoreface profile but a shift in the profile of the upper shoreface and beach that indicates landward movement of sand. This is consistent with the rollover process. Shell debris and shell lags are ubiquitous in cores collected from the upper surface, and record episodes of storm erosion (Fig. 8). The reason for the shallowness (~2 m) of this surface remains uncertain.

The millennial timescale overwash flux for Follets Island is about 2300 m^3/year (~0.23 m^3/m/year) (Wallace et al. 2010). Compared to the current rate of ~15,200 m^3/year (1.52 m^3/m/year), the historical rate is about an order of magnitude faster than the long-term rate. In addition, grain size analyses of the bay sediment qualitatively indicate that distal overwash fluxes have been much higher recently than they were on the millennial timescale; sand content in the present bay sediment is significant, while it is negligible where the bay sediment outcrops on the shoreface. Our estimates of total overwash volume deposited in ~70 years is ~1,064,000 m^3 (overwash flux ~1.52 m^3/m/year). A total volume of ~2,100,000 m^3 (3.0 m^3/m/year) of sand was eroded from the shoreface and beach over the same period of observation. Thus, overwash processes account for a little over half of the sand produced by shoreline erosion in historical time. The other half is likely being transported farther west via alongshore transport (Wallace et al. 2010) and spread out in the shoreface and downdrift beaches. The barrier is estimated to have translated landwards to the present location at a rate of 0.17–0.27 m/year during the past 3 ka, which is an order of magnitude slower than the current rate.

The back-barrier accommodation is 40,500,000 m^3 (the areal extent of Christmas Bay is ~27,000,000 m^2 and water depth averages 1.5 m). The volume of sand in Follets Island is ~14,000,000 m^3 (5,500,000 m^3 sand for the barrier and 8,500,000 m^3 sand in the back-barrier). Thus, back-barrier accommodation is about three times greater than the volume of sand in Follets Island.

Back-barrier morphology, vegetation, and substrate slope also control overwash rates. Barrier islands with low-gradient substrates and back-barrier accommodation space migrate rapidly (Swift and Moslow 1982; Pilkey and Davis 1987; Cowell et al. 2003; Storms and Swift 2003; Stolper et al. 2005; Donnelly et al. 2006; FitzGerald et al. 2008; Moore et al. 2010; Brenner et al. 2015). Overwash is removing and transporting half of the available sand landwards from the undernourished barrier. Therefore, this depletion will likely cause barrier over-stepping (negative sediment budget) during sea-level rise (Cowell et al. 1995; Stolper et al. 2005).

Because only about half of the eroded shoreline sand is deposited as overwash, the barrier is getting lower and narrower, which will likely lead to increases in overwash flux in the future (Schwartz 1975; Cowell et al. 2003; Stolper et al. 2005; Rosati et al. 2006; FitzGerald et al. 2008; Park and Edge 2011). Low-gradient, narrow barrier islands are prone to overwash and therefore to multiple breaches, especially during accelerated sea-level rise, potentially leading to barrier disintegration and break up (such as identified for pre-historical time along the North Carolina Outer Banks by Mallinson et al. this volume). Given that accommodation of Christmas Bay greatly exceeds sand available in the barrier island system and that sand supply rates are diminished, the island will likely transition from a subaerial barrier to subaqueous shoals in the foreseeable future, similar to environments like

Table 2 Input parameter values used in Fig. 12

Parameter	Units	Value
Maximum overwash flux	$m^3/m/year$	10, 20, 30
Shoreface response rate	$m^3/m/year$	5,000
Equilibrium shoreface slope	–	0.02
Shoreface toe depth	m	10
Equilibrium island width	m	400
Equilibrium island height	m	2
Back-barrier lagoon slope	m	10^{-4}
Sea-level rise rate	mm/year	0–10

the Chandeleur Islands and the central Mexico coast. Extrapolating the historical fluxes of overwash and shoreline erosion rates, we estimate that Follets Island will likely drown in ~260 years (see Sect. 4.3.2). This estimate, however, does not account for the effect of accelerated sea-level rise and barrier narrowing.

Storm frequency along the Texas coast does not appear to have increased in historical time relative to the late Holocene (Wallace and Anderson 2010), although stronger but fewer storms are projected globally by the end of the century (Lin et al. 2012; Woodruff et al. 2013). Storms dominate shoreface erosion, but the interplay between sea-level rise and sediment supply is the main driver of the long-term rate of shoreline retreat (Woodruff et al. 2013). Therefore, storms are not the sole cause of increased erosion and washover of Follets Island.

Most of the barriers of the Texas Coast were formed less than 5000 years ago when the sea-level rise rate in the northern Gulf of Mexico region decreased from an average rate of 1.4 mm/year to about 0.4–0.6 mm/year (Milliken et al. 2008; Anderson et al. 2014). Current sea-level rise in the region is estimated to be ~3.0 mm/year (NOAA 2015), or about five times the rate when most Texas barriers were formed. This does not account for subsidence, which depends on rates of compaction of Holocene sediments (Törnqvist et al. 2008), and more than double sea-level rise rates locally.

Field observations from Rodriguez et al. (this volume) suggest an abrupt increase in the rate of sea-level rise makes barrier islands vulnerable to overwash leading to reductions in the width and height of a barrier and increasing the rate of shoreline retreat. Additionally, recent modeling efforts (Moore et al. 2010; Lorenzo-Trueba and Ashton 2014; Cowell and Kinsela this volume; Murray and Moore this volume; Ashton and Lorenzo-Trueba this volume) emphasize the sensitivity of barrier island response to sea-level rise. In particular, using generic island characteristics similar to those used by Lorenzo-Trueba and Ashton (2014) (see Table 2), we find that a change in sea-level rise rate from 1 to 10 mm/year can result in a 4-fold increase in the magnitude of shoreline retreat within a 100-year time period (Fig. 12). This result does not depend on the maximum overwash flux used as an input in the model. Although more analysis is needed, we suggest that the acceleration in sea-level rise

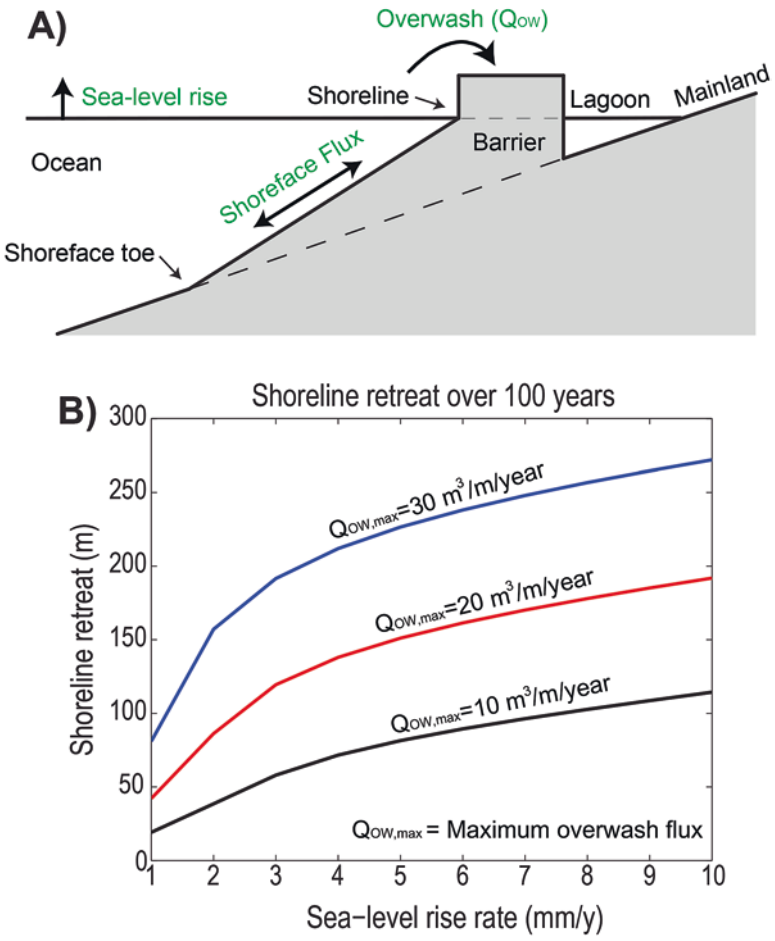

Fig. 12 (**a**) Barrier model setup and components (Lorenzo-Trueba and Ashton 2014). Note the strong exaggeration of the vertical scale. (**b**) Shoreline retreat during barrier landward migration as a function of the sea-level rise rate. Input parameter values are included in Table 2

has played a significant role on the unprecedented rate of shoreline erosion of Follets Island.

Diminished sand supply is likely also contributing to the unprecedented erosion on Follets Island. Sand supply from the east is regulated by dynamic processes operating within the San Luis Pass tidal inlet/delta complex, and sand rarely discharges from the inlet towards Follets (Wallace and Anderson 2013). The east end of Follets Island has experienced significant erosion during historical time (Fig. 2a) and this sand is moving west (Wallace et al. 2010). In addition, diversion of the Brazos River mouth from its pre-1929 location at Surfside Beach and construction of jetties at the former river mouth (at the west end of Follets Island) have blocked sand delivery from the west (Morton and Pieper 1975) (Fig. 1). The State of Texas

has undertaken several beach nourishment projects at Surfside Beach in recent decades only to have nourishment sands disappear within months of when these projects where completed.

Follets Island could transition from a rollover subaerial barrier to subaqueous shoals within the next few centuries. Exactly when this will happen depends on the number and magnitude of storms that will impact the island during this time. Regardless, the role of the island as a natural barrier to storm impact on inland areas will significantly diminish. Our volume and flux estimates indicate that sustaining the island by beach nourishment would require volumes of sand that currently do not exist in the nearshore zone as little sand exists seaward of the upper shoreface to a distance of approximately 40 km offshore (Anderson et al. 2014). Given the paucity of sand available to Follets Island and high rates of overwash, sand nourishment would have to come from sources on the continental shelf that are far removed from the island.

6 Conclusions

Follets Island is the thinnest barrier island and one of the fastest retreating islands on the Texas coast. Landward translation of the island is manifest as a surface of erosion, ~1.5 m deep, which is a sharp, planar surface that separates back-barrier deposits from overlying shoreface-foreshore deposits. Our results show that current shoreline erosion rates for Follets Island are unprecedented, with current rates being as much as an order of magnitude faster than the long-term (millennial) rate. This increase was associated with an increase in sand overwash rates over historic relative to geologic time.

Results show that the washover flux for the island accounts for at least half the volume of sand produced by shoreline erosion. Accelerated sea-level rise and diminished sand supply are considered the key causes of unprecedented shoreline erosion of the barrier.

At the current rate of shoreline retreat and overwash, coupled with the diminished sand supply and large back-barrier accommodation of Christmas Bay, Follets Island could transition from a rollover subaerial barrier to subaqueous shoals in the next few centuries. Its role as a barrier to storm impact is being significantly diminished. Barriers similarly impacted by accelerated sea-level rise and reduced sand supply could suffer the same fate.

Acknowledgments The research was funded by the Shell Center for Sustainability, Rice University. The radiocarbon dating was funded by a BP scholarship. We wish to thank Rodrigo Fernández for assistance in the field. We also wish to thank the two anonymous reviewers, in addition to Laura Moore and Brad Murray, whose comments greatly improved the manuscript.

References

Anderson J, Milliken K, Wallace D et al (2010) Coastal impact underestimated from rapid sea level rise. EOS Trans Am Geophys Union 91:205–206

Anderson JB, Wallace DJ, Simms AR et al (2014) Variable response of coastal environments of the northwestern Gulf of Mexico to sea-level rise and climate change: implications for future change. Mar Geol 352:348–366

Appleby PG (1998) Dating recent sediments by 210Pb: problems and solutions. In: Dating of sediments and determination rate, vol. STUK-A145, Helsinki, pp 7–24

Appleby PG, Oldfield F (1983) The assessment of 210Pb data from sites with varying sediment accumulation rates. Hydrobiologia 103:29–35

Ashton AD, Lorenzo-Trueba J (2018) Morphodynamics of barrier response to sea-level rise. In: Moore LJ, Murray AB (eds) Barrier dynamics and response to changing climate. Springer, New York

Bernard HA, Major CF Jr, Parrot BS (1959) The Galveston Barrier Island and environments: a model for predicting reservoir occurrence and trend. Trans Gulf Coast Assoc Geol Soc 9:221–224

Bernard HA, Major CF Jr, Parrot BS et al (1970) Recent sediments of Southeast Texas: a field guide to the Brazos alluvial and deltaic plains and the Galveston barrier island complex. University of Texas, Bureau of Economic Geology Guidebook 11, Austin, TX, p 132

Boyd R, Penland S (1984) Shoreface translation and the Holocene stratigraphic record: examples from Nova Scotia, the Mississippi Delta and eastern Australia. Mar Geol 60:391–412

Brenner OT, Moore LJ, Murray AB (2015) The complex influences of back-barrier deposition, substrate slope and underlying stratigraphy in barrier island response to sea-level rise: insights from the Virginia Barrier Islands, Mid-Atlantic Bight, U.S.A. Geomorphology 246:334–350

Bruun P (1954) Coastal erosion and development of beach profiles. Tech. Rep. Memo 44, U.S. Army Corps of Eng., Vicksburg, MS

Bruun P (1962) Sea-level rise as a cause of shore erosion. J Waterway Harbor Coast Eng Div 88:117–132

Carlin J, Dellapenna T, Figlus J et al (2015) Investigating morphological and stratigraphic changes to the submarine shoreface of a transgressive Barrier Island: Follets Island, Northern Gulf of Mexico. In: Wang P, Rosati JD, Cheng J (eds) Coastal sediments: the proceedings of the coastal sediments 2015. World Scientific, Singapore

Carruthers EA, Lane PD, Evans RL et al (2013) Quantifying overwash flux in barrier systems: an example from Martha's Vineyard, Massachusetts, USA. Mar Geol 343:15–28

Cowell PJ, Kinsela MA (2018) Shoreface controls on barrier evolution and shoreline change. In: Moore LJ, Murray AB (eds) Barrier dynamics and response to changing climate. Springer, New York

Cowell PJ, Roy PS, Jones RA (1995) Simulation of large-scale coastal change using a morphological behaviour model. Mar Geol 126:45–61

Cowell PJ, Stive MJF, Niedoroda AW et al (2003) The coastal-tract (part 2): applications of aggregated modeling of lower-order coastal change. J Coast Res 19:828–848

Dean RG, Maurmeyer EM (1983) Models for beach profile response. CRC handbook of coastal processes and erosion. CRC Press, Boca Raton, pp 151–165

Donnelly C, Kraus N, Larson M (2006) State of knowledge on measurement and modeling of coastal overwash. J Coast Res 22:965–991

Faure G (1986) Principles of isotope geology. Wiley, New York, p 589

FitzGerald DM, Fenster MS, Argow BA et al (2008) Coastal impacts due to sea-level rise. Annu Rev Earth Planet Sci 36:601–647

FitzGerald DM, Hein C, Hughes Z, Kulp M, Georgiou I, Miner M (2018) Runaway barrier island transgression concept: global case studies. In: Moore LJ, Murray AB (eds) Barrier dynamics and response to changing climate. Springer, New York

Gibeaut JC, White WA, Hepner T et al (2000) Texas Shoreline Change Project: Gulf of Mexico shoreline change from the Brazos River to Pass Cavallo. Bureau of Economic Geology, The University of Texas at Austin, Report to the Texas Coastal Coordination Council and the General Land Office, contract no. NA870Z0251, p 32

Harter C, Figlus J, Dellapenna T (2015) The role of hurricanes on the morphological evolution of a sediment-starved barrier island along the upper Texas coast: Follets Island. In: Wang P, Rosati JD, Cheng J (eds) Coastal sediments: the proceedings of the coastal sediments 2015. World Scientific, Singapore

Inman DL, Dolan R (1989) The Outer Banks of North Carolina: budget of sediment and inlet dynamics along a migrating barrier system. J Coast Res 5(2):193–237

Leatherman SP (1983) Shoreline mapping: a comparison of techniques. Shore Beach 7:28–33

Lin N, Emanuel K, Oppenheimer M et al (2012) Physically based assessment of hurricane surge threat under climate change. Nat Clim Chang 2(6):462–467

Lorenzo-Trueba J, Ashton AD (2014) Rollover, drowning, and discontinuous retreat: distinct modes of barrier response to sea-level rise arising from a simple morphodynamic model. J Geophys Res Earth 119:779–801

Mallinson D, Culver S, Leorri E, Mitra S, Mulligan R, Riggs S (2018) Barrier Island and estuary co-evolution in response to Holocene climate and sea-level change: Pamlico Sound and the Outer Banks Barrier Islands, North Carolina, USA. In: Moore LJ, Murray AB (eds) Barrier dynamics and response to changing climate. Springer, New York

McBride RA, Byrnes MR (1997) Regional variations in shore response along barrier island systems of the Mississippi River delta plain: historical change and future prediction. J Coast Res 13:628–655

Milliken KT, Anderson JB, Rodriguez AB (2008) A new composite Holocene sea-level curve for the northern Gulf of Mexico. In: Anderson JB, Rodriguez AB (eds) Response of Upper Gulf Coast Estuaries to Holocene climate change and sea-level rise. Geological Society of America Special Paper 443, pp 1–11

Moore LJ, List JH, Williams SJ et al (2010) Complexities in barrier island response to sea level rise: insights from numerical model experiments, North Carolina Outer Banks. J Geophys Res 115:F03004. https://doi.org/10.1029/2009JF001299

Moore LJ, Patsch K, List JH et al (2014) The potential for sea-level-rise-induced barrier island loss: insights from the Chandeleur Islands, Louisiana, USA. Mar Geol 355:244–259

Morton RA (1994) Texas barriers. In: Davis RA (ed) Geology of Holocene barrier island systems. Springer, New York, pp 75–114

Morton RA, Amdurer M (1974) Environmental geology in coastal zone development: an analysis of physical properties and processes. University of Texas, Bureau of Economic Geology, Austin, p 103

Morton RA, Paine J G (1985) Beach and vegetation-line changes at Galveston Island, Texas: erosion, deposition, and recovery from Hurricane Alicia. The University of Texas at Austin, Bureau of Economic Geology, Geological Circular 85-5, p 39

Morton RA, Pieper MJ (1975) Shoreline changes on Brazos Island and South Padre Island (Mansfield Channel to mouth of the Rio Grande). The University of Texas at Austin, Bureau of Economic Geology Geological Circular 75-2, p 39

Morton RA, Sallenger AH (2003) Morphological impacts of extreme storms on sandy beaches and barriers. J Coast Res 19:560–573

Morton RA, Gibeaut JC, Paine JG (1995) Meso-scale transfer of sand during and after storms: implications for prediction of shoreline movement. Mar Geol 126:161–179

Morton RA, Miller TL, Moore LJ (2004) National assessment of shoreline change: part 1: historical shoreline changes and associated coastal land loss along the U.S. Gulf of Mexico. U.S. Geological Survey Open-file Report 2004-1043, p 45

National Oceanic and Atmospheric Administration (2015) Tides and Currents. http://tidesandcurrents.noaa.gov. Accessed 4 Jul 2015

Murray AB, Moore LJ (2018) Geometric constraints on long-term barrier migration: from simple to surprising. In: Moore LJ, Murray AB (eds) Barrier dynamics and response to changing climate. Springer, New York
Niedoroda AW, Swift DJP, Figueiredo AG et al (1985) Barrier island evolution, middle Atlantic shelf, USA Part 2: evidence from the shelf floor. Mar Geol 63(1–4):363–396
Paine JG (1993) Subsidence of the Texas coast: inferences from historical and late Pleistocene sea levels. Tectonophysics 222:445–458
Paine JG, Sojan M, Tiffany C (2012) Historical shoreline change through 2007, Texas Gulf Coast: Rates, contributing causes, and Holocene context. Gulf Coast Assoc Geol Soc J 1:13–26
Paine JG, Caudie TL, Andrews JR (2017) Shoreline and sand storage dynamics from annual airborne LIDAR surveys, Texas Gulf coast. J Coast Res 33(3):487–506
Park YH, Edge BL (2011) Beach erosion along the northeast Texas coast. J Coast Res 27:502–514
Pilkey OH, Davis, TW (1987) An analysis of coastal recession models: North Carolina coast. Society of Economic and Paleontologists and Mineralogists, pp 59–68
Reimer PJ, Bard E, Bayliss A et al (2013) IntCal13 and Marine13 radiocarbon age calibration curves 0–50,000 years cal BP. Radiocarbon 55:1869–1887
Rodriguez AB, Fassell ML, Anderson JB (2001) Variations in shoreface progradation and ravinement along the Texas coast, Gulf of Mexico. Sedimentology 48:837–853
Rodriguez AB, Anderson JB, Siringan FP et al (2004) Holocene evolution of the east Texas coast and inner continental shelf: along strike variability in coastal retreat rates. J Sediment Res 74:405–421
Rodriguez AB, Yu W, Theuerkauf EJ (2018) Abrupt increase in washover deposition along a transgressive barrier island during the late 19th century acceleration in sea-level rise. In: Moore LJ, Murray AB (eds) Barrier dynamics and response to changing climate. Springer, New York
Rosati JD, Stone GW, Dean RG et al (2006) Restoration of barrier islands overlying poorly -consolidated sediments, south-central Louisiana. Gulf Coast Assoc Geol Soc Trans 56:727–740
Schwartz RK (1975) Nature and genesis of some storm washover deposits. U.S. Army Corps of Engineers, Coastal Engineering Research Center Technical Memorandum No. 61, p 69
Simms AB, Anderson JB, Blum M (2006) Barrier-island aggradation via inlet migration: Mustang Island, Texas. Sediment Geol 187:105–125
Siringan FP, Anderson JB (1994) Modern shoreface and inner-shelf storm deposits off the East Texas coast, Gulf of Mexico. J Sediment Res 64:99–110
Stéphan P, Suanez S, Fichaut B (2012) Long-term morphodynamic evolution of the Sillon de Talbert gravel barrier (Brittany, France). Shore Beach 80(1):19–36
Stive MJF, de Vriend HJ (1995) Modelling shoreface profile evolution. Mar Geol 126:235–248
Stolper D, List JH, Thieler ER (2005) Simulating the evolution of coastal morphology and stratigraphy with a new morphological-behaviour model (GEOMBEST). Mar Geol 218(1):17–36
Storms JEA, Swift DJP (2003) Shallow-marine sequences as the building blocks of stratigraphy: Insights from numerical modelling. Basin Res 15(3):287–303
Swift DJP (1976) Continental shelf sedimentation. In: Stanley DJ, Swift DJP (eds) Marine sediment transport and environmental management. Wiley, New York, pp 311–350
Swift DJP, Moslow TF (1982) Holocene transgression in South-Central Long Island, New York: discussion. J Sediment Res 52(3):1014–1019
Swift DJP, Niedoroda AW, Vincent CE et al (1985) Barrier island evolution, Middle Atlantic Shelf U.S.A., part 1: shoreface dynamics. Mar Geol 63:331–361
Taha ZP, Anderson JB (2008) The influence of valley aggradation and listric normal faulting on styles of river avulsion: a case study of the Brazos River, Texas, USA. Geomorphology 95:429–448
Thieler ER, Pilkey OH, Young RS et al (2000) The use of mathematical models to predict beach behavior for US coastal engineering: a critical review. J Coast Res 16:48–70
Törnqvist TE, Wallace DJ, Storms JEA et al (2008) Mississippi Delta subsidence primarily caused by compaction of Holocene Strata. Nat Geosci 1:173–176

Wallace DJ, Anderson JB (2010) Evidence of similar probability of intense hurricane strikes for the Gulf of Mexico over the late Holocene. Geology 38:511–514

Wallace DJ, Anderson JB (2013) Unprecedented erosion of the upper Texas Coast: response to accelerated sea-level rise and hurricane impacts. Geol Soc Am Bull 125:728–740

Wallace DJ, Anderson JB, Rodriguez AB (2009) Natural versus anthropogenic mechanisms of erosion along the upper Texas coast. In: Kelley JT, Pilkey OH, Cooper JAG (eds) America's most vulnerable coastal communities. Geological Society of America Special Paper 460, pp 137–147

Wallace DJ, Anderson JB, Fernández RA (2010) Transgressive ravinement versus depth of closure: a geological perspective from the upper Texas coast. J Coast Res 26:1057–1067

Wilkinson BH (1975) Matagorda Island, Texas: the evolution of a Gulf coast barrier complex. Geol Soc Am Bull 86:959–967

Wilkinson BH, Basse RA (1978) Late Holocene history of the central Texas coast from Galveston Island to Pass Cavallo. Geol Soc Am Bull 89:1592–1600

Woodruff JD, Irish JL, Camargo SJ (2013) Coastal flooding by tropical cyclones and sea-level rise. Nature 504(7478):44–52

Role of the Foredune in Controlling Barrier Island Response to Sea Level Rise

Chris Houser, Patrick Barrineau, Brianna Hammond, Brooke Saari, Elizabeth Rentschler, Sarah Trimble, Phil Wernette, Bradley Weymer, and Shelby Young

Abstract The height, volume, and alongshore extent of the foredune are primary controls on the response of barrier islands to the elevated storm surge that accompanies hurricanes and extra-tropical storms. In this respect, the ability of the foredune to recover following a storm determines whether a barrier island can maintain elevation as sea level rises and the island migrates landward through the redistribution of sediment to the back of the island through washover and breaching. This chapter provides a review of a body of recent fieldwork on the role of the foredune in controlling island transgression. It is argued that the role of the foredune to control washover and island transgression is analogous to that of a variable resistor in an electrical circuit, with the strength of the resistor dependent on the ability of the dune to recover in height and extent following each storm. Recovery of the foredune requires that sediment removed to the nearshore during a storm be returned to the beachface through the landward migration and welding of the innermost bars where it is eventually transported to the backshore and trapped by vegetation. Field observations from Padre Island in Texas, Santa Rosa Island in Florida, and Assateague Island in Virginia suggest that the recovery of dune height can be modeled using a sigmoidal growth curve, and that recovery can take up to a decade. The slow rate of

C. Houser (✉)
Department of Earth and Environmental Sciences, University of Windsor,
401 Sunset Avenue, Windsor, Ontario, Canada, N9B 3P4
e-mail: chouser@uwindsor.ca

P. Barrineau • B. Hammond • E. Rentschler • S. Trimble • P. Wernette • S. Young
Department of Geography, Texas A&M University, College Station, TX 77843, USA
e-mail: barrineaux@gmail.com; brianna.mj.hammond@gmail.com; t.rentschlar@gmail.com; trimblesm@gmail.com; wernett9@tamu.edu; slyoung221@gmail.com

B. Saari
Department of Environmental Studies, University of West Florida,
Pensacola, FL 32514, USA

B. Weymer
Department of Geology and Geophysics, Texas A&M University,
College Station, TX 77843, USA
e-mail: brad.weymer@gmail.com

L.J. Moore, A.B. Murray (eds.), *Barrier Dynamics and Response to Changing Climate*, https://doi.org/10.1007/978-3-319-68086-6_6

dune recovery suggests that the resiliency of barrier islands to sea level rise is dependent on whether there is a change in the frequency and magnitude of storm events or an interruption to the exchange of sediment among the nearshore, beach, and dune. Ultimately, the height and volume of the foredune can be controlled by the framework geology (to varying degrees), which determines beach and nearshore state through the availability and texture of sediment and structural controls. In this respect, the response of barrier islands to sea level rise can be expected to vary regionally and alongshore as a reflection of diverse framework geology. The local response to sea level rise depends on the ability of the dune to recover following storms. Assuming no new sediment from alongshore or offshore sources, an increase in the frequency of washover will limit the ability of the dune to recover, and recent field evidence suggests that a change in dune height and volume is self-reinforcing, which suggests a lack of island resiliency. Further testing is required to determine how the field observations and modeling described in this chapter from a select group of barrier islands around the United States are applicable to other islands and consistent throughout the evolution of a barrier island.

Keywords Foredunes • Beach-dune interaction • Sediment supply • Recovery • Resiliency • Transgression • Assateague island • Santa Rosa Island • Storm surge • Storm frequency • Sea level rise

1 Introduction

Throughout much of the world, barrier islands and spits have become an important part of the cultural and economic landscape. Development in support of recreation and navigation now dominates many barrier islands (Nordstrom 2000). A large number of barrier islands are found along the Atlantic and Gulf coasts of the United States where there is a wide flat coastal plain fronted by a wide continental shelf, but they are also found along numerous coastlines worldwide (see Stutz and Pilkey 2011). Barrier islands tend to be in a state of transgression (landward retreat) in response to a combination of eustatic sea level rise and local land subsidence (together yielding relative sea level rise, in most places), which threaten the cultural and economic development on those islands (Houser 2009), but provide ecologically important ecosystems along backbarrier shorelines such as habitat for endangered waterfowl (Godfrey and Godfrey 1973). Barrier islands are considered resilient with a rise in sea level if they are able to maintain elevation, width and volume (see Godfrey and Godfrey 1973; Hosier and Cleary 1977), and ecological function, which in turn depends on the frequency and extent of washover (see also Ashton and Lorenzo-Trueba this volume, Murray and Moore this volume, Odezulu et al. this volume, and Rodriguez et al. this volume). The potential for washover and breaching and the rate of island transgression depend on the height and alongshore extent of coastal dunes relative to the elevation of the storm surge (Thieler and Young 1991; Sallenger 2000; Morton 2002; Nott 2006; Houser et al. 2008a, Masetti

et al. 2008), which is dependent on the availability of sediment from alongshore and offshore sources to maintain the height and volume of the foredune over longer timescales (Hequette and Ruz 1991; Psuty 1992; Schwab et al. 2000; Houser et al. 2008a, b).

Barrier island resiliency, or the ability of an island to return to its previous equilibrium state (Woodroffe 2007), is dependent on the rate of post-storm dune recovery and frequency of following storms. This recovery is directly dependent on sediment exchange among nearshore, beach, and dune that is initiated with the landward migration and welding of the innermost nearshore bars. Recovery is also dependent on the ability of effective dune-building vegetation to colonize and expand within the backshore. The time required for the dune to recover to its pre-storm height and volume, or to a height that prevents significant erosion and breaching during the next storm event, depends on the level of impact and can range anywhere from a couple of weeks and months for minor scarping to almost a decade in areas where the dune was completely overwashed. Due to the disparate timescales of erosion by elevated storm surge and post-storm recovery, the resiliency of barrier islands is sensitive to changes in the frequency of storm events. A rapid succession of (even relatively weak) storms may lead to widespread erosion and washover that can leave an island especially vulnerable to further overtopping for decades (see Houser and Hamilton 2009). If the subsequent storms occur when most of the sediment remains in the nearshore or in a recently recovered beach profile, the recovery will be delayed but it is possible for the dune to recover to its pre-storm height and volume at or near its original position. The rate at which the dune recovers ultimately depends on the rate at which the nearshore and beach are restored to their pre-storm equilibrium state (Houser et al. 2015). Since the dune is relatively small and potentially discontinuous during recovery, the threshold for storm surge to exceed the dune crest elevation is lower. As a consequence, there is a greater potential for washover during subsequent storms and a loss of the recovered sediment to be moved landward and made unavailable for further recovery. Without an adequate supply of sediment from alongshore or offshore sources, the recovery of the dune may be limited or delayed by the lack of available sediment despite the recovery of the nearshore and beach to their pre-storm configuration. There is only a finite amount of sediment that is limited by moisture (tidal and groundwater) and lag, which means that new sediment needs to be supplied from the landward migration of nearshore bars (Aagaard et al. 1998, 2004, 2007; Anthony et al. 2006; Houser and Ellis 2013) or from adjacent areas alongshore. Results from Weymer et al. (2015) suggest that the divergence of sediment during a storm is reflected in the dune morphology and structure and can persist for decades after a storm, particularly where the framework geology varies alongshore (see Lentz and Hapke 2011; Houser 2012). If the recovery of the largest dunes is limited, or frequently interrupted by storm surge, there is the potential for the island to transition from large continuous dunes, in which transgression is controlled and the island is resilient, to small discontinuous dunes that represent a new equilibrium state prone to extensive washover, breaching, and even drowning (Fig. 1). This conceptual model, based on the field studies described in this review, is consistent with the numerical modeling results of Duran Vinent and Moore (2015), who found

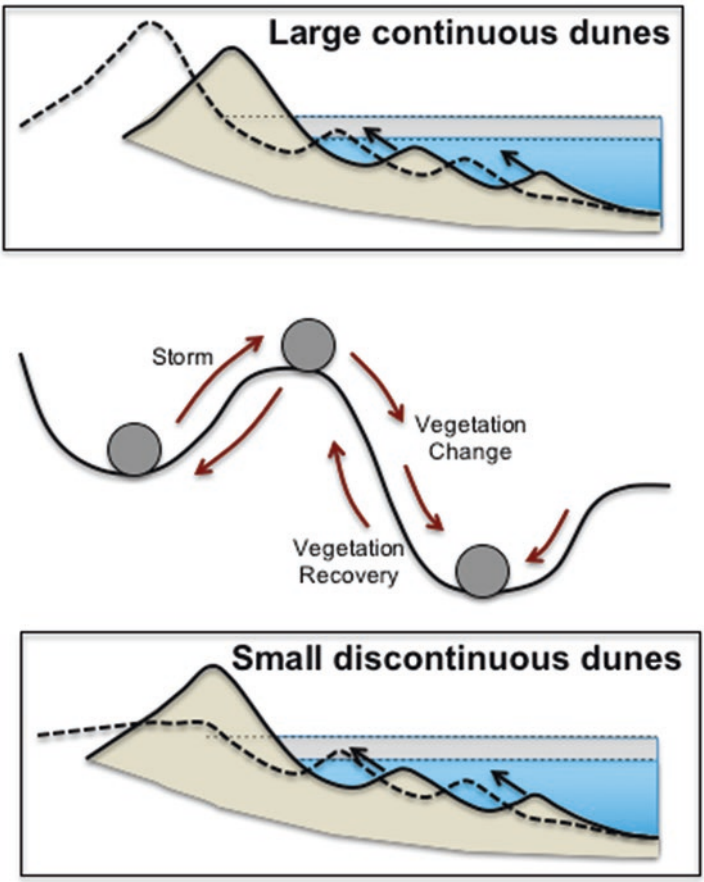

Fig. 1 Equilibrium states possible with barrier island response to storm frequency and magnitude, and sea level rise depending on the complex eco-geomorphic feedback that determines the exchange of sediment among the nearshore, beach, and dune. A barrier island will remain resilient in an equilibrium state characterized by large, continuous dunes if the exchange of sediment is able to keep pace with the rise in sea level. Otherwise, the island will transition towards an equilibrium state characterized by small, discontinuous dunes

that islands tend to be high in elevation (i.e., large continuous dunes) when the biophysical processes driving dune recovery dominate. When storm erosion is frequent and extensive, islands can enter a low-elevation state (characterized by small discontinuous dunes) that makes the island susceptible to erosion and washover during relatively mild storm conditions.

The resiliency of a sandy barrier island and the potential for the island to maintain elevation, width, and volume as sea level rises depend on a dune that limits but does not completely eliminate washover. In this respect, the role of the foredune in moderating barrier island transgression is analogous to that of a variable resistor in an electrical circuit and the response of barrier islands to sea level rise depends on

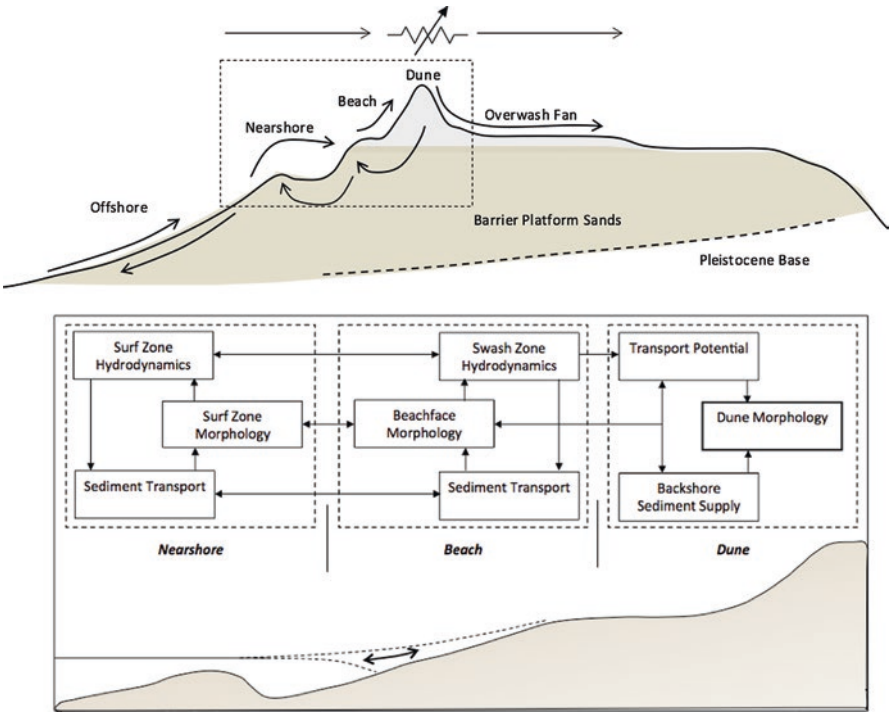

Fig. 2 Schematic of the dune as a variable resistor to the landward transport of sediment in response to rising sea levels and the feedback among the processes of the nearshore, beach, and dune that determine the strength of that resistor

the continued function and strength of that resistor. If the dune is tall (compared to the storm surge elevation for that region) and continuous alongshore, it can be considered a strong resistor that is able to limit washover, which in turn promotes island narrowing (e.g., Lorenzo-Trueba and Ashton 2014; Timmons et al. 2010) and dune scarping leading to blowout development (Davidson-Arnott 2005). In contrast, a dune that is relatively short or exhibits considerable variability alongshore can be considered a weak resistor that allows for washover and island breaching. The strength of the dune as a resistor of washover varies in both time and space and ultimately depends on how sediment is exchanged among nearshore, beach, and dune. Our understanding of that interaction is complicated by the need and difficulty to link aeolian, swash, and nearshore processes over a sequence of erosional and accretionary periods of varying frequency, magnitude, and timing (Fig. 2). Predictions of beach-dune sediment budgets and morphological change based on empirical relationships are not reliable at the smallest spatial and temporal scales (Sherman et al. 1998) and tenuous when extrapolated to the scales relevant to our understanding of island transgression (Davidson-Arnott and Law 1990, 1996; Davidson-Arnott et al. 2005). The purpose of this chapter is to explore the role of the foredune in barrier island response to relative sea level rise and to identify the

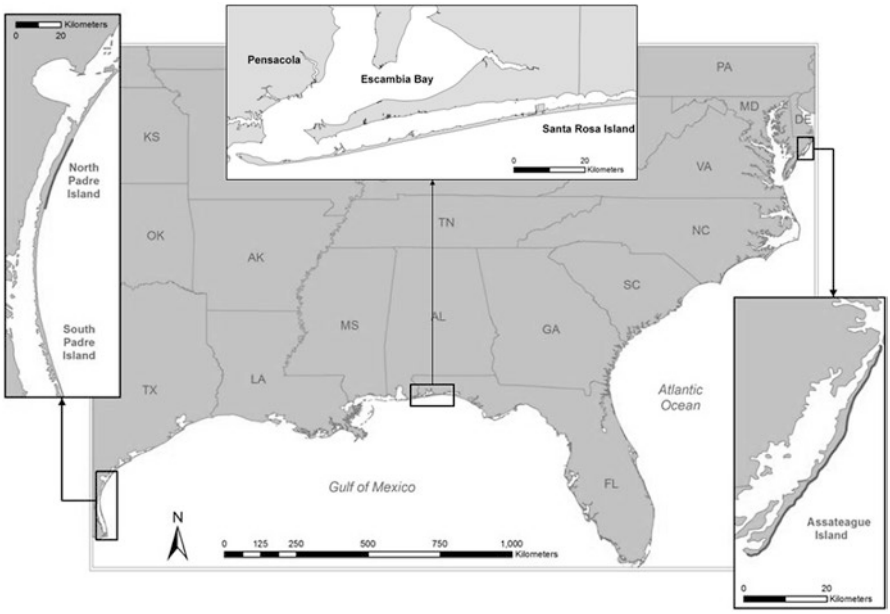

Fig. 3 Map showing location of the primary study sites referred to in this review: Padre Island in Texas, Santa Rosa Island in Florida, and Assateague Island in Virginia

multi-scale controls on the continued function and strength of this important but often overlooked (variable) resistor of island transgression. The review focuses on the results of recent field studies conducted by the authors at Padre Island in Texas, Santa Rosa Island in Florida, and Assateague Island in Virginia (Fig. 3). How and if the results of these studies are appropriate to other barrier islands and if their relationships observed hold true through time remains unclear and represents an important avenue of future research.

2 Controls on Dune Height

In general, coastal dune development is dependent on an adequate supply of sediment from the nearshore or alongshore (Swift 1976), transport of sediment from the beachface to the backshore (Bauer and Davidson-Arnott 2003), and vegetation to capture that sediment (Nickling and Davidson-Arnott 1990; Davidson-Arnott 2005; Davidson-Arnott et al. 2005). In this respect, differences in the rate of development and foredune morphology reflect differences in the wind regime, wave climate, temperature and precipitation, littoral sediment supply, sediment size and mineralogy, and vegetation type and density (see Olson 1958; Jennings 1964; Ritchie 1972; Short and Hesp 1982; Pye 1982, 1983; Hesp 1988; Klijn 1990; Davidson-Arnott et al. 2008; Bauer et al. 2009; Zarnetske et al. 2012, 2015; Moore et al. this volume;

Ruggiero et al. this volume). Field evidence suggests that the alternation between erosional and accretionary phases in the beach-dune system throughout the Holocene depended on the temporal variability of storm frequency and magnitude (Orford et al. 1999), sediment supply (FitzGerald et al. 2000), and/or sea-level change (Storms et al. 2002). Many coastal dune systems in Western Europe developed during the Little Ice Age, in response to a combination of low sea level and strong winds (Clemmensen and Murray 2006; Klijn 1990; Pye and Neal 1993; Clemmensen et al. 2001; Wilson et al. 2001, 2004; Clarke et al. 2002; Dawson et al. 2004; Matthews and Briffa 2005) capable of transporting available sediment across the wide exposed shoreface (Aagaard et al., 2007). A similar pattern of dune building and erosion has also been observed around the Great Lakes in response to variations in lake level (Olson 1958; Loope and Arbogast 2000; Arbogast et al. 2002, 2004; Hansen et al. 2010). In other words, the baseline potential for the foredune to act as a variable resistor to island transgression reflects the local relationship between sediment supply and sea level rise and fall (see Pilkey and Stutz 2000).

2.1 Role of the Geologic Framework

The majority of barrier islands are found along passive margins and are underlain by older stratigraphic units from the Pleistocene beneath and/or seaward of the shoreface interacted with modern morphodynamic processes (Riggs et al. 1995; see also Murray and Moore this volume). The supply and texture of sediment to these barrier islands is largely dependent on the framework geology, which determines (to some degree) the morphology of the shoreface and exerts considerable controls on contemporary beach-dune interaction. The morphology of the nearshore-beach-dune system has been suggested to be controlled by framework geology at multiple scales by affecting the alongshore distribution of sediment and slope of the nearshore and beach (e.g., Riggs et al. 1995; Houser and Mathew 2011), although the spatial correlations (or lack thereof) between sub-surface features and surface morphology are not well understood and can be masked by alongshore transport gradients. Honeycutt and Krantz (2003) identified three ways in which the framework geology influences shoreline-change rates and nearshore morphology: (1) Differential erosion of underlying sediments creates alongshore variations in shoreline-change rates, (2) Relict topographic highs and lows slow and hasten shoreline retreat, respectively, and (3) Relict deposits of sediment supply local beaches with sand. While framework geology has been observed as an important control on East and Gulf Coast barrier islands, alongshore sediment transport can overwhelm the imprint of framework geology. In the absence of variations in bathymetry and/or sediment supply and texture, small-scale variations in the shoreline will ultimately be dependent on large-scale gradients over long timescales (see Lazarus et al. 2011).

Previous studies have investigated the relationships between offshore bathymetry and alongshore variations in beach-dune morphology (e.g., McNinch 2004; Browder and McNinch 2006; Houser 2009; Houser and Mathew 2011). For example,

McNinch (2004) investigated the relationships between a series of shore-oblique ridges and swales identified in offshore bathymetry to alongshore variations in beach-dune morphology. The location of transverse bars coincides with Pleistocene paleochannels that were infilled by gravels during the Holocene transgression. Portions of the coast fronted by these transverse gravel bars corresponded with hotspots of shoreline erosion, which were suggested to be caused by wave refraction and focusing on the bars and energy diffusion along the intervening troughs. Browder and McNinch (2006) proposed that the framework geology in this region is a product of the interaction between the hydrologic regime and relict channel fill sediments. Working along the same section of coast, Lazarus et al. (2011) also noted a high degree of spatial correlation between the framework geology and coastal evolution and morphology at large spatial and temporal scales. Given that dune morphology can be directly related to nearshore and beach morphology (e.g., Short and Hesp 1982; Houser and Mathew 2011), it is reasonable to presume that dune morphology would most closely reflect the framework geology over broad spatial and temporal scales.

At Santa Rosa Island in northwest Florida, Houser et al. (2008a, b) used a combination of LiDAR-derived DEMs, seismic surveys, GPR transects, and cores to investigate the role of transverse ridges and swales on dune response and recovery from Hurricane Ivan in 2004. The ridges and swales are superimposed on lower order Pleistocene features and appear to be reinforced and possibly even accreted during storms. Areas of the island located landward of the transverse ridges had taller and more continuous dunes, while areas of the island coincident with the swales had lower, discontinuous dunes (Fig. 4) and also exhibited a greater shoreline retreat historically (Houser et al. 2008a, b). The ridges are spatially coherent and stratigraphically similar to the cuspate spits along the backbarrier shoreline following the initial formation of the island through progradation and aggradation (Houser 2012). Horizontal layers of mud within the ridges appear to be associated with the development of seagrass beds, salt marsh, and maritime forest at the cuspate spits and associated shoals. In this respect, Houser (2012) proposes a model in which the initial development of cuspate spits along the backbarrier shoreline and island transgression leads to the formation of the mud-core ridges, analogous to the surface imprint left by the treads of a tire. As the ridge and swale bathymetry developed on the shoreface, it reinforced the variation in dune height and storm response that controls the amount of sediment that reaches the back of the island through washover. In other words, the alongshore variation in beach and dune morphology on Santa Rosa Island is a reflection of the framework geology, which is in turn a reflection of the alongshore variation in dune morphology that developed during the Holocene. The end result is an alongshore-alternating transition from high-elvevation dunes at the cuspate headlands to low-elevation dunes between headlands with an associated variation in storm response (Fig. 5).

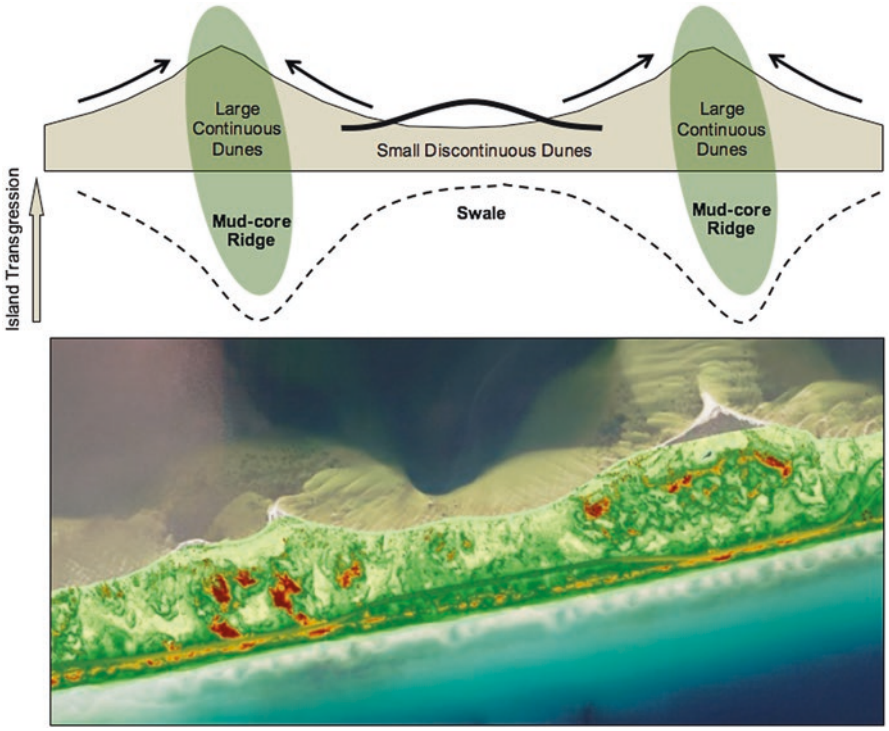

Fig. 4 Conceptual model of the spatial relationships between the framework geology and island morphology in response to sea level rise (from Houser 2012) and a representative LiDAR (Light Detection and Ranging) digital elevation model showing alongshore variation in dune and island morphology

3 Beach-Dune Interaction

As outlined by Pye (1990), coastal dune development for a given geologic framework is dependent on a supply of sediment that in many cases results from the landward migration and welding of the innermost nearshore bars (see also Swift 1976; Aagaard et al. 2004; Houser 2009), a sufficient wind and fetch for the transport of sediment from the beachface to the backshore (Bauer and Davidson-Arnott 2003), and vegetation to capture the sediment transferred from the nearshore to the beach to the backshore (Nickling and Davidson-Arnott 1990; Davidson-Arnott 2005; Davidson-Arnott et al. 2005). The development and recovery of foredunes has been suggested to depend on the synchronization of transport potential (i.e., the wind) and the availability of sediment from the nearshore, both of which may be affected by rising sea level and a change in the frequency and/or magnitude of storms (Houser 2009). The dynamic nature of the foredune is the reason that this resistor to island transgression is considered variable.

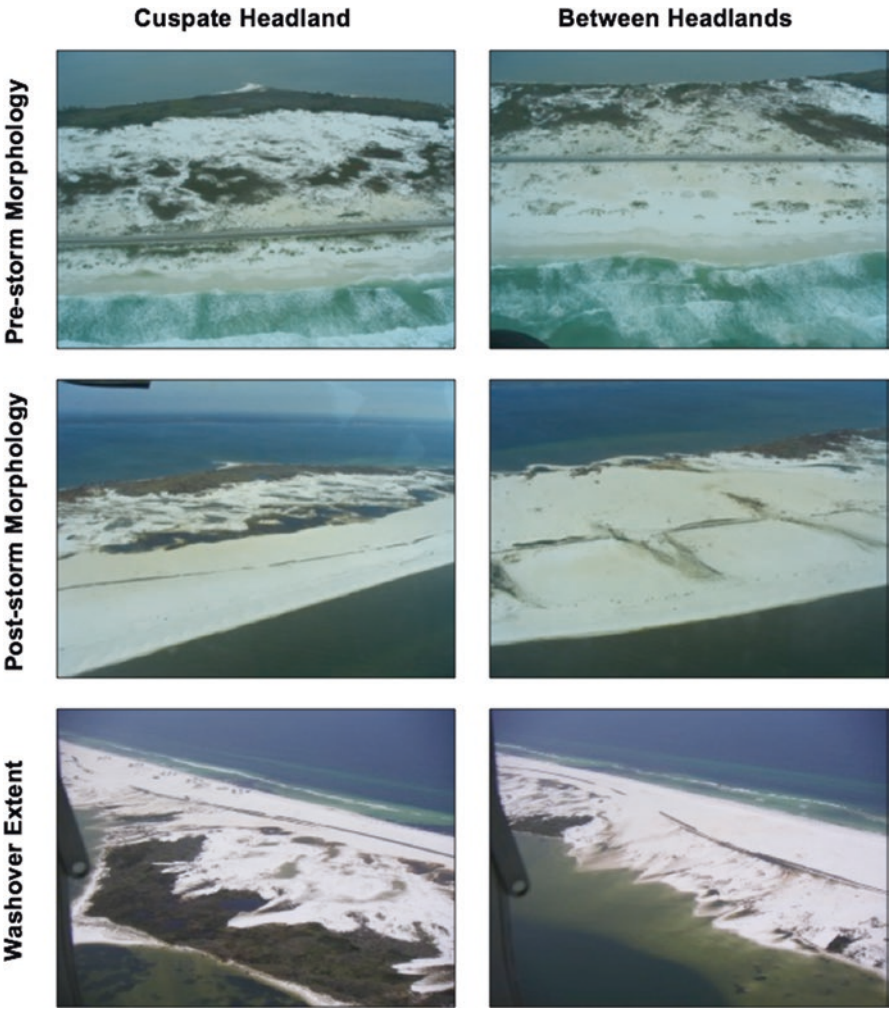

Fig. 5 Oblique aerial photographs of storm impact from Hurricanes Ivan (2004) and Dennis (2005) showing pre- and post-storm island morphology at the cuspate headlands and between headlands. Also shown is the extent of washover at and between the headlands

3.1 Sediment Supply from the Nearshore

In many cases, the sediment required for beach and dune recovery comes from the landward migration and welding of the bar(s) (Aagaard et al. 1998; Aagaard et al. 2006; Christiansen and Davidson-Arnott 2004; Aagaard et al. 2004; Houser and Greenwood 2005, 2007) or from sediment delivered by surf zone circulation processes and deposited by swash processes (Ruessink and Jeuken 2002; Pritchard and Hogg 2005; Lapinskis 2005; Houser and Barrett 2010). Bar migration is a response

to wave breaking at the crest of the bar, even if only a small fraction of the waves are breaking (Houser and Greenwood 2005, 2007). Bars migrate offshore in response to large cross-shore gradients in the sediment transport induced by quasi-steady, near-bottom, offshore flows (bed return flow), and group-bound long waves. Onshore bar migration is a response to sediment transport by incident gravity waves, with the direction of transport determined by the asymmetry between the onshore wave velocity and the offshore wave velocity in the absence of a strong bed return flow. The behavior of the innermost bars is dependent on the transformation of the wave field by the bars farther offshore (see Houser and Greenwood 2005); only when the outermost bar moves offshore is the innermost bar able to move offshore as wave breaking intensifies on its crest (see Houser and Greenwood 2005). Since storm waves are dissipated through breaking on nearshore bars and berms, their energy is reduced and the beach, backshore, and dunes are afforded some protection during a storm or subsequent storms. In this respect, the supply of sediment from the nearshore to the beachface depends on the frequency and sequencing of storm and calm-wave events, with the spatial and temporal patterns of sediment transport directed (to varying degrees) by that morphology (e.g., Wright and Short 1984).

Landward migration of subtidal and intertidal bars on the gently sloping dissipative shoreface of Skallingen, Denmark, is a consequence of a persistent onshore-directed transport, particularly within the intertidal zone (Houser and Greenwood 2007; Houser et al. 2006) and a relatively weak undertow currents (Aagaard et al. 2004). The persistent landward migration of the bars suggests that dune development on this eroding coast is a reflection of the near-continuous sediment supply from offshore rather than a beach state that promotes aeolian transport across the beach and backshore. However, the landward migration of the subtidal and intertidal bars at Skallingen is not representative of the offshore bar migration observed further south on the Dutch Coast (see Ruessink and Kroon 1994; Wijnberg and Terwindt 1995) and in New Zealand (Shand 2003) or the cyclical bar migration observed at Duck North Carolina (Lippmann and Holman 1990) and northwest Florida (Houser et al. 2013). In the absence of intertidal bars welding to the beach, the recovery of the beachface and backshore is dependent on the swash emplacement of sediment advected landward through the inner-nearshore (Hughes et al. 1997; Butt et al. 2004; Jackson et al. 2004; Pritchard and Hogg 2005). Recent evidence from Houser and Barrett (2010) suggests that the balance between erosional and accretionary swash depends on the seaward boundary condition of the swash zone. Specifically, the hydrodynamics, sediment transport, and evolution of the swash zone vary in response to the evolution of the nearshore (see Wright and Short 1984); as the nearshore evolves during and following storms, so will the swash zone and the availability of sediment for the dune (Houser and Barrett 2010).

A conceptual model developed by Davidson-Arnott (2005) suggests that sea level rise alone should have no impact on the availability of sediment from the nearshore for dune development and recovery. Unlike the Bruun rule, the model predicts a net landward migration of subtidal and intertidal bars to maintain an equilibrium profile in which the bars are positioned at the breakpoint (see Fig. 1; High Island). Rising sea levels, however, will allow relatively small storms to scarp the dunes,

with the sediment being transferred back to the littoral budget. Wind over a scarped dune increases the transport of sediment from the seaward face of the dune to the crest and over to the landward (lee) slope (see Psuty 1992; Law and Davidson-Arnott 1990; Nickling and Davidson-Arnott 1990; Davidson-Arnott and Law 1996; Aagaard et al. 1998, 2004; Ollerhead et al. 2013) and hastened through the development of blowouts (Hesp 2002; Jewell et al. 2014). However, it is not clear how an increase in the frequency and/or magnitude of storm events capable of overwashing and breaching the dune will affect the response of the nearshore profile and the ability of sediment to be transferred from the nearshore to the dune, and whether that may transition the island to a new equilibrium characterized by small discontinuous dunes (Fig. 1).

3.2 Transport Potential

The amount of sediment transported from the beach to the dune is partly dependent on the morphodynamic state of the beach and nearshore as determined by the sediment texture and the incident wave energy (Short and Hesp 1982). In general, there is less flow disturbance and greater sediment transport off and across dissipative beaches (Hsu 1977; Sherman et al. 1998; Kaimal and Finnigan 1994). In contrast, the wind is accelerated across the foreshore and berm crest on steep reflective beaches, leading to flow separation landward of the crest (Bauer et al. 1996) and the inability of the boundary layer to adjust (Short and Hesp 1982), which limits sediment transport. Intermediate beaches exhibit considerable variability in form from relatively steep beachface at the reflective end of the spectrum to relatively flat at the dissipative end of the spectrum. Where there are bar structures on the beachface, the boundary layer is unable to adjust, thereby limiting sediment transport (Short and Hesp 1982; Houser et al. 2009). In general, intermediate beaches tend to be associated with parabolic dune fields, while reflective and dissipative beaches tend to be associated with small dune fields or transgressive dune fields respectively (Short and Hesp 1982). As observed by Hesp et al. (2005), growth of the dune can lead to a stagnation point directly at the base of the dune that promotes deposition and the landward expansion of the dune or the development of a new dune system. Similar results are presented in the modeling work of Duran and Moore (2013).

The transport potential is not just dependent on whether or not the nearshore and beach are dissipative or reflective. Morton et al. (1994) observed that the narrow beach width on developed beaches limited dune recovery. In response to this and similar observations, Bauer and Davidson-Arnott (2003) present a model to show that in some settings oblique winds are largely responsible for transport of sediment from beach to dune, assuming that there is an unlimited supply of sediment in the backshore and across the beach. The amount of sediment transferred to the dune, then, partly depends on the orientation of the beach relative to the predominant wind, which means that the transport of sediment from the beach to the dune as the profile migrates landward is sensitive to changes in the local wind climate and how

the beach width varies seasonally. A change in beach width may also result from the alongshore migration of sand waves (Stewart and Davidson-Arnott 1988; Ruessink and Jeuken 2002), which provides more sediment for aeolian transport and greater protection to the dune toe during storms. In lacustrine environments, the width of the backshore is also closely tied to water levels, such that low water levels promote dune recovery and progradation, whereas high water levels allow even moderate storms to erode the foredune and reset the recovery (Saunders and Davidson-Arnott 1990). In the same way, changes in sea level at storm, seasonal, and decadal scales will also affect the beach width, which can in turn alter the transport potential (Bauer and Davidson-Arnott 2003), the availability of sediment available for transport (Davidson-Arnott and van Heyningen 2003), and the potential for erosion of the dune toe (Davidson-Arnott 1988). As wind speeds increase above threshold for aeolian transport, the potential for storm surge capable of flooding the beach increases. It is, therefore, reasonable to expect that there is a narrow spatial or temporal window in which sediment can be transported to the dune before the storm surge extends into the backshore and the transport system begins to shut down (see Delgado-Fernandez and Davidson-Arnott 2011).

3.3 Vegetation

The type of vegetation present on a barrier island depends on the amount of sediment being transported from beach to dune and the rate of sand accretion (Maun 1998). Woody shrubs and herbaceous plants are partially to fully intolerant of burial and sand blasting, while grasses can thrive with intermediate rates of burial (Nickling and Wolfe 1994; Maun 1998). As a consequence, the ability of dune vegetation to capture sediment and promote vertical growth relies on the degree to which a species is burial-tolerant, which in turn is controlled by the sediment transport potential at a particular location (Ranwell 1958; Hewett 1970; Van der Valk 1974; Moreno-Casasola 1986; Sykes and Wilson 1990; Zhang and Maun 1989; Kent et al. 2001; Maun 2004). Dune vegetation can be classified into three categories: dune builders, burial-tolerant stabilizers (or maintainer species), and burial-intolerant stabilizers (Miller et al. 2010). The plant communities found in different geomorphic control regimes of barrier islands are dependent on the individual species response and adaptations to stresses placed on plants by the coastal dune environment (Zhang and Maun 1992; Maun 1996; Amsberry et al. 2000; Feagin and Wu 2007). Areas prone to washover because dune height or greater storm surge potential typically have low-profile dunes covered by burial-tolerant vegetation, while areas with less frequent washover have burial-intolerant vegetation and larger dunes (Stallins and Parker 2003; Wolner et al. 2013). Dune-builder species and burial-tolerant stabilizers are both well-adapted to salt exposure; the former are able to grow vertically in response to limited burial, and the latter are adapted to frequent burial. Burial-tolerant species are capable of quickly colonizing the exposed sand of overwash

terraces by creeping low to the ground and are often the first vegetation types to recover to their pre-storm extent.

It follows that vegetation type is controlled by the frequency of disturbance on a barrier island (Wolner et al. 2013). Dunes that experience frequent overwash are colonized by maintainer species that have adjusted to frequent disturbance through a shorter lifespan and the production of numerous offspring. If there is insufficient time for plant communities to recover following a storm, there is the potential for maintainer species to become the dominant vegetation cover (Wolner et al. 2013). Since the low profile of maintainer species does not promote the deposition of sediment transferred from the beach to the backshore as rapidly as dune builders, frequent disturbance increases the dominance and extent of maintainer species leading to low dunes that increase the frequency of washover (Stallins and Parker 2003; Wolner et al. 2013). In contrast, dune-building species dominate where there is limited disturbance due to the limited time required for these species to expand, primarily through rhizomes, and for the new seedlings to grow to a size capable of promoting the deposition of sediment and rapid dune growth. The different growth strategies and tolerance to burial create an eco-geomorphic feedback that reinforces the height, extent, and volume of the foredune and determine its strength as a resistor to island transgression, with different species giving rise to different dune shapes (see Ruggiero et al. this volume). In other words, an increase in the frequency and/or magnitude of storm surge has the potential to promote burial-tolerant species and the development of low dunes and a new equilibrium state (Hosier and Cleary 1977; Stallins and Parker 2003; Wolner et al. 2013), though this low dune state may also be achieved by feedbacks between the growth rate of dunes and storm frequency alone, without the aid of maintainer species (Duran Vinent and Moore 2015; Moore et al. this volume).

4 Foredune Erosion and Recovery

The impact of storm surge depends on the elevation and duration of the surge relative to the elevation of the dune toe and crest (Sallenger 2000). Assuming no new sources of sediment from offshore or alongshore sources, foredune height is dependent on the time elapsed since the most recent storm, the magnitude of change induced during that event, and the rate of post-storm recovery (Houser and Hamilton 2009; Houser et al. 2015). Storms can have a range of impacts, from minor scarping at the base of the dune to overwash and/or breaching (Sallenger 2000; Hesp 2002); the length of time required for recovery depends on the degree of storm impact (Fig. 6). This suggests that the height, volume, and extent of the dune is sensitive to changes in the frequency and/or magnitude of storm events. As an example of how a change in storm frequency can affect an island, the storm surge of Hurricanes Dennis and Katrina at Santa Rosa Island should have only resulted in minor dune scarping had it not been for the loss of dune height during Hurricane Ivan the year before. Because the time between events was insufficient for the dunes to recover,

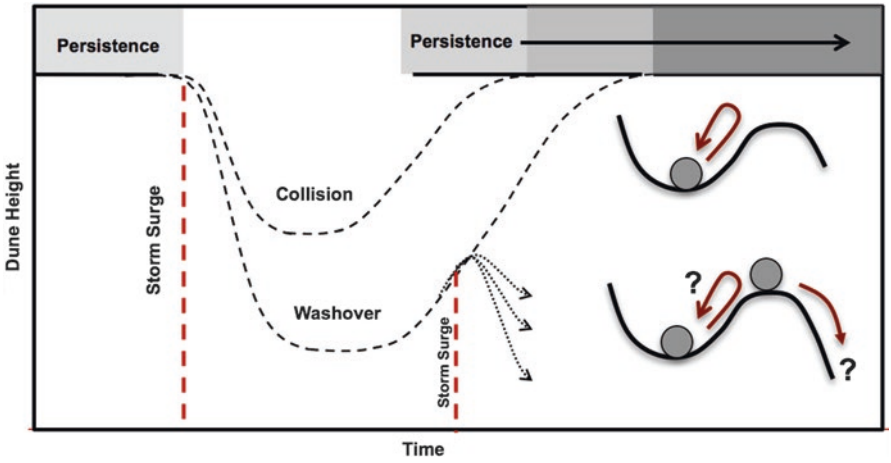

Fig. 6. Change in dune height as a consequence in response to storms of different impact (swash, collision, and washover; Sallenger 2000) and the long-term persistence of a high-island state dependent on the frequency of storm events

the storm surge of Hurricanes Dennis and Katrina caused widespread washover and erosion, damaging infrastructure that had been recently repaired (Houser 2009). If several storms occur in quick succession and limit dune recovery, there is the potential for a loss of island resiliency and rapid transgression (see Houser and Hamilton 2009).

Results from Galveston Island, Texas (Morton et al. 1994), and Santa Rosa Island, Florida (Houser et al. 2015), suggest that post-storm dune recovery can take up to 10 years following a storm that causes extensive washover. Post-storm recovery of dune crest (D_c), height (D_H), and volume (D_v) to their pre-storm state or some long-term equilibrium height can be described using the growth model of Verhulst (1838):

$$\frac{dN}{dt} = rN\left[1-\left(\frac{N}{K}\right)\right]$$

where N is a system attribute (i.e., dune height), r is the growth rate, t is the time elapsed since the last disturbance, and K is the upper boundary (asymptote) of dune growth. Integration of Eq. 1 gives:

$$N_t = \frac{KN_o}{\left(K-N_o\right)e^{-n}+N_o}$$

where N_t is the height of the dune at time t, N_o is the initial height of the dune ($t=0$), and e is the base of the natural logarithm (see Hugenholtz and Wolfe 2005). The sigmoidal curve reflects the slow recovery of the beach and backshore to provide a

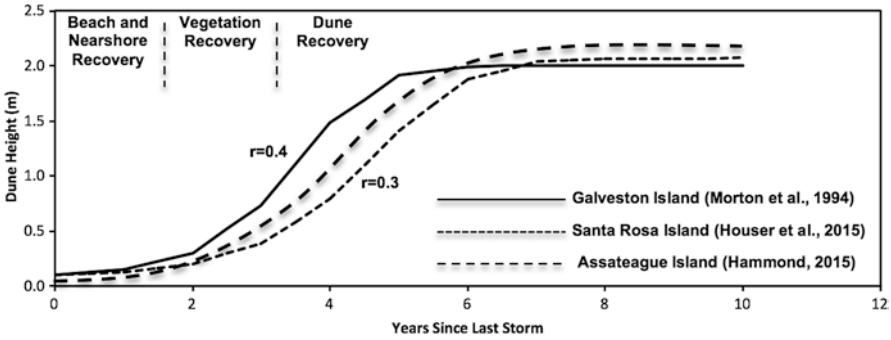

Fig. 7 Dune height recovery curves for similarly sized dunes on Galveston Island (Morton et al. 1994), Santa Rosa Island (Houser et al. 2015), and Assateague Island (Hammond 2015). Also shown is the approximate timing for recovery of the beach and nearshore (Stages 1 and 2; Morton et al. 1994), recovery of dune-building vegetation (Stage 3), and recovery of the dune to its pre-storm height (Stage 4)

supply of sediment to be captured by the vegetation that needs to recolonize the eroded area (Rentschlar 2014) before the dune can recover. As observed by Houser et al. (2015), recovery of island volume through the landward migration of the innermost bars can take up to 2 years followed by the recovery of vegetation up to 5 years after the storm (Fig. 7). Results from Hammond (2015) suggest that sections of Assateague Island National Seashore with relatively small pre-storm dunes recovered within ~3 years, but ceased to recover further due to the lack of sediment for further dune development. This suggests that there is a limit to recovery in low sections of the island. In contrast, the largest dunes continued to recover after 3 years, suggesting that the height of recovered dunes is related to the height of the pre-storm dunes. This in turn determines how much sediment is transferred landward and seaward during storms and the potential for vegetation to persist.

The sigmoidal nature of the recovery curves presented in Fig. 7 can be described with respect to the four stages of dune recovery following a storm event described by Morton et al. (1994). The first stage of recovery begins immediately after the storm and can last a few weeks or up to a year, depending on the severity of the storm (Sallenger 2000). This stage is characterized by berm reconstruction and steepening of the beach face. Specifically, sediment is returned to the beachface and the beach undergoes gradual accretion as the innermost bar migrates landward and welds to the beachface, leading to a steep beach ridge in reflective environments or a low-gradient berm in more dissipative environments. As noted, landward migration of nearshore bars is driven by the waves as they shoal across the bar during fair-weather conditions (Elgar et al. 2001; Houser et al. 2006), with recovery and beach welding taking a season or even several years following a large storm or multiple storms in succession (Lee et al. 1998). The second stage of recovery involves sediment deposition in the backshore and lengthening of the available fetch. This can either occur between storms, when winds tend to be below the transport thresh-

old, or during storms, through the landward migration of subtidal and intertidal bars (Houser and Greenwood 2005, 2007), the alongshore migration of sandwaves (Law and Davidson-Arnott 1990, 1996), or in response to lake levels (Saunders and Davidson-Arnott 1990). As the beach widens, the amount of available dry sediment increases, allowing for transport from the beach to the dune system.

Stage 3 is characterized by aeolian transport across the beach and backshore to the embryo dune when either dune building or maintainer species have been able to colonize. Since storm winds capable of entraining sediment are usually accompanied by elevated water levels (Ruz and Meur-Ferec 2004; Delgado-Fernandez and Davidson-Arnott 2011) and precipitation (Keijsers et al. 2012), it is reasonable to assume that sediment only becomes available to the dunes when the backshore expands and allows for the development/recovery of a dune ramp (Christiansen and Davidson-Arnott 2004). While aeolian transport is possible as soon as the upper-beach and any washover deposits become dry, the expansion of the backshore is required to increase the fetch length, which controls the amount of sediment exchanged from the beach to the dune (Davidson-Arnott 1988; Davidson-Arnott and Law 1990, 1996; Bauer and Davidson-Arnott 2003; Houser 2009). The rate of aeolian transport to the recovering dune is complicated by the presence of a moist sand surface (c.f., Namikas and Sherman 1995; McKenna Neuman 2003; Jackson and Nordstrom 1997; Wiggs et al. 2004), surface crusting (c.f., Leys and Eldridge 1998; Rice and McEwan 2001), topographic variability (c.f., Iversen and Rasmussen 1999; Hesp et al. 2005), and flotsam including woody debris (c.f., Walker and Barrie 2006; Eamer and Walker 2010), seasonal berm colonizers, shell lag (Wolner et al. 2013), and seaweed (Houser et al. 2012). Depending on how the availability of sediment and the transport potential are synchronized (see Houser 2009), this part of the recovery can take several years.

Stage 4 occurs after the initial establishment of vegetation and involves the growth of "*taller, wider, continuous, and more densely vegetated*" dunes (Morton et al. 1994). Depending on the extent to which the roots and rhizomes are impacted, this stage of recovery can take two to eight years if the roots and rhizomes are not destroyed during the disturbance (Brodhead and Godfrey 1979; Houser et al. 2013). The faster the vegetation emerges, the more likely it will remain viable (Maun 2009) and the dunes can recover faster. Vegetation recovery after Hurricane Opal depended on the presence of seed banks, vegetation fragments, and rhizomes that survived the storm (Snyder and Boss 2002). This is consistent with Hesp (1988) who argued that the morphology of the incipient foredune is dependent on the mode of beach colonization, plant density, and distribution, and that the species available for recolonization are, in turn, dependent on the beach state. The biodiversity and total number of plants present on a beach decreases with an increase in the frequency of storms (Gornish and Miller 2010; Miller et al. 2010), with a transition to maintainer species that are ineffective dune builders (Hosier and Cleary 1977; Stallins and Parker 2003; Wolner et al. 2013; Duran Vinent and Moore 2015). The rate of vegetation and dune recovery is fastest for maintainer species, but ultimately the height of the dune is limited if dune builders do not become established (Rentschlar 2014; Hammond 2015).

4.1 Dune Recovery at Santa Rosa Island

The recovery of Santa Rosa Island after Hurricane Ivan in 2004 exhibited considerable variability alongshore in response to the presence of the ridge and swale bathymetry (Fig. 8) and the persistence of vegetation within the Fort Pickens section of the Gulf Islands National Seashore (Houser and Hamilton 2009). The largest dunes landward of the shoreface ridges limit washover penetration and most of the sediment eroded from the dunes during a storm was transported seaward and deposited as nearshore bars. In contrast, the sections of the island landward of the swales had relatively small discontinuous dunes leading to overwash to the backbarrier shoreline and in some cases beyond. Because of greater overwash frequency, narrow sections of the island were dominated by maintainer species and dune recovery was limited due to the lack of sediment available from the nearshore and limited aeolian transport potential. Although recovery was limited overall, the rate of recovery was faster in narrow sections of the island compared to the wider sections of the island that experienced limited overwash.

Recovery was faster in the Fort Pickens section of the Gulf Islands National Seashore due to the persistence of vegetation despite this section being immediately east of the storm track for Hurricane Ivan (Houser and Hamilton 2009). The persistence of vegetation occurred along the low-profile backbarrier dune that had developed landward of the primary access road to Fort Pickens. Shoreline retreat caused this dune to become the most landward form due to shoreline retreat during Hurricanes Ivan, Dennis, and Katrina, and growth of the dune was initiated as soon as the beach and backshore recovered. Saari (2015) examined the relative importance of sediment supply, transport potential, and the presence of vegetation across areas of Santa Rosa Island that experienced different levels of storm impact. Sections of the island that experienced only beach and backshore erosion exhibited limited aeolian transport, but exhibited continued growth of the dune due to the presence of topographic gradients and vegetation cover. In contrast, the areas of the island that experienced extensive overwash and breaching also experienced greater aeolian transport, but little to no deposition due to the lack of topographically forced transport gradients and vegetation cover.

4.2 Storm Frequency and Sequencing

Although it has been shown that an increase in the frequency and/or magnitude of storms has the potential to promote burial-tolerant species and the development of a new low-dune equilibrium state (Hosier and Cleary 1977; Stallins and Parker 2003; Wolner et al. 2013; Duran Vinent and Moore 2015), it is not clear how the equilibrium state of the island depends on the sequencing of those storms. A simple model was developed for this review to examine how storm sequencing may affect island response to sea level rise. Following Larson et al. (2004), the erosion of the dune is

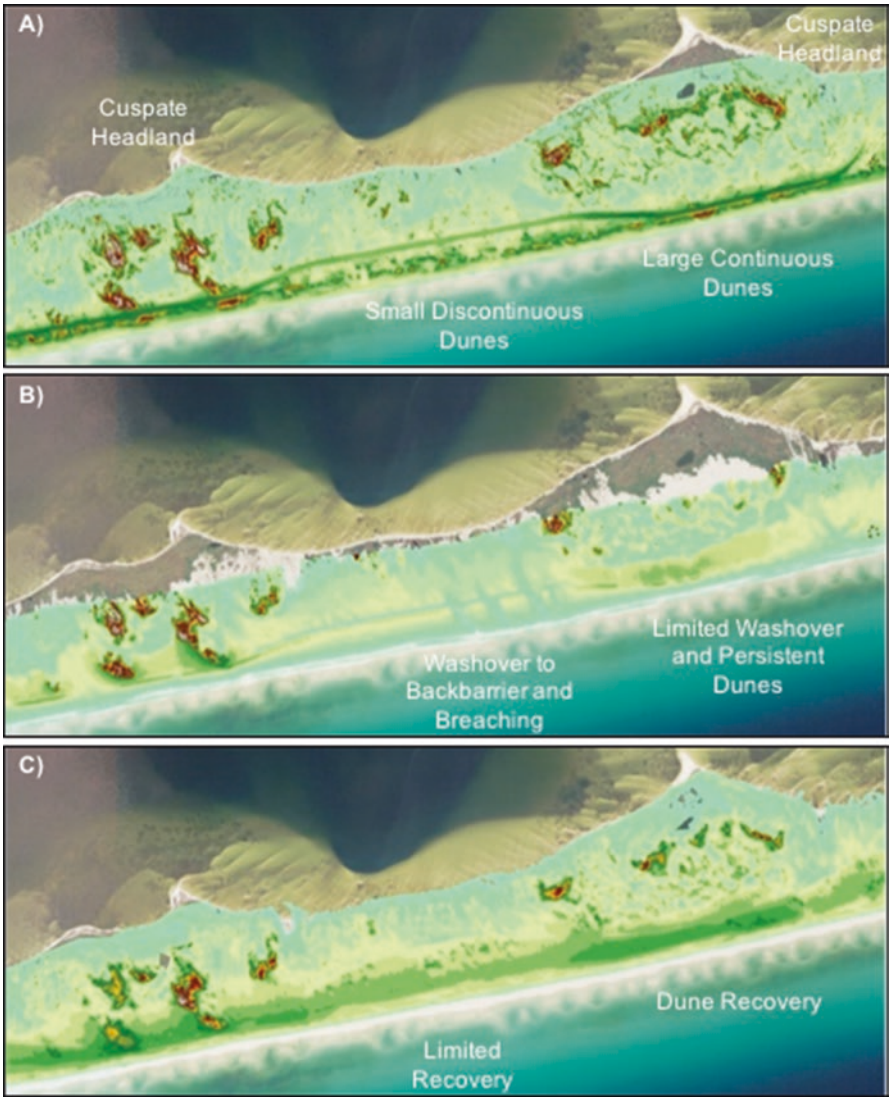

Fig. 8. Alongshore variability of storm response and recovery at Santa Rosa Island corresponding to the "sections of island with large dunes at the cuspate headlands and the relatively low-elevation sections of the island between headlands." Shown is the LiDAR digital elevation model for (**a**) Pre-Hurricane Ivan (May 2004), (**b**) Post-Hurricane Ivan (September 2004), and (**c**) post-storm recovery in 2010

estimated using "wave impact theory" in which it is assumed that there is a linear relationship between the strength of the swash bores impacting the dune and the volume of sediment eroded from the average dune on Santa Rosa Island before Hurricane Ivan made landfall. Recovery from that point was based on the recovery

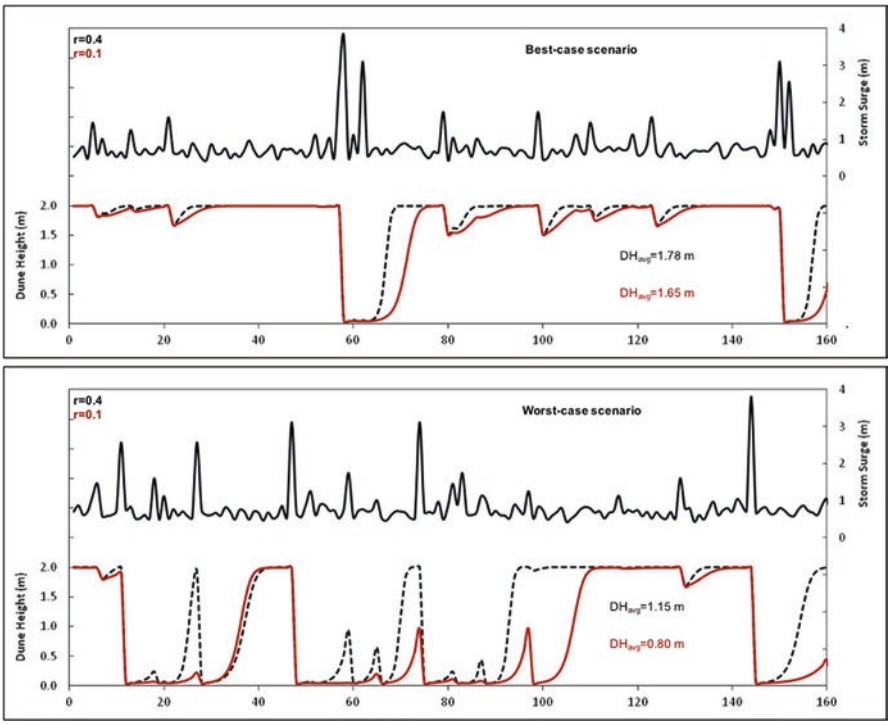

Fig. 9. Modeled variation in dune height for different rates of recovery ($r = 0.4$ and $r = 0.1$) and randomized maximum annual water levels for Pensacola. Shown are the 'best-case' and 'worst-case' scenarios based on the clustering of the storm surge events

curves for Galveston Island and Santa Rosa Island (Fig. 9). The 1% annual maximum coastal water level presented by Xu and Huang (2008) was used as a first order approximation of the storm surge elevation responsible for the erosion of the dune. The storm surge data was extended to 160 years and randomized and resampled to create different storm surge histories. Results of this analysis suggest that the sequencing of storm events has important implications for the long-term average height of the foredune and the potential for rapid island transgression. The "best-case scenario," in which the average dune height is maximized over time, has storms clustered, while the "worst-case scenario" has the storms distributed throughout the 160-year period. While the dunes in the "best-case scenario" remain small or non-existent during the storm cluster, there is considerable time after the storms for sediment to return from offshore and alongshore sources and dune-building vegetation to re-establish, allowing the dune to return to its pre-storm height. In the "worst-case scenario," erosion and washover are more frequent and dune recovery is interrupted, leading to smaller average dune heights. As previously noted, the threshold for storm surge to exceed the dune crest elevation is lower when the dune is relatively small and potentially discontinuous during recovery. As a consequence, there

is a greater potential for washover during subsequent storms and a loss of the recovered sediment to be moved landward and made unavailable for further recovery. This is consistent with the observations of Houser and Hamilton (2009) following the clustering of Hurricanes Ivan, Dennis, and Katrina. In contrast, distributed storms continually reset dune recovery, thereby maintaining small, discontinuous dunes and, possibly, promoting colonization by vegetation that is ineffective at dune building (see Wolner et al. 2013). The dunes with the slower rate of recovery are most sensitive to a change in storm sequencing that may result from intensification of atmospheric teleconnections including ENSO and AMO (Park et al. 2010). Similarly, Duran Vinent and Moore (2015) found that islands tend to be high in elevation (i.e., large continuous dunes) when the biophysical processes driving dune recovery dominate. As storm frequency increases, islands can enter a low-elevation state (characterized by small, discontinuous dunes) that makes the island susceptible to erosion and washover during relatively mild storm conditions. While the recovery curves presented in Fig. 9 are consistent with previous modeling efforts and field studies, further studies are required to determine if dunes recover in similar ways at other locations.

4.3 Alongshore Variability and Lateral Erosion

As noted and shown in Figs. 4 and 7, the foredune is not uniform and can exhibit considerable variability, in height, volume, and alongshore extent as a result of variations in overwash history, sediment supply, transport potential, and anthropogenic forcing (see Thieler and Young 1991; Hesp 2002; Houser et al. 2008a, b; Houser and Mathew 2011; Houser et al. 2012). Variations in the duneline can occur over alongshore length scales tens of meters to several kilometers (see Wetzell 2003; Houser et al. 2008a, b), with the susceptibility of the island to washover correlated to the variations in dune height and volume (Cleary and Hosier 1979). The dependency of recovery mechanisms on the pre-storm dune height and storm impact scale suggests that response and recovery are reinforced processes once alongshore variations in dune height first develop (Weymer et al. 2015). Modeling results suggest that small variations in the height of an otherwise alongshore uniform foredune act as overwash conduits and are unstable, leading to a more variable duneline that is more susceptible to change by subsequent storms (Houser 2013; Duran Vinent and Moore 2015). The vertical erosion of the gaps in the duneline is limited and eventually replaced by a lateral expansion that erodes adjacent dunes (Fig. 10). In this respect, the response of a barrier island to an increase in sea level and/or an increase in storm activity is not only influenced by variations in dune height, but also by the alongshore continuity of dunes. The increase in height variability along the duneline may be a type of "*flickering*" (or increased variability) observed to occur with changes in climate (see Grootes et al. 2002) and may be diagnostic of a weakening of the role of the dune as a resistor to sea level rise and suggests that an island may experience rapid transgression in the future. Not only does an increase in prevalence of

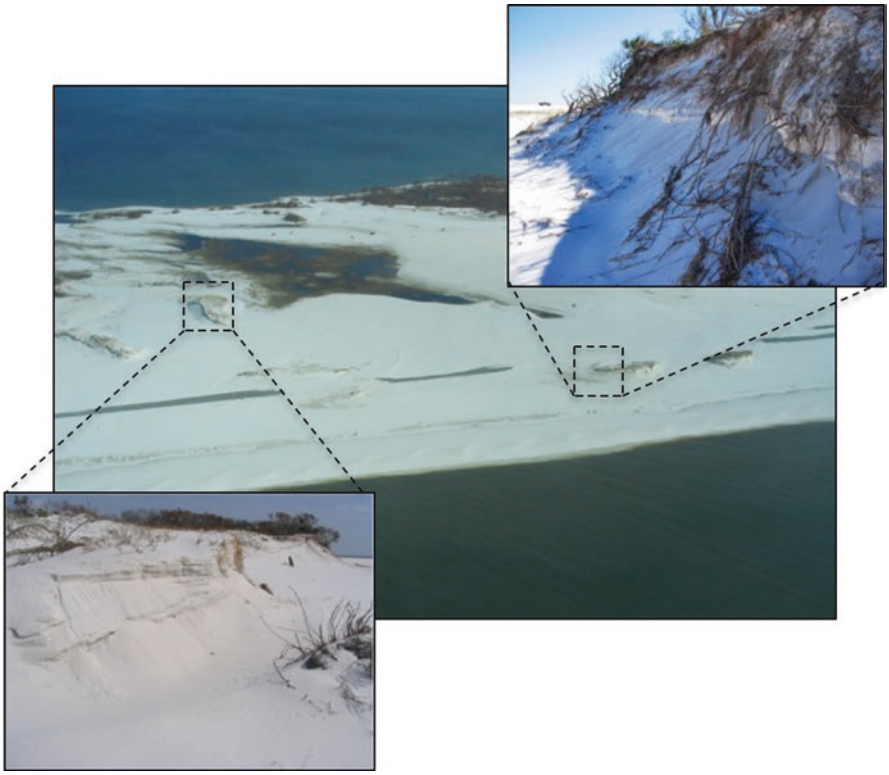

Fig. 10 Lateral (or alongshore) erosion of dunes by washover on Santa Rosa Island that persisted during Hurricane Ivan

washover conduits lead to an increase in washover, associated lateral erosion leads to an overall decrease in island elevation and an increase in the potential for washover to extend along the island. Further study is required to determine whether alongshore variability in the height of the dune line (spatial flickering) is in fact diagnostic of a barrier island system moving to a new equilibrium state susceptible to rapid transgression.

5 Anthropogenic Impact to Dune Recovery

Alterations to island morphology (specifically dune height and extent) can reinforce and even amplify, to varying degrees, the vulnerability of a barrier island, and commercial and residential development, to storm waves and surge (Nordstrom 2000), through changes in the aeolian transport potential, sediment supply, and vegetation cover. For example, damage to County Road 399 along Santa Rosa Island was highly variable alongshore after Hurricane Ivan (2004), ranging from areas

Fig. 11 Damage to road on Santa Rosa Island following Hurricane Ivan. Damage to the road was extensive in the narrow sections of the island (between headlands) leading to a lag of shell, gravel, and asphalt that further limited dune recovery (Houser 2009)

exhibiting little or no damage in the widest sections of the island (landward of the transverse ridges) to areas where the road was completely breached in the narrowest sections of the island (Houser 2009). The road was largely passable following Hurricane Ivan and was rebuilt just before Hurricane Dennis made landfall. Damage to the road in the narrow sections of the island resulted in a lag deposit of shell, gravel, and asphalt (Fig. 11) that further limited aeolian transport and the recovery of the dunes. Further to the west, a "knickpoint effect" along the access road created a swale that was reinforced when the road surface and debris lag were removed, leading to a discontinuity in aeolian transport from the beach to the recovering dunes (Houser et al. 2008a, b). Despite the persistence of vegetation on the dune, aeolian transport was not saturated and the gradients in transport were more

reflective of the expanding fetch and topographic acceleration then by drag imposed on the wind by the vegetation, which would have otherwise led to deposition of sand. As a consequence, the vegetation was heavily abraded by the sediment in transport and the dune began to erode.

Recent evidence suggests that driving on the beach can also affect the height and extent of the foredune. Driving on the backshore and on the dune can seriously impact vegetation cover and only 70–105 vehicle passes are required to completely eliminate vegetation (Brodhead and Godfrey 1979). Roots and rhizomes that were not destroyed took upwards of 8 years to grow into plants with the same biomass as a control group unaffected by vehicles. The inability for the vegetation to recover from the effects of vehicular traffic has been a problem at Assateague Island National Seashore (south of where the Ocean City Inlet has an influence on the island), where driving was previously permitted within designated areas of the beach, but not on the backshore and dune. However, erosion of the beach, backshore, and dune during storms has led to the road being placed farther landward in some locations (pre-storm backshore), which limits the ability of vegetation in those areas to recover (Houser et al. 2012). Combined with compaction of the beachface and backshore, driving at Assateague Island National Seashore has resulted in dune toe and crest elevations that are significantly lower than adjacent areas where driving is not permitted. A similar impact has been observed at Padre Island National Seashore where the beachface is legally recognized as a state highway. Driving on the beach has resulted in considerably lower dune toe and crest elevations through compaction of the beach, which has increased the frequency of dune scarping and resulted in the development of blowouts (Jewell et al. 2014; Fig. 12). The blowouts have resulted in a loss of sediment volume from the beach and dune system and an increase in the variability of the dune line. As a consequence, the driving section of the island is more susceptible to sea level rise and/or an increase in storm activity.

By completely removing plant and the root systems, sand mining impacts vegetation and dune recovery even more seriously than vehicle traffic. Partridge (1992) found that vegetation had not returned to a previously mined community, even 40 years after the disturbance. Anthropogenic impacts to dune recovery also arise from the emplacement of jetties and groins that limit (or resist) the transport of sediment alongshore. This is evident at Assateague Island, where the emplacement of a jetty downdrift from Ocean City, MD in 1935 has significantly limited the availability of sediment provided by alongshore sediment transport, resulting in the rapid transgression of the northern part of the island (Leatherman 1976). Specifically, the lack of sediment has limited post-storm recovery and reinforced a low island state, prompting recession at rates ranging from 11 to 12.2 m $year^{-1}$ (Thornberry-Ehrlich 2005). Similarly, Morton et al. (1994) noted that recovery at Galveston Island was limited in those areas where alongshore sediment supply was interrupted by a groin or a jetty.

Fig. 12 Blowout through the foredune at Padre Island National Seashore resulting from increased scarping with driving on the beach leading to a loss of dune volume and a reduction in dune crest elevation

6 Summary

Barrier islands are considered to be resilient if they are able to maintain elevation and morphology as they migrate landward through the landward redistribution of sediment during storms capable of overwashing or breaching the dunes, or through aeolian transport and blowouts where the dunes are regularly scarped. In this chapter, we provided a review of recent fieldwork that examined the role of the foredune in controlling barrier island transgression with sea level rise. We argue that the foredune is analogous to a variable resistor in an electrical circuit such that the rate of transgression is greater for islands of low elevation (analogous to a weak resistor) and the rate of transgression is lower for islands with large dunes (analogous to strong resistor). The strength of the resistor is determined by the ability of foredunes to develop in both height and extent, which is, in turn, dependent on the availability of sediment from the recovery of the nearshore beach, the aeolian transport potential from beach to dune, and the distribution and density of dune-building vegetation. In this respect, the height, volume, and extent of the dune and its ability to act as a resistor to island transgression are reinforced by a complex eco-geomorphic feedback that appears to be sensitive to the preexisting morphology of the barrier

island, changes in the frequency and/or magnitude of storm events, and the sequencing of those storms. An increase in alongshore variability of the height of the dune line (suggested in this review as a possible example of spatial flickering) may be an early warning that an island is about to transition to a new equilibrium low-elevation state characterized by rapid transgression. Further study is required to understand how the relatively small-scale behavior of the foredune affects and is affected by island transgression over much longer timescales and how the dune behaves as a variable resistor responsible for island resiliency as it transgresses. While the field results are consistent with recent modeling efforts (see Duran and Moore 2013; Duran Vinent and Moore 2015; Moore et al. this volume), there is a need to examine how the results from Padre Island in Texas, Santa Rosa Island in Florida, and Assateague Island in Virginia examined in this study are applicable to other barrier islands, and if the behaviors and relationships are consistent through time with changes in climate, anthropogenic forcing, and changes in storm frequency and magnitude.

References

Aagaard T, Nielsen J, Davidson-Arnott R, Greenwood B, Nielsen N (1998) Coastal morphodynamics at Skallingen, SW Denmark: high-energy conditions. Dan J Geogr 98:20–30

Aagaard T, Davidson-Arnott RGD, Greenwood B, Nielsen J (2004) Sediment supply from shoreface to dunes-linking sediment transport measurements and long term morphological evolution. Geomorphology 60:205–224

Aagaard T, Hughes M, Møller-Sørensen R, Andersen S (2006) Hydrodynamics and sediment fluxes across an onshore migrating intertidal bar. J Coast Res 22:247–259

Aagaard T, Orford J, Murray A (2007) Environmental controls on coastal dune formation; Skallingen Spit, Denmark. Geomorphology:29–47

Amsberry L, Baker MA, Ewanchuk PJ, Bertness MD (2000) Clonal integration and the expansion of Phragmites australis. Ecol Appl 10:1110–1118

Anthony EJ, Ruz MH, Vanhee S (2006) Morphodynamics of intertidal bars on a megatidal beach, Merlimont, northern France. Mar Geol 208:73–100

Arbogast AF, Hansen E, Van Oort M (2002) Reconstructing the geomorphic evolution of large coastal dunes along the southeastern shore of Lake Michigan. Geomorphology:241–255

Arbogast AF, Schaetzl RJ, Hupy JP, Hansen EC (2004) The Holland Paleosol aninformal pedostratigraphic unit in the coastal dunes of southeastern Lake Michigan. Can J Earth Sci 14:1385–1400

Ashton AD, Lorenzo-Trueba J (2018) Morphodynamics of barrier response to sea-level rise. In: Moore LJ, Murray AB (eds) Barrier dynamics and response to changing climate. Springer, New York

Bauer BO, Davidson-Arnott RGD (2003) A general framework for modeling sediment supply to coastal dunes including wind angle, beach geometry, and fetch effects. Geomorphology 49:89–108

Bauer BO, Davidson-Arnott RGD, Nordstrom KF, Ollerhead J, Jackson NL (1996) Indeterminacy in eolian sediment transport across beaches. J Coast Res 12:641–653

Bauer BO, Davidson-Arnott RGD, Hesp PA, Namikas SL, Ollerhead J, Walker IJ (2009) Aeolian sediment transport on a beach: surface moisture, wind fetch, and mean transport. Geomorphology 105(1):106–116

Brodhead JM, Godfrey PJ (1979) The effects of off-road vehicles on coastal dune vegetation in the Province Lands, Cape Cod National Seashore. Massachusetts, Environmental Institute

Browder AG, McNinch JE (2006) Linking framework geology and nearshore morphology: correlation of paleo-channels with shore-oblique sandbars and gravel outcrops. Mar Geol 231:141–162

Butt T, Russell P, Puleo J, Miles J, Masselink G (2004) The influence of bore turbulence on sediment transport in the swash and inner surf zones. Cont Shelf Res 24:757–771

Christiansen MB, Davidson-Arnott R (2004) Rates of landward sand transport over the foredune at Skallingen, Denmark and the role of dune ramp. Dan J Geogr 104:31–43

Clarke M, Rendell H, Tastet J, Clave B, Masse L (2002) Late-Holocene sand invasion and North Atlantic storminess along the Aquitaine coast, southwest France. Holocene:231–238

Cleary WJ, Hosier PE (1979) Geomorphology, washover history, and inlet zonation: Cape Lookout, NC to Bird Island, NC. In: Letherman SP (ed) Barrier islands—from the Gulf of St. Lawrence to the Gulf of Mexico. Academic, New York

Clemmensen LB, Murray A (2006) The termination of the lastmajor phase of aeolian sand movement, coastal dunefields, Denmark. Earth Surf Process Landf 31:795–808

Clemmensen L, Pye K, Murray A, Heinemeier J (2001) Sedimentology, stratigraphy and landscape evolution of a Holocene coastal dune system, Lodbjerg, NW Jutland, Denmark. Sedimentology 48:3–27

Davidson-Arnott RGD (1988) Temporal and spatial controls on beach–dune interaction, Long Point, Lake Erie. In: Psuty NP (ed) Journal of Coastal Research Special Issue, vol 3. C.E.R.F, Florida, pp 131–136

Davidson-Arnott RG, Law MN (1996) Measurement and prediction of long-term sediment supply to coastal foredunes. J Coast Res 12:654–663

Davidson-Arnott R (2005) Conceptual model of the effects of sea level rise on sand coasts. J Coast Res 21:1166–1172

Davidson-Arnott RGD, Law MN (1990) Seasonal patterns and controls on sediment supply to coastal foredunes, Long Point, Lake Erie. In: Nordstrom K, Psuty N, Carter RWG (eds) Coastal dunes: processes and geomorphology. Wiley, New York, pp 177–200

Davidson-Arnott RGD, Law MN (1996) Measurement and prediction of long-term sediment supply to Coastal Foredunes. J Coast Res 12:654–663

Davidson-Arnott RGD, van Heyningen A (2003) Migration and sedimentology of longshore sandwaves, Long Point, Lake Erie, Canada. Sedimentology 50:1123–1137

Davidson-Arnott RGD, MacQuarrie K, Aagaard T (2005) The effect of wind gusts, moisture content and fetch length on sand transport on a beach. Geomorphology 68:115–129

Davidson-Arnott RG, Yang Y, Ollerhead J, Hesp PA, Walker IJ (2008) The effects of surface moisture on aeolian sediment transport threshold and mass flux on a beach. Earth Surf Process Landf 33(1):55

Dawson S, Smith E, Jordan J, Dawson AG (2004) Late Holocene coastal sand movements in the Outer Hebrides, N.W. Scotland. Mar Geol 210:281–306

Delgado-Fernandez I, Davidson-Arnott R (2011) Meso-scale aeolian sediment input to coastal dunes: the nature of aeolian transport events. Geomorphology 126:217–232

Duran O, Moore LJ (2013) Vegetation controls on the maximum size of coastal dunes. Proc Natl Acad Sci U S A 110:17217–17222

Duran Vinent OD, Moore LJ (2015) Barrier island bistability induced by biophysical interactions. Nature Climate Change *5*(2):158–162

Eamer JBR, Walker IJ (2010) Quantifying sand storage capacity of large woody debris on beaches using LiDAR. Geomorphology 118:33–47

Elgar S, Gallagher EL, Guza RT (2001) Nearshore sandbar migration. J Geophys Res 106:11623–11627

Feagin RA, Wu XB (2007) The spatial patterns of functional groups and successional direction in a coastal dune community. Rangel Ecol Manage 60:417–425

FitzGerald DM, Buynevich IV, Fenster MS, McKinlay PA (2000) Sand dynamics at the mouth of a rock-bound, tide-dominated estuary. Sedimentary Geology 131:25–29

Godfrey PJ, Godfrey MM (1973) Comparison of ecological and geomorphic interactions between altered and unaltered barrier island systems in North Carolina, Coastal Geomorphology. State University, New York, pp 239–257
Gornish ES, Miller TE (2010) Effects of storm frequency on dune vegetation. Glob Chang Biol 16:2668–2675
Grootes PA, White JWC, Barlow LK (2002) The 'flickering switch' of late Pleistocene climate change. Clim Change Nat Clim Change Proxy-Climate Data 3:119
Hammond B (2015) Rate of post-Hurricane Barrier Island recovery. MSc thesis, Texas A&M University, 85 pp
Hansen EC, Fisher TG, Arbogast AF, Bateman M (2010) Geomorphic history of low perched, transgressive dune groups along the southeastern shore of Lake Michigan. J Aeolian Res 1:111–127
Hequette A, Ruz M (1991) Spit and barrier island migration in the southeastern Canadian Beaufort Sea. J Coast Res 7:677–698
Hesp PA (1988) Surfzone, beach and foredune interactions on the Australian southeast coast. J Coast Res Spec Issue 3:15–25
Hesp PA (2002) Foredunes and blowouts: initiation, geomorphology and dynamics. Geomorphology 48:245–268
Hesp PA, Davidson-Arnott R, Walker I, Ollerhead J (2005) Flow dynamics over a foredune at Prince Edward Island, Canada. Geomorphology 65(1-2):71–84
Hewett DG (1970) The colonization of sand dunes after stabilization with marram grass (Ammophila arenaria). J Ecol 58:653–668
Honeycutt MG, Krantz DE (2003) Influence of the geologic framework on spatial variability in long-term shoreline change, Cape Henlopen to Rehoboth Beach, Delaware. J Coast Res 38:147–167
Hosier PE, Cleary WJ (1977) Cyclic geomorphic patterns of washover on a barrier island in southeastern North Carolina. Environ Geol 2:23–31
Houser C (2009) Synchronization of transport and supply in beach-dune interaction. Prog Phys Geogr 33:733–746
Houser C (2012) Feedback between ridge and swale bathymetry and barrier island storm response and transgression. Geomorphology 173/174:1–16
Houser C (2013) Alongshore variation in beach-dune morphology: implications for barrier island response. Geomorphology 199:48–61
Houser C, Barrett G (2010) Divergent behavior of the swash zone in response to different foreshore slopes and nearshore states. Mar Geol 271(1):106–118
Houser C, Ellis J (2013) Beach and dune interaction. Treat Geomorphol 10:267–288
Houser C, Greenwood B (2005) Profile response of a lacustrine multiple-barred nearshore to a sequence of storm events. Geomorphology 69:118–137
Houser C, Greenwood B (2007) Onshore migration of a swash bar. J Coast Res 23:1–14
Houser C, Hamilton S (2009) Sensitivity of post-hurricane beach and dune recovery to event frequency. Earth Surf Process Landf 34:613–628
Houser C, Mathew S (2011) Variability in foredune height depends on the alongshore correspondence of transport potential and sediment supply. Geomorphology 125:62–72
Houser C, Greenwood B, Aagaard T (2006) Divergent response of an intertidal swash bar. Earth Surf Process Landf 31:1775–1791
Houser C, Hapke C, Hamilton S (2008a) Controls on coastal dune morphology, shoreline erosion and barrier island response to extreme storms. Geomorphology 100:223–240
Houser C, Hobbs C, Saari B (2008b) Post-hurricane airflow and sediment transport over a recovering dune. J Coast Res 24:944–953
Houser C, Labude B, Haider L, Weymer B (2012) Impacts of driving on the beach: case studies from Assateague Island and Padre Island National Seashores. Ocean Coast Manag 71:33–45
Houser C, Arnott R, Ulzhöfer S, Barrett G (2013) Nearshore circulation over transverse bar and rip morphology with oblique wave forcing. Earth Surf Process Landf 38:1269–1279

Houser C, Wernette P, Rentschlar E, Jones H, Hammond B, Trimble S (2015) Post-storm beach and dune recovery: implications for barrier island resilience. Geomorphology 234:54–63
Hsu SA (1977) Boundary-layer meteorological research in the coastal zone. In: Walker HJ (ed) Geoscience and man. School of Geoscience, LSU, Baton Rouge, pp 99–111
Hugenholtz C, Wolfe S (2005) Biogeomorphic model of dunefield activation and stabilization on the northern Great Plains. Geomorphology 70:53–70
Hughes MG, Masselink G, Brander RW (1997) Flow velocity and sediment transport in the swash zone of a steep beach. Mar Geol 138:91–103
Iversen JD, Rasmussen KR (1999) The effect of wind speed and bed slope on sand transport. Sedimentology 46:723–731
Jackson NL, Nordstrom KF (1997) Effects of time-dependent moisture content of surface sediments on aeolian transport rates across a beach, Wildwood, New Jersey, USA. Earth Surf Process Landf 22:611–621
Jackson NL, Masselink G, Nordstrom KF (2004) The role of bore collapse and local shear stresses on the spatial distribution of sediment load in the uprush of an intermediate-state beach. Mar Geol 203:109–118
Jennings JN (1964) The question of coastal dunes in tropical humid climates. Z GEomorphol Sondehelt NF 8:150–154
Jewell M, Houser C, Trimble S (2014) Initiation and evolution of blowouts within Padre Island National Seashore. Ocean Coast Manag 95:156–164
Kaimal JC, Finnigan JJ (1994) Atmospheric boundary layer flows: their structure and measurement. Oxford University, New York. 289 pp
Keijsers JGS, Poortinga A, Riksen MJPM, Groot de AV (2012) Connecting aeolian sediment transport with foredune development. In: NCK-days 2012: crossing borders in coastal research, 13 March 2012–16 March 2012, Enschede, the Netherlands.
Kent M, Owen NW, Dale P, Newnham RM, Giles TM (2001) Studies of vegetation burial: a focus for biogeography and biogeomorphology? Prog Phys Geogr 25:455–482
Klijn JA (1990) The younger dunes in the Netherlands; chronology and causation. Catena Suppl 18:89–100
Lapinskis J (2005) Long-term fluctuations in the volume of beach and foredune deposits along the coast of Latvia. Baltica 18:38–43
Larson M, Erikson L, Hanson H (2004) An analytical model to predict dune erosion due to wave impact. Coast Eng 51(8):675–696
Law MN, Davidson-Arnott RGD (1990) Seasonal controls on aeolian processes on the beach and foredune. In: Proc. symposium on coastal sand dunes. NRC, Ottawa, pp 49–67
Lazarus E, Ashton A, Murray AB, Tebbens S, Burroughs S (2011) Cumulative versus transient shoreline change: dependencies on temporal and spatial scale. J Geophys Res 116:F02014. https://doi.org/10.1029/2009JF001611
Leatherman SP (1976) Barrier island dynamics: overwash processes and solian transport. In: Coastal engineering proceedings.
Lee G, Nicholls RJ, Birkemeier WA (1998) Storm-driven variability of the beach-nearshore profile at Duck, North Carolina, USA, 1981-1991. Mar Geol 148:163–177
Lentz EE, Hapke CJ (2011) Geologic framework influences on the geomorphology of an anthropogenically modified barrier island: assessment of dune/beach changes at Fire Island, New York. Geomorphology 126:82–96
Leys JF, Eldridge DJ (1998) Influence of cryptogamic crust disturbance to wind erosion on sand and loam rangeland soils. Earth Surf Process Landf 23:963–974
Lippmann TC, Holman RA (1990) The spatial and temporal variability of sand bar morphology. J Geophys Res 95:11,575–11,590
Loope W, Arbogast A (2000) Dominance of a ~150-year cycle of sand-supply change in late Holocene dune building along the eastern shore of Lake Michigan. Quatern Res 54(3):414–422
Lorenzo-Trueba J, Ashton AD (2014) Rollover, drowning, and discontinuous retreat: distinct modes of barrier response to sea-level rise produced by a simple morphodynamic model. Case Rep Med 119:779–801. https://doi.org/10.1002/2013JF002941

Masetti R, Fagherazzi S, Montanari A (2008) Application of a barrier island translation model to the millennial-scale evolution of Sand Key, Florida. Cont Shelf Res 28:1116–1126
Matthews JA, Briffa KR (2005) The 'Little Ice Age': reevaluation of an evolving concept. Geogr Ann 87A:17–36
Maun MA (1996) The effects of burial by sand on survival and growth of Calamovilfa longifolia. Ecoscience 3(1):93–100
Maun M (1998) Adaptations of plants to burial in coastal sand dunes. Can J Bot 76(5):713–738
Maun MA (2004) Burial of plants as a selective force in sand dunes. In: Martínez ML, Psuty NP (eds) Coastal dunes: ecology and conservation ecological studies, vol 171. Springer, Berlin, pp 119–135
McKenna Neuman C (2003) Effects of temperature and humidity upon the entrainment of sedimentary particles by wind. Bound Layer Meteorol 108:61–89
McNinch JE (2004) Geologic control in the nearshore: shore-oblique sandbars and shoreline erosional hotspots, Mid-Atlantic Bight, USA. Mar Geol 211:121–141
Miller TE, Gornish ES, Buckley HL (2010) Climate and coastal dune vegetation: disturbance, recovery and succession. Plant Ecol 206:97–104
Moore LJ, Goldstein EB, Vinent OD, Walters D, Kirwan M, Rebecca L, Brad Murray A, Ruggiero P (2018) The role of ecomorphodynamic feedbacks and landscape couplings in influencing the response of barriers to changing climate. In: Moore LJ, Murray AB (eds) Barrier dynamics and response to changing climate. Springer, New York
Moreno-Casasola P (1986) Sand movement as a factor in the distribution of plant communities in a coastal dune system. Vegetation 65:67–76
Morton RA (2002) Factors controlling storm impacts on coastal barriers and beaches—a preliminary basis for near real-time forecasting. J Coast Res 18:486–501
Morton RA, Paine JG, Gibeaut JC (1994) Stages and durations of post-storm beach recovery, southeastern Texas coast. J Coast Res 10:884–908
Murray AB, Moore LJ (2018) Geometric constraints on long-term barrier migration: from simple to surprising. In: Moore LJ, Murray AB (eds) Barrier dynamics and response to changing climate. Springer, New York
Namikas SL, Sherman DJ (1995) A review of the effects of surface moisture content on aeolian sand transport. In: Tchakerian VP (ed) Desert aeolian processes. Chapman & Hall, London, pp 269–293
Nickling WG, Davidson-Arnott RGD (1990) Aeolian sediment transport on beaches and coastal dunes. In: Proceedings symposium on coastal sand dunes. NRC, Ottawa, pp 1–35
Nickling WG, Wolfe SA (1994) The morphology and origin of nabkhas, region of Mopti, Mali, West Africa. J Arid Environ 28:13–30
Nordstrom KF (2000) Beaches and dunes of developed coasts. Cambridge University Press, Cambridge. 356 pp
Nott J (2006) Tropical cyclones and the evolution of the sedimentary coast of Northern Australia. J Coast Res 22:49–62
Odezulu CI, Lorenzo-Trueba J, Wallace DJ, Anderson JB (2018) Follets Island: a case of unprecedented change and transition from rollover to subaqueous shoals. In: Moore LJ, Murray AB (eds) Barrier dynamics and response to changing climate. Springer, New York
Ollerhead J, Davidson-Arnott R, Walker IJ, Mathew S (2013) Annual to decadal morphodynamics of the foredune system at Greenwich Dunes, Prince Edward Island, Canada. Earth Surf Process Landf 38:284–298
Olson JS (1958) Lake Michigan dune development 3: lake level, beach and dune oscillations. J Geol 66:473–483
Orford J, Cooper J, Jackson D, Malvarez G, White D (1999) Extreme storms end thresholds on foredune stripping at Inch Spit, South-West Ireland. In: Proceedings of coastal sediments '99, pp 1852–1866
Park J, Obeysekera J, Irizarry-Ortiz M, Barnes J, Park-Said W (2010) Climate links and variability of extreme sea-level events at Key West, Pensacola, and Mayport, Florida. J Waterw Port Coast Ocean Eng 136:350–356

Partridge TR (1992) Vegetation recovery following sand mining on coastal dunes at Kaitorete Spit, Canterbury, New Zealand. Biol Conserv 61:59–71
Pilkey OH, Stutz M (2000) Seawalls and sandbags: geotimes, p 26–27
Pritchard D, Hogg AJ (2005) On the transport of suspended sediment by a swash event on a plane beach. Coast Eng 52:1–23
Psuty NP (1992) Spatial variation in coastal fordune development. In: Carter RWG, Curtis TGF, Sheehy-Skeffington MJ (eds) Coastal dunes: geomorphology, ecology and management for conservation. Rotterdam, Balkema, pp 3–13
Pye K (1982) Morphological development of coastal dunes in a humid tropical environment, Cape Bedford and Cape Flattery. North Queensland. Geogr Ann A 64:213–227
Pye K (1983) Dune formation on the humid tropical sector of the North Queensland Coast, Australia. Earth Surf Process Landf 8(4):371–381
Pye K (1990) Physical and human influences on coastal dune development between the Ribble and Mersey estuaries, northwest England. In: Nordstrom KF, Psuty NP, Carter RWG (eds) Coastal dunes: form and process. Wiley, Chichester, pp 339–359
Pye K, Neal A (1993) Late Holocene dune formation on the Sefton Coast, Northwest England. Dyn Environ Context Aeolian Sediment Syst:201–217
Ranwell DS (1958) Movement of vegetated sand dunes at Newborough Warren, Anglesey. J Ecol 46:83–100
Rentschlar E (2014) Quantifying vegetation recovery on Santa Rosa Island. MSc thesis. Department of Geography, Texas A&M University, 105 pp
Rice MA, McEwan IK (2001) Crust strength: a wind tunnel study of the effect of impact by saltating particles on cohesive soil surfaces. Earth Surf Process Landf 26:721–733
Riggs SR, Cleary WJ, Snyder SW (1995) Influence of inherited geologic framework on barrier shoreface morphology and dynamics. Mar Geol 126:213–234
Ritchie W (1972) The evolution of coastal sand dunes. The Scottish Geographical Magazine 88:19–35
Rodriguez AB, Yu W, Theuerkauf EJ (2018) Abrupt increase in washover deposition along a transgressive barrier island during the late 19th century acceleration in sea-level rise. In: Moore LJ, Murray AB (eds) Barrier dynamics and response to changing climate. Springer, New York
Ruessink BG, Jeuken MCJL (2002) Dunefoot dynamics along the Dutch coast. Earth Surf Process Landf 27:1043–1056
Ruessink BG, Kroon A (1994) The behaviour of a multiple bar system in the nearshore zone of Tershelling, the Netherlands: 1965-1993. Mar Geol 121:187–197
Ruggiero P, Hacker S, Seabloom E, Zarnetske P (2018) The role of vegetation in determining dune morphology, exposure to sea-level rise, and storm-induced coastal hazards: a U.S. Pacific Northwest perspective. In: Moore LJ, Murray AB (eds) Barrier dynamics and response to changing climate. Springer, New York
Ruz MH, Meur-Ferec C (2004) Influence of high water levels on aeolian sand transport: upper beach/dune evolution on a macrotidal coast, Wissant Bay, northern France. Geomorphology 60:73–87
Saari BR (2015) Post-hurricane interactions between vegetation dynamics, dune recovery and physical gradients on barrier islands. MSc thesis, Department of Environmental Studies, University of West Florida, pp 71
Sallenger AH (2000) Storm impact scale for barrier islands. J Coast Res 16:890–895
Saunders KE, Davidson-Arnott RGD (1990) Coastal dune response to natural disturbances. In: Proc. symposium on coastal sand dunes. NRC, Ottawa, pp 321–345
Schwab WC, Thieler ER, Allen JR, Foster DS, Swift BA, Denny JF (2000) Influence of inner-continental shelf geologic framework on the evolution and behavior of the barrier-island system between Fire Island inlet and Shinnecock Inlet, Long Island, New York. J Coast Res 16:408–422
Shand RD (2003) Relationships between episodes of bar switching, cross-shore bar migration and outer bar degeneration at Wanganui, New Zealand. J Coast Res 19:157–170

Sherman DJ, Jackson DWT, Namikas SL, Jinkang W (1998) Wind-blown sand on beaches: an evaluation of models. Geomorphology 22:113–133
Short A, Hesp PA (1982) Wave–beach–dune interaction in southeast Australia. Mar Geol 48:259–284
Snyder R, Boss C (2002) Recovery and stability in barrier island plant communities. J Coast Res 18:530–536
Stallins JA, Parker AJ (2003) The influence of complex systems interactions on barrier island dune vegetation pattern and process. Ann Assoc Am Geographers 93:13–29
Stewart CJ, Davidson-Arnott RGD (1988) Morphology, formation and migration of longshore sandwaves; Long Point, Lake Erie. Can Mar Geol 81:63–77
Storms JEA, Weltje GJ, van Dijke JJ, Geel CR, Kroonenberg SB (2002) Process-response modeling of wave-dominated coastal systems: simulating evolution and stratigraphy on geological timescales. J Sediment Res 7:226–239
Stutz ML, Pilkey OH (2011) Open-ocean barrier islands: global influence of climatic, oceanographic, and depositional settings. J Coast Res 27(2):207–222
Swift JP (1976) Coastal sedimentation. In: Stanley DJ, Swift DJP (eds) Marine sediment transport and environmental management. Wiley, New York, pp 255–310
Sykes MT, Wilson JB (1990) An experimental investigation into the response of New Zealand sand dune species to different depths of burial by sand. Acta Bot Neerl 39:171–181
Thieler ER, Young RS (1991) Quantitative evaluation of coastal geomorphological changes in South Carolina after Hurricane Hugo. J Coast Res 8:187–200
Thornberry-Ehrlich TL (2005) Assateague Island National Seashore Geologic Resource Managment Issues Scoping Summary. National Park Service, 25p
Timmons EA, Rodriguez AB, Mattheus CR, DeWitt R (2010) Transition of a regressive to a transgressive barrier island due to back-barrier erosion, increased storminess, and low sediment supply: Bogue Banks, North Carolina, USA. Mar Geol 278(1):100–114
Van der Valk AG (1974) Environmental factors controlling the distribution of forbs on foredunes in Cape Hatteras National Seashore. Can J Bot 52:1057–1073
Verhulst PF (1838) Notice sur la loi que la population suit dans son accroissement. Corresp Math Phys Publ Que 10:113–121
Walker I, Barrie J (2006) Geomorphology and sea-level rise on one of Canada's most sensitive coasts: Northeast Graham Island, British Columbia. J Coast Res 31:220–226
Wetzell LM (2003) Simple models for predicting dune erosion hazards along the Outer Banks of North Carolina. MS thesis, University of South Florida
Weymer BA, Houser C, Giardino R (2015) Poststorm evolution of beach-dune morphology: Padre Island National Seashore, Texas. J Coast Res 31:634–644
Wiggs GFS, Baird AJ, Atherton RJ (2004) The dynamic effects of moisture on the entrainment and transport of sand by wind. Geomorphology 59:13–30
Wijnberg KM, Terwindt JHJ (1995) Extracting decadal morphological behavior from high-resolution, long-term bathymetric surveys along the Holland coast using eigenfunction analysis. Mar Geol 126:301–330
Wilson P, Orford JD, Knight J, Braley SM, Wintle AG (2001) Late-Holocene (post-4000yr BP) coastal dune development in North Umberland, northeast England. Holocene 11:215–229
Wilson P, McGourty J, Bateman M (2004) Mid- to late-Holocene coastal dune event stratigraphy for the north coast of Northern Ireland. Holocene 14:406–416
Wolner CWV, Moore LJ, Young DR, Brantley ST, Bissett SN, McBride RA (2013) Ecomorphodhamic feedbacks and barrer island response to disturbance: insights from the Virginia Barrier Islands, Mid-Atlantic Bight, USA. Geomorphology 199:115–128
Woodroffe CD (2007) The natural resilience of coastal systems: primary concepts. In: McFadden L, Penning-Rowsell E, Nicholls RJ (eds) Managing coastal vulnerability. Elsevier, Amsterdam, pp 45–60
Wright LD, Short AD (1984) Morphodynamic variability of surf zones and beaches: a synthesis. Mar Geol 56:93–118

Xu S, Huang W (2008) Frequency analysis for predicting 1% annual maximum water levels along Florida coast, US. Hydrol Process 22:4507–4518

Zarnetske PL, Hacker SD, Seabloom EW, Ruggiero P, Killian JR, Maddux TB, Cox D (2012) Biophysical feedback mediate effects of invasive grasses on coastal dune shape. Ecology 93(6):1439–1450. https://doi.org/10.1890/11-1112.1

Zarnetske PL, Ruggiero P, Seabloom EW, Hacker SD, 2015. Coastal foredune evolution: the relative influence of vegetation and sand supply in the US Pacific Northwest. J R Soc Interface 20150017. https://doi.org/10.1098/rsif.2015.0017

Zhang J, Maun MA (1989) Seed dormancy of Pannicum virgatum L. on the shoreline sand dunes of Lake Erie. Am Midl Nat 122:77–87

Zhang J, Maun M (1992) Effects of burial in sand on the growth and reproduction of Cakile edentula. Ecography 15:296–302

Part II
Mechanisms of Barrier Response to Changing Climate

Geometric Constraints on Long-Term Barrier Migration: From Simple to Surprising

A. Brad Murray and Laura J. Moore

Abstract Considerations of mass conservation, sediment budgets, and geometry lead to insights regarding how barriers respond to sea-level rise. We begin with relatively simple insights, which facilitate more surprising conclusions as more complicated cases are considered. The simplest case assumes: (1) a constant depth beyond which sediment transport is negligible; (2) a lack of gradients in net long-term alongshore sediment flux that add or remove sediment; (3) shoreface erosion into a substrate that produces sediment which is all sufficiently coarse to remain in the nearshore system; and (4) a spatially uniform slope across which a barrier migrates (i.e., the substrate slope). In this case, the migration trajectory for the barrier shorelines—the ratio between the rates of sea-level rise and landward transgression—parallels the average slope of the barrier and shoreface profile (the surface over which active sediment transport occurs). In the next simplest case, substrates composed partly of fine sediment (which is lost to the nearshore system when the substrate is eroded) cause a reduction of the slope of the migration trajectory, because more landward migration is required for each increment of sea-level rise in this case. Gradients in net alongshore sediment transport also cause adjustments to the migration trajectory (although the adjustment depends on the rate of relative sea-level rise). Analysis shows that even with a gradient in net alongshore sediment transport, in the long term, barrier geometry adjusts until the trajectory parallels the (spatially uniform) slope of the substrate. When a barrier is eroding into material that was deposited in back-barrier bay or marsh environments, surprising results come from considerations of geometry and conservation of mass. In this case, the effects of substrate slope on barrier migration trajectory become indirect and time-lagged. In addition, depending on the relative compositions of marsh and bay deposits, feedbacks tend to either produce a stable bay/marsh width and barrier geometry, or a runaway widening or narrowing of the back-barrier environment.

A.B. Murray (✉)
Division of Earth and Ocean Sciences, Nicholas School of the Environment, Center for Nonlinear and Complex Systems, Duke University, Durham, NC, USA
e-mail: abmurray@duke.edu

L.J. Moore
Department of Geological Sciences, University of North Carolina at Chapel Hill, Chapel Hill, NC, USA
e-mail: laura.moore@unc.edu

L.J. Moore, A.B. Murray (eds.), *Barrier Dynamics and Response to Changing Climate*, https://doi.org/10.1007/978-3-319-68086-6_7

When substrate slope (or alongshore-transport gradients or substrate composition) varies as the barrier migrates landward, numerical investigation is required to determine how the migration trajectory varies with time.

Keywords Generalized Bruun Rule • Barrier migration • Substrate slope • Shoreface depth • Equilibrium profile • Overwash • Geometry • Barrier evolution • Shoreline erosion • Numerical modeling • Analytical modeling • Conservation of mass • Barrier response to sea-level rise • Barrier migration trajectory • Back-barrier depth

1 Introduction

We focus in this chapter on narrow barriers that are migrating landward, and the response of these "transgressive" barriers to sea-level rise. We take a long-term view, addressing timescales that are long compared to both the return period of strong storms (i.e., decades to centuries), and possible shifts between alternate "high" and "low" stable states triggered by stochastic storm sequences (Duran Vinent and Moore 2015; Moore et al. this volume). The resulting analyses, arising from the constraints imposed by geometry and the conservation of mass, apply generically, to a range of barrier types, including those composed of sand and those composed of gravel (which we refer to collectively as "coarse" sediment).

Although barriers responding to sea-level rise move vertically as well as horizontally, first consider the horizontal component of barrier migration separately (which could occur in nature where relative sea level is steady, driven by an ongoing loss of sediment). Prolonged shoreline erosion leads to horizontal barrier migration: The shoreline moves landward where storm-driven overwash and/or gradients in wave-driven alongshore sediment transport remove sediment from the beach and shallow seabed (in and near the surf zone; for background information, please see Preface of this volume). When a barrier becomes sufficiently narrow, overwash deposition can extend to the landward edge of the barrier, tending to maintain a minimum barrier width related to the cross-shore extent of the largest overwash events (Leatherman 1979). Thus, in the long term, the open-ocean shoreline and the landward bay-facing shoreline (i.e., landward edge) of a migrating barrier will tend to move landward at the same rate.

Understanding the vertical component of barrier migration in response to sea-level rise requires consideration of sediment transport during storms. Although extreme storms in which water levels "inundate" a barrier can remove sediment (Sallenger 2000; Sallenger et al. 2007), less extreme storm events, which produce "overwash," deposit sediment on the barrier. On balance, in the long term, transgressive barriers can gain elevation as the result of these storm effects. (In addition, sandy barriers can gain elevation through eolian dune growth between overwash events, and the sediment making up the dunes is then redistributed during overwash

events; e.g., Donnelly et al. 2006.) In the absence of relative sea-level rise (RSLR), the elevation of a transgressive barrier will tend to approach a maximum, related to the maximum elevation to which storm waves can move sediment (tide level plus storm surge plus wave set up plus wave run up; Sallenger 2000; Stockdon et al. 2006). Although dune growth can add elevation, dunes are transient features (e.g., Houser et al. this volume; Moore et al. this volume).

If sea level is rising, the processes affecting barrier elevation change, but only slightly. Rising sea level tends to decrease barrier elevation relative to sea level, therefore increasing the frequency of overwash events and overwash deposition rates. Therefore, a negative feedback arises, in which the rate of overwash deposition increases as the RSLR increases. In the long term, this feedback tends to produce a steady state in which the elevation of the barrier increases at the same rate that sea level rises. In this case, relative to sea level (a moving frame of reference), barrier elevation remains constant, at approximately the maximum elevation to which storm waves can move sediment (much as would occur in the absence of RSLR).

For a transgressive barrier that is translating both horizontally and vertically, migration occurs along a slope equal to the ratio of the RSLR rate and the landward migration rate; both the shoreline and the landward edge of the barrier migrate along lines parallel to this slope (Fig. 1). Here, we will address what determines this migration "trajectory"—i.e., how much landward movement (including shoreline erosion) occurs for each increment of RSLR. In Sects. 2 and 3, we introduce background material and provide an intuitive explanation of a broadly applied framework (stemming originally from Bruun 1962) for analyzing how shoreline erosion relates to sea-level rise. Our analysis applies this framework to barrier migration trajectories (an exercise inspired originally by the results of the Shoreface Translation Model; Roy et al. 1994; Cowell et al. 1995). We start with the simplest set of assumptions in Sects. 2 and 3, to review how considerations of mass conservation and the tendency for barrier geometry to remain constant lead to basic insights about the factors that determine how barrier migration changes over time—including the tendency for the trajectory to approach a steady state (Roy et al. 1994; Wolinsky and Murray 2009; Moore et al. 2010). We then consider cases in which the simplifying assumptions are relaxed, leading to further insights, which become progressively more surprising as further complexities are considered. We sequentially introduce factors that influence barrier migration trajectory, and how it evolves over the long term, including: in Sect. 4, the composition of the "substrate" over which the barrier migrates; in Sect. 5, "external" losses or gains of sediment (e.g., from gradients in alongshore transport, or in some cases from onshore sediment flux from a shallow continental shelf; e.g., Cowell and Kinsela this volume); and, in Sect. 6, the cross-shore extent of back-barrier environments such as marshes or shallow bays, and the thickness and composition of the resulting deposits. In this contribution, we also present graphical illustrations of how trajectories evolve (as introduced by Moore et al. 2010), under the assumption that some or all of these factors remain constant. Finally, in Sect. 7, we introduce the need for numerical analyses to address barrier evolution in more complicated, realistic situations.

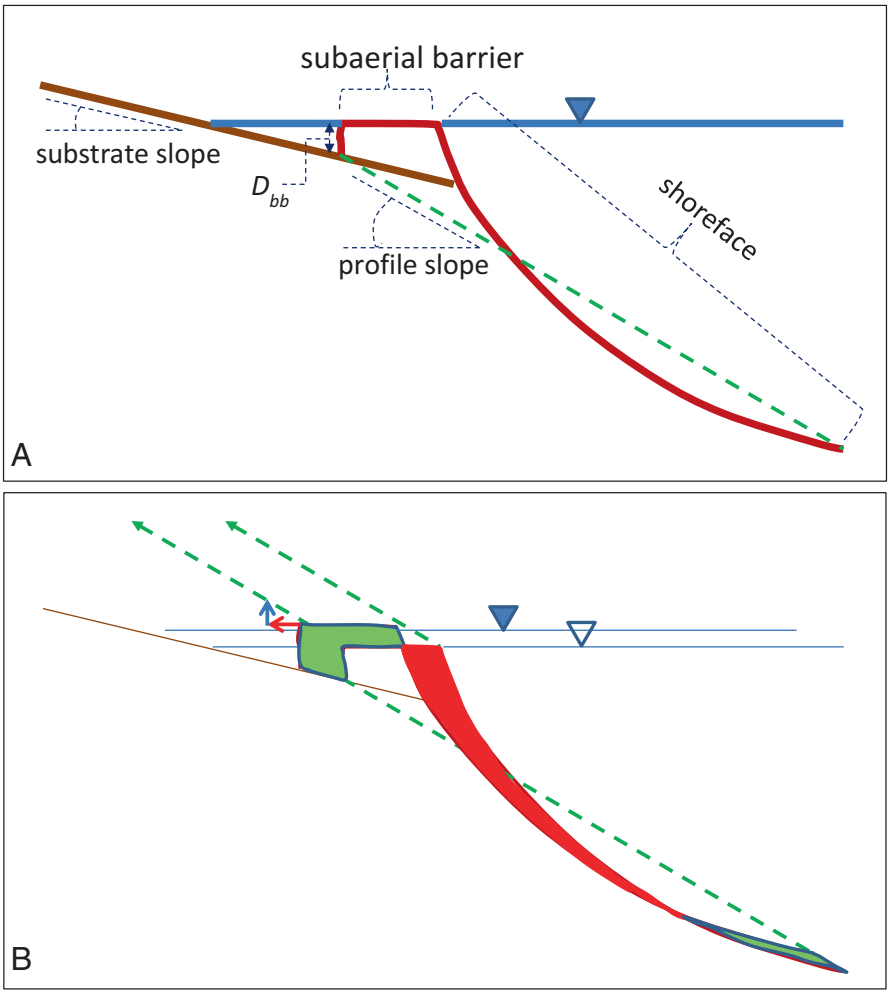

Fig. 1 A transgressive barrier, migrating upward and landward in response to relative sea level rise (RSLR). (**a**) Schematic diagram showing the subaerial barrier and shoreface extents, the substrate and average barrier profile slopes, and the back-barrier depth, D_{bb}. The green dotted line shows the average slope of the active barrier profile. Blue triangle indicates sea level. (**b**) Shows the profile at two different times, before and after the amount of RSLR indicated by the blue horizontal lines and triangles (open triangle indicates sea level at the earlier time). Red area indicates where sediment was made available through shoreface erosion, and the green area shows where deposition occurred. The red arrow shows the amount of horizontal translation—barrier retreat, R—while the solid blue arrow shows the amount of vertical translation, which together define the migration trajectory, along which points on the profile (e.g., the seaward and landward barrier shorelines and shoreface toe) migrate, as shown by the dotted green arrows. Note the vertical exaggeration in this (and subsequent) figures; the cross-shore scale is kilometers, while the vertical scale is tens of meters. (Graphical interpretation of the barrier migration trajectory after Moore et al. 2010)

2 Background

2.1 Cross-shore Shoreface-Barrier Profile

The visible, subaerial portion of a barrier is part of a larger system; it is intimately connected to the nearshore seabed. Wave processes tend, in the long term, to create a characteristic equilibrium cross-shore shoreface profile (extending down to the depth below which waves move little sediment, which is a fuzzy, time-dependent boundary; Preface, this volume; and e.g., Hallermeier 1981; Stive and de Vriend 1995; Ortiz and Ashton 2016). Considered in isolation, nearshore waves tend to sweep coarse sediment toward shore (e.g., Fredsøe and Deigaard 1992), creating a pile of sediment, with gentle slopes extending along the nearshore seabed (Fig. 1) upward to approximately the long-term limit of wave influence—i.e., the top of the barrier (excluding aeolian dune-building processes). The local slopes of the sediment surface tend to adjust, in the long term, to be sufficiently steep to prevent further net onshore sediment transport. These "equilibrium slopes" depend on the strength of wave influence locally (as well as the grain size of the sediment), so that the local equilibrium slopes tend to decrease as the depth increases with distance offshore (e.g., Dean 1977, 1991; Fredsøe and Deigaard 1992). Thus, the equilibrium shoreface profile composed of these equilibrium slopes tends to exhibit a concave-upward shape (Fig. 1). (This heuristic description of the shoreface profile neglects surf zone currents, and the storm-driven temporal fluctuations in the shape of the landward-most portions of the profile; e.g., Lee et al. 1988.)

The subaerial barrier, shaped by storm-driven overwash (and possibly aeolian processes), with a maximum elevation related to the height above sea level to which storm waves can reach, can be thought of as the top portion of the surface of active sediment transport. In what follows, the term "barrier profile" includes both the shoreface and subaerial barrier components of the equilibrium profile (except where otherwise specified). This barrier profile extends from the seaward toe of the shoreface (at the shoreface depth) to the long-term landward extent of overwash deposition (at the bay depth immediately behind the barrier, the back-barrier depth; Fig. 1a).

2.2 Landward Profile Translation and Sediment Excavation

Losses of sediment from the beach, dunes, and surf zone, either from storm-driven overwash or gradients in alongshore sediment transport, can drive prolonged shoreline erosion. This erosion tends to propagate across the entire shoreface, through reductions of the shoreface slopes, which allow waves to sweep sediment onshore (please see the Preface, this volume). Because the tendency for waves to sweep sand onshore extends to the toe of the shoreface over long timescales, the oceanward portion of the barrier profile (the shoreface, beach, and dunes) tends to move landward in unison with the shoreline. Assuming the storm/wave climate remains

approximately constant, and the erosion is sufficiently gradual, the shape of the profile remains approximately constant (maintaining near equilibrium slopes). Each increment of landward translation of the beach, dunes, and shoreface, R, liberates a quantity of sediment (a volume of sediment per unit alongshore length, or an area in cross-shore profile; Fig. 2a). This quantity is equal to $R * H$ (Bruun 1962), where H is the height of the barrier profile (Fig. 2a). This relationship does not depend on the shape of the barrier profile. To understand the lack of dependence on shape, consider first the limiting case of a rectangular shoreface, for which the eroded area is clearly $R * H$ (Fig. 2a). If that area is sliced into thin horizontal slabs, those slabs can be slid horizontally by different amounts to reproduce the area between any shoreface shape and its landward-translated equivalent (Fig. 2b). In other words, as long as the shape remains constant over time, the eroded area = $R * H$. If the material underlying the shoreface—the "substrate"—isn't already mobile sediment, then as erosion exposes that material, physical, chemical, and biological processes tend to weather it into its component pieces (i.e., sand, silt, clay), converting it into transportable sediment. What the substrate is composed of affects the migration trajectory (as we discuss in Sect. 4), but for now we ignore this complication.

If erosion of the profile is associated with a migrating barrier, then some of the sediment made available by beach, dune, and shoreface erosion is used to move the barrier landward (Fig. 1b). Thus, the effective height, H_{eff}, of the barrier profile—the height of the part of the profile that contributes new sediment to the nearshore system as the barrier migrates—is the difference between back-barrier depth and shoreface depth (Fig. 2c, d).

2.3 *Response to Sea-Level Rise: Qualitative Concept*

RSLR induces horizontal and vertical shifts in the entire barrier profile through increases in the rate of overwash events and overwash deposition on the barrier (as well as the inlet-related processes that move sediment from the front to the back of a barrier). This removes sediment from the beach and upper shoreface, causing the shoreline and shoreface to translate landward (please see the Preface, this volume). Overwash deposition tends to raise the elevation of the barrier at a rate equal to the rate of RSLR (over timescales longer than the characteristic overwash return interval). In addition, the shoreface portion of the profile moves upward at that same rate (as the tendency for waves to sweep sediment toward shore tends to maintain an equilibrium profile). To understand this point, consider that the equilibrium slopes that define the shoreface profile are a function of depth relative to sea level. Therefore, starting at the shoreline and moving offshore, the sequence of equilibrium slopes are always the same—independent of the absolute elevation of sea level (relative to some datum). In the limit of high rates of RSLR, the lower parts of the shoreface may not adjust to changing sea level rapidly enough to keep up. Cowell and Kinsela (this volume) and Ashton and Lorenzo-Trueba (this volume) consider this case, although we neglect it in this chapter.

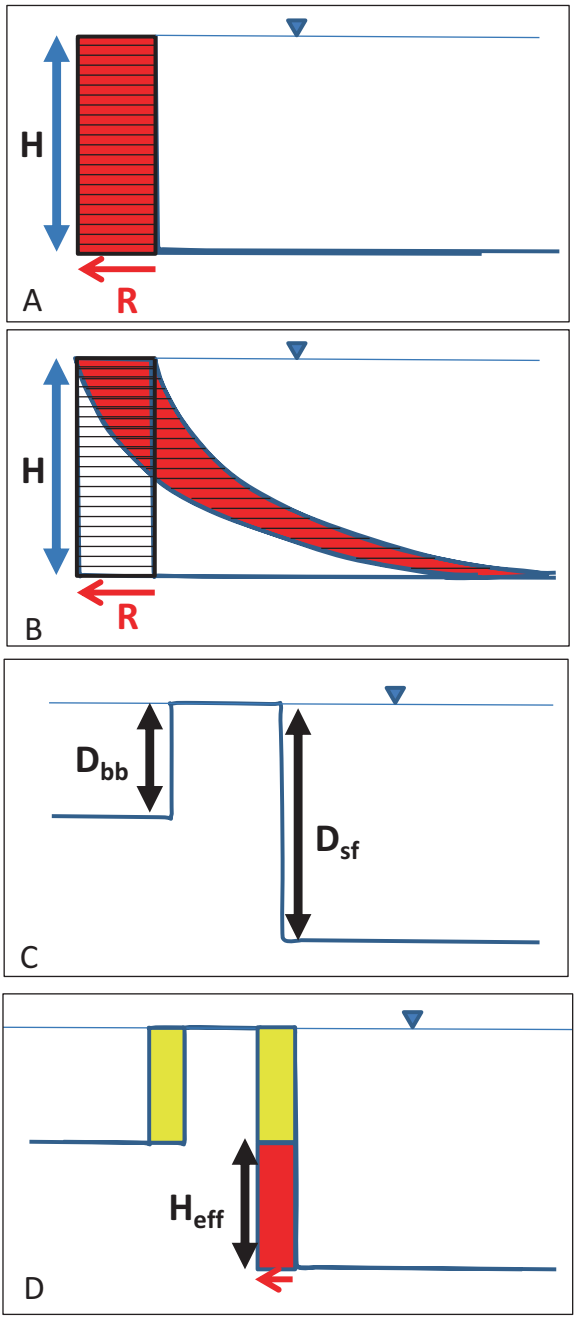

Fig. 2 Sediment produced by landward barrier translation. (**a**) For a hypothetical rectangular shoreface (e.g., the limiting case of a concave shoreface with very high concavity), the area (volume/unit alongshore distance) eroded equals $R * H$. (**b**) This eroded area is independent of the shape of the shoreface (concave shoreface profile shown here), as long as the shape remains constant; sliding the slabs composing the eroded area for the rectilinear profile horizontally by different amounts reproduces the eroded area for the concave profile. (**c**) A hypothetical rectilinear barrier profile, showing the shoreface and back-barrier depths, D_{sf} and D_{bb}. (**d**) Because area eroded above the elevation of (sea level—D_{bb}) equals the area deposited above (sea level—D_{bb}), the net sediment produced by landward translation equals $R * (D_{sf} - D_{bb})$, or $R * H_{eff}$, where H_{eff} is the effective height of the barrier profile $(D_{sf} - D_{bb})$

In other words, relative to the reference point of the shoreline, which is moving upward and landward with RSLR, both the subaerial and subaqueous portions of the barrier profile will tend to retain a constant shape. (In one exception to this tendency to retain a constant shape, the depth of the water into which overwash is deposited at the landward edge of the barrier profile, D_{bb} (Fig. 2b) will tend to change as sea-level rises, as we discuss in the next section.) In the analytic/geometric framework we are assuming, we consider in the next three sections, how the distance that the barrier profile moves landward for a given amount of RSLR—which defines the migration trajectory—is determined by a balance between the amount of coarse sediment (sand and/or gravel) needed to raise the elevation of the barrier profile where deposition occurs (chiefly the subaerial portion of the profile) and the amount of coarse sediment available from erosion of the seaward portion of the barrier profile (with the possible addition of sources or sinks from outside the cross-shore profile, as discussed below).

3 Simplest Migration Scenario: Generalized Bruun Rule for Barriers, and Long-Term Consequences

3.1 Assumptions

The simplest scenario for barrier migration involves several assumptions: (1) the depth of the shoreface—the depth to which erosion occurs as the shoreface moves landward—remains constant (an assumption relaxed in Cowell and Kinsela this volume); (2) all sediment produced by shoreface erosion is sufficiently coarse to remain in the high-energy nearshore system (relaxed in Sect. 4); (3) sediment is conserved within the cross-shore profile, with no net sources or sinks from outside the profile (i.e., there are no gradients in net alongshore sediment transport, as in Sect. 5, or cross-shore fluxes from the continental shelf, as in Cowell and Kinsela, and Ashton and Lorenzo-Trueba this volume); (4) deposition in the back-barrier bay is negligible (relaxed in Sect. 6); and (5) the slope of the substrate over which the barrier progressively migrates is spatially uniform (relaxed in Sects. 6 and 7).

3.2 Generalized Bruun Rule for Barriers

To derive the ratio between an increment of RSLR(S) and the associated landward migration (R), we first consider the vertical and horizontal movements separately, in a sequence of thought experiments. As described in Sect. 2.2, if the barrier profile only shifts landward (by R), this produces an amount of sediment equal to $R * H_{\text{eff}}$. Conversely, if the barrier profile is just elevated by an amount, S, this requires an amount of sediment equal to $S * L$, where L is the horizontal length of the profile

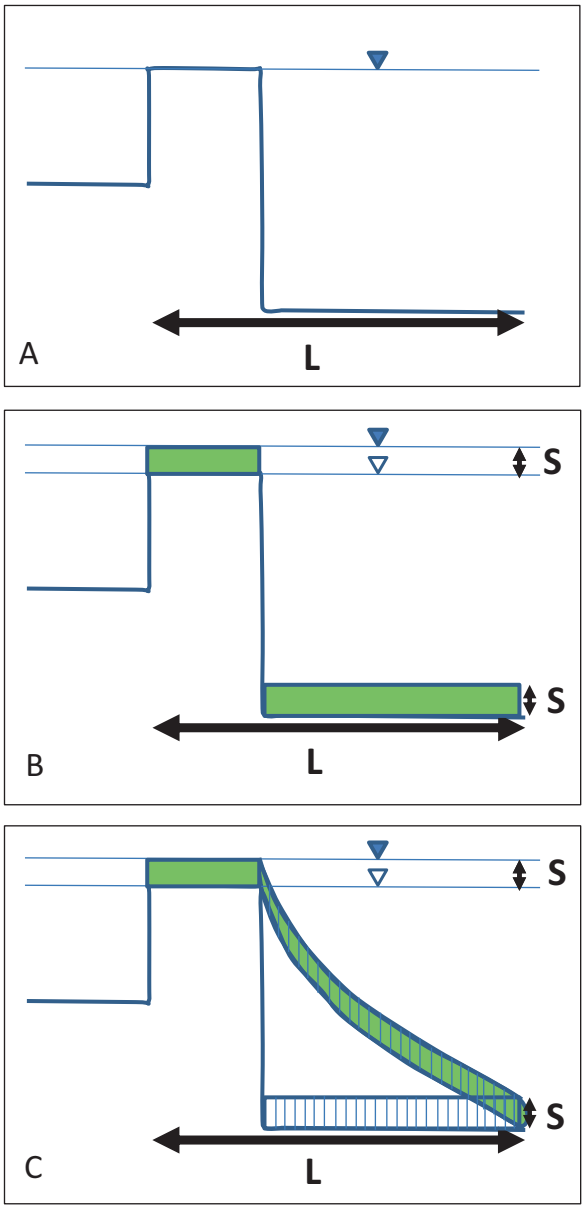

Fig. 3 Sediment required for vertical barrier translation. (**a**) The length of the profile, *L*, includes the lengths of the shoreface and the subaerial barrier. (**b**) Raising the profile requires *L* * *S*, where *S* is the amount of SLR (depicted by difference between the lines denoted by the blue triangles; the open triangle shows the earlier sea level). (**c**) This sediment area (volume/unit alongshore distance) is independent of profile shape, as long as the shape remains constant (see Fig. 2 caption)

(including subaerial and subaqueous portions; Fig. 3a, b). As in the case of the considerations of shoreface erosion in Sect. 2.2, this result is clear for a profile with a rectangular shoreface, but it also applies to profiles of any shape, as long as the shape remains constant; Fig. 3c. In addition, this analysis applies to a snapshot in time, during which H_{eff} and L can be considered constant. Over time, these variables can change, as we discuss in Sect. 3.2. Now, if the barrier profile is first shifted

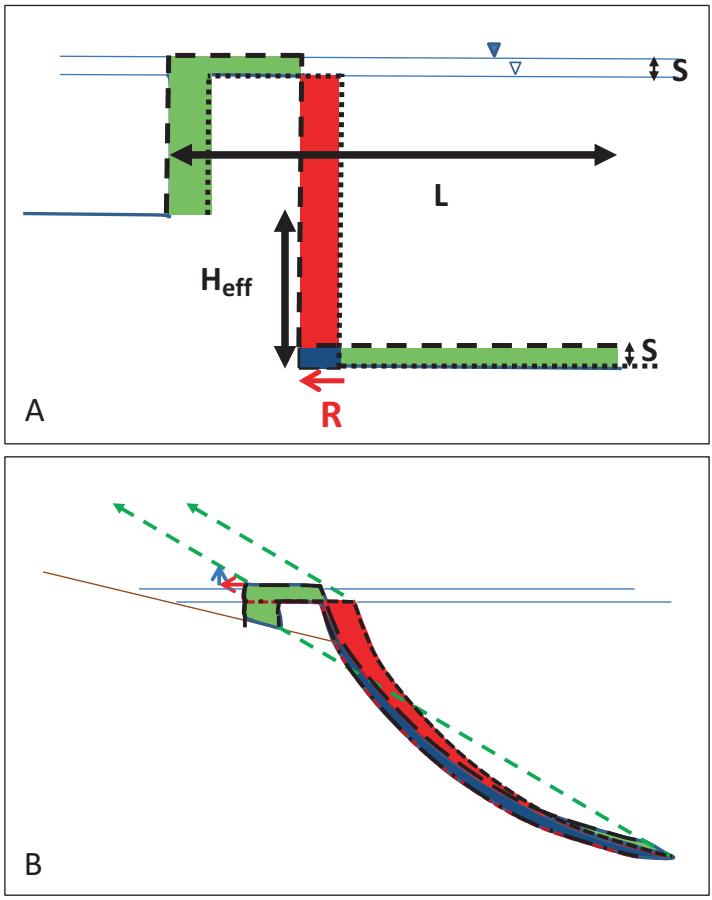

Fig. 4 Combining horizontal and vertical barrier translations, as a barrier responds to RSLR. (**a**) Neglecting sources/sinks of sediment from outside the cross-shore profile, the net area (volume/unit alongshore distance) of sediment eroded, shown in red, must equal the net area deposited, shown in green. The net area eroded equals ($R * H_{eff}$, minus the area of the blue rectangle in the corner), while the net area deposited equals ($L * S$ minus the area of the blue rectangle in the corner). Equating these quantities, the blue rectangle in the corner drops out, and therefore $R * H_{eff} = L * S$, or $S/R = H_{eff}/L$. (**b**) The same analysis applies to a less simplified geometry, although the blue area that does not contribute to the net eroded area or the net deposited area has a different shape

horizontally, and then the resulting sediment derived from shoreface erosion is used to raise the profile vertically, $R * H_{\text{eff}} = S * L$, or, rearranging:

$$R = S * \left(L / H_{\text{eff}} \right) \tag{1}$$

In this last thought experiment, we applied the horizontal and vertical components of the profile migration sequentially—but how might the answer (Eq. 1) be

different for the more realistic case in which both horizontal and vertical components occur simultaneously? Figure 4a, which uses a schematic rectangular shoreface for clarity, shows that, *relative to the sequential-motion thought experiment*, there is an area not subjected to net erosion in the combined-motion thought experiment. The deficit in net erosion in the combined-motion thought experiment is indicated by the dark rectangle in the bottom corner of the shoreface in Fig. 4a. Similarly, relative to the sequential experiment, an area in the combined-motion experiment is not subjected to net deposition (the same rectangle in the bottom corner of the shoreface). However, the deficit in erosion (relative to the sequential-motion experiment) is equal to the deficit in deposition (relative to the sequential experiment). Thus, these deficits cancel out, leaving the result of the sequential-motion thought experiment—Eq. 1—intact. Figure 4b demonstrates graphically that this result also holds for a less-schematized profile geometry.

In Eq. 1, L/H_{eff} is the inverse of the average slope of the barrier profile. L is typically on the order of kilometers, H_{eff} is typically on the order of 10s of meters, and L/H_{eff} typically ranges from a few hundred to a thousand (e.g., Moore et al. 2010; Lorenzo-Trueba and Ashton 2014). Because L/H_{eff} is a large number, a small amount of RSLR and associated cross-shore sediment fluxes can cause a relatively large amount of barrier migration, including shoreline erosion.

Bruun (1962) originally derived an expression similar to Eq. 1, but applied it only to the shoreface—i.e., involving the average slope of the shoreface, rather than the entire barrier profile. The concepts of constant geometry and conservation of mass introduced by Bruun can be extended to include either beach-backing cliffs or overwash plains and barriers (e.g., Dean and Maumeyer 1983; Davidson-Arnott 2005; Wolinsky and Murray 2009; Rosati et al. 2013), which is more appropriate than the original Bruun Rule when considering timescales that are sufficiently long for cliff erosion or overwash to occur. Equation (1) is the generalization specific to barrier coasts (e.g., Wolinsky and Murray 2009).

3.3 Long-Term Consequences

Equation 1 defines the slope of the migration trajectory: $S/R = H_{eff}/L$ (Fig. 5a). However, this trajectory only applies to a snapshot in barrier evolution, because as the barrier migrates along the trajectory, H_{eff} will tend to change. To see how this occurs, first consider Fig. 5a, which illustrates that as the barrier profile migrates, the shoreface toe, the shoreline, and the subaerial landward edge of the barrier all migrate along parallel trajectories. However, if the slope of these trajectories is steeper than the slope of the (spatially uniform) substrate the barrier is migrating across, the depth of the water behind the barrier (D_{bb}) will increase over time, as Fig. 5b shows. This increase in the back-barrier depth decreases H_{eff}, which, in turn, leads to a shallowing of the average slope of the barrier profile. Thus, over time, the slope of the migration trajectory decreases (Fig. 5b)—and the trajectory slope must continue to decrease as long as it remains steeper than the substrate slope. As the

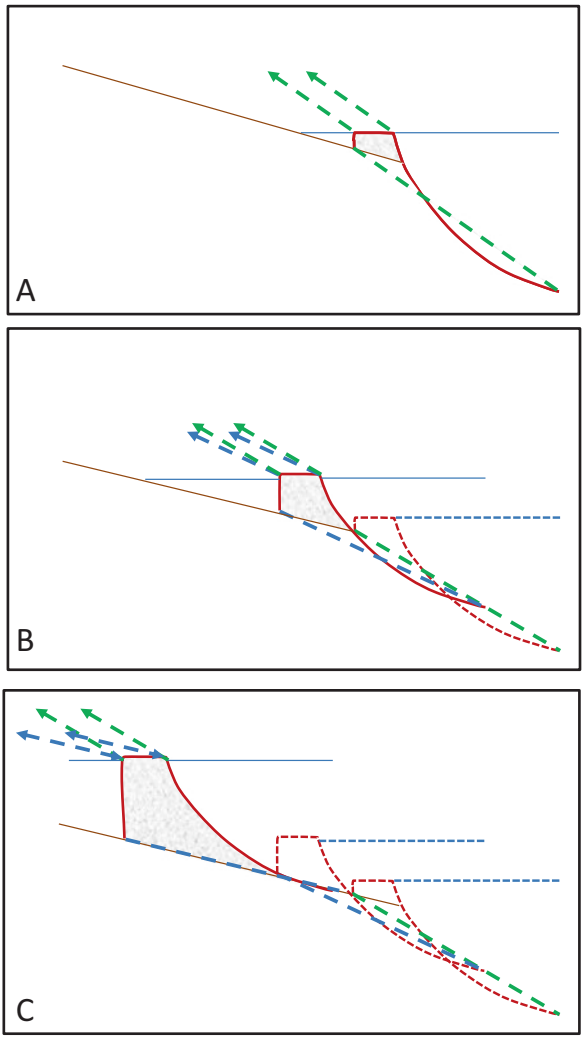

Fig. 5 Long-term adjustments to the barrier geometry—barrier volume, back-barrier depth, and average profile slope—as a barrier migrates across a constant-slope substrate. (**a**) The average profile slope (green dashed line) and barrier migration trajectory (shown for both the seaward and landward edges of the barrier; green dashed lines with arrows) parallel each other. Note that the slope of the migration trajectory is steeper than the slope of the substrate in this hypothetical initial geometry. (**b**) At a later time, the back-barrier depth has increased, which decreases the average profile slope (blue dashed line) and migration-trajectory slope (blue dashed lines with arrows). (**c**) Eventually, the migration-trajectory slope approaches the substrate slope, producing a steady state back-barrier depth and migration trajectory slope. (After Wolinsky and Murray 2009; Moore et al. 2010)

trajectory slope approaches the substrate slope, the rate of change of H_{eff}, and therefore the rate of change of the trajectory slope, decreases (holding RSLR rate constant). In this way, the trajectory slope asymptotically approaches the substrate slope (Fig. 5c) (Moore et al. 2010). (In this case, it is the slope of the substrate evaluated at the landward edge of the barrier that controls the evolution of the barrier migration trajectory. In contrast, in Sect. 6, where we consider back-barrier deposition and spatially varying substrate slope, both the substrate slope at the landward edge of back-barrier deposition and at the point of intersection with the shoreface control the barrier migration trajectory. When the substrate slope is spatially uniform, of course, all three of these slopes are the same.)

Once the trajectory slope converges to the substrate slope, the geometry of the barrier ceases to change with time (Wolinsky and Murray 2009; Moore et al. 2010). The asymptotic approach to steady state occurs over a timescale that depends on the rate of RSLR; Wolinsky and Murray (2009) show analytically that the adjustment requires a sufficient amount of RSLR—an amount that is commensurate with the height of the profile (H_{eff}). The configuration in which the barrier migration trajectory equals the substrate slope, and the geometry of the barrier (relative to the moving reference of sea level) is in steady state, represents a dynamically stable equilibrium; perturbing the migration-trajectory slope (or the substrate slope) triggers a negative feedback that tends to bring the system back to the steady state (as in the thought experiment above).

With the simplifying assumptions in this scenario, the geometry of the barrier approaches the configuration often depicted in textbooks: a large body of sand, perched on top of the underlying substrate (Fig. 5c; Roy et al. 1994). In this configuration, the barrier "rolls" across the substrate as sea level rises, as sand moves from the seaward to the landward portions of the profile (via overwash or barrier bypassing through inlets, and associated onshore sediment flux on the shoreface; e.g., Leatherman 1979; Rodriguez et al. this volume; Preface, this volume). However, this configuration is only an end member possibility; as we will see in Sect. 5, barriers will commonly evolve toward a state in which part of the shoreface is incised into the underlying substrate (e.g., Fig. 5a, b), so that each increment of landward translation tends to excavate new sediment that is added to the nearshore system (e.g., with incision being driven by a divergence in net alongshore sediment flux; Sect. 5).

4 The Effect of Shoreface Composition on Barrier Response to RSLR

We have so far assumed that all of the new sediment added from shoreface erosion is available to the island system as the profile moves upward and landward. However, prolonged landward translation will ultimately expose the underlying substrate on the shoreface; the tendency of waves to sweep sediment toward shore, interacting with shoreface slopes, creates gradients in cross-shore sediment fluxes on the shoreface (Preface, this volume) that can uncover the underlying substrate. Once exposed, the substrate (if lithified) weathers into transportable sediment (via physical, biological, and chemical weathering processes). If all of the resulting substrate-derived sediment is sufficiently coarse, relative to the energy conditions of the coast in question (i.e., sand and/or gravel), it will remain in the nearshore system. In this case, each increment of landward translation, R, produces an amount of sediment equal to $R * H_{eff}$, as assumed in deriving Eq. 1. However, some substrates consist, at least partly, of material that weathers into finer sediment (i.e., silt and clay, weathering out from a muddy back-barrier deposit, or lithified rock with a mudstone or shale component, or mud from former deltaic deposits). In this case, the fine fraction of the sediment produced by shoreface erosion is lost from the nearshore system

(advecting and or/diffusing into some lower-energy environment). In this case, each increment of landward translation produces a reduced amount of sediment available for deposition as the barrier-shoreface profile migrates.

We can quantify this effect and incorporate it into the framework of Eq. 1 (Wolinsky and Murray 2009): The amount of coarse sediment produced by an increment of landward translation is equal to $(R * H_{eff}) * F$, where F is the fraction of the sediment produced by shoreface erosion that is coarse enough to remain in the nearshore system (the "coarse fraction," ranging from 0 to 1). Here, F is an average of the coarse fraction over H_{eff} (Fig. 2b). Figure 5a illustrates that the portion of the shoreface spanned by H_{eff} will in general include both mobile sand and outcrop of the underlying substrate (i.e., the "transgressive ravinement surface" in stratigraphic terminology).

The portion of the shoreface consisting of outcropping substrate is the result of the previous migration history of a barrier (Brenner et al. 2015). In addition, the composition of the substrate depends on the history of deposition in the back-barrier environment as well as the migration history of the barrier (Brenner et al. 2015), as we discuss in Sect. 6. However, in this section, for simplicity we take the average composition of the shoreface (over H_{eff}) to be an extrinsic constraint.

Taking F as an input, we can calculate how much landward translation is needed to meet the demands of raising the profile; $(R * H_{eff}) * F = S * L$, or, rearranging:

$$R = S^* \left(L / H_{eff} \right)^* \left(1 / F \right) \tag{2}$$

Then, relative to results of Eq. 1, the slope of the barrier migration trajectory is reduced if $F < 1$:

$$S / R = \left(H_{eff} / L \right)^* F \tag{3}$$

A thought experiment analogous to that in Sect. 3.2 leads to the conclusion that even if $F < 1$, given a sufficient amount of RSLR, the barrier profile will tend to adjust qualitatively as it does when $F = 1$, toward a state in which the migration trajectory parallels the slope of the substrate (with the same barrier volume that would occur if $F = 1$; Fig. 5c).

5 The Effect of Sediment Losses (or Gains) on Barrier Response to RSLR

The trajectory is also modified when the sediment supply/loss rate, from sources other than shoreface erosion, is not 0. For example, in most shoreline locations, gradients in net alongshore sediment transport cause either a net gain (when the rate of sediment transport into a shoreline segment is greater than the rate at which sediment is transported out; a convergence of net sediment flux) or a net loss (when the rate of sediment transport into a shoreline segment is lower than the rate at which

sediment is transported out; a divergence of net sediment flux). (Note that "convergence" and "divergence" do not necessarily imply a directional convergence or divergence; the net flux can be moving in the same direction on either end of a shoreline segment, but with different magnitudes.)

A divergence of net alongshore sediment transport induces landward translation of the barrier profile (please see Sect. 2.2; the Preface, this volume; and Roy et al. 1994). This additional component of horizontal translation is in addition to the landward motion associated with RSLR (e.g., Moore et al. 2010) and equates to a reduction in the slope of the migration trajectory (Fig. 6). This shallowing of the migration-trajectory slope alters the geometry that a barrier tends to develop in the long term (compared to the case without net sediment loss). For example, imagine starting with a barrier that consists entirely of mobile sediment, perched on top of the substrate. In the absence of a net sediment loss, this geometry is a stable steady state, in which the migration-trajectory slope parallels the substrate slope (e.g., Fig. 6a, blue arrow), as outlined in Sect. 3. However, adding a sediment loss increases shoreline and shoreface erosion—i.e., increasing the landward translation of the barrier profile that occurs during each increment of RSLR. This increased landward translation reduces the slope of the migration trajectory, so that it is lower than that of the substrate (Fig. 6a, red arrow). As a result, over time, the back-barrier depth (D_{bb}) will decrease, and the toe of the shoreface will become incised into the substrate as the barrier profile moves landward (Fig. 6c, purple arrow). Because the elevation of the shoreface toe (relative to sea level) remains constant, while the elevation of the landward end of the barrier profile relative to sea level increases (corresponding to the decrease in back-barrier depth), the average slope of the barrier profile increases over time. Therefore, as the barrier evolves from this hypothetical initial state, the trajectory slope will steepen (Fig. 6, green and purple arrows). As long as the slope of the migration trajectory is lower than the substrate slope, the back-barrier depth will continue to decrease and a greater proportion of the shoreface will erode into the substrate as the barrier profile migrates. As in Sect. 3, these changes in profile geometry (barrier volume, D_{bb}) will, again, ultimately cause the trajectory slope to approach the slope of the substrate (Fig. 6c).

However, in the case of a net sediment loss, the steady-state geometry that produces a migration trajectory parallel to the substrate slope features a shoreface that partly erodes the substrate as it moves landward. In fact, steady state is only possible when enough of the shoreface is eroding into the substrate to produce new sediment (as distinguished from the mobile sediment already atop the substrate; Fig. 6) at a rate equal to the rate at which sediment is being lost. For a given average barrier profile slope, the vertical extent of the shoreface that needs to be actively eroding into the substrate depends on the substrate composition (through its effect on the average shoreface sediment composition F) and on the rate at which sediment is being lost (e.g., how large the gradient in net alongshore sediment transport is).

In the case of a net sediment gain—either from a convergence of net alongshore sediment transport (Moore et al. 2010), or from onshore sediment flux from a shallow continental shelf (Cowell and Kinsela this volume)—the added component of horizontal translation is in the seaward direction (as the sediment gain in the beach and upper shoreface decreases shoreline erosion, and the rest of the profile responds;

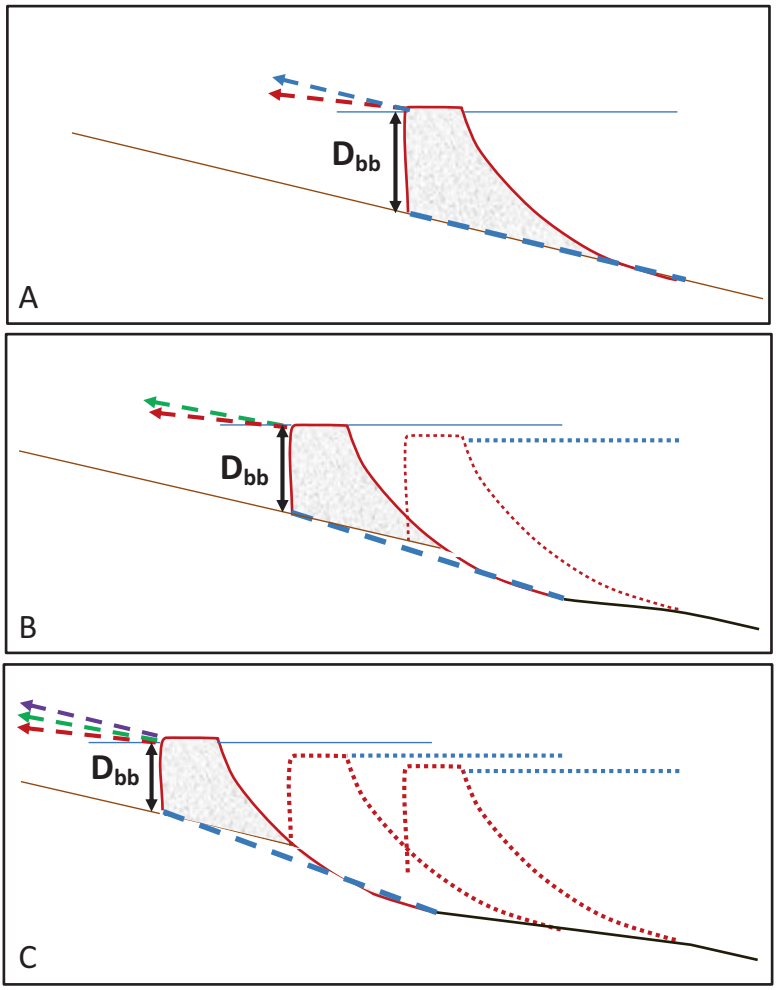

Fig. 6 Long-term adjustments to the barrier geometry and migration trajectory when sediment is being lost from the cross-shore profile (e.g. when there is a gradient in net alongshore sediment transport). (**a**) In a hypothetical initial condition the average slope of the barrier profile (blue dashed line) equals the slope of the substrate (brown line). However, because of the negative sediment budget the slope of the migration trajectory (red dashed line with arrow) will be lower than the average profile slope (which otherwise sets the migration trajectory slope). (**b**) Consequently, the back-barrier depth decreases over time, and the average profile slope increases (blue dashed line), tending to increase the slope of the migration trajectory (green arrow, relative to the red arrow that shows the migration trajectory in (**a**)). Note that the toe of the shoreface becomes incised into the substrate, so that shoreface erosion tends to bring new sediment into the nearshore system. (**c**) At a later time the slope of the migration trajectory (purple dashed line with arrow) has approached the slope of the substrate, so that the back-barrier depth and migration trajectory have approached steady state. Note that this steady state is reached when the profile is incised into the substrate far enough for the landward to retreat feed new sediment into the nearshore system at a rate that equals the rate at which sediment is lost from the cross-shore profile (e.g. the divergence of the net alongshore sediment flux)

please see Sect. 2.2 and the Preface, this volume). This tends to increase the slope of the migration trajectory. (We do not consider in this chapter the case in which sediment is added rapidly enough to cause shoreline progradation, and a widening barrier, which Cowell and Kinsela this volume and Moore et al. this volume examine).

In Sects. 3 and 4, the slope of the barrier migration trajectory was a kinematic result, independent of the RSLR rate (because both horizontal and vertical translation rates are proportional to RSLR). However, when sediment losses or gains are considered, the trajectory slope does depend on RSLR rate. More precisely, it depends on the relative magnitudes of RSLR rate and the rate of horizontal translation induced by the sediment loss or gain. By definition, the migration-trajectory slope is the ratio of the rate of vertical translation (equal to RSLR rate) and the rate of horizontal translation. In the case of a sediment loss or gain, the horizontal translation rate results from two independent contributions: RSLR causes horizontal translation with a rate proportional to RSLR rate (Eq. 3); and a sediment loss/gain causes horizontal translation at a rate that depends on the rate of sediment loss or gain (which is in general independent of RSLR rate). For example, consider the case of a divergence in net alongshore sediment flux, Q_s. The sediment loss rate, dQ_s/dx (where x is the alongshore coordinate), must equal the rate at which coarse sediment is produced, which is $F * H_{eff}$ multiplied by the horizontal translation rate arising from the sediment loss. Therefore, rearranging this equation, the contribution to the horizontal translation rate equals $(1/F) * (1/H_{eff}) * (dQ_s/dx)$.

How much the slope of the migration trajectory is altered by a sediment loss or gain, relative to the effect produced by RSLR alone (Eq. 3), depends on the relative magnitudes of the horizontal translation rates related to RSLR and to dQ_s/dx. When RSLR rate is relatively low, so that the rate of landward retreat related to RSLR (Eq. 3) is small compared to the rate of horizontal translation related to the external sediment loss or gain rate, then the trajectory is strongly affected by the loss or gain—and vice versa. We can quantify this within the analytical framework by adding the two components of horizontal translation together, where the sediment gain/loss term represents a gradient in net alongshore sediment transport (and where we have treated the increments of landward retreat, RSLR, and time as differentials, *dR, dS, and dt*):

$$dR = dS * (1/F) * (L/H_{\text{eff}}) + (1/F) * (1/H_{\text{eff}}) * (dQ_{\text{s}}/dx) * dt. \quad (4)$$

Or, rearranging:

$$dS/dR = (H_{\text{eff}}/L) * F * \left[1 - (1/dR) * (1/F) * (1/H_{\text{eff}}) * (dQ_{\text{s}}/dx) * dt\right]. \quad (5)$$

Then, substituting *dS*/(RSLR rate) for *dt* makes clear that the trajectory depends on the balance between RSLR rate and the magnitude of the gradient in net alongshore sediment transport:

$$dS/dR = \left(H_{\text{eff}}/L\right)*F \\ *\left[1-\left(1/F\right)*\left(1/H_{\text{eff}}\right)*\left(dQ_s/dx\right)*\left(dS/dR\right)*\left(1/\text{RSLR rate}\right)\right] \quad (6)$$

Even though (6) is not an explicit equation for the trajectory (because *dS/dR* appears on both sides), it does show that the trajectory slope: (1) reduces to the pure RSLR response either when RSLR rate is very high or the gradient in net alongshore sediment transport is very small (so that the second term in the brackets approaches 0); and (2) will approach 0 (pure horizontal translation) either when RSLR rate is very low or the gradient in net alongshore sediment transport is very high (so that the second term in the brackets approaches 1).

6 The Effect of Back-Barrier Deposition, Deposit Thickness, and Composition

6.1 Coupling Between Back-Barrier Deposition and Barrier Migration Trajectory

In this section, we consider the case in which deposition occurs in the environments landward of a barrier, typically marshes and/or shallow bays (elaborating on the results from Brenner et al. 2015). Where such deposition occurs, a barrier moves across these deposits as it migrates landward. In this case, the substrate cropping out on the shoreface will consist at least partly of back-barrier deposits (Fig. 7a), which typically have $F < 1$. We will assume that back-barrier deposition keeps up with RSLR (e.g., Marani et al. 2007; Mariotti and Fagherazzi 2010); that sediment is supplied to the back-barrier environment (from rivers and/or the coastal ocean) at a rate that is sufficient to fill the accommodation space as fast as it is created by RSLR.

In this case, the influence of the substrate slope on the barrier migration trajectory is different than in the cases considered so far. In Sects. 3–5, the relationship between the slope of the migration trajectory and the slope of the substrate at the landward edge of the barrier profile (Fig. 4) determines whether the depth of the water into which the barrier migrates increases or decreases as the barrier migrates landward. Changes in this back-barrier depth, then, equate to changes in H_{eff} and therefore to changes in the barrier migration trajectory. However, when back-barrier deposition occurs, and keeps up with RSLR, then the depth of water into which the barrier migrates remains constant (defined by the steady-state depth of the marsh or bay, relative to sea level), and therefore, H_{eff} remains constant in time and is not influenced by the substrate slope.

Even in the case of back-barrier deposition, substrate slope influences the barrier migration trajectory. In this case, however, the influence is modulated by the effect of the thickness of the back-barrier deposit (Brenner et al. 2015). To understand this modulated influence, we pose a thought experiment: Consider a case in which the

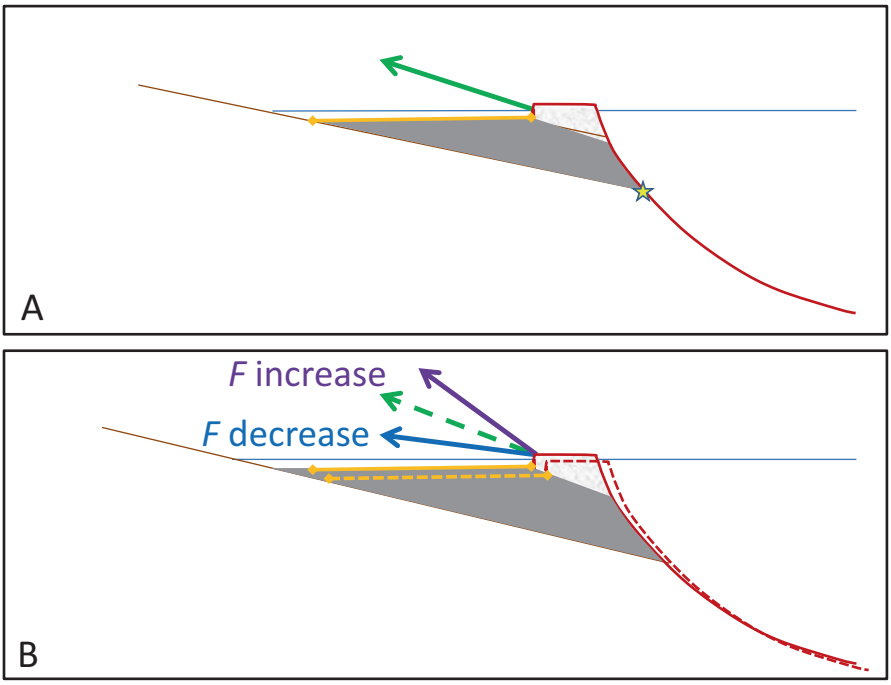

Fig. 7 Barrier migration trajectory (green arrow) depends on the thickness of the back-barrier deposit. (**a**) The migration trajectory, influenced by the composition of the back-barrier deposit (gray) and the thickness of that deposit on the shoreface, is steeper than the substrate slope in this hypothetical condition. Yellow line shows the width of the back-barrier deposition at this snapshot, and the star shows where the contact between the substrate and the back-barrier deposit (i.e. the substrate slope beneath the back-barrier deposit) intersects the shoreface. (**b**) The effects of a thicker back-barrier deposit where it outcrops on the shoreface (i.e. a wider back-barrier environment, for a constant substrate slope) depends on whether the back-barrier deposit is coarser than the underlying substrate (purple arrow) or finer than the underlying substrate (blue arrow). The green dashed line shows the initial trajectory. Dashed yellow line and dashed barrier-shoreface profile show the back-barrier width and barrier profile location in the snapshot shown in (**a**). The solid yellow line depicts the width of the back-barrier in (**a**), at the elevation of the top of the back-barrier deposit in the snapshot shown in (**b**) (i.e. it is the dashed yellow line translated along the barrier migration trajectory), showing that the back-barrier in the snapshot shown in (**a**) is narrower than the back-barrier in the snapshot shown in (**b**). (After Brenner et al. 2015)

substrate slope is lower than the slope of the current barrier migration trajectory (Fig. 7a). In this case, the cross-shore width of the back-barrier environment increases with time (Fig. 7b). With the assumption (for now) that the substrate slope is spatially uniform, widening of the back-barrier environment corresponds to a thickening of the back-barrier deposit where it outcrops on the shoreface (Fig. 7b). Therefore, a low substrate slope, relative to the slope of the barrier migration trajectory, means that the proportion of the shoreface consisting of back-barrier deposits increases over time.

The proportion of the shoreface composed of back-barrier deposits, combined with the composition of the back-barrier deposit, affects the average shoreface composition, *F* (Sect. 4). Thus, the thickness of the back-barrier deposit, which depends in part on the barrier migration trajectory, in turn, affects barrier trajectory (Sect. 4); a coupling between the thickness of the back-barrier deposit and the barrier migration trajectory. The long-term consequences of this coupling depend on the composition of the back-barrier deposit relative to the composition of the underlying substrate (Brenner et al. 2015).

6.2 Negative Feedback

If the back-barrier deposit weathers into sediment consisting of a smaller proportion of coarse material (hereafter referred to as "less coarse") than the underlying substrate, then thickening the outcrop of the back-barrier deposit on the shoreface decreases the coarse sediment fraction liberated by shoreface erosion (*F*), and therefore decreases the slope of the migration trajectory (Fig. 7b, blue arrow). The decreased slope of the trajectory then decreases the rate at which the back-barrier environment widens and therefore the rate at which the deposit thickens. As long as the slope of the barrier migration trajectory is greater than the substrate slope, the widening and thickening continue, and the slope of the migration trajectory continues to decrease. As the slope of the barrier migration trajectory approaches the substrate slope, back-barrier widening slows to a halt (Brenner et al. 2015).

In a parallel thought experiment, consider the situation in which the back-barrier deposit is less coarse than the underlying substrate, as above, but initially the substrate slope is steeper than the slope of the barrier migration trajectory. In this case, the back-barrier environment narrows and the thickness of the back-barrier deposit on the shoreface decreases over time. The resulting increase in the coarse fraction of sediment liberated by shoreface erosion (*F*) will steepen the barrier migration trajectory. Ultimately, the outcrop of the back-barrier deposit on the shoreface will become sufficiently thin for the slope of the barrier migration trajectory to approach the substrate slope.

These considerations reveal that if the back-barrier deposit is less coarse than the underlying substrate, the barrier/back-barrier system will tend to approach a dynamic equilibrium defined by: (1) a barrier migrating along a trajectory parallel to the substrate slope (as in Sects. 3–5), (2) a steady-state thickness of the back-barrier deposit on the shoreface; and (3) a steady-state back-barrier width, determined by a combination of the substrate slope and the composition of the back-barrier deposit relative to the composition of the underlying substrate. This dynamic equilibrium state is stable (as was the case in Sects. 3–5); if the thickness of the back-barrier deposit on the shoreface is perturbed from the equilibrium value, the barrier migration-trajectory slope will be perturbed as well, and a negative feedback will tend to return the system to the equilibrium (as in the thought experiments above; Brenner et al. 2015).

6.3 Positive Feedback

Now, consider the case in which the back-barrier deposit is *coarser than* the underlying substrate. A steady-state configuration is still theoretically possible; some value of the thickness of the back-barrier deposit on the shoreface will produce a barrier migration-trajectory slope equal to the substrate slope. However, in this case the equilibrium is unstable. Starting from this equilibrium condition, If the back-barrier deposit thickness on the shoreface is perturbed so that it is slightly thicker than the equilibrium value, the slope of the barrier migration trajectory will become steeper than the substrate slope, so that the proportion of the shoreface consisting of back-barrier deposit increases. Then, the average shoreface composition becomes increasingly coarse. This increase in F causes the barrier trajectory to steepen (Fig. 7b), which increases the difference between the migration-trajectory slope and the substrate slope. Thus, the back-barrier will continue to widen, at an ever-increasing rate (Brenner et al. 2015).

Conversely, if the back-barrier deposit thickness on the shoreface is perturbed so that it is slightly lower than the equilibrium value, the barrier-trajectory slope will be less steep than the substrate slope, leading to narrowing the back-barrier environment, further decreasing the thickness of the back-barrier deposit and leading to ever more rapid back-barrier narrowing, in a runaway feedback (Brenner et al. 2015). This positive feedback, which pushes the barrier/back-barrier system away from the equilibrium state, will not operate indefinitely. In the case of narrowing, the barrier would ultimately become welded to the mainland.

In the case of runaway widening, ultimately the back-barrier deposit will extend to the base of the shoreface. If this happens, the migration trajectory becomes disconnected from the substrate slope entirely. However, before runaway widening goes too far in any actual barrier landscape, the assumptions we make in this section are likely to break down. As the back-barrier environment widens, RSLR creates accommodation space at an increasing rate. In many actual barrier landscapes, the rate of sediment input from rivers, tidal inlets, and overwash is finite, preventing back-barrier deposition from keeping up with RSLR indefinitely.

Where back-barrier deposits are predominantly muddy, as is common in marshes and shallow bays, the negative feedback in Sect. 6.2 will be more likely to occur than the positive feedback in Sect. 6.3. The positive feedback, which requires back-barrier deposits to be coarser than the underlying substrate, is probably relevant for fewer actual barrier landscapes. However, some bay environments, with high-energy waves or tidal currents, can feature a high proportion of sand, and some substrates can consist of material that weathers into predominantly fine sediment, so that the positive feedback is possible.

6.4 Timescalesof Migration-Trajectory Adjustments

When back-barrier deposition is occurring, it is the thickness of the back-barrier deposit where it outcrops on the shoreface that needs to adjust to produce the equilibrium state. As an examination of Fig. 7 demonstrates, changes in this thickness arise directly from the difference between the slope of the contact between the back-barrier deposit and the overlying sandy barrier (which is a record of the slope of the barrier migration trajectory through time) and the slope of the substrate, where these slopes intersect the shoreface. If these two slopes are not equal, adjustments to the migration trajectory related to changes in thickness of the back-barrier deposit on the shoreface occur with no delay. However, starting from a hypothetical initial condition in which back-barrier deposits are absent, developing a back-barrier deposit with a sufficient thickness for the slope of the barrier migration trajectory to equal the substrate slope (i.e., dynamic equilibrium) would take time. Developing the equilibrium thickness would require an amount of RSLR commensurate with the equilibrium thickness. Therefore, the characteristic time to come to approach equilibrium would scale with this thickness divided by RSLR rate.

A different timescale arises if the slope of the substrate varies in space, so that the slope of the substrate under the back-barrier deposit is different where it intersects the shoreface than it is at the landward edge of the back-barrier deposit (Fig. 8a). As discussed in Sect. 6.1, assuming back-barrier deposition keeps up with sea-level rise, the slope of the substrate at the landward edge of the back-barrier deposit, in relation to the slope of the migration trajectory, determines the rate of change of the back-barrier width. However, the slope of the migration trajectory is only coupled directly to the slope of the substrate where it intersects the shoreface. The slope of the substrate at the landward edge of the back-barrier deposit (at a snapshot in time as an island migrates) will not affect the barrier migration trajectory until much later—until the barrier has migrated landward (and upward) far enough for the point on the substrate slope corresponding to the former landward edge of back-barrier deposition to crop out on the shoreface (Fig. 8b,c). In other words, the barrier migration trajectory will not begin to adjust to a change in the substrate slope (at the landward edge of back-barrier deposition) until after a time that scales with the width of the back-barrier environment divided by the horizontal translation rate ($dR/dt = dS * (1/F) * (L/H_{eff})$).

To examine barrier evolution when substrate slope is highly variable, as occurs in many actual barrier systems (e.g., Moore et al. 2010), requires numerical modeling, which we discuss in the next section.

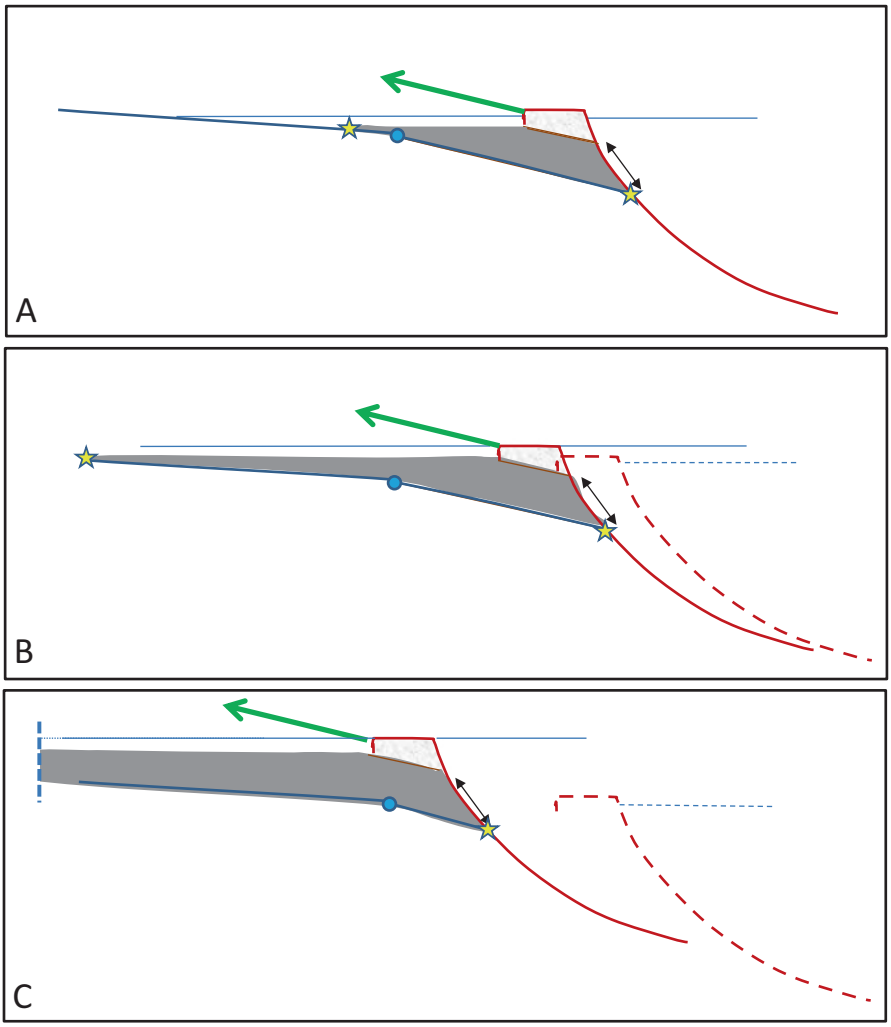

Fig. 8 Time-lagged adjustment of migration trajectory to substrate slope changes. (**a**) In this thought experiment, the migration trajectory is adjusted to the substrate slope where it intersects the shoreface. However, the substrate slope is not uniform; it becomes lower at the location near the current mainland shoreline, highlighted by the blue circle. Yellow stars show the substrate slope at the locations of the landward edge of the back-barrier deposit and at the intersection with the shoreface. (**b**) At a later time, the location of the change in substrate slope (blue circle) is in the middle of the back-barrier environment, and the back-barrier environment is widening. However, the thickness of the back-barrier deposit where it outcrops on the shoreface has not yet changed, so the barrier trajectory has not yet been affected. Dotted lines show the initial profile and sea level. (**c**) At a time shortly before the location of the change in substrate slope (blue circle) outcrops on the shoreface, after which the thickness of the back-barrier deposit on the shoreface will increase, and the barrier migration trajectory will respond. If the composition of the back-barrier deposit is less coarse then the substrate, then the migration trajectory will ultimately adjust to be parallel to the new substrate slope

7 Toward the Real World: Numerical Modeling

The scenarios considered above involve three key assumptions (either implicitly or explicitly): (1) that the slope of the substrate is uniform in space, and therefore constant in time as the barrier migrates across it (with the exception of Sect. 6.4); (2) that the composition of the substrate underlying the barrier (Sects. 3–5) or the back-barrier deposits (Sect. 6) is spatially constant; and (3) that depth of the seaward toe of the shoreface remains constant. These assumptions simplify the analyses, clarifying the basic insights about barrier behavior to be gleaned from considering idealized geometry and conservation of mass. However, these assumptions are not likely to apply strictly in any actual coastline setting, and considering barrier response to RSLR in a more realistic way is also beneficial. Relaxing these assumptions requires numerical modeling.

Numerical modeling of long-term barrier response to sea-level change, driven primarily by the constraints of geometry and conservation of mass as described above, started with the Shoreface Translation Model (Roy et al. 1994; Cowell et al. 1995). The BARSIM model (Storms et al. 2002; Storms 2003) features an analytical representation of a decrease in the response timescale of the shoreface with depth, representing long-term lower shoreface sediment fluxes (e.g., Stive and De Vriend 1995), leading to changes in the effective depth of the shoreface toe as a function of migration rate (e.g., Cowell and Kinsela this volume). Ashton and Lorenzo-Trueba have recently introduced a numerical model including shoreface dynamics—sediment fluxes on the shoreface as a function of the shoreface slope—and the consequent time lags between the responses of the subaerial and subaqueous portion of the barrier profile (Lorenzo-Trueba and Ashton 2014; Ashton and Lorenzo-Trueba this volume).

A complementary model, GEOMBEST (Stolper et al. 2005; Moore et al. 2010), which also treats variations in shoreface response rates with depth and variations in substrate characteristics, has proven useful especially for exploring barrier migration as influenced by variations in substrate slope, substrate erodibility, and substrate composition. In GEOMBEST, the substrate is represented as distinct strata (e.g., Fig. 9) that in general have different compositions and erodibilities (maximum erosion rates), which can be represented as realistically as can be justified based on available sediment-core data and geophysical data. The erosion-rate limitation can lead to a change in the geometry of the shoreface as a function of migration rate. In addition, resolving distinct strata allows the composition of the shoreface, averaged over the strata outcropping on the shoreface, to change as the migration trajectory brings the shoreface into contact with different units. GEOMBEST experiments based on actual barriers can be used to explore the conditions under which variations in substrate composition and slope prevent the approach to equilibrium described in Sects. 3–6—i.e., preventing the slope of the barrier migration trajectory from adjusting to the slope of the substrate (Fig. 10; Moore et al. 2010; Brenner et al. 2015).

Other insights from GEOMBEST experiments include how barrier geometry (e.g., back-barrier depth and barrier sand volume) and landward migration rates of

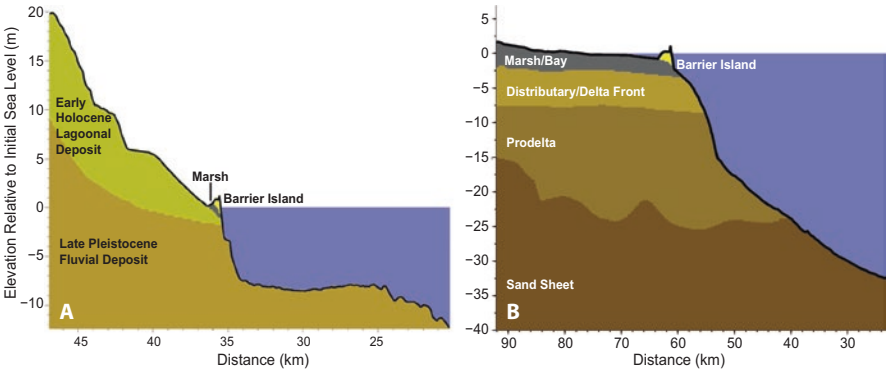

Fig. 9 GEOMBEST initial conditions, representing generalized stratigraphic units and substrate/island morphologies, based on best-available sediment-core, geophysical, topographic and bathymetric data, for (**a**) Northern Metompkin, Island, Virginia and (**b**) North Chandeleur Island, Louisiana. Reprinted from Brenner et al. (2015) and Moore et al. (2014), respectively, with permission from Elsevier

particular barrier chains are likely to change, in response to scenarios of increased rates of RSLR (e.g., Moore et al. 2010)—and under what conditions barriers may cease to persist in the long term (e.g., Moore et al. 2014), leading to barrier drowning or "overstepping" (e.g., Mellett and Plater this volume). In particular, barriers in deltaic environments face multiple challenges. The substrate composition tends to be dominated by fine material, and RSLR rates tend to be high. In addition, on abandoned delta lobes where sediment supply rates are low, back-barrier deposition will ultimately not be able to keep up with RSLR, so that back-barrier depths increase over time (contrary to the assumption in Sect. 6). The Chandeleur Islands off of southeast coast of Louisiana provide a striking example of barrier evolution in such an environment (e.g., Penland et al. 1985; McBride et al. 1992; Fearnley et al. 2009), highlighting the important role of substrate sediment composition and changes in back-barrier width and depth in determining island response to sea-level rise (Moore et al. 2014). The example of the Chandeleurs also highlights that spatial (and temporal) changes in substrate composition, as well as changes in back-barrier width—which can't be addressed with the analytical approaches outlined in previous chapters—can play key roles in barrier evolution.

8 Discussion

Though we have focused in this chapter on cross-shore variability, substrate slope and composition, as well as back-barrier depth, can vary significantly and abruptly alongshore (e.g., Brenner et al. 2015). In addition, although the sediment supply/loss from outside the cross-shore profile (Sect. 5) can encompass the effects of gradients in net alongshore sediment transport, the features that give rise to such

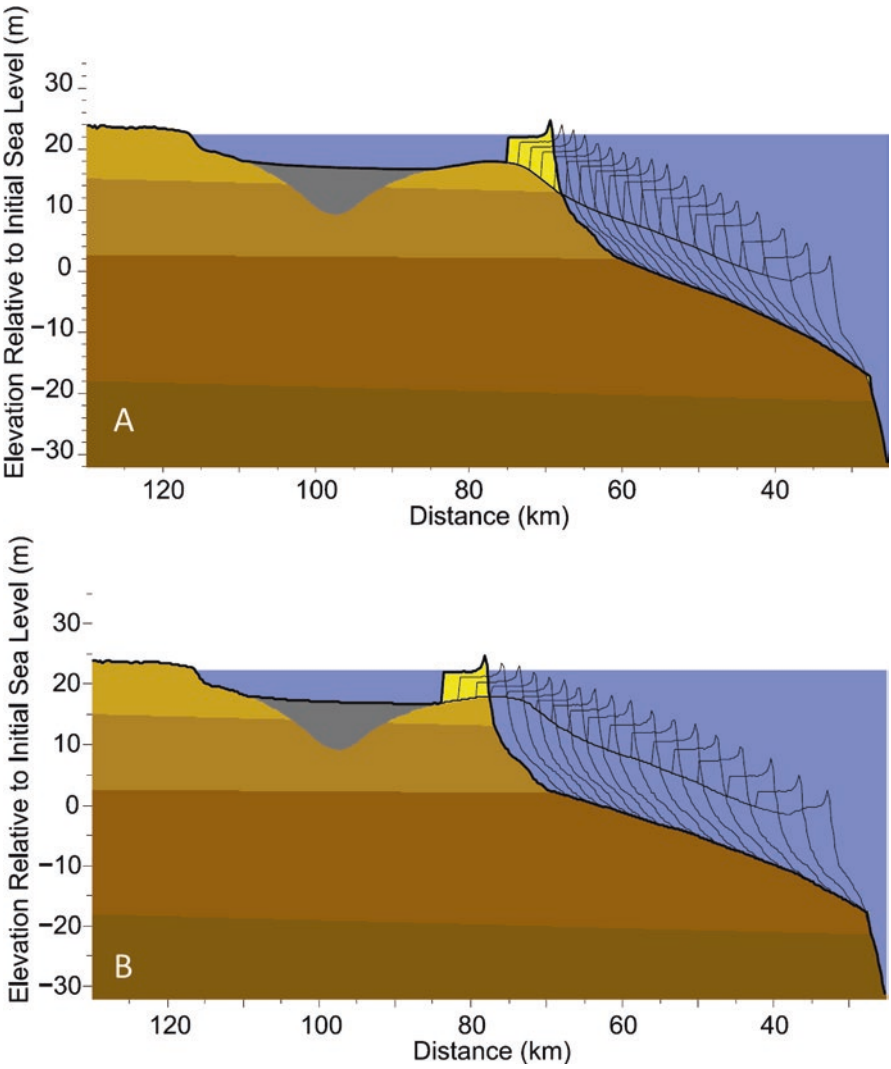

Fig. 10 (**a**) The final time step in an 8500-year GEOMBEST simulation of a generalized stretch of barrier along the Outer Banks, NC. Each trace represents a 500-year time increment and the modern barrier island appears in yellow. The initial surface is shown as a thin black line above the bold black line, which represents the modern shelf surface. The line of traces shows the migration trajectory the barrier has been following, which is approximately parallel to the substrate it has been traversing across. (**b**) The final time step in an 8500-year simulation for the same barrier under different conditions (i.e., a greater rate of sediment loss from gradients in alongshore sediment transport), which result in the barrier migrating farther landward by the end of the simulation than in (**a**). In this case, the traces show a shallowing of the migration trajectory but the migration trajectory, as shown by the several last traces, is not in equilibrium with the substrate slope landward of the barrier at the end of the simulation. From Moore et al. (2010)

gradients can vary significantly alongshore leading to alongshore variations in the sediment/loss rate. For example, coastline curvature can vary significantly even along an approximately straight shoreline (e.g., Lazarus et al. 2011), and the proximity to tidal inlets and effects of wave-shadowing by promontories tend to be localized (e.g., Barkwith et al. 2014). If the factors driving cross-shore barrier migration vary alongshore, consequent alongshore variations in migration rates will feed back upon the evolution of plan-view coastline shape, which partly drives cross-shore migration. Thus, to fully address coastline and barrier evolution, models focusing primarily on cross-shore processes/profiles need to be coupled to models addressing alongshore-extended domains.

However, despite the potential effect of alongshore variations in driving factors on cross-shore migration rates, gradients in net alongshore sediment transport tend to smooth most coastlines and therefore to homogenize shoreline-change rates (Valvo et al. 2006)—and migration trajectories—alongshore. We can consider the variables in the cross-shore focused analysis presented here to represent alongshore averages (i.e., substrate composition, substrate slope, sediment gain/loss rate, and back-barrier deposit composition; e.g., Cowell et al. 2003; Moore et al. 2010). Therefore, the main insights from the simplified scenarios considered in Sects. 3–6 likely apply to actual coastlines broadly, as tendencies guiding long-term barrier evolution. In particular, if RSLR is sufficiently gradual and substrate composition and slope sufficiently uniform, we can expect that after an amount of RSLR commensurate with the height of the profile (Wolinsky and Murray 2009), the geometry of the cross-shore profile will tend to adjust in a way that leads the migration trajectory to become approximately parallel to the slope of the substrate. If the slope of the substrate is approximately spatially uniform, then this slope corresponds to the slope of the landscape the barrier is migrating across, in the very long term. This tendency means that the slope of the landscape ultimately dictates the rate at which the shoreline (and barrier) moves landward as sea level rises. From a geological perspective, this result seems intuitive—if sea level rises far enough, how could the slope of the landscape not determine future coastline positions in the very long term? However, this intuitive, long-term result can seem to be at odds with shorter-term predictions based on the analytical framework of the generalized Bruun rule (e.g., Wolinsky and Murray 2009). The analysis recapitulated here shows how the very long-term intuition is consistent with the analytical framework (e.g., Figs. 5 and 6, and Eqs. 3 and 6).

Thought experiments analogous to those presented here lead to complementary insights for coastline types other than barriers. For example, if the substrate (i.e., landscape) slope is steeper than the slope of the shoreface, and sea level is rising, a cliffed coastline results (Wolinsky and Murray 2009). In addition, after sea level has risen far enough (commensurate with the height of the profile), the height of the cliff will adjust toward a steady-state value—a value that produces a migration trajectory parallel to the landscape (Eq. 6, where H_{eff} represents the height of the shoreface plus the cliff height). Thus, whether a barrier or rocky coastline develops depends on the slope of the landscape (averaged over a sufficient scale). Early numerical experiments using the Shoreface Translation Model (Roy et al. 1994) imply these

conclusions, which are verified and explained by analytical modeling (Wolinsky and Murray 2009) and graphical/geometric framework presented here. Additionally, if back-barrier narrowing leads to a barrier welding to the mainland (Sect. 6.3), the cross-shore extent of overwash deposition will become limited by the space available (rather than maintaining a constant value related to the strength of the largest characteristic storms, as we have assumed in the rest of the chapter). As long as the shoreline migration-trajectory slope differs from the substrate slope, the cross-shore extent of overwash deposition will change over time. Consequently, the effective length of the profile, and therefore the migration trajectory, will change over time. In this case, thought experiments analogous to those presented here demonstrate that the migration trajectory will ultimately adjust to parallel the substrate slope, as in the previous cases.

In Sects. 3–6, we presented theoretical analyses, meant to explore the tendencies for long-term barrier evolution that geometry and conservation of mass impose. Although these tendencies will never be exactly manifest on actual barriers, which are also affected by spatial/temporal variations in substrate slope and composition (as well as other factors discussed in Sect. 6 and 7), the relevance of these long-term tendencies could be tested by strategic comparison with large-scale stratigraphic evidence. For example, if in the long term a barrier migration trajectory adjusts to approximately parallel the substrate slope, the condition of the substrate over which the barrier has migrated should depend on the sediment budget (averaged over the long term): If the sediment budget is balanced (i.e., no net sediment gain or loss from outside the cross-shore profile), the substrate should (on average) neither be eroded by the passage of the barrier or covered with barrier-related sediments (Fig. 5c, extrapolated further in time). If a net sediment loss exists (e.g., from a gradient in net alongshore sediment transport), the substrate should exhibit an erosion surface—a "transgressive ravinement surface" (Fig. 6C)—and if a net sediment gain exists (e.g., from a gradient in net alongshore sediment transport or onshore sediment flux from a shallow continental shelf), a sheet of shoreface sediment should remain on top of the substrate as the barrier migrates past.

The long-term analysis we have focused on, which involves a constant time-averaged profile shape, excludes dynamics that drive important variations in barrier-profile shape and barrier response to climate change on human timescales, including cycles of dune destruction (during major overwash or inundation events) and dune growth (e.g., Houser et al. this volume)—as well as associated longer-term shifts between high- and low-island states related to recently illuminated barrier bistability (Vinent Duran and Moore 2015). In addition, we have neglected the effects of human development and management practices on barriers (e.g., McNamara and Werner 2008; McNamara and Lazarus this volume), which can prevent or change the cross-shore sediment fluxes that drive barrier evolution in our analyses. For example, coastal development and dune maintenance can curtail overwash fluxes and overwash deposition, which can lead to barrier narrowing and ultimately, potentially, drowning (e.g., McNamara and Werner 2008; Magliocca et al. 2011; Lorenzo-Trueba and Ashton 2014; Rogers et al. 2015).

9 Conclusions

Under conditions in which the shape of a cross-shore barrier profile (including the subaerial and subaquesous portions) tends to remain approximately constant, conservation of mass constrains how barriers migrate in response to relative sea-level rise. The factors determining the rate of landward barrier migration, relative to the rate of relative sea-level rise (RSLR), can be understood intuitively as well as expressed analytically. A framework for analyzing this "barrier migration trajectory" (the generalized "Bruun Rule") can be extended to include the effects of: (1) variable composition of the substrate over which a barrier migrates; (2) a loss or gain of sediment from alongshore or the continental shelf; and (3) sediment deposition in back-barrier environments. This analytical framework can be used to address how barrier migration trajectories, and the geometry of barrier systems, tend to evolve over time. The slope of the barrier migration trajectory (i.e., the rate of RSLR divided by the rate of landward migration) tends, in most cases, to approach the slope of the substrate (either evaluated at the landward edge of the barrier, or in the case of back-barrier deposition, at the edge of the back-barrier deposit, if not spatially uniform) over time. If the substrate slope is spatially uniform, a dynamic equilibrium results in which the barrier and back-barrier geometries remain constant, relative to the frame of reference of sea level. The characteristics of the steady-state geometry depend on the sediment loss rate, and on the composition of back-barrier deposits. When substrate slope, substrate composition, or sediment gain/loss rates vary in space and/or time, the steady state is never attained and numerical investigations are needed to address how the constraints of geometry and the conservation of mass influence barrier evolution.

Acknowledgments The authors thank Dylan McNamara and Michael Kinsela for helpful reviews and feedback that assisted in improving this manuscript.

References

Ashton AD, Lorenzo-Trueba J (2018) Morphodynamics of barrier response to sea-level rise. In: Moore LJ, Murray AB (eds) Barrier dynamics and response to changing climate. Springer, New York

Barkwith A, Thomas CW, Limber PW, Ellis MA, Murray AB (2014) Coastal vulnerability of a pinned, soft-cliff coastline. Part I, assessing the natural sensitivity to wave climate. Earth Surf Dyn 2:295–308

Brenner OT, Moore LJ, Murray AB (2015) The complex influences of back-barrier deposition, substrate slope and underlying stratigraphy in barrier island response to sea-level rise: insights from the Virginia Barrier Islands, Mid-Atlantic Bight, U.S.A. Geomorphology 246:340–350. https://doi.org/10.1016/j.geomorph.2015.06.014

Bruun P (1962) Sea-level rise as a cause of shore erosion. J Waterw Harb Div 88(1):117–132

Cowell PJ, Kinsela MA (2018) Shoreface controls on barrier evolution and shoreline change. In: Moore LJ, Murray AB (eds) Barrier dynamics and response to changing climate. Springer, New York

Cowell PJ, Roy PS, Jones RA (1995) Simulation of large-scale coastal change using a morphological behaviour model. Mar Geol 126(1–4):45–61

Cowell PJ, Stive MJ, Niedoroda AW, de Vriend HJ, Swift DJ, Kaminsky GM, Capobianco M (2003) The coastal-tract (part 1): a conceptual approach to aggregated modeling of low-order coastal change. J Coast Res 19(4):812–827

Davidson-Arnott RG (2005) Conceptual model of the effects of sea level rise on sandy coasts. J Coast Res 21(6):1166–1172

Dean RG (1977) Equilibrium beach profiles: US Atlantic and Gulf coasts. Department of Civil Engineering and College of Marine Studies, University of Delaware

Dean RG (1991) Equilibrium beach profiles: characteristics and applications. J Coast Res 7(1):53–84

Dean RG, Maurmeyer EM (1983) Models for beach profile response. In: Komar PD (ed) CRC handbook of coastal processes and erosion. CRC Press, Boca Raton, pp 151–165

Donnelly C, Kraus N, Larson M (2006) State of knowledge on measurement and modeling of coastal overwash. J Coast Res 224:965–991

Duran Vinent O, Moore LJ (2015) Barrier island bistability induced by biophysical interactions. Nat Clim Chang 5(2):158–162

Fearnley S, Miner MD, Kulp M, Bohling C, Penland S (2009) Hurricane impact and recovery shoreline change analysis of the Chandeleur Islands, Louisiana, USA: 1855–2005. Geo-Mar Lett 29:455–466

Fredsøe J, Deigaard R (1992) Mechanics of coastal sediment transport, vol 3. World Scientific, Singapore

Hallermeier RJ (1981) A profile zonation for seasonal sand beaches from wave climate. Coast Eng 4:253–277

Houser C, Barrineau P, Hammond B, Saari B, Rentschler E, Trimble S, Wernette P, Weymer B, Young S (2018) Role of the foredune in controlling barrier island response to sea level rise. In: Moore LJ, Murray AB (eds) Barrier dynamics and response to changing climate. Springer, New York

Lazarus E, Ashton A, Murray AB, Tebbens S, Burroughs S (2011) Cumulative versus transient shoreline change: dependencies on temporal and spatial scale. J Geophys Res Earth Surf 116(F2):2156–2202. https://doi.org/10.1029/2010JF001835

Leatherman SP (1979) Migration of Assateague Island, Maryland, by inlet and overwash processes. Geology 7(2):104–107

Lee GH, Nicholls RJ, Birkemeier WA (1988) Storm-driven variability of the beach-nearshore profile at Duck, North Carolina, USA, 1981–1991. Mar Geol 148(3):163–177

Lorenzo-Trueba J, Ashton AD (2014) Rollover, drowning, and discontinuous retreat: distinct modes of barrier response to sea-level rise arising from a simple morphodynamic model. J Geophys Res Earth Surf 119(4):779–801

Magliocca NR, McNamara D, Murray AB (2011) Long-term, large-scale effects of artificial dune construction along a barrier island coastline. J Coast Res 27:918–930

Marani M, D'Alpaos A, Lanzoni S, Carniello L, Rinaldo A (2007) Biologically-controlled multiple equilibria of tidal landforms and the fate of the Venice lagoon. Geophys Res Lett 34:L11402. https://doi.org/10.1029/2007GL030178

Mariotti G., Fagherazzi S (2010) A numerical model for the coupled long-term evolution of salt marshes and tidal flats. J Geophys Res Earth 115(F1)

McBride RA et al (1992) Analysis of barrier shoreline change in Louisiana from 1853 to 1939. In: Williams SJ et al (eds) Miscellaneous 1-2150-A. U.S. Geological Survey, Reston

McNamara DE, Lazarus ED (2018) Barrier islands as coupled human–landscape systems. In: Moore LJ, Murray AB (eds) Barrier dynamics and response to changing climate. Springer, New York

McNamara, D. E., Werner, B. T. (2008). Coupled barrier island–resort model: 1. Emergent instabilities induced by strong human-landscape interactions. J Geophys Res Earth 113(F1).

Mellett CL, Plater AJ (2018) Drowned barriers as archives of coastal-response to sea-level rise. In: Moore LJ, Murray AB (eds) Barrier dynamics and response to changing climate. Springer, New York

Moore LJ, List JH, Williams SJ, Stolper D (2010) Complexities in barrier island response to sea level rise: insights from numerical model experiments, North Carolina Outer Banks. J Geophys Res Earth 115(F3)

Moore LJ, Patsch K, List JH, Williams SJ (2014) The potential for sea-level-rise-induced barrier island loss: insights from the Chandeleur Islands, Louisiana, USA. Mar Geol 355:244–259

Moore LJ, Goldstein EB, Vinent OD, Walters D, Kirwan M, Rebecca L, Murray AB, Ruggiero P (2018) The role of ecomorphodynamic feedbacks and landscape couplings in influencing the response of barriers to changing climate. In: Moore LJ, Murray AB (eds) Barrier dynamics and response to changing climate. Springer, New York

Ortiz AC, Ashton AD (2016) Exploring shoreface dynamics and a mechanistic explanation for a morphodynamic depth of closure. J Geophys Res Earth Surf 121(2):442–464

Penland S, Sutter JR, Boyd R (1985) Barrier island arcs along abandoned Mississippi River deltas. Mar Geol 63:197–233

Rodriguez AB, Yu W, Theuerkauf EJ (2018) Abrupt increase in washover deposition along a transgressive barrier island during the late 19th century acceleration in sea-level rise. In: Moore LJ, Murray AB (eds) Barrier dynamics and response to changing climate. Springer, New York

Rogers LJ, Moore LJ, Goldstein EB, Hein CJ, Lorenzo-Trueba J, Ashton AD (2015) Anthropogenic controls on overwash deposition: evidence and consequences. J Geophys Res Earth 120(12):2609–2624

Rosati JD, Dean RG, Walton TL (2013) The modified Bruun Rule extended for landward transport. Mar Geol 340:71–81

Roy PS, Cowell PJ, Ferland MA, Thom BG (1994) Wave-dominated coasts. In: Carter RWG, Woodroffe CD (eds) Coastal evolution: late quaternary shoreline morphodynamics. Cambridge University Press, Cambridge, pp 121–186

Sallenger AH Jr (2000) Storm impact scale for barrier islands. J Coast Res 16(3):890–895

Sallenger A, Wright CW, Lillycrop J (2007) Coastal-change impacts during Hurricane Katrina: an overview. In: Kraus N, Rosati JD (eds) Coastal sediments '07: proceedings of the sixth international symposium on coastal engineering and science of coastal sediment processes. American Society for Civil Engineers, Reston, pp 888–896

Stive MJ, De Vriend HJ (1995) Modelling shoreface profile evolution. Mar Geol 126(1–4):235–248

Stockdon HF, Holman RA, Howd PA, Sallenger AH (2006) Empirical parameterization of setup, swash, and runup. Coast Eng 53(7):573–588

Stolper D, List JH, Thieler ER (2005) Simulating the evolution of coastal morphology and stratigraphy with a new morphological-behaviour model (GEOMBEST). Mar Geol 218(1–4):17–36

Storms JE (2003) Event-based stratigraphic simulation of wave-dominated shallow-marine environments. Mar Geol 199(1–2):83–100

Storms JE, Weltje GJ, Van Dijke JJ, Geel CR, Kroonenberg SB (2002) Process-response modeling of wave-dominated coastal systems: simulating evolution and stratigraphy on geological timescales. J Sediment Res 72(2):226–239

Valvo LM, Murray AB, Ashton A (2006) How does underlying geology affect coastline change? An initial modeling investigation. J Geophys Res Earth Surf 111(F2):F02025

Wolinsky MA, Murray AB (2009) A unifying framework for shoreline migration: 2. Application to wave-dominated coasts. J Geophys Res Earth Surf 114(F01009). doi:https://doi.org/10.1029/2007JF000856

Shoreface Controls on Barrier Evolution and Shoreline Change

Peter J. Cowell and Michael A. Kinsela

Abstract Barriers exist in a continuum of forms, which are fundamentally governed by processes that shape the shoreface to determine the envelope available for sediment *accommodation*. This envelope is contained between the shoreface and underlying surface defined by the continental shelf and coastal plain (i.e., the substrate). Barrier form also depends on coastal change that is constrained, following reasonably well-established principles, by the volume and type of sediment *supply* (or loss) and rates of change in sea level that modify the shoreface and associated accommodation potential. While the shoreface is therefore significant to barrier form and behavior, processes that shape the shoreface itself remain poorly understood. In particular, systematic long-term evolution of the shoreface, which is evident in geological data, indicates not only a time-varying morphology, but also a lagged response to environmental change. Such shoreface evolution has implications for barrier evolution (and vice versa). In this chapter, we review (1) relations between shoreface and barrier form, (2) limits to knowledge on shoreface behavior and insights from depositional records from which systematic changes over time can be inferred, and (3) exploratory experiments on the morphodynamic timescale of shoreface change. The third part of the review derives from results of experimental modeling of combined shoreface and barrier evolution constrained by geologic data. The numerical experiments demonstrate that, on intermediate timescales (decades to centuries) that are most relevant to coastal management and planning, adjustments are dominated by sediment exchanges between the beach and shallower portions of the shoreface in response to rapid changes in boundary conditions, especially sea level. Significant morphodynamic hysteresis can be expected from the partial adjustment of lower shoreface geometry during sea-level change,

P.J. Cowell
School of Geosciences, Faculty of Science, The University of Sydney,
Sydney, NSW, Australia
e-mail: peter.cowell@sydney.edu.au

M.A. Kinsela (✉)
School of Geosciences, Faculty of Science, The University of Sydney,
Madsen Building (F09), Sydney, NSW 2006, Australia

Department of Coastal and Marine Science, Office of Environment and Heritage,
59 Goulburn Street, Sydney, NSW 2000, Australia
e-mail: michael.kinsela@sydney.edu.au

L.J. Moore, A.B. Murray (eds.), *Barrier Dynamics and Response to Changing Climate*, https://doi.org/10.1007/978-3-319-68086-6_8

resulting in ongoing barrier evolution and shoreline migration after the stabilization of boundary conditions.

Keywords Climate change • Coastal barrier • Coastal evolution • Encroachment • Lagged response • Morphodynamic hysteresis • Morphodynamic model • Morphologic inheritance • Morphologic-response timescale • Prograded barrier • Sea-level rise • Sediment transport • Sediment-accommodation • Shoreface dynamics • Shoreface geometry

1 Introduction

In this chapter, we extend the examination of shoreface-translation effects on barriers and back-barrier deposits (Murray and Moore this volume) to account for how the shoreface geometry, and time-dependent changes in that geometry (i.e., morphologic response), affect barrier form and behavior. The shoreface refers partly or wholly to the subaqueous surface expression of the barrier front, extending from the landward limit of wave run-up, to a position offshore that is generally considered to define the limit of significant wave influence on seabed morphology. Allowing for time dependence raises questions about the rates and extent of shoreface change on different timescales. We address this issue particularly for the intermediate timescales (decades to a few centuries) that are of greatest relevance in coastal management.

In examining the effects of shoreface geometry, the emphasis is on the barrier *complex* in aggregate. These depositional complexes comprise not only the littoral sediment wedge beneath the shoreface and beach (herein termed the barrier front), but also back-barrier deposits, where present, depending on shoreface-related *accommodation c*ontrols and sediment supply (Fig. 1). Accommodation is a concept drawn from sedimentology (e.g., Swift and Thorne 1991) that we apply to define the

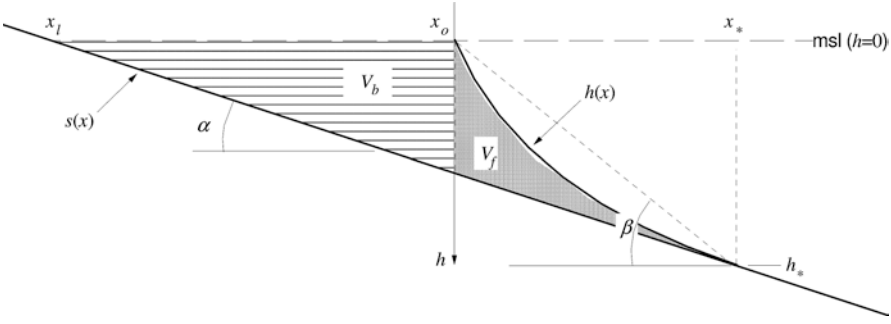

Fig. 1 Simplified definition sketch of potential sediment accommodation with respective volumes, V_f and V_b, for the *barrier front* and *back-barrier*, created by the geometric relationship between the shoreface and substrate underlying the barrier complex

space available for potential deposition within the barrier complex under the prevailing energy regime (Cowell et al. 2003a). The barrier complex is an undifferentiated aggregation of barrier-front and back-barrier deposits, with the latter comprising all depositional environments landward of the beach. A distinction is made here with other chapters in this volume, in which the term back-barrier is restricted to describing all environments landward of the sandy part of the barrier, including dune and washover sands.

In reality, washover is one of the two types of barrier deposits attributable to sand-bypassing from the shoreface to the back-barrier basin, driven by marine flows: the other type being flood-tide delta deposits (Swift and Thorne 1991; Cowell et al. 2003a). The flood tide and waves entering tidal inlets are generally capable of displacing sand much further landward within back-barrier basins (kilometers) than is possible through washover processes, especially for coasts with higher tidal ranges.

During barrier evolution, alongshore migration of tidal inlets, or their intermittent breaching and closure, can make flood-tide delta lobes ubiquitous alongshore behind the barrier, especially during periods of strong sea-level rise when the subaerial extent of transgressive barriers tends to be reduced in width and height. Further landward, on most barrier coasts, back-barrier deposits tend to transition irregularly into finer estuarine lagoonal sediments and fluvial bayhead deltas, with peat deposits on the margins of the mainland where it emerges from beneath the coastal sediments (Roy et al. 1994).

Conceptual aggregation of the fine and coarse deposits (muddy and sandy facies, respectively) into an undifferentiated barrier complex provides for simplification of the principles outlined in this chapter. As in concepts outlined by others (Murray and Moore this volume), our initial work on this subject differentiated between the littoral sand wedge and the back-barrier mud deposits, on the basis of contrasting assumptions about their fate whenever a landward translating shoreface erodes into and reworks these deposits (Cowell et al. 1992, 1995). The assumptions were that the sandy facies are conserved, subject to littoral-transport gradients, while the muddy facies are winnowed away and lost to seaward beyond the retreating shoreface. Such shoreface translation and sediment reworking occur systemically under transgressive conditions (Roy et al. 1994; Murray and Moore this volume).

Subsequently, however, research by others showing that the seabed can be a dominant source of lagoonal mud could no longer be ignored: e.g., mud deposited behind barriers in Holland (Beets et al. 1992, 2000) and in northern Australia (Woodroffe et al. 1989). Relic lagoonal mud buried beneath barriers, and subsequently eroded from the seabed by a retreating shoreface, therefore seems likely in part or whole to be maintained in suspension until advected back through tidal inlets to settle out in the more quiescent lagoonal environments. Contrary to earlier assumptions, therefore, the net effect over time is for lagoonal mud to be volumetrically preserved within the accommodation space created by barriers.

Based on this documented behavior, in later application of shoreface-translation principles to Holocene evolution of barriers on the Netherlands coast (7000–5800 BP), we treated the entire back-barrier, including the sandy facies of washover and flood-tide delta deposits, and muddy facies of the lagoonal basin, as an undifferenti-

ated sediment body (Cowell et al. 1999b). The veracity of this approach was supported by the modeled shoreface translation, which took the transgressive barrier to within 1.5% of its final position on the Holland coast at present, relative to the 80 km over which the barrier retreated in response to post-glacial rising sea level (Cowell et al. 2003b). This final position is evident in preserved barrier deposits that have been cored and radiocarbon-dated (van der Valk 1992).

Of significance to principles on time-dependent geometry of shorefaces, explored in this chapter, the Netherlands modeling entailed progressive growth in shoreface dimensions with sea-level rise (Cowell et al. 2003b). This growth was imposed in recognition of the expanding fetch distances for wave generation that occurred when the initially emergent North Sea floor was progressively flooded during post-glacial sea-level rise. The modeling demonstrated that barrier behavior was entirely regulated by the coupling between the time-varying shoreface dimensions, resulting changes to back-barrier accommodation, and the rate of littoral sediment supply available to occupy this accommodation.

To expedite analysis and modeling, the barrier complex can be simplified in two dimensions (a cross-shore profile), through alongshore averaging of morphologies and facies according to *coastal tract* concepts (Cowell et al. 2003a, b). Gross 2D representation is applicable to both barrier island and bay barrier complexes. In nature, barrier-front sediments not only merge with back-barrier deposits, the sediment mass beneath the shoreface and beach in transgressive barriers are back-barrier deposits, or underlying strata (Thom 1984; Roy et al. 1994). At and immediately beneath the seabed and beach face, however, the barrier-front deposits take on marine sand attributes (e.g., assemblages of marine shells and their fragments) due to shallow reworking by nearshore, surfzone, overwash, and tidal inlet processes (Thom 1984). The three-dimensional distribution of barrier-front and back-barrier sediment facies within barrier systems, due to cross-shore and alongshore energy gradients, can also be aggregated in two dimensions for efficient modeling (e.g., Storms et al. 2002).

The most compelling sign of functional integration for the barrier complex lies in mutual dependence of the barrier front and back-barrier: one cannot exist without the other. More specifically, the location, dimensions, and form of the barrier and back-barrier are mutually dependent (Fig. 2). Although barriers provide a fundamental boundary condition controlling the existence of a lagoon and its associated deposits, the barrier front itself, and its location, depends strongly upon the rate of estuarine infill. With reduced sediment supply to the back-barrier, the littoral sediment wedge is located further landward (Cowell et al. 2003b; Walters et al. 2014), while reduced vertical dimensions of the shoreface also limit the width and potential thickness of back-barrier deposits, reflecting accommodation constraints (Fig. 1). The interdependence is universal, unless sediment bypassing between the shoreface and back-barrier is precluded: e.g., where stable dunes prevent tidal inlet formation and washover processes everywhere along the coast, such as has been the case on the central Netherlands coast since 5800 BP despite ongoing relative sea-level rise (Cowell et al. 2003b).

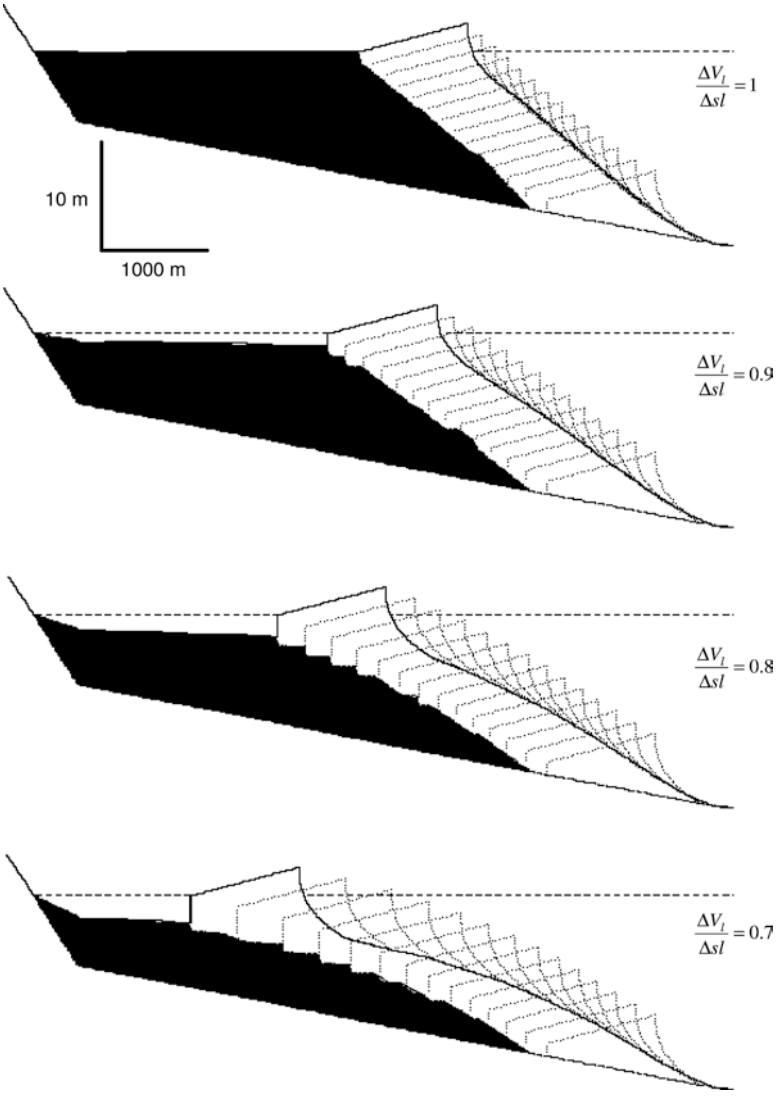

Fig. 2 Mutual dependence of barrier front and lagoon deposition rates, V_l, as a proportion of accommodation created by sea-level rise, Δsl = 1 m per time step for 14 steps; positive sand supply alongshore at $dq_s/dy = -2$ m³/m/year

The purpose of this chapter is to explore the effects of shoreface-related accommodation constraints on the size and form of barriers. The focus is on effects on barrier form, dimensions, and behavior that can be inferred from changes through time in the shoreface geometry. This extends the principles outlined by Murray and Moore (this volume) who show how barriers respond to changes in boundary conditions (principally, sea-level rise and sediment supply) based on the simplifying

assumption of time-invariant shoreface geometry. The assumption of instantaneous and complete morphologic response of the shoreface to changing boundary conditions is likely to be more quantitatively meaningful for simulating deposition at very long timescales (Cant 1991; Nummedal et al. 1993) and allows for analytical solutions to predict shoreline migration (Wolinsky and Murray 2009; Murray and Moore this volume). However, here we relax this assumption to account for the effects on barriers due to systematic changes in shoreface geometry over decades to millennia: i.e., the timescales of greatest relevance to understanding barrier response to climate change. Ashton and Lorenzo-Trueba (this volume) also relax this assumption using a different, complementary approach.

We begin by summarizing axiomatic shoreface-related sediment-accommodation controls on barrier size and form in Sect. 2. From this, a key question of this chapter arises: what potential exists for time-dependent change in shoreface geometry (i.e., morphologic response)? Evidence from geological records and sediment budget analyses indicate that shoreface geometry can evolve systematically over the long term, and that evolution may lag any driving change in system boundary conditions (Cowell et al. 1995, 2001, 2003b; Kinsela et al. 2016).

Unfortunately, as we describe in Sect. 3, little is known about shoreface dynamics that can be used to predict such time-dependent behavior, especially in response to sea-level rise. The main limitations concern the application of sediment-transport theory and observations over timescales of years or more, where cumulative effects of small residual sediment fluxes are of critical importance, but cannot be resolved relative to the error bounds of sediment-transport models. The depositional record, however, contains evidence of shoreface geometry spanning millennia, which may provide an opportunity to downscale inferences on the nature and rate of shoreface evolution over the long term (Cowell et al. 1995, 2001). In Sect. 4, therefore, we explore the sensitivity of barrier and shoreline change to timescale effects in evolving shoreface geometry.

The dependence on timescale of shoreface morphologic response has critical implications for forecasting future barrier response to climate change. The degree of uncertainty that currently exists in probabilistic shoreline change forecasts, chiefly due to our limited understanding of the shoreface (Cowell et al. 2006; Stive et al. 2009), tends to be difficult for decision-makers to manage. While more precise (i.e., seemingly less uncertain), the accuracy of predictions that are based on the commonly applied simplifying assumptions, such as a depth-restricted shoreface response (e.g., closure depth limited to the upper shoreface) or instantaneous adjustment across the entire shoreface domain, may not be acceptable for all settings and forcing scenarios. Thus, timescale effects on changing shoreface geometry will be of critical interest to coastal managers seeking the most accurate representations of future barrier behavior and shoreline change.

As shoreface sediment transport remains so notoriously poorly understood due to observational and theoretical constraints, we use numerical morphodynamic- and morphologic-behavior modeling, grounded in geological evidence of past barrier evolution (e.g., Mellett and Plater this volume) to explore the sensitivity of barrier

form and shoreline change to timescale-dependent shoreface morphologic response. In Sect. 4, we consider the sensitivity of shoreface geometry, and critical shoreface depths, to rates of sea-level change that are consistent with past (late Quaternary) change and projected sea-level rise due to climate change (e.g., IPCC 2013). The premise of the exploratory modeling is that, in many settings, an assumption of time-invariant shoreface geometry may be invalid for these rates of sea-level change. The exploratory modeling highlights challenges in forecasting shoreline change at the intermediate timescales (decades to centuries) that are most relevant to managing and planning for the impacts of climate change on barriers, but also demonstrates opportunities to apply evidence from the depositional records of past barrier evolution to understand and model future barrier-shoreface evolution.

2 Shoreface-Accommodation Controls on Barrier Form and Dimensions

A classification-based approach to the geomorphology and geology of coastal barriers has tended to blind scientists to the possibility of unified principles. A process-based approach ideally should lead more naturally to the development of unified theory: a central tradition in physics. But, research on physics of coastal processes has tended to concentrate on scales much smaller than those characterizing barriers overall. Integrating details of process theory over time and space scales relevant to barrier form and behavior have proven impractical, for reasons given in Sect. 3.

In contrast, the *sequence-stratigraphy* paradigm from sedimentary geology offers a way forward. Despite the arcane terminology attached to this paradigm, it provides, at least, the basis for a unified theory of coastal deposits more relevant to the inherent space-time scales of barrier dynamics. It does so by placing concepts of sediment accommodation and supply at its core (e.g., Curray 1964; Sloss 1962), as expounded more specifically for barriers in texts focusing on shallow-marine deposition (Swift and Thorne 1991), and through *coastal tract* concepts (Cowell et al. 2003a). These principles provide an overarching framework within which the scale hierarchy of processes can be organized, down to details of sediment transport at grain-scale. The framework thereby allows coastal barriers, in all their textbook typologies, to be viewed through unified general principles.

In the specific context of coastal barriers, we can envisage barriers per se to be one realization, a reference form, in a continuum of wave-dominated littoral sediment bodies that can be differentiated simply in terms of their shoreface-related accommodation versus sediment supply (or loss) conditions (Fig. 3). The former controls the potential volume available for deposition, while the latter determines whether sufficient sediments, of a type compatible with the depositional environment, are available for that deposition.

The total marine accommodation potential of barriers (i.e., ignoring their aeolian superstructure; see Houser et al. this volume, Moore et al. this volume, Ruggiero

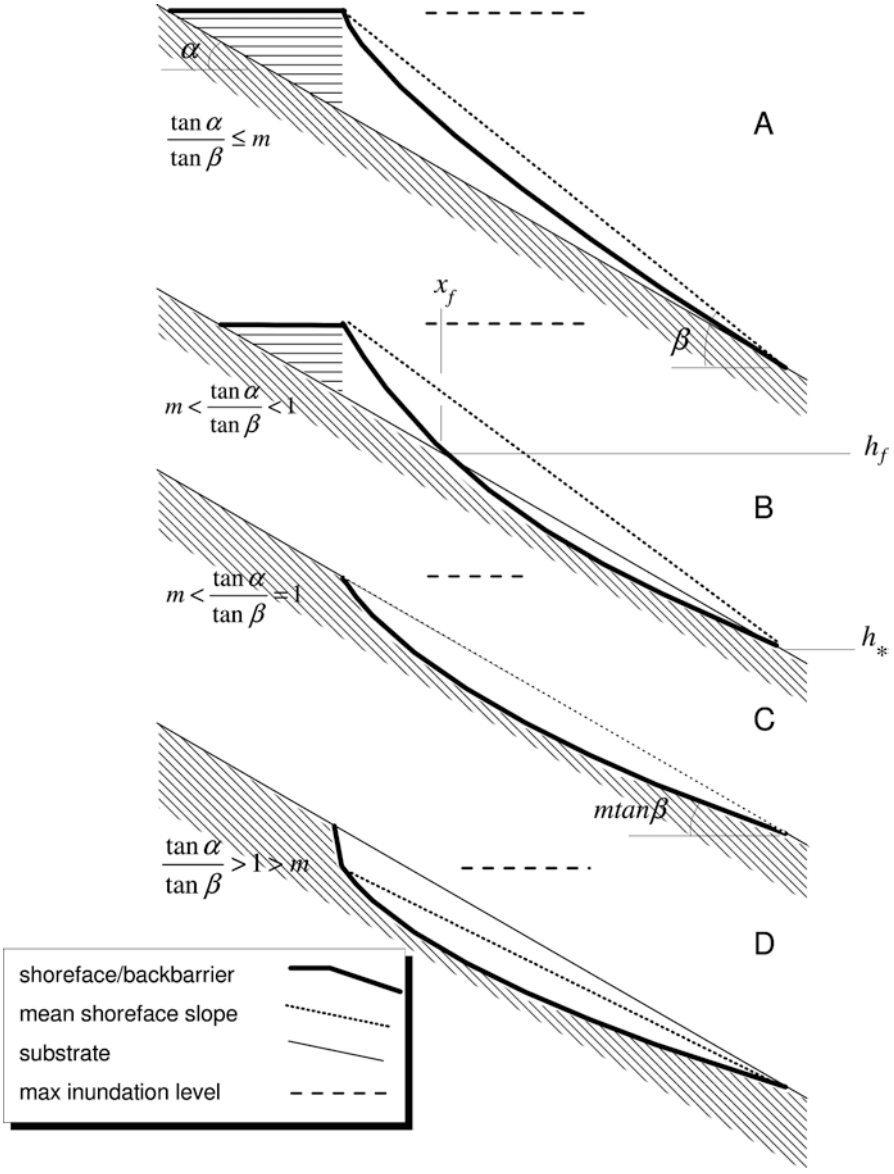

Fig. 3 Continuum of barrier forms and dimensions constrained by controls on shoreface-related accommodation defined by the envelope formed above the substrate to the barrier complex: (**a**) positive accommodation shoreface, extending to the water-depth limit, h_*, and back-barrier; (**b**) *partial encroachment* of the shoreface into the substrate, with mixed (positive and negative) shoreface-accommodation and reduced back-barrier accommodation; (**c**) *full encroachment* of shoreface into substrate with negative accommodation and back-barrier fully truncated by mainland; (**d**) *full encroachment* with cliff formation in friable mainland substrate

et al. this volume for treatment of this realm) is a function of the comparative geometry of the shoreface, $h(x)$, and the underlying surface, $s(x)$, upon which the barrier complex rests (hereafter referred to as the *substrate*):

$$V_{total} = V_f + V_b \tag{1}$$

where V_f and V_b are the constituent accommodation volumes, respectively, of the barrier-front and back-barrier deposits:

$$V_f = \int_{x_o}^{x_*} \left[s(x) - h(x) \right] dx \tag{2}$$

and

$$V_b = \int_{x_o}^{x_l} s(x) dx \tag{3}$$

for the variables defined in Fig. 1, in which x_o is the horizontal origin of the coordinate system, and where $s(x)$ represents the substrate.

Any set of geographically appropriate functions can be applied to calculate these volumes. If no analytic functions are thought appropriate, then digital surfaces measured through hydrographic and seismic surveys are just as applicable. In that case, principles for calculating sediment accommodation from the equations given above can be applied using computational numerical methods rather than analytical solutions: i.e., contention over appropriate choice of morphostratigraphic representation is not an impediment to application of these principles. GIS methods can be applied to spatial data covering the shoreface and substrate along any given tract of coast without alongshore averaging, although the results will, in principle, will be identical to that obtained from computing accommodation volumes after alongshore averaging of data. Therein lies the computational advantage of aggregating the morphology using coastal tract principles (Cowell et al. 2003a).

An alongshore-averaged representation, however, can be adopted to help convey clarity on shoreface-related barrier accommodation principles. For an idealized shoreface, $h = \left(h_* / x_*^m \right) x^m$ of conventional form (e.g., Cowell et al. 1999a), α, the barrier-front volume can be simplified to

$$\begin{aligned} V_f &= x_* h_* - \frac{x_*^2 \tan\alpha}{2} - \int_{x_o}^{x_*} \frac{h_*}{x_*^m} x^m dx \\ &= x_* \left(\frac{m}{m+1} h_* - \frac{x_*}{2} \tan\alpha \right) \end{aligned} \tag{4}$$

and, the back-barrier accommodation can be rewritten only in terms of shoreface variables as

$$V_b = \frac{x_l}{2}\left(h_* - x_* \tan\alpha\right) = \frac{x_*^2}{2}\left(\frac{\tan\beta}{\tan\alpha} - 1\right)\left(\tan\beta - \tan\alpha\right) \quad (5)$$

per unit length of coastline, where $\tan\beta = h_*/x_*$ is the mean shoreface slope. The total barrier accommodation (Eq. 1), therefore, can also be expressed entirely in terms of shoreface variables:

$$V_{total} = x_*\left(\frac{m}{m+1}h_* - \frac{x_*}{2}\tan\alpha\right) + \frac{x_*^2}{2}\left(\frac{\tan\beta}{\tan\alpha} - 1\right)\left(\tan\beta - \tan\alpha\right) \quad (6)$$

Thus, the dimensions and volume of any alongshore-averaged barrier morphology diminish as the mean slope of the shoreface decreases relative to that of the substrate (i.e., $V_{total} \to 0$ as $\frac{\tan\alpha}{\tan\beta} \to 1$, and $V_{total} \to \infty$ as $\alpha \to 0$). The barrier-front-volume also decreases as the shoreface concavity increases (decreasing m): shoreface concavity being classically associated with wave-dominated coasts (Conaglia 1889; Niedoroda et al. 1984; Cowell et al. 1999a). For the case shown in Fig. 1, shoreface concavity does not affect back-barrier accommodation. More generally, however, shoreface concavity needs to be taken into account when considering the continuum of littoral sediment bodies that includes barriers (Fig. 3).

At the seaward limit of the shoreface (x_*,h_*), the slope of the idealized shoreface is $m \tan\beta$. Consequently, three sets of conditions can be defined (Tortora et al. 2009) with respect to sediment accommodation beneath classical wave-dominated shorefaces (i.e., with concave-up surfaces, $0 < m < 1$):

1. Fully positive accommodation, in which $\tan\alpha \le m \tan\beta$ or $\frac{\tan\alpha}{\tan\beta} \le m$ (Figs. 1 and 3a).
2. Mixed (positive and negative) accommodation (with *partialencroachment* into the substrate), in which $\tan\beta > \tan\alpha > m \tan\beta$: i.e., $m < \frac{\tan\alpha}{\tan\beta} < 1$ (Fig. 3b).
3. Fully negative accommodation (*full encroachment*), in which $\tan\alpha \ge \tan\beta$ or $\frac{\tan\alpha}{\tan\beta} \ge 1 > m$ (Fig. 3c, d).

These three conditions relate to "barrier-" and "encroachment modes" defined by Cowell et al. (1995) under transgressive conditions. Of these modes, encroachment involves erosion by the shoreface into the substrate: the available accommodation is negative where this occurs and is thus potentially a sediment source (Fig. 3b–d).

With partial encroachment, accommodation beneath the shoreface is positive at water depths above the point (x_f,h_f,) where the substrate first outcrops midway along the shoreface (Figs. 3b and 4e). This intersection is the toe of the barrier sediment wedge beneath the shoreface and occurs where

$$x_t^m - \frac{x_*^{m-1}}{\tan\beta}\left[h_* + \left(x_t - x_*\right)\tan\alpha\right] = 0 \tag{7}$$

That is, the substrate outcrop point with partial encroachment occurs at x_f,h_f:

$$x_f^m - \frac{x_*^{m-1}}{\tan\beta}\left[h_* + \left(x_f - x_*\right)\tan\alpha\right] = 0, h_* + \left(x_f - x_*\right)\tan\alpha \quad 0 < m < \frac{\tan\alpha}{\tan\beta} < 1 \tag{8}$$

From Fig. 3, it is visually evident that, in the general case, both barrier-front and back-barrier accommodations depend on x_f,h_f rather than x_*,h_*, which is applicable only to the special condition of barriers with full positive accommodation (Fig. 3a). Replacing x_*,h_* with x_f,h_f in Eqs. 2, 5, and 6 provides general applicability in which total accommodation potential for sediment in barriers, excluding aeolian superstructure, depends entirely on both the dimensions and concavity of the segment of shoreface forming the surface of the barrier front.

Equation 6 also is a formal expression of the concept that barrier genesis occurs through mainland-beach detachment (Hoyt 1967). That is, barrier formation requires development of a shoreface with a storm berm at its apex that produces an emergent highpoint in marine deposits offshore from the primal shoreline associated with marine flooding of the land surface.

3 Shoreface Dynamics: The Missing Link

3.1 Sediment-Transport Processes

Although concepts underpinning simplistic models exist to explain shoreface dynamics and form (Niedoroda, et al. 1984; Wright 1995; Cowell et al. 1999a), knowledge is far from definitive. Early theories put forward to explain the typically concave shoreface geometry considered a balance between onshore- and offshore-directed sediment transport (Cornaglia 1889; Fenneman 1902) and uniform wave energy dissipation to the shoreline (Johnson 1919). Collations of upper shoreface geometry measurements by Bruun (1954) and Dean (1977), for example, provided data for the further development of null-point (advection-diffusion) and entropy-maximizing models (Wright 1995). More recent efforts to understand and predict the relationship between sediment-transport processes and shoreface form (and response) have applied energetics-based models to predict wave-driven sediment transport (Aagaard and Sorensen 2012; Ortiz and Ashton 2016) and empirically derived shoreface sediment-transport models (Aagaard and Hughes 2017).

Nevertheless, our understanding of the governing processes that control shoreface morphology remains limited by the accessibility and complexity constraints that impair direct observations of sediment transport on the shoreface. One fundamental aspect that is well-established is that the influence of wave energy on sediment

entrainment and transport decreases with increased water depth across the shoreface, and that relationship has a pronounced influence on the geometry of the shoreface (Niedoroda and Swift 1981; Niedoroda et al. 1984; Wright 1995).

The limits to knowledge are not surprising given practical limitations in measuring sediment-transport processes, especially in wave-dominated shallow-marine environments. Observational records of shoreface evolution are typically restricted to the upper shoreface, where rapid rates of surface response and accessibility allow for surface change to be measured over annual to decadal timescales (Birkemeier 1985; Nicholls et al. 1998). Beyond the upper shoreface, surface response rates are usually too gradual to allow for the detection of surface change at observational timescales, within the envelope of measurement uncertainty. Exceptions to this may occur where the shoreface is sufficiently far from equilibrium, due to either natural or anthropogenic processes, to drive relatively high rates of surface response across the mid to lower shoreface (e.g., Patterson 2012).

On the timescales relevant to barrier formation and evolution (i.e., decades to millennia), the variability in intensity and direction of flows through time, especially for wind waves and swell, is problematic for physics-based explanations and predictions of shoreface dynamics. Detailed measurements of inner-shelf boundary layer flows show that this variability exists even during the course of individual storm events (Wright 1995). Aggregating the effects of such variability on sediment transport over decades to millennia would be challenging enough even if gross transport rates were relevant over the long term, and errors in calculations of gross sediment-transport rates were small over short time intervals (seconds to minutes). The problem is greatly compounded by the fact that it is net transport resulting from tiny residuals between onshore and offshore fluxes, and their gradients, that are relevant for barrier evolution over the long term. The magnitude of these residuals compared to errors in sediment-transport calculations is the real issue of relevance to predicting barrier-shoreface evolution from first principles.

3.2 Geological Evidence

Unfortunately, sediment-transport theory and measurement for combined waves and currents is accurate only to within one to two orders of magnitude (Davies et al. 2002). The error bands are comparable, or much greater than, the actual transport residuals required to produce changes in the shoreface and barriers, which are evident from both historical and geological studies of these sediment bodies. Radiometrically calibrated results of seismic and coring investigations on barriers and shorefaces in southeast Australia (Thom 1984; Roy et al. 1997) have been used to infer magnitudes of time-averaged transport residuals under reasonably stable sea levels and sediment supply conditions that have prevailed over the past few millennia (Cowell et al. 2001, 2003a). These data form the basis for numerical exploration of rates of change in shoreface-related accommodation controls on barrier form and

volumes reported in the following section. An understanding of these rates is critical for sober forecasts of barrier response to sea-level rise, especially for cases in which the shoreface partially encroaches into the substrate.

Encroachment of the lower shoreface into preexisting substrate has been demonstrated as a primary source of sediment supply for barrier progradation in southeast Australia and elsewhere (Roy et al. 1994; Cowell et al. 1995, 2001, 2003b; Kinsela et al. 2016). The sedimentology and radiometric age structures of barriers and their shorefaces in southeast Australia also reveal that outcropping of the substrate on the lower shoreface ($m < \tan \alpha / \tan \beta < 1$) is not only common, but is the result of the evolution in shoreface geometry over the past 6000 years of roughly stable sea level (Thom and Roy 1985). Shoreface sand supply has ensued over millennia of near stable sea level in some cases, or in the case of the central Netherlands barrier coast, even with steadily rising relative sea level, on the order of 5 m during the past 5000 years (Cowell et al. 2003b). Thus, shoreface geometry not only varies geographically along many coasts, in ways that are not yet well-understood, it also changes systematically at long timescales (millennia), even under stable boundary conditions.

The depositional records of coastal barriers may preserve detailed histories of shoreface evolution, indirectly in the gross dimensions and morphology of the barrier, and directly as buried paleo-shoreface reflector surfaces, which can be mapped using sub-surface imaging techniques such as ground-penetrating radar and high-resolution seismic reflection (e.g., Roy et al. 1997; Fig. 4). Both indirect and direct lines of evidence can be used to interpret coupled barrier-shoreface evolution where the geochronology of the barrier is known. Recent advances in geochronology techniques (e.g., optically stimulated luminescence) and the resolution of sub-surface imaging have revealed the depositional records of prograded coastal barriers in unprecedented detail, enabling detailed reconstructions of paleo-depositional controls and barrier deposition, and the integration of barrier evolutionary processes across observable and long-term (millennial) timescales (e.g., Goodwin et al. 2006; Tamura 2012; Dougherty 2014; Costas et al. 2016; Oliver et al. 2017). In settings where the prevailing depositional controls are known or can be approximated, these records offer the most promising insights to the process and timescales of coupled barrier-shoreface evolution.

However, the interpretation of geological evidence alone often tells only part of the evolutionary story, as the spatial and chronological precision necessary to form detailed reconstructions of lower shoreface evolution in particular may still exceed the range and resolution of available techniques. Furthermore, shoreface evolution involves sediment transfers between the upper and lower shoreface (Cowell et al. 2003a), and usually only the region that experienced accretion (as opposed to erosion) is preserved in the depositional record. An exception is where shoreface lowering can be estimated from the thickness of a coarse sediment lag, which is a condensed deposit derived from the underlying parent material containing a measurable concentration of coarse clasts (Cowell et al. 1995, 2001). In principle, this potential line of evidence exists wherever the shoreface encroaches into the substrate. In practice, however, the method requires the presence of a suitable coarse

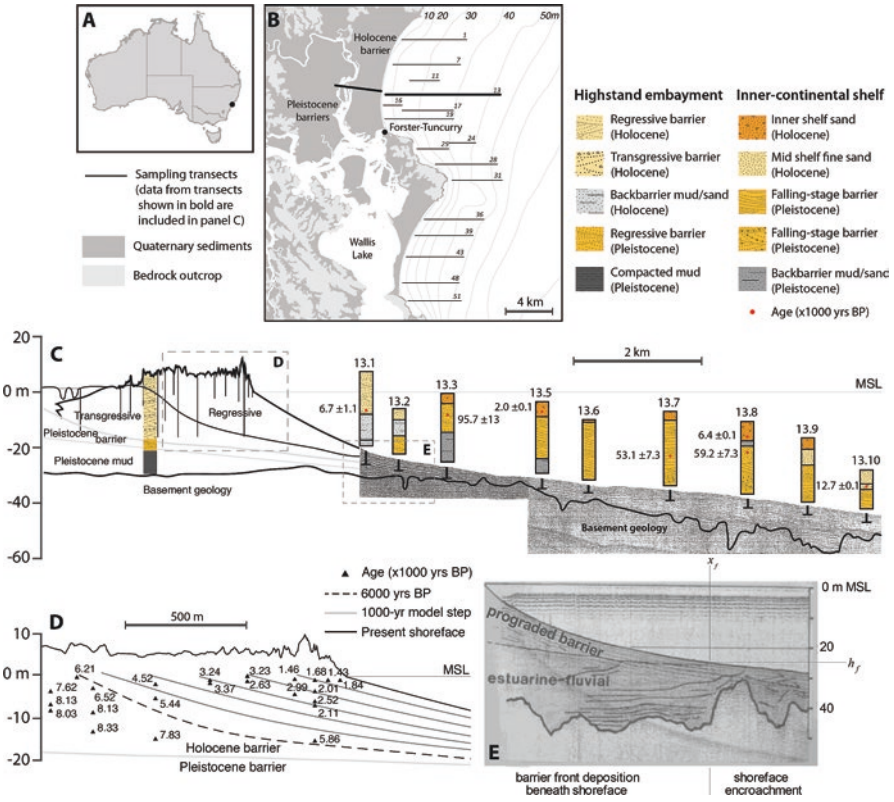

Fig. 4 The Forster-Tuncurry coastal barrier systems and geological data referred to in the text. (**a**) Location in southeastern Australia. (**b**) The northern embayment features a horizontally stacked series of Pleistocene and Holocene barriers, which have been sampled along onshore and offshore transects using coring, geochronology, and sub-surface imaging (ground-penetrating radar and seismic reflection) techniques (Roy et al. 1997). (**c**) The Holocene barrier complex includes a core of transgressive facies that is buried beneath the sand wedge of regressive facies. The Holocene barrier overlies Pleistocene barrier sand, and the regressive facies blends into a coarse inner-shelf sand sheet in around 24 m water depth. (**d**) The radiocarbon geochronology of the Holocene barrier shows a relatively steady rate of progradation from over 6000 years ago to present. Barrier progradation during the past 6000 years was simulated using the BARSIM model, as shown by 1000-year (1-kyr) increment model shoreface profiles. (**e**) Enlarged seismic record showing the toe of the barrier-front sediment wedge at its intersection with the regions of positive shoreface accommodation and encroachment into the substrate further offshore (x_f, h_f). The regressive barrier deposits below mean sea level (MSL) are shoreface facies, because the barrier has prograded through the late Holocene, following the termination of post-glacial sea-level rise along this coast. Backbarrier facies would otherwise be expected on the retrogradational shoreface of a transgressive barrier. Adapted from Kinsela et al. (2016) and Roy et al. (1997)

fraction within the finer sand matrix of the underlying parent material, such as along much of the coast of southeast Australia (Fig. 4). If, for example, the substrate comprises aeolian sand deposits, coarser clasts are most likely to be absent.

3.3 Knowledge Gaps

Reflection on the geological evidence and the uncertainties in shoreface dynamics raises the key question: what will really happen to shorefaces as sea-level rise continues into the future? It seems contrary to reason that partially encroached shorefaces (e.g., Fig. 4) should suddenly begin sequestering sand from adjacent barriers as sea level rises, as is presupposed by Bruun's (1962) model, instead of continuing to supply sand to the barrier as has been the case for millennia. Rather, lower shorefaces on some coasts are likely to continue supplying sand to adjacent beaches despite rising sea level, at least up until the sea attains some elevation high enough for the supply process to cease. On low-gradient coasts, barrier rollover processes such as overwash can maintain stable shoreface geometry as the barrier migrates over the preexisting substrate without encroachment ($\tan\alpha \leq m \tan\beta$), and without any sediment transfer from the upper to lower shoreface as sea level rises. However, in settings where the shoreface tends to become a sink for beach sand as sea level rises, what rates can be expected for the transfer of sand from the beach to the shoreface, and to what water depths on the lower shoreface?

The principles outlined in Sect. 2 imply that adjustments to shoreface geometry have consequences for barrier accommodation, and thus also for barrier evolution and shoreline change. In the context of predicting barrier response to climate change, the existing limits to knowledge regarding shoreface adjustment in response to sea-level rise include:

1. The total volume of shoreface sediment accommodation generated by sea-level rise;
2. The rate of barrier-shoreface sediment exchange relative to the rate of sea-level rise; and
3. The significance of lagged shoreface response following the stabilization of sea level.

The first of these limits affects accuracy in predicting the ultimate sediment redistribution across the barrier front in response to a recorded or projected sea-level change (and also the total shoreline change commitment associated with shoreface adjustment). This is the least problematic, as geological evidence suggests that the total response can be reasonably well-estimated using shoreface-translation techniques applied to the entire shoreface and barrier, while also taking into account sediment supply (and loss) constituents (Cowell et al. 1995). These shoreface-translation techniques compute the cross-shore sediment balance while accounting for other gains and losses of sediments, including alongshore-transport residuals. However, solving the cross-shore balance only describes the ultimate limits of barrier response and shoreline migration: it does not explicitly incorporate rates or timescale of change.

The second aspect concerns the prediction of shoreline change at an intermediate time during sea-level change: e.g., how far may the shoreline retreat in response to sea-level rise during a civil planning period (e.g., 50 years)? Where applicable, this depends on how much sediment is lost from the barrier to newly generated shoreface accommodation within that time frame, or, how much of the total potential shoreface sediment-accommodation volume is actually filled? This will depend on the rate of sediment exchange between the barrier and shoreface, which is controlled by shoreface sediment dynamics that remain poorly understood. Considering that sea-level rise driven by global climate change is projected to continue beyond the present century (IPCC 2013), addressing this second aspect of uncertainty may be the most useful for managing shoreline change within current lifetimes.

The third limit to knowledge concerns the time required for complete barrier-shoreface response to sea-level change (and the total shoreline change commitment) to be realized and is a product of the first two points above. If an instantaneous response of the entire shoreface to sea-level rise is not feasible, due to the balance between the rate of sea-level rise and the progressive decrease in shoreface sediment-transport rates with increasing water depth, then sediment redistribution and shoreline change must persist for some amount of time following the stabilization of sea level. Therefore, hysteresis must exist if sea-level change is ongoing. Addressing the third limit to knowledge provides an ultimate time horizon for coastal management and planning initiatives, for the case of sea-level stabilization within civil planning periods. This could be realized, for example, in the case of rapid reduction and mitigation of greenhouse gas emissions within the next one or two decades (IPCC 2013).

The fundamental concept to emphasize here is that the spatial scale of morphological change is intimately related to the timescale. This is demonstrated, for example, in long-term shoreface measurement datasets, which show that the depth limit of shoreface morphological change (i.e., the so-called closure depth) increases with the observation timescale (Nicholls et al. 1998). The implication of the morphologic-response timescale is that, if wave-driven sediment transport is the predominant control on shoreface evolution (Niedoroda and Swift 1981), the water depth limit to which the shoreface response to sea-level change is instantaneous (i.e., occurs within an annual timescale) will vary depending on the rate of sea-level change. For example, the limit of shoreface morphological change may become shallower for faster rates of sea-level rise. While surf zone sediment-transport processes may support seabed adjustment at short timescales (seasons to years), beyond the surf zone, rates of shoreface response diminish with wave-driven sediment entrainment and transport toward the seaward limit of the shoreface (at x_*,h_*).

In the context of the impact of climate change on barriers, uncertainty around shoreface response is one of the greatest challenges to research in coastal geoscience, both in terms of difficulty and importance to coastal management. In Sect. 4, we present numerical experiments based on geological data, which demonstrate opportunities to apply depositional records to explore past barrier-shoreface evolution and the future response of barriers to global climate change.

4 Lower Shoreface Change and Barrier Evolution

The large horizontal extent of the lower shoreface, relative to other depositional features of the barrier system, means that minor vertical adjustments in the shoreface surface imply significant sediment exchanges with adjacent sources or sinks (e.g., the barrier complex), with implications for barrier evolution (Cowell et al. 2003a). Systematic changes in shoreface geometry through time (i.e., statistical non-stationarity) may drive barrier evolution without change in boundary conditions (in a static system), or otherwise without variation in the rate of change in boundary conditions (in a stable dynamic system). This implies that barrier evolution may not be directly proportional to a change in boundary conditions (e.g., sea-level rise). In this section, we explore the potential for statistical non-stationarity in shoreface geometry, for rates of sea-level change representative of the late Quaternary and future sea-level rise projections.

Shoreface geometry is "maintained" where rates of morphologic response equal or exceed the rate of sea-level change, and thus shoreface geometry is statistically stationary (Niedoroda and Swift 1981). As such, the majority of shoreline response that is additional to passive inundation during sea-level rise may be associated with morphologic change in that region. To reliably predict barrier evolution and shoreline change at a future point in time, therefore, the limit of shoreface maintenance (i.e., the extent across the shoreface to which geometry is statistically stationary) during sea-level rise must be known. Slower rates of morphologic response across the remainder of the shoreface imply a lesser contribution to sediment exchange between the barrier and shoreface (and shoreline change) from that area during sea-level change. Determining the extent of shoreface maintenance, and the significance of lower shoreface contributions to the barrier sediment budget, requires an improved understanding of depth-dependent shoreface morphologic-response rates relative to projected rates of sea-level rise.

The depth dependence of shoreface morphologic-response timescales (i.e., the time required for complete adjustment to new boundary conditions) is a fundamental consideration in modeling barrier response at the intermediate timescales (decades to centuries) relevant to managing and planning for the impacts of climate change. While idealized barrier behavior can be demonstrated analytically using the simplifying assumption of time-invariant shoreface geometry (Wolinsky and Murray 2009; Murray and Moore this volume), the idealized behavior may only provide a first-approximation of barrier response at intermediate timescales. This is because the simplifying assumption is violated where the rate of relative sea-level rise exceeds shoreface morphologic-response rates, which decrease with increasing water depth. Sensitivity to this factor may have significant effects on predictive models of barrier evolution, because of the relatively large horizontal dimensions of the shoreface (Cowell et al. 2003b).

4.1 Framework for Investigating Shoreface Morphologic-Response Timescales

Fixed (time-invariant) definitions of the shoreface domain, whether based on morphological measurements (Birkemeier 1985; Nicholls et al. 1998), empirical relationships (Hallermeier 1981), or sedimentary evidence (Fig. 4e), are all inflexible for changing boundary conditions (dynamic systems). Empirically derived definitions are biased by relatively short observation timescales and by the relative stability of boundary conditions during the historical period. That is, all historical observations have been made under particular relative sea-level conditions, which are projected to change significantly in the present century due to global mean sea-level rise (IPCC 2013). As an alternative, we use morphologic-response timescale concepts to construct a framework with which to quantify shoreface response to sea-level change.

Long-term observations of shoreface bathymetry change are rare, and thus little is known about the morphologic-response timescales of most shorefaces, beyond what can be gleaned from the modern geometry and sediment distribution. Hallermeier (1981) proposed analytical equations, based on shoreface profile observations, wave climate statistics, and sediment characteristics, to define limits for the upper and lower shoreface or "shoal zone." The inner (d_l) and outer (d_i) shoal zone water-depth limit equations were intended to approximate the annual limit of profile variability (defined by $\delta h < 0.3$ m), and the typical annual limit of significant cross-shore sand transport due to waves, respectively. Hallermeier (1981) reasoned that if d_i captured the effective limit of cross-shore sediment transport at annual timescales, it might represent an appropriate morphological scale for predicting coastal erosion in response to sea-level change, using Bruun's (1962) model. Bruun assumed that sediment flux rates across the shoreface are sufficiently rapid to maintain time-invariant shoreface geometry during sea-level rise and that the shoreface translates upward and landward at the same pace as rising sea level.

Consideration of the above prompts the two key questions that we consider in this section:

1. To what extent may the shoreface respond fully (i.e., "instantaneously" on this timescale) to sea-level rise, for the rates and duration of current global projections?
2. Does partial (sub-instantaneous) shoreface response occur beyond that limit, and if so, what does that mean for barrier evolution and shoreline change in response to sea-level rise?

A more robust conceptualization of instantaneous response is that morphological change in that region is rapid enough to allow the annually averaged shoreface morphology to fully adjust to the annual range in wave conditions: giving rise to the term *active zone* (Stive and de Vriend 1995). Farther offshore, on the lower shoreface, progressively decreasing rates of wave-driven sediment entrainment and transport imply that rates of shoreface adjustment decrease with increasing water depth (Niedoroda et al. 1984; Wright 1995). Shoreface evolution and barrier response during sea-level

change are likely to be sensitive to depth-varying rates of shoreface morphologic response beyond the active zone, because of the large spatial scale of the lower shoreface for typical concave geometry, relative to the upper shoreface and beach.

In modeling the observed evolution of the Holland coast during the Holocene and recent historical past, Stive and de Vriend (1995) reasoned that, at annual timescales, time-invariant shoreface geometry is limited to the active zone, where morphologic-response rates greatly exceed rates of change in forcing. They also reasoned, however, that the active zone should extend deeper across the shoreface for longer observation timescales or reduced rates of change in boundary conditions. Their modeling of recent historical coastal evolution suggested that for short timescales (years to a decade), upper shoreface change and barrier evolution could be reliably predicted on the basis of a static sediment balance. That is, techniques that translate time-invariant shoreface geometry limited to the upper shoreface may yield meaningful predictions. However, without detailed and long-term measurement records across the lower shoreface, appropriate dimensions of the active zone for longer timescales remain elusive.

We borrow concepts from Hallermeier (1981) and Stive and de Vriend (1995) in our framework for investigating shoreface morphologic-response timescales (Fig. 5):

- The *upper shoreface*, which is affected by wave breaking and surf zone processes, extends to a limiting water depth (h_c), beyond which rates of sediment flux and morphological change are too gradual to support instantaneous shoreface response at *annual timescales*;
- The *active shoreface*, which extends to a limiting water depth (h_a) and implicitly includes the upper shoreface, and is characterized as having statistically stationary geometry at the *observation (or simulation) timescale* and for the rates of change in boundary conditions; and
- The *lower shoreface*, which is affected by wave shoaling, extends from the active shoreface limit to a limiting water depth (h_*) beyond which rates of sediment flux and morphological change diminish at negligible rates towards wave base (h_w), where profile response is immeasurable or otherwise insignificant at the *observation (or simulation) timescale.*

The rationale for defining the active shoreface emerges from the traditional perception of the upper and lower shoreface domains as time-independent morphological domains, which does not support a domain that is characterized by statistically stationary geometry (featuring necessarily timescale-dependent dimensions). While the active shoreface may be subject to fluctuating vertical adjustment about a mean profile in response to high frequency variability in boundary conditions, geometry variance is constant about a stationary mean and may be considered noise when modeling barrier evolution at intermediate to long timescales (decades to millennia). As the upper shoreface is characterized by statistical stationarity at annual timescales, the active shoreface limit (h_a) is anticipated to vary between h_c and h_* (Fig. 5).

Beyond h_a, sub-instantaneous response implies that the lower shoreface is characterized by lagged evolution, and the hysteresis is anticipated to increase with depth. The lower shoreface may therefore experience morphological inheritance:

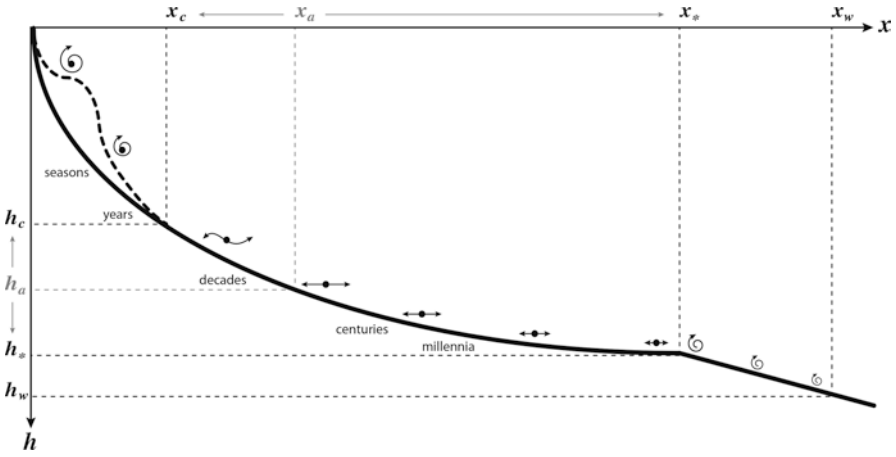

Fig. 5 Definition of shoreface domains in relation to morphologic-response timescales. Moving from wave base (h_w) towards the shore (right to left), waves begin to interact with the seabed as it shoals. Above the lower shoreface limit (h_*), wave action is sufficient to drive cross-shore sediment transport resulting in meaningful seabed change at long timescales (centuries to millennia), with sediment fluxes increasing with decreasing water depth. Above the active shoreface limit (h_a), sediment flux rates are sufficient to support time-invariant shoreface geometry, at the observation or simulation timescale, and for the prevailing rates of change in boundary conditions (e.g., sea level). Above the upper shoreface limit (h_c), sediment flux rates support shoreface response to changing boundary conditions at annual timescales (instantaneous response). As such, $h_c < h_a < h_*$. The dashed line represents the surf zone morphology, which fluctuates at very short timescales (weeks to seasons) in response to time-varying wave conditions, and which can be considered noise in the context of intermediate- to long-term (decades to millennia) barrier-shoreface evolution. Adapted from Kinsela and Cowell (2015)

i.e., the partial adoption of antecedent substrate morphology into the shoreface geometry under conditions of shoreface encroachment (Figs. 3b and 4e). Encroachment involves a sustained surface relaxation toward equilibrium that persists after stabilization of boundary conditions. The relaxation contributes to prolonged shoreline change following sea-level rise, due to ongoing sediment redistribution driven by lagged shoreface response: a phenomenon evident in the depositional histories of barriers in the central Netherlands and southeastern Australia (Cowell et al. 2003b; Kinsela et al. 2016).

The global sea-level highstand experienced during the late Holocene means that many barriers have been subject to stable or only subtly changing (in the case of subsidence or tectonics) sea level during that time, relative to the rapid sea-level rise experienced in the early Holocene. The principles outlined above, determined from past behavior, provide insights into future response. At intermediate (decadal to centennial) to long (centennial-millennial) timescales, the upper shoreface can be anticipated to respond "instantaneously" (i.e., at annual timescales) to sea-level rise, while the lower shoreface can be anticipated to respond at progressively reduced rates with increasing water depth. However, the sensitivity of active shoreface dimensions and depth-dependent rates of lower shoreface response, to the rate of sea-level change, remains largely unknown. The remainder of this chapter explores this relationship through experimental simulations.

4.2 Exploring Shoreface Response to Sea-Level Change

Morphologic- and morphodynamic-behavior models provide a means to explore coupled barrier-shoreface evolution at the intermediate to long timescales of interest here, without a complete understanding of shoreface sediment-transport processes. Such models use behavior rules and lumped parameters to describe the morphologic response to changing boundary conditions, without simulating the physics of shoreface sediment transport (Cowell et al. 1995; Storms 2003; Stolper et al. 2005; Moore et al. 2010; Lorenzo-Trueba and Ashton 2014). We use a morphodynamic-behavior model and a detailed geological dataset from southeastern Australia (Fig. 4) to resolve the shoreface evolution that drove the deposition of a Holocene prograded barrier. We then apply the model to explore shoreface response to rates of sea-level change experienced during the late Quaternary and projected in response to present climate change.

The BARSIM model applied here uses computationally efficient process-response functions to simulate erosion and deposition across the barrier and shoreface, and through time, the formation of sedimentary strata (Storms et al. 2002; Storms 2003). Time-averaged sediment transport and morphologic evolution are described by behavior rules that control depth-dependent rates of shoreface erosion and grain-size-dependent sediment travel distances. The model is particularly suited to investigating shoreface response to sea-level change, because shoreface morphology evolves freely through depositional interactions between the erosion and sedimentation functions.

Behavior models can be calibrated using depositional records of past barrier evolution to ensure that the simulated rates of morphologic evolution reflect the natural setting. We calibrate the shoreface-erosion efficiency parameter in BARSIM using the dimensions and geochronology of the Holocene prograded barrier at Tuncurry in southeastern Australia (Fig. 4), through inverse simulations to reproduce the observed barrier dimensions and age structure (Kinsela and Cowell 2015). The radiocarbon geochronology indicates relatively consistent rates of progradation over the past 6000 years (Fig. 4d), despite relatively stable late-Holocene sea levels in this region. Sensitivity testing was carried out to assess the feasibility of possible sediment supply scenarios, based on detailed geological investigations of the barrier complex and adjacent depositional features (Roy et al. 1994, 1997). The scenario featuring a dominant sand supply from the shoreface to the barrier, with a secondary alongshore sand supply, was the only scenario that generated simulated barrier-shoreface morphology, and barrier geochronology, consistent with the geological evidence (Kinsela et al. 2016).

We apply the calibrated model in a series of hypothetical experiments to investigate shoreface morphologic-response timescales. The experiments consider the evolution of shoreface geometry in response to steady rates of sea-level change (0.5, 1, 2.5, and 5 mm/year) across a linear substrate. To isolate the simulated morphologic response to sea-level change from any influence from the initial shoreface geometry, which was equivalent to the modern shoreface geometry at Tuncurry

(Fig. 4c), the experiments simulate falling sea level across a linear continental shelf substrate with a slope consistent with the gradient of the lower shoreface at Tuncurry (0.15°). This approach removes any potential for morphological inheritance of the initial substrate into the evolving shoreface geometry, which may occur where substrate morphology is variable and the rate of sea-level change exceeds morphologic-response rates (i.e., beyond the active shoreface). Aside from sea level, all model variables and parameters are held constant throughout the simulations and the sediment budget is balanced, such that there are no net gains or losses.

Normalized shoreface geometries derived using a moving reference frame show the simulated shoreface evolution during translation across the linear continental shelf substrate, in response to sea-level change at constant rates of 0.5, 1, 2.5, and 5 mm/year (Fig. 6a-d). The total adjustment from the initial shoreface geometry (black line) to the final geometry (red line) is shown, along with ten equivalent sea-level change increments between each scenario (gray lines). The normalized shoreface geometries adjust for the relative vertical adjustment due to sea-level change and horizontal translation due to sediment redistribution, enabling the visualization and analysis of shoreface geometry alone. Divergence between the normalized profiles within each simulation indicates the depth at which shoreface maintenance (time-invariant geometry) ceased, based on the model parameterization and simulated rate of sea-level change. Seaward of the divergence, the rate of sea-level change exceeds the threshold sediment flux and morphologic-response rate required to maintain stable shoreface geometry. Therefore, the divergence point also marks the depth limit of the active shoreface (h_a) in each scenario (Fig. 6).

From more than 30 years of deep-water wave measurements at Crowdy Head (40 km north-east of Tuncurry), the annual mean significant wave height (H_s) at Tuncurry is 1.6 m ($\sigma = 0.65$ m). Using Hallermeier's (1981) approximation for the inner shoal zone depth limit ($d_l \approx 2H_s + 11\sigma$), or the limit of significant (i.e., $\delta h > 0.3$ m) morphological change at annual timescales, $d_l = 10$ m at Tuncurry. Similarly, using Hallermeier's empirical equation for the outer shoal zone depth limit (d_i), or the limit of significant cross-shore wave-driven sediment transport at annual timescales, $d_i = 35$ m at Tuncurry. In Fig. 6, h_c and h_* are defined using the d_l and d_i values as calculated for Tuncurry, respectively. The question then arises, how to define the active shoreface depth limit (h_a) to distinguish between time-invariant and time-varying shoreface geometry?

A pragmatic approach to objectively determine h_a between the simulations is to use a fixed shoreface adjustment threshold. While Hallermeier's shoal zone depth limits were devised for annual timescales, they are often applied as time-independent limits of the upper and lower shoreface. Hallermeier's empirical equations for d_l were intended to estimate the depth beyond which $\delta h < 0.3$ m at annual timescales. In contrast, using a fixed shoreface adjustment threshold (e.g., $\delta h > 0.3$ m) to detect morphologic response between initial and final shoreface geometries in the simulations (Fig. 6), provides a means to identify h_a that implicitly accounts for variation in the rate of sea-level change between the experiments. Applying that threshold to the simulated shoreface geometry, the active shoreface depth limit (h_a) decreases (i.e., becomes shallower) for increasing rates of sea-level change. That is, the measured h_a in the

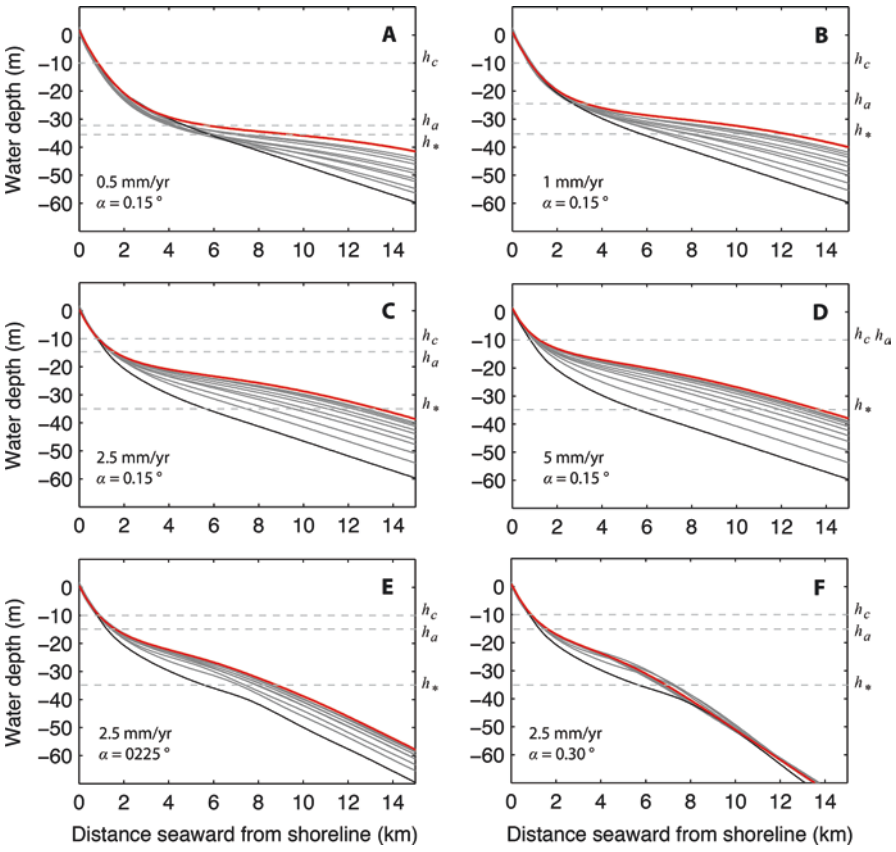

Fig. 6 Normalized shoreface morphology from numerical simulations exploring the influences of the rate of sea-level change and substrate slope on shoreface geometry. Panels **a**–**d** consider increasing rates of sea-level change from 0.5 to 5 mm/year, for shoreface translation across a linear substrate of slope 0.15°. Panels **e** and **f** consider a rate of sea-level change of 2.5 mm/year (as in **c**), for shoreface translation across linear substrate slopes of 0.225° and 0.3°, respectively. The initial (black line) and final (red line) shoreface geometry is shown with intermediate geometries corresponding to 8-m sea-level change increments (gray lines). The upper (h_c), active (h_a), and lower (h_*) shoreface limits are shown for each case. Adapted from Kinsela and Cowell (2015)

simulations was 32, 25, 15, and 10 m, for increasing rates of sea-level change of 0.5, 1, 2.5, and 5 mm/year, respectively (Fig. 6a–d). Based on the model parameterization and rates of sea-level change considered, therefore, h_a decreased from the vicinity of the lower shoreface depth limit (h_*) to the upper shoreface depth limit (h_c) for this setting, as defined using Hallermeier's (1981) empirical shoal zone equations.

Simulations were also carried out to explore the sensitivity of shoreface evolution to the substrate slope. Specifically, the experiment featuring a 2.5 mm/year rate of sea-level change (Fig. 6c) was repeated with linear shelf gradients of 0.225° and 0.3° (compared to 0.15°). The results suggest that both the depth limit and geometry of the active shoreface are insensitive to the substrate slope within the representative

range for this region. That is, h_a remains unchanged between panels c, e, and f in Fig. 6. However, the geometry of the lower shoreface (spanning h_a to h_*) is observed to contract for steeper substrate slopes, meaning that the cross-shore extent becomes reduced. This is to be expected, as h_* defined using Hallermeier's outer shoal zone limit (d_i) equation varies with the wave climate and sediment characteristics only, which were consistent between all simulation experiments.

Comparison between the simulations shown in Fig. 6 demonstrates that while active shoreface geometry may be independent of the preexisting substrate, lower shoreface evolution is sensitive to the preexisting substrate, and thus lower shoreface geometry in modern settings may reflect the preexisting substrate. In the context of barrier response to climate change, this suggests that morphological inheritance may persist across the lower shoreface, where the rate of sea-level rise exceeds depth-dependent residual sediment flux and morphologic-response rates. Furthermore, the reduced extent of the lower-shoreface encroachment zone in steeper shelf settings suggests that in such settings, depth-dependent lower shoreface response may be of less significance to the coastal sediment budget during sea-level rise.

4.3 Implications for Barrier Response to Climate Change

The exploratory simulations described above provide some interesting insights regarding the potential significance of depth-dependent lower shoreface response to barrier evolution and shoreline response to present and future sea-level rise. Contraction of the active shoreface from the vicinity of h_* to h_c for increasing rates of sea-level change, from 0.5 to 5 mm/year, suggests that the active (time-invariant) shoreface encroachment zone, which represents most of the sediment transfer between sub-aerial barrier and shoreface during sea-level change, should decrease as the rate of sea-level rise accelerates. On the other hand, the lower shoreface, which is characterized by depth-dependent morphologic-response rates, morphological inheritance, and lagged behavior, expands as the rate of sea-level rise accelerates. The simulations thus demonstrate the potential for increasing hysteresis in the barrier-shoreface system with accelerating sea-level rise.

This raises an important question: how well do barrier response models that are based on time-invariant shoreface geometry assumptions reflect sediment budget considerations raised by an active shoreface that varies in dimensions with change in the rate of sea-level rise? Considering the projected acceleration in sea-level rise through the present century and beyond (IPCC 2013), it may be expected that such models will under- or over-predict shoreline change, depending on the shoreface depth to which time-invariant geometry is assumed (the so-called closure depth) and the nature of time-varying h_a in reality.

To investigate this, we present results from a morphologic-behavior model (Cowell et al. 1995), which compare the influence of time-invariant and time-varying active shoreface dimensions on predicted shoreline change at Tuncurry

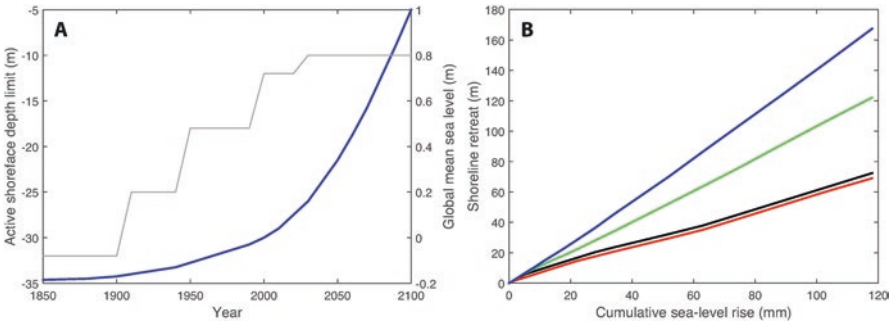

Fig. 7 Comparison of shoreline retreat predictions for the period 1850–2100 using a geometric shoreface translation model with fixed (time-invariant) and dynamic (time-varying) active shoreface dimensions. Panel **a** shows the sea-level rise scenario (blue, right axis) and the dynamic active shoreface depth limit (gray, left axis); panel **b** shows predicted shoreline retreat based on fixed active shoreface limits of 10 m (red), 25 m (green), and 35 m (blue), and based on the time-varying active shoreface limit described in **a** (black)

(Fig. 4), in response to recorded and projected sea-level rise over the period 1850–2100 attributed to global climate change. The model simulates shoreface encroachment and shoreline change relative to a modern dune-scarp position at Tuncurry, adjusted to account for the observed historical sea-level rise. The historical global mean sea-level rise applied in the model was from Church and White (2011), while the projected sea-level rise was the Intermediate scenario of Sweet et al. (2017). Their Intermediate scenario features a relatively modest acceleration in sea-level rise through the present century, resulting in global mean sea level rise of 1 m at 2100, relative to the year 2000 (Fig. 7a). The scenarios presented by Sweet et al. (2017) are based on sea-level rise projections from IPCC (2013), which have been updated to reflect recent advances in scientific understanding of accelerated ice losses. It should be noted that the Intermediate scenario of Sweet et al. (2017) lies within a range of possible scenarios for this century and beyond, which result in projected global mean sea-level rise at 2100 between 0.3 m (no acceleration) and 2.5 m (rapid acceleration).

We apply the morphologic-behavior model with time-invariant shoreface geometries that reflect the present-day shoreface at Tuncurry. We first carry out separate simulations with fixed active shoreface depth limits (h_a) of 10, 25, and 35 m. The simulations compare predicted shoreface encroachment and shoreline retreat, if the active shoreface extends across the upper shoreface ($h_a = h_c = 10$ m), to a position midway across the shoreface ($h_a = 25$ m), or across the full extent of the shoreface ($h_a = h_* = 35$ m). In a separate experiment, we vary h_a throughout the simulation reflecting change in the rate of sea-level rise. Based on the simulation results shown in Fig. 6, we decrease h_a from 32 m to 10 m throughout the simulation, as sea-level rise accelerates through the simulation period from 0.5 to 15 mm/year (Fig. 7a). We limit contraction of the active shoreface to $h_a = h_c = 10$ m, even as the rate of sea-level rise exceeds 5 mm/year (beyond 2010), in recognition that, by definition, the upper shoreface responds to variation in boundary conditions at annual timescales

(i.e., instantaneously). While there likely exists a threshold rate of sea-level rise, beyond which instantaneous shoreface response retreats into the surf zone, the identification of that threshold is beyond the scope of our simulations.

As anticipated, variation in the active shoreface dimensions has a profound influence on the predicted shoreface encroachment and associated shoreline response to sea-level rise. At 2100, the predicted shoreline retreat in response to the sea-level rise scenario, for fixed h_a values of 10, 25, and 35 m, was 69 m (red line), 122 m (green line), and 167 m (blue line), respectively (Fig. 7b). The predicted shoreline retreat based on time-varying h_a proportionate to the rate of sea-level rise (Fig. 7a) was 72.5 m as indicated by the black line (Fig. 7b). The similarity between predictions based on time-varying active shoreface dimensions and an active shoreface restricted to the upper shoreface ($h_a = h_c = 10$ m) emerges from the fact that the vast majority of sea-level rise in the 1850–2100 scenario occurs after 2025, when the accelerating rate of sea-level rise exceeds 5 mm/year, and thus h_a in our model converges on h_c (Fig. 7a). The result suggests that $h_a = h_c$ may be a reasonable assumption for predicting shoreline retreat driven by shoreface encroachment in response to accelerating sea-level rise within the present century, based on our model parameterization derived from the simulations presented in Fig. 6. The result is consistent with previous suggestions that lower shoreface response timescales may be on the order of millennia (Stive and de Vriend 1995).

An interesting and unanticipated implication of the dynamic shoreface experiment, in which h_a converges on h_c, is the prospect of an enhanced sand supply from the shoreface to the barrier, upon the slowing and stabilization of sea-level rise. That is, if shoreface encroachment was largely restricted to above h_c for the rest of this century, a geometric inflection may develop in the shoreface beyond h_c. Perhaps contrary to intuition, the effect of this on barrier sediment budgets could be most pronounced in lower gradient settings, because of the higher rates of shoreface translation associated with sea-level change across lower gradient substrates (Roy et al. 1994). The outcome would be a mid-shoreface sand body that could provide an onshore-directed sand supply upon the stabilization of sea-level rise, as the lagged response of the lower shoreface acts to reduce system hysteresis. This hypothesized response would be comparable to the shoreface evolution that supplied barrier progradation at Tuncurry following Holocene post-glacial sea-level rise (Kinsela et al. 2016).

The simulations described in this section have explored the sensitivity of barrier evolution and shoreline change to the relationship between shoreface morphologic-response timescales and the rate of sea-level change, which emerges from depth-dependent residual sediment flux and morphologic-response rates. The findings raise questions regarding the balance between barrier evolution and shoreline change driven by "instantaneous" barrier-shoreface sediment transfers during sea-level rise, and lagged sediment transfers resulting from system hysteresis upon (and following) sea-level stabilization. While these questions remain difficult to resolve due to the limited observation and knowledge base on shoreface dynamics, the experiments highlight the potential sensitivity of barrier evolution and shoreline change to the nature of the acceleration and stabilization of sea-level rise over the

present century and beyond, not simply the magnitude of sea-level rise at the end of a particular civil planning period (e.g., 2100).

The findings also hint that the actual response of barriers and shorelines upon the stabilization of sea-level rise may be sensitive to multi-year to inter-decadal fluctuations in wave climate. For example, a constructive wave climate may moderate shoreline retreat through enhanced sand supply from the shoreface to the barrier, while a destructive wave climate could result in the redistribution of a mid-shoreface sand body across newly generated accommodation space on the lower shoreface. Therefore, even if $h_a = h_c$ is an appropriate assumption for predicting shoreline response to sea-level rise due to instantaneous barrier-shoreface sediment transfers, it implicitly ignores the potential for sustained barrier evolution and shoreline change, driven by lagged lower shoreface response beyond the slowing or stabilization of sea-level rise. This highlights the need for further development of predictive models to account for the sensitivity of barrier-shoreface response to variation in the rate of sea-level rise over the coming decades and centuries.

5 Conclusions

In this chapter, we have reviewed barrier evolution and shoreline migration driven by shoreface response to sea-level change, and by lagged shoreface evolution following the stabilization of boundary conditions caused by morphodynamic hysteresis that emerges from protracted morphologic-response timescales across the lower shoreface. The primary conclusions drawn from the review are as follows:

1. Controls on shoreface-related accommodation constrain barrier form and dimensions, which means that adjustments in shoreface geometry over time necessarily cause changes in the associated barrier complex and barrier shoreline location.
2. Time lags exist in shoreface adjustment to changes in boundary conditions, such as sea-level rise, due to increasingly long morphologic-response timescales across the lower shoreface. The hysteresis is especially significant on intermediate timescales of decades to centuries, which are of most relevance to planning for and managing barrier evolution and shoreline migration in response to climate change.
3. Present limits to knowledge on shoreface dynamics and sediment transport hinder reliable predictions of coupled barrier-shoreface evolution from first principles at intermediate timescales (decades to centuries). While morphologic- and morphodynamic-behavior models offer promising means to predict barrier evolution and shoreline migration, the accurate parameterization of depth-dependent shoreface morphological response timescales is key to reliable predictions. In particular, the extent of instantaneous shoreface response (time-invariant geometry), which varies with the rate of sea-level change, must be determined to predict barrier evolution and shoreline migration during sea-level rise.

4. Build-up of the effects of rate-dependent morphodynamic hysteresis across the lower shoreface during sea-level change means that coupled barrier-shoreface evolution may persist beyond the slowing and stabilization of sea-level rise, and the nature of ongoing shoreline migration may be sensitive to the influences of wave climate variability on shoreface dynamics and sediment redistribution between the upper and lower shoreface.

5.1 Shoreface-Related Accommodation Constraints on Barrier Form and Volume

We show in Sect. 2 that barrier form and potential for accommodation of sediments depends exclusively on shoreface geometry relative to the geometry of the substrate underlying the barrier complex. Adjustments in shoreface geometry therefore necessarily affect barrier form and accommodation. Although we demonstrate the shoreface-related controls on sediment accommodation analytically, to illustrate the concepts using a simplified albeit conventional representation of shoreface geometry, it is important to note that the principles are axiomatic. That is, the principles also apply if the shoreface and substrate geometry were based on natural settings, which could be generated through the spatial averaging of their surfaces as mapped using hydrographic and seismic survey techniques.

The principles also reveal that alongshore-averaged barrier morphology belongs to a continuum of forms that tends to become a mainland beach as the back-barrier width becomes infinitesimal whenever the substrate attains a steepness equivalent to that of the mean slope of the shoreface. For intermediate ratios of substrate to shoreface slope, the barrier-front accommodation only extends part way down the shoreface to a point where the substrate outcrops, due to the encroachment of the shoreface into the substrate. This encroachment is possible only where the substrate comprises loose sediments or readily erodible sedimentary rocks. If the encroaching shoreface encounters areas of hard material (e.g., bedrock or strongly indurated sand), which cannot be eroded at the same rate as encroachment into the surrounding loose substrate, then the hard substrate will form reef outcrops in the encroachment zone of the shoreface.

Where the substrate comprises loose sediments, however, encroachment into the substrate by a translating shoreface creates a source of sediment that can be supplied to the barrier: with the fine fraction likely being deposited in the back-barrier, and the sand fraction incorporated into the tidal delta, washover, and prograded shoreface deposits of the barrier. The axiomatic geometric relations do not, however, provide an immediate indication of the rates of such sediment displacements across the shoreface, which gives rise to uncertainty in the morphologic-response timescales of coupled barrier-shoreface evolution.

5.2 Challenges in Forecasting Barrier Evolution: Lagged Shoreface Response

The shoreface response to sea-level rise is perhaps the greatest uncertainty in forecasting future barrier evolution and shoreline migration due to climate change. Even as projections of sea-level rise become more reliable over the coming decades and centuries, the readjustment of coastal sediment budgets to permanently raised sea level, and consequent shoreline migration, both remain difficult to predict with only an elementary understanding of shoreface dynamics and morphologic-response timescales. Our findings demonstrate a relationship between the rate of sea-level rise, the extent of the active shoreface (time-invariant geometry), and the resulting shoreline change, which is based on a model parameterization guided by past coastal evolution:

1. For slow rates of sea-level change, the shoreline change commitment for a given magnitude sea-level change is mostly experienced *during* sea-level change, and all other forcing held constant, shoreline stability should return shortly after the stabilization of sea level;
2. For rapid rates of sea-level change, the shoreline change commitment for the same magnitude sea-level change is only partially experienced during sea-level change, and even with all other forcing held constant, shoreline change *following* the stabilization of sea-level will be significant and prolonged.

Based on current projections of accelerating sea-level rise through the present century, the active shoreface may become increasingly restricted to the upper shoreface, where rates of morphologic response are sufficient for complete adjustment to varying boundary conditions at annual timescales. This suggests that predictive models that apply time-invariant shoreface geometry limited to the upper shoreface may provide reasonable estimates of barrier response and shoreline migration during sea-level rise, but increasingly poor estimates of the ultimate barrier evolution and shoreline change commitment into the future. Conversely, the assumption of time-invariant geometry across the entire shoreface may lead to overestimation of barrier response and shoreline migration during sea-level rise, but more informative estimates of the ultimate limits of barrier evolution and shoreline change. Amidst this uncertainty around the evolution of shoreface geometry during sea-level rise, our simulations highlight opportunities to apply evidence of past shoreface behavior and barrier response stored in depositional records, to refine forecasts of future barrier response to climate change.

Depth-dependent residual sediment flux rates across the shoreface mean that sea-level rise generates morphodynamic hysteresis where the rate of rise exceeds the slowest morphologic-response rates (i.e., on the lower shoreface). The morphodynamic hysteresis is rate-dependent, because the effects of hysteresis build up for faster rates of sea-level rise as the active shoreface contracts (i.e., the extent of instantaneous response reduces), thereby expanding the lower shoreface, which is characterized by depth-dependent morphologic-response rates. Thus, the self-regulatory

morphodynamic system behavior is experienced at rates proportional to the rate of system disturbance (sea-level change). Morphodynamic hysteresis results in lagged shoreface response (and thus ongoing barrier evolution and shoreline change) that continues beyond the stabilization of sea level. Determining the balance of barrier-shoreface sediment transfers that occur during sea-level rise, and those that will persist after sea-level rise, is paramount to coastal management and planning. This can be estimated if the time-varying dimensions of the active shoreface can be approximated.

The coupled barrier-shoreface behavior that we have described in this chapter considers time-averaged barrier and shoreline response driven by barrier-shoreface sediment transfers caused by sea-level rise. Understanding the time-averaged response is of crucial importance to planning for the coastal impacts of climate change. However, just as severe storms contribute to significant shoreline variability around a time-averaged position, episodic processes such as floods and mega-rips may allow for sediment-bypassing of the upper shoreface during sea-level rise, contributing to variability in barrier-shoreface evolution and shoreline change around the time-averaged response. Furthermore, while continuous barrier behaviors (e.g., encroachment and rollover) may drive significant and nonlinear shoreline migration, more abrupt shoreline change may arise from discontinuous behaviors (e.g., overstepping and drowning). The switch from continuous to discontinuous barrier behavior occurs where sediment-exchange thresholds between the shoreface, barrier, and back-barrier environments are exceeded, which is explored by Mellett and Plater (this volume) and Ashton and Lorenzo-Trueba (this volume).

Acknowledgments Laura Moore and Brad Murray provided valuable comments on the manuscript, although the authors remain responsible for any shortcomings.

References

Aagaard T, Hughes MG (2017) Equilibrium shoreface profiles: a sediment transport approach. Mar Geol 390:321–330. https://doi.org/10.1016/j.margeo.2016.12.013

Aagaard T, Sorensen P (2012) Coastal profile response to sea level rise: a process-based approach. Earth Surf Process Landf 37:354–362. https://doi.org/10.1002/esp.2271

Ashton AD, Lorenzo-Trueba J (2018) Morphodynamics of barrier response to sea-level rise. In: Moore LJ, Murray AB (eds) Barrier dynamics and response to changing climate. Springer, New York

Beets DJ, van der Valk L, Stive MJF (1992) Holocene evolution of the coast of Holland. Mar Geol 103:423–443

Beets DJ, Adam JF, van der Spek A (2000) The Holocene evolution of the barrier and the back-barrier basins of Belgium and the Netherlands as a function of late Weichselian morphology, relative sea-level rise and sediment supply. Neth J Geosci 79:3–16

Birkemeier WA (1985) Field data on seaward limit of profile change. J Waterw Ports Coasts Ocean Eng 111:598–602

Bruun P (1954) Coastal erosion and the development of beach profiles. Beach Erosion Board, USACE, Washington, p 79

Bruun P (1962) Sea level rise as a cause of shore erosion. J Waterw Harb Div 88:117–130

Cant DJ (1991) Geometric modelling of facies migration: theoretical development of facies successions and local unconformities. Basin Res 3:51–62. https://doi.org/10.1111/j.1365-2117.1991.tb00139.x

Church JA, White NJ (2011) Sea-level rise from the late 19th to the early twenty-first century. Surv Geophys 32:585–602. https://doi.org/10.1007/s10712-011-9119-1

Cornaglia P (1889) On beaches. In: Fisher JS, Dolan R (eds) Beach processes and coastal hydrodynamics. Benchmark papers in geology, vol 39. Dowden, Hutchins and Ross, Stroudsberg, pp 11–26

Costas S, Ferreira Ó, Plomaritis TA, Leorri E (2016) Coastal barrier stratigraphy for Holocene high-resolution sea-level reconstruction. Sci Rep 6:38,726. https://doi.org/10.1038/srep38726

Cowell PJ, Roy PS, Jones RA (1992) Shoreface translation model: computer simulation of coastal-sand-body response to sea level rise. Math Comput Simul 33:603–608

Cowell PJ, Roy PS, Jones RA (1995) Simulation of large-scale coastal change using a morphological behavior model. Mar Geol 126:45–61

Cowell PJ, Hanslow DJ, Meleo JF (1999a) The shoreface. In: Short AD (ed) Handbook of beach and shoreface morphodynamics. Wiley, New York, pp 39–71

Cowell PJ, Roy PS, Cleveringa J, de Boer PL (1999b) Simulating coastal systems tracts using the shoreface translation model. Soc Econ Palaeontol Miner Spec Publ 62:165–175

Cowell PJ, Stive MJF, Roy PS, Kaminsky GM, Buijsman MC, Thom BG, Wright LD (2001) Shoreface sand supply to beaches. In: Edge BL (ed) Coastal engineering 2000—proceedings of 27th international coastal engineering conference, Sydney, pp 2495–2508

Cowell PJ, Stive MJF, Niedoroda AW, de Vriend HJ, Swift DJP, Kaminsky GM, Capobianco M (2003a) The coastal-tract (part 1): a conceptual approach to aggregated modeling of low-order coastal change. J Coast Res 19:812–827

Cowell PJ, Stive MJF, Niedoroda AW, Swift DJP, de Vriend HJ, Buijsman MC, Nicholls RJ, Roy PS, Kaminsky GM, Cleveringa J, Reed CW, de Boer PL (2003b) The coastal-tract (part 2): applications of aggregated modeling of lower-order coastal change. J Coast Res 19:828–848

Cowell PJ, Thom BG, Jones RA, Everts CH, Simanovic D (2006) Management of uncertainty in predicting climate-change impacts on beaches. J Coast Res 22:232–245

Curray JR (1964) Transgressions and regressions. In: Miller RL (ed) Papers in marine geology. Macmillan, New York, pp 175–203

Davies AG, van Rijn LC, Damgaard JS, van de Graaff J, Ribberink JS (2002) Intercomparison of research and practical sand transport models. Coast Eng 46:1–23

Dean RG (1977) Equilibrium beach profiles: U.S. Atlantic and Gulf coasts. Department of Civil Engineering, University of Delaware, Newark

Dougherty AJ (2014) Extracting a record of Holocene storm erosion and deposition preserved in the morphostratigraphy of a prograded coastal barrier. Cont Shelf Res 86:116–131. https://doi.org/10.1016/j.csr.2013.10.014

Fenneman NM (1902) Development of the profile of equilibrium of the subaqueous shore terrace. J Geol 10:1–32

Goodwin ID, Stables MA, Olley JM (2006) Wave climate, sand budget and shoreline alignment evolution of the Iluka-Woody Bay sand barrier, northern New South Wales, Australia, since 3000 yr BP. Mar Geol 226:127–144

Hallermeier RJ (1981) A profile zonation for seasonal sand beaches from wave climate. Coast Eng 4:253–277

Houser C, Barrineau P, Hammond B, Saari B, Rentschler E, Trimble S, Wernette P, Weymer B, Young S (2018) Role of the foredune in controlling barrier island response to sea level rise. In: Moore LJ, Murray AB (eds) Barrier dynamics and response to changing climate. Springer, New York

Hoyt JH (1967) Barrier island formation. Geol Soc Am Bull 78:1123–1136

Intergovernmental Panel on Climate Change (IPCC) (2013) Climate change 2013: the physical science basis. In: Stocker TF, Qin D, Plattner G-K, Tignor M, Allen SK, Boschung J, Nauels A, Xia Y, Bex V, Midgley PM (eds) Contribution of working group I to the fifth assessment report of the intergovernmental panel on climate change. Cambridge University Press, Cambridge, p 1535

Johnson DW (1919) Shore processes and shoreline development. Wiley, New York
Kinsela MA, Cowell PJ (2015) Controls on shoreface response to sea level change. In: Proceedings of coastal sediments '15, San Diego, World Scientific Publishing, 2015
Kinsela MA, Daley MJA, Cowell PJ (2016) Origins of Holocene coastal strandplains in Southeast Australia: shoreface sand supply driven by disequilibrium morphology. Mar Geol 374:14–30. https://doi.org/10.1016/j.margeo.2016.01.010
Lorenzo-Trueba J, Ashton AD (2014) Rollover, drowning, and discontinuous retreat: distinct modes of barrier response to sea-level rise arising from a simple morphodynamic model. J Geophys Res Earth 119:779–801. https://doi.org/10.1002/2013JF002941
Mellett CL, Plater AJ (2018) Drowned barriers as archives of coastal-response to sea-level rise. In: Moore LJ, Murray AB (eds) Barrier dynamics and response to changing climate. Springer, New York
Moore LJ, List JH, Williams SJ, Stolper D (2010) Complexities in barrier island response to sea level rise: Insights from numerical model experiments, North Carolina Outer Banks. J Geophys Res 115:F03004. https://doi.org/10.1029/2009JF001299
Moore LJ, Goldstein EB, Vinent OD, Walters D, Kirwan M, Rebecca L, Murray AB, Ruggiero P (2018) The role of ecomorphodynamic feedbacks and landscape couplings in influencing the response of barriers to changing climate. In: Moore LJ, Murray AB (eds) Barrier dynamics and response to changing climate. Springer, New York
Murray AB, Moore LJ (2018) Geometric constraints on long-term barrier migration: from simple to surprising. In: Moore LJ, Murray AB (eds) Barrier dynamics and response to changing climate. Springer, New York
Nicholls RJ, Birkemeier WA, Lee GH (1998) Evaluation of depth of closure using data from Duck, NC, USA. Mar Geol 148:179–201
Niedoroda AW, Swift DJP (1981) Maintenance of the shoreface by wave orbital currents and mean flow—observations from the Long Island coast. Geophys Res Lett 8:337–340
Niedoroda AW, Swift DJP, Hopkins TS, Ma CM (1984) Shoreface morphodynamics on wave-dominated coasts. Mar Geol 60:331–354
Nummedal D, Riley GW, Templet PL (1993) High-resolution sequence architecture: a chronostratigraphic model based on equilibrium profile studies. In: Posamentier HW, Summerhayes CP, Haq BU, Allen GP (eds) Sequence stratigraphy and Facies associations. Blackwell Scientific Publications, Oxford, pp 55–68
Oliver TSN, Tamura T, Hudson JP, Woodroffe CD (2017) Integrating millennial and interdecadal shoreline changes: morpho-sedimentary investigation of two prograded barriers in southeastern Australia. Geomorphology 288:129–147. https://doi.org/10.1016/j.geomorph.2017.03.019
Ortiz AC, Ashton AD (2016) Exploring shoreface dynamics and a mechanistic explanation for a morphodynamic depth of closure. J Geophys Res Earth 121(2):442–464. https://doi.org/10.1002/2015JF003699
Patterson DC (2012) Shoreward sand transport outside the surf zone, northern gold coast, Australia. In: Proceedings of 33rd international conference on coastal engineering, Santander, 2012
Roy PS, Cowell PJ, Ferland MA, Thom BG (1994) Wave dominated coasts. In: Carter RWG, Woodroffe CD (eds) Coastal evolution: late quaternary shoreline morphodynamics. Cambridge University Press, Cambridge, pp 121–186
Roy PS, Zhuang WY, Birch GF, Cowell PJ, Congxiang L (1997) Quaternary geology of the Forster-Tuncurry coast and shelf southeast Australia. Geological Survey of New South Wales. Department of Mineral Resources, Sydney
Ruggiero P, Hacker S, Seabloom E, Zarnetske P (2018) The role of vegetation in determining dune morphology, exposure to sea-level rise, and storm-induced coastal hazards: a U.S. Pacific Northwest perspective. In: Moore LJ, Murray AB (eds) Barrier dynamics and response to changing climate. Springer, New York
Sloss LL (1962) Stratigraphical models in exploration. J Sediment Petrol 32:415–422
Stive MJF, de Vriend HJ (1995) Modeling shoreface profile evolution. Mar Geol 126:235–248

Stive MJF, Cowell PJ, Nicholls RJ (2009) Impacts of global environmental change on beaches, cliffs and deltas. In: Slaymaker O, Spencer T, Embleton-Hamann C (eds) Geomorphology and global environmental change. International Association of Geomorphologists. Cambridge University Press, Cambridge, pp 158–179

Stolper D, List JH, Thieler ER (2005) Simulating the evolution of coastal morphology and stratigraphy with a new morphological-behaviour model (GEOMBEST). Mar Geol 218:17–36

Storms JEA (2003) Event-based stratigraphic simulation of wave-dominated shallow-marine environments. Mar Geol 199:83–100

Storms JEA, Weltje GJ, van Dijke JJ, Geel CR, Kroonenberg SB (2002) Process-response modeling of wave-dominated coastal systems: simulating evolution and stratigraphy on geological timescales. J Sediment Res 72:226–239

Sweet WV, Kopp RE, Weaver CP, Obeysekera J, Horton RM, Thieler ER, Zervas C (2017) Global and regional sea level rise scenarios for the United States. Technical Report NOS CO-OPS 083. National Oceanic and Atmospheric Administration (NOAA), Silver Spring, pp 55

Swift DJP, Thorne JA (1991) Sedimentation on continental margins, I: a general model for shelf sedimentation. In: Swift DJP, Oertal GF, Tillman RW, Thorne JA (eds) Shelf sand and sandstone bodies—geometry, facies and sequence stratigraphy. Blackwell Scientific Publications, Oxford, pp 3–31

Tamura T (2012) Beach ridges and prograded beach deposits as palaeoenvironmental records. Earth Sci Rev 114:279–297

Thom BG (1984) Transgressive and regressive stratigraphies of coastal sand barriers in southeast Australia. Mar Geol 56:137–158

Thom BG, Roy PS (1985) Relative sea levels and coastal sedimentation in southeast Australia in the Holocene. J Sediment Petrol 55:257–264

Tortora P, Cowell PJ, Adlam K (2009) Transgressive coastal systems (1st part): barrier migration processes and geometric principles. J Mediterranean Earth Sci 1:1–13

van der Valk L (1992) Mid- and Late-Holocene coastal evolution in the beach-barrier area of the western Netherlands. Ph.D thesis, Vrije Universiteit, Amsterdam

Walters D, Moore LJ, Duran Vinent O, Fagherazzi S, Mariotti G (2014) Interactions between barrier islands and backbarrier marshes affect island system response to sea level rise: insights from a coupled model. Case Rep Med 119:2013–2031. https://doi.org/10.1002/2014JF003091

Wolinsky MA, Murray AB (2009) A unifying framework for shoreline migration: 2. Application to wave-dominated coasts. J Geophys Res Earth Surf 114:F01009. https://doi.org/10.1029/2007jf000856

Woodroffe CD, Chappell J, Thom BG, Wallensky E (1989) Depositional model of a macrotidal estuary and floodplain, South Alligator River, Northern Australia. Sedimentology 36:737–756

Wright LD (1995) Morphodynamics of inner continental shelves. CRC Press, Boca Raton

Morphodynamics of Barrier Response to Sea-Level Rise

Andrew D. Ashton and Jorge Lorenzo-Trueba

Abstract Barrier response to sea-level rise involves a dynamic interplay between the shoreface and the subaerial portion affected by overwashing. Focusing on feedbacks between these two, here we discuss a morphodynamic approach to modeling barrier transgression. In contrast with the steady transgression portrayed by morphokinematic models (which transport mass based on geometric considerations), a simple morphodynamic model predicts two modes of long-term barrier failure: width and height drowning. For barriers that survive sea-level rise, a most likely mode of barrier motion consists of punctuated and abrupt periodic transgression of the shelf, which can arise even from constant driving conditions. These intermittently migrational barriers spend most of their existence staying essentially in place, a stark contrast to the continuous behavior suggested by morphokinematic models of barrier retreat. Even small perturbations to a barrier system traversing the shelf in dynamic equilibrium can kick-start an oscillating retreat. Looking alongshore, shoreline interconnectivity can have a significant effect on shoreline behavior across both space and time. Overall, our morphodynamic modeling results motivate a need to investigate the internal dynamics of barrier systems to understand the full range of past and potential future response of barrier systems to sea-level rise.

Keywords Barrier rollover • Overwash • Shoreface • Width drowning • Height drowning • Periodic retreat • Dynamic equilibrium • Alongshore connectivity • Alongshore transport • Moving boundary

A.D. Ashton, Ph.D. (✉)
Department of Geology and Geophysics, Woods Hole Oceanographic Institution, Woods Hole, MA, USA
e-mail: aashton@whoi.edu

J. Lorenzo-Trueba, Ph.D.
Department of Earth and Environmental Studies, Montclair State University, Montclair, NJ, USA
e-mail: jorge.lorenzo@montclair.edu

L.J. Moore, A.B. Murray (eds.), *Barrier Dynamics and Response to Changing Climate*, https://doi.org/10.1007/978-3-319-68086-6_9

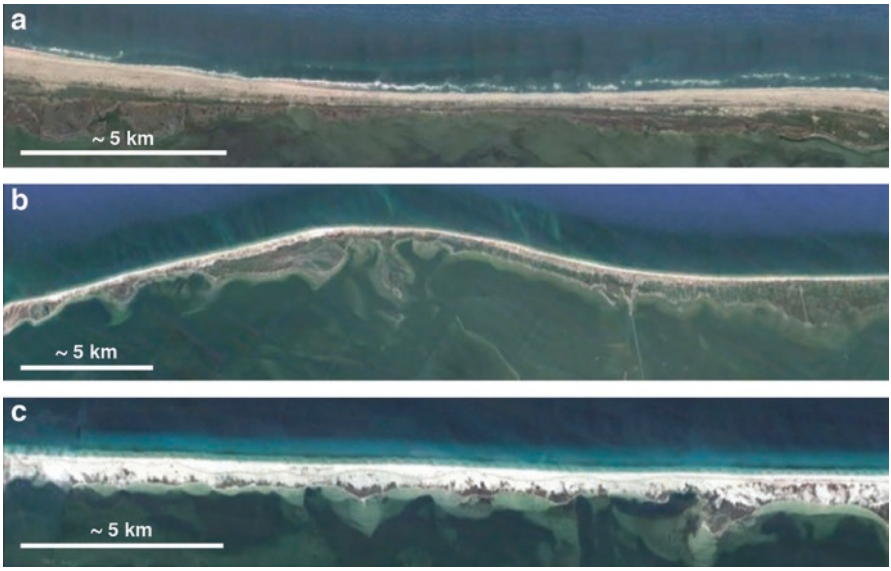

Fig. 1 Aerial images of barrier islands in different states of overwash and with differing shoreline curvature: (**a**) Hatteras Island, North Carolina, USA (35°N 75°W), (**b**) St. George Island, Florida, USA (30°N 85°W), and (**c**) Santa Rosa Island, Florida, USA (30°N 87°W). Images courtesy of Google Earth

1 Introduction

Coastal barriers are dynamic landforms; their long-term evolution can generally be understood through interactions between the alongshore and cross-shore domains. The wave-dominated shoreface and the overwashing subaerial barrier represent local cross-shore systems—these are linked along the coast through littoral transport (Fig. 1). The long-term response of coastal barriers to rising sea level is landward movement. If local sediment budgets are closed, with no net alongshore transport gradients or other potential sources and sinks of sediment, sea-level rise is expected to drive a long-term rollover response, in which barriers move landward through movement of sediment from the front to the back of the barrier (e.g., Houser et al. this volume; Odezulu et al. this volume; Rodriguez et al. this volume; Murray and Moore this volume; Moore et al. this volume).

Many barriers experiencing modern, typically slow (1–3 mm/year) rates of local sea-level rise, however, are not currently rolling over and are often wider and higher than typical threshold widths and heights that would accommodate large overwash sediment fluxes (Leatherman 1979, 1983). This suggests that eventually, as relative sea level rises, barriers are likely to abruptly transition into a new dynamic rollover state. Such threshold behaviors, often expressed in conceptual models of barrier evolution (Leatherman 1983), are typically absent in many of the mathematical and numerical models constructed to capture and predict barrier response to sea-level

rise and other environmental changes. Here, using a simple morphodynamic model of barrier evolution (Lorenzo-Trueba and Ashton 2014), we demonstrate that threshold behaviors can emerge from internal feedbacks within coupled shoreface-overwash dynamics, and that changes to the back-barrier can affect these behaviors. Furthermore, we show model results in which coupling of barrier profiles along a coastline can result in a cascade of threshold behaviors alongshore, with barrier segments alternatingly rolling over or aggrading in place based upon local histories and conditions, but also influenced by changes in barriers at a distance.

In this chapter, we first discuss three components of barrier behavior: the shoreface, the overwashing subaerial portion, and the alongshore-coupled system. We then provide a framework representing a commonly used morphokinematic approach to modeling barrier evolution, which we then contrast with a morphodynamic model that does not suppose that overwash maintains barrier width. We then present results from a simplified morphodynamic model (Lorenzo-Trueba and Ashton 2014) that demonstrates four potential modes of barrier evolution: dynamic equilibrium rollover common in other models, two mechanisms for drowning (one driven by insufficient overwash and the other arising from an excess of overwash), and a periodic retreat driven by feedbacks between the shoreface and overwashing system. We then examine simple cases of changes to regional geometry behind the barrier (i.e., in the "back-barrier") to show how transitions in the back-barrier environment could amplify threshold behaviors already arising in the simple model. By coupling barrier profiles alongshore, we further demonstrate that threshold dynamics can be communicated alongshore and, depending on the interconnectivity of the shoreline (strength of shoreline smoothing, or diffusivity), can lead to either in-step or out-of-phase dynamic responses along a slightly irregular coast line. Overall, model results reveal that a simple morphodynamic framework can give rise to threshold barrier behaviors, including the possibility of barrier rollover that is discontinuous over time, exhibiting episodes of rapid rollover interspersed with long periods of quiescent behavior.

2 Dynamic Processes Affecting Barriers

Barrier systems consist of different components, the shoreface, overwashing barrier, and the littoral system, each controlled by their own set of dynamics (Fig. 2).

2.1 Shoreface Evolution

Shoaling waves, interacting with the seabed, constantly move sediment on- and offshore. The surf zone, where waves break, is constantly dynamic, moving the shoreline back and forth in response to daily changes in wave climate, tempered by the preexisting beach state. Models of seasonal to interannual shoreline change can

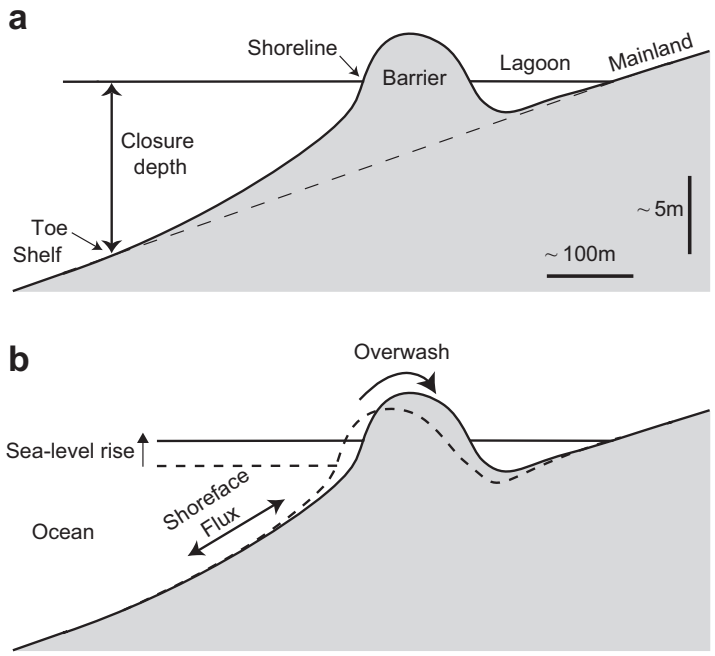

Fig. 2 Typical cross-section of a barrier system demonstrating (**a**) key components and (**b**) the process domains. As with all plots of barrier profiles shown here, note the strong exaggeration of the vertical scale

capture shoreline oscillations by considering movement of sediment to and from the shoreline to an offshore sand bar or reservoir—these short-term models typically capture shoreline movement about a presumed mean shoreline location or assume a constant rate of long-term erosion (Yates et al. 2009; Splinter et al. 2014).

Offshore of the surf zone, shoaled, unbroken waves move bed sediment; this region of wave-driven bed agitation is often referred to as the lower shoreface (Wright 1995) and is concave up (Dean 1991). Although there are many offered explanations for the controls on this shape, perhaps the most straightforward approaches suggest a balance between onshore- and offshore-directed sediment transport (Bowen 1980; Stive and de Vriend 1995). Moving offshore to deeper portions of the profile, as wave influence weakens, processes that can drive sediment onshore similarly weaken. If offshore sediment transport is dependent on gravity, bed equilibrium slopes will be smaller moving offshore (Bowen 1980), particularly when considering that many waves affecting the lower shoreface may not be fully shoaled (Ortiz and Ashton 2016).

As the effect of waves continues to weaken with distance offshore, the outer edge of the shoreface is typically demarked using a "depth of closure" of the active profile. Debate exists in terms of both the presence of such an offshore profile limit and how to quantify that depth based on the relevant timescales, given that wave-driven

sediment transport often occurs across shelves beyond most delineated closure depths (Hallermeier 1981; Stive et al. 1991; Wright et al. 1991; Cooper and Pilkey 2004). Recently, Ortiz and Ashton (2016) argued that the closure depth could be set by considering morphologic evolution, whereby the rate of change of the bed in response to changes at the shoreline becomes overwhelmingly slow—as with other closure depth estimates (see also Cowell and Kinsela this volume), this morphodynamic closure depth depends on the timescale of interest.

In terms of long-term evolution, if the shoreface can be considered a system that is driven towards an equilibrium form due to onshore wave-driven sediment transport (by processes such as wave velocity asymmetry and bed streaming) and offshore gravity-driven sediment transport (Bowen 1980), this leads to general understanding of the expected shoreface response to perturbation. First, an increase of sea level should oversteepen a shoreface that was previously at equilibrium, driving offshore sediment transport (Bruun 1962; Stive and de Vriend 1995; Ortiz and Ashton 2016). Similarly, accumulation of sediment within the surf zone, perhaps from alongshore transport gradients, should also result in offshore transport which spreads this sediment across the shoreface. Processes that remove sediment from the upper profile, such as overwash and aeolian processes, should drive onshore sediment transport from the lower profile (Davidson-Arnott 2005; Donnelly et al. 2006).

2.2 Overwash

Overwash moves sediment from offshore up and over a barrier. This exclusively onshore flux is often storm-driven and can occur through overtopping or as a result of breaching or a temporary inlet opening (Leatherman 1979; Donnelly et al. 2006). Although overwash can occur on most barriers for a large enough storm, sediment fluxes are most frequent and significant for low and narrow barriers, such that Leatherman (1979, 1983) introduced the concept of an equilibrium barrier width, whereby vigorous overwash initiates when barriers become sufficiently thin (on the order of 300–500 m) and low. Overwash is therefore considered to be controlled primarily by the width and height of a barrier. Importantly, this subaerial control suggests that the shoreface state (in terms of under- or oversteepening) is unlikely to significantly affect overwash fluxes except that an eroding shoreline should lead to thinning of a barrier, which could then lead to initiation of overwashing.

2.3 Alongshore Sediment Transport

Profiles of sandy coastlines at different alongshore locations can be considered to be tied together by alongshore sediment transport, such that a pronounced change in one alongshore location, such as rapid overwash, can be communicated to alongshore neighbors, both up- and downdrift. Gradients in alongshore sediment

transport typically act to diffuse (smooth) the plan-view shape of a shoreline (Pelnard-Consideré 1956). At any one profile location, even small gradients in alongshore sediment transport can overwhelm sea-level signals (Cowell et al. 1995), and often littoral sediment budgets must be considered to understand long-term barrier trajectories (Moore et al. 2010).

The strength of diffusive shoreline smoothing depends not only on wave energy, but also wave approach angle (Ashton and Murray 2006a). In extreme cases, a wave climate dominated by high-angle waves approaching from more than ~42° between crests and the shoreline, assuming shore-parallel contours and neglecting more complex refraction effects (e.g., Falqués and Calvete 2005; Falqués et al. 2017), can lead to shoreline instability (Ashton et al. 2001; Ashton and Murray 2006b), which can in turn affect the stability of barriers to breaching (Walton and Dean 1973).

However, even in the case where a shoreline is expected to be diffusive due to dominance by low-angle waves, the spread of wave approach angles affects the net smoothing rate of a shoreline. For the same wave energy, even in the absence of a net transport direction, a coast with a broader distribution of wave approach angles will have a lower shoreline diffusivity than a coast where waves approach directly onshore (Ashton and Murray 2006b; Ashton et al. 2016). A coast with higher shoreline diffusivity will be more strongly coupled or interconnected alongshore—changes at one profile location will be more rapidly communicated to the neighboring coastal segments.

3 Morphokinematics Versus Morphodynamics of Barrier Response to Sea-Level Rise

In the absence of sediment transport, shoreline recession due to an increase in sea level should be minimal, tied to the slope of the beach itself. However, waves move sediment and, on a wave-dominated coast, bath-tub scenarios vastly underestimate the expected shoreline retreat expected from a given amount of sea-level rise. Perhaps the best-known model of coastal response to sea-level rise is the Bruun Rule (Bruun 1962, 1983) which, by assuming that the shoreface maintains its shape relative to sea level and assuming conservation of mass, posits that for a given rise in sea level the shoreline will retreat at a rate based upon the slope of the shoreface.

The original Bruun Rule (which addresses only the shoreface and is referred to within this chapter as the "shoreface Bruun Rule" for clarity) can be explained geometrically (see Murray and Moore this volume). However, the shoreface Bruun Rule does not rest solely on geometric assumptions—it is also congruent with our general understanding of shoreface dynamics discussed above: increased water levels lead to oversteepening of the shoreface, which drives an offshore sediment flux. This flux abates when the profile is in equilibrium at the new water level. Despite this basis in shoreface dynamics, the shoreface Bruun Rule can be classi-

fied as a "morphokinematic" model, whereby the system changes to obey mass conservation and geometric rules without specifically factoring for rates of mass flux. For example, shoreline retreat predicted by the shoreface Bruun Rule depends only on the quantity of sea-level rise and is independent of the rate of rise—there is no dynamic rate and no flux needs to be computed to institute the Bruun rule.

Limitations of the shoreface Bruun rule that arise when inundation surpasses the shore spurred the development of modifications to the Bruun rule for barrier island geometries (Dean and Maurmeyer 1983; Rosati et al. 2013), resulting in a "generalized Bruun Rule" that includes the subaerial barrier as part of the profile (Murray and Moore this volume). Wolinsky and Murray (2009) provide a full and robust mathematical morphokinematic framework applied broadly to Bruun-type rules (including those addressing cliffed as well as barrier coastal geometries), clearly showing that, at steady state, shoreline recession should exactly equal the slope upland of the geometry-maintaining coastal system (Murray and Moore this volume). These generalized Bruun rules are similarly morphokinematic and are not sensitive to rates of sea-level rise. The only steady-state situation in which long-term recession exactly matches the trajectory indicated by the shoreface Bruun rule is a case in which the upland slope exactly equals the shoreface slope (Zhang et al. 2004). Shape-preserving morphokinematics underlie several numerical models of barrier response to sea-level rise (Cowell et al. 1995; Stolper et al. 2005; Moore et al. 2010).

There remains, however, an apparent mechanistic paradox in terms of sediment transport pathways for geometric, morphokinematic models. To demonstrate this apparent paradox, here we present results from a simple numerical model of mass conservation to demonstrate the general behavior of a barrier system within such models. In this numerical model, by delineating an equilibrium profile and barrier shape, the effects of sea-level rise can be rapidly computed using a modern computer by applying a mass conservation approach (similar to the approach used in other models (Cowell et al. 1992; Stolper et al. 2005). Starting from an initial configuration of a barrier with its entire shoreface atop a constantly sloping back-barrier, the barrier shape can be raised by an incremental sea-level rise. This new artificial profile contains more mass than the previous profile. Iteratively, the model numerically steps this barrier landwards until the mass removed equals the mass lost, reproducing landwards barrier rollover (Fig. 3a).

Changing the shoreface slope has no effect on the retreat rate of the modeled barrier system (Fig. 3d), whereas reducing the regional back-barrier slope increases shoreline recession (Fig. 3e), at the rate of 1/slope. In this example, the shoreface slope does not affect the retreat rate because we start from an initial condition in which the shoreface is "perched" atop the regional slope—the model starts in a configuration of long-term dynamic equilibrium (see also Murray and Moore this volume). The long-term behavior is in agreement with analytical formulations (Wolinsky and Murray 2009).

Looking between time slices, the change in elevation along the profile shows erosion of the shoreface and deposition on and behind the barrier. As the model is based on mass conservation, integration over the change in elevation shows what fluxes would be needed to produce these bed changes (assuming the outermost

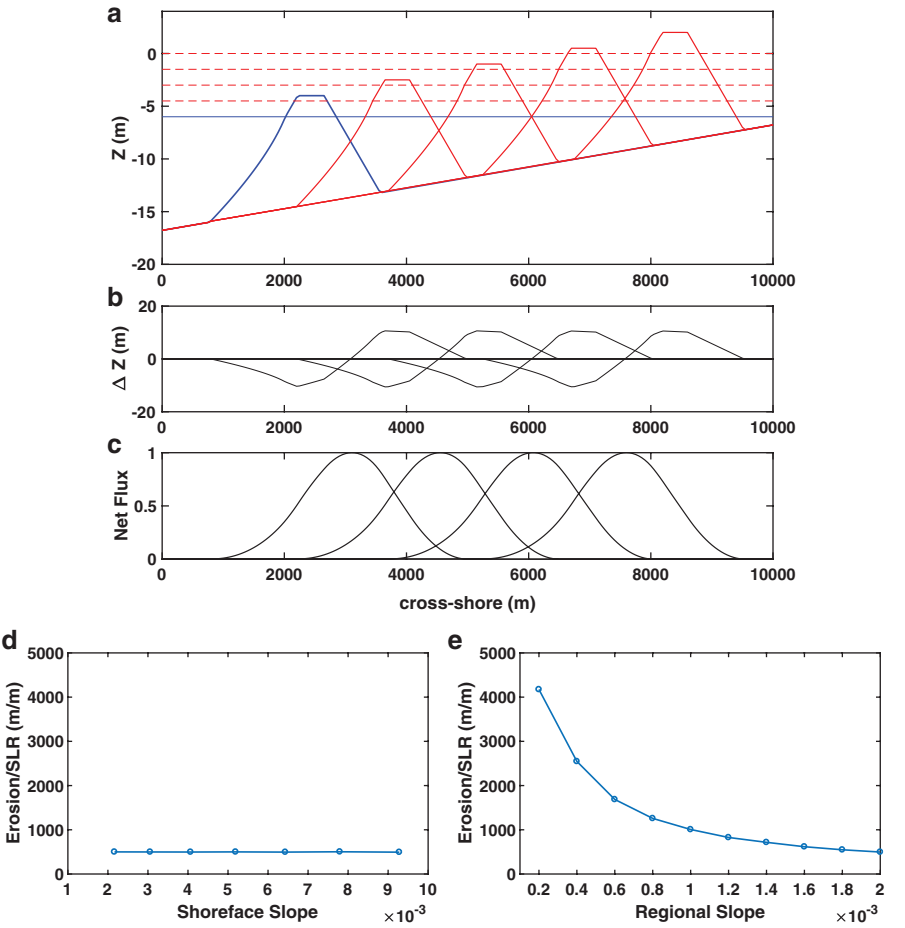

Fig. 3 Results from a simple morphokinematic model of barrier roll-over response to sea-level rise, showing (**a**) barrier location for 1 m sea level increments, (**b**) change in height over those increments, and (**c**) net flux computed from those height changes. Also shown are the effect of (**d**) shoreface slope and (**e**) regional backbarrier slope on the rate of shoreline recession

boundaries are closed, which they clearly should be for this example). Erosion of the shoreface and deposition of the barrier would result from a landward flux over both the barrier and the shoreface.

These results pose a possible conundrum—although morphokinematic in nature, the behavior of the shoreface Bruun rule is in accordance with basic understanding of shoreface dynamics. Rising sea level oversteepens the shoreface and sediment moves offshore. The results shown in Fig. 3, however, suggest that sea-level rise must drive shoreface sediment onshore during rollover. The simple parsimonious answer is that, as overwash removes sediment from the upper shoreface, the shoreface becomes understeepened, routing sediment onshore even as sea level rise

(without the overwash effect) would be expected to send sediment offshore (see also Murray and Moore this volume). If the interaction between an overwashing barrier and the shoreface is instantaneous (or close to it), there is no conundrum—the shoreface slopes become understeepened because of the overwash effect rather than oversteepened from the direct sea-level-rise effect—and morphokinematic approaches capture barrier dynamics. However, as discussed above, the processes controlling overwash and shoreface processes are distinct and may not occur on the same timescales. Barrier rollover requires intimate coupling between the shoreface and the overwashing barrier; however, different timescales for the shoreface and overwashing systems could complicate the coupling. For example, the sediment deficit at the shoreline driven by overwashing of the barrier may not be instantly communicated to the lowermost shoreface (Ortiz and Ashton 2016; Cowell and Kinsela this volume), which would affect long-term barrier dynamics.

As another example, what if the flux of sediment overwashing the barrier does not occur at a sufficient rate to move a barrier onshore in a rollover state? A simple first morphodynamic model of barrier evolution (Ashton and Ortiz 2011), based on the main principles underlying the simplified model presented below, shows how the rate of overwash can affect barrier response to sea-level rise (Fig. 4). A barrier that can overwash rapidly maintains its subaerial shape with sea-level rise, but with rapid shoreline recession. Although this model uses a rather ad hoc relationship for shoreface dynamics, the shoreface slope is clearly reduced, which leads to onshore sediment transport. Without overwash, a Bruun Rule response leads to slight shoreline recession, even as the barrier itself loses height. Changing the rate of overwash directly affects the amount of shoreline recession during sea-level rise (Fig. 4).

4 A Simplified Morphodynamic Model of Barrier Evolution

Motivated to better understand the coupled dynamics of the shoreface and overwashing system, we developed a simple morphodynamic model of barrier evolution. The objective of our approach is to study the potential effects of delays in shoreface response to shoreline change as well as the effect of potential limitations on overwash fluxes. Here we describe the basic model processes—a full description, along with the constituent equations, can be found in Lorenzo-Trueba and Ashton (2014). The model tracks the movement of three key barrier locations: the shoreface toe, the shoreline, and the back-barrier location, along with the barrier height (Fig. 5). These variables change due to sediment transport in the shoreface, sediment transported as overwash, and in response to passive sea-level rise (Fig. 2).

The model does not capture many processes and complexities that can affect barrier evolution, including aeolian processes, vegetative feedbacks, and lithological controls. As the model dynamics are abstractions and parameterizations of shoreface dynamics, we expressly call this model “simple.” Despite this simplicity, model behavior is based upon sediment fluxes determined by feedbacks between constituent model components, and in this manner, the model is fully “dynamic.” The model

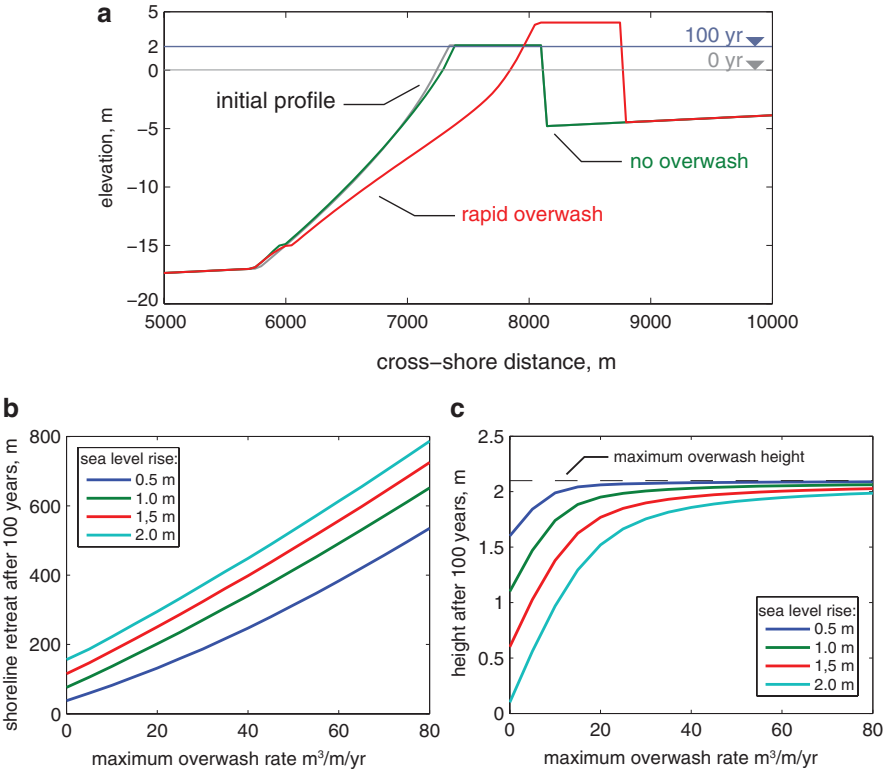

Fig. 4 Results from a simple morphodynamic model of (**a**) barrier response to a 1 m sea-level rise over 100 years with and without overwash, also plotted the initial, 'equilibrium' profile shape. Dependence of (**b**) shoreline retreat and (**c**) barrier height on overwash rate for different sea-level-rise scenarios

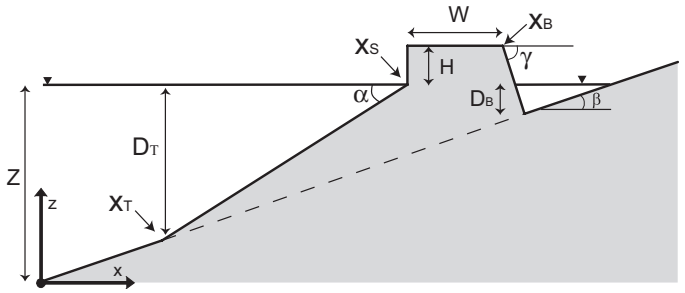

Fig. 5 Morphodynamic barrier model set-up and components

itself bears resemblance to other dynamic models of barrier evolution, such as those by Storms et al. (2002) and Masetti et al. (2008).

On the shoreface, sediment is moved between the shoreline and the shoreface toe. We approximate the concave shoreface as a single unit with equilibrium slope, α_e, and fluxes are linearly proportional to the difference between the actual slope and the equilibrium slope. A steep shoreface sends sediment offshore; a shallow shoreface sends sediment onshore. Although fluxes tend to drive the shoreface to equilibrium, our approach does not presume an ad hoc relaxation of morphology. Instead, the slope-based flux is derived from models of shoreface dynamics that suggest the first-order flux term for shoreface sediment transport, when driven out of equilibrium, is proportional to the slope deviation from equilibrium (Bowen 1980; Stive and de Vriend 1995; Ortiz and Ashton 2016). The linear approximation of the shoreface itself, of course, is a simplification, yet it captures exchanges between the shoreline and the lower shoreface. For high shoreface response rates, K (m^3/m/year), rapid profile response is akin to a morphokinematic model. Slow shoreface responses could result in response lags. It is also interesting to note that our slope-based flux, based on the shoreface dynamics, does resemble the shoreface evolution formulation used by Masetti et al. (2008). Fluxes in that model are based upon diffusion of the distance from a presumed equilibrium profile location—the use of a second derivative translates the distance term to a term in which fluxes are proportional to the difference from an equilibrium slope.

Overwash is initiated when a barrier becomes thinner than its critical width (and if the barrier is below a critical height)—overwash increases as barriers become thinner and lower. Sediment is deposited on top and behind the barrier proportionately based upon the departure from critical width and height (Jiménez and Sánchez-Arcilla 2004). Because of the low slope of the shelves and coastal plains that barriers sit atop, deposition preferentially occurs in the back-barrier region (Ashton and Ortiz 2011; Lorenzo-Trueba and Ashton 2014). Most essential to our approach is the presumption of a maximum rate of barrier overwash, $Q_{ow,max}$ (m^3/m/year). We test a broad parameter space of potential maximum overwash rates—results for large overwash rates can be interpreted if our presumption of a maximum rate seems unreasonable.

Sea-level rise is implemented by reducing the barrier height without moving the shoreline. The model conserves mass by moving the barrier toe landwards, which also allows the model to capture the phenomenon of shoreface oversteepening despite the schematization of a linear shoreface.

5 Morphodynamic Barrier Response to Sea-Level Rise

Starting with initial conditions of a barrier in static equilibrium for a constant sea level, we run this model over 1000 years for different rates of sea-level rise, $\dot{Z}$, and for different slopes of the regional back-barrier, β (representing the exogenous variables). Lorenzo-Trueba and Ashton (2014) offer a larger parameter space exploration,

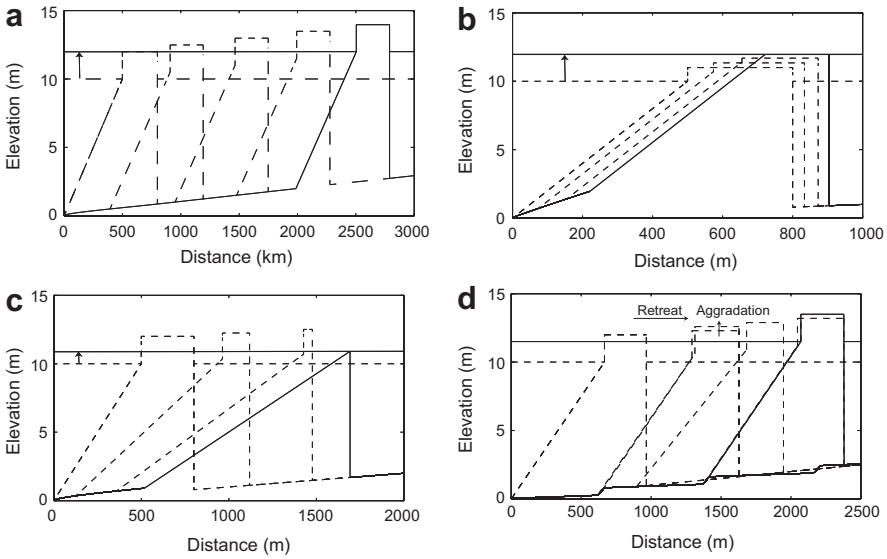

Fig. 6 Profile evolution of modeled barrier systems response demonstrating four main modes of response: (**a**) dynamic equilibrium, (**b**) height drowning, (**c**) width drowning, and (**d**) periodic retreat. Reproduced from Lorenzo-Trueba and Ashton (2014)

showing how the main internal controls on morphodynamic barrier response are the shoreface response rate and the maximum overwash rate.

5.1 Modes of Barrier Response

The morphodynamic model produces four distinct modes of barrier transgression with rising sea level (Fig. 6). The most familiar is a dynamic equilibrium, a constant rollover barrier whose width, height, and shoreface slope become constant (Fig. 6a). This state, whose characteristics can be determined analytically (Lorenzo-Trueba and Ashton 2014), takes the form of a damped oscillation from the initial conditions.

There are two modes of barrier failure, or drowning, representing run-away behavior (Fig. 6b). If overwash rates are low, the barrier cannot maintain itself above sea level, a phenomenon we term "height drowning." In this case, insufficient rates of overwash (see also Fig. 4) do not allow the barrier to maintain itself as sea levels rise. This is perhaps the most intuitive mode of barrier collapse, arising in the model from the imposed limit on the maximum overwash rate (e.g., Fagherazzi et al. 2003; Masetti et al. 2008).

The other mode of barrier drowning, however, is perhaps not as obvious. As sea level rises, barriers can only maintain their elevation and width by overwashing.

Overwash, however, drives rapid shoreline recession with sediment constantly filling the back-barrier. If the rate of sediment resupply from the shoreface to the shoreline itself does not keep sufficient pace (an onshore flux that would slow shoreline recession), the sediment deficit caused by rapid overwashing drives barrier narrowing until the barrier disappears, which we term "width drowning." Although both overwash and shoreface dynamics are treated as continuous processes in our model, in nature both the overwash and the shoreface will be most active during the same storm events. Conceptually, width drowning would represent a case where a barrier becomes exceedingly low and narrow such that overwash occurs frequently, during small storms and high tides, not just during the large storms that also rework the lower shoreface (Ortiz and Ashton 2016). Both drowning responses, and in particular this width drowning, are not predicted by morphokinematic approaches.

The fourth, and most common, response we classify is an oscillatory behavior, whereby the barrier system retreats rapidly then remains in place, which we term "periodic retreat" (Fig. 6d). In essence, this limit cycle behavior switches between both of the "drowning" stages—rapid overwash-driven recession alternating with in-place drowning (Fig. 7). Lags between the two stages continue to drive barrier dynamics. Rapid overwash, while reducing barrier width, flattens the shoreface, driving sediment onshore. This onshore flux reduces shoreline retreat, until the barrier attains a width sufficient to stop overwashing. Cessation of overwash, in conjunction with continued onshore transport from the lower shoreface, widens the barrier. Slowly, as sea level rises, the shoreline recedes in a shoreface-Bruun-type response as there is no overwash of the wide barrier. Once this persistent shoreline erosion sufficiently narrows the barrier to reactivate the overwash system, the shoreline retreats rapidly, renewing the cycle.

Note that this oscillatory behavior is not unique to the simplified scheme in the Lorenzo-Trueba and Ashton (2014) model that only tracks key barrier locations; for example, it emerged from a discretized model with similar components (Ashton and Ortiz 2011). Also, threshold behavior can be observed in the Masetti et al. (2008, Fig. 8) model; the dynamics of the threshold behavior in this model are not fully explored, with the authors attributing the behavior as a response to transitions to steep morphology of the regional back-barrier. The oscillations we produce are fully autogenic (Fig. 8), developing with a back-barrier of a constant slope.

We run simulations for 1000 years. If none of the above responses can be quantified during the 1000-year model runs, we classify this as a "mixed" behavior. In some cases, the barrier is drowning, but has failed to do so over one millennia. In other cases, periodic retreat might be occurring, but with a similarly millennial period. Also, perhaps a slow oscillation towards dynamic equilibrium from the initial conditions does not complete within the model run.

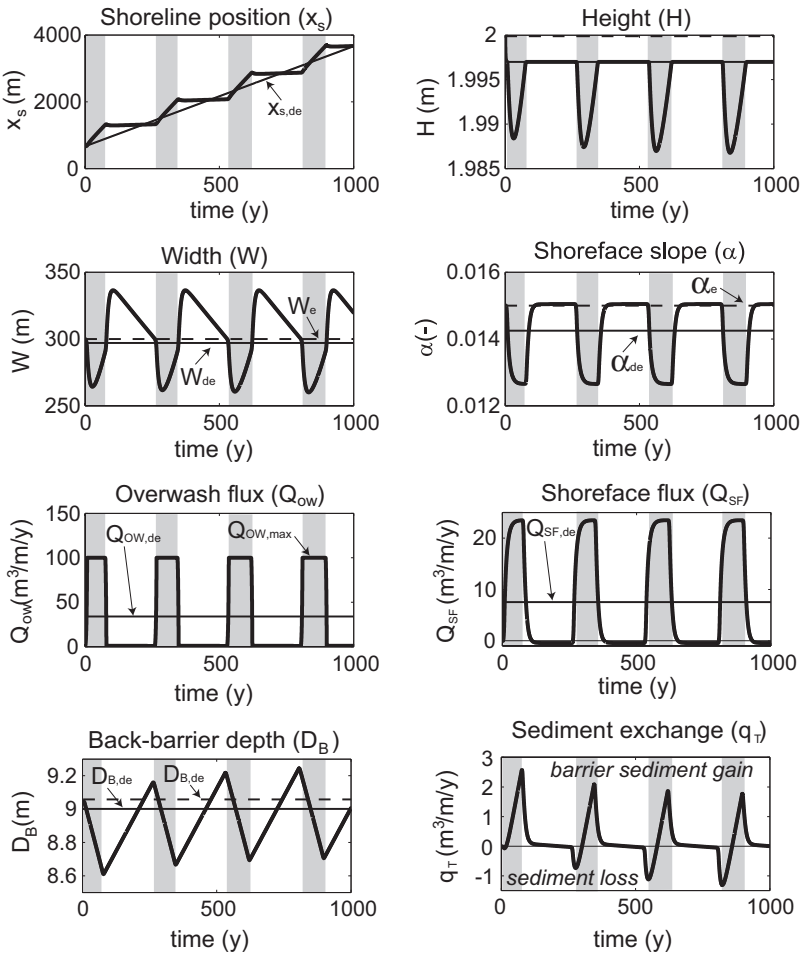

Fig. 7 Time evolution of key variables for a barrier system undergoing "periodic retreat." Shaded regions correspond to transgressive intervals. Reproduced from Lorenzo-Trueba and Ashton (2014)

5.2 Controls on Barrier Response

We explore how modeled barrier behaviors are affected by the exogenous factors of sea-level rise rate (Fig. 8) and back-barrier slope (Fig. 9) across a parameter space of internal system characteristics: shoreface response rate and maximum overwash rate. Perhaps most importantly, dynamic equilibrium, the mode that most resembles the results of morphokinematic models, is rare, constrained in parameter space such that it is only prevalent for steeper back-barriers (Fig. 9). Intuitively, height

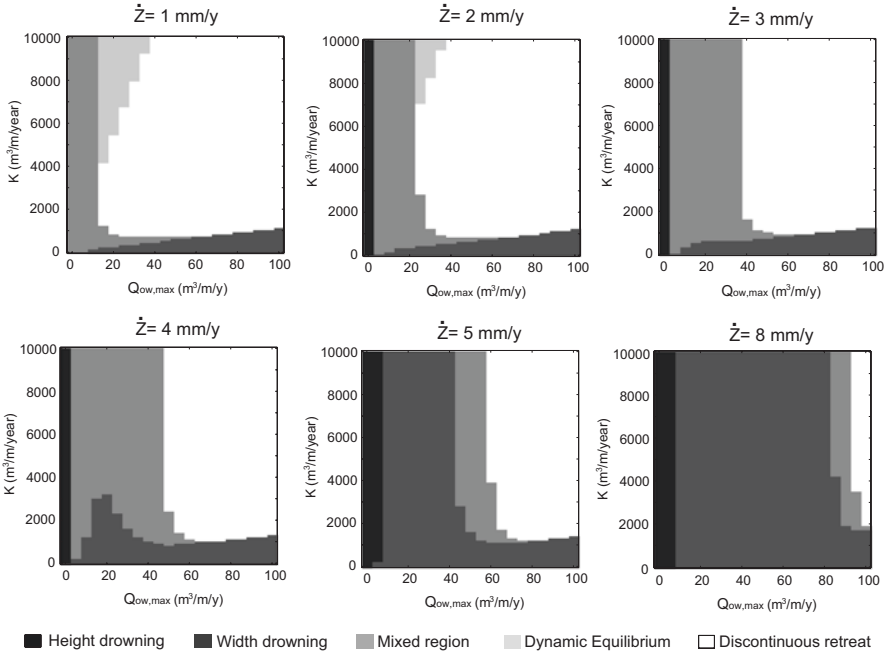

Fig. 8 Regime diagrams as a function of the maximum overwash flux $Q_{\mathrm{ow,max}}$ and the shoreface flux constant K for different values of the sea-level rise rate $\dot{Z}$. The back-barrier lagoon slope is $\beta = 0.001$. Reproduced from Lorenzo-Trueba and Ashton (2014)

drowning occurs when maximum overwash rates are low, and width drowning is predicted for slow shoreface response rates. For slow rates of sea-level rise and moderate back-barrier slopes, periodic retreat (and in some cases the less defined "mixed behavior") tends to dominate.

Focusing on barrier survival, increased rates of sea-level rise increase drowning responses (Fig. 8). For higher sea-level-rise rates, height drowning for low maximum overwash rates expands slightly. More obvious, however, is the expansion of the zone of predicted width drowning, which grows significantly for higher rates of sea-level rise. Similarly, even for a moderate rate of sea-level rise (2 mm/year), shallower back-barrier slopes tend towards width drowning, replacing dynamic equilibrium and periodic behaviors predicted for steeper back-barriers. Regions of barrier failure grow mostly at the expense of periodic retreat. The time to drowning depends on many variables (Lorenzo-Trueba and Ashton 2014), but we do note that for moderate sea-level rise rates (for example, 3 mm/year), the time to drowning of modeled barriers is on the order of 100's of years.

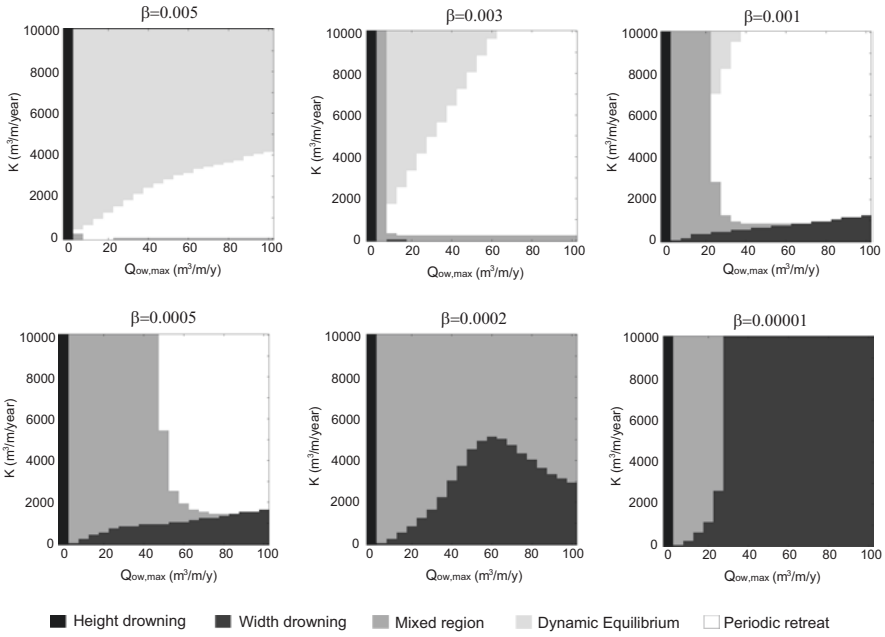

Fig. 9 Regime diagrams as a function of the maximum overwash flux $Q_{\mathrm{ow,max}}$ and the shoreface flux constant K for different values of the backbarrier lagoon slope β. The sea-level rise rate is $\dot{Z} = 0.002$. Reproduced from Lorenzo-Trueba and Ashton (2014)

5.3 *Threshold Response to Back-Barrier Geometry*

Using our model, we previously investigated the modes of barrier retreat over a constantly sloping back-barrier (or shelf/coastal plain). What happens if there are changes in the regional slope behind the barrier? Here we present a first set of experiments investigating the effects of a steady change in the back-barrier slope. In similar scenarios, geometric considerations suggest that shoreline trajectory should gradually change across such a transition—this smooth change is not complete until sea level has risen the entire height of the shoreface itself (Wolinsky and Murray 2009; Moore et al. 2010; Murray and Moore this volume).

As a barrier in the process of width drowning transgresses onto a steeper back-barrier slope (Fig. 10), it experiences a decrease in back-barrier accommodation depth, and the drowning trajectory can be reversed, with the barrier transitioning to periodic retreat as shelf slope steepens (Fig. 9). During width drowning, the barrier was losing volume from the shoreface toe to the shelf. The transition away from drowning, which requires addition of mass to the barrier itself, is accomplished through ravinement (erosion) of the shelf (Fig. 10). Periodic retreat creates a series of stepwise incisions in the steeper shelf.

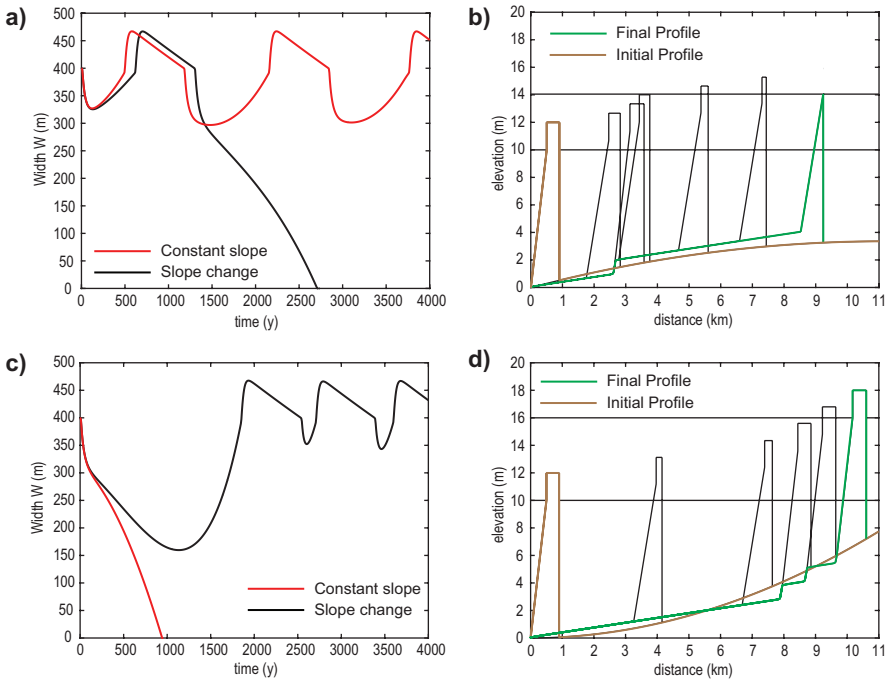

Fig. 10 Modeled barrier response to a change in regional slope behind the barrier. (**a**) Width and (**b**) profile view of a barrier trangressing over a constant backbarrier slope versus a linear slope decrease. (**c**) Width and (**d**) profile view of a barrier trangressing over a constant backbarrier slope versus a linear slope increase. For model parameters, see Table 1

An increase in back-barrier accommodation depth, from a flattening of the back-barrier shelf, should increase the likelihood of barrier drowning. For example, a barrier experiencing periodic retreat can transition to width drowning as back-barrier slopes decrease (Fig. 10). In this scenario, the barrier accomplishes a full periodic oscillation before transitioning towards breakdown. Width drowning, driven by loss of barrier sediment, smears a large depositional sand body across the shelf from the abandoned shoreface toe.

The morphodynamic barrier system is also sensitive to small perturbations in the back-barrier. For example, when a barrier transgressing a shelf/coastal plain in dynamic equilibrium experiences a small perturbation in the back-barrier depth, it can transition to periodic retreat (Fig. 11). Here we add a small negative perturbation (for example, a relict channel); similar behavior occurs for a positive perturbation. Model results demonstrate how even slight perturbations can lead to threshold changes in barrier behavior. For example, if a small perturbation could transition a barrier from dynamic equilibrium to periodic retreat, this suggests that some of the behaviors we identify in parameter space (Figs. 8 and 9) could be metastable. The presence of such a phenomenon, whereby modes of barrier

Table 1 Input parameters used in Fig. 10

Parameter	Symbol	Units	Fig. 1a & b (top)	Fig. 2c & d (down)
Shoreface response rate	K	$m^3/m/year$	2000	2000
Equilibrium shoreface slope	α	–	0.02	0.02
Shoreface toe depth	D_t	m	10	10
Equilibrium island width	W	m	400	400
Equilibrium island height	H	m	2	2
Back barrier lagoon slope	B	m	$6 * 10^{-4}$ to 10^{-5} over 11 km	10^{-5} to $1.4 * 10^{-3}$ over 11 km
Sea level rise	$\dot{Z}$	mm/year	1.5	1.5
Maximum overwash flux	$Q_{ow,max}$	$m^3/m/year$	50	50
Maximum deficit volume	$V_{d,max}$	m^3/m	100	100

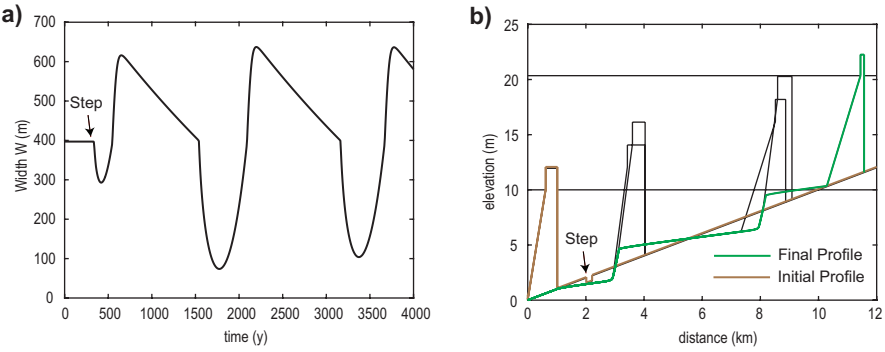

Fig. 11 (**a**) Width and (**b**) profile view of response of a barrier system transgressing in dynamic equilibrium to a "step" perturbation in the backbarrier. For model parameters, see Table 2

behavior might depend on initial conditions and local minima in phase space, requires further investigation (Fig. 11).

6 Alongshore Coupling

With the emergence of dynamic cross-shore profile behavior, the next question is: how does alongshore connectivity affect barrier evolution? For the next set of model experiments, we connect cross-shore profiles alongshore (spaced every 200 m), starting with a straight coast. These profiles are connected through alongshore

Table 2 Input parameters used in Fig. 11

Parameter	Symbol	Units	Value
Shoreface response rate	K	$m^3/m/year$	2000
Equilibrium shoreface slope	α	–	0.02
Shoreface toe depth	D_t	m	10
Equilibrium island width	W	m	400
Equilibrium island height	H	m	2
Back barrier lagoon slope	B	m	10^{-3}
Sea level rise	$\dot{Z}$	mm/year	3
Maximum overwash flux	$Q_{ow,max}$	$m^3/m/year$	100
Maximum deficit volume	$V_{d,max}$	m^3/m	100
Step length	Δx	m	200
Step depth/height	Δy	m	2

transport; as this transport occurs in the surf zone, sediment deposition and accretion are implemented by depositing or eroding sediment at the shoreline and conserving mass. Deposition will tend towards shoreface oversteepening and erosion will tend towards flattening of the shoreface—the shoreface then dynamically responds to these changes at the shoreline. Alongshore transport is treated as a diffusional process (Pelnard-Consideré 1956; Larson et al. 1987; Ashton and Murray 2006a), scaled using the CERC (Komar 1971) formula based on waves with 1 m height and 8 s period.

As discussed above, for a given (effective) wave height, shoreline diffusivity depends on the wave angle. For a distribution of waves (and the same wave height), there is a stronger diffusivity for waves approaching directly onshore (with no net transport) and weaker diffusivity as wave approach angle increases (increasing wave angle) (Ashton and Murray 2006b). High-angle waves do not smooth the coastline, with strongest anti-diffusivity for the largest angle waves. Here we model a wave climate dominated by diffusive low-angle waves. Whether or not there is a net direction of transport, wider distributions of wave angles will reduce the effective diffusivity of the shoreline (Ashton et al. 2016), a phenomenon we implement by reducing the effective diffusivity by a fraction d. In terms of the cross-shore profiles, the shoreline diffusivity represents the "connectivity" of the coast. For the same input of wave energy, shorelines with a large d will be more tightly coupled alongshore than coasts with smaller d. However, as wave heights are the same for both cases, we would expect the shoreface dynamics to be the same for both cases. Our interest is in the dynamics that arise when one part of the coastline overwashes, and how this affects the neighboring coasts as shoreline change is transmitted along the coast (Fig. 12).

Model simulations start with a shoreline consisting of barriers at equilibrium width, connected with periodic boundary conditions. With moderate regional/back-barrier slope ($\beta = 0.001$) and a significant maximum overwash flux ($Q_{ow,max} = 100\ m^3/m/year$), these barrier profiles are expected to respond to the sea-level rise forcing of

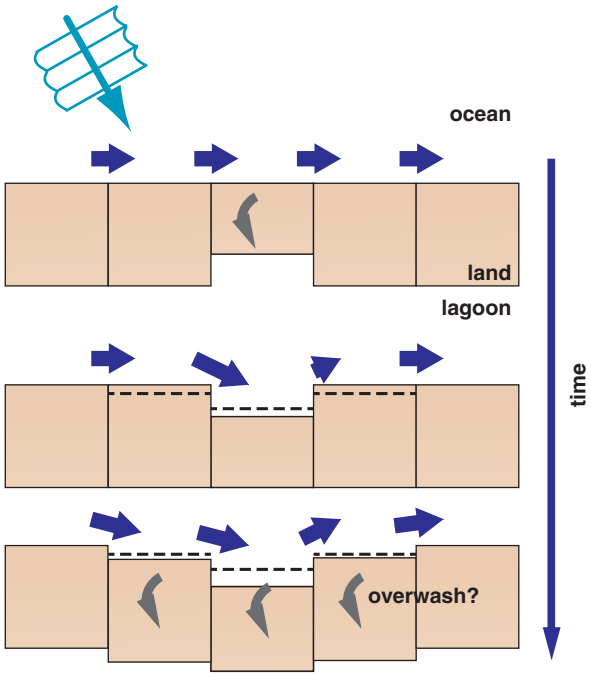

Fig. 12 Conceptual diagram of alongshore coupling. Arrows represent relative alongshore sediment transport fluxes (assuming a low-angle, diffusive wave climate)

4 mm/year with a periodic retreat (Fig. 8). The initial coast is perturbed by reducing the width of the barrier within the middle of the model domain.

The entire coast begins vigorously rolling over landwards (Fig. 13). The initially wider barrier eventually stops rolling over, even as the thin section continues to overwash. The differences in the shoreline location, however, are transmitted alongshore (notice the smooth curvature of the coast), and soon the entire coast is periodically retreating in sync.

With weaker alongshore coupling, asynchronous barrier retreat persists for much longer (Fig. 14). As a result, there are periods when the shoreline of the initially rapidly eroding coast stays in place and eventually becomes landward of other portions of the coast, with offsets that can last for hundreds of years. In this case, the shoreline and barrier location reflect a complex history of interconnected behavior. These new model results demonstrate how continued understanding of barrier dynamics requires understanding of variability in both the cross-shore and alongshore directions.

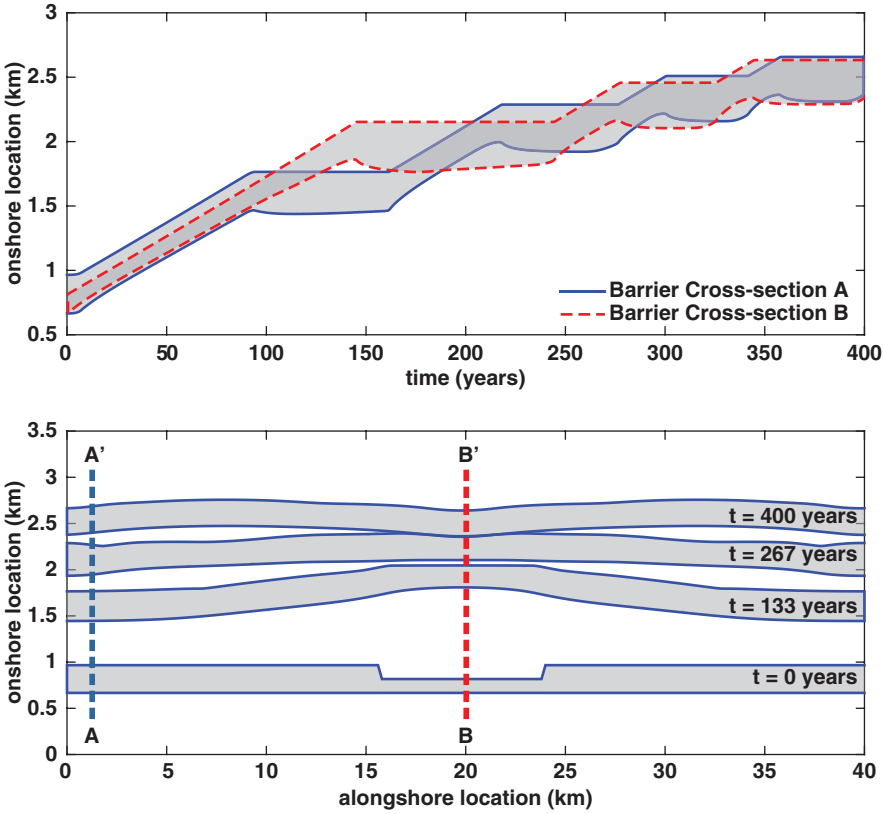

Fig. 13 Barrier island evolution with a constant sea-level-rise rate of 4 mm/year and strong alongshore coupling ($d = 0.5$). Top: time evolution of the ocean and backbarrier shorelines. Bottom: plan views of the barrier at different time intervals

7 Discussion

The dynamics explored here prompt a few key questions. How could we determine if the dynamic, threshold behaviors prominent in the model results have occurred (or could occur) for natural barriers? Furthermore, if periodic behavior might be the most common mode of barrier transgression, why do the results of morphokinematic models provide reasonable long-term trajectories of barrier across several thousands of years? For example, our results suggest that development of a dynamic equilibrium, which most approximates the behavior of morphokinematic models, requires steep back-barrier slopes and slow sea-level rise rates, also occurring most often when the shoreface responds quickly. Otherwise, dynamic equilibrium rollover is not expected, particularly for gentle slopes and faster sea-level rise rates.

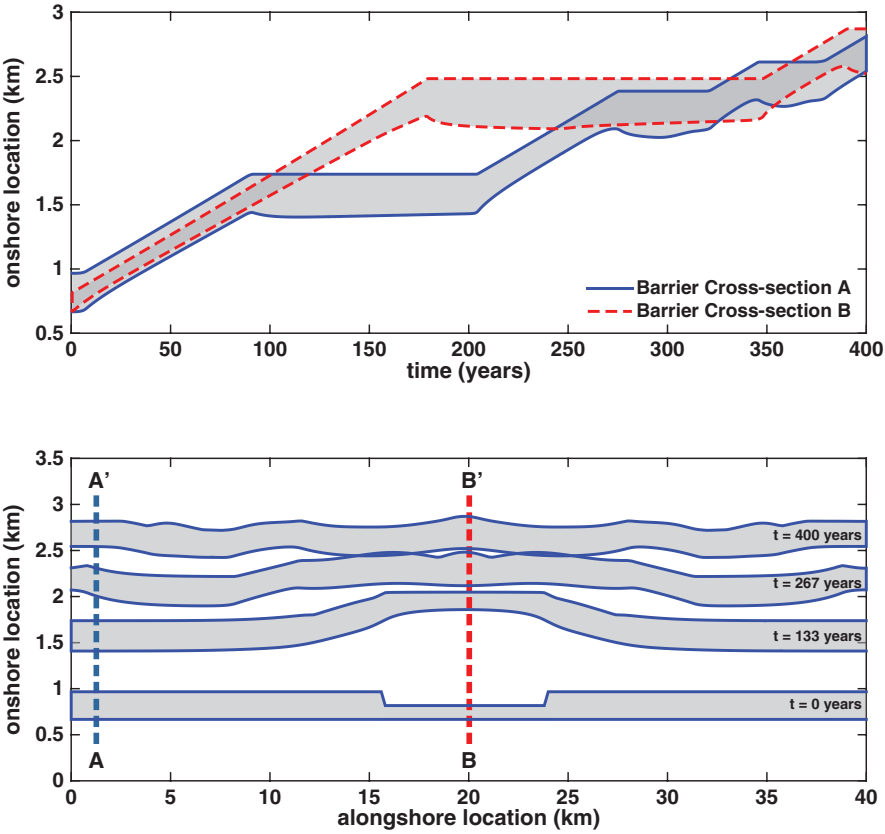

Fig. 14 Barrier island evolution with a constant sea-level-rise rate of 4 mm/year and weak alongshore coupling ($d = 0.1$). Top: time evolution of the ocean and backbarrier shorelines. Bottom: plan views of the barrier at different time intervals

Perhaps, although morphokinematic models may be constrained in their ability to reproduce the exact timing and location of barriers transgressing a shelf, the underlying fundamental rigor of mass balance provides a long-term constraint on barrier position. For example, when our model displays periodic retreat, the most common behavior within our parameter space, the long-term trajectory is that of the back-barrier, a finding that also arises from the mass balance underlying the morphokinematic approach (Wolinsky 2009; Wolinsky and Murray 2009; Moore et al. 2010; Murray and Moore this volume). Although long-term trajectories would be the same, decadally averaged rates of change and, indeed, gross barrier behavior arising from each approach could still be dramatically different. Over the long term, barriers that survive sea-level rise must tend towards the long-term trajectory determined by the regional slope, tempered by lithologic control (non-beach-compatible sediments such as muds and peats underlying many barrier islands can affect the

long-term trajectories) (Stolper et al. 2005; Moore et al. 2010, 2014). However, despite similarity in long-term trends, our modeling results suggest that the specifics of barrier transgression across the shelf may depart significantly from the continuous predictions suggested by the results of morphokinematic models. A barrier that spends most of its time not transgressing is perhaps fundamentally different than a smoothly moving system—morphokinematic models may generally reproduce the past history or future behavior of barriers, but care should be taken in interpreting not only predicted barrier location, but also the style of retreat.

An apt analogy may be the fable of the tortoise and the hare. Both animals began and ended a race at approximately the same time, and therefore, traversed the course with similar average speeds. Their detailed trajectories, however, are quite different. Slow and steady, the tortoise lumbered along at a constant rate. On the other hand, the hare raced ahead rapidly, rested in the middle, and then chased to (not quite) catch up with the tortoise.

Can the morphodynamic results be tested? Perhaps over the late Holocene, sea-level rise rates were sufficiently slow such that overwash fluxes did not outpace shoreface response, in which case, associated lags may not have occurred. However, the most significant impediment to determining past behavior modes could be that barrier islands themselves (both in reality and definitely in models) tend to leave little sedimentologic evidence behind other than an ravinement (erosional) surface. However, when remnants of barrier facies and sand bodies are found on continental shelves, they are often presumed to be left behind by a rapid sea-level-rise event (Gardner et al. 2005; Mellett et al. 2012; Mellett and Plater this volume). Modeled barriers undergoing periodic retreat, even with a constant rate of sea-level rise, would be expected to leave alternating zones of shoreface deposition and shelf ravinement—large-scale periodic depositional features across the shelf could potentially be remnants of an autogenically episodic transgression.

For the model cases we present here in which sediment budgets are closed, the long-term trajectory of a barrier in dynamic equilibrium is the same as one experiencing periodic retreat. Despite this similarity, the system in dynamic equilibrium "glides" across the shelf without gaining or losing mass, whereas the periodically retreating barrier interacts with the shelf, alternately incising and depositing sediment (Figs. 3, 6, and 11). Such interactions with the shelf could have other implications for a barrier's trajectory—for the model experiments presented here we assume that the shelf consists of the same non-cohesive sand that is barrier-compatible. If a barrier is transgressing over a shelf of mixed cohesive and non-cohesive sediment, periodic retreat would result in a net incision of the shelf, with inflated sand bodies left behind.

For the model results shown here, the initial configuration is a barrier that is not yet rolling over, yet precariously perched at the equilibrium threshold where sea-level rise would initiate rollover. Many modern barriers (particularly those that are developed) are currently wider (on the order of 1 km or more) than threshold overwash widths (critical barrier widths tend to be on the order of 300–500 m, but this should vary locally; Leatherman 1983; Jiménez and Sánchez-Arcilla 2004). Some modern barriers have experienced several thousand years of slowly rising sea level

conditions and have grown wide, either through alongshore transport gradients or addition of sediment from other sources, such as rivers, or potentially from onshore sediment transport from the lower shoreface toe, a morphologic remnant from previous rapid transgression (Fig. 7) (e.g., Cowell and Kinsela this volume).

In many cases, even as shoreline erosion rates are significant, they are insufficient for long-term maintenance of the barrier shape (Carruthers et al. 2013), which could presage a threshold towards entering a rollover mode (Leatherman 1979, 1983). The dynamic modeling framework here can capture the dynamics of a transition to rapid overwash—sea-level rise will drive shoreface erosion (in the manner of the shoreface Bruun rule) until the barrier is thin, at which point overwash will take over. After a rapid rollover period, once overwash stalls, barriers would then continue to widen until the cycle starts again. Changes of the width of barriers over time should have both dynamic and ecologic impacts (Theuerkauf and Rodriguez 2017). Furthermore, episodic narrowing has significant implications for front-to-back resettlement management strategies on developed barriers (McNamara and Lazarus this volume), particularly as overwash volumes can depend on the amount and type of development on top of barriers (Rogers et al. 2015).

Overall, as evidence of barrier transgression remains scant on the shelf, the specifics of how barriers moved onshore may remain a mystery. However, our morphodynamic modeling framework offers the potential to understand how the process of transgression may have occurred, suggesting foremost that unforced oscillations might not only occur, but also should be expected. How such oscillations may interact with intervals of rapid sea-level rise and the stochastic nature of storms, as well as the potential dynamic influence of lithology and back-barrier sedimentation, remains the focus of future investigations.

Our simple model assumes a barrier fully composed of sandy sediments, and future efforts can benefit from rich insights gained from previous morphokinematic models that account for environmental complexities, such as lithological variation, lagoonal sedimentation, and the influence of back-barrier marsh development (Cowell et al. 1995; Stolper et al. 2005; Moore et al. 2010, this volume; Walters et al. 2014). Two such examples couple the dynamic barrier framework with the dynamics of marsh growth and edge erosion (Walters et al. 2014; Lorenzo-Trueba and Mariotti 2017).

Furthermore, interactions with aeolian processes that build dunes atop barriers are similarly prone to autocyclic and threshold behaviors (Moore et al. this volume; Ruggiero et al. this volume), and overwash processes remain an important next avenue of research. This includes the effects of dune rebuilding (Priestas and Fagherazzi 2010) and reworking of the subaerial barrier by rainfall and runoff (Fagherazzi and Priestas 2012). Importantly, whether or not modern barriers are prone to threshold behavioral changes will be important for understanding barrier evolution over the coming centuries as global sea level rise quickens and storm and wave climates possibly change.

8 Conclusions

Using a simple morphodynamic model of barrier evolution, we demonstrate that the coupled shoreface-overwash system that comprises barriers can exhibit complex dynamics. Model results suggest that dynamic equilibrium rollover can develop as barriers cross the shelf; however, oscillatory behavior and drowning tend to be more common responses. Furthermore, slight geometric perturbations, in both the cross- and alongshore, can cause abrupt transitions in barrier behavior. This suggests that the smooth transgressive behavior expected from conceptual and analytical models, which is quantified and visualized in numerical morphokinematic models, may give an unreasonable expectation of gentle and smooth progressive transgression of barrier systems as sea level rises. The presence of threshold behaviors affects interpretations of relict barrier deposits, as we demonstrate that changes in external forcing, such as rapid sea-level-rise events, are not necessary for barriers to transition from a stable configuration to a rapid rollover state.

Acknowledgments This research was funded by National Science Foundation grants CNH-0815875 and CNH-85850300, as well as Strategic Environmental Research and Development Program grant RC-1702. We thank Alejandra Ortiz, Jaap Nienhuis, and Daniel Ciarletta for thoughtful conversations. The manuscript was improved by thoughtful reviews from Peter Ruggiero and an anonymous reviewer. We also thank the editors of the book for their thoughtful input and patience.

References

Ashton AD, Murray AB (2006a) High-angle wave instability and emergent shoreline shapes: 1. Modeling of sand waves, flying spits, and capes. J Geophys Res Earth Surf 111:F04011. https://doi.org/10.1029/2005JF000422

Ashton AD, Murray AB (2006b) High-angle wave instability and emergent shoreline shapes: 2. Wave climate analysis and comparisons to nature. J Geophys Res Earth Surf 111:F04012. https://doi.org/10.1029/2005JF000423

Ashton AD, Ortiz AC (2011) Overwash controls coastal barrier response to sea-level rise. In: Coastal sediments '11. Miami, Florida, pp 230–243

Ashton A, Murray AB, Arnoult O (2001) Formation of coastline features by large-scale instabilities induced by high-angle waves. Nature 414:296–300. https://doi.org/10.1038/35104541

Ashton AD, Nienhuis J, Ells K (2016) On a neck, on a spit: controls on the shape of free spits. Earth Surf Dyn 4:193–210. https://doi.org/10.5194/esurf-4-193-2016

Bowen AJ (1980) Simple models of nearshore sedimentation. Beach profiles and longshore bars. In: McCann SB (ed) The coastline of Canada. Geological survey of Canada, pp 1–11

Bruun P (1962) Sea-level rise as a cause of shore erosion. Proc ASCE. J Waterw Harb Div 88:117–130

Bruun PER (1983) Review of conditions for uses of the Bruun rule of erosion. Water 7:77–89

Carruthers EA, Lane DP, Evans RL et al (2013) Quantifying overwash flux in barrier systems: an example from Martha's vineyard, Massachusetts. USA Mar Geol 343:15. https://doi.org/10.1016/j.margeo.2013.05.013

Cooper JAG, Pilkey OH (2004) Sea-level rise and shoreline retreat: time to abandon the Bruun rule. Glob Planet Change 43:157–171

Cowell PJ, Kinsela MA (2018) Shoreface controls on barrier evolution and shoreline change. In: Moore LJ, Murray AB (eds) Barrier dynamics and response to changing climate. Springer, New York

Cowell PJ, Roy PS, Jones RA (1992) Shoreface translation model: computer simulation of coastal-sand-body response to sea level rise. Math C Simul 33:603–608

Cowell PJ, Roy PS, Jones RA (1995) Simulation of large-scale coastal change using a morphological behavior model. Mar Geol 126:45–61

Davidson-Arnott RGD (2005) Conceptual model of the effects of sea level rise on Sandy coasts. J Coast Res 216:1166–1172. https://doi.org/10.2112/03-0051.1

Dean RG (1991) Equilibrium Beach profiles: characteristics and applications. J Coast Res 7:53–84

Dean RG, Maurmeyer EM (1983) Models for beach profile response. In: Komar PD (ed) Handbook of coastal processes and erosion. CRC Press, Boca Raton, pp 151–165

Donnelly C, Kraus NC, Larson M (2006) State of knowledge of measurement and modeling of coastal overwash. J Coast Res 224:965–991. https://doi.org/10.2112/04-0431.1

Fagherazzi S, Priestas AM (2012) Back-barrier flooding by storm surges and overland flow. Earth Surf Process Landforms 37:400–410. https://doi.org/10.1002/esp.2247

Fagherazzi S, Wiberg PW, Howard AD (2003) Modeling barrier island formation and evolution. In: Proceedings of the international conference on coastal sediments 2003. CD-ROM published by World Scientific Publishing Corp. And East Meets West Productions, Corpus Christi, Texas, USA. St. Petersburg, Florida. ISBN 981-238-422-7

Falqués A, Calvete D (2005) Large-scale dynamics of sandy coastlines: diffusivity and instability. J Geophys Res 110. https://doi.org/10.1029/2004JC002587

Falqués A, Ribas F, Idier D, Arriaga J (2017) Formation mechanisms for self-organized kilometer-scale shoreline sand waves. J Geophys Res Earth Surf 122:1121–1138. https://doi.org/10.1002/2016JF003964

Gardner JV, Dartnell P, Mayer LA et al (2005) Shelf-edge deltas and drowned barrier–island complexes on the northwest Florida outer continental shelf. Geomorphology 64:133–166. https://doi.org/10.1016/j.geomorph.2004.06.005

Hallermeier RJ (1981) A profile zonation for seasonal sand beaches from wave climate. Coast Eng 4:253–277

Houser C, Barrineau P, Hammond B, Saari B, Rentschler E, Trimble S, Wernette P, Weymer B, Young S (2018) Role of the foredune in controlling barrier island response to sea level rise. In: Moore LJ, Murray AB (eds) Barrier dynamics and response to changing climate. Springer, New York

Jiménez JA, Sánchez-Arcilla A (2004) A long-term (decadal scale) evolution model for microtidal barrier systems. Coast Eng 51:749–764

Komar PD (1971) The mechanics of sand transport on beaches. J Geophys Res 76:713–721

Larson M, Hanson H, Kraus NC (1987) Analytical solutions of the one-line model of shoreline change, technical report CERC-87-15

Leatherman SP (1979) Migration of Assateague Island, Maryland, by inlet and overwash processes. Geology 7:104–107

Leatherman SP (1983) Barrier dynamics and landward migration with Holocene sea-level rise. Nature 301:415–417

Lorenzo-Trueba J, Ashton AD (2014) Rollover, drowning, and discontinuous retreat: distinct modes of barrier response to sea-level rise arising from a simple morphodynamic model. J Geophys Res Earth Surf 119:779–801. https://doi.org/10.1002/2013JF002941

Lorenzo-Trueba J, Mariotti G (2017) Chasing boundaries and cascade effects in a coupled barrier-marsh-lagoon system. Geomorphology 290:153–163. https://doi.org/10.1016/j.geomorph.2017.04.019

Masetti R, Fagherazzi S, Montanari A (2008) Application of a barrier island translation model to the millennial-scale evolution of sand key, Florida. Cont Shelf Res 28:1116–1126. https://doi.org/10.1016/j.csr.2008.02.021

McNamara DE, Lazarus ED (2018) Barrier islands as coupled human–landscape systems. In: Moore LJ, Murray AB (eds) Barrier dynamics and response to changing climate. Springer, New York

Mellett CL, Plater AJ (2018) Drowned barriers as archives of coastal-response to sea-level rise. In: Moore LJ, Murray AB (eds) Barrier dynamics and response to changing climate. Springer, New York

Mellett CL, Hodgson DM, Lang A et al (2012) Preservation of a drowned gravel barrier complex: a landscape evolution study from the north-eastern English Channel. Mar Geol 315–318:115–131. https://doi.org/10.1016/j.margeo.2012.04.008

Moore LJ, List JH, Williams SJ, Stolper D (2010) Complexities in barrier island response to sea level rise: insights from numerical model experiments, North Carolina Outer Banks. J Geophys Res 115:F03004. https://doi.org/10.1029/2009jf001299

Moore LJ, Patsch K, List JH, Williams SJ (2014) The potential for sea-level-rise-induced barrier island loss: insights from the Chandeleur Islands, Louisiana, USA. Mar Geol 355:244–259. https://doi.org/10.1016/j.margeo.2014.05.022

Moore LJ, Goldstein EB, Vinent OD, Walters D, Kirwan M, Rebecca L, Brad Murray A, Ruggiero P (2018) The role of ecomorphodynamic feedbacks and landscape couplings in influencing the response of barriers to changing climate. In: Moore LJ, Murray AB (eds) Barrier dynamics and response to changing climate. Springer, New York

Murray AB, Moore LJ (2018) Geometric constraints on long-term barrier migration: from simple to surprising. In: Moore LJ, Murray AB (eds) Barrier dynamics and response to changing climate. Springer, New York

Odezulu CI, Lorenzo-Trueba J, Wallace DJ, Anderson JB (2018) Follets Island: a case of unprecedented change and transition from rollover to subaqueous shoals. In: Moore LJ, Murray AB (eds) Barrier dynamics and response to changing climate. Springer, New York

Ortiz AC, Ashton AD (2016) Exploring shoreface dynamics and a mechanistic explanation for a morphodynamic depth of closure. J Geophys Res F Earth Surf 121:442. https://doi.org/10.1002/2015JF003699

Pelnard-Consideré R (1956) Essai de theorie de l'evolution des formes de rivage en plages de sable et de galets. 4th Journees l'Hydraulique, Les Energies la Mer III:289–298

Priestas AM, Fagherazzi S (2010) Morphological barrier island changes and recovery of dunes after Hurricane Dennis, St. George Island, Florida. Geomorphology 114:614–626. https://doi.org/10.1016/j.geomorph.2009.09.022

Rodriguez AB, Yu W, Theuerkauf EJ (2018) Abrupt increase in washover deposition along a transgressive barrier island during the late 19th century acceleration in sea-level rise. In: Moore LJ, Murray AB (eds) Barrier dynamics and response to changing climate. Springer, New York

Rogers LJ, Moore LJ, Goldstein EB et al (2015) Anthropogenic controls on overwash deposition: evidence and consequences. J Geophys Res F Earth Surf 120:2609. https://doi.org/10.1002/2015JF003634

Rosati JD, Dean RG, Walton TL (2013) The modified Bruun rule extended for landward transport. Mar Geol 340:71–81. https://doi.org/10.1016/j.margeo.2013.04.018

Ruggiero P, Hacker S, Seabloom E, Zarnetske P (2018) The role of vegetation in determining dune morphology, exposure to sea-level rise, and storm-induced coastal hazards: a U.S. Pacific Northwest perspective. In: Moore LJ, Murray AB (eds) Barrier dynamics and response to changing climate. Springer, New York

Splinter KD, Turner IL, Davidson MA et al (2014) A generalized equilibrium model for predicting daily to interannual shoreline response. J Geophys Res Earth Surf 119:1936–1958. https://doi.org/10.1002/2014JF003106

Stive MJF, de Vriend HJ (1995) Modelling shoreface profile evolution. Mar Geol 126:235–248. https://doi.org/10.1016/0025-3227(95)00080-I

Stive MJF, Nicholls RJ, deVriend HJ (1991) Sea-level rise and shore nourishment—a discussion. Coast Eng 16:147–163

Stolper D, List JH, Thieler ER (2005) Simulating the evolution of coastal morphology and stratigraphy with a new morphological-behaviour model (GEOMBEST). Mar Geol 218:17–36. https://doi.org/10.1016/j.margeo.2005.02.019

Storms JEA, Weltje GJ, Van Dijke JJ et al (2002) Process-response modeling of wave-dominated coastal systems: simulating evolution and stratigraphy on geological timescales. J Sediment Res 72:226–239

Theuerkauf EJ, Rodriguez AB (2017) Placing barrier-island transgression in a blue-carbon context. Earth's Futur 5:789. https://doi.org/10.1002/2017EF000568

Walters D, Moore LJ, Duran Vinent O et al (2014) Interactions between barrier islands and backbarrier marshes affect island system response to sea level rise: insights from a coupled model. J Geophys Res Earth Surf 119:2013–2031. https://doi.org/10.1002/2014JF003091

Walton Jr. TL, Dean RG (1973) Application of littoral drift roses to coastal engineering problems

Wolinsky MA (2009) A unifying framework for shoreline migration: 1. Multiscale shoreline evolution on sedimentary coasts. J Geophys Res 114:F01009

Wolinsky MA, Murray AB (2009) A unifying framework for shoreline migration: 2. Application to wave-dominated coasts. J Geophys Res 114:F01009

Wright LD (1995) Morphodynamics of inner continental shelves. CRC Press, Boca Raton

Wright LD, Boon JD, Kim SC, List JH (1991) Modes of cross-shore sediment transport on the shoreface of the Middle Atlantic Bight. Mar Geol 96:19–51. https://doi.org/10.1016/0025-3227(91)90200-N

Yates ML, Guza RT, O'Reilly WC (2009) Equilibrium shoreline response: observations and modeling. J Geophys Res 114:C09014. https://doi.org/10.1029/2009jc005359

Zhang K, Douglas BC, Leatherman SP (2004) Global warming and coastal erosion. Clim Chang 64:41–58. https://doi.org/10.1023/B:CLIM.0000024690.32682.48

The Role of Ecomorphodynamic Feedbacks and Landscape Couplings in Influencing the Response of Barriers to Changing Climate

Laura J. Moore, Evan B. Goldstein, Orencio Durán Vinent, David Walters, Matthew Kirwan, Rebecca Lauzon, A. Brad Murray, and Peter Ruggiero

Abstract Because barriers are low-lying and dynamic landforms, they are especially sensitive to changing environmental conditions. The continued existence of barriers will depend on the degree to which these landforms can maintain elevation above sea level while also migrating landward. We are increasingly learning that ecomorphodynamic interactions (i.e., interactions between morphology, fluid dynamics, and/or sediment transport with biological processes) as well as couplings between barrier and back-barrier environments play a critical role in determining how barrier systems will evolve as sea level rises, storm intensity increases, and the species composition of coastal vegetation changes in the future. For example, the effectiveness of storms in building elevation and moving a barrier landward is determined, in large part, by the morphology of the coastal foredune (i.e., the seaward-most dune), which is itself a product of couplings between vegetation and sediment transport processes. The cross-shore and alongshore shape of coastal foredunes, in the presence of shoreline erosion or shoreline accretion, is influenced by the distance from the shoreline that vegetation can grow, the rates of lateral and vertical vegetation growth of dune-building vegetation, as well as the dependence of

L.J. Moore, Ph.D. (✉) • E.B. Goldstein, Ph.D.
Department of Geological Sciences, University of North Carolina at Chapel Hill, Chapel Hill, NC, USA
e-mail: laura.moore@unc.edu; evan.goldstein@unc.edu

O.D. Vinent, Ph.D. • D. Walters, M.S. • M. Kirwan, Ph.D.
Department of Physical Sciences, Virginia Institute of Marine Sciences, Gloucester Point, VA, USA
e-mail: oduranvinent@tamu.edu; davidwalters@usgs.gov; kirwan@vims.edu

R. Lauzon, B.A • A.B. Murray, B.A., B.I.S., M.S., Ph.D.
Division of Earth and Ocean Sciences, Nicholas School of the Environment, Duke University, Durham, NC, USA
e-mail: rebecca.lauzon@duke.edu; abmurray@duke.edu

P. Ruggiero, Ph.D.
College of Earth, Ocean, and Atmospheric Sciences, Oregon State University, Corvallis, OR, USA
e-mail: pruggier@coas.oregonstate.edu

L.J. Moore, A.B. Murray (eds.), *Barrier Dynamics and Response to Changing Climate*, https://doi.org/10.1007/978-3-319-68086-6_10

vegetation growth on dune slope. In addition, as storm frequency increases relative to the rate at which dunes can grow, dunes, and therefore local barrier elevation, may become bistable, tending to be in either a high dune/barrier or low dune/barrier state. When dunes are low, storms can effectively increase barrier elevation and move a barrier landward over time leading also to the potential for increased connectivity to back-barrier marshes, which are vulnerable to drowning as sea level rises. In this case, sand delivered to back-barrier marshes can, for a time, allow back-barrier marshes to persist under conditions in which they would otherwise disappear, thereby benefitting the entire barrier-marsh system. Here we provide a synthesis of model results—tested against observations—that demonstrate these findings, illustrating the importance of feedbacks between vegetative and sediment transport processes, and couplings between landscape units, in influencing the future evolution of barrier-marsh systems.

Keywords Ecomorphodynamics • Beach grasses • Dune grasses • *Ammophila breviligulata* • *Uniola paniculata* • *Spartina patens* • Coastal barriers • Barrier islands • Backbarrier marsh • Foredunes • Morphodynamics • Barrier migration • Hummocky dunes • Sea-level rise • Virginia • East coast

1 Introduction

As low-lying landforms, barrier islands and barrier spits are vulnerable to changing conditions, such as climate change-induced sea-level rise (e.g., Stocker et al. 2013; Sallenger et al. 2012; Kopp et al. 2014), increases in the frequency of the most intense hurricanes and tropical storms (e.g., Knutson et al. 2010; Emanuel 2013) (as well as the changes in wave climate that are likely to occur as a result, e.g., Moore et al. 2013; Johnson et al. 2015), and the potential for changes in the species composition of foundational dune-building vegetation. Traditionally, the overall long-term evolution of a barrier system—whether it is growing seaward (prograding) or migrating landward (retrograding, transgressive)—has been thought to depend primarily on the balance between how sea level is changing locally (i.e., relative sea-level change) and sediment supply (e.g., Curray 1960; FitzGerald et al. 2008). When the rate of sediment supply is sufficiently large to overcome relative sea-level rise (or when sea level is falling), a barrier will tend to prograde seaward, widening in the seaward direction and leading to the formation of multiple dune ridges through time—e.g., some barriers in Oregon and Washington (Ruggiero et al. 2016) and the ends of rotational barrier islands on mixed-energy coasts, such as the Virginia Eastern Shore (personal observation). When the rate of sea-level rise and the rate of sediment supply are in balance, although storms may occasionally cause shoreline or dune erosion, barrier shoreline position will tend to be stable and the landform itself will remain stationary over time. In contrast, and as is most common today, barriers for which the rate of sediment supply is not sufficient to overcome the effects of relative sea-level rise will tend to become narrower as their seaward

shoreline erodes (moves landward) over time, leading to an increased frequency of dune erosion and overwash and the potential for landward barrier migration (e.g., Assateague Island, VA; Leatherman 1979).

Overwash occurs when the combination of tides, storm surge, and waves brings water levels above the highest cross-shore point on the profile, which is often the seaward-most dune, known as the foredune (e.g., Sallenger 2000, see also Rodriguez et al. this volume). The overwash process removes sand from the front of a barrier, depositing it on the top or back side, building barrier elevation, and facilitating landward migration of the landform toward higher elevations (e.g., Hayden et al. 1980). As barriers migrate landward, they tend to maintain an equilibrium in which barrier elevation relative to sea level is near constant. Although landward barrier migration is a prerequisite for the continued persistence of these landforms, it is in direct conflict with their current use in developed areas, and, as a result, migration is often prevented from occurring (e.g., see McNamara and Lazarus this volume). When a barrier is no longer able to build upward and migrate landward sufficiently rapidly to maintain elevation relative to sea level, disintegration, drowning, and potential conversion to a subaqueous shoal become likely (e.g., FitzGerald et al. 2006; Moore et al. 2010, 2014; Rogers et al. 2015; Ashton and Lorenzo-Trueba this volume; Mellett and Plater this volume; Odezulu et al. this volume).

Contributing to the balance between changes in sea level and changes in sediment supply over long time scales (i.e., centuries to millennia) are the effects of substrate slope, substrate erodibility, substrate composition, and the potential for important contributions of sediment from the shoreface (see Murray and Moore this volume and Cowell and Kinsela this volume). Further, it is becoming increasingly clear that changes in the intensity and frequency of coastal storms, as well as shifts in the geographic distribution of important species of dune vegetation, also play a critical role in determining barrier state by influencing processes at shorter time scales (i.e., annual to centurial), especially as a barrier approaches the threshold for transition from one state to another (e.g., stable to landward migrating or migrating to disintegrating/drowning). These factors influence barrier state at shorter time scales because barrier morphology—especially the size, shape, and alongshore continuity of the coastal foredune—plays a fundamental role in determining how a barrier will respond to changes in forcing: dune morphology dictates whether or not overwash will occur during storms (e.g., Sallenger 2000; Houser et al. 2008, this volume) and how connected the beach/dune system is to the back-barrier (e.g., Walters et al. 2014; Brenner et al. 2015). Not only does barrier topography determine how a barrier will respond to changes in forcing, in developed areas dune topography is also critical in determining vulnerability to flooding and erosion hazards in the face of intensifying and/or more frequent storms and rising sea level; a role that is increasingly of interest to coastal communities (Elko et al. 2016).

In recent decades, the coastal science community has made significant progress in understanding the effect of barrier morphology on the impact of storms and vice versa (i.e., the two-way coupling between morphology and storm impacts; e.g., Morton 2002; Morton and Sallenger 2003; Stockdon et al. 2007; Roelvink et al. 2009). Emerging only more recently is a better mechanistic understanding of the

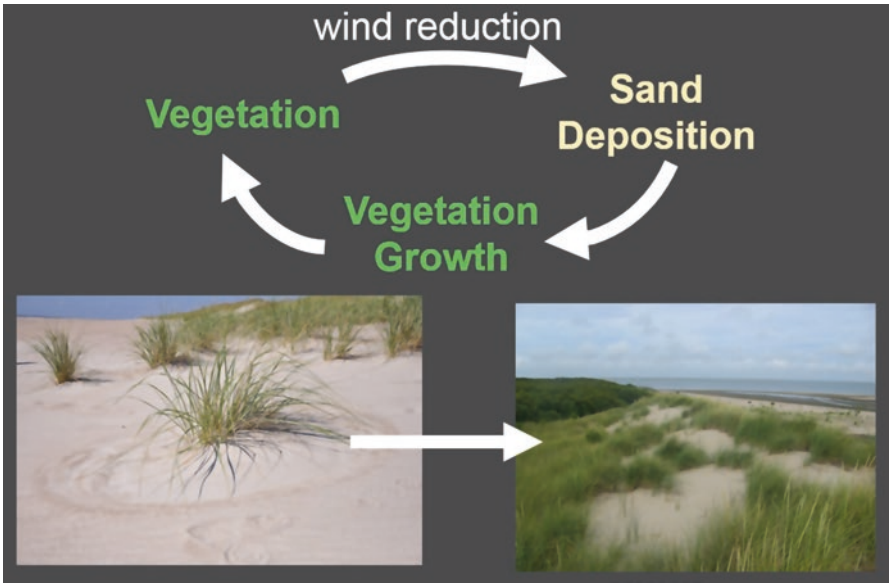

Fig. 1 An illustration of the feedback between vegetation and sand deposition that gives rise to the formation of coastal foredunes

processes and couplings that are responsible for the initial building, and recovery, of barrier topography via the formation of coastal foredunes (see also Ruggiero et al. this volume). Like dune erosion, dune-building also arises from a two-way coupling, in this case, between vegetation and aeolian sediment transport processes (e.g., Short and Hesp 1982; Hesp 1988, 1989). Vegetation slows sand-laden wind blowing across the back beach causing sand to accumulate in the vicinity of vegetation. Burial by sand then stimulates the growth of dune-building plants (e.g., Disraeli 1984; Ehrenfeld 1990; Maun 1998; Maun and Perumal 1999), further enhancing deposition in a positive (i.e., self-reinforcing) feedback that gives rise to the formation of dunes on the timescale of years (Fig. 1). Both the coupling between morphology and storm impacts and the feedback that gives rise to coastal dunes will be affected by climate-change induced shifts in storminess, wind intensity and/or frequency, precipitation, sea level, and the species composition of dune-building grasses. In addition, key processes operating in one component of the landscape have the potential to affect both adjacent and nonadjacent landscape units via connections and couplings that operate between components of the coastal system. Here, we provide a synthesis, based primarily on our results from numerical model experiments, of: (1) the ecological and morphodynamic (i.e., "ecomorphodynamic") factors that control the morphology of coastal foredunes; (2) what we are coming to understand about the effects of foredune morphology on long-term barrier response to changing climate; and (3) our emerging understanding of the role of connectivity among landscape units in altering how barrier systems respond to changing conditions.

2 Vegetation Control of Dune Morphology

A growing body of quantitative, largely observational, work has examined species-specific control on foredune morphology along the U.S. West Coast (Seabloom and Wiedemann 1994; Hacker et al. 2012; Zarnetske et al. 2012, 2013; Ruggiero et al. this volume). Hacker et al. (2012) present results that connect U.S. Pacific Northwest dune-grass species morphology, or growth form, to the resulting dune morphology. Ongoing species invasion, which results in changing species dominance and changes to dune morphology, is therefore impacting protective services provided by dunes (e.g., Seabloom et al. 2013; Zarnetske et al. 2015).

Building on earlier work (e.g., Godfrey 1977; Godfrey et al. 1979), there has been renewed interest in investigating species-specific control of foredune morphology on the U.S. East Coast (e.g., Stallins and Parker 2003; Stallins 2005; Wolner et al. 2013). The primary dune-building grass species on the U.S. East Coast are *Ammophila breviligulata* (American Beachgrass), which tends to dominate from Virginia northward, and *Uniola paniculata* (Sea Oats), which tends to dominate from North Carolina southward (Fig. 2; Woodhouse et al. 1977; Duncan and Duncan 1987; Lonard et al. 2011). The mid-Atlantic region is the transition

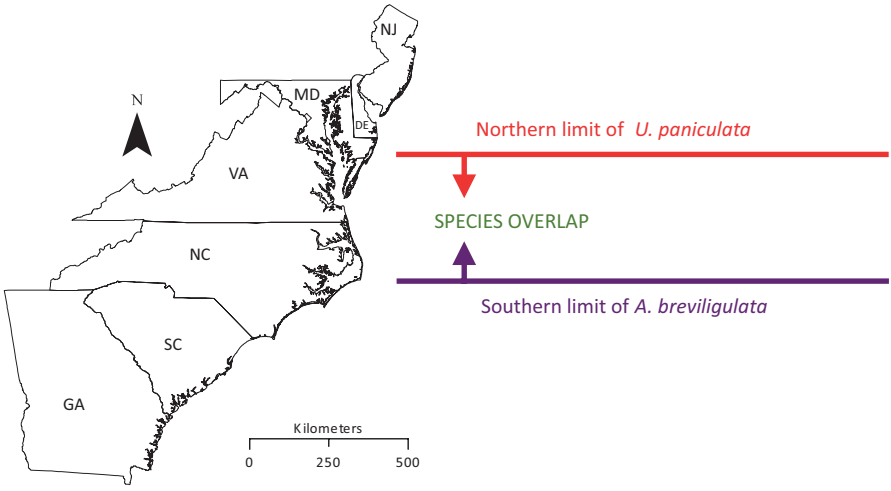

Fig. 2 A literature review and field observations suggest that the U.S. mid-Atlantic region is the transition zone between the two foredune grasses *Uniola paniculata* and *Ammophila breviligulata*. Plantings of *A. breviligulata* in NC tend to die as a result of blight, pests, drought intolerance, and intolerance of high temperature (Seneca 1972; Singer et al. 1973; Van Der Valk 1975; Woodhouse et al. 1977; Odum et al. 1987; Duncan and Duncan 1987; Seliskar and Huettel 1994). *U. paniculata* appears to be restricted in northward extent by temperature (Seneca 1972; Godfrey 1977; Duncan and Duncan 1987) though northern expansion of the range has been observed (Stalter and Lamont 1990, 2000; Zinnert et al. 2011)

zone between the two species. In the U.S. Southeast, *A. breviligulata* tends to succumb to intolerance of drought, high temperatures, pests, and blight (Seneca 1972; Singer et al. 1973; Van Der Valk 1975; Woodhouse et al. 1977; Odum et al. 1987; Duncan and Duncan 1987; Seliskar and Huettel 1994). Temperature constraints determine the northward extent of *U. paniculata* (Seneca 1972; Godfrey 1977; Duncan and Duncan 1987), though range expansion has been observed (Stalter and Lamont 1990, 2000; Zinnert et al. 2011) and competition between *A. breviligulata* and *U. paniculata* tends to favor *U. paniculata* (Brown et al. 2017; Harris et al. 2017).

The change in species dominance from north to south along the U.S. East Coast appears to impact foredune morphology—observational work has demonstrated that dunes in the northeast tend to be alongshore continuous, whereas dunes in the southeast tend to be hummocky and irregular (Godfrey 1977; Godfrey et al. 1979). Later in this chapter, we explore, quantitatively, a hypothesis that this geographical difference in dune morphology may be the result of differences in the lateral growth rates of the dominant species, summarizing results from Goldstein et al. (2017).

Two other dune-building grasses are commonly found on U.S. East Coast foredunes, occasionally with high local abundance, most notably, *Spartina patens*, which is also a common marsh grass (Godfrey 1977; Lonard et al. 2010)—and *Panicum amarum* (Lonard and Judd 2011). From our anecdotal observations of the Virginia and North Carolina coast, these two grasses appear to be most commonly associated with low embryo dunes, though the role of these grasses in dune formation is not well-understood.

2.1 Maximum Potential Dune Height

To investigate coastal foredune dynamics and the factors that determine dune size and formation time, Durán and Moore (2013) reformulated and expanded a legacy code (previously developed by Durán and Herrmann 2006 and Durán et al. 2008 to study the effects of vegetation on desert dunes) to simulate dune formation in the coastal barrier environment. The resulting new, spatially explicit, numerical model (Durán and Moore 2013; Durán Vinent and Moore 2015b) consists of a series of differential equations representing the physical and biological processes affecting sand transport on a vegetated, sandy surface, in the presence of a shoreline, at low tide. At each time step, the model resolves the fluid dynamics of the wind, as well as the reduction in shear stress induced by the presence of vegetation, to determine the shear stress exerted at the sand surface across the model domain. Where the shear stress is above the critical threshold necessary for sand transport, the model calculates a sand flux, from which, based on the principles of mass conservation, the model calculates the resulting rate of erosion or accretion of the sand surface. Using a parameter relating rates of surface erosion and accretion to changes in vegetation growth, the percentage of the domain that is covered in vegetation and the locations

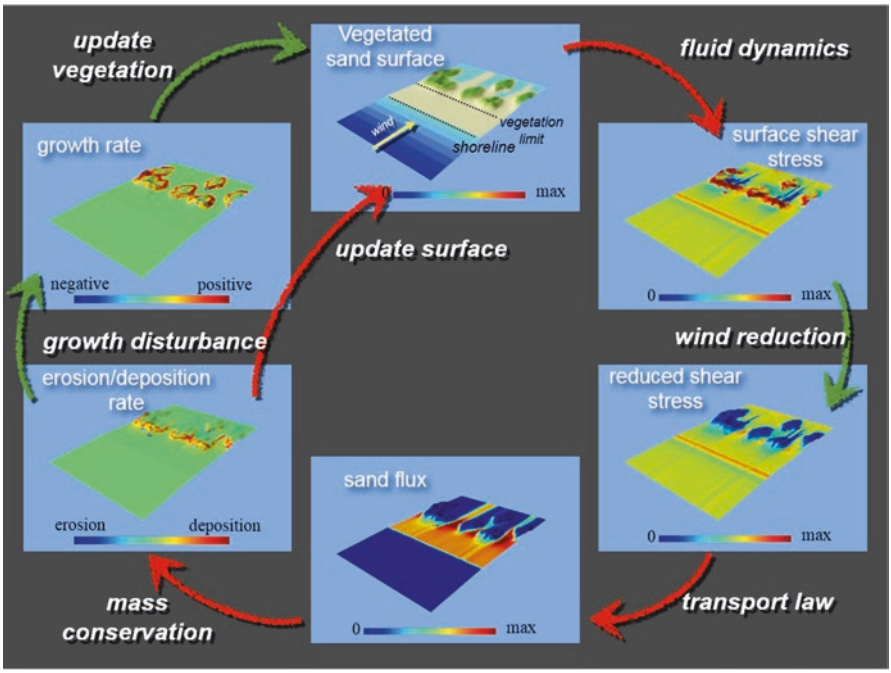

Fig. 3 The Coastal Dune Model consists of a series of differential equations that simulate the co-evolution of vegetation and a sandy surface. At each timestep, the model iterates through the steps depicted in this schematic

where vegetation grows are updated and the model iterates through successive time steps (Fig. 3). In a typical simulation, sand transport begins above the water line and continues across the beach into the backshore under a constant wind (for simplicity and generalization) where it is trapped by dune-building vegetation leading to formation of a foredune. For a description of the specific equations and a more extensive description of this version of the model, please see Durán and Moore (2013).

Using this model, Durán and Moore (2013) found that the formation of dunes is eventually limited by a negative feedback between wind flow and topography such that, for a given set of conditions, there is a maximum potential dune height that can be achieved. As a result of the negative feedback, steady-state foredunes are scale invariant, which allows derivation of scaling relations for maximum dune height and dune formation time—two parameters that are critical to barrier evolution across a range of time scales. Durán and Moore (2013) found that the rate of dune formation is controlled by the sand flux from the beach to dunes (which is related to, but not the same as the sand flux from the nearshore to the beach, e.g., Psuty 1992) (Fig. 4a): higher rates of sand flux (e.g., resulting, for example, from faster or more frequent winds and dryer conditions) lead to faster rates of dune formation.

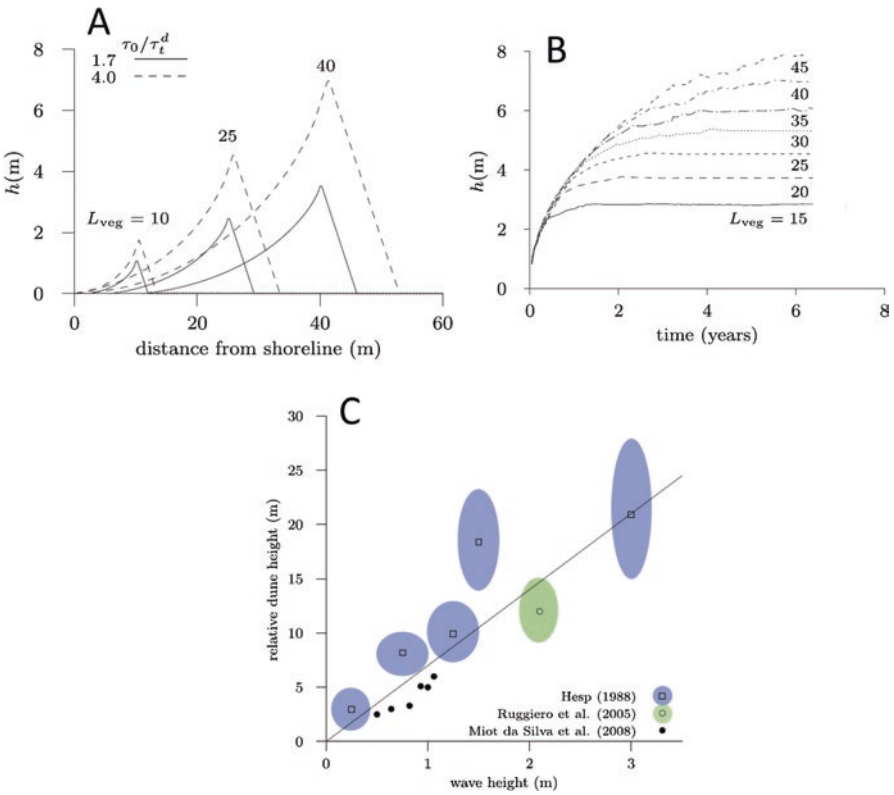

Fig. 4 Results from numerical model simulations demonstrate that (**a**) dune formation time decreases as the sand flux rate increases and (**b**) dune size increases as the distance from the shoreline that dune-building vegetation becomes established (L_{veg}) increases. (**c**) A collection of observations of dune size relative to wave height indicating that larger dunes are associated with dissipative beaches. Figures originally published in Durán and Moore (2013)

Contrary to what was previously assumed, Durán and Moore (2013) also found that the size of coastal foredunes is not related to sand flux magnitude, but is instead a function of the distance from the shoreline that dune-building vegetation can grow, a distance they call L_{veg} (Fig. 4b). The farther from the shoreline that dune-building vegetation establishes, the larger a dune can grow before it steers the wind above the surface of the beach, reducing the shear stress below the critical threshold for transport thereby causing dune growth to cease. These results offer an explanation for the observed relationship between beach type and foredune size, in which large (small) foredunes are found on dissipative (reflective) beaches, regardless of whether the associated sand supply rate is large or small (Fig. 4c). Higher waves associated with dissipative beaches increase the disturbance of dune-building grass species, lengthening L_{veg}, and shifting foredune formation landward, leading to larger foredunes.

2.2 Hummockiness

The model experiments discussed so far include vegetation growth parameterizations for a single generic dune species. However, individual species of dune-building grasses vary in their growth rate (vertical and lateral), shape (basal and frontal area), and propagation style (seed vs. rhizome), and these factors exert control on foredune morphology (e.g., Hacker et al. 2012; Hesp 2004; see also Ruggiero et al. this volume). We have focused on the U.S. Atlantic coast and used the Coastal Dune Model to study the relationship between species of vegetation (and variations in vegetation properties) and alongshore foredune morphology (Goldstein et al. 2017). Here, we consider the two dominant dune-building grasses on the U.S. Atlantic coast, *Uniola paniculata* and *Ammophila breviligulata*. In addition to differing in geographic range, these grasses differ in their lateral growth rate: *U. paniculata* grows more slowly in the lateral direction than Ammophila (Godfrey 1977). Additionally, qualitative observations by Godfrey and coworkers (Godfrey and Godfrey 1976; Godfrey 1977; Godfrey et al. 1979) suggest that dunes dominated by *U. paniculata* are "hummocky" (more height variation in the alongshore direction) compared to dunes dominated by *A. breviligulata* (which tend to be more consistent in height, and thus more continuous, alongshore).

Goldstein et al. (2017) use the Coastal Dune Model, with an improved vegetation growth routine presented in Moore et al. (2016), to investigate if hummockiness (i.e., variability in alongshore dune height) is a function of lateral propagation rate. As the plant lateral propagation rate decreases, Goldstein et al. (2017) observe that alongshore foredune height becomes increasingly variable. However, in all model experiments, regardless of lateral propagation rate, the foredune eventually coalesces, forming a continuous dune ridge of equal elevation. Experiments indicate that the timescale for coalescing is inversely related to lateral propagation rate. This work suggests that "hummockiness" is a transient phase, and that the timescale for the development and loss of hummockiness is related to the lateral growth rate of dunes (which is set by the lateral growth rate of vegetation; Fig. 5). However, the finding that hummocky dunes always coalesce if given sufficient time suggests that species-specific differences in lateral growth rates alone are not sufficient to explain hummockiness that persists through time.

A more complete explanation for the persistence of hummocky coastal foredunes requires combining our finding that coalescing timescales lengthen with decreasing lateral vegetation growth rate, with the suggestion by Godfrey (1977) that low areas (and therefore hummocks) are maintained by overwash during high-water events. Thus, the persistence of hummocky dunes along the U.S. southeast coast suggests that the recurrence time for high-water events tends to be shorter than the time it takes for low areas to grow vertically (via the coalescing of hummocks). Climate change may lead to a northward shift of the warm season, slowly laterally propagating dune grass *U. paniculata* (Zinnert et al. 2011; Stalter and Lamont 1990, 2000), and an increase in the frequency of high-water events. Such changes would lead to a higher potential for hummocky dunes to persist northward of their current distribution and for longer periods of time, increasing vulnerability to overwash and enhancing connectivity with back-barrier environments in these areas.

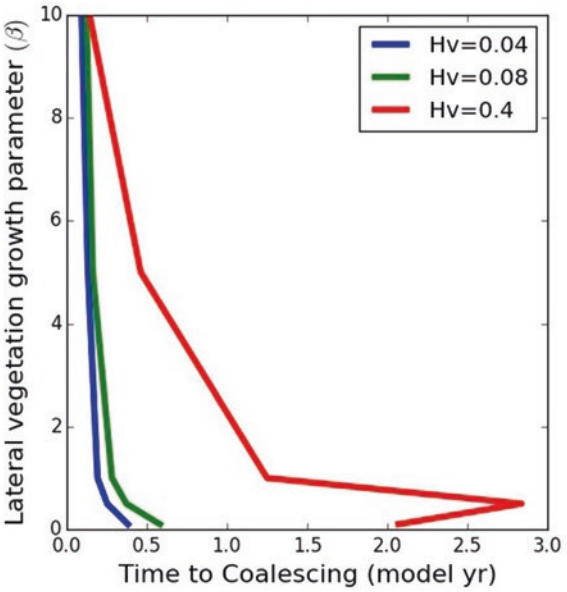

Fig. 5 Time to coalescing of hummocky coastal dunes as a function of lateral propagation rate (β) and plant growth rate (Hv). From Goldstein et al. (2017) and reprinted without changes under the Creative Commons Attribution 4.0 International license (CC BY 4.0; http://www.earth-surface-dynamics.net/about/licence_and_copyright.html)

2.3 Number, Spacing, and Size of Multiple Dunes

In addition to species-specific controls on dune shape in the alongshore direction, on barriers where the shoreline progrades seaward, limits on the lateral growth of vegetation appear to play an important role in determining cross-shore dune shape—setting the number, spacing, and size of multiple dunes (Moore et al. 2016). Researchers have long recognized that multiple dune ridges can form on progradational coasts in association with variations in beach and dune sediment supply (e.g., Hesp 1984; Psuty 1986), local tectonic activity (e.g., Goff et al. 2008), and/or sea level (e.g., Orford et al. 2000). In addition to providing protection from coastal storms—dune ridges have also been considered valuable indicators of local and regional changes in climate, sea level, and earthquake activity (e.g., Wells and Goff 2007; Goff et al. 2008).

Early work by Hesp (1984) cites evidence for the formation of incipient foredunes seaward of the primary foredune along a prograding coast in response to the colonization of new areas by dune-building vegetation. The conceptual model of beach–dune interactions of Psuty (1986, 1988) assumes that sediment supply to the beach and dune drives the formation of multiple dune ridges. Psuty (1986) hypothesizes that rapid beach progradation leads to a series of low foredune ridges, whereas slower rates of progradation allow for the development of a single, larger foredune. Moore et al. (2016) set out to investigate the role of vegetation in determining the morphology of multiple coastal dunes using a version of the Coastal Dune Model that includes lateral vegetation growth (as discussed in the section above) and shoreline progradation.

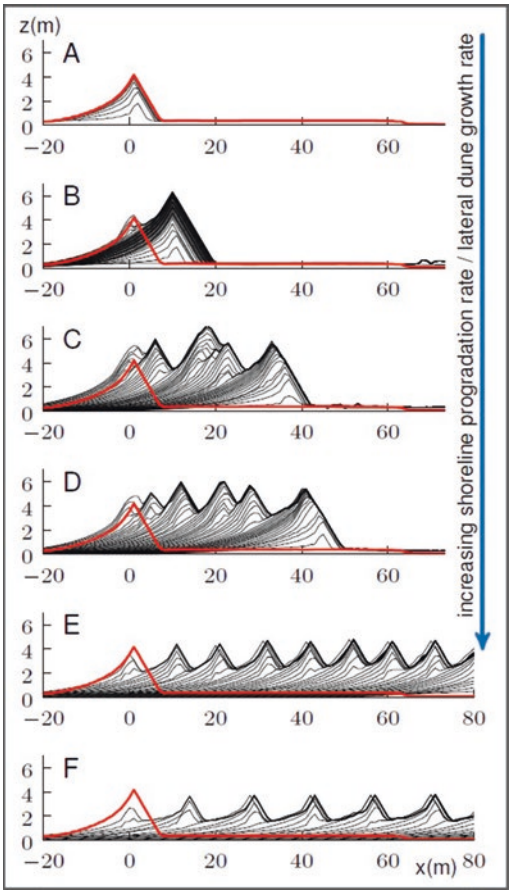

Fig. 6 Dune profile evolution in association with shorelines that are prograding at different rates. For comparison, the steady-state dune profile for a stable shoreline position is highlighted in *red* with its crest centered at $x = 0$. Progradation occurs to left as in Fig. 7, and $x = 0$ corresponds to the crest position of the newest foredune. Mean sea level corresponds to $z = 0$. From Moore et al. (2016) and reprinted with changes under the Creative Commons license (CC-BY; https://creativecommons.org/licenses/by/3.0/us/)

In addition to adding lateral vegetation growth, Moore et al. (2016) also added to the model the key assumption that steeper dune slopes reduce the lateral growth of rhizomes as they propagate from higher to lower areas and that, at slopes steeper than 15 degrees (derived from observations), lateral propagation of vegetation ceases. In the model, this feedback leads to the formation of multiple dunes by allowing the colonization of vegetation by propagules (seeds or rhizome fragments) seaward of the foredune to give rise to an incipient dune as suggested by Hesp (1984). Analysis of model results leads to the finding that dune morphology depends on the ratio between the rate of shoreline progradation and the rate at which the dune ridge propagates seaward due to vertical dune growth. When shoreline progradation rates are slower than the lateral dune growth rate, dunes are taller than they would be under stable shoreline conditions, and ridges tend to overlap (Fig. 6b–d). In contrast, when progradation rates are faster than the lateral dune growth rate, dunes are smaller, tend to be periodic, and are more widely spaced (i.e., Fig. 6e, f). These results compare well with observations of dune growth and

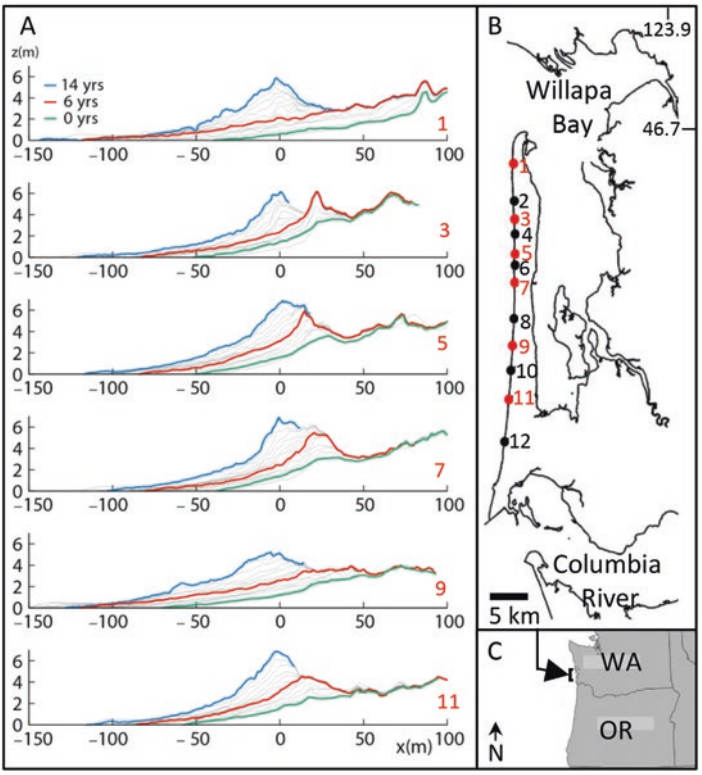

Fig. 7 Beach and foredune topographic profiles collected quarterly since A.D. 1997 using real-time kinematic differential GPS surveying techniques (Ruggiero et al. 2005) demonstrate the successive development of coastal foredunes along Long Beach Peninsula, Washington State (Fig. 1), over a 15-year time period. From Moore et al. (2016) and reprinted without changes under the Creative Commons license (CC-BY; https://creativecommons.org/licenses/by/3.0/us/)

morphology derived from a > 15-year dataset of dune growth from the Long Beach Peninsula in Washington State, where in some cases the progradation rate is slower than the lateral dune growth rate and dune ridges overlap as in Fig. 6a–d (Fig. 7; Moore et al. 2016).

Overall, these findings suggest that internal dune dynamics alone (even in the absence of variations in sediment supply or relative sea level) are sufficient to give rise to multiple dune fields and that vegetative processes play a key role in determining the number, spacing, and size of dune ridges in a multiple dune field. Because the amount of protection from storms that dunes provide depends on these characteristics (especially dune height), understanding when and where a single large dune ridge is likely to form, as opposed to multiple lower dune ridges, is important. Given the findings of Moore et al. (2016), the relationship between shoreline progradation rate and lateral dune growth rate also provides a means for predicting the height, number, and spacing

of multiple dunes under different conditions. For example, in places where the flux of sand to dunes is low, well-defined multiple dune ridges may form even at relatively slow rates of shoreline progradation, while in locations where the rate of shoreline progradation is slower than the rate of lateral dune growth, new ridges will typically become superimposed on one another to form large complex foredune shapes.

3 Factors Controlling Dune and Barrier State Across Scales

The ecomorphodynamic interactions that give rise to dunes also play an important role in determining how the sandy component of barrier topography evolves as conditions change, with implications for connectivity to other parts of the barrier system. To investigate the effects of changing forcing on dune—or local, barrier—state, Durán Vinent and Moore (2015a) simulated multiple cycles of dune erosion and recovery using a simple formulation for storms (following Larson et al. 2004) and by imposing the occurrence of periodic high-water events drawn randomly from a probability distribution in which small high-water events are frequent and large high-water events are relatively infrequent. Within the model, Durán Vinent and Moore (2015a, b) represent dune growth as a logistic process (Fig. 8a; consistent

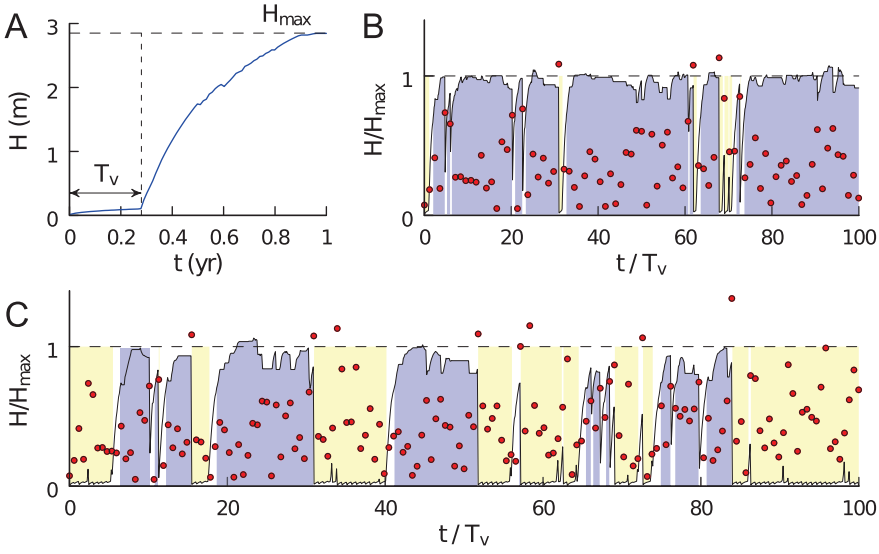

Fig. 8 (**a**) Evolution of island elevation with vegetation following a storm. T_v is the vegetation recovery time. (**b**) Evolution of dune elevation (H) relative to maximum potential dune height (H_{max}) as a function of time rescaled by T_v for vulnerability index = 0.9 (**b**) and 2 (**c**). *Red symbols* denote extreme events, values above 1 are higher than H_{max} and lead to overwash. High state elevations are shown in *blue* and low state elevations are shown in *yellow*. Figure modified from Durán Vinent and Moore (2015a)

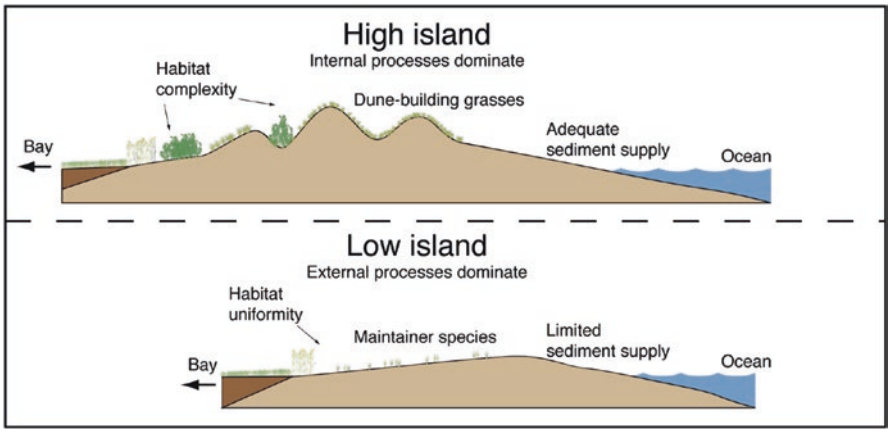

Fig. 9 An illustration of the generalized differences between high and low dune/island states. Figure drafted by Luke Cole

with the empirical findings of Houser et al. 2015, this volume) that proceeds slowly in the initial stages as aeolian processes build the barrier to an elevation that will support the growth of dune-building vegetation. Once dune-building vegetation becomes established, the self-reinforcing interactions between sediment transport and vegetation promote rapid dune-building, (if it proceeds uninterrupted) to a local maximum potential dune height (Durán and Moore 2013).

Model results indicate that the dynamics of barrier elevation are controlled by the ratio of the time it takes for vegetation to recover following a storm to the return period of high-water events. Durán Vinent and Moore (2015a) call this ratio the "vulnerability" index. When this index is less than one, high-water events occur infrequently relative to the vegetation recovery time. In this case (Fig. 8b), vegetation will tend to establish before the next high-water event leading to rapid dune growth, low vulnerability to the next storm, and near continuous maintenance of dunes near their maximum height. In contrast, when the period of high-water events is equal to or shorter than the vegetation recovery time, meaning the vulnerability index is equal to or greater than one, (Fig. 8c), low areas typically cannot recover prior to the next high-water event and tend to remain vulnerable. However, even when the vulnerability index is equal to or greater than one, high areas will be less prone to overwash, and if partially eroded during a high-water event, will quickly recover toward the high-elevation state, as long as some elevation and vegetation remain. In this latter scenario, barriers are bistable; feedbacks reinforce both the high elevation state and the low elevation state (Fig. 9), so that both are stable. Intermediate states in such a bistable system are relatively less frequent, since the paired feedbacks tend to push the system toward either of the two stable states. Thus, a barrier with a vulnerability index in the bistable range will tend to exhibit a bimodal distribution of local elevations, with a dominance of high values and/or low values, but relatively fewer intermediate values. At very high values of the vulnerability index, high-water events occur so frequently relative to the vegetation

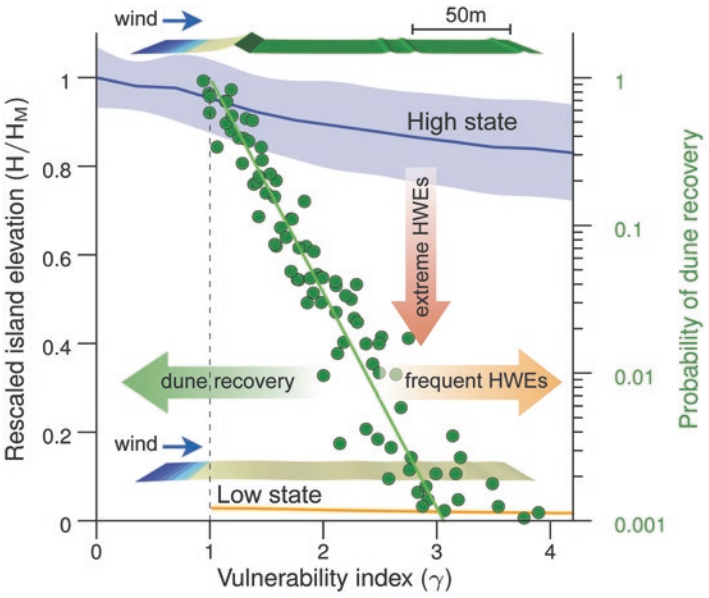

Fig. 10 Equilibrium states for dune/island elevation and the probability of dune recovery (*green symbols*) as a function of the vulnerability index, for varying winds, RSLR rates, and vegetation sensitivities (see Durán Vinent and Moore 2015a for details). The *green line* is an exponential fit for the recovery probability (defined as the inverse of the average number of HWEs spent in the low state). *Blue* and *orange lines* are average values for the stable high and low states, respectively; the *blue shadow* area on either side of the line represents data dispersion. The onset of bistability occurs when the probability of dune recovery decreases below 1 (*dashed line*). Processes leading to a transition between alternative states (*arrows*) are shown for reference. Figure modified from Durán Vinent and Moore (2015a)

recovery time that local barrier elevation can become perpetually trapped in the low state. In this way, local barrier state is controlled by the competing effects of storm erosion, sea-level rise, and the ecomorphodynamic interactions that build dunes (Duran Vinent 2015a; Fig. 10).

This quantification of barrier dynamics, with the possibility for local barrier elevation to be bistable, is supported by data from the Virginia Barrier Islands, U.S., where empirical evidence reveals that low and high barriers occur with greater frequency than barriers of intermediate elevation (Durán Vinent and Moore 2015a, 2016). This provides a broader context for considering barrier response to climate change and the likelihood of potentially abrupt transitions in barrier state, as well as the dynamics of connections to back-barrier environments.

In addition to the spatially explicit, process-based model of Durán Vinent and Moore (2015a), a coarse-grained description of the foredune-storm system was modeled by Goldstein and Moore (2016). Using entirely different mathematics from Durán Vinent and Moore (2015a), Goldstein and Moore (2016) constructed a one-dimensional model of dune growth and destruction using a single impulsive

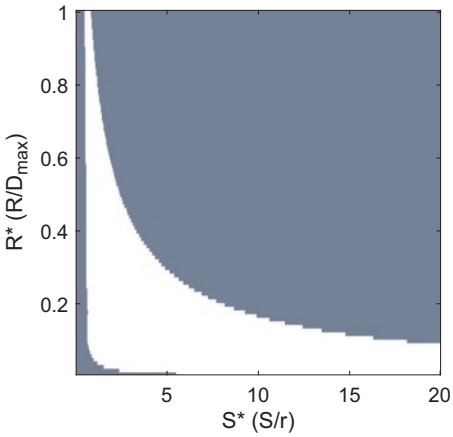

Fig. 11 Stability diagram in $S^* - R^*$ parameter space. S^* is the nondimensional storm frequency (the ratio between storm frequency and the intrinsic growth rate of the dune). R^* is the nondimensional total water level (ratio between characteristic storm height and the maximum dune height). *Grey regions* contain a single attracting state. The bistable region is shown in *white*. From Goldstein and Moore (2016)

differential equation reduced to a discrete time map. The mathematical model was built from empirical formulations for the logistic growth of foredunes (Houser et al. 2015, this volume) and the storm-driven destruction of dunes (Long et al. 2014). By varying two nondimensional parameters (the nondimensional storm frequency and magnitude), bistable behavior appears in a non-negligible region of parameter space (Goldstein and Moore 2016; Fig. 11).

Beyond presenting a simplified model of the foredune system, Goldstein and Moore (2016) compiled observational studies from the U.S. East Coast. Barrier island dunes from MD, VA, NC, and FL plot in the bistable region of model parameter space, which is consistent with the persistence of low overwash flats and high-resistant dunes, even on the same island, in these regions. These states were long lasting (decadal) and durable (through several major storm events), suggesting that these observations represent stable attracting states, consistent with model predictions.

4 Couplings Between Barriers and Back-Barrier Marshes

Many barrier islands and barrier spits are backed by marshes on the bayward side. When back-barrier marshes are present and barriers/dunes are sufficiently low to permit barrier migration, connections between the sandy part of barriers and back-barrier marshes can play an important role in determining how the barrier-marsh system responds to changing conditions. As described below, overwash sand can contribute to the vertical accretion (building upward) of back-barrier marshes

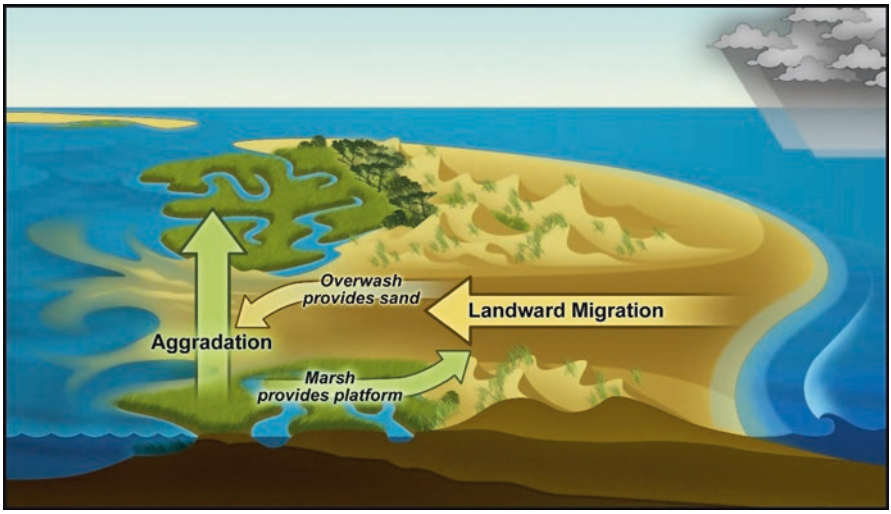

Fig. 12 Illustration of the two-way interactions between sandy barrier islands and back-barrier marshes, in which overwash sand provides a source of sediment to assist with marsh aggradation and the marsh provides a platform onto which the barrier migrates

responding to sea-level rise (Fig. 12). In turn, marsh soils influence barrier migration rates by providing a platform onto which the sandy part of a barrier migrates, and by affecting the sand content of the eroding shoreface when marsh deposits become exposed (described below, Brenner et al. 2015; Murray and Moore this volume).

4.1 Effect of Back-Barrier Marshes on Barrier Migration Rate

Brenner (2012) and Brenner et al. (2015) explored couplings between the sandy part of a barrier and back-barrier environments using GEOMBEST (Stolper et al. 2005; Moore et al. 2010, 2014), a morphological-behavior model which simulates the evolution of barrier morphology and stratigraphy in response to changes in sediment supply and sea-level rise over timescales of decades to millennia. Within GEOMBEST, barrier migration is driven primarily by the constraints of geometry and conservation of mass; the profile translates vertically (to keep pace with sea level) and horizontally (to produce the sediment needed via shoreface erosion) with the tendency to evolve toward a user-specified/data-derived equilibrium morphology, when conditions allow. The model includes adjustments for external sediment supply or loss; variable substrate erodibility and composition; and inputs derived from geologic/geomorphic data (see Stolper et al. 2005; Moore et al. 2010 and Brenner et al. 2015 for a complete model description).

In the absence of back-barrier marsh sedimentation, the slope of the landscape across which a barrier migrates (the "substrate slope") directly influences barrier

volume and migration rate (Moore et al. 2010). The influence of substrate slope becomes indirect and time-lagged when a back-barrier marsh is present. Low substrate slopes landward of the back-barrier marsh environment, relative to the slope of the present barrier trajectory (the ratio between the RSLR rate and the rate of landward barrier migration), tend to produce widening of the back-barrier environment, and therefore eventually lead to thickening of the back-barrier deposit that the barrier migrates over (and vice versa) (Brenner et al. 2015). Depending on whether or not the back-barrier deposit is more or less sand-rich than the underlying substrate, changes in back-barrier width caused by changes in the slope of the substrate can lead to either a negative or a positive feedback that either produces a stable back-barrier width, or that reinforces either back-barrier widening or back-barrier narrowing/thinning. See Murray and Moore (this volume) for a more complete discussion of these feedbacks and their relationship to other geometric considerations.

Additional modeling by Walters et al. (2014) suggests that the presence of a marsh directly behind a barrier causes a reduction in the rate of landward barrier migration by reducing the accommodation space that the barrier must fill. This is evidenced by experiments conducted in an expanded version of GEOMBEST (GEOMBEST+), which includes marsh accretion processes to explicitly address couplings between the sandy portion of a barrier and back-barrier marshes (Walters et al. 2014). The deposition of fine-grained suspended sediment from an external source, such as a river or exchange through tidal inlets, and locally derived organic material into the back-barrier basin was simulated such that a marsh platform can persist behind the barrier under conditions in which the rate of sea-level rise was balanced by the accretion rate, which depends on the rate of sediment input. By varying the rate of fine-grained sediment input to the back-barrier basin, GEOMBEST+ simulations demonstrated that the landward rate of barrier migration can be reduced 30% by the presence of a back-barrier marsh as compared to an empty basin with the same relative sea-level rise rate (Fig. 13) (Walters et al. 2014). These model experiments addressed barrier evolution over timescales that are too short for the shoreface-composition feedbacks described in the previous section to influence barrier migration rates.

4.2 Effect of Barrier Dynamics on Back-Barrier Marshes

In addition to the effect of marshes on barrier migration, there is also an effect of barrier migration on the morphology and resilience of back-barrier marshes. During storms, sand eroded from the barrier can be deposited on the back-barrier marsh as overwash (De Groot et al. 2011). Thus, a migrating barrier provides the marsh with an important source of sediment that assists marshes in keeping pace with sea-level rise.

Exploratory modeling with GEOMBEST+ offers quantitative insight into the conceptual link between barrier migration, overwash, and marsh sedimentation, and the conditions under which marsh-barrier connectivity influences the persistence

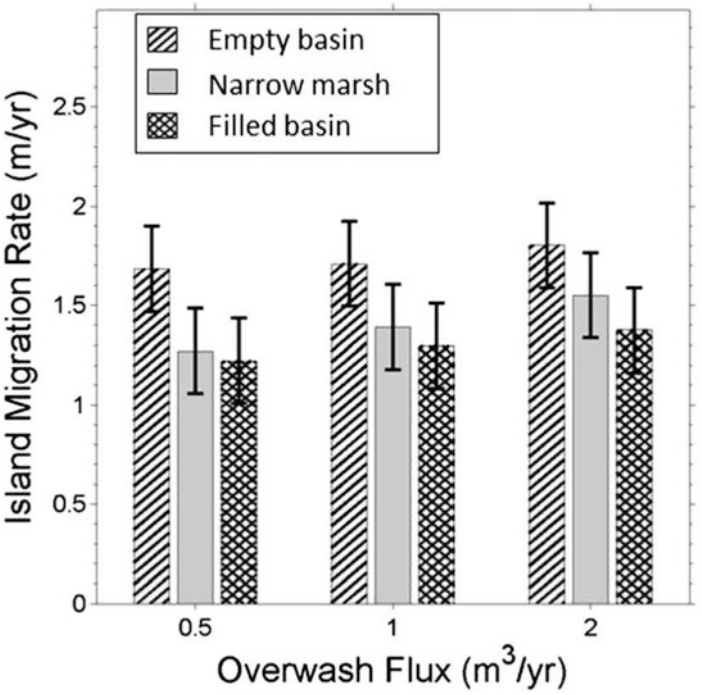

Fig. 13 Plot of shoreline migration rate from 1000 year GEOMBEST+ simulation with a 4 mm/year relative sea-level rise rate and different back-barrier environments (empty basin to marsh-filled basin; muddy to sandy). Error bars show one standard deviation from the mean. From Walters et al. (2014)

of back-barrier marshes. In GEOMBEST+, marshes form and evolve from a combination of organic and fine-grained sediment deposition driven by back-barrier, tidal inundation. Additionally, GEOMBEST+ simulates overwash as a flux that transports sand from the barrier shoreface and deposits it behind the barrier in increments that decay exponentially with distance from the barrier. The inclusion of overwash flux allows the back-barrier to evolve dynamically, such that marshes occur when the rate of sea-level rise can be balanced by the deposition of fine-grained suspended sediment, organic material, and sand from overwash (Walters et al. 2014).

To investigate the role of overwash in aiding marsh response to sea-level rise, GEOMBEST+ simulations addressed marsh and barrier evolution under a range of suspended sediment input, sea-level rise, and overwash scenarios. In these model experiments, the marsh keeps pace with the rate of sea-level rise when the rate of sediment deposition into the basin (Basin Accretion Rate or BAR) is greater than or equal to the rate of sea-level rise (RSLR), and thus the ratio between the BAR and RSLR (BAR/RSLR) is equal to or greater than 1. However, if RSLR is greater than BAR, and the ratio of BAR/RSLR is less than 1, the marsh will be starved of

sediment, leading to conditions that favor marsh inundation. Results from GEOMBEST+ simulations also show that marshes close to the barrier are able to persist even at BAR/RSLR ratios less than 1 when overwash fluxes are high, suggesting that overwash increases the resilience of narrow (100–500 m) back-barrier marshes under conditions of sea-level rise rates and suspended sediment concentrations in which they would otherwise disappear. Consistent with this finding, a comparison to the back-barrier marshes of the Virginia Coast Reserve (VCR) indicates that narrow back-barrier marshes occur frequently at a statistically significant rate in the same range of widths as predicted by the GEOMBEST+ simulations (Fig. 14).

How might the results of Walters et al. (2014) be altered if erosion of marsh edges from wave attack, as well as vertical drowning, could potentially reduce or remove persistent narrow marshes? To address this question, Lauzon et al. (in revision) added marsh-edge erosion by waves to the GEOMBEST+ formulation. Wave height and period are limited by the fetch and depth of the bay (e.g., Young and Verhagen 1996). Wind directions are not explicitly addressed. Instead, assuming for simplicity that the cross-shore component of the wind is sometimes in the seaward direction and sometimes in the landward direction, the cross-shore bay width serves as a proxy for fetch, without distinguishing between landward and seaward portions of the bay. Following Mariotti and Fagherazzi (2013), Lauzon et al. (in revision) include erosion of the bay bottom and marsh scarps from wave forces. The rate at which waves tend to vertically erode the bed depends on bed shear stress, calculated using linear wave theory (Dean and Dalrymple 1991). The rate at which waves tend to horizontally erode the marsh edge depends on the wave power delivered to the marsh edge (e.g., Schwimmer 2001; Marani et al. 2011). However, sediment deposition tends to cause vertical accretion of the bed and lateral progradation of the marsh edge as formulated by Walters et al. (2014). The net result of wave erosion combined with deposition determines the rates of change of bed elevation and marsh-edge position. Consistent with Walters et al. (2014), sediment eroded from the bay bottom or marsh edge is subsequently available for redeposition. This redeposition occurs on the marshes and, if sediment is left over after enough is deposited on the marshes to keep up with SLR, on the marsh edges.

In the absence of SLR, bay depths rapidly approach a steady state in which the rate that waves tend to erode the bed is balanced by the rate of deposition. When SLR is included, steady state bay depths are slightly greater than without SLR, which allows net deposition rates to equal the rate of SLR, because wave-related shear stress tends to decrease with depth (beyond a depth which produces the maximum shear stress; Fagherazzi et al. 2006). However, the bay depths are in dynamic equilibrium; as the width (and therefore fetch) of the bay changes, the depths adjust (Fig. 15).

Perhaps counterintuitively, adding wave erosion to the experiments of Walters et al. (2014) increases, rather than decreases, the prevalence and extent of narrow back-barrier marshes, at least temporarily. This result arises mainly from two mechanisms. In one, as recognized previously (e.g., Mariotti and Carr 2014), the sediment eroded at marsh edges can provide additional sediment for deposition on the top of marsh platforms, tending to delay marsh drowning. The other mechanism

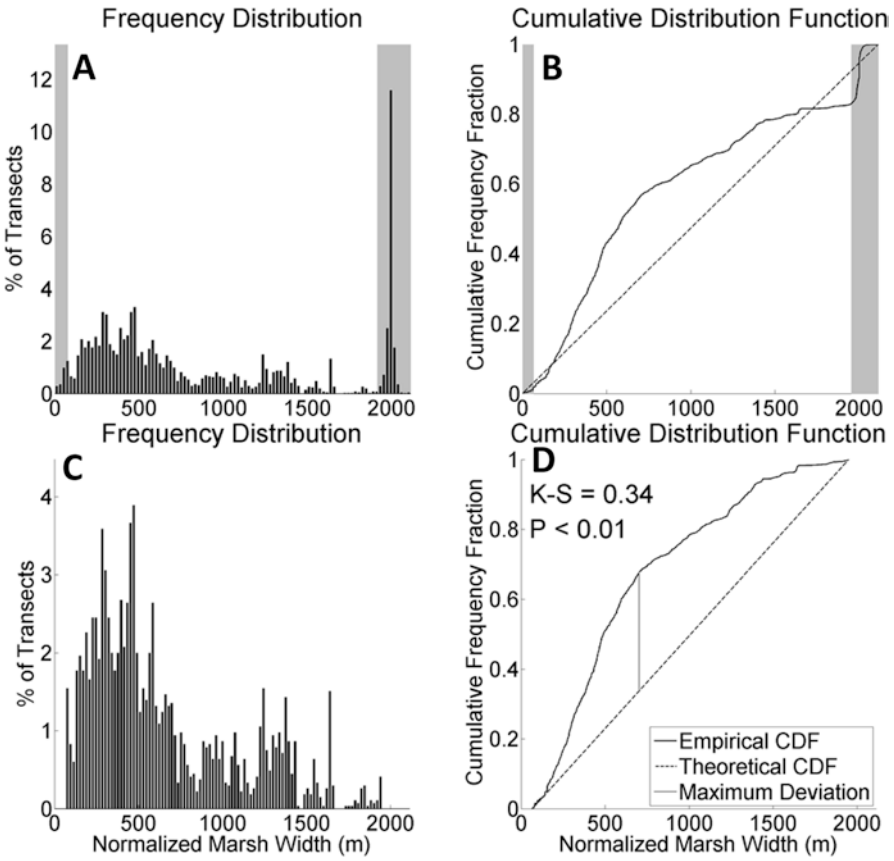

Fig. 14 (**a**) Frequency distribution of back-barrier marsh width measurements from remote sensing observations of the entire Virginia Barrier Islands. Measurements are normalized to a basin size of 2000 m by dividing the raw measurements of the back-barrier marsh width by the basin width, and multiplying by 2000 m. (**b**) Cumulative distribution function of the back-barrier marsh widths. *Gray bars* indicate the range of widths within which basins are completely filled with marsh (>1950 m) based on the maximum deviation of the cumulative distribution function from the standard uniform distribution, or completely empty of marsh (<67 m) based on the range derived from model experiments. (**c**) Frequency distribution for the intermediate widths that are not associated with the boundary condition peaks. (**d**) Cumulative distribution function of the intermediate widths, showing that the maximum deviation from a standard uniform distribution occurs at 702 m. This deviation of the cumulative distribution function from the hypothetical distribution over widths from 150 to 700 m is statistically significant (99% confidence level) according to the Kolmogorov–Smirnov test. From Walters et al. (2014)

involves the organic component of tidal marshes, assumed to compose 50% of the marsh deposit in GEOMBEST+ (Walters et al. 2014). The fraction of eroded marsh sediment that is organic is not conserved in GEOMBEST+, representing loss to decomposition and/or distant dispersal. When marshes drown in GEOMBEST+, extensive portions of the marsh can be converted to deeper-water bay environments,

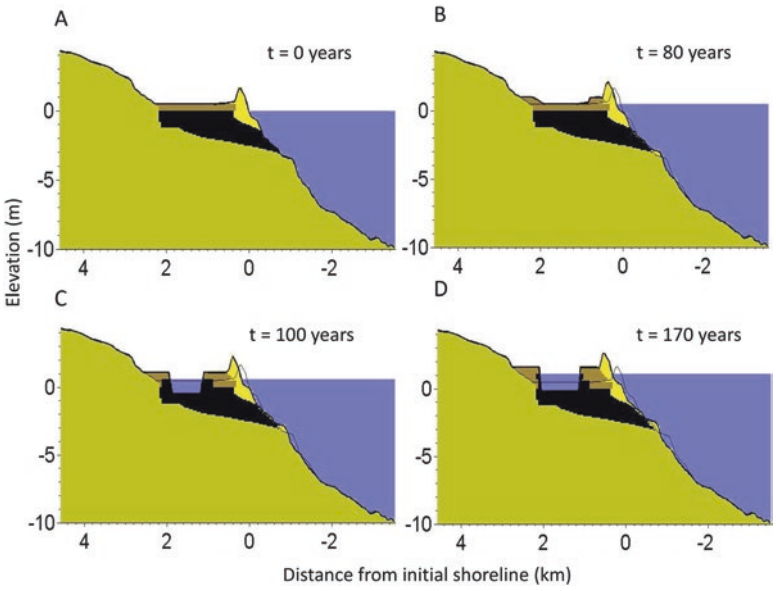

Fig. 15 Evolution of an initially full marsh over 1 m of RSLR. (**a**) Initial condition of a full marsh. (**b**) The center of the marsh, farthest from the sediment sources, cannot maintain its elevation. (**c**) The center of the marsh drowns, and as waves begin to form in the resulting bay it quickly deepens and widens, eroding the marsh edge. (**d**) Final condition of a narrow marsh (~475 m wide) after 1 m of RSLR. The black outline on **b**, **c**, and **d** shows the initial landscape. From Lauzon et al. (in revision)

with the loss of 50% of the marsh deposits eroded. With the addition of wave-edge erosion, since marsh drowning is reduced, this sediment loss is reduced. (Marsh-edge erosion still consumes marsh deposits, engendering loss of organic sediment, but the volume of loss is small compared with the results of converting large areas of marsh into bay.)

If rates of sediment delivery to the back-barrier basin (e.g., from overwash, rivers, tides) are sufficiently high, then deposition on marsh edges can overcome the tendency for marsh-edge erosion, causing net progradation of the marsh edge (Mariotti and Fagherazzi 2013) (e.g., Fig. 16). The rate of net sediment import into the back-barrier environment relative to the rate at which accommodation space is created (SLR rate multiplied by the back-basin area) determines whether marsh edges erode or prograde, and at what rate. For cases in which sedimentation of marsh surfaces and the bay bottom keep up with SLR, if the rate of net sediment delivery is less than the rate space is created, geometry and the conservation of mass dictate that marsh edges must be eroding (e.g., Ganju et al. 2017). If sediment is being delivered faster than space is being created, marsh edges must be prograding (e.g., Redfield 1972). The insight that the erosion or progradation rate of the marsh edge can be predicted based on sediment budget and geometry considerations alone also applies when a back-barrier basin is open to sediment exchange through an inlet—as long as the net rate of sediment import or export can be determined at a snap shot in time (Lauzon et al. in revision).

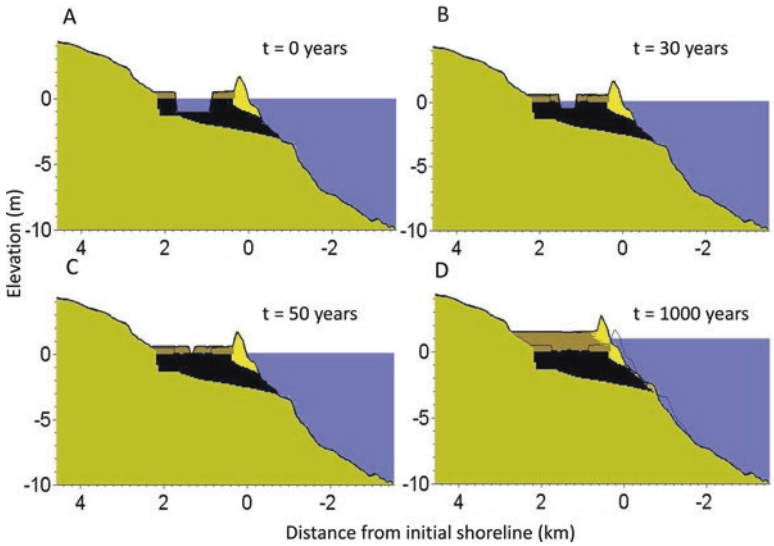

Fig. 16 An example of a prograding marsh beyond 1 m of RSLR. (**a**) Initial condition of a narrow marsh. (**b**) The marsh quickly progrades. (**c**) The basin fills with marsh. (**d**) The marsh accretes at the rate of sea level rise leading to a final condition of a full basin after 1 m of RSLR. The black outline on **b**, **c**, and **d** shows the initial landscape

4.3 Effects of Overwash on Marshes: Experimental Results

While the deposition of overwash sand onto marsh platforms may enhance the rate at which marshes build vertically, burial of marsh vegetation with sand may also lead to plant mortality that may take decades to recover from (Osgood et al. 1995). To investigate the conditions under which overwash benefits or harms marsh vegetation, a field experiment was conducted to determine how marsh productivity responded to overwash deposition events of varying thickness (Walters and Kirwan 2016). Small sections of existing *Spartina alterniflora* marsh were buried with various depths of barrier sand in mesocosms. The results of this field experiment showed the plants responded positively to small amounts of burial (5–10 cm) by increasing their belowground productivity, while larger amounts of burial (c > 15 cm) led to reduced productivity or mortality (Fig. 17).

These results suggest that back-barrier marshes are well-adapted to the natural process of barrier migration, as they are able to survive and flourish under conditions in which thin sheets of overwash are deposited over the marsh surface by frequent, low-magnitude storm events. However, thicker overwash deposits due to higher magnitude storms can lead to a decrease in marsh resiliency due to vegetation mortality. This finding emphasizes that the couplings between barriers and back-barrier marshes are strengthened under natural conditions where a low barrier rolls over through the process of frequently occurring, low-magnitude overwash events. This leads to enhanced marsh productivity and resilience to sea-level rise, which in turn can help slow the rate of barrier migration. Alternatively, where bar-

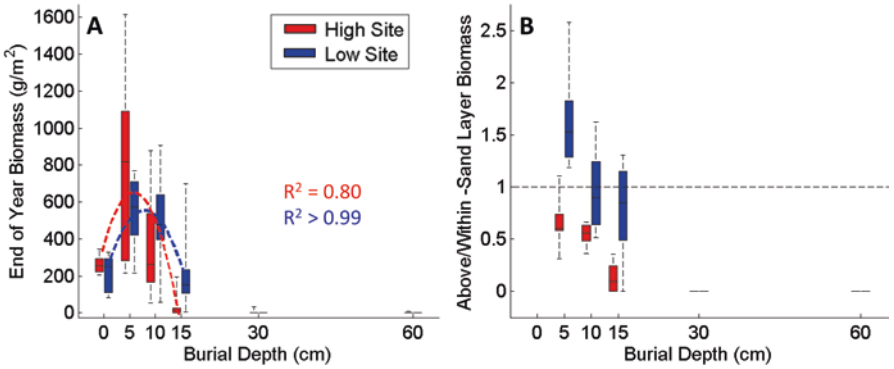

Fig. 17 (**a**) Box and whisker plot of end of year biomass versus burial depth for each experimental treatment. Biomass represents the total living biomass above and within the sand layer across each replicate burial depth. *Dashed lines* represent best quadratic fits for high site ($y = -0.61x^2 + 7.57x + 22.59$, $R^2 = 0.80$, $p = 0.11$) and low site ($y = -0.42x^2 + 6.21x + 16.10$, $R^2 > 0.99$, $p < 0.01$). (**b**) Box and whisker plot of the ratio of above-sand layer biomass to within-sand layer biomass. From Walters and Kirwan (2016) and reprinted without changes under the Creative Commons license (CC-BY; https://creativecommons.org/licenses/by/3.0/us/)

rier dunes are artificially maintained at greater heights, only large magnitude storm events result in overwash. Thus, artificial dune heightening simultaneously leads to a reduction of frequent, thin layer sand deposition that enhances marsh resilience to SLR, while still allowing large magnitude overwash events that lead to plant mortality. This could ultimately reverse the natural tendency for storms to increase marsh and barrier resilience.

5 Summary and Implications

We are increasingly learning that in addition to the important long-term (centurial to millennial) roles of sediment supply and sea-level rise, shorter-term (annual to centurial) ecomorphodynamic interactions (i.e., interactions between morphology, fluid dynamics, and/or sediment transport with biological processes)—as influenced by changes in the intensity and/or frequency of storms and changes in the geographic distribution of dune-building vegetation, as well as couplings between barrier and back-barrier marsh environments—play a critical role in determining how barrier-marsh systems will evolve in the future. For example, the effectiveness of storms in increasing landform elevation and moving a barrier landward is determined, in large part, by the morphology of the coastal foredune (i.e., the seaward-most dune line), which is itself a product of couplings between vegetation and sediment transport processes.

In the cross-shore dimension, the maximum potential height that a coastal foredune can achieve is a function of the distance from the shoreline that dune-building vegetation can grow. The farther from the shoreline that vegetation becomes estab-

lished, the taller the foredune can become before steering the wind sufficiently above the beach to reduce the shear stress below the critical shear stress necessary for sand to be transported into the dune, at which point dune growth ceases. In the alongshore dimension, the rate of lateral vegetation growth relative to the rate of vertical vegetation growth at least partially determines whether alongshore dune morphology will tend to remain hummocky (and therefore allow transfer of sand from the front to the interior/back of a barrier during moderate storms) or tend to be characterized by a relatively more resistant, alongshore-continuous foredune ridge. Likewise, at larger spatial and temporal scales, interactions between the rate of lateral vegetation growth, as potentially controlled by dune slope, can explain the spacing, number, and size of multiple dunes that form in the presence of shoreline progradation. Where the ratio of the shoreline progradation rate to the lateral dune growth rate is large, dunes tend to be smaller and widely spaced. In contrast, in areas where the ratio of the shoreline progradation rate and the lateral dune growth rate is small, dunes tend to be larger and more closely spaced or exhibit a morphology typified by overlapping complex dune forms.

The morphology of barrier dunes directly influences the coupled evolution of barriers and back-barrier marshes through time, especially as conditions change. For low and narrow barriers, overwash supplies the marsh with sediment that can be important for maintaining a back-barrier marsh fringe in the face of sea-level rise and edge erosion. The marsh, in turn, tends to reduce barrier migration rates by providing a platform for the sandy part of the barrier to migrate across. The strength of this stabilizing feedback may depend on the frequency and magnitude of overwash events, because frequent, low-magnitude deposition events are more likely to benefit marshes than infrequent, high magnitude events. Therefore, the response of barriers to changing climate depends not only on the morphology of the barrier itself, but on ecomorphodynamic feedbacks operating throughout and across the barrier-marsh system as a whole.

These ecomorphodynamic feedbacks combine with the characteristics of the underlying substrate (i.e., slope, thickness, and composition) to influence the topographic state of dunes and barriers. Topographic state, in turn, determines how connected the frontal, sandy portion of a barrier is to the back-barrier, whether marsh, lagoon, or shallow bay. Where dunes are high, the effects of small overwash events are filtered; where dunes are low, even small storms may make important contributions of sediment to back-barrier environments. In developed areas, residences and commercial structures are also efficient filters, potentially starving the barrier interior of overwash contributions that are essential for barrier landforms to persist in the future (Rogers et al. 2015). These factors highlight the importance of considering the height of natural dunes when planning rebuilding and restoration efforts following storms. Artificially constructing dunes that are higher than natural conditions, although attractive as green infrastructure and an alternative to more permanent measures, will be more efficient filters of overwash events with possibly significant consequences, as they alter the natural processes that would otherwise allow barriers to persist as sea level rises and the most intense storms become more frequent. Striking a balance between the desire to preserve coastal habitation in its current form and the need for barriers to move landward and upward to maintain

equilibrium with sea level and storm conditions as they change more and more rapidly is a major challenge coastal communities will face in the very near term. Failing to strike this balance before a barrier becomes so out of equilibrium that a major storm causes deterioration of the landform that is infeasible to repair may lead to barrier loss altogether.

When barriers are complex, consisting of a series of dune ridges separated by swales, connectivity with back-barrier environments is unlikely and the evolution of the barrier system as conditions change is likely to be focused at the ocean and bay margins. More research is necessary to understand how such complex topography might alter the dynamics of barrier-marsh evolution as conditions change in the future.

Where barriers are low and narrow, evolution of the barrier-marsh system may also be influenced by connections between back-barrier marshes and processes in the bay behind. For example, the presence of seagrass has the potential both to decrease marsh-edge erosion by reducing wave energy and to increase marsh-edge erosion by sequestering sediment. Whether the effect of seagrass presence (or absence) on wave energy, or sediment availability, wins out, and under what conditions, is the subject of ongoing work. In such cases, there is the potential for state changes in one part of the landscape (e.g., a change from seagrass to no seagrass) to cause state changes in nonadjacent landscape units (e.g., a transition from high to low on the sandy part of the barrier) via connectivity with landscape units in between (e.g., the marsh). The potential for such a cascade of state changes is important to consider as we seek to better understand the effect of changing climate on these low-lying and highly connected landscapes (Fig. 18).

A better understanding of the time scale for, and morphological evolution of, dune recovery as a function of key factors that vary with location (e.g., wind speed and direction, precipitation, sediment availability, species composition, etc.) and under a range of likely future sea-level rise and storm scenarios will be helpful in predicting the future vulnerability of barriers and the communities they host to

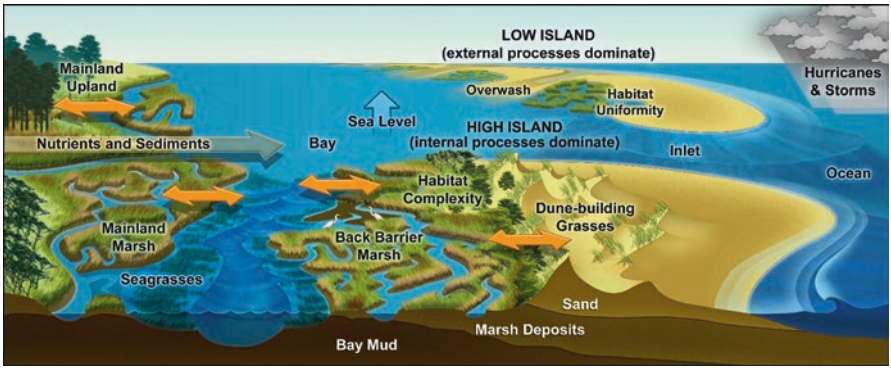

Fig. 18 Landscape-scale interactions and potential for cascading state changes brought about by couplings between adjacent and nonadjacent landscape units

undesirable (from the human perspective) transitions in state. Advancing our understanding of the potential for changes in state to cascade across the coastal landscape as well as the regional or local characteristics that affect this potential, and the mechanisms involved, will be important to assessing the future holistic behavior of barrier-marsh-bay systems. It is also essential to expand our understanding of the ways in which the natural dynamics focused on in this chapter will interact with and be affected by (i.e., coupled with) human coastal dynamics, especially as changing conditions lead to consideration of more extreme defensive measures (see McNamara and Lazarus this volume). Perhaps most challenging, but ultimately, most important, there is a critical need to develop creative ways to maintain or re-establish the natural and essential connection among the frontal beach-dune system, the interior, and back-barrier marsh components—especially where development and protective measures have severed this connection. This will be challenging and may require a type and range of collective thinking on the part of scientists, managers, and community members that has not yet emerged, but that will become essential in years to come.

Acknowledgments The work presented in this chapter was originally funded by the Virginia Coast Reserve Long-term Ecological Research Program (National Science Foundation DEB 123773), the Department of Energy's Office of Science through the Coastal Center of the National Institute for Climatic Change Research at Tulane University, the Geomorphology and Land use Dynamics Program of the National Science Foundation (EAR 1324973 and EAR 1053151), and the University of North Carolina at Chapel Hill. The authors thank Andrea D'Alpaos and Jorge Lorenzo-Trueba for helpful reviews and feedback that assisted in improving this manuscript.

References

Ashton AD, Lorenzo-Trueba J (2018) Morphodynamics of barrier response to sea-level rise. In: Moore LJ, Murray AB (eds) Barrier dynamics and response to changing climate. Springer, New York

Brenner O (2012) The complex influences of back-barrier deposition, substrate slope and underlying stratigraphy in barrier island response to sea-level rise: Insights from the Virginia Barrier Islands, Mid-Atlantic Bight, USA. Masters thesis, University of Virginia, Charlottesville, VA

Brenner OT, Moore LJ, Murray AB (2015) The complex influences of back-barrier deposition, substrate slope and underlying stratigraphy in barrier island response to sea level rise: Insights from the Virginia Barrier Islands, Mid-Atlantic Bight, U.S.A. Geomorphology 246(1):334–350. https://doi.org/10.1016/j.geomorph.2015.06.014

Brown JK, Zinnert JC, Young DR (2017) Emergent interactions influence functional traits and success of dune building ecosystem engineers. Journal of Plant Ecol. https://doi.org/10.1093/jpe/rtx033

Cowell PJ, Kinsela MA (2018) Shoreface controls on barrier evolution and shoreline change. In: Moore LJ, Murray AB (eds) Barrier dynamics and response to changing climate. Springer, New York

Curray JR (1960) Sediments and history of the Holocene transgression, continental shelf, northwest Gulf of Mexico. In: Shepard FP, Phleger FB, van Andel TH (eds) Recent sediments, northwest Gulf of Mexico. Am. Assoc. Petrol. Geol, Tulsa, pp 221–266

Dean RG, Dalrymple RA (1991) Water wave mechanics for engineers and scientists. World Scientific, Singapore
De Groot AV, Veeneklaas RM, Bakker JP (2011) Sand in the salt marsh: contribution of high-energy conditions to salt-marsh accretion. Mar Geol 282(3–4):240–254
Disraeli DJ (1984) The effect of sand deposits on the growth and morphology of Ammophila Breviligulata. J Ecol 72:145–154
Duncan WH, Duncan MB (1987) The Smithsonian guide to seaside plants of the Gulf and Atlantic Coasts from Louisiana to Massachusetts. Smithsonian Institution Press, Washington, DC
Durán O, Herrmann HJ (2006) Vegetation against dune mobility. Phys Rev Lett 97(18):188001
Durán O, Silva M, Bezerra L, Herrmann H, Maia L (2008) Measurements and numerical simulations of the degree of activity and vegetation cover on parabolic dunes in northeastern Brazil. Geomorphology 102(3–4):460–471
Durán O, Moore LJ (2013) Vegetation controls on the maximum size of coastal dunes. Proc Natl Acad Sci 110(43):17217–17222. https://doi.org/10.1073/pnas.1307580110
Durán Vinent O, Moore LJ (2015a) Bistability of barrier islands induced by biophysical interactions. Nat Clim Chang 5:158–162
Durán Vinent, O, Moore LJ (2015b) Coastal Dune Model, v1.0. https://doi.org/10.5281/zenodo.16161
Durán Vinent O, Moore LJ (2016) Reply to comment on bistability of barrier islands induced by biophysical interactions. Nat Clim Chang 6:6
Ehrenfeld JG (1990) Dynamics and processes of barrier island vegetation. Reviews in Aquatic Sciences
Elko N, Brodie K, Stockdon H, Nordstrom K, Houser C, McKenna K, Moore L, Rosati J, Ruggiero P, Thuman R, Walker I (2016) Dune management challenges on developed coasts. Shore Beach 84(1):15–28
Emanuel KA (2013) Downscaling CMIP5 climate models shows increased tropical cyclone activity over the 21st century. Proc Natl Acad Sci 110(30):219–224
Fagherazzi S, Carniello L, D'Alpaos L, Defina A (2006) Critical bifurcation of shallow microtidal landforms in tidal flats and salt marshes. Proc Natl Acad Sci 103(22):8337–8341
FitzGerald DM, Buynevich I, Argow B (2006) Model of tidal inlet and barrier island dynamics in a regime of accelerated sea-level rise. J Coast Res Spec Issue 39:789–795
FitzGerald DM, Fenster MS, Argow BA, Buynevich IV (2008) Coastal Impacts Due to Sea-Level Rise. Annu Rev Earth Planet Sci 36:601–647. https://doi.org/10.1146/annurev.earth.35.031306.140139
Ganju NK, Defne Z, Kirwan ML et al (2017) Spatially integrative metrics reveal hidden vulnerability of microtidal salt marshes. Nat Commun 8:14156
Godfrey PJ, Godfrey MM (1976) Barrier island ecology of Cape Lookout National Seashore and vicinity, North Carolina (NPS Scientific Monograph Series No. 9). National Park Service, Cape Hatteras Natl. Seashore, NC
Godfrey P (1977) Climate, plant response and development of dunes on barrier beaches along the US East Coast. Int J Biometeorol 21(3):203–215
Godfrey PJ, Leatherman SP, Zaremba R (1979) A geobotanical approach to classification of barrier beach systems. Academic Press:Pp:99–126
Goff J, McFadgen B, Wells A, Hicks M (2008) Seismic signals in coastal dune systems. Earth Sci Rev 89:73–77
Goldstein EB, Moore LJ (2016) Stability and bistability in a one-dimensional model of coastal foredune height. J Geophys Res Earth Surf 121(5):964–977. https://doi.org/10.1002/2015JF003783
Goldstein EB, Moore LJ, Durán Vinent O (2017) Vegetation controls on maximum coastal foredune hummockiness and annealing time. Earth Surf Dynam Discuss. https://doi.org/10.5194/esurf-2017-2
Hacker SD et al (2012) Subtle differences in two non-native congeneric beach grases significantly affect their colonization, spread, and impact. Oikos 121:138–148
Hayden BP, Dolan R, Ross P (1980) Barrier island migration. In: Coats DR, Vitek JD (eds) Thresholds in Geomorphology. George Allen and Unwin, Ltd., London, UK, pp 363–384

Harris AL, Zinnert JC, Young DR (2017) Differential response of barrier island dune grasses to species interactions and burial. Plant Ecol 218(5):609–619
Hesp PA (ed) (1984) Foredune Formation in Southeast Australia. Academic Press, New York
Hesp P (1988) Surfzone, beach, and foredune interactions on the Australian South East Coast. J Coast Res (Special issue 3):15–23
Hesp P (1989) A review of the biological and geomorphological processes in the initiation and development of incipient foredunes. Proc R Soc Edinb 96:191–202
Hesp PA (2004) Coastal dunes in the tropics and temperate regions: location, formation, morphology and vegetation processes. In: Coastal dunes. Springer, Berlin/Heidelberg, pp 29–49
Houser C, Hapke C, Hamilton S (2008) Controls on coastal dune morphology, shoreline erosion and barrier island response to extreme storms. Geomorphology 100(3):223–240
Houser C, Wernette P, Rentschlar E, Jones H, Hammond B, Trimble S (2015) Post-storm beach and dune recovery: Implications for barrier island resilience. Geomorphology 234(1):54–63. https://doi.org/10.1016/j.geomorph.2014.12.044
Houser C, Barrineau P, Hammond B, Saari B, Rentschler E, Trimble S, Wernette P, Weymer B, Young S (2018) Role of the foredune in controlling barrier island response to sea level rise. In: Moore LJ, Murray AB (eds) Barrier dynamics and response to changing climate. Springer, New York
Johnson J, Moore LJ, Ells K, Murray B, Adams P, Jaeger J, MacKensize R (2015) Recent shifts in coastline change and shoreline stabilization linked to storm climate change. Earth Surf Process Landf 40:569–585. https://doi.org/10.1002/esp.3650
Knutson TR et al (2010) Tropical cyclones and climate change. Nat Geosci 3(3):147–163
Kopp RE et al (2014) Probabilistic 21st and 22nd century sea-level projections at a global network of tide-gauge sites. Earth's Future 2(8):383–406
Larson M, Kubota S, Erikson K (2004) Swash-zone sediment transport and foreshore evolution: field experiments and mathematical modeling. Mar Geol 212(14):61–79
Lauzon R, Moore LJ, Murray AB, Walters D, Kirwan M, Fagherazzi S (in revision) Enhanced persistence of narrow marshes in the presence of wave 1 erosion for coupled marsh-barrier island systems reveals geometric 2 constraints on marsh evolution. J Geophys Res Earth Surf
Leatherman SP (1979) Migration of Assateague Island, Maryland, by inlet and overwash processes. Geology 7:104–107
Lonard RI, Judd FW (2011) The biological flora of coastal dunes and wetlands: Panicum amarum S. Elliott and Panicum amarum S. Elliott var. amarulum (AS Hitchcock and MA Chase) P. Palmer. J Coast Res 27(2):233–242
Lonard RI, Judd FW, Stalter R (2010) The biological flora of coastal dunes and wetlands: Spartina patens (W. Aiton) GH Muhlenberg. J Coast Res 26:935–946
Lonard RI, Judd FW, Stalter R (2011) Biological flora of coastal dunes and wetlands: Uniola paniculata L. J Coast Res 27(5):984–993
Long JW, de Bakker ATM, Plant NG (2014) Scaling coastal dune elevation changes across storm-impact regimes. Geophys Res Lett 41:2899–2906. https://doi.org/10.1002/2014GL059616
Marani M et al (2011) Understanding and predicting wave erosion of marsh edges. Geophys Res Lett 38(21)
Mariotti G, Carr J (2014) Dual role of salt marsh retreat: long-term loss and short-term resilience. Water Resour Res 50(4):2963–2974
Mariotti G, Fagherazzi S (2013) Critical width of tidal flats triggers marsh collapse in the absence of sea-level rise. Proc Natl Acad Sci U S A 110(14):5353–5356
Maun MA (1998) Adaptations of plants to burial in coastal sand dunes. Can J Bot 738:713–738
Maun MA, Perumal J (1999) Zonation of vegetation on lacustrine coastal dunes: effects of burial by sand. Ecol Lett:14–18
McNamara DE, Lazarus ED (2018) Barrier islands as coupled human–landscape systems. In: Moore LJ, Murray AB (eds) Barrier dynamics and response to changing climate. Springer, New York
Mellett CL, Plater AJ (2018) Drowned barriers as archives of coastal-response to sea-level rise. In: Moore LJ, Murray AB (eds) Barrier dynamics and response to changing climate. Springer, New York

Moore LJ, List JH, Williams SJ, Stolper D (2010) Complexities in barrier island response to sea-level rise: insights from model experiments. J Geophys Res Earth Surf. https://doi.org/10.1029/2009JF001299

Moore LJ, McNamara DE, Murray AB, Brenner O (2013) Observed changes in hurricane-driven waves explain the dynamics of modern cuspate shorelines. Geophys Res Lett 40(22):5867–5871. https://doi.org/10.1002/2013GL057311

Moore LJ, Patsch K, Williams SJ, List JL (2014) Barrier islands poised for geomorphic threshold crossing in response to rapid sea-level rise: insights from Numerical Model Experiments, Chandeleur Islands, Louisiana, USA. Mar Geol 355(1):244–259. https://doi.org/10.1016/j.margeo.2014.05.022

Moore LJ, Ruggiero P, Durán O (2016) Vegetation control allows autocyclic formation of multiple dunes. Geology 44(7). https://doi.org/10.1130/G37778.1

Morton RA (2002) Factors controlling storm impacts on coastal barriers and beaches—apreliminary basis for near real-time forecasting. J Coast Res 18(3):486–501

Morton RA, Sallenger AH (2003) Morphological impacts of extreme storms on sandy beaches and barriers. J Coast Res 19(3):560–573

Murray AB, Moore LJ (2018) Geometric constraints on long-term barrier migration: From simple to surprising. In: Moore LJ, Murray AB (eds) Barrier dynamics and response to changing climate. Springer, New York

Odezulu CI, Lorenzo-Trueba J, Wallace DJ, Anderson JB (2018) Follets Island: a case of unprecedented change and transition from rollover to subaqueous shoals. In: Moore LJ, Murray AB (eds) Barrier dynamics and response to changing climate. Springer, New York

Odum WE, Smith TJ, Dolan R (1987) Suppression of natural disturbance: long-term ecological change of the outer banks of North Carolina. In: Turner MG (ed) Landscape Heterogeneity and Disturbance. Springer, New York, NY, pp 123–134

Orford JD, Wilson P, Wintle AG, Knight J, Braley S (2000) Holocene coastal dune initiation in Northumberland and Norfolk, eastern UK: climate and sea-level changes as possible forcing agents for dune initiation. In: Shennan I, Andrews J (eds) Holocene land-ocean interaction and environmental change around the North Sea, vol 166. Geological Society, London, pp 197–217

Osgood DT, Santos M, Zieman J (1995) Sediment physico-chemistry associated with natural marsh development on a storm-deposited sand flat. Mar Ecol Prog Ser 120:271–283

Psuty NP (1986) A Dune/Beach interaction model and dune managemetn. Thalassas 4(1):11–15

Psuty NP (1988) Sediment budget and dune/beach interaction. J Coast Res 3(special issue): 1–4

Psuty NP (1992) Spatial variation in coastal foredune development. In: Proceedings of the 3rd european dune congress, Balkema, Rotterdam, The Netherlands, pp 3–13

Redfield AC (1972) The development of a New England Salt Marsh. Ecol Monogr 42(2):201–237. https://doi.org/10.2307/1942263

Rodriguez AB, Yu W, Theuerkauf EJ (2018) Abrupt increase in washover deposition along a transgressive barrier island during the late nineteenth century acceleration in sea-level rise. In: Moore LJ, Murray AB (eds) Barrier dynamics and response to changing climate. Springer, New York

Roelvink D, Reniers A, van Dongeren A, Van Theil deVries J, McCall R, Lescinski J (2009) Modeling storm impacts on beaches dunes and barrier islands. Coast Eng 56(11–12): 1133–1152. https://doi.org/10.1016/j.coastaleng.2009.08.006

Rogers L, Moore LJ, Goldstein EB, Hein C, Lorenzo-Trueba J, Ashton A (2015) Anthropogenic controls on overwash deposition: evidence and consequences. J Geophys Res Earth Surf 120(12):2609–2624. https://doi.org/10.1002/2015JF003634

Ruggiero P, Kaminsky GM, Gelfenbaum G, Voigt B (2005) Seasonal to interannual morphodynamics along a high-energy dissipative littoral cell. J Coast Res 21(3):553–578

Ruggiero R, Kaminsky GM, Gelfenbaum G, Cohn N (2016) Morphodynamics of prograding beaches: a synthesis of seasonal- to century-scale observations of the Columbia River littoral cell. Mar Geol 376:51–68. https://doi.org/10.1016/j.margeo.2016.03.012

Ruggiero P, Hacker S, Seabloom E, Zarnetske P (2018) The role of vegetation in determining dune morphology, exposure to sea level rise, and storm-induced coastal hazards: A U.S. Pacific Northwest perspective. In: Moore L, Murray B (eds) Barrier dynamics and the impact of climate change on barrier evolution. Springer

Sallenger AH Jr (2000) Storm impact scale for barrier islands. J Coast Res 16(3):890–895

Sallenger AH, Doran KS, Howd PA (2012) Hotspot of accelerated sea-level rise on the Atlantic Coast of North America. Nat Clim Chang 2(12):884–888

Schwimmer RA (2001) Rates and processes of marsh shoreline erosion in Rehoboth Bay, Delaware, U.S.A. J Coast Res 17(3):672–683

Seabloom EW, Ruggiero P, Hacker S, Mull J, Zarnetske P (2013) Invasive grasses, climate change, and flood risk in coastal ecosystems. Glob Chang Biol 19(3):824–832. https://doi.org/10.1111/gcb.12078

Seabloom EW, Wiedemann AM (1994) Distribution and effects of Ammophila breviligulata Fern. (American Beach Grass) on the foredunes of the Washington Coast. J Coast Res 10:178–188

Seliskar DM, Huettel RN (1994) Nematode involvement in the dieout of Ammophila breviligulata (Poaceae) on the Mid-Atlantic coastal dunes of the United States. J Coast Res 9(1):97–103

Seneca ED (1972) Seedling response to salinity in four dune grasses from the outer banks of North Carolina. Ecology 53(3):465–471

Short AD, Hesp PA (1982) Wave, beach and dune interactions in southeastern Australia. Mar Geol 48:259–284

Singer R, Lucas LT, Warren TB (1973) The marasmius-blight fungus. Mycologia 65(2):468–473

Stallins JA (2005) Stability domains in barrier island dune systems. Ecol Complex 2:410–430

Stallins JA, Parker AJ (2003) The influence of complex systems interactions on barrier island dune vegetation pattern and process. Ann Assoc Am Geogr 93(1):13–29

Stalter R, Lamont SE (1990) The vascular flora of Assateague Island, Virginia. Bull Torrey Bot Club 117(1):48–56. https://doi.org/10.2307/2997128

Stalter R, Lamont SE (2000) Vascular flora of fisherman Island, Virginia. J Torrey Bot Soc 127(4):324–332. https://doi.org/10.2307/3088651

Stockdon HF, Sallenger AH, Holman RA, Howd PA et al (2007) A simple model for the spatially-variable coastal response to hurricanes. Mar Geol 238(1–4):1–20. https://doi.org/10.1016/j.margeo.2006.11.004

Stocker TF et al (2013) IPCC, 2013: climate change 2013: the physical science basis. Cambridge University Press, Cambridge, U.K

Stolper D, List JH, Thieler ER (2005) Simulating the evolution of coastal morphology and stratigraphy with a new morphological-behaviour model (GEOMBEST). Mar Geol 218:17–36. https://doi.org/10.1016/j.margeo.2005.02.019

Van Der Valk AG (1975) The floristic composition and structure of foredune plant communities of cape hatteras national seashore. Chesap Sci 16(2):115–126

Walters D, Moore LJ, Durán O, Fagherazzi S, Mariotti G (2014) Interactions between barrier Islands and back-barrier marshes affect island system response to sea level rise: insights from a coupled model. J Geophys Res Earth Surf 119:2013–2031. https://doi.org/10.1002/2014JF0033091

Walters D, Kirwan M (2016) Optimal hurricane overwash thickness for maximizing marsh resilience to sea level rise. J Ecol Evol 6(9):2948–2956. https://doi.org/10.1002/ece3.2024

Wells A, Goff J (2007) Coastal dunes in Westland, New Zealand, provide a record of paleoseismic activity on the Alpine fault. Geol Soc Am 35(8):731–734. https://doi.org/10.1130/G23554A.1

Wolner CV, Moore LJ, Young DR, Brantley ST, Bissett SN, McBride RA (2013) Ecomorphodynamic feedbacks and barrier island response to disturbance: Insights from the Virginia Barrier Islands, Mid-Atlantic Bight, USA. Geomorphology 199:115–128. https://doi.org/10.1016/j.geomorph.2013.03.035

Woodhouse WW, Seneca ED, Broome SW (1977) Effect of species on dune grass growth. Int J Biometeorol 21(3):256–266

Young IR, Verhagen LA (1996) The growth of fetch limited waves in water of finite depth. Part 1. Total energy and peak frequency. Coast Eng 29:47–78

Zarnetske PL et al (2012) Biophysical feedback mediates effects of invasive grasses on coastal dune shape. Ecology 93(6):1439–1450. https://doi.org/10.1890/11-1112.1

Zarnetske PL, Gouhier TC, Hacker SD, Seabloom EW, Bokil VA (2013) Indirect effects and facilitation among native and non-native species promote invasion success along an environmental stress gradient. J Ecol 101(4):905–915

Zarnetske PL, Ruggiero P, Seabloom EW, Hacker SD (2015) Coastal foredune evolution: the relative influence of vegetation and sand supply in the US Pacific Northwest. J R Soc Interface 12(106):20150017. https://doi.org/10.1098/rsif.2015.0017

Zinnert JC, Shiflett SA, Vick JK, Young DR (2011) Woody vegetative cover dynamics in response to recent climate change on an Atlantic Coast barrier island using Landsat TM imagery. Geocarto Int 26:595–612. https://doi.org/10.1080/10106049.2011.621031

The Role of Vegetation in Determining Dune Morphology, Exposure to Sea-Level Rise, and Storm-Induced Coastal Hazards: A U.S. Pacific Northwest Perspective

Peter Ruggiero, Sally Hacker, Eric Seabloom, and Phoebe Zarnetske

Abstract Coastal foredunes are often the "first line of defense" for backshore infrastructure from the hazards of erosion and flooding, and they are key components of coastal ecosystems. The shape and growth characteristics of coastal foredunes, typically characterized by simple morphometrics such as dune toe and crest elevations, and dune volume, are a product of both physical and biological forces. By influencing foredune shape, these forces ultimately affect the exposure of human populations and ecosystems to extreme storms and sea-level rise. In this chapter, we synthesize field surveys and a suite of interdisciplinary laboratory, mesocosm, and computer modeling experiments that examine the relative role of vegetation in determining dune geomorphology in the U.S. Pacific Northwest (PNW). We focus on how dunes of different shapes result in variable levels of exposure to coastal hazards. Results suggest that PNW dune shape is primarily a function of sediment supply and the geographic distribution of two species of non-native beach grasses (*Ammophila arenaria* and *A. breviligulata*). Over recent decades, *A. breviligulata* (American beachgrass) has increased its dominance over *A. arenaria* (European

P. Ruggiero, Ph.D. (✉)
College of Earth, Ocean, and Atmospheric Sciences, Oregon State University, Corvallis, OR, USA
e-mail: pruggier@coas.oregonstate.edu

S. Hacker, Ph.D.
Department of Integrative Biology, Oregon State University, Corvallis, OR, USA
e-mail: hackers@science.oregonstate.edu

E. Seabloom, Ph.D.
Department of Ecology, Evolution, and Behavior, University of Minnesota, St. Paul, MN, USA
e-mail: seabloom@umn.edu

P. Zarnetske, Ph.D.
Department of Forestry, Fisheries and Wildlife, Michigan State University, East Lansing, MI, USA

Ecology, Evolutionary Biology, and Behavior Program, Michigan State University, East Lansing, MI, USA
e-mail: plz@anr.msu.edu

L.J. Moore, A.B. Murray (eds.), *Barrier Dynamics and Response to Changing Climate*, https://doi.org/10.1007/978-3-319-68086-6_11

beachgrass) on dunes where it was originally planted and has actively spread to new sites formerly dominated by *A. arenaria*. A species-specific biophysical feedback occurs between sand deposition and beach grass growth habit, resulting in distinctly different dune geomorphologies in locations dominated by these different grass species. The dense, vertical growth habit of *A. arenaria* allows it to capture more sand, produce more vertical tillers, and build taller, narrower dunes, while the less dense, lateral growth habit of *A. breviligulata* is more suited for building shorter but wider dunes. The species-specific feedbacks, along with invasion dynamics, have a first order effect on the region's exposure to coastal hazards, in the present day and under a range of climate change and invasion scenarios. These findings draw on insights from geomorphology, ecology, and coastal engineering to assess coastal barrier vulnerability in light of global change.

Keywords Beach grasses • *Ammophila arenaria* • *Ammophila breviligulata* • Coastal barriers • Ecomorphodynamics • Foredunes • Morphodynamics • Oregon • Pacific Northwest • Sea-level rise • Washington

1 Introduction

The Indian Ocean and Tōhoku tsunamis, Hurricanes Katrina and Rita, and most recently Hurricane Sandy and Typhoon Haiyan have reinforced the notion that coastal communities are highly vulnerable to damages caused by flooding and erosion. Hurricane Sandy, in particular, provided a wake-up call to the damages that can be sustained when storms and high water levels converge on unprepared coastal populations. These extreme flooding events will likely become more frequent due to global climate change (e.g., IPCC 2014). Alongshore variability in destruction from flooding during extreme storm events (e.g., Stockdon et al. 2007) also has highlighted the value of natural barriers formed by coastal ecosystems, so-called *green infrastructure*, in reducing flooding vulnerability (e.g., Duarte et al. 2013). Although coastal zones support large human populations worldwide and contribute significantly to the economic welfare of countries, we know surprisingly little about how climate change and extreme events will interact with coastal ecosystems, such as along coastal barriers, and ultimately affect the sustainability of coastal communities and habitats.

Extreme events and chronic stressors associated with climate change, such as intense storms, tsunamis, and sea-level rise (SLR), can have severe impacts on humans and the ecosystem services upon which they depend. Further, there is growing recognition that coastal dunes provide critical ecosystem services (Fig. 1; Barbier et al. 2011); they are the first line of defense against flooding (e.g., Sallenger 2000; Ruggiero et al. 2001; Feagin et al. 2005; Seabloom et al. 2013), provide conservation value for native species (Gutierrez et al. 2012), and are an important draw for recreation (Guerry et al. 2012). The coastal protection properties of dunes are

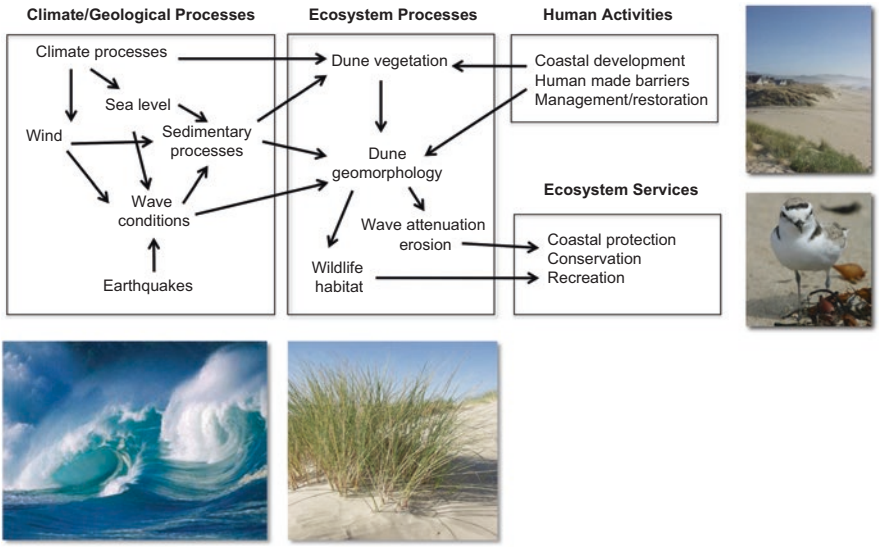

Fig. 1 The relationships between physical processes, ecosystem processes, and human activities important to the ecosystem services provided by coastal dunes

intrinsically linked to the interaction and feedbacks between sediment supply and vegetation in these systems (e.g., Hesp 1989; Ruggiero et al. 2011; Hacker et al. 2012; Zarnetske et al. 2012; Duran and Moore 2013, 2015). Climate change and other human-caused perturbations can influence these feedbacks, significantly affecting the structural and functional role of these ecosystems and the services they provide (Seabloom et al. 2013; Duarte et al. 2013). In particular, we know that climate alters physical drivers through the hydrodynamics of wind and water, including both chronic trends and extreme events that alter sediment deposition and coastal flooding (Fig. 1). Likewise, climate affects ecosystem processes when warming, altered precipitation, and extreme storms modify the distribution and abundance of coastal vegetation, such as dune-building plants. These dynamics can also be altered by socioeconomic factors including coastal development, shoreline armament and beach nourishment, recreation, raw material extraction such as sand mining, and even ocean energy generation (e.g., Carter 1990; Pye and Tsoar 1990; Nordstrom et al. 2011; Martinez and Psuty 2004; Kim et al. 2012, Elko et al. 2016). Taken together, the interactions between climate, geological processes, ecosystem processes, and socioeconomic factors all influence the ecosystem services provided by coastal dunes (Fig. 1).

Coastal dunes of the U.S. Pacific Northwest (PNW, Oregon and Washington, Fig. 2) are an excellent system in which to explore how climate change affects interactive ecomorphodynamics and community-scale adaptive hazard planning in coastal socio-ecological systems. The PNW coastline is characterized by significant gradients in both the physical (e.g., sediment supply) and the ecological (e.g., grass cover dominance, growth patterns) parameters that are thought to be of primary

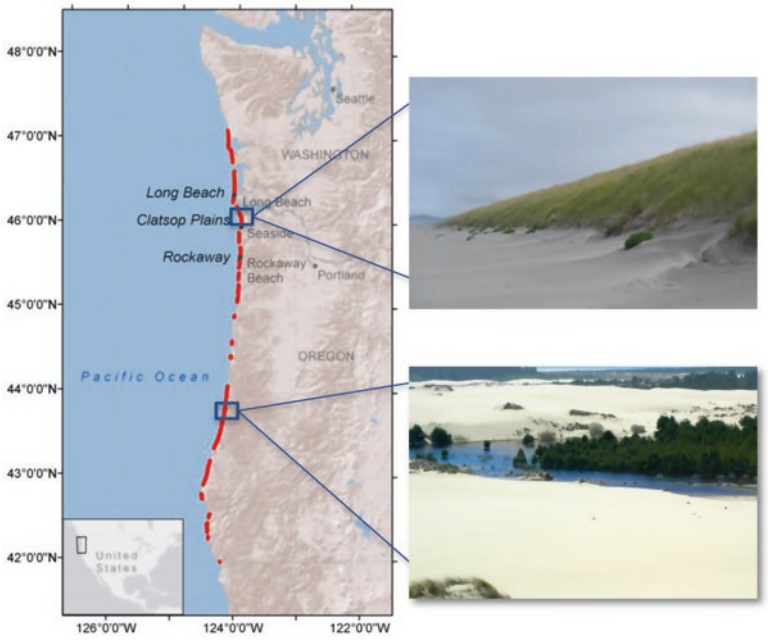

Fig. 2 Map of the dune-backed beaches along the Washington and Oregon coastlines (modified from Mull and Ruggiero 2014). The locations of the Long Beach Peninsula (WA), Clatsop Plains (OR), and Rockaway Beach (OR) littoral cells, areas highlighted in Fig. 6, are shown. Inset photos of dunes are from the Clatsop Plains (*top*) and the Oregon Dunes National Recreation Area (*bottom*)

importance to dune geomorphology (Cooper 1958; Ruggiero et al. 2005; Hacker et al. 2012; Zarnetske et al. 2015). Further, various stakeholder sectors in the region are working to define appropriate climate change adaptation strategies (Lipiec 2015; Mills 2015), particularly those involving green engineering solutions, as seas rise (e.g., NRC 2012), storms intensify (e.g., Ruggiero 2013), and coastal populations continue to increase.

In the following sections, we review recent work performed on the coastal dune systems of the PNW that synthesizes field surveys and a suite of laboratory, mesocosm, and computer modeling experiments (Fig. 3) to examine the role of vegetation in determining dune geomorphology and, therefore, exposure to coastal hazards. We conclude by discussing the implications of our findings for improving conceptual and numerical models of beach-dune interactions with an ultimate goal of improving coastal management decision making. The work described here is inherently interdisciplinary and draws on insights from geomorphology, ecology, and coastal engineering to assess coastal barrier vulnerability in light of global change.

Fig. 3 Field, lab, and mesocosm techniques used to investigate PNW foredune ecomorphodynamics. (**a**) Schematic of airborne lidar data being collected, (**b**) topographic beach profile collection, (**c**) quadrat for beach grass ecological surveys, (**d**) mesocosm experiment, (**e**) wind tunnel experiment setup, (**f**) alternative beach mapping techniques, (**g**) representative PNW foredune

2 Study Area Description

The PNW coast is tectonically active, being a so-called "collisional coast" (sensu Inman and Nordstrom 1971), located onshore of where the eastward moving Juan de Fuca and Gorda plates collide with the North American plate. Due to this setting, the PNW is subject to both near-field Cascadia Subduction Zone earthquakes and tsunamis (Atwater 1996) and far-field (distant) tsunami events. The region's geology also results in the coast being comprised of a series of segmented sandy littoral cells with alternating stretches of erosion-resistant rocky headlands and more easily eroded dune-backed or bluff-backed beaches (Fig. 2; Komar et al. 2013). Modern rates of relative SLR in this region are strongly affected by tectonics with significant alongshore variations in vertical land motions. While some stretches of the coast are being submerged by a net rise in relative sea level (central Oregon and southwest Washington), other areas are presently experiencing land uplift at rates faster than

the increase in sea level, resulting in emergent coastlines (southwest Oregon and northwest Washington, Komar et al. 2011).

The wave climate of the PNW is recognized for its severity, with winter storms commonly generating deep-water significant wave heights (SWH) greater than 10 m (about one event of this magnitude per year) and the largest storms in the region having generated SWHs in the range of 14–15 m (Allan and Komar 2002). Deep-water SWHs and spectral peak periods have annual averages of about 2 m and 10 seconds (s), respectively. High, long-period waves (averaging about 3 m in height and 12–13 s in period), high water levels, and a west-southwest direction of wave approach characterize the winter months (November through February), whereas small waves (1-m SWHs and 8-s periods), low water levels, and wind and waves from the west-northwest are typical for summer (May through August) (Ruggiero et al. 2005). Strong El Niño events, occurring approximately once every 20 years, are typified by an increased frequency of storms tracking from the south-southwest and higher than typical sea levels (Komar 1986; Kaminsky et al. 1998). The most recent strong El Niños of 1982–1983, 1997–1998, and 2015–2016 resulted in significant hotspot beach erosion and severe dune scarping along much of the region (e.g., Revell et al. 2002). Increasing wave heights have been observed in the northeastern Pacific using instrumented NOAA buoys along the U.S. West Coast (Allan and Komar 2000, 2006; Méndez et al. 2006; Menéndez et al. 2008; Komar et al. 2009; Ruggiero et al. 2010; Seymour 2011) and from satellite altimetry (Young et al. 2011). For the coast of the PNW over the period of wave buoy observations (approximately 30 years), Ruggiero (2013) found that wave height increases have had a more significant role in the increased frequency of dune overtopping and erosion than has the rise in sea level over that same period.

Nearly 45% of the coast in Oregon and Washington consists of sandy beaches backed by dunes (Fig. 2), including the Oregon Dunes National Recreation Area, the largest dune sheet in North America (~240 km long and 3 km wide). Prior to the early 1900s, these habitats lacked extensive dune-building vegetation and were exposed to shifting sand environments that provided little barrier between the ocean and coastal communities. To stabilize these areas, two non-native beach grasses were introduced over a 40–60-year time span. The grasses included *Ammophila arenaria* from Europe and *A. breviligulata* from the U.S. Atlantic and Great Lakes. These early green infrastructure projects resulted in a complete state change in coastal dune systems (Wiedemann and Pickart 2004). Prior to the invasion of these species, native dune plants (including the native beach grass, *Elymus mollis*) formed small hillocks or short, parallel ridges depending on sand supply. In contrast, *A. arenaria* created stable foredunes, with dune ridges reaching as high as 15 meters and serving to intercept and stabilize sand and decrease sand supply to the backshore (Cooper 1958; Hacker et al. 2012). By the 1950s, *A. arenaria* had colonized the entire Pacific coast, from Canada to Mexico, and *A. breviligulata* had expanded from focused plantings in southwest Washington into northwest Oregon. While these early green infrastructure projects successfully provided increased sand stabilization and protection services for coastal communities, one unintended consequence of the *Ammophila* invasion was the displacement of a number of native dune

species along the Pacific coast including the federally threatened Western snowy plover and the state-endangered Pink sandverbena (Zarnetske et al. 2010). Additional consequences of these new foredune ridges included an increase in the prevalence of wetlands behind dunes and deflation plains, as well as an increase in the area of forested and shrub habitats. Management of coastal dunes in Oregon and Washington has been complicated by the presence of both species of non-native beach grasses. *Ammophila breviligulata* has displaced *A. arenaria* throughout much of Washington and continues to spread south along the Oregon coast (Seabloom and Wiedemann 1994; Hacker et al. 2012).

3 U.S. Pacific Northwest Beach and Foredune Morphometrics

The alongshore variability of beach and foredune geomorphology within the PNW has been primarily evaluated via the extraction of quantitative morphometric parameters from lidar data (Fig. 3a; Mull and Ruggiero 2014). We have developed automated methods (modified from the approaches of Elko et al. 2002 and Stockdon et al. 2009 to be relevant for the U.S. West Coast) to objectively and accurately extract parameters such as the horizontal and vertical locations of the foredune toe (*dtoe*), the foredune crest (*dhigh*), and the foredune heel (*dheel*) from individual cross-shore beach profiles derived from gridded lidar data (Fig. 4). The *dhigh* elevation is taken as the most shoreward dune crest with a minimum elevation drop in the backshore of 0.60 m (a necessary distinction due to significant areas in the PNW with multiple dune ridges). *dheel* is the local minimum between *dhigh* and a subsequent (more landward) dune crest (if present). *dtoe* is the maximum difference between the measured profile and the profile detrended with a cubic function in the extent between the horizontal location of mean high water (MHW) and *dhigh*. The dune volume, *V*, is the numerically integrated area between the profile and the horizontal line at the elevation of *dtoe*.

Foredune shape and evolution within some areas of the PNW is being monitored in situ with Real Time Kinematic Differential Global Positioning System (RTK DGPS) surveying techniques (Fig. 3b, f; Ruggiero et al. 2005, http://nvs.nanoos.org/BeachMapping). Topographic beach profiles are typically measured by walking from the landward side of the primary foredune ridge, over the dune crest, to wading depth during spring low tides. To resolve the interannual- to decadal-scale variability of the region's foredunes, beach profiles have been collected quarterly (since 1997) at ~50 locations along the Columbia River littoral cell (CRLC; Fig. 2), nominally distributed in the alongshore at approximately 3 km. The procedures used to extract morphometric parameters from the lidar data were also applied to the beach profiles collected in situ.

Littoral-cell-averaged beach and foredune morphometrics are summarized in Fig. 5 for the majority of dune-backed beaches in the PNW (Mull and Ruggiero 2014). We focus here on backshore beach slopes (computed between the horizontal

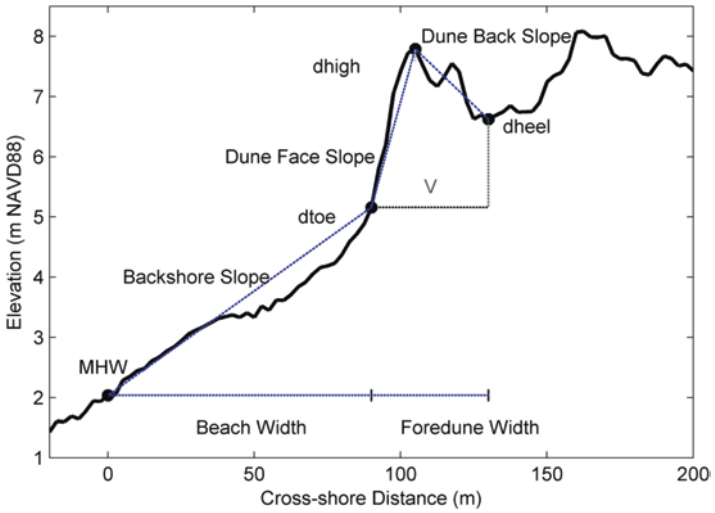

Fig. 4 An example of a lidar-derived cross-shore profile and the beach and foredune morphometric parameters extracted from the profile (modified from Mull and Ruggiero 2014)

location of MHW and the horizontal position of *dtoe*, Fig. 5b), *dhigh* elevations, and *dtoe* elevations (Fig. 5c) as these parameters are used in subsequent estimates of exposure to overtopping during high water events (e.g., Sallenger 2000). Backshore beach slopes in the region are typically fairly mild, ranging from 0.02 to 0.06, as much of the PNW can be characterized as morphodynamically dissipative (Wright and Short 1983; Ruggiero et al. 2005). Cell-averaged dune toe elevations range from ~4.7 to 5.7 m mean lower low water (MLLW) with relatively minimal variability. Average dune crest elevations are more variable, ranging from 7 to 13.6 m MLLW throughout the region.

Sediment supply to both beaches and dunes is an important parameter in beach-dune interaction models (e.g., Psuty 1992). Here we take decadal-scale, end-point shoreline change rates (SCR, Fig. 5d) as a proxy for sediment supply to the beaches of the PNW. SCRs were computed based on proxy-based shorelines (e.g., interpreted position of the average high water line) derived from aerial photography (1967 for Oregon and 1980s for Washington) and datum-based shorelines (e.g., position of MHW) extracted from 2002 lidar data (Ruggiero et al. 2013). The methods of Moore et al. (2006) and Ruggiero and List (2009) were employed to correct for the proxy-datum bias associated with these differently derived shoreline positions. The littoral-cell averaged SCRs shown in Fig. 5d reveal relatively stable shorelines in southern Oregon, modestly retreating shorelines in central Oregon, and rapidly prograding shorelines in northwest Oregon and southwest Washington within the CRLC. Note the relatively low dune heights in areas experiencing rapid shoreline progradation.

To explore intra-cell variability, extracted beach and dune morphometrics along three representative PNW littoral cells, Long Beach Peninsula (WA), Clatsop Plains (OR), and Rockaway (OR), are shown in Fig. 6 with values smoothed in the

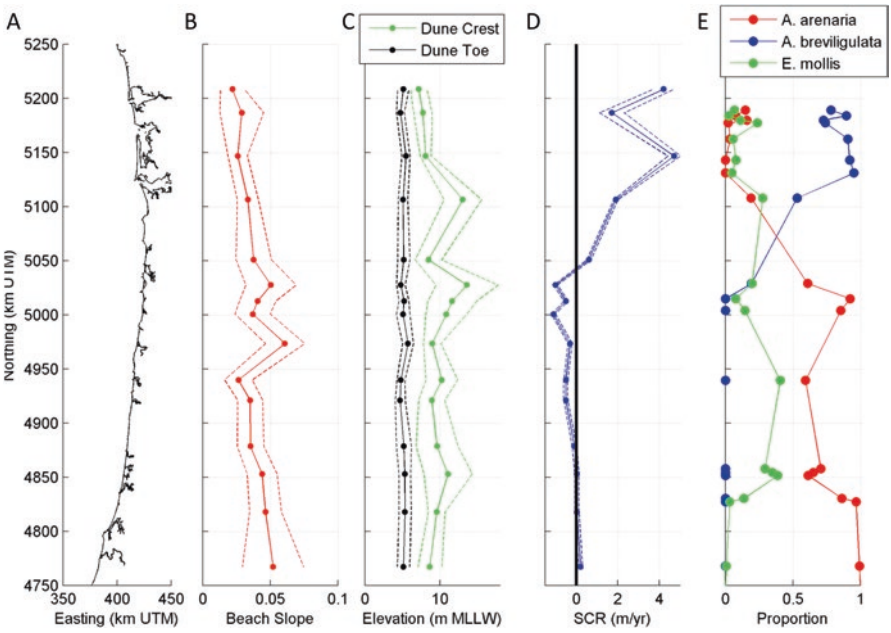

Fig. 5 Summary of beach and dune morphometrics for the Oregon and southern Washington coasts using lidar-derived cross-shore profiles from 2002. (**a**) Map of PNW, (**b**) backshore beach slope, (**c**) dune toe and dune crest elevations, (**d**) decadal-scale shoreline change rates, (**e**) mean proportional abundance for two non-native and one native beach grass species. Panels **b**, **c**, and **d** illustrate littoral-cell averages (*filled circles* and *solid lines*) and variability (±1 standard deviation, *dashed lines*)

alongshore direction over a length scale of 250 m to reduce noise and small-scale variability. In general, the *dtoe* elevations are similar in all three littoral cells. The *dhigh* elevations are similar at Long Beach and Rockaway, while the dunes are taller and more variable in height at Clatsop Plains. On average, the backshore is slightly steeper at Rockaway than Long Beach or Clatsop Plains.

4 Relative Importance of Sand Supply and Beach Grasses to Dune Geomorphology

The availability of synoptic lidar data (Mull and Ruggiero 2014), the long-term beach monitoring program described above (Ruggiero et al. 2005), as well as a co-located dune ecology monitoring program (Seabloom and Wiedemann 1994; Hacker et al. 2012) have allowed us to examine the relative role of biological (e.g., grass distribution and abundance) and physical (e.g., sediment supply) mechanisms governing foredune evolution (Zarnetske et al. 2015).

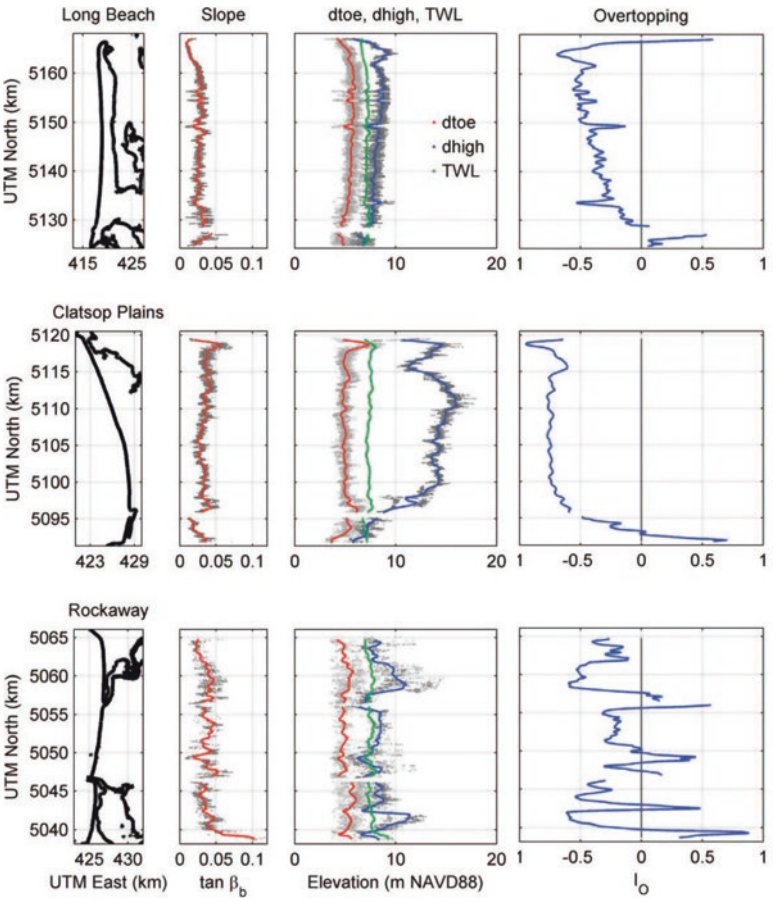

Fig. 6 (*first (left) panel*) Alongshore position of data. (*second panel*) Backshore slopes in *dark gray* and backshore slopes that have been smoothed in the alongshore direction (*red*). (*third panel*) dtoe elevations in *light gray* and dhigh elevations in *dark gray*, with both parameters smoothed in the alongshore (*red* and *blue*, respectively). Smoothed TWL elevations for the March 2–4 1999 storm event are shown in *green*. (*fourth (right) panel*) Overtopping index (modified from Mull and Ruggiero 2014)

To specifically document the colonization, spread, and dominance of the two invasive beach grass species through time, we measured plant community cover, composition, and *Ammophila* spp. tiller density at 18 locations across the region (Fig. 5e). We measured the plant morphology of the three beach grass species collected (where present) on each of several transects at each location. Grasses were collected by placing a quadrat on the upper face of the foredune (Fig. 3c) next to the transect in monocultures of each species (where present) and digging up all the plants including as much as 50 cm of the belowground stem or rhizome. Individual plants (defined as one or more tillers attached to a single proximal rhizome) were counted within each quadrat. Individual plants of each species (where present) were

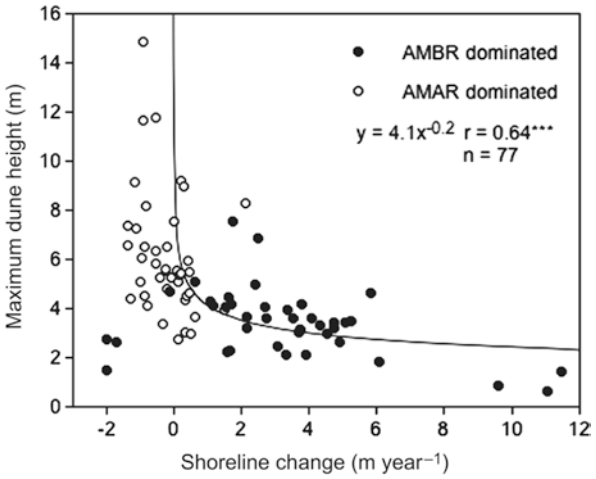

Fig. 7 Relationship between maximum foredune height and shoreline change rate for transects dominated by *A. breviligulata* (AMBR, *dark circles*) and *A. arenaria* (AMAR, *open circles*). The line represents a negative exponential relationship for all transects combined (***$p < 0.0001$) (from Hacker et al. 2012)

extracted, including at least 50 cm of the rhizome, on the upper face of the foredune along the transect. We measured tiller density (tillers per rhizome), tiller height (cm), tiller weight (g), length of primary rhizome internodes and lateral versus vertical secondary rhizomes produced at the nodes and terminating in tillers. Hacker et al. (2012) give more detail on ecological survey methods.

Ammophila breviligulata had a higher proportional cover at sites north of Fort Stevens, OR (just south of the Columbia River), while *A. arenaria* was present at all sites and had higher proportional cover at Cape Lookout and south where *A. breviligulata* was absent (Fig. 5e; Hacker et al. 2012). The native *Elymus mollis* was present at low to moderate proportional cover at all sites, was most abundant at the central Oregon sites, and least abundant at northern and southern sites. Hacker et al. (2012) found that between 1988 (Seabloom and Wiedemann 1994) and 2006, *A. breviligulata* increased in abundance by 36% and colonized an additional 10 km of coast to the south. During this same 19-year period, *A. arenaria* decreased in abundance by 43% and *E. mollis* increased by 11%. For a given area, *E. mollis* had the lowest density of plants compared to *A. arenaria* and *A. breviligulata*, which did not differ. For a given plant, tiller density was lowest for *E. mollis* compared to *A. arenaria* and *A. breviligulata*, which did not differ. In addition, *A. arenaria* plants had significantly fewer lateral rhizomes compared to *A. breviligulata* or *E. mollis* plants.

Foredunes dominated by *A. breviligulata* were about half the height (Fig. 7), nearly twice the width, and half as steep as those dominated by *A. arenaria*. They also typically occurred in areas with higher sand deposition and greater SCRs than those dominated by *A. arenaria*. Transects with highly positive or negative SCRs had shorter foredunes compared to those with rates near zero and were dominated by *A. breviligulata* (Fig. 7). Importantly, even after controlling for sediment supply—within a restricted range of SCRs of ±2 m or less—*A. arenaria* foredunes were taller, narrower, and steeper than those with *A. breviligulata*, even though the grass cover did not differ. In general, field observations suggest that *A. arenaria* can be characterized as having thinner stems, higher density, and a primarily vertical growth form,

as opposed to *A. breviligulata's* thicker stems, lower density, and horizontal growth forms (Hacker et al. 2012). To investigate the detailed dynamics associated with why different grass species are associated with differently shaped foredunes, we performed two controlled experiments that are described in the next section.

4.1 Species-Specific Feedbacks

To assess the growth of the three grass species found in PNW foredunes in response to different levels of sand deposition, we performed a species interaction mesocosm experiment (Fig. 3d; Zarnetske et al. 2012) in spring 2007 at the Hatfield Marine Science Center (Newport, Oregon). We planted 41 permeable geotextile bags with 15 adult plants (grass mixtures or monocultures) in Oregon beach sand. We planted the bags with a constant density; mixture bags had five plants per species and the monoculture bags had 15 plants of a single species. After allowing the plants to establish for 3 months, the bags were subjected to one of four treatments of vertical beach sand deposition—where rates of deposition reflected observations on PNW foredunes (Ruggiero et al. 2005, 2011). We measured growth responses for each species in each bag at the start and end of the experiment. These measurements included tillers m^{-2}, tiller growth form (determined by the tiller angle from the main rhizome; a right angle was deemed more lateral spreading growth, an acute angle was deemed more vertical growth), total plant dry biomass m^{-2}, and rhizome internode lengths (a proxy for growth response to deposition, measured on the first 16 internodes on the rhizomes of four random tillers per species–bag combination).

To characterize the dune-building capacity of each beach grass species, we constructed a moveable bed wind tunnel at the O.H. Hinsdale Wave Research Laboratory (HWRL), Corvallis, Oregon, USA, and performed a series of sand capture efficiency experiments (Fig. 3e; Zarnetske et al. 2012). Three thousand adult beach grass tillers with intact rhizomes were collected along the Oregon coast and planted in 1 m^2 boxes filled with Oregon beach sand. Each of the three beach grass species were planted at three densities reflecting the range of tiller densities found in the field on coastal foredunes in the PNW. We subjected 28 boxes (three replicates per species by density combination, one sand-only box) to two different wind conditions (low and high) and assessed sand capture efficiency by dividing the mass of sediment trapped in each box by the mass provided to the box during each experimental run.

Results from the moveable bed wind tunnel experiments (Zarnetske et al. 2012) suggest that increasing tiller density increased sand capture efficiency. Under different experimental densities, the native grass (*E. mollis*) had higher sand capture efficiency compared to the *Ammophila* congeners on an equal density basis. However, the greater densities of non-native grasses under PNW field conditions indicate that they have greater potential to capture more sand overall. The mesocosm experiment looked at plant growth responses to sand deposition and found that, in response to increasing sand supply rates, *A. arenaria* produced higher-density vertical tillers

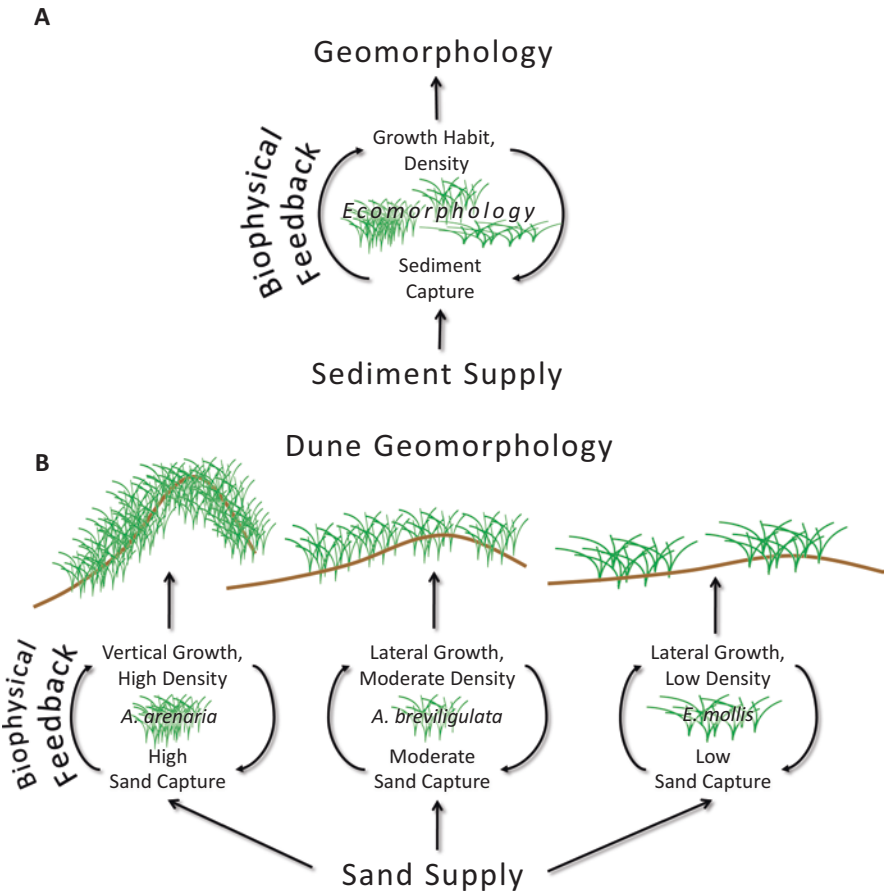

Fig. 8 (**a**) Conceptual diagram showing the important biophysical feedback between vegetation and sediment in coastal foredune systems. Vegetation characteristics (growth habit, density) and sediment supply form the basis for the sediment capture process, which is continually modified through feedbacks between vegetation growth and sediment capture. (**b**) Expected feedbacks and resulting dune geomorphology for this coastal dune study system based on data from Hacker et al. (2012) for native beach grass (*Elymus mollis*) and two non-native grass species, (*Ammophila arenaria* and *Ammophila breviligulata*) (from Zarnetske et al. 2012)

(characteristic of higher sand capture efficiency), while *A. breviligulata* and *E. mollis* responded with lower-density lateral tiller growth (characteristic of lower sand capture efficiency).

Combined, these ecomorphodynamic experiments and our field observations (Fig. 3g) provide evidence for a species-specific two-way biophysical feedback between sand deposition, growth habit, and growth-habit-mediated sand capture efficiency, resulting in distinctly different dune geomorphologies for PNW foredunes (Fig. 8). First, differences in the form (growth habit and density) of species lead to initial differences in function (sediment capture ability). Second, species

vary in their growth response to sediment deposition. Third, deposition-induced changes in plant growth further alter sediment capture. The feedback reinforces species-specific sediment capture ability, eventually resulting in differences in dune shape with *A. arenaria* building taller, narrower dunes, *A. breviligulata* building lower, wider dunes, and *E. mollis* building the shortest and widest dunes. Zarnetske et al. (2012) suggested that two, non-mutually exclusive, ecological mechanisms exist for these differences: (1) the species differ in their ability to capture sand and (2) the species differ in their growth habit in response to sand deposition.

4.2 Retrospective Analysis

Given the measureable species-specific effect on dune shape described above, an important next step was determining the extent to which the vegetation influenced dune shape over time. To address this question, Zarnetske et al. (2015) assessed the relative importance of sand supply and changes in beach grass species in shaping foredunes across a 100 km stretch of the CRLC at both interannual and decadal time scales. The majority of the coastline within the CRLC has been prograding over the last two decades (Fig. 5d), such that in some locations new foredune features have developed seaward of the historical foredune (Fig. 9; Ruggiero et al. 2011, 2013, 2016). Beaches along the Long Beach Peninsula have exhibited shoreline advances of approximately 4 m/year, with the foredunes accumulating sand at rates of well over 10 m^3/m/year. While net onshore-directed cross-shore sediment transport within the surf zone and cross-shore feeding from a shoreface out of equilibrium with forcing conditions (Kaminsky et al. 2010) may each be partially responsible for the sediment supplied to the beaches and dunes during this period, gradients in alongshore sediment transport are primarily responsible for the large supply of sediment available to the beaches, and subsequently to the dunes via aeolian sediment transport processes (Ruggiero et al. 2016).

Over the two decades of CRLC foredune evolution studied by Zarnetske et al. (2015), the dominant vegetation switched from *A. arenaria* to *A. breviligulata*. From 1988 to 2009, the overall proportion of vegetation cover and *A. breviligulata* abundance in the CRLC increased by an average of 1% per year (21% total for the 21-year timeframe). The combination of physical (e.g., sand supply rates) and biotic (e.g., abundance and composition of the plant community) forces was important in explaining the variation in foredune shape across both interannual- and decadal-scales; however, the relative importance of sand supply and vegetation varied with temporal scale and location within the CRLC (Fig. 10). At interannual timescales, sand supply rates explained the majority of change in both foredune height and width. However, at decadal scales, change in vegetation explained the majority of the change in foredune width, whereas sand supply rates explained most of the change in foredune height. In areas with lower shoreline change rates (<±2.0 m/year), the change in vegetation explained the majority of decadal changes in both foredune width and height (Fig. 10).

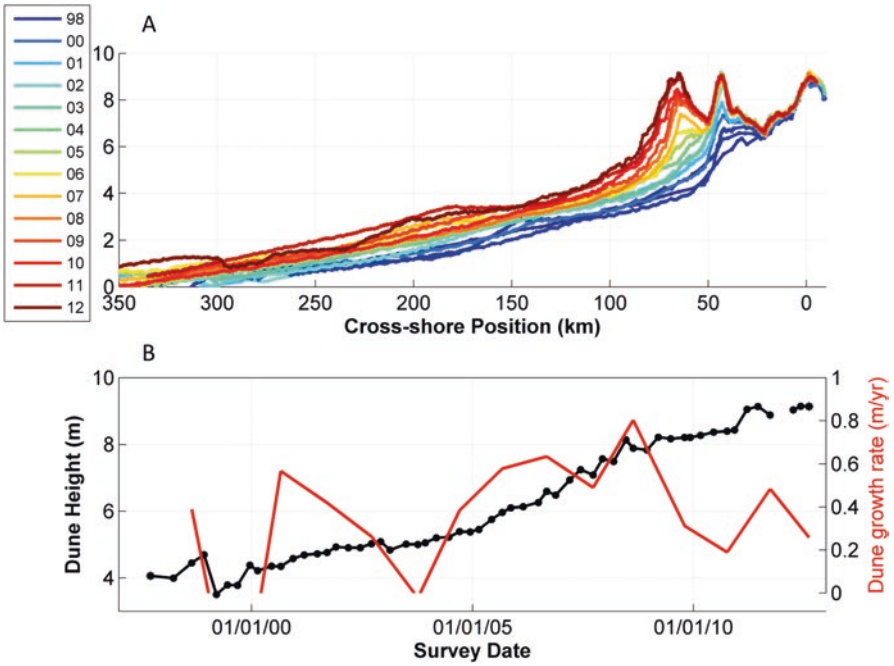

Fig. 9 (**a**) Evolution of foredune geomorphology between 1998 and 2012 for a CRLC beach profile along the Long Beach Peninsula, WA; (**b**) Time evolution of the elevation of the location of the 2012 dune crest position (*black line*) and the vertical growth rate (VGR) at this position (*red line*).

5 Implications to Coastal Protection Services

To assess the risk to overtopping of PNW dune-backed beaches for present-day conditions and possible future climate change and beach grass invasion scenarios, we used the simple Storm Impact Scaling model of Sallenger (2000). In the Storm Impact Scaling model, four storm-impact regimes, or thresholds for coastal change, are defined to provide a framework for examining the relative magnitudes of coastal change likely to occur. Here we focus only on one of the regimes; overtopping, which occurs when extreme storm-induced total water levels (TWLs) are greater than the crest elevation of the foredune, *dhigh*.

Extreme coastal total water levels (TWL) are the result of interactions between multiple oceanographic, hydrological, geological, and meteorological forcings that act over a wide range of scales (e.g., astronomical tide, wave setup, wind setup, large-scale storm surge, precipitation, fluvial discharges, monthly mean sea level, vertical land motions, etc.). At any given time, the elevation of the TWL, relative to a fixed datum, is comprised of at least four components such that

$$\mathrm{TWL} = \mathrm{MSL} + \eta_A + \eta_{\mathrm{NTR}} + R \tag{1}$$

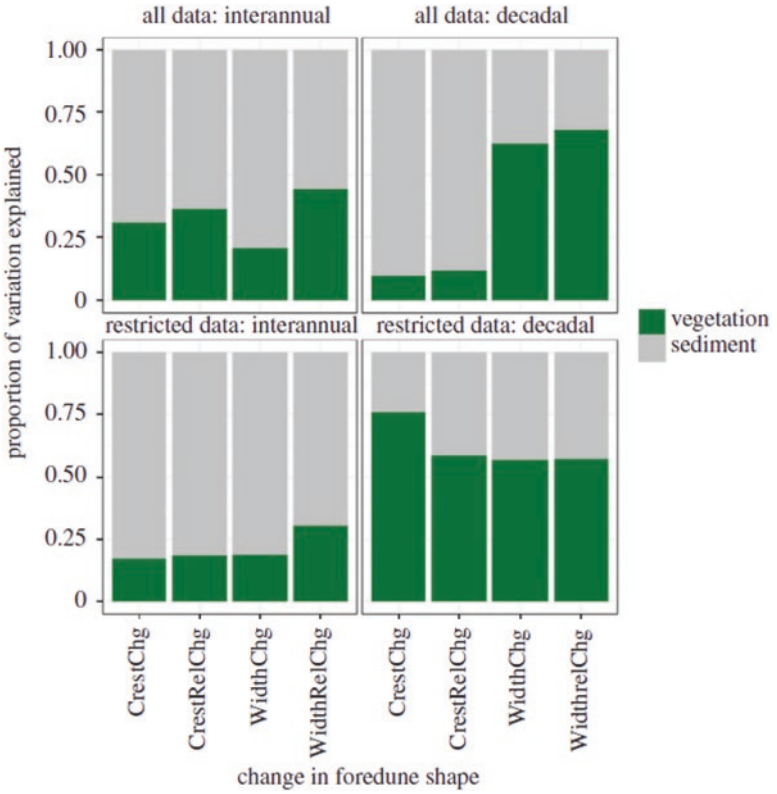

Fig. 10 The overall proportion of variation in change in foredune shape that was explained by all vegetation versus sand explanatory variables for the full and restricted (±2.0 m/year SCR) sets of CRLC field observational data (from Zarnetske et al. 2015)

where MSL is the mean sea level, η_A is the deterministic astronomical tide, η_{NTR} is the non-tidal residual, or any elevation change to the water level not due to the tide, and R is a wave-induced component, called wave runup. Here, wave runup is computed using the empirical relation of Stockdon et al. (2006) for the 2% exceedance percentile of extreme wave runup and is parameterized by the backshore beach slope, the deep-water SWH, and the deep-water wave length. Ultimately, exposure to overtopping can be synthesized with an overtopping index, I_o, given as

$$I_O = \frac{\mathrm{TWL} - dhigh}{dhigh - dtoe} \tag{2}$$

in order to compare relative vulnerability between study areas (Mull and Ruggiero 2014). Positive values of I_o indicate overtopping and negative values indicate that no overtopping occurred. An overtopping index value of one indicates that the TWL exceeds *dhigh* by approximately one dune height.

Mull and Ruggiero (2014) used an event selection approach to examine the potential for dune overtopping during a major extratropical cyclone, with an approximately 30-year return period, that struck the PNW coastline between March 2–4, 1999 (Allan and Komar 2002). During the storm, SWHs, peak spectral periods (T_p), and non-tidal residuals exceeded 12 m, 16 s, and 1 m, respectively. Estimates of the overtopping index were made in the event that the maximum storm conditions measured in the region impacted the entire coastline directly, in order to identify specific dune-backed areas in the PNW that are particularly vulnerable to overtopping. For example, the extreme TWLs produced during this event are shown for three sample locations in Fig. 6 based on dune morphometrics extracted from 2002 lidar data. The overtopping index results for these three sites suggest that there is a relatively high exposure to overtopping in the southern portion of Clatsop Plains and at Rockaway Beach. These areas are developed with significant infrastructure directly behind the foredunes that would be immediately impacted by overtopping. An index that is close to 0, but still negative, indicates that a profile will not be overtopped for these storm conditions, but may be overtopped during a more extreme design storm (i.e., a storm with a 100-year return period rather than a 30-year return period). Mean overtopping indices for each littoral cell (not shown) confirm that of the three littoral cells compared here, Rockaway is the most vulnerable littoral cell to overtopping, and that Clatsop Plains is the least vulnerable to overtopping.

Seabloom et al. (2013) also examined the potential for the region's foredunes to be overtopped, but instead used hydrodynamic conditions extrapolated to the 100-year storm event (SWH = 14.5 m). In this study, the potential for overtopping was estimated for three grass invasion scenarios (Historical, Current, and Future), three wave period scenarios (Decreasing, Current Conditions, and Increasing), three wave height scenarios (Decreasing, Current Conditions, and Increasing), and three sea-level scenarios (No Change, Slow Rise, and Rapid Rise) for a total of 81 combinations. Since our earlier work had suggested that invasion of coastal dune systems by *A. breviligulata* had reduced the height of coastal foredunes previously dominated by *A. arenaria* (Seabloom and Wiedemann 1994; Hacker et al. 2012), the beach grass invasion scenarios represented (1) historical conditions in which all dunes were dominated by *A. arenaria* and dune heights were higher, (2) current conditions in which *A. breviligulata* dominates most areas in Washington and northern Oregon and dune heights were as measured, and (3) possible future conditions in which all dunes are dominated by *A. breviligulata* and dune heights are lower than the present day. The climate change scenarios represented approximately 40 years of increasing or decreasing storminess (e.g., Ruggiero et al. 2010; Young et al. 2011) and a range of region-specific SLR projections (NRC 2012).

Seabloom et al.'s (2013) quantification of the relative exposure to storm-wave-induced dune overtopping posed by the *A. breviligulata* invasion in the face of projected multi-decadal changes in sea level and storm intensity is summarized in Fig. 11. Changes in wave period during the analyzed extreme event were the primary driver of changes in exposure to flooding (I_o), accounting for 16% of the total variability (Fig. 11a). Invasion accounted for an additional 8% of the variability in exposure to flooding. Wave height (Fig. 11b) and SLR (Fig. 11c) accounted for only

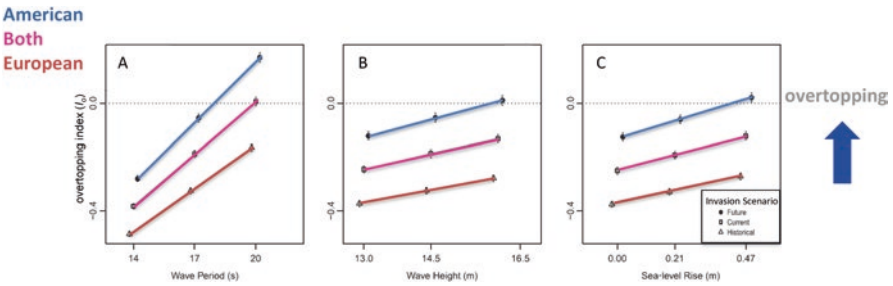

Fig. 11 Effects of wave period (**a**), wave height (**b**), and sea-level rise (**c**) on the overtopping index under different beach grass invasion scenarios. Positive overtopping index values indicate conditions in which foredunes will be overtopped during storms. Invasion scenarios represent the following: Historical (*Ammophila arenaria* only), Current (*A. breviligulata* in the north and *A. arenaria* in the south), and Future (*A. breviligulata* only). Overtopping index values are averaged across all transects and all sea-level rise scenarios. Error bars represent 1 SEM (modified from Seabloom et al. 2013)

1.4% and 1.7% of the variability in flooding exposure, respectively. While altered storm intensity was the largest driver of overtopping extent, the invasion by *A. breviligulata*, which lowers dune heights, tripled the number of areas in the PNW vulnerable to overtopping and posed a fourfold larger exposure than SLR over multi-decadal time scales.

6 Implications for Enhancing Beach-Dune Interaction Models

The work described herein demonstrates the tight linkages that can occur between the biotic and abiotic forces that govern the development of geomorphology, especially in highly dynamic systems like coastal foredunes. In our PNW case study, we demonstrate that the invasion of two novel grass species continues to alter dune geomorphology and ultimately the coastal protection services the dunes provide. The impact of the grasses, though, appears to be dependent on sand supply, suggesting that the impacts of the beach grass invasions are context-dependent. Foredunes in the northern sites where *A. breviligulata* dominates are shorter and wider compared to sites in the south where *A. arenaria* dominates. Many of the beaches in the northern part of the region are prograding, primarily due to massive offshore sand remobilization following the construction of jetties at the mouths of the Columbia River and Grays Harbor (Kaminsky et al. 2010). In contrast, the SCR is lower at the southern sites (erosional or stable) where *A. arenaria* dominates, resulting in foredunes that are taller and narrower (Fig. 5). Examining these results in the context of existing conceptual beach-dune interaction models provides insights into the processes involved in foredune growth or foredune recovery following storm events

(see Houser et al. this volume and Houser and Ellis 2013 for a detailed review of such models).

Short and Hesp (1982) developed one of the earliest beach-dune interaction models. Using data from the high energy, microtidal Australian coastline, they argued that dissipative surf zones had the highest potential wave-driven onshore transport, while reflective beaches had the lowest. Dissipative beaches have the lowest mobility, the widest fetch, and the lowest beach slopes, whereas reflective beaches have steep beach slopes and short fetches, limiting transport of sediment to dunes. According to Short and Hesp (1982), these transport rates determine the potential size of foredunes which are correspondingly largest on dissipative beaches and smallest on reflective beaches. In the PNW, the lowest dune heights are found in the northern sub-cells of the CRLC –North Beach, Grayland Plains, and the Long Beach Peninsula. Due to fine, Columbia River-derived sand (D_{50} ~ 0.2 mm), these beaches are modally dissipative (Wright and Short 1983). In contrast to what might be expected from the Short and Hesp (1982) model, the dunes in these littoral cells are among the lowest in the PNW (Fig. 5), a result most likely due to the relatively high rates of sediment supply.

Psuty's (1992) beach-dune model assumes that sediment supply is the driving factor for foredune evolution. When sediment supply to the beach is large, foredune development is limited by the possibility of prograding beaches and the development of new, seaward foredunes that limit the supply of sediment to the now relict foredune. Rapid beach progradation leads to a series of low foredune ridges, while lower rates of progradation allow for the development of a single, larger foredune. Psuty's (1992) model suggests that when the beach sediment budget is just negative (due to cross-shore exchange of sediment from the beach to the dune), foredune development (dune volume growth or crest height increase) is at a maximum (blue curve in Fig. 12). When sediment supply to the beach is such that the beach sediment budget is significantly negative (due to sediment losses offshore or alongshore), the availability of sediment for aeolian transport to dunes is limited and foredune growth is halted and the features are susceptible to erosion and overwash (e.g., see Rodriguez et al. this volume).

Missing from the simple conceptual models of Short and Hesp (1982) and Psuty (1992) are the impacts of beach grasses and our findings show that these impacts can be significant. We have found that, for a given sand supply (beach sediment budget), foredunes dominated by *A. breviligulata* are lower than foredunes dominated by *A. arenaria* due to differences in the ability of *A. breviligulata* to accumulate sand (Hacker et al. 2012; Zarnetske et al. 2012). Thus, it appears that both the beach grass introductions and inherent variability in sand supply along the coast have resulted in the present day foredune structure, which varies widely throughout the region (Fig. 5c; Hacker et al. 2012; Mull and Ruggiero 2014). We can qualitatively test the Psuty (1992) model by using data derived from the CRLC (Fig. 12). As mentioned above, SCR can be taken as a proxy for Psuty's "beach sediment budget" and foredune vertical growth rate (VGR, Fig. 9) as a proxy for "foredune sediment budget." Examining this phase space in Fig. 12 (along with a least squares second order polynomial fit to the data, not shown) suggests that the shape of Psuty's

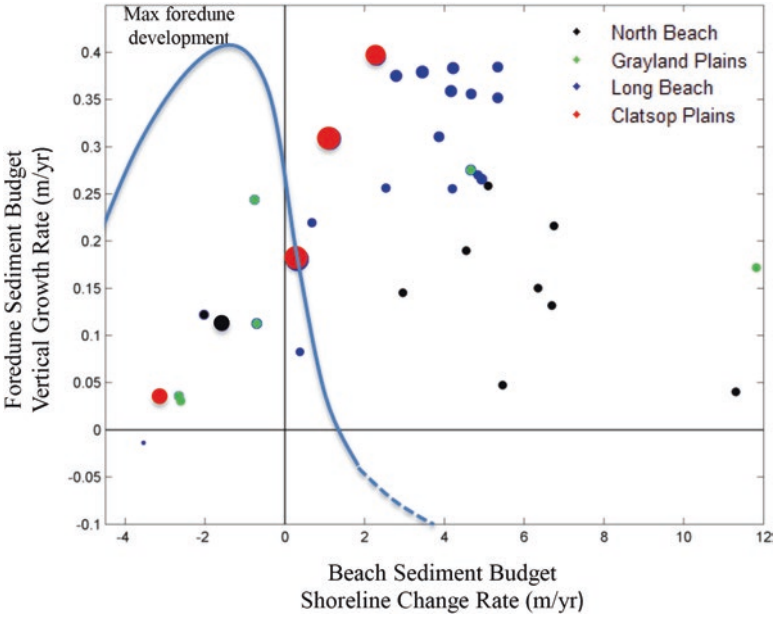

Fig. 12 Relationship between foredune vertical growth rate, a proxy for foredune sediment budget, and shoreline change rate, a proxy for beach sediment budget, along the CRLC. The size of the symbols is proportional to the height of the dunes. The symbol colors indicate which sub-cell within the CRLC the data are derived from. Note that dunes at least partially dominated by *A. arenaria* have larger foredunes than those dominated by *A. breviligulata*. The *blue curve* is the conceptual model of Psuty (1992) in which the location within the four quadrants of the phase plane dictates the relative rate of foredune development

model describing foredune development is qualitatively correct. Interestingly, at least for the CRLC data, the apex of maximum foredune development is shifted to the right. This result is possibly due to the relatively high rates of sediment supply available along the CRLC in recent decades.

The largest dunes in the CRLC (largest circles in Fig. 12) are in the Clatsop Plains, a sub-cell with relatively modest shoreline change rates. These dunes also have the highest vertical growth rates for a given shoreline change rate. While the other three sub-cells of the CRLC are dominated by *A. breviligulata*, the foredunes of Clatsop Plains have approximately even distributions of *A. breviligulata* and *A. arenaria* (Hacker et al. 2012; Fig. 5e). Therefore, the species-specific feedbacks described above coupled with the sediment supply model of Psuty (1992) provide a reasonable explanation of the factors important to dune shape variability along the PNW. This information is beginning to be incorporated into more sophisticated, process-based dune-building models (e.g., Duran and Moore 2013, 2015; Moore et al. 2016, this volume) to expand the plant-scale sediment capture mechanisms described here to ecosystem-scale dynamics. These models, in turn, can potentially assist in coastal management, restoration, and engineering decisions.

7 Synthesis and Conclusions

Here we have reviewed a dramatic case where the invasion of two species of beach grasses, coupled with alongshore variability in sand supply, have created a range of foredunes shapes along the PNW coast. Whereas the dune grass species appear almost identical in the field, they differ in morphology and growth form, their abundance and distribution along the coast, and their potential to impact coastal dune shape. Few studies have used variability in dune vegetation and sand supply across such large spatial scales to explore the functional two-way processes that play a role in determining dune geomorphology. However, as envisioned by Murray et al. (2008), data concerning both physical and biological change at relatively large scales, such as those reported here, are necessary to parameterize and ultimately place ecomorphodynamic models on solid empirical footing. Data collected in the PNW has revealed that the two grass species are associated with significantly different foredune shapes that are likely controlled by a combination of variability in sand supply along the coast and subtle differences in the congeners' morphology and growth form.

In addition to the field studies, we used a mesocosm experiment to look at plant growth responses to sand deposition and found that, in response to increasing sand supply rates, *A. arenaria* produced higher-density vertical tillers (characteristic of higher sand capture efficiency), while *A. breviligulata* and *E. mollis* responded with lower-density lateral tiller growth (characteristic of lower sand capture efficiency). To investigate sand capture, we used a moveable bed wind tunnel experiment and found that increasing tiller density increased sand capture efficiency and that, under different experimental densities, the native grass had higher sand capture efficiency compared to the *Ammophila* congeners. However, the greater natural densities of non-native grasses under field conditions suggest that they have greater potential to capture more sand overall. Together, the field data, wind tunnel experiment, and mesocosm experiment results provide evidence for species-specific biophysical feedbacks between sand deposition, growth habit, and growth-habit-mediated sand capture efficiency, leading to the documented differences in the shapes of dunes dominated by the two grass invaders along the PNW coast. Further, our observations show that at decadal scales and with modest sand supply, vegetation changes controlled the evolution of foredune geomorphology, while at shorter time scales, sand supply processes outweighed the effects of vegetation.

It is possible that further invasion by *A. breviligulata* will eventually lower foredune heights along the entire PNW coast. Under future climate change, species invasions, sand supply, SLR, and changes in storminess are all likely to interact in ways that make coastal protection uncertain, especially across different spatial and temporal scales. Consequently, interdisciplinary studies like these are increasingly important to provide novel insights that can help anticipate changes to coastal protection. In particular, the results of these studies can be used to help make predictions about how foredune shape will change in relation to changes in vegetation, sand supply, and climate change impacts such as sea-level rise and possible changing storminess patterns.

Acknowledgments The field, mesocosm, and laboratory observations described in this manuscript are the result of the hard work by many individuals from Oregon State University, the Evergreen State College, the Washington Department of Ecology, the Oregon Department of Geology and Mineral Industries, and the U.S. Geological Survey. Funding for the work synthesized in this paper was provided by the U.S. Environmental Protection Agency (EPA/NCER 83383601-0), Oregon Sea Grant (NA060AR4170010, NA10OAR4170010), the National Science Foundation (IGERT NSF award 0333257), the National Oceanic and Atmospheric Administration (NOAA award NA15OAR4310243), the Northwest Association of Networked Ocean Observing Systems (NANOOS), the O.H. Hinsdale Wave Research Laboratory, and a Mamie Markham Research Grant (Hatfield Marine Science Center). This manuscript benefited greatly from thorough reviews of Evan B. Goldstein and an anonymous reviewer.

References

Allan JC, Komar PD (2000) Are ocean wave heights increasing in the eastern North Pacific? EOS Trans Am Geophys Union 81(47):561–567

Allan JC, Komar PD (2002) Extreme storms on the Pacific Northwest coast during the 1997–98 El Niño and 1998 La Niña. J Coast Res 18(1):175–193

Allan JC, Komar PD (2006) Climate controls on US West Coast erosion processes. J Coast Res 22:511–529

Atwater BF (1996) Coastal evidence for great earthquakes in western Washington. In: Rogers AM, Walsh TJ, Kockelman WJ, Priest GR (eds), Assessing earthquake hazards and reducing risk in the Pacific Northwest, vol 1. U.S. Geological Survey Professional Paper 1560, pp 77–90

Barbier E, Hacker SD, Kennedy C, Koch E, Stier AD, Silliman B (2011) The value of estuarine and coastal ecosystem services. Ecol Monogr 81:169–193

Carter RWG (1990) Coastal environments: an introduction to the physical, ecological and cultural systems of coastlines. Academic Press, London, UK

Cooper WS (1958) Coastal sand dunes of Oregon and Washington. Mem Geol Soc Am 72:169

Duran O, Moore L (2013) Vegetation controls on the maximum size of coastal dunes. PNAS 110(43):17217–17222. https://doi.org/10.1073/pnas.1307580110.Emanuel

Duran O, Moore LJ (2015) Bistability of barrier islands induced by biophysical interactions. Nat Clim Chang 5(2):158–162

Duarte CM, Losada IJ, Hendriks IE, Mazarrasa I, Marba N (2013) The role of coastal plant communities for climate change mitigation and adaptation. Nat Clim Chang 3. https://doi.org/10.1038/nclimate1970

Elko N, Sallenger AH, Guy K, Stockdon H, Morgan K (2002) Barrier island elevations relevant to potential storm impacts: 1. Techniques. Open File Report 02-287, U.S. Geological Survey, St. Petersburg, FL, 6p

Elko N, Brodie K, Stockdon H, Nordstrom K, Houser C, McKenna K, Moore L, Rosati J, Ruggiero P, Thuman R, Walker I (2016) Dune management challenges on developed coasts. Shore Beach 84(1):1–14

Feagin RA, Sherman DJ et al (2005) Coastal erosion, global sea-level rise, and the loss of sand dune plant habitats. Front Ecol Environ 3(7):359–364

Guerry AD, Ruckelshaus MH, Arkema K, Bernhardt JR, Guannel G, Kim CK, Marsik M, Papenfus M, Toft JE, Verutes G, Wood SA, Beck M, Chan F, Chan KMA, Gelfenbaum G, Gold BD, Halpern BS, Labiosa WB, Lester SE, Levin PS, McField M, Pinsky ML, Plummer M, Polasky S, Ruggiero P, Sutherland DA, Tallis H, Day A, Spencer J (2012) Modeling benefits from nature; using ecosystem services to inform coastal and marine spatial planning. Int J Biodivers Sci Ecosyst Serv Manag 8(1–2):107–121. https://doi.org/10.1080/21513732.2011.647835

Gutierrez JL et al (2012). Physical ecosystem engineers and the functioning of estuaries and coasts. In: Heip CHR et al (eds) Functioning of estuaries and coastal ecosystems, vol 7. In: Wolanski E, McLusky D (series eds) The treatise on estuarine and coastal science. Elsevier

Hacker S, Zarnetske P, Seabloom E, Ruggiero P, Mull J, Gerrity S, Jones C (2012) Subtle differences in two non-native congeneric beach grasses significantly affect their colonization, spread, and impact. Oikos 121(1):138–148. https://doi.org/10.1111/j.1600-0706.2011.01887.x

Hesp P (1989) A review of the biological and geomorphological processes in the initiation and development of incipient foredunes. Proc R Soc Edinb 96:191–202

Houser C, Ellis J (2013) Beach and dune interaction. In: Shroder J (Editor in Chief), Sherman DJ (ed) Treatise on geomorphology. Coastal geomorphology, vol 10. Academic Press, San Diego, CA, pp 267–288

Houser C, Barrineau P, Hammond B, Saari B, Rentschler E, Trimble S, Wernette P, Weymer B, Young S (2018) Role of the foredune in controlling barrier island response to sea level rise. In: Moore LJ, Murray AB (eds) Barrier dynamics and response to changing climate. Springer, New York

Inman DL, Nordstrom CE (1971) On the tectonic and morphologic classification of coasts. J Geol 79(1):1–21

IPCC (2014) Climate change 2014: impacts, adaptation and vulnerability. Contributions of Working Group II to the Fifth Assessment Report of the Intergovernmental Panel on Climate Change, Cambridge University Press, New York

Kaminsky GK, Ruggiero P, Buijsman MC, Gelfenbaum G (2010) Historical evolution of the Columbia River littoral cell. Mar Geol. https://doi.org/10.1016/j.margeo.2010.02.006

Kaminsky GM, Ruggiero P, Gelfenbaum G (1998) Monitoring coastal change in southwest Washington and Northwest Oregon during the 1997/98 El Niño. Shore Beach 66(3):42–51

Kim C-K, Toft JE, Papenfus M, Verutes G, Guerry AD et al (2012) Catching the right wave: evaluating wave energy resources and potential compatibility with existing marine and coastal uses. PLoS One 7(11):e47598. https://doi.org/10.1371/journal.pone.0047598

Komar PD (1986) The 1982–83 El Niño and erosion on the coast of Oregon. Shore Beach 54(2):3–12

Komar PD, Allan JC, Ruggiero P (2009) Ocean wave climates—Trends and variations due to Earth's changing climate. In: Kim YC (ed) Handbook of coastal and ocean engineering. World Scientific, Singapore, pp 971–975

Komar PD, Allan JC, Ruggiero P (2011) Sea level variations along the US Pacific Northwest coast: tectonic and climate controls. J Coast Res 5(27):808–823. https://doi.org/10.2112/JCOASTRES-D-10-00116.1

Komar PD, Allan JC, Ruggiero P (2013) Chapter 21: U.S. Pacific Northwest Coastal Hazards: Tectonic and Climate Controls. In: Finkl C (ed) Coastal hazards, pp 587–674

Lipiec E (2015) Assessing coastal community adaptation scenarios in the face of climate change: a Tillamook county, Oregon, example. M.S. thesis, Oregon State University

Martinez ML, Psuty NP (2004) Coastal dunes: ecology and conservation. Springer, London

Méndez FJ, Menéndez M, Luceño A, Losada IJ (2006) Estimation of the long-term variability of extreme significant wave height using a time-dependent peak over threshold (POT) model. J Geophys Res Oceans 111(C7):C07024

Menéndez M, Méndez FJ, Losada IJ, Graham NE (2008) Variability of extreme wave heights in the northeast Pacific ocean based on buoy measurements. Geophys Res Lett 35(22):L22607

Mills A (2015) Exploring the impacts of climate and management on coastal community vulnerability through alternative future scenarios. M.S. thesis, Oregon State University

Moore LJ, Ruggiero P, List JH (2006) Comparing mean high water and high water line shorelines: should proxy-datum offsets be incorporated in shoreline change analysis? J Coast Res 22(4):894–905

Moore L, Duran O, Ruggiero P (2016) Vegetation control allows autocyclic formation of multiple dunes on prograding coasts. Geology 4(7):559–462. https://doi.org/10.1130/G37778.1

Moore LJ, Goldstein EB, Vinent OD, Walters D, Kirwan M, Rebecca L, Brad Murray A, Ruggiero P (2018) The role of ecomorphodynamic feedbacks and landscape couplings in influencing the response of barriers to changing climate. In: Moore LJ, Murray AB (eds) Barrier dynamics and response to changing climate. Springer, New York

Mull J, Ruggiero P (2014) Estimating storm-induced dune erosion and overtopping along U.S. West Coast beaches. J Coast Res 30(6):1173–1187. https://doi.org/10.2112/JCOASTRES-D-13-00178.1.

Murray AB, Knaapen MAF, Tal M, Kirwan ML (2008) Biomorphodynamics: physical-biological feedbacks that shape landscapes. Water Resour Res 44:W11301

Nordstrom KF, Jackson NL, Kraus NC, Kana TW, Bearce R, Bocamazo LM, Young DR, DeButts HA (2011) Enhancing geomorphic and biologic functions and values on backshores and dunes of developed shores: a review of opportunities and constraints. Environ Conserv 38:288–302

NRC (2012) Sea level rise for the Coasts of California, Oregon, and Washington: past, present, and future, s.l.: Committee on Seal Rise in California, Oregon, and Washington: Board of Earth Sciences and Resources; Ocean Studies Board; Division on Earth and Life Studies

Psuty NP (1992) Spatial variation in coastal foredune development. Proceedings of the 3rd European dune congress, Balkema, Rotterdam, The Netherlands, pp 3–13

Pye K, Tsoar H (1990) Aeolian Sand and Sand Dunes. Unwin Hyman, London, UK

Revell DL, Komar PD, Sallenger AH (2002) An application of LIDAR to analyses of El Niño erosion in the Netarts Littoral Cell, Oregon. J Coast Res 18(4):792–801

Rodriguez AB, Yu W, Theuerkauf EJ (2018) Abrupt increase in washover deposition along a transgressive barrier island during the late nineteenth century acceleration in sea-level rise. In: Moore LJ, Murray AB (eds) Barrier dynamics and response to changing climate. Springer, New York

Ruggiero P, Komar PD, McDougal WG, Marra JJ, Beach RA (2001) Wave runup, extreme water levels and the erosion of properties backing beaches. J Coast Res 17(2):407–419

Ruggiero P, Kaminsky GM, Gelfenbaum G, Voigt B (2005) Seasonal to interannual morphodynamics along a high-energy dissipative littoral cell. J Coast Res 21(3):553–578

Ruggiero P, List JH (2009) Improving accuracy and statistical reliability of shoreline position and change rate estimates. J Coast Res 25(5):1069–1081

Ruggiero P, Komar PD, Allan JC (2010) Increasing wave heights and extreme-value projections: the wave climate of the U.S. Pacific Northwest. Coast Eng 57:539–552. https://doi.org/10.1016/j.coastaleng.2009.12.005

Ruggiero P, Mull J, Zarnetske P, Hacker S, Seabloom E (2011) Interannual to decadal foredune evolution. In: Proceedings of coastal sediments 2011. ASCE, Miami, FL, pp 698–711

Ruggiero P (2013) Is the intensifying wave climate of the U.S. Pacific Northwest increasing flooding and erosion risk faster than sea level rise? J Waterw Port Coast Ocean Eng. https://doi.org/10.1061/(ASCE)WW.1943-5460.0000172

Ruggiero P, Kratzmann MA, Himmelstoss EG, Reid D, Allan J, Kaminsky G (2013) National assessment of shoreline change: historical shoreline change along the Pacific Northwest Coast. U.S. Geological Survey Open-File Report 2012-1007, 62p

Ruggiero P, Kaminsky G, Gelfenbaum G, Cohn N (2016) Morphodynamics of prograding beaches: a synthesis of seasonal- to century-scale observations of the Columbia River littoral cell. Mar Geol 376:51–68. https://doi.org/10.1016/j.margeo.2016.03.012

Sallenger AH (2000) Storm impact scale for barrier islands. J Coast Res 16:890–895

Seabloom E, Ruggiero P, Hacker S, Mull J, Zarnetske P (2013) Invasive grasses, climate change, and flood risk in coastal ecosystems. Glob Chang Biol. https://doi.org/10.1111/gcb.12078

Seabloom EW, Wiedemann AM (1994) Distribution and effects of Ammophila breviligulata Fern. (American Beach Grass) on the foredunes of the Washington Coast. J Coast Res 10:178–188

Seymour RJ (2011) Evidence for changes to the northeast Pacific wave climate. J Coast Res 27(1):194–201

Short A, Hesp P (1982) Wave, beach and dune interactions in Southeastern Australia. Mar Geol 48:259–284

Stockdon HF, Holman RA, Howd PA, Sallenger AH Jr (2006) Empirical parameterization of setup, swash, and runup. Coast Eng 53(7):573–588

Stockdon HF, Sallenger AH, Holman RA, Howd PA (2007) A simple model for the spatially-variable coastal response to hurricanes. Mar Geol 238:1–20

Stockdon HF, Doran KS, Sallenger AH (2009) Extraction of LiDAR-based dune crest elevations for use in examining the vulnerability to beaches during inundation during hurricanes. J Coast Res 53:59–65

Wiedemann AM, Pickart AJ (2004) Temperate zone coastal dunes. In: Martinez M, Psuty N (eds) Coastal dunes: ecology and conservation. Springer, Berlin, pp 53–65

Wright LD, Short AD (1983) Morphodynamics of beaches and surf zones in Australia. In: Komar PD (ed) CRC handbook of coastal processes and erosion. CRC Press, Boca Raton, FL, pp 35–64

Young IR, Ziegler S, Babanin AV (2011) Global trends in wind speed and wave height. Science 332(6028):451–455

Zarnetske PL, Seabloom EW, Hacker SD (2010) Non-target effects of invasive species management: beach grass, birds, and bulldozers in coastal dunes. Ecosphere 1:13

Zarnetske PL, Ruggiero P, Seabloom EW, Hacker SD (2015) Coastal foredune evolution: the relative influence of vegetation and sand supply in the US Pacific Northwest. J R Soc Interface 12(106):20150017. https://doi.org/10.1098/rsif.2015.0017

Zarnetske PL, Hacker SD, Seabloom EW, Ruggiero P, Killian JR, Maddux TB, Cox D (2012) Biophysical feedback mediates effects of invasive grasses on coastal dune shape. Ecology 93(6):1439–1450. https://doi.org/10.1890/11-1112.1

Barrier Islands as Coupled Human–Landscape Systems

Dylan E. McNamara and Eli D. Lazarus

Abstract In recent decades, coastal development has transformed barrier systems around the world. The longest, most intensively developed chain of barriers extends along the Atlantic and Gulf Coasts of the U.S., where mean population density is the highest in the country. There are nearly 300 barrier islands between Maine and Texas, and of these, at least 70 are intensively built-up. Concentrated development exists and continues despite the fact that barrier islands are transient landscapes, not only over geologic time scales of millennia, but also within human and economic time scales of centuries to decades. Populated barrier islands are inherently vulnerable to natural hazards such as sea-level rise, cumulative erosion, and storm events; this vulnerability drives humans to actively modify barrier geometry and environments. The most common manipulations are beach nourishment, to mitigate shoreline erosion, and increases to dune height or seawall construction to prevent flooding and damage from overwash during storm events. Over time scales of years to decades, hazard-mitigation actions impact natural, spatio-temporal barrier processes such as washover deposition and planform transgression, which in turn affect future efforts to manage, control, or prevent changes to barrier morphology. Through their maintenance and persistence, interventions against coastal hazards represent a significant dynamical component of developed barrier-island system evolution, such that, within the past century, human actions and natural barrier-island processes have become dynamically coupled. This coupling leads to steady-state barrier-island behaviors that are new. A fundamental way to understand how developed barrier islands will respond to climate change over decadal time scales is to treat these settings as strongly coupled human–natural systems. Dynamical demonstration of coupled-system behavior suggests new avenues for less reactionary and more holistic coastal management perspectives for barrier systems and raises questions about whether and how society may adapt to coastal change. Over time scales

D.E. McNamara (✉)
Department of Physics and Physical Oceanography, Center for Marine Science, University of North Carolina, Wilmington, NC, USA
e-mail: mcnamarad@uncw.edu

E.D. Lazarus
Environmental Dynamics Lab, Geography and Environment Unit, University of Southampton, Southampton, UK
e-mail: E.D.Lazarus@soton.ac.uk

L.J. Moore, A.B. Murray (eds.), *Barrier Dynamics and Response to Changing Climate*, https://doi.org/10.1007/978-3-319-68086-6_12

longer than centuries, human interventions may be coupled only weakly to long-term barrier dynamics. Short of major technological advancements or sweeping decisions to transform these environments into comprehensively geoengineered terrains, high-density development on U.S. barrier islands will eventually have to change—perhaps radically—from its current configuration.

Keywords Coupled system • Developed coasts • Beach nourishment • Coastal adaptation • Soft-engineering • Geoengineering • Coastal management • Beach economics • Coastal property • Common-pool resources

1 Introduction

For developed barrier islands around the world, hazard and risk are both increasing. Intensifying and often compounded coastal hazards include sea-level rise, storm flooding, and shoreline erosion (which can be a function of sea-level rise and changes in wave climate). Likewise, risk is increasing as a function of population density and infrastructure development in coastal zones worldwide. As a result, coastal environments—and barrier islands, especially—are being transformed by management decisions, hazard-mitigation interventions, and deliberate manipulation of coastal morphology. In economics, risk is typically defined as the likelihood of a hazard event (where hazard is a physical change of a given magnitude driven by a natural event or process) multiplied by the value of assets and infrastructure susceptible to damage from that event. A recent report by the U.S. National Research Council defines coastal risk "as the potential for coastal hazards, such as storm surge–induced flooding and wave attack, to cause adverse effects on human health and well-being; economic conditions; social, environmental, and cultural resources; infrastructure; and the services provided within a community" (NRC 2014: 1). Coastal management and engineering interventions to reduce risk and mitigate hazard impacts often have unintended consequences, including complex feedbacks between human activities and physical coastal change that researchers are just beginning to understand (Nordstrom 2000; Kirwan and Megonigal 2013; Temmerman et al. 2013; Stive et al. 2013; Temmerman and Kirwan 2015; Lazarus et al. 2016).

Barrier islands comprise approximately 10% of the world's open-ocean coastline, and more than 400 barrier islands fringe the seaboards of the United States; collectively, they represent 24% of barrier-island shoreline length worldwide, a quantity more than twice the next highest national total (Mexico; 11%) (Stutz and Pilkey 2011). There are nearly 300 barrier islands between Maine and Texas—nearly 2.5 times more than on the Pacific Coast—accounting for over 16,800 km^2 (~6500 mi^2) of land area, or 1.5% of coastal shoreline county area along the Atlantic and Gulf Coasts. Of these, at least 70 are intensively developed. Between 1945 and 1975, barrier-island land used for urban development increased by 153% (over

~500 km^2 or ~200 mi^2); in 1975, urban development comprised 14% of Atlantic and Gulf Coast barrier-island land area, when the national average was only 3% (Dolan and Lins 2000). In many states, especially throughout the Mid-Atlantic, barrier islands host a disproportionate amount of high-value housing stock (Nordstrom 2000).

Moreover, these same places have experienced marked increases in population. According to a NOAA report on recent Census data (NOAA 2013), the mean percent historic population change for "coastal shoreline counties" in the U.S. (defined as "counties that are directly adjacent to the open ocean, major estuaries, and the Great Lakes") increased by 39% between 1970 and 2010, but coastal shoreline counties along the U.S. Eastern Seaboard and Gulf Coast sustained a 62% increase. (The U.S. mean for all counties was 52%.) Mean population density in Atlantic and Gulf Coast shoreline counties (556 people mi^{-2}) already exceeds the mean density of coastal shoreline counties more generally (446 people mi^{-2}) and the mean density nationally (105 people mi^{-2}). (Note that the U.S. Census calculates density in terms of square miles, by convention.) Of the total number of housing units in the U.S. in 2010, 39% were in coastal shoreline counties, along with 42% of all U.S. seasonal homes. Nearly four million new housing units appeared in coastal shoreline counties between 2000 and 2010, representing an 8% increase overall; seasonal units increased by 18%. At last count, 52% of U.S. households with an annual household income greater than $150,000 were in coastal shoreline counties.

The transient nature of the barrier landscape (e.g., FitzGerald et al. 2008) makes development on barrier systems inherently vulnerable to natural coastal hazards and drives humans to actively modify barrier geometry and environments. One way barriers absorb the hydrodynamic energy of coastal storms is through overwash. When tide, surge, wave set-up, and swash combine during a storm into an elevated water level that exceeds barrier height, shallow overland flow—overwash—travels across the barrier, carrying sediment with it (Sallenger 2000). Over long time scales (10^2–10^3 year), overwash enables barriers to maintain their height and width relative to sea level (Leatherman 1979a, b, 1983). Over short time scales (<10^2 year), overwash can result in inland flooding and constitutes a hazard (e.g., Rogers et al. 2015). The most common manipulations of barrier shorelines are beach nourishment, to mitigate shoreline erosion, and increases to dune height or seawall construction to prevent flooding and damage from overwash during storm events. As human interventions modify the natural environment to make it more accommodating for development, those modifications affect spatio-temporal changes resulting from natural physical processes (see FitzGerald et al. this volume; Houser et al. this volume; Moore et al. this volume; Murray and Moore this volume; Odezulu et al. this volume; Rodriguez et al. this volume), which in turn affect subsequent interventions. For example, beach nourishment and dune construction alter the distribution of barrier overwash (and washover) in space and time, barrier height and width, and spatial patterns of change in planform shoreline position. Interfering in these natural barrier processes and traits in turn affects subsequent management and engineering decisions regarding future nourishment projects. The ubiquity, maintenance, and persistence of beach nourishment, dune construction, cliff stabilization, and

seawalls, jetties, and other structures mean that interventions and modifications now function as intrinsic morphodynamic components of the developed barrier system—and thus control how developed barrier islands evolve as landforms.

Over intermediate time scales of years to decades, human actions and barrier-island processes are therefore dynamically coupled. Werner and McNamara (2007: 399) describe the constituent parts of a human–landscape system in which dynamic coupling is particularly strong:

> "…human–landscape coupling should be strongest where fluvial, oceanic or atmospheric processes render significant stretches of human-occupied land vulnerable to large changes and damage, and where market processes assign value to the land and drive measures to protect it from damage. These processes typically operate over the (human) medium scale of perhaps many years to decades over which landscapes become vulnerable to change and over which markets drive investment in structures, evaluate profits from those investments and respond to changes in conditions."

On barrier islands, coupling leads to dynamical states into which the developed coastal system may evolve, termed "attractors", which represent a subset of its possible configurations, such as states characterized by high-density infrastructure, high property value, and significant investment in mitigation practices. Present attractors for developed barriers may also include chaotic evolution of beach width (Lazarus et al. 2011), "sucker" and "free-rider" dynamics among neighboring coastal towns (detailed below in Sect. 2.1) (Williams et al. 2013), and complex spatial connections between locations separated by long distances within regional-scale littoral cells (where a "cell" is a closed sediment system of sources, transport, and sinks) (Slott et al. 2008, 2010; McNamara et al. 2011; Ells and Murray 2012; Murray et al. 2013).

As external forcing such as sea-level rise and rates of coastal erosion increase, dynamical attractors for barrier islands are likely to become unstable. For example, recent work suggests that property markets may anticipate the increasingly precarious nature of barrier-island real estate as sea level rises, and perhaps drive divestment from barrier-island property (McNamara and Keeler 2013). If divestment from developed barrier islands turns into abandonment, it is not clear what the future of these environments will be. Ancient examples of coastal development, abandonment, and reoccupation are at best distant analogs for modern society (Dunning et al. 2012; Turner and Sabloff 2012). Conceptual frameworks for spatio-temporal patterns in tourist-driven economies still struggle to resolve more than one iteration of a boom-bust cycle (Butler 2006). Some work has suggested that after abandonment, the evolution of "fresh", less precarious (albeit temporarily) natural barrier-island sites entices renewed development, such that development pressures shift across and within a given barrier system in space and time (McNamara and Werner 2008a). This posited boom-and-bust attractor emerges over long time scales, making it difficult to constrain (McNamara and Werner 2008b). However, its dynamical demonstration suggests new avenues for less reactionary and more holistic coastal management perspectives for barrier systems and raises questions about whether and how society may adapt to coastal change, whether through abandonment or reinforcement of economic drivers to continue intensifying coastal development.

Traditional approaches to understanding decadal- to centennial-scale evolution of coastal systems have either treated human activity as a perturbation to physical dynamics, or treated physical change as a perturbation to human activity. However, both are unidirectional treatments of cause and effect and cannot address the feedback-driven, coupled dynamics of change along developed coastlines (Nordstrom 1994, 2000; Lazarus et al. 2016). In this chapter, we address coupled dynamics: specifically, we elaborate on beach nourishment as a specific linking mechanism in the coupled dynamics of developed barrier islands and examine how this coupled system evolves to current configurations with unanticipated emergent behaviors. We also explore some controlling factors on the timing of destabilization of coupled coastal systems as sea level rises and erosion increases. Finally, we summarize work that evolves coupled coastal systems over longer time scales and discuss what potentially "decoupled" developed coastal systems (if natural dynamics become completely dominated by engineering, or if coastal development becomes too expensive to maintain) might mean for future coastal vulnerability to extreme events.

2 Beach Nourishment and Coupled Coastal Dynamics

Figure 1 illustrates beach nourishment as a coupled human–landscape system (Werner and McNamara 2007). Natural spatial and temporal patterns of shoreline erosion and accretion are a function of net cross-shore and alongshore sediment flux, driven by storm impacts, waves, and other physical transport processes. With coastal development comes the introduction of economic value: beach width becomes a source of natural capital, and proximity to that source of capital affects the values and prices of other assets, from real estate to commercial businesses (Smith et al. 2009). A wide beach is more valuable to a coastal town, both directly and indirectly, than a narrow one. However, when shoreline erosion impinges upon that development, the real or prospective damage spurs investment in coastal defense and hazard mitigation (e.g., beach nourishment, dune reconstruction). So-called "soft-engineering" strategies like beach nourishment, which typically involves importing sand from a source outside the immediate littoral system and depositing it on a reach of eroding shoreline, tend to be preferable to "hard-engineering" options like seawalls because, relative to the latter, the former sustains the natural capital provided by a consistently wide beach (Pilkey and Wright 1988). Paradoxically, investment in coastal defense then encourages further investment in development and infrastructure (Nordstrom 1994; Mileti 1999; Bagstad et al. 2007; Werner and McNamara 2007; Smith 2013; Armstrong et al. 2016). In Florida, single-family shorefront houses in nourishment zones are larger and more numerous than in non-nourishment zones, indicating intensified development in areas known to be at risk (Armstrong et al. 2016). Natural physical impacts on the developed coastal zone (e.g., persistent erosion) may last or intensify over several years to decades, requiring repeated mitigation cycles. For example, the first reported beach-nourishment project on Wrightsville Beach, near Wilmington, North

Fig. 1 Schematic of a developed barrier coastline as a coupled human–landscape system. (*1*) Natural processes of wave-driven sediment transport (Q_s) drive physical coastal changes in space and time; (*2*) development capitalizes on economically viable coastal real estate; (*3*) chronic or event-driven natural hazards damage coastal development and infrastructure, prompting (*4*) interventions to mitigate or prevent damage in the future. Such interventions modify the physical landscape, altering sediment fluxes in (*1*), pushing the cycle to iterate. Reprinted with permission from Elsevier from Lazarus et al. (2016), An evolving research agenda for human–coastal systems. Geomorphology, 256, 81–90

Carolina, was in 1939, and the beach has been rebuilt several times a decade since the 1980s; likewise, Virginia Beach, Virginia, has undergone several nourishment episodes per decade since the 1950s (PSDS 2015). In the U.S. Pacific Northwest, the more common—and controversial—coastal intervention has involved "grading" the tops of high-standing dune systems to allow better views of the ocean, a practice that has completely altered much of the region's natural dune ecology (Nordstrom 2000). Nor are these dynamics limited to the U.S. In Europe, beach nourishment has been ongoing for decades, with trends similar to those observed in U.S. coastal management (Hanson et al. 2002).

As these interventions modify the natural condition of the coastline, and as those changes in turn inform subsequent interventions, the reciprocal feedbacks inherent in beach nourishment as a mitigation strategy mean that an artificially nourished coastal zone functions as a fundamentally coupled human–landscape system. Although beach nourishment is a common mitigation strategy that engineers (Dean and Dalrymple 2002), geomorphologists (Nordstrom 1994, 2000), and economists (Smith et al. 2009; Gopalakrishnan et al. 2011; Hoagland et al. 2012; Jin et al. 2013) have studied in depth, dynamical insight into how persistent nourishment affects economic value of coastal assets and alters coastal response to changes in natural forcing (e.g., storminess, wave climate, sea-level rise) is only beginning to come into focus.

2.1 Modelling the Coupled Economic–Physical System

Recent work has applied dynamic optimization, a perspective that addresses how the behaviors of dynamical systems change as a function of external inputs and internal feedbacks, to explore conditions in which beach-nourishment cycles are economically optimal (Smith et al. 2009). This approach borrows from forestry (Hartman 1976), where tree growth rate, timber value, and fixed costs associated with harvesting yield a time interval between sequential harvests that optimizes the net benefits of the timber stock—that is, the money the timber earns at market minus the fixed costs. Mapped onto beach nourishment, this conceptual framework suggests that erosion rate, the economic value associated with beach width, and the fixed costs of a nourishment project likewise yield a time interval between nourishment episodes that optimizes the net benefits (earnings minus costs) that a coastal town receives. If the town nourishes too frequently, cumulative fixed costs (e.g., permitting, sand acquisition, dredging and earth-moving equipment, labor) exceed the value the beach earns back over the same time period. Oppositely, waiting too long between nourishment episodes means the town loses the revenue it would have earned from a wider beach.

Nourishing at intervals that optimize net economic benefits can be viewed as an emergent state—an attractor in the developed barrier coastline system—that arises once faster-scale market dynamics begin steering nourishment episodes to maximize returns. Although the optimization approach does not explicitly simulate all of the dynamics that drive the coastline into its emergent configuration, exploring how this particular attractor changes with external conditions reveals insight into its functional dependence on environmental forcing. Analytical work on the emergent dynamics of optimal states has raised some fraught implications, even in these deliberately simplified coastal systems.

One implication is the potential for a runaway feedback in which nourishment frequency increases with nourishment cost (Smith et al. 2009), catalyzing a kind of arms race among neighboring towns for access to beach-nourishment material and infrastructure. In the analysis by Smith et al. (2009), nourishment frequency might increase for several reasons, including if the variable costs of nourishment—the price of sand, for example—increase: "when variable costs increase, the relative importance of fixed costs [e.g., permitting, dredge contracting] decrease, reducing the incentive to delay future nourishment" (p. 63). Indeed, the cost of nourishment, indexed as the price of sand per unit volume, has been increasing over recent decades, as has the volume of sand used for beach nourishment and the number of nourishment episodes (Trembanis et al. 1999; Valverde et al. 1999; PSDS 2015). Another implication is the spatial effect of disparities in property values among a series of towns alongshore. McNamara et al. (2011) model a developed coastal system in which different towns alongshore have different tax bases, but all share access to a single reservoir of nourishment sand. As the reservoir of available sand dwindles, the cost of sand increases. If a "wealthy" town is situated in a zone of chronic erosion, their nourishment-cycle calculus (Smith et al. 2009) means that

they will nourish more frequently, driving up the cost of sand faster—and at the expense of non-wealthy towns also in need of beach nourishment. (Conversely, if a wealthy town is situated in a zone with low rates of shoreline erosion, the sand reservoir lasts longer and appears more equitable.) However, as the cost of sand increases, towns with lower property values will likely lose the nourishment arms race to wealthier towns elsewhere, further diminishing property values where they are already low and increasing them where they are already high. A third implication is that the relative contributions of physical, economic, and policy factors to coastal property value could open pathways to potentially rapid property value collapse, whereby the removal of extant government subsidies that reduce effective beach-nourishment costs for coastal towns could undercut property values by as much as 60% (McNamara et al. 2015).

A similar approach also has been extended to numerical models that couple agent-based decision-making to large-scale coastline behavior (Lazarus et al. 2011; Jin et al. 2013; Williams et al. 2013). These studies explore how complex shoreline behavior—spatial behaviors beyond the analytically tractable treatment of shoreline evolution—alters the emergent, optimized coastal–economic state. In one set of simulations, a series of towns alongshore share the same initial beach conditions and property values, but manager agents make nourishment decisions independently of each other. The model shows that spatially myopic nourishment ultimately destabilizes long-term coastline behavior: despite individual manager agents determining and following nourishment schedules that are economically optimal, the system overall transitions into chaotic evolution, with sensitivity to initial conditions and the disappearance of any periodicity in nourishment patterns in space and time (Lazarus et al. 2011). As gradients in alongshore sediment transport increase erosion rates in some places and slow them in others, spatio-temporal patterns of nourishment change as different towns nourish out of sync. The introduction of such variability in the beach-width data that a given manager agent must interpret means that agents are constantly recalculating the nourishment interval that yields an economic optimum. Collectively, the entire (model) developed coastline then departs from its economic optimum (and does not return to it). Spatially myopic nourishment is characteristic of most U.S. East Coast nourishment programs (Smith et al. 2009; Lazarus et al. 2011).

Subsequent simulations for other complex coastline configurations (Murray and Ashton 2013), such as the cuspate planform of the North Carolina coast, have shown that not only does modeled erosion mitigation result in spatial patterns of shoreline erosion and accretion that differ significantly from the spatial patterns that would otherwise occur under natural conditions, but also that sites of sustained nourishment intervention are not necessarily a simple reflection of background erosion patterns (Slott et al. 2010; Ells and Murray 2012; Hapke et al. 2013; Williams et al. 2013; Johnson et al. 2015). Shifts in spatial patterns of erosion and accretion can result in a chronic system of “suckers”, who experience exacerbated erosion rates and compensate with more frequent nourishment, and “free-riders”, who benefit from extra sand (and lower erosion rates, if not shoreline accretion) supplied by their updrift neighbors. When linked to property value, these persistent differences

in beach width can drive disparities in town property values alongshore that eventually span orders of magnitude (Williams et al. 2013).

2.2 Developed Coastlines and Common-Pool Resources

The "suckers" and "free-riders" problem brings beach nourishment into a broader discourse regarding the social and natural dynamics of common-pool resource systems (Lazarus et al. 2016). Common-pool resources are characterized by their open accessibility to users, who must find ways to share the resource, or not; different user groups may use the same resource in different ways. Common-pool resources range from agricultural land and fishing grounds to the Earth's atmosphere. In Hardin's (1968) "tragedy of the commons" narrative, local farmers pasture their cows on the town common; because each farmer always has the same incentive to pasture one more cow, the common soon becomes crowded with cows, who graze it bare, and the arrangement of open access to a shared resource ultimately fails. Other resource economists have generated a huge body of counter-examples (Ostrom et al. 1999; Dietz et al. 2003) in which social institutions, often self-organized, prevent resource collapse and correct inequities among users. But common-pool resources in which the resource flows in a particular direction or otherwise moves in space and time while user groups remain spatially fixed constitute "asymmetrical commons" (Ostrom and Gardner 1993) and represent a particularly difficult kind of dynamical problem.

For example, consider an irrigation system (Freeman 1990). Water flows downstream from an upstream source, with farmers distributed along its route. Too much water use or leaky infrastructure upstream limits the quantity of water available to farmers downstream. If farmers upstream fix the leaks in their irrigation works, farmers downstream benefit even if their own irrigation works are in disrepair. The unidirectional movement of the resource (from upstream down) means that, in the first case of imbalance, farmers upstream lack an incentive to account for farmers downstream, and in the second case, farmers downstream have every incentive to free-ride on infrastructural upkeep by farmers upstream (who become the suckers in this hypothetical system).

On developed coastlines, and developed barriers in particular, beach nourishment and hard structures can have both local and nonlocal effects on shoreline change within a common littoral cell in which sand (and, by extension, beach width) is the shared resource (Stone and Kaufman 1988). For coastal segments in which net alongshore sediment flux has a predominant direction, emplacement of sand-trapping hard structures like groynes and jetties affect sand supply immediately downdrift. But by modifying the planform shape of the coastline, they also affect gradients in alongshore sediment flux over significant distances in both directions, especially where wave forcing conditions are more spatially symmetric (Ells and Murray 2012). These nonlocal effects then play out along the length the littoral cell in the economic decisions individual towns must make regarding subsequent miti-

gation actions. As shoreline management decisions in one place become an indirect function of similar but uncoordinated actions elsewhere, an emergent attractor results (at least when optimization functions as the primary coupling mechanism between the system's physical and economic components) (Lazarus et al. 2011). This attractor is ultimately characterized by unequal access to nourishment sand as a resource, as towns with high property values can afford mitigation when less wealthy towns cannot, and thus, the wealthy towns gain significant advantages in withstanding coastal hazard. Although theoretical, this insight has important implications for policy as it suggests that a more holistic management approach is necessary to avoid rapid depletion of coastal sediment resources and severe economic disparities in defense capacity even across coastal towns within the same region (McNamara et al. 2011; Williams et al. 2013). Likewise, predictions that a loss of property value can result from reductions in nourishment subsidies and increased costs of insurance suggest that changes in coastline mitigation practices should be made with caution (McNamara et al. 2015).

3 Inundation and Abandonment: An Attractor Disappears

Although beach nourishment tempers short-term erosion hazard and dune construction can prevent damage from small and intermediate storm events, both mitigation actions interfere with the processes of barrier transgression and neither ultimately will protect developed barrier islands from inundation as sea level rises. Given this fate, recent numerical modeling has explored specific controlling factors that influence the timing of when developed barriers, as they are presently configured with high property value, dense infrastructure, and frequent mitigation efforts, will cease to be stable or viable as coupled systems (McNamara and Keeler 2013). The modeling work focuses on the roles that coastal property markets, measured observations of coastal change, and belief among market agents in projections of future climate-change play in altering the long-term behavior of a generic, developed barrier system. This use of agent decision-making, which approaches key questions in current discourse on coastal vulnerability and adaptation to climate change (NRC 2014), divides a coastal real estate market into agents who range from those who take climate-change predictions into account and those who do not (Phillips 2012). Given data on historical trends and scientific model predictions about environmental characteristics associated with barrier island and storm behavior (e.g., erosion rates, storm impacts, storm recurrence intervals), individual agents weigh the available information differently to decide how much to pay for a shorefront property and how much to spend on coastal defense. The results show that, relative to agents with little belief in climate-change predictions, informed property owners invest heavily in defensive measures in the short term. However, they abandon coastal real estate when price volatility becomes so significant that they no longer think defensive expenditures are worthwhile. Their exit from the market has a striking effect (McNamara and Keeler 2013: 561):

> "The amount of property damage is larger when model predictions do not inform beliefs, and the magnitude of this difference rises as the rate of SLR [sea-level rise] increases….As non-believers [in projected environmental change] are more likely to own property during periods of high risk, this highlights an important equity issue. Disaster assistance typically represents income transfers from taxpayers as a whole to affected populations…, and the systematic selection of…non-believers into the property market means that broader society is funding repairs for damages that the average citizen would not have suffered."

How private markets anticipate increasing risk and guide adaptive behavior is a key component of policy discussions on coastal adaptation (NRC 2014), especially at the social scale of local residents and community land-use planning processes, and remains a major challenge in future research into developed-coastline dynamics (Lazarus et al. 2016).

3.1 Modeling the Decision to Abandon: Physical Forcing

To extend this previous work on the abandonment of developed barriers, here we investigate other factors that may influence when the coastal home-owner agents in the McNamara and Keeler (2013) coupled model choose to abandon coastal property. The model begins with an initial physical barrier-island state similar to barriers found along the North Carolina Outer Banks, USA. As in the original model, agents can buy and sell coastal properties located on the modeled barrier island. Simulations are run for two sea-level rise scenarios: a "low" scenario in which sea level rises at 3 mm/year, and a "high" scenario in which sea level rises at 10 mm/year. (For specific details of all model dynamics, see McNamara and Keeler 2013.)

First, we examine how an increase in mean storm surge height impacts (a) the time that elapses before coastal inhabitants abandon their property, and (b) the total damage that occurs prior to abandonment. Simulations are run at both sea-level-rise rates. Results show that for rates under both the low and high scenarios, time to abandonment is reduced as mean storm surge height increases (Fig. 2). The amount of damage that occurs prior to abandonment increases significantly with larger increases in mean storm surge height. However, the amount of damage is not a strong function of the rate of sea-level rise; the cumulative damage that occurs in the lead-up to abandonment, when the barrier is precariously low, constitutes the majority of the total damage suffered, which suggests abandonment is driven by additive damage rather than any single event.

3.2 Modeling the Decision to Abandon: Policy Forcing

To examine the role that policy plays in abandonment, we introduce a subsidy for beach-nourishment costs into the model. Historically, the cost of most beach-nourishment projects along the U.S. East Coast has been subsidized by the government at a rate of 66% (NOAA 2006). When simulations are run with the nourishment subsidy ranging from 0 to 60% for the low and high rates of sea-level rise, time to

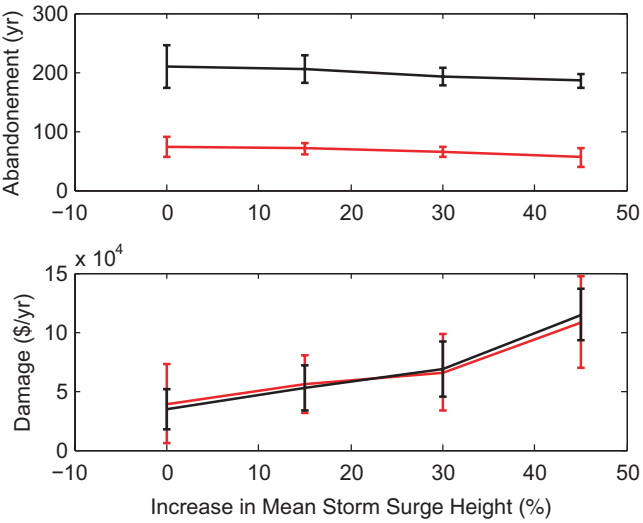

Fig. 2 Results from a coupled real estate market-physical barrier island model showing elapsed time before abandonment and associated total damage sustained as a function of percent increase in mean storm surge height. *Red* and *black* lines denote high and low sea-level rise scenarios, respectively. Error bars reflect the 95% confidence interval from 20 model simulations at each parameter value

abandonment and the amount of damage prior to abandonment both increase as the subsidy increases (Fig. 3). This result again raises issues of equity: given that the nourishment subsidy, as well as emergency repairs in the wake of major storms, is funded from taxes paid by national populace, not just local coastal property owners, tandem increases in both expenditures would likely draw political fire (Pilkey and Dixon 1996).

3.3 Modeling the Decision to Abandon: Psychological Forcing

Finally, to examine how individual perceptions of environmental change might impact abandonment, we run a suite of simulations in which "belief" in forward-looking, "science-based" forecasts increases across all agents. The impact of belief in "science-based" projections is more evident when the rates of sea-level rise are high. In that case, increasing the weight agents give to their belief in forecasts of barrier evolution causes both time to abandonment and damage to decrease (Fig. 4). This result highlights that when the rate of sea-level rise is high, the ability of agents to adapt rapidly to the prospect of significantly diminished future returns (which they do when their belief in science-based forecasts is high), rather than to simply rely on past observations, can affect the total amount of damage sustained prior to barrier abandonment.

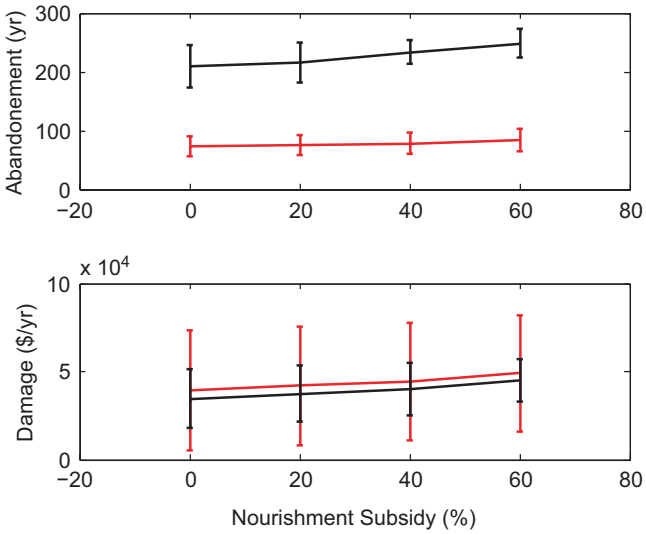

Fig. 3 Results from a coupled real estate market-physical barrier island model model showing elapsed time before abandonment and associated total damage sustained as a function of percent increase in nourishment subsidy. *Red* and *black* lines denote "high" and "low" sea-level rise scenarios, respectively. Error bars reflect the 95% confidence interval from 20 model simulations at each parameter value

These extensions of the coupled modeling by McNamara and Keeler (2013) bring to focus the range of forcing factors that control the timing of systemic instability under conditions representative of developed barriers today. Coastal research typically focuses on sea-level rise rates when considering the fate of populated barrier islands. Although sea-level rise is certainly an important factor, other physical forcing (e.g., storm surge size), policy forcing (e.g., rate of nourishment subsidy), and psychological forcing (e.g., belief in forward-looking models) can play a prominent, if not dominant, role in steering the path toward (or away from) destabilization of the barrier-island attractor and subsequent barrier abandonment.

4 Boom, Bust, Repeat: An Attractor Emerges

Modeling the long-term dynamics of developed coastlines and coastal-resort economies over time scales on the order of centuries, rather than decades, reveals a potential emergent behavior—one of boom and bust cycles—that could play out beyond the time when initial abandonment occurs. For example, McNamara and Werner (2008a) coupled a three-dimensional numerical model of barrier-island evolution with an agent-based model of tourism development. The basic structure of the model routine is the same as the cycle shown in Fig. 1. Natural physical processes (e.g., nearshore bar migration, alongshore sediment transport, dune growth,

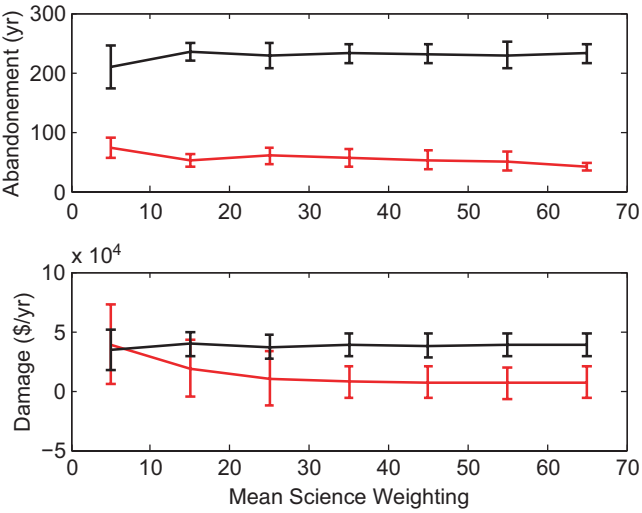

Fig. 4 Results from a coupled real estate market-physical barrier island model model showing elapsed time before abandonment and associated total damage sustained as a function of the mean weight a given agent lends to "science-based" forecasts of barrier-island change. *Red* and *black* lines denote "high" and "low" sea-level rise scenarios, respectively. Error bars reflect the 95% confidence interval from 20 model simulations at each parameter value

sea-level rise) rework the barrier island in between storm events. Meanwhile, heterogeneous economic agents, divided into developers, hotel owners, and tourists, interact in a simulated market for tourism real estate. A policy agent in each shoreline cell alongshore tracks beach width and decides when to implement beach and dune nourishment; if nourishment will result in a net gain in revenue and property appreciation (relative to no nourishment) after costs, then the nourishment project goes ahead. Because populous locations in the model generate significantly more revenue relative to the cost of a nourishment project, they are more likely to replenish (Valverde et al. 1999). In addition to shoreline erosion from sea-level rise, the barrier island is also subject to storm events of differing severity, in which overwash, driven by storm surge (see also Murray and Moore this volume; Houser et al. this volume; Moore et al. this volume; Rodriguez et al. this volume; Odezulu et al. this volume), causes barrier erosion and property damage to which the economic and policy agents respond.

Like in other simulated markets with complex behavior (Arthur 1999), agents track market indicators (e.g., tourist population, numbers of hotel rooms, room rental price, hotel selling price) and make decisions that maximize their own utility functions. Developer agents decide to build a hotel of a certain size (e.g., number of rooms) if its construction will maximize profit (projected sale price minus cost). Hotel-owning agents bid on hotels for sale if the projected appreciation and revenue of those hotels exceed the future return of a risk-free investment (Clayton 1997). The offered purchase price for a hotel is found by setting total demand to the number of hotel rooms offered by developer agents. The economic agents are in turn

coupled to the physical model by tourist agents seeking to maximize their own utility functions, which depend on a combination of economic and beach parameters (e.g., whether the beach town is a familiar or unfamiliar destination, beach width, total vacation cost per day). Within a model year, tourist agents decide whether or not to vacation, and if so, which beaches to visit; hotel agents adjust room price to maximize revenue; and developer agents decide based on anticipated market behavior whether or not to build new hotels. If damaged in a storm, hotels are rebuilt only if projected revenue outweighs costs for the coming year. This rule means that sections of barrier may be abandoned and return to an effectively "undeveloped" state. However, if an unprotected barrier segment remains undamaged long enough for developer agents to project profits there, new building initiates.

In the model, this cycle of resort development, coastal defense, and economic collapse continues episodically, predicting an emergent boom-and-bust pattern in the dynamical behavior of a developed barrier island. Moreover, the pattern oscillates in both space and time. The boom phases are associated with thriving tourism and significant investment in mitigation against rising sea level; the bust phases correspond to complete destruction of resort-town infrastructure. Imminent bust cycles are also signaled (Scheffer 2009) by exaggerated modifications to barrier geometry: a marked narrowing of barrier width and decrease in barrier elevation relative to sea level as beach and dune nourishment prevent the island from overwashing as it would under natural circumstances. (During a bust phase, the island translates landward but rebuilds width and elevation via overwash.) An unintended consequence of mitigating against coastal hazard by filtering out the cumulative impacts of small-scale storms is that large storm events overwhelm barrier defenses and become even more destructive (Werner and McNamara 2007; McNamara and Werner 2008a; Lazarus 2014; Rogers et al. 2015). Despite its abstractions, the model showed good agreement when tested against the historical development of Ocean City, Maryland (McNamara and Werner 2008b), and although data records remain either short or sparse, early signs of this long-term behavioral, boom-bust-repeat pattern may be appearing at other developed barrier locations along the U.S. East Coast (Pilkey et al. 1998; McNamara and Werner 2008a).

5 Conclusions

Recent work by Hapke et al. (2013) investigating historical (~150 years) and recent (25–30 years) measurements of regional-scale shoreline change along the New England and Mid-Atlantic coasts of the U.S. arrives at a startling conclusion. The authors find

> "a strong correlation…between rates of shoreline change and amount of human development over long time periods and large spatial scales. Even moderate amounts of development are associated with reduced erosion indicating that activities associated with protecting and preserving human infrastructure have a substantial and long-lasting impact. The influence of development also appears to override the geomorphological signal of shoreline

> behavior, an important consideration for interpretations of investigations of change along developed coasts. Only along sparsely developed coasts does the shoreline respond as expected with respect to the coastal geomorphology" (Hapke et al. 2013: 169).

Johnson et al. (2015) reach a similar conclusion at the smaller spatial scale of a coastal cape. The fact that intensively developed coastlines behave differently in general from natural coastlines is not a surprise: in Japan, in Belgium, and the Netherlands, and in regions of Italy and the U.S. (Nagao 1991; Kabat et al. 2009; Nordstrom 1994, 2000), researchers have documented the transition of coastlines from natural systems to "human artifacts that bear little resemblance to the coast that formerly existed" (Nordstrom 2000: 16). In this case, the surprise is the effective masking—through sediment diversion, nourishment, and shoreline hardening—of natural geomorphic shoreline-change signals along thousands of kms of coastline. Unlike in the Netherlands, for example, which introduced as part of its national policy framework for coastal defense a comprehensive beach-nourishment program to fix and maintain indefinitely the 1990 position of the Dutch shoreline (Hillen and Roelse 1995), the U.S. Eastern Seaboard reflects no such coordinated policy, planning, or integrated coastal management on any comparable scale. If, as Hapke et al. (2013: 169) conclude, "naturally forced variations in rates of shoreline change through time may only be detectable within sparsely developed stretches of coastline," then empirical, analytical, quantitative consideration of humans as principal agents of large-scale coastal geomorphic change (Hooke 1994, 2000; Hooke et al. 2012; Haff 2003, 2010, 2012) is a scientific imperative for future coastal sustainability, not just a theoretical exercise (Lazarus et al. 2016).

Whether signals of natural coastal hazards are obscured by gradual, incremental interventions or massive geoengineering works matters to the dynamics of the developed coastal system (Lazarus 2014). Technological interventions, including hazard defenses, buffer human enterprise—the development and infrastructure that supports societal functions and activity—from natural variability and allow otherwise naturally inhospitable places to be not only inhabitable, but comfortable. (Beach nourishment and seawalls aside, imagine South Florida without air conditioning.) However, hazard defenses that evolve incrementally tend to be reactionary—for example, raising levee height based on the magnitude of the last storm to overtop them (Werner and McNamara 2007), or expanding the width of a beach enough to lend shorefront protection but not so much that tourists get discouraged by a long trek to the water's edge (Smith et al. 2009). By comparison, massive hazard defenses designed for very long time scales (Kabat et al. 2009) may so overwhelm faster-acting natural processes that the system may appear "decoupled": defenses over-engineered for short time scales (< decades) may be so effective at preventing damage that the hazard component of the coupled human–natural system shown in Fig. 1 (step 3) is functionally bypassed (Lazarus 2014). However, the unintended consequence of filtering out frequent, minor hazard events is that the coupled human–natural system becomes vulnerable to infrequent, major, more destructive events (Werner and McNamara 2007; Lazarus 2014). By extension, once a coupled system has evolved toward a state of low frequency, high magnitude hazard exposure, hazard mitigation requires constant maintenance to compensate

for increased risk (Lazarus 2014). Consider that in 1953, when a disastrous North Sea winter storm struck the U.K., Dutch, and Belgian coasts, the extensive—and predominantly earthen—Dutch flood-defense infrastructure had languished without maintenance during and after the Second World War (Gerritsen 2005). Furthermore, when the strength of background forcing increases (e.g., rising sea level or increasing storminess), events that were once extreme become more likely to occur, putting further strain on the resources demanded by the highly coupled attractor.

For the barriers islands of the U.S. East Coast, given the evident dominance of human interference in patterns of natural coastal sediment flux, the next advances into understanding quantitatively the dynamics of developed coastlines will stem from empirical and analytical investigations of the economic and policy instruments and social processes of decision-making that directly and indirectly affect coastal management and, in turn, the ways in which developed coastal environments evolve. Direct measurement of anthropogenic controls on storm-driven overwash and washover in developed shorefront zones (Rogers et al. 2015) offers a promising answer to a long-standing data gap (Nordstrom 1994). Investigations into the intrinsic and external factors, from beach width to tax and insurance subsidies, that influence coastal property values—and the effects those values have on coastal management and policy—comprise another fast-expanding area (Landry et al. 2003; Kriesel and Landry 2004; Bagstad et al. 2007; Bin et al. 2008; Smith et al. 2009; Gopalakrishnan et al. 2011; Landry and Jahan-Parvar 2011; Jin et al. 2015). Still another underexplored tool for dynamical insight is agent-based modeling with agent behaviors that better capture the psychology of decision-making and adaptive learning, which would represent a departure from agents guided by rule-based optimization of utility functions (Lazarus et al. 2016). Overall, future work on developed coastlines needs to be rich in data analysis of social (including economic) and physical parameters and engage nonlinear approaches capable of resolving causal drivers, lags, and coupling in complex, dynamical human–landscape systems (Sugihara et al. 2012).

Acknowledgments D.E.M. acknowledges funding support from NSF grants (EAR-0952120 and EAR-1053113). E.D.L. acknowledges funding support from Welsh Government and HEFCW through the Sêr Cymru National Research Network for Low Carbon, Energy and the Environment RESILCOAST Project, and from the UK NERC BLUEcoast project (NE/N015665/2). We thank the Editors, Marty Smith, and two anonymous reviewers for constructive comments on the chapter manuscript.

References

Armstrong SB, Lazarus ED, Limber PW, Goldstein EB, Thorpe C, Ballinger RC (2016) Indications of a positive feedback between coastal development and beach nourishment. Earth's Future 4:626–635

Arthur WB (1999) Complexity and the economy. Science 284:107–109

Bagstad KJ, Stapleton K, D'Agostino JR (2007) Taxes, subsidies, and insurance as drivers of United States coastal development. Ecol Econ 63:285–298

Bin O, Kruse JB, Landry CE (2008) Flood hazards, insurance rates, and amenities: evidence from the coastal housing market. J Risk Insur 75:63–82
Butler R (ed) (2006) The tourism area life cycle, vol 1. Channel View Publications, Clevedon
Clayton J (1997) Are housing price cycles driven by irrational expectations? J Real Estate Financ Econ 14:341–363
Dean RG, Dalrymple RA (2002) Coastal processes with engineering applications. Cambridge University Press, Cambridge
Dietz T, Ostrom E, Stern PC (2003) The struggle to govern the commons. Science 302:1907–1912
Dolan R, Lins H (2000) The Outer Banks of North Carolina. U.S. Geological Survey Professional Paper, Report 1177-B (4th printing)
Dunning NP, Beach TP, Luzzadder-Beach S (2012) Kax and kol: collapse and resilience in lowland Maya civilization. Proc Natl Acad Sci U S A 109:3652–3657
Ells K, Murray AB (2012) Long-term, non-local coastline responses to local shoreline stabilization. Geophys Res Lett 39:L19401
FitzGerald DM, Fenster MS, Argow BA, Buynevich IV (2008) Coastal impacts due to sea-level rise. Annu Rev Earth Planet Sci 36:601–647
FitzGerald DM, Hein C, Hughes Z, Kulp M, Georgiou I, Miner M (2018) Runaway barrier island transgression concept: global case studies. In: Moore LJ, Murray AB (eds) Barrier dynamics and response to changing climate. Springer, New York
Freeman DM (1990) Designing local irrigation organization for linking water demand with supply. In: Sampath RK, Young RA (eds) The social, economics and institutional issues on Third World management. Westview Press, Boulder, pp 111–140
Gerritsen H (2005) What happened in 1953? The Big Flood in the Netherlands in retrospect. Phil Trans R Soc A 363:1271–1291
Gopalakrishnan S, Smith MD, Slott JM, Murray AB (2011) The value of disappearing beaches: a hedonic pricing model with endogenous beach width. J Environ Econ Manag 61:297–310
Haff PK (2003) Neogeomorphology, prediction, and the Anthropic landscape. In: Wilcock PR, Iverson RM (eds) Prediction in geomorphology, Geophysical Monograph No 135. American Geophysical Union, Washington, DC, pp 15–26
Haff PK (2010) Hillslopes, rivers, plows, and trucks: mass transport on Earth's surface by natural and technological processes. Earth Surf Process Landf 35:1157–1166
Haff PK (2012) Technology and human purpose: the problem of solids transport on the earth's surface. Earth Syst Dynam 3:417–431
Hanson H, Brampton A, Capobianco M, Dette HH, Hamm L, Laustrup C, Lechuga A, Spanhoff R (2002) Beach nourishment projects, practices, and objectives—a European overview. Coast Eng 47:81–111
Hapke CJ, Kratzmann MG, Himmelstoss EA (2013) Geomorphic and human influence on large-scale coastal change. Geomorphology 199:160–170
Hartman R (1976) The harvesting decision when a standing forest has value. Econ Inq 14:52–58
Hardin G (1968) The tragedy of the commons. Science 162:1243–1248
Hillen R, Roelse P (1995) Dynamic preservation of the coastline in the Netherlands. J Coast Conserv 1:17–28
Hoagland P, Jin D, Kite-Powell HL (2012) The costs of beach replenishment along the U.S. Atlantic Coast. J Coast Res 28:199–204
Hooke RLB (1994) On the efficacy of humans as geomorphic agents. GSA Today 4:224–225
Hooke RLB (2000) On the history of humans as geomorphic agents. Geology 28:843–846
Hooke RLB, Martin-Duque JF, Pedraza J (2012) Land transformation by humans: a review. GSA Today 22:4–10
Houser C, Barrineau P, Hammond B, Saari B, Rentschler E, Trimble S, Wernette P, Weymer B, Young S (2018) Role of the foredune in controlling barrier island response to sea level rise. In: Moore LJ, Murray AB (eds) Barrier dynamics and response to changing climate. Springer, New York

Jin D, Ashton AD, Hoagland P (2013) Optimal responses to shoreline changes: an integrated economic and geological model with application to curved coasts. Nat Resour Model 26:572–604
Jin D, Hoagland P, DK A, Qiu J (2015) Shoreline change, seawalls, and coastal property values. Ocean Coast Manag 114:185–193
Johnson JM, Moore LJ, Ells K, Murray AB, Adams PN, MacKenzie RA, Jaeger JM (2015) Recent shifts in coastline change and shoreline stabilization linked to storm climate change. Earth Surf Process Landf 40:569–585
Kabat P, Fresco LO, Stive MJF et al (2009) Dutch coasts in transition. Nat Geosci 2:450–452
Kirwan ML, Megonigal JP (2013) Tidal wetland stability in the face of human impacts and sea-level rise. Nature 504:53–60
Kriesel W, Landry C (2004) Participation in the national flood insurance program: an empirical analysis for coastal properties. J Risk Insur 71:405–420
Landry CE, Jahan-Parvar MR (2011) Flood insurance coverage in the coastal zone. J Risk Insur 78:361–388
Landry CE, Keeler AG, Kriesel W (2003) An economic evaluation of beach erosion management alternatives. Mar Resour Econ 18:105–127
Lazarus ED (2014) Threshold effects of hazard mitigation in coastal human–environmental systems. Earth Surf Dyn 2:35–45
Lazarus ED, Ellis MA, Murray AB, Hall DM (2016) An evolving research agenda for human–coastal systems. Geomorphology 256:81–90
Lazarus ED, McNamara DE, Smith MD, Gopalakrishnan S, Murray AB (2011) Emergent behavior in a coupled economic and coastline model for beach nourishment. Nonlinear Process Geophys 18:989–999
Leatherman SP (1979a) Barrier dune systems: a reassessment. Sediment Geol 24:1–16
Leatherman SP (1979b) Migration of Assateague Island, Maryland, by inlet and overwash processes. Geology 7:104–107
Leatherman SP (1983) Barrier dynamics and landward migration with Holocene sea-level rise. Nature 301:415–417
McNamara DE, Keeler A (2013) A coupled physical and economic model of the response of coastal real estate to climate risk. Nat Clim Change 3:559–562
McNamara DE, Werner BT (2008a) Coupled barrier island–resort model: 1. Emergent instabilities induced by strong human-landscape interactions. J Geophys Res Earth Surf 113:F01016. https://doi.org/10.1029/2007JF000840
McNamara DE, Werner BT (2008b) Coupled barrier island–resort model: 2. Tests and predictions along Ocean City and Assateague Island National Seashore, Maryland. J Geophys Res Earth Surf 113:F01017. https://doi.org/10.1029/2007JF000841
McNamara DE, Gopalakrishnan S, Smith MD, Murray AB (2015) Climate adaptation and policy-induced inflation of coastal property value. PLoS One 10:e0121278. https://doi.org/10.1371/journal.pone.0121278
McNamara DE, Murray AB, Smith MD (2011) Coastal sustainability depends on how economic and coastline responses to climate change affect each other. Geophys Res Lett 38:L07401. https://doi.org/10.1029/2011GL047207
Mileti D (1999) Disasters by design. National Academy Press, Washington, DC
Moore LJ, Goldstein EB, Vinent OD, Walters D, Kirwan M, Rebecca L, Brad Murray A, Ruggiero P (2018) The role of ecomorphodynamic feedbacks and landscape couplings in influencing the response of barriers to changing climate. In: Moore LJ, Murray AB (eds) Barrier dynamics and response to changing climate. Springer, New York
Murray AB, Ashton AD (2013) Instability and finite-amplitude self-organization of large-scale coastline shapes. Phil Trans R Soc A 371:20120363
Murray AB, Gopalakrishnan S, McNamara DE, Smith MD (2013) Progress in coupling models of human and coastal landscape change. Comput Geosci 53:30–38
Murray AB, Moore LJ (2018) Geometric constraints on long-term barrier migration: From simple to surprising. In: Moore LJ, Murray AB (eds) Barrier dynamics and response to changing climate. Springer, New York

Nagao Y (1991) Coastlines of Japan. American Society of Civil Engineers, New York
NOAA (National Oceanic and Atmospheric Administration) (2006) Beach nourishment: A guide for local government officials. NOAA Coastal Services Center. Available via https://coast.noaa.gov/archived/beachnourishment/html/human/law/index.htm. Accessed 5 Jan 2015
NOAA (2013) U.S. Population living at the coast. Available via http://stateofthecoast.noaa.gov/population/welcome.html. Accessed 5 Jan 2015
Nordstrom KF (1994) Beaches and dunes of human-altered coasts. Prog Phys Geogr 18:497–516
Nordstrom KF (2000) Beaches and dunes of developed coasts. Cambridge University Press, Cambridge
National Research Council (NRC) (2014) Reducing coastal risk on the East and Gulf Coasts. National Academies Press, Washington, DC
Odezulu CI, Lorenzo-Trueba J, Wallace DJ, Anderson JB (2018) Follets Island: a case of unprecedented change and transition from rollover to subaqueous shoals. In: Moore LJ, Murray AB (eds) Barrier dynamics and response to changing climate. Springer, New York
Ostrom E, Gardner R (1993) Coping with asymmetries in the commons: self-governing irrigation systems can work. J Econ Perspect 7:93–112
Ostrom E, Burger J, Field CB, Norgaard RB, Policansky D (1999) Revisiting the commons: local lessons, global challenges. Science 284:278–282
Phillips L (2012) Sea versus senators. Nature 486:450
Pilkey OH, Dixon KL (1996) The corps and the shore. Island Press, Washington, DC
Pilkey OH, Wright HL III (1988) Seawalls versus beaches. J Coast Res SI 4:41–64
Pilkey OH et al (1998) The North Carolina shore and its barrier islands. Duke University Press, Durham
PSDS (Program for the Study of Developed Shorelines) (2015) Beach nourishment database. Available via http://psds.wcu.edu/projects-research/beach-nourishment/. Accessed 5 Jan 2015
Rodriguez AB, Yu W, Theuerkauf EJ (2018) Abrupt increase in washover deposition along a transgressive barrier island during the late nineteenth century acceleration in sea-level rise. In: Moore LJ, Murray AB (eds) Barrier dynamics and response to changing climate. Springer, New York
Rogers LJ, Moore LJ, Goldstein EB, Hein CJ, Lorenzo-Trueba J, Ashton AD (2015) Anthropogenic controls on overwash deposition: evidence and consequences. J Geophys Res Earth Surf 120:2609–2624. https://doi.org/10.1002/2015JF003634
Sallenger AH Jr (2000) Storm impact scale for barrier islands. J Coast Res 16:890–895
Scheffer M (2009) Critical transitions in nature and society. Princeton University Press, Princeton, NJ
Slott JM, Murray AB, Ashton AD (2010) Large-scale responses of complex-shaped coastlines to local shoreline stabilization and climate change. J Geophys Res Earth Surf 115:F03033. https://doi.org/10.1029/2009JF001486
Slott JM, Smith MD, Murray AB (2008) Synergies between adjacent beach-nourishing communities in a morpho-economic coupled coastline model. Coast Manag 36:374–391
Smith K (2013) Environmental hazards: assessing risk and reducing disaster, 6th edn. Routledge, London
Smith MD, Slott JM, McNamara DE, Murray AB (2009) Beach nourishment as a dynamic capital accumulation problem. J Environ Econ Manag 58:58–71
Stive MJ, de Schipper MA, Luijendijk AP, Aarninkhof SG, van Gelder-Maas C, van Thiel de Vries JS, de Vries S, Henriquez M, Marx S, Ranasinghe R (2013) A new alternative to saving our beaches from sea-level rise: the sand engine. J Coast Res 29:1001–1008
Stone K, Kaufman B (1988) Sand rights: a legal system to protect the 'shores of the sea'. Shore Beach 56:7–14
Stutz ML, Pilkey OH (2011) Open-ocean barrier islands: global influence of climatic, oceanographic, and depositional settings. J Coast Res 27:207–222
Sugihara G, May R, Ye H et al (2012) Detecting causality in complex ecosystems. Science 338:496–500

Temmerman S, Kirwan ML (2015) Building land with a rising sea. Science 349:588–589
Temmerman S, Meire P, Bouma TJ, Herman PM, Ysebaert T, De Vriend HJ (2013) Ecosystem-based coastal defence in the face of global change. Nature 504:79–83
Trembanis AC, Pilkey OH, Valverde HR (1999) Comparison of beach nourishment along the US Atlantic, Great Lakes, Gulf of Mexico, and New England shorelines. Coast Manag 27:329–340
Turner BL II, Sabloff JA (2012) Classic Period collapse of the Central Maya Lowlands: insights about human–environment relationships for sustainability. Proc Natl Acad Sci U S A 109:13908–13914
Valverde HR, Trembanis AC, Pilkey OH (1999) Summary of beach nourishment episodes on the US east coast barrier islands. J Coast Res 15:1100–1118
Werner BT, McNamara DE (2007) Dynamics of coupled human-landscape systems. Geomorphology 91:393–407
Williams ZC, McNamara DE, Smith MD, Murray AB, Gopalakrishnan S (2013) Coupled economic-coastline modeling with suckers and free riders. J Geophys Res Earth Surf 118:887–899

Index

L.J. Moore, A.B. Murray (eds.), *Barrier Dynamics and Response to Changing Climate*, https://doi.org/10.1007/978-3-319-68086-6